THE CONTRIBUTION OF THE ELECTRON MICROSCOPE TO MOLECULAR BIOLOGY

James Robinson Harris

Doctor of Science
University of Edinburgh
1981

NON-ENZYMIC PROTEINS

CONTENTS

This article will apppear, in a slightly modified form, in Volume 2 of Electron Microscopy of Proteins (Harris, J.R., ed.), due to be published by Academic Press late in 1981.

I. INTRODUCTION

In this chapter, the application of negative staining electron microscopy to a limited and somewhat arbitrary selection of non-enzymic proteins and polypeptides will be presented. Data will be drawn from the published studies of several groups and supplemented by published and previously unpublished data of the author. In general, the isolation and purification techniques used to obtain the proteins in a state suitable for electron microscopic study will not be discussed, but this information will be readily available from the reference material.

Most of the studies to be described have employed conventional bright field transmission electron microscopy, without adopting the minimal exposure techniques currently used by certain workers in an attempt to minimize molecular irradiation damage and which are likely to be used more widely in the future, with the increasing availability of instrumental systems for specimen protection. Nevertheless, some studies using dark field transmission and scanning transmission electron microscopy, and single sideband phase contrast interference transmission electron microscopy will also be included. Although most of the electron microscopic studies on proteins have been performed on multi-subunit molecules of molecular weight greater than approximately 100 000, attempts have been made to define the folding of the polypeptide chain, i.e., tertiary structure, within single subunit molecules of lower molecular weight, but with little success . It is, therefore, pertinent to discuss the interesting, although controversial, high resolution electron microscopic studies of Ottensmeyer and his colleagues, who have investigated small proteins and polypeptides using dark field transmission electron microscopy of unstained molecules.

One approach used by these workers, which is significantly different from that of the others under discussion in this chapter, requires the selection of electron optical images of individual polypeptides for subsequent manual construction of regular arrays of similarly orientated molecules, from which an optical diffraction pattern was produced. After filtering, this diffraction pattern to produce signal to noise enhancement, superior reconstructed images of the polypeptides were obtained. The possible value of this approach, its limitations and its application to other systems will be discussed.

11. FERRITIN AND APOFERRITIN

(i) FERRITIN

The iron storage protein ferritin has for many years been subject to study by electron microscopy, initially in relation to its complex hydrous ferric oxide core, but more recently emphasis has also been placed on its multi-subunit hollow sherical shell of protein. Ferritin has been used an a tracer for investigating the permeability of extracellular spaces and the integrity of membrane systems (Brown and Harris, 1970) and as a label for membrane antigens after conjugation with specific antibodies, these various functions being facilitated by the inherent electron opaque iron core of the molecule. Current opinion maintains that the spherical protein shell of ferritin and apoferritin from which the iron has been chemically removed, has 24 identical subunits of molecular weight approximately 18 500. The intact ferritin molecule has an external diameter of approximately 12 nm, but the internal diameter is more difficult to determine precisely owing to the variable and irregular dimensions of the hydrous ferric oxide core (Haggis, 1965). Figures between 6 to 7 nm would appear to be reasonable for the internal diameter of the

spherical shell. Fig. 1 shows randomly spread arrays of horse spleen ferritin negatively stained with sodium phosphotungstate and uranyl acetate. The variable electron density of the the core of the molecules is very distinct, indicating the variable iron content and that the negative stain has not, in the case of sodium phosphotungstate, appreciably penetrated the iron-deficient molecules. Had the negative stain penetrated the hollow core of the iron-deficient molecules, it would be very difficult to distinguish them from the iron rich molecules owing to the comparable density of this stain and ferric oxide. Massover and Cowley (1975), using sodium tetraborate as the negative stain have shown that the presence of apoferritin in ferritin populations can be revealed when the stain does penetrate the protein shell (Fig. 2), because the borate stain has considerably less density (mass thickness) than the ferric oxide but greater density than the protein shell.

If no negative stain is added to the spread ferritin molecules their location is readily detectable, but the protein shell cannot be visualized, so any apoferritin present would go undetected. This becomes particularly apparent when oligomers of ferritin are studied, there being discrete gaps between groups of iron cores. Williams and Harrison (1968) fractionated the mixture of naturally occuring ferritin oligomers by gel filtration chromatography and starch gel electrophoresis, as shown in Figs. 3 and 4. Dimers, trimers, tetramers and pentamers can be detected in which the iron cores are clearly seen to be spaced by the 'invisible' electron transparent protein shells. These workers did in fact resort to the study of unstained ferritin because they feared that the oligomers might dissociate in the presence of negative stain. This does not appear

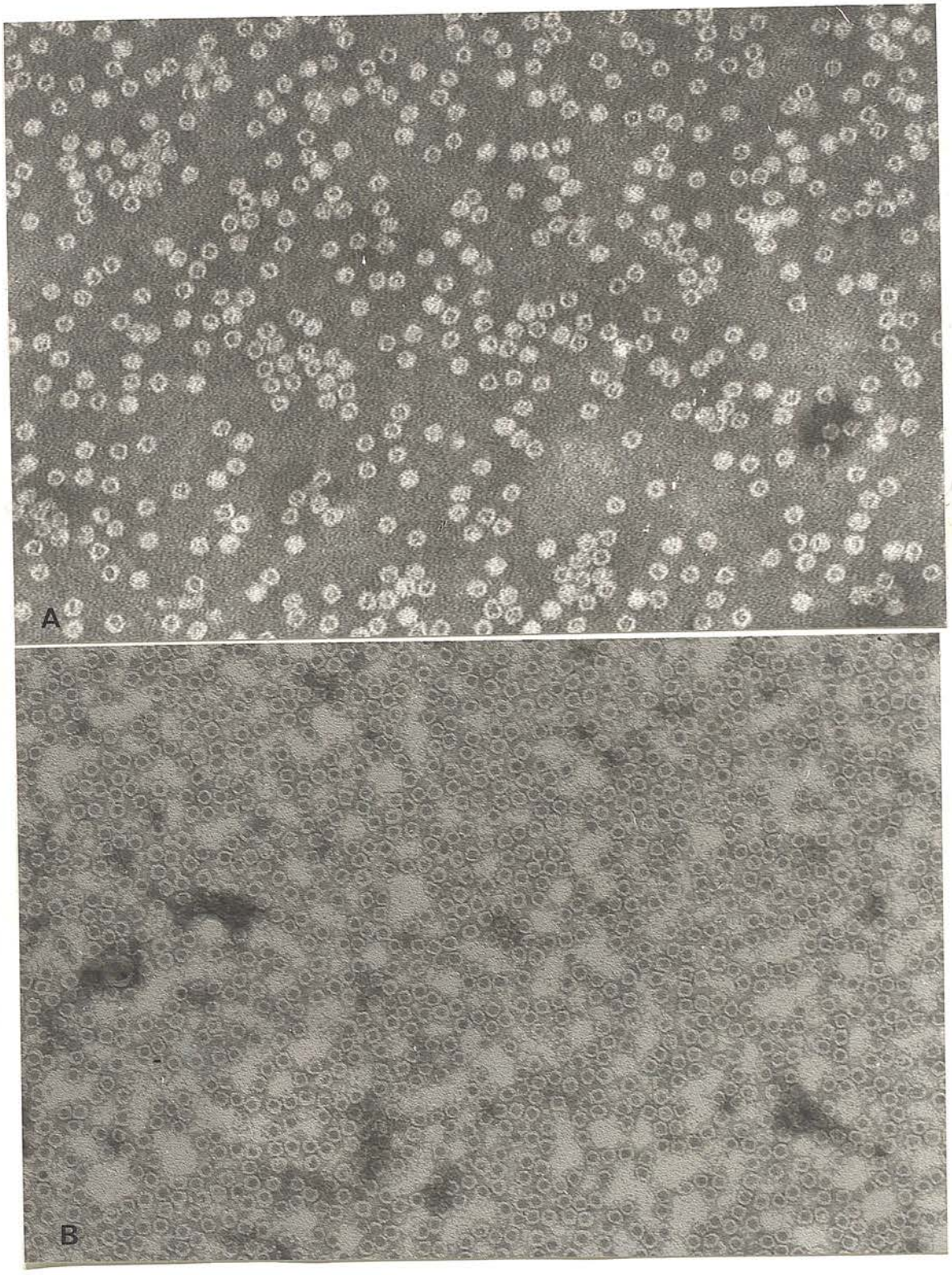

Fig. 1: Horse spleen ferritin, negatively stained (A) with sodium phosphotungstate (pH 7.0) and (B) with uranyl acetate (pH 4.5). x 210 000.

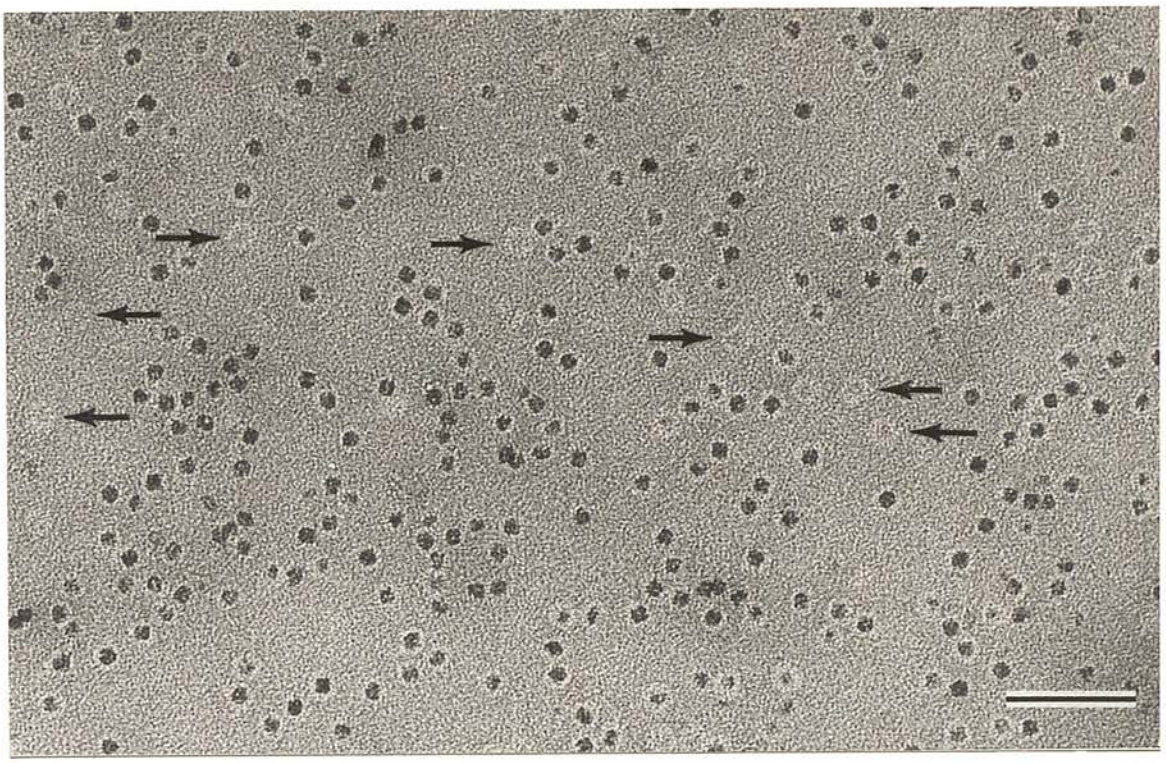

Fig. 2: Horse spleen ferritin, negatively stained with 5% sodium borate. Arrows indicate appoferritin present in the samples. The scale marker indicates 50 nm. By courtesy of W.H. Massover, previously unpublished micrograph.

Fig. 3: Unstained horse spleen ferritin, showing the oligomer-rich fraction obtained by Sephadex G-200 gel filtration chromatography. The iron cores reveal the location of monomers, dimers, trimers and higher oligomers. By the courtesy of M.A. Williams and with the permission of The Biochemical Society. From Williams and Harrison (1968). x 282 000.

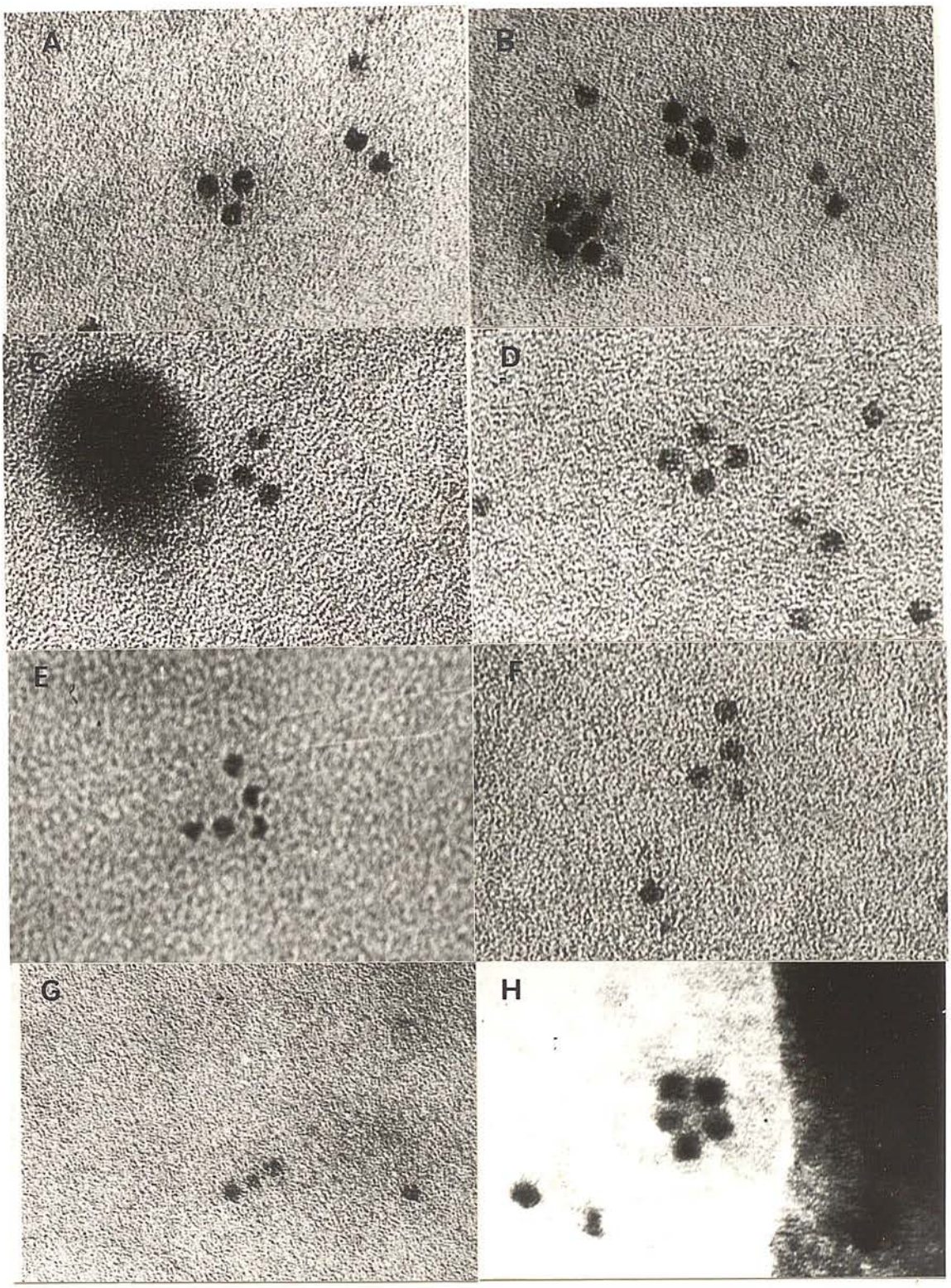

Fig. 4: Unstained oligomers of horse spleen ferritin at higher electron optical magnifications. Note the discrete spacing of the iron cores by the 'invisible' protein shells of the ferritin monomers. By courtesy of M.A. Williams. With permission of The Biochemical Society, from Williams and Harrison (1968). A to F, x 564 000; G, x 426 000; H, x 750 000.

to happen (see below, on apoferritin oligomers), the groups of molecules being particularly stable and only separate form one another when fairly drastic procedures such as ultrasonication or treatment with acetic acid are employed. Further ultrastructural detail of the ferritin molecule has been revealed by the recent studies of Massover (1978a and 1978b). In particular, the attachment of broken protein shells to the iron core has been clearly revealed (Fig. 5), following a variety of disruptive treatments such as freeze-thawing, strong ultrasonication, boiling and cooling, drying and rehydrating. Although the claim was made that some indication of the individual subunits of the protein shell of ferritin could be detected (Figs. 6 and 7), it is the opinion of the present author that the fundamental nature of image formation from a hollow spherical shell resulting from the summated protein thickness parallel to the electron beam will undoubtedly detract from the possibility of directly visualizing subunits of molecular weight 18 500 within the intact molecule. Nevertheless, it is likely that inthe future electron microscopy will have a contribution to make to the study of ferritin dissociation and reassociation, and investigations on single and small groups of subunits are a distinct probability.

An interesting approach has been used by Fromherz (1971) to produce a regular monolayer of ferritin molecules, by adsorption onto a lipid monolayer containing stearic acid methyl ester and eicosic trimethyl ammonium bromide (4:1). To the author's knowledge this work has not been further expanded, but it is of relevance in relation to the application of the carbon-film negative staining technique of Horne and Pasquali-Ronchetti (1974), which has been used to produce regular arrays of apoferritin molecules (see below).

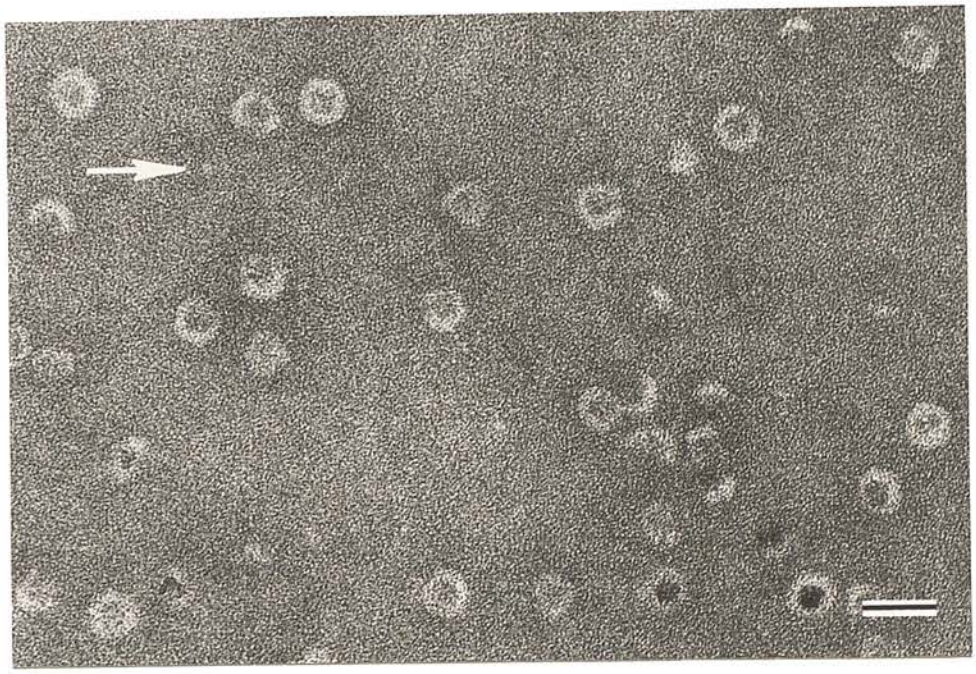

Fig 5: Horse spleen ferritin negatively stained with 2% sodium silicotungstate (pH 7.0) after being frozen and thawed. A significant number of broken protein shells are present and dispersed fragments are also apparent; one of these (arrow) is approximately the size of a single protein subunit of the ferritin shell. The scale marker indicates 20 nm. From Massover (1978b), with permission of Academic Press.

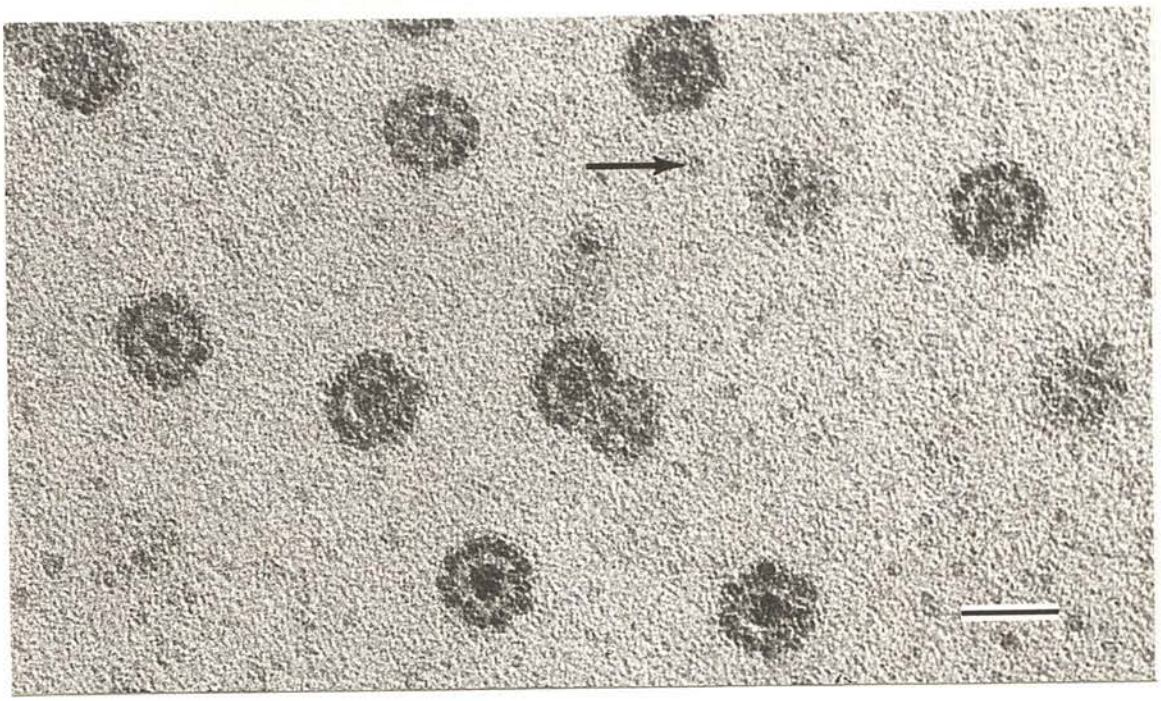

Fig. 6: Horse spleen ferritin deposited onto a carbon film and rotary shadowed (10° at 120 rpm) with uranium. Many separate deposits of metal indicating the subunits of the protein shell are positioned around the perimeter of most molecules; single deposits (arrows) on the carbon substrate could represent dissociated subunits. The scale marker indicates 20 nm. From Massover (1978a), with permission of the Microscopical Society of Canada.

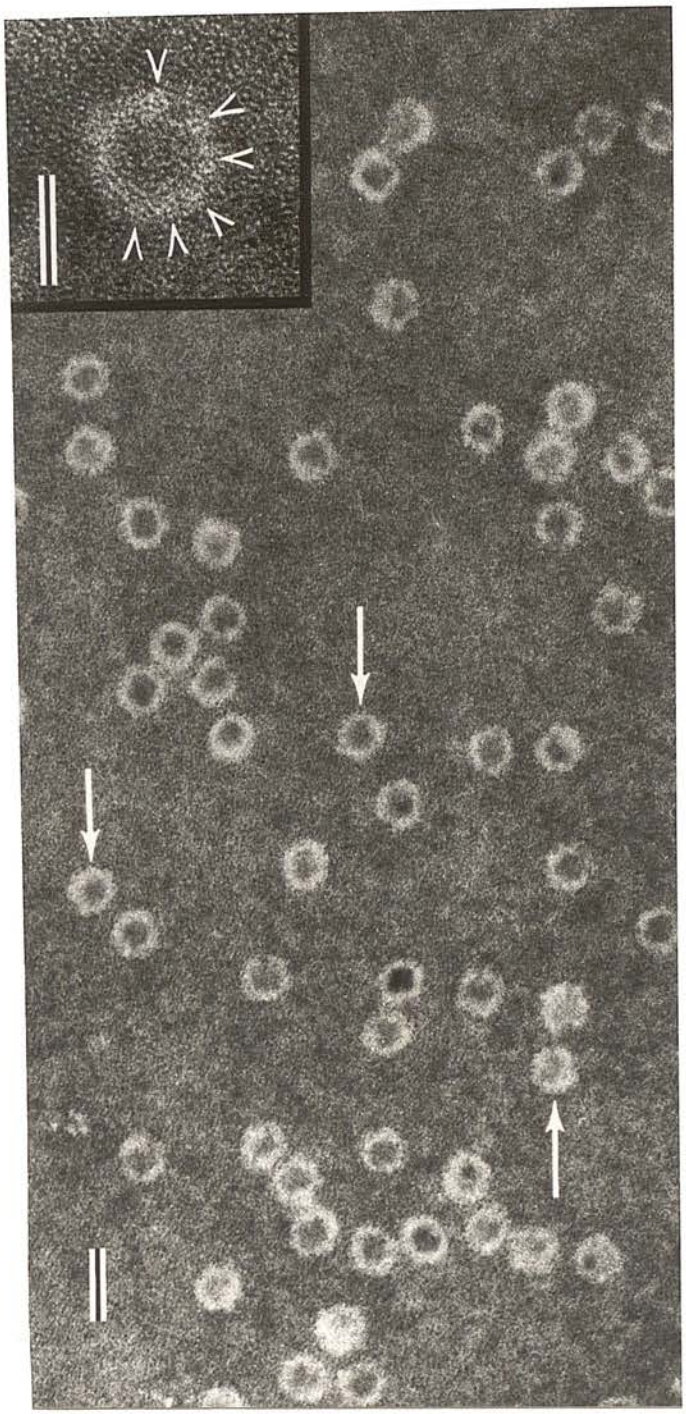

Fig. 7: Horse spleen ferritin deposited onto a carbon film and negatively stained with 2% sodium silicotungstate (pH 7.0). Some molecules(e.g., arrows) show distinct scalloping of their outer perimeter. The scale marker indicates 20 nm. Insert; horse spleen ferritin stripped by thioglycolate treatment, indicating subunit structure within the protein shell (arrow heads). The scale marker indicates 10 nm. From Massover (1978a), with the permission of the Microscopical Society of Canada.

(ii) Apoferritin

Following the removal of the hydrous ferric oxide core of the ferritin molecule by chemical reduction, the protein shell remains intact, as do the oligomers which are apparently extremely stable groups of molecules (Bjork, 1973; Williams and Harrison, 1968). Electron microscopic studies have been performed on purified apoferritin oligomers isolated by gel slicing of 5% polyacrylamide gels following electrophoretic separation, with subsequent electrophoretic elution and concentration of the oligomers using the equipment manufactured by Universal Scientific Ltd., London. This work is complementary to that of Williams and Harrison (1968) on ferritin, mentioned above, but shows a superior purity of the dimer and trimer fractions, and also reveals oligomers with six and more molecules. Representative electron micrographs of the apoferritin monomer, dimer, trimer, tetramer and higher oligomers are shown in Figs. 8 to 12. Despite the fact that Williams and Harrison (1968) showed the ferritin oligomers to resist disruption by a wide variety of dissociating agents, they included no negatively stained material in their study. In our hands, using neutralized phosphotungstic acid and ammonium molybdate, no evidence has been obtained to suggest that these negative stains might split the apoferritin oligomers. Prolonged ultrasonication with efficient cooling, ineither a water bath-type apparatus or the M.S.E. 150 W probe-type apparatus, has been found to slowly separate the oligomers, as shown by the breakdown of purified trimer into dimer and monomer with increasing time (Fig. 13). Trace amounts of the subunits are also detectable by polyacrylamide gel electrophoresis, indicating dissociation of the protein shells, in agreement with the observations of Massover (1978b).

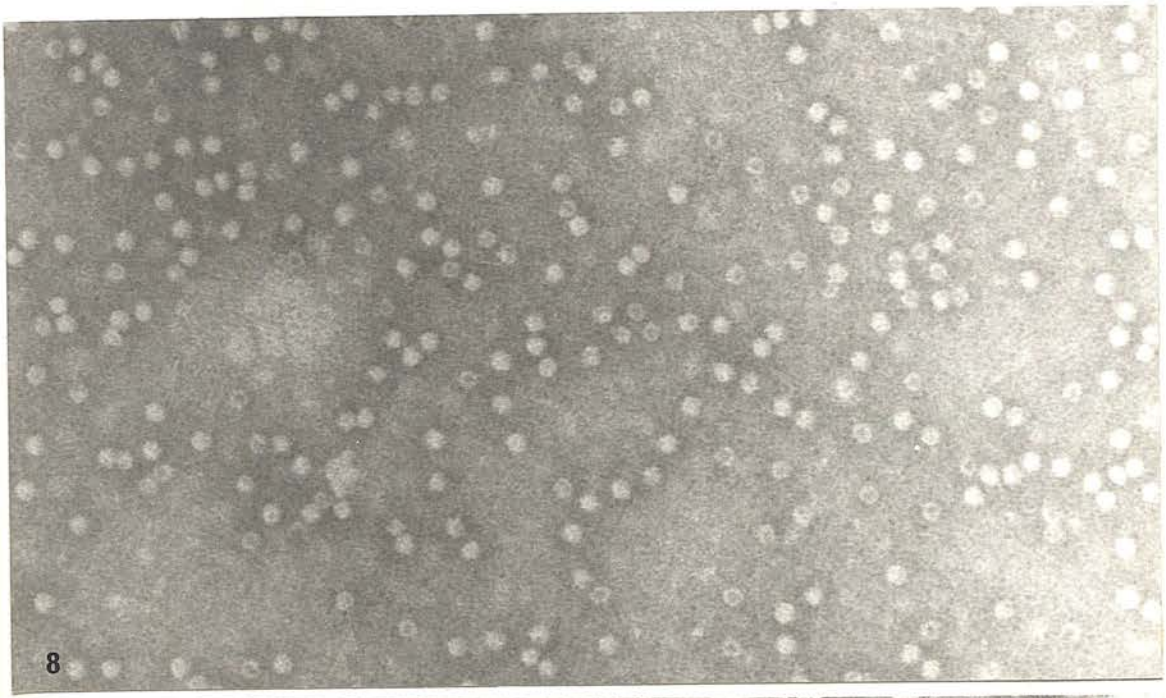

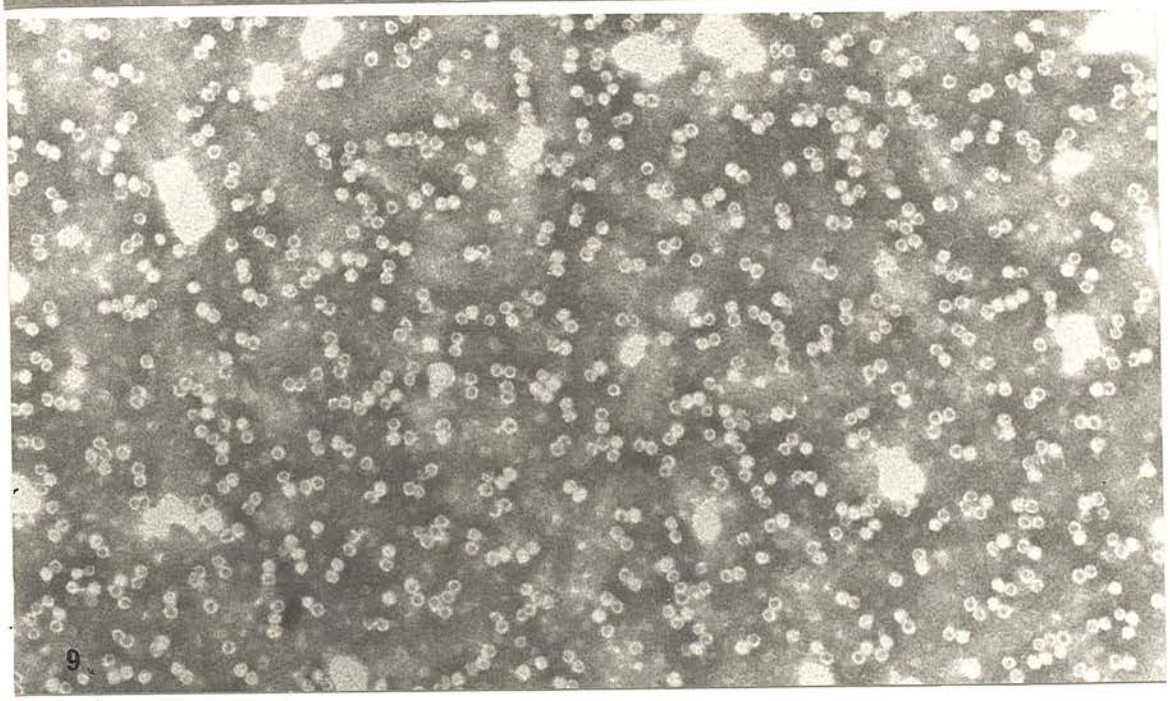

Figs 8 to 12: Horse spleen apoferritin, fractionated by polyacrylamide gel electrophoresis, negatively stained with 2% sodium phosphotungstate (pH 7.0). Fig. 8 shows the monomer band; Fig. 9, the dimer band; Fig. 10, the trimer band; Fig. 11, a mixture of trimers and tetramers; Fig. 12, the topmost slice, containing predominantly tetramers, although some trimers and pentamers are also present, indicating breakdown of the oligomers. x 198 000; x 150 000; x 198 000; x 198 000 and x 198 000, respectively.

10

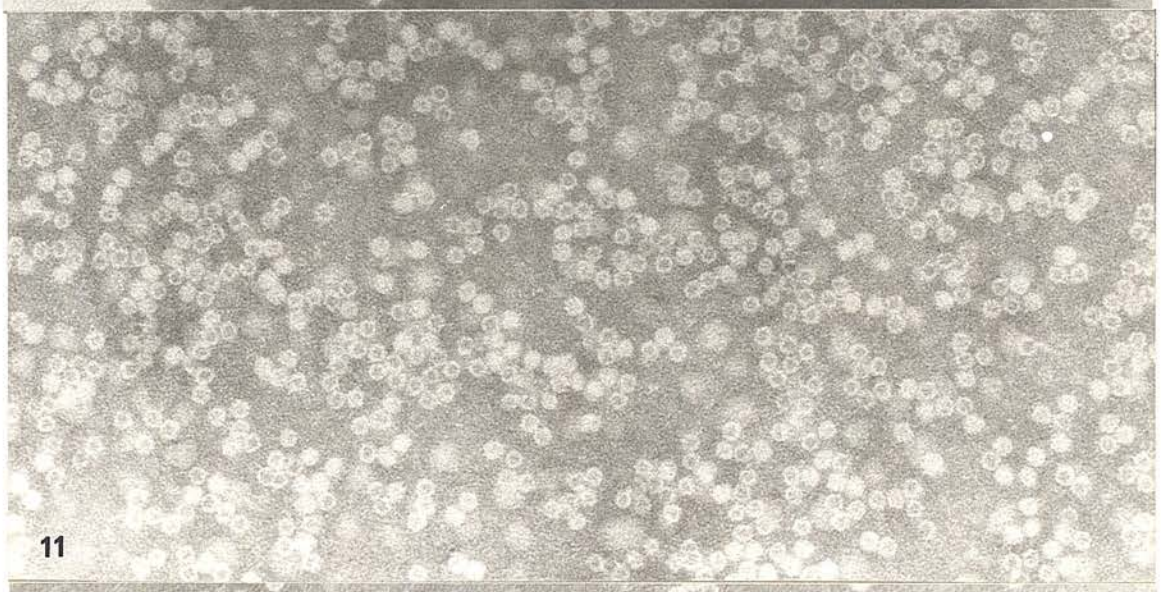

11

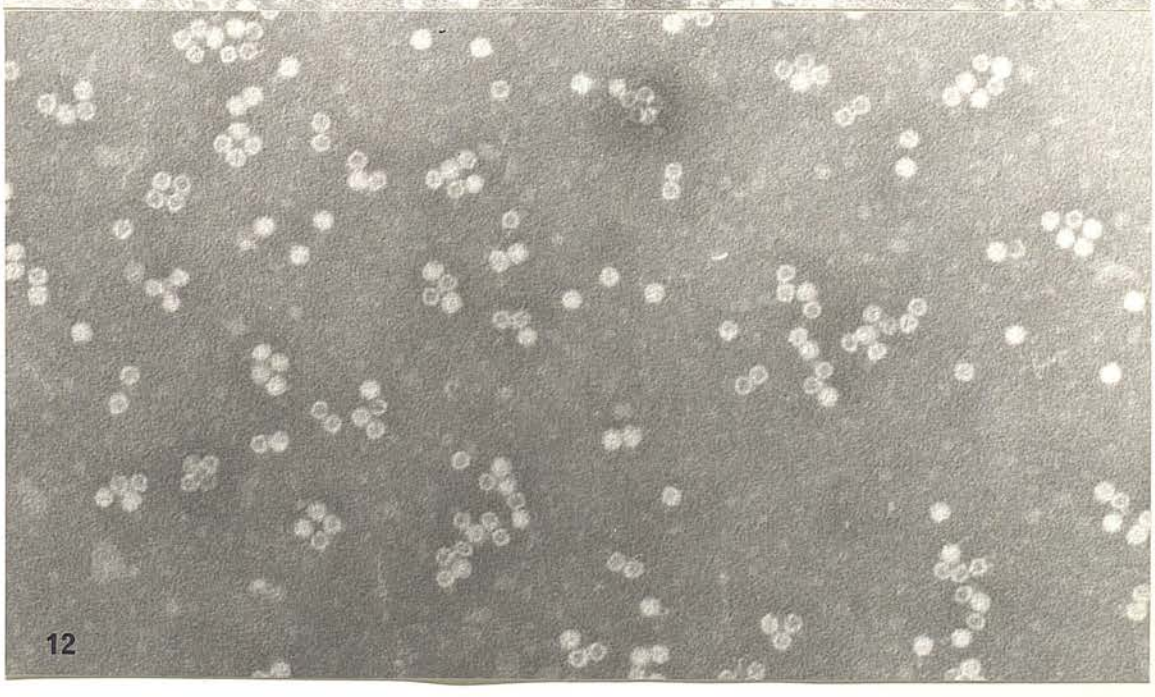

12

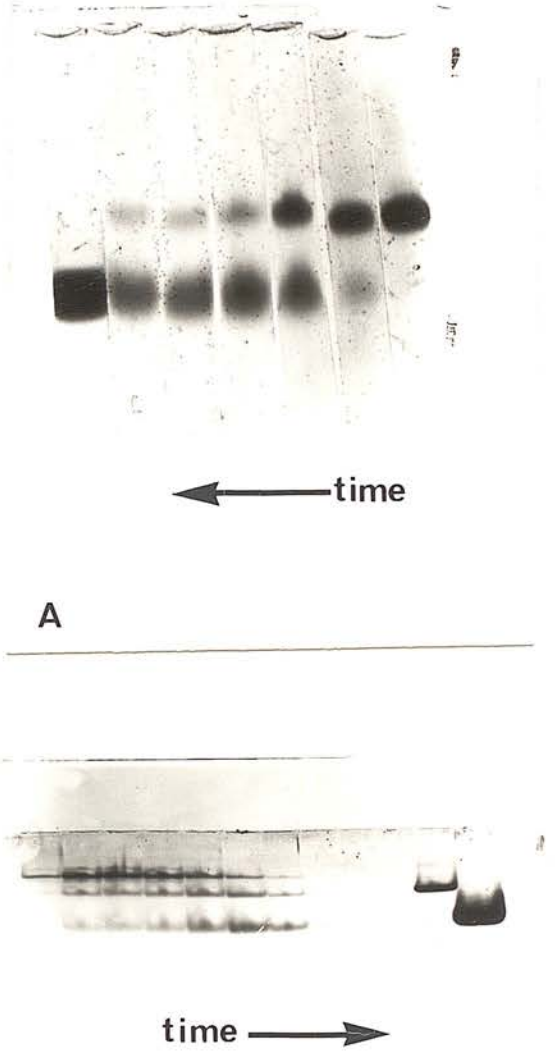

Fig. 13: (A) Polyacrylamide gel electrophoresis on 5% tube gels, showing the progressive breakdown of apoferritin dimer with increasing ultrasonication time. (B) Polyacrylamide gel electrophoresis on a 3% to 30% slab gel, showing the progressive breakdown of an apoferritin trimer-rich fraction into dimer and monomer with increasing time of ultrasonication.

The electron optical shadowing technique, termed single sideband phase contrast interference (Harris and Kerr, 1976) has been used to study apoferritin, as shown in Fig. 14. In this instance, although there is an increased image contrast, the technique does not appear to offer any distinct advantage over conventional bright field transmission electron microscopy (cf. the use of this technique to study the Bordetella pertussis '22S antigen' and human erythrocyte cylindrin, section VII).

Application of the carbon-film negative staining technique of Horne and Pasquali-Ronchetti (1974) to apoferritin solutions, either as purchased from Calbiochem Ltd or Sigma (London) Ltd which contain more than 90% apoferritin monomer, or after purification of the monomer by preparative polyacrylamide gel electrophoresis, has shown that the molecules have a strong tendency to form randomly packed arrays, and limited regions containing regular mono-layer and multi-layer arrays (Harris, 1978). Fig.15 shows a region where the apoferritin molecules are forming random mon-, di-, and multi-layer molecular arrays. By manual search, regions containing an almost perfect hexagonal packing of molecules within a mono-layer can be detected (Fig. 16). With increasing protein concentration (up to approximately 5 mg / ml) there is a pronounced tendency for multi-layer arrays to be formed, and within these regions it is possible to detect complex, yet regular electron optical images, produced by the partial overlapping of molecules in two or more layers, as shown in Fig. 17.

III. Thyroglobulin

Thyroglobulin, the iodinated glycoprotein secreted by the thyroid gland, has a molecular weight of approximately 670 000 and a sedimentation

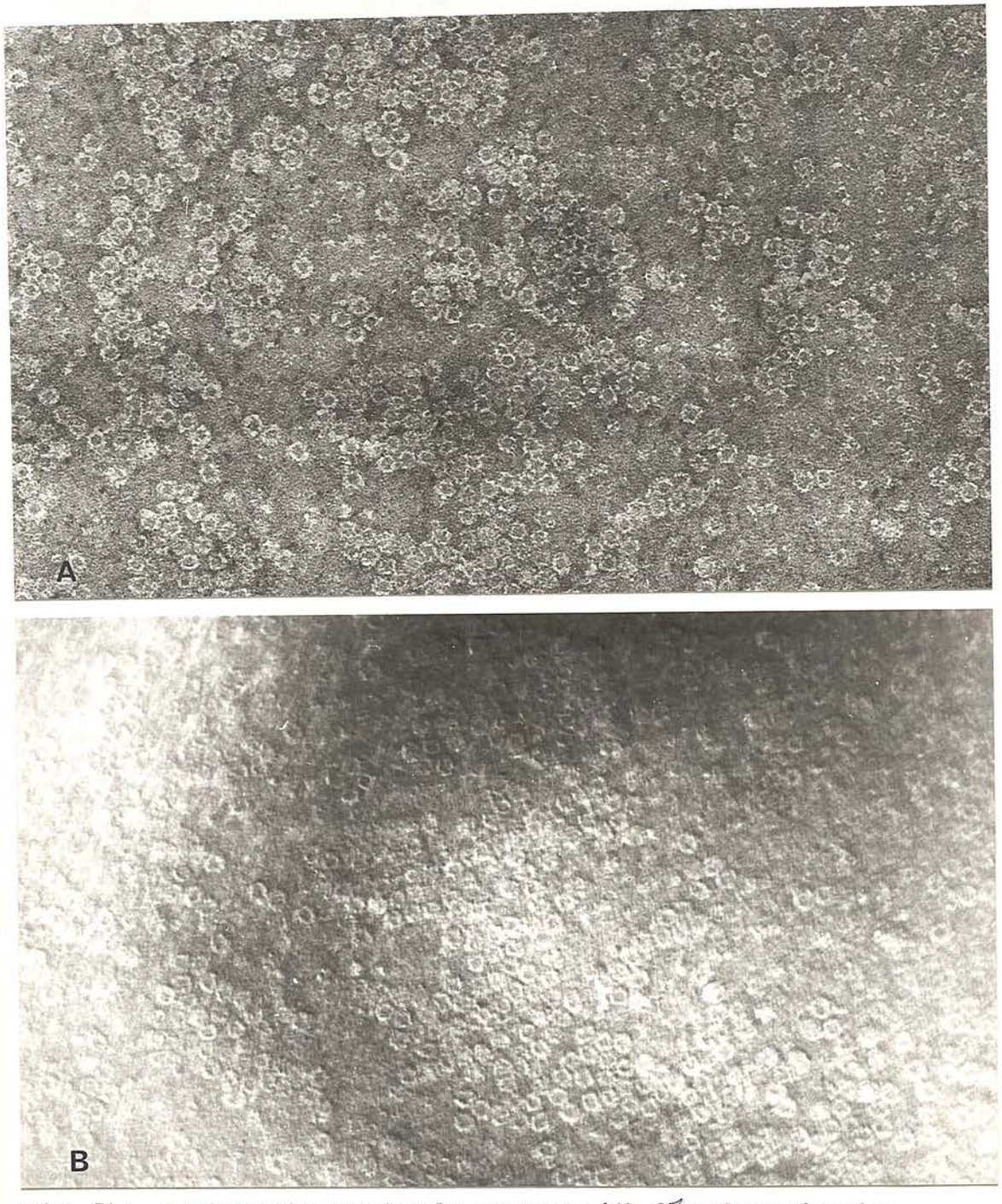

Fig. 14: Apoferritin negatively stained with 2% sodium phosphotungstate (pH 7.0). (A) The conventional bright field transmission image. (B) the single sideband phase contrast interference image. x 270 000. By courtesy of Philips Electron Optics Applications Laboratory, Pye Unicam, Cambridge.

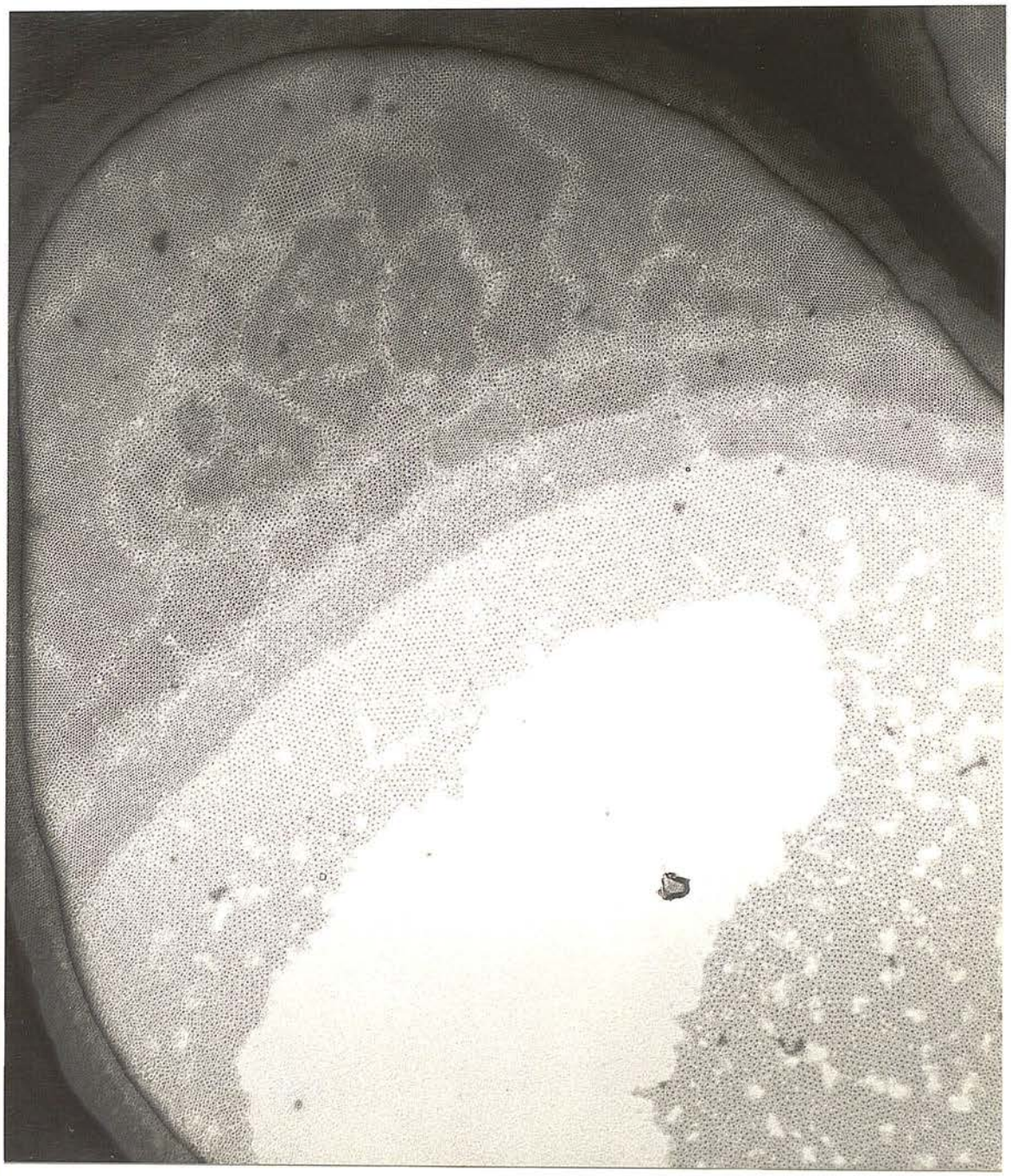

Fig. 15: Apoferritin spread on freshly cleaved mica after mixing with 2% ammonium molybdate (pH 7.0), for the negative staining-carbon film technique of Horne and Pasquali Ronchetti (1974). After drying and coating with a thin layer of carobon, the carbon layer with attached molecules was floated onto 2% uranyl acetate (pH 4.5) and picked up on a perforated carbon film. Mono- and multi-layer regions of random and ordered molecular arrays are present. x 75 000.

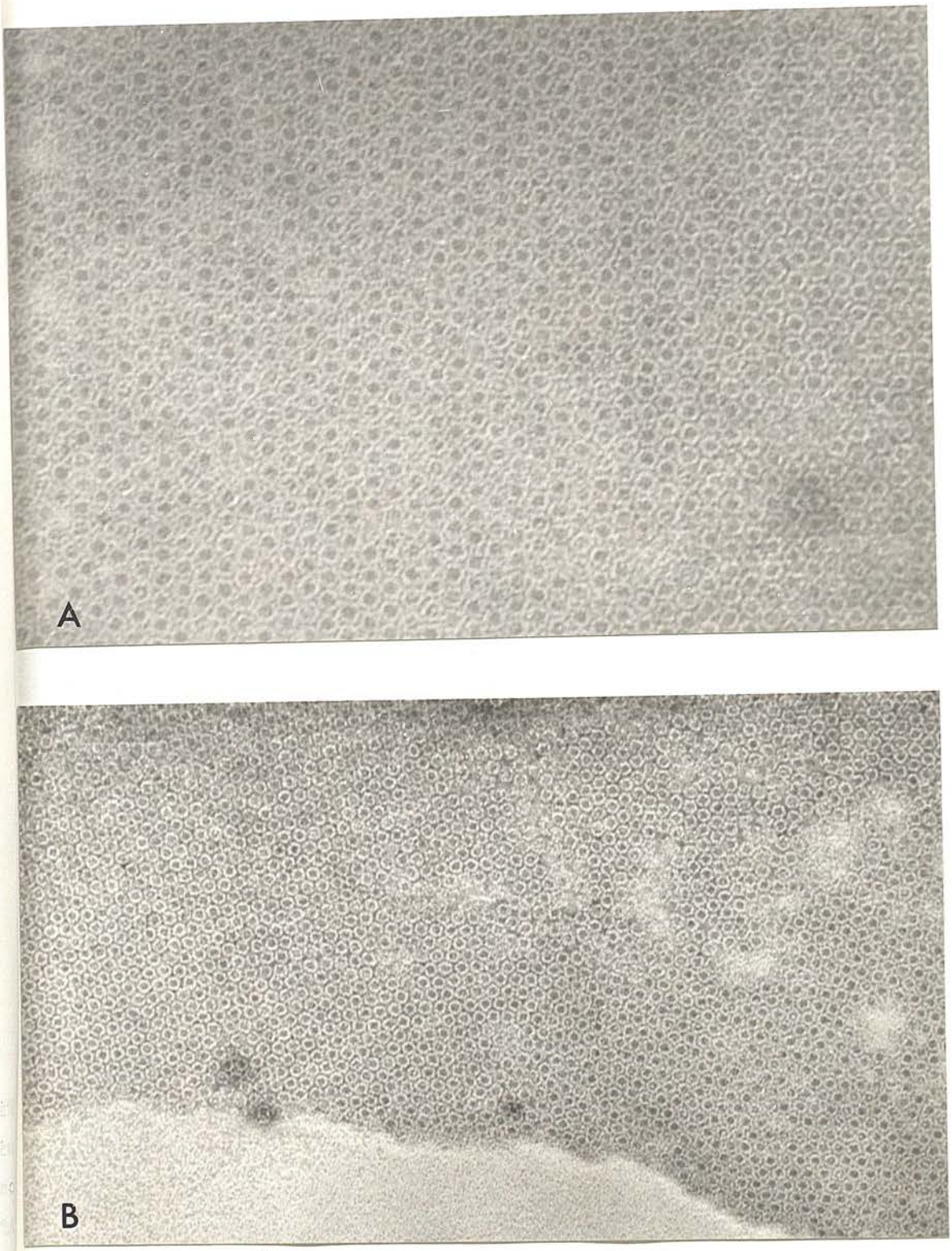

Fig. 16 Apoferritin prepared as for Fig. 15. Regions containing almost regular monolayer hexagonally packed molecular arrays are shown; (A) x 400 000, (B) x 200 000.

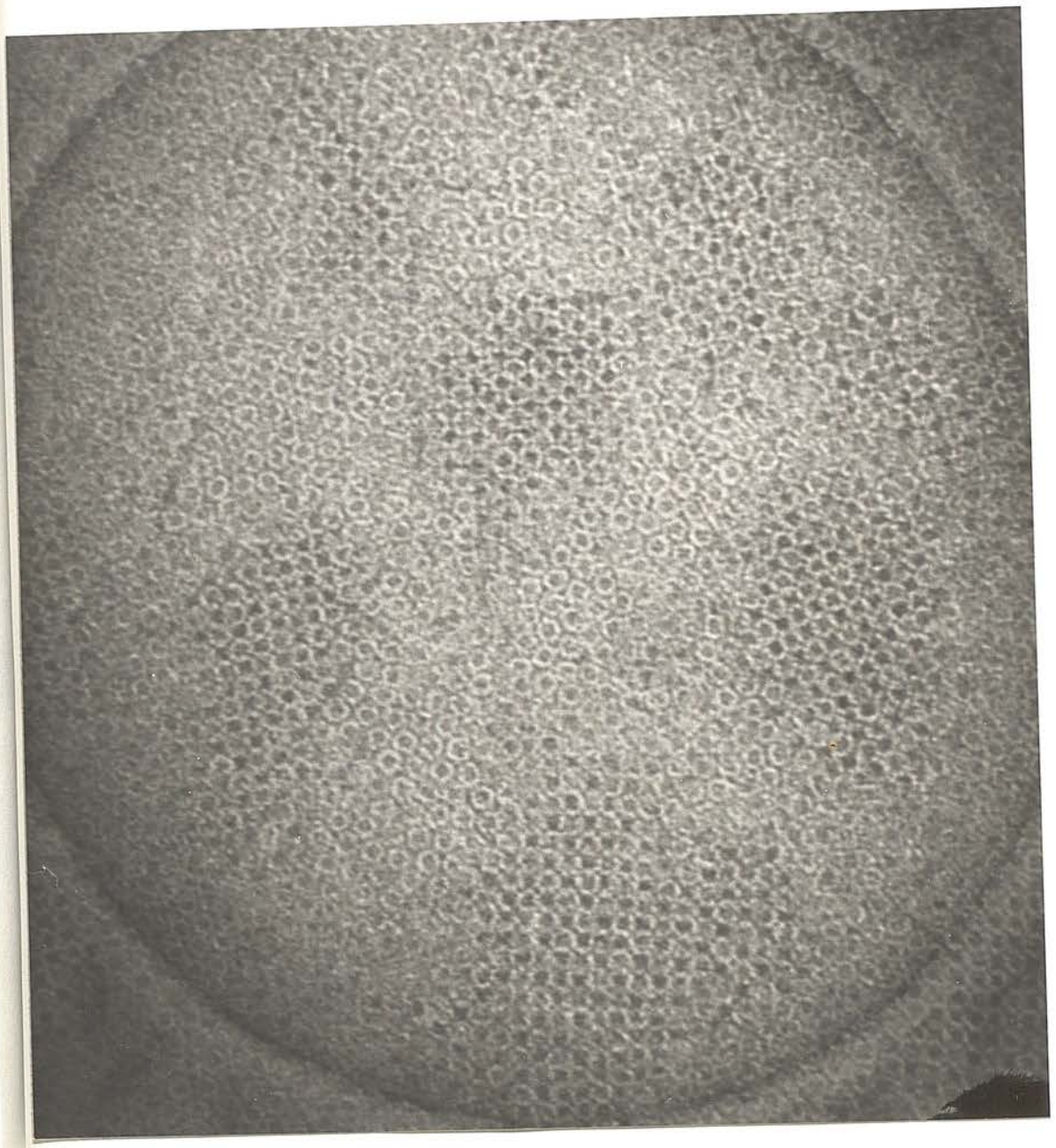

Fig. 17: Apoferritin prepared as in Fig. 15. A region containing discrete regions showing multilayer molecular arrays, x 300 000

coefficient of 19S. It is one of the few proteins, the study of which by negative staining transmission electron microscopy has benefited markedly from prior fixation with glutaraldehyde. The elegant studies of Berg and her colleagues using bovine, rat and human thyroglobulin (Berg, 1973; Berg, 1975; Berg and Ekholm, 1975; Berg, 1978) have shown that ammonium molybdate (pH 6.8) is particularly disruptive towards thyroglobulin, whereas sodium phosphotungstate and sodium silicotungstate (pH 6.0) are not. Brief fixation (1 to 3 min) in approximately 0.75% glutaraldehyde prior to ammonium molybdate negative staining enabled intact ovoid molecules, 30 nm in length and 15 nm in diameter, to be detected, which appeared very similar to those revealed by silicotungstate and phosphotungstate staining (Fig. 18). From these electron optical images of thyroglobulin a tentative two subunit model has been constructed by Berg, as shown in Fig. 19. Under conditions of low iodination in vivo, obtained in rats by feeding an iodine deficient diet or administration of propylthiouracil, and from human goiterous thyroid tissue, it was found that in the electron microscope very few ovoid molecules were present. However, a high proportion of compact cylindrical molecules of length approximately 23 nm and diameter approximately 13.5 nm were present and also a more porous cylindrical molecule of length approximately 15 nm and diameter approximately 20 nm. Fig. 20 shows thyroglobulin from low iodinated rat thyroid gland, revealing the two cylindrical forms, and likewise thyroglobulin from human goiterous thyroid gland reveals the cylindrical molecules (Fig. 21), but the ovoid molecules are also present (Berg, 1975). There is considerable evidence to suggest that under conditions of low iodination thyroglobulin has an increased tendency to be dissociated. Thus, there is a likelihood that the 19S region of protein selected

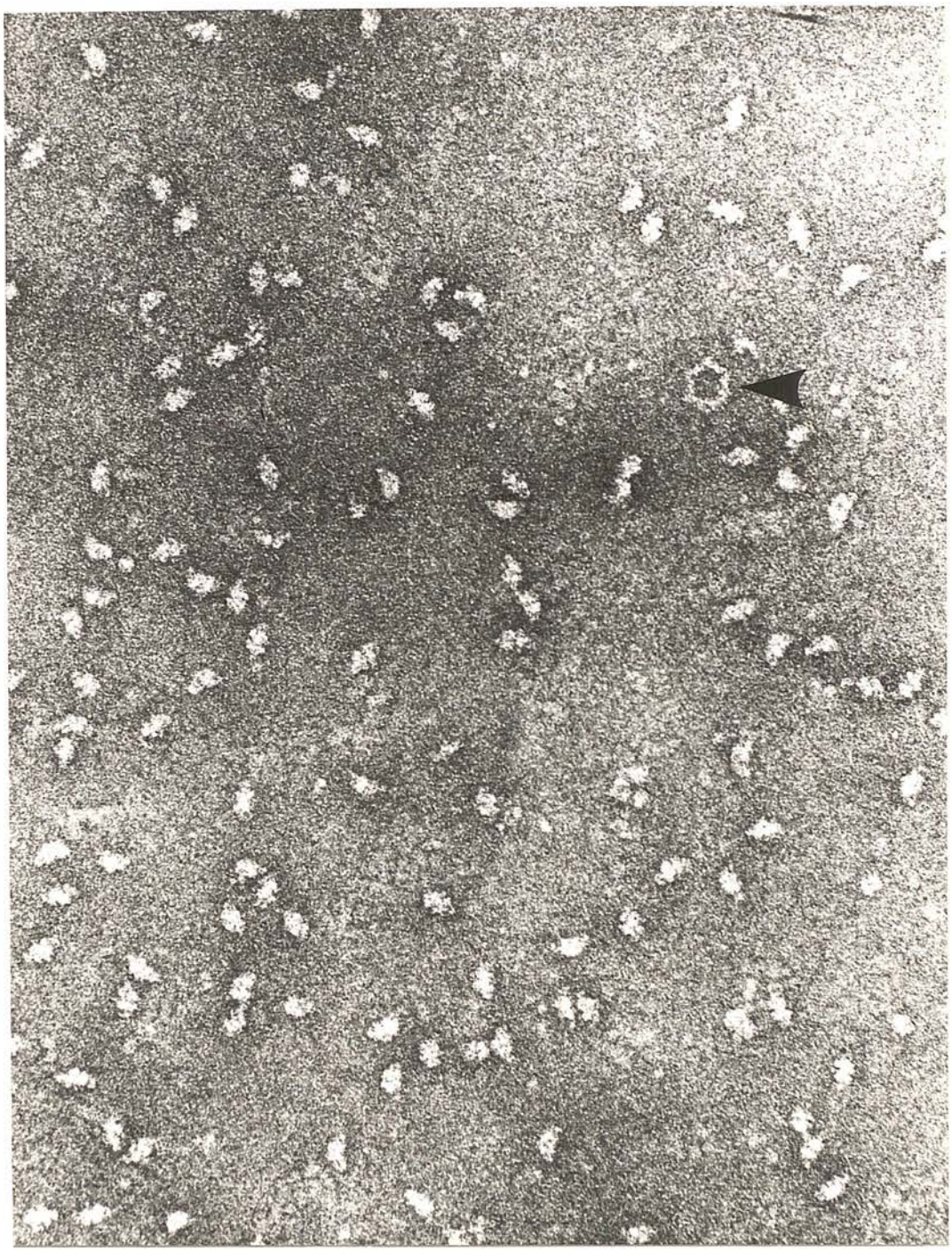

Fig. 18: Thyroglobulin from normal human thyroid (iodine content 0.3%), purified by glycerol gradient centrifugation, stabilized for 3 mins in 0.75% glutaraldehyde. Negatively stained with 2% ammonium molybdate (pH 6.8). × 200 000. From Berg (1975), with the permission of Academic Press.

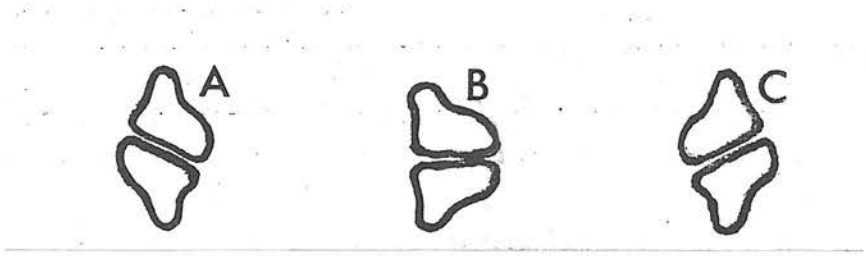

Fig. 19: A diagrammatic representation of normal human thyroglobulin showing the molecule in three possible orientations. The molecule appears as two subunits, giving electron optical images which depend on the orientation around the long axis of the molecules, A and C being mirror images, whilst B represents an intermediate position. Re-drawn from Berg (1978).

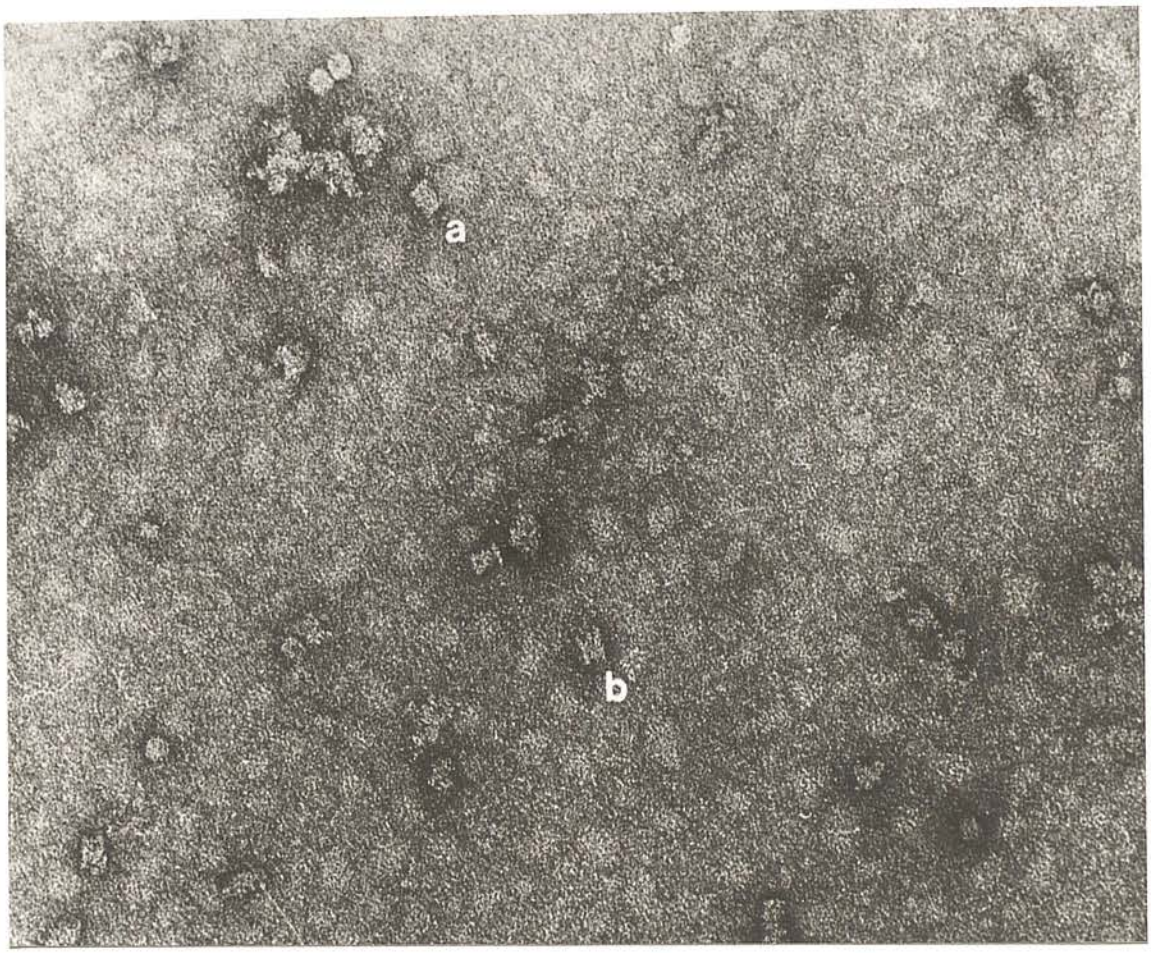

Fig. 20: Low iodinated thyroglobulin from propylthiouracil-treated rats. The two types of cylindrical molecules are indicated: (a) the compact cylinder and (b) the more porous cylinder. Negatively stained with 2% ammonium molybdate (pH 6.8). x 200 000
From Berg and Ekholm (1975) with the permission of Elsevier North Holland Biomedical Press.

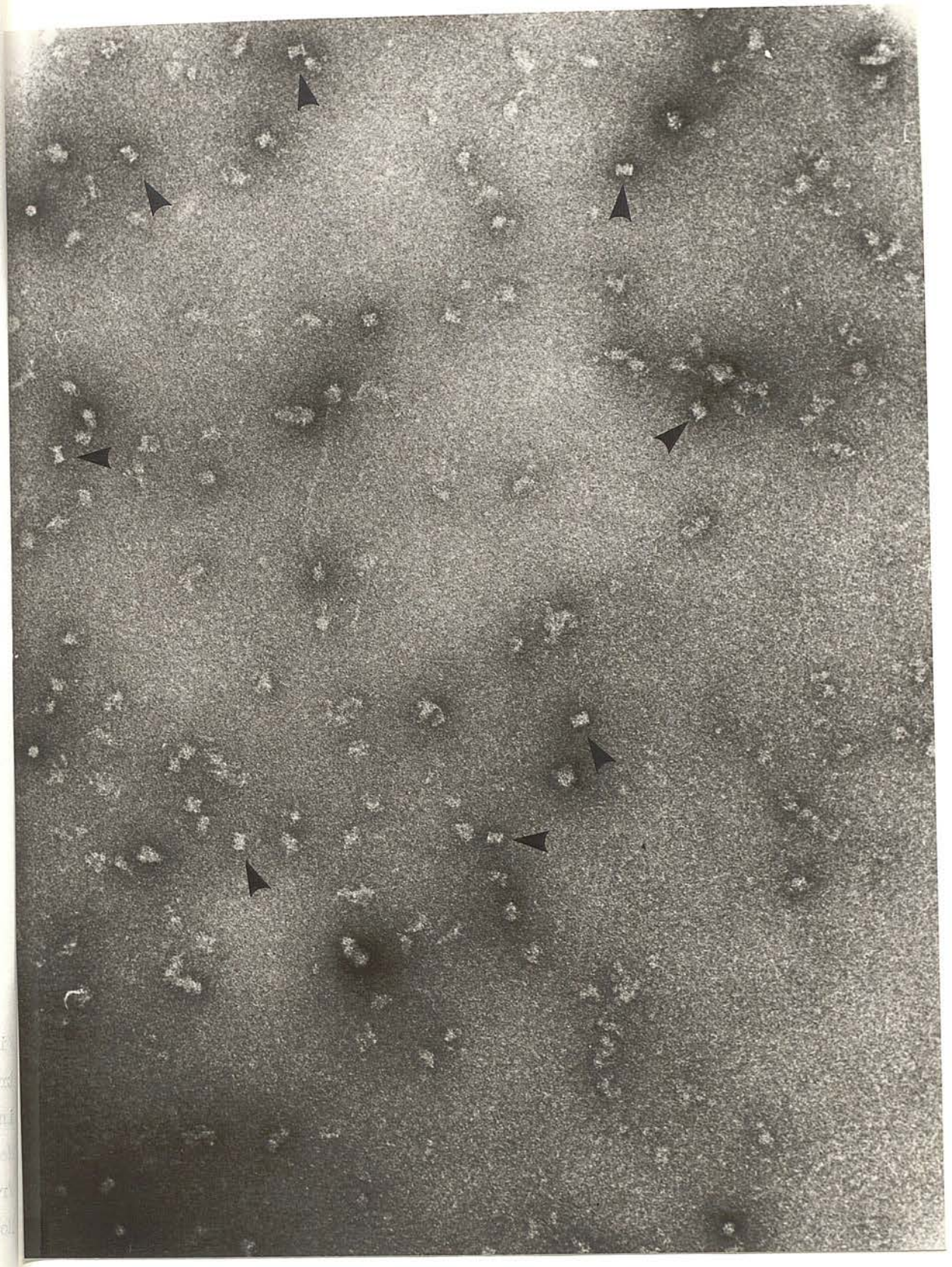

Fig. 21: Thyroglobulin from low iodinated human thyroid gland (iodine content 0.02%), negatively stained with 2% ammonium molybdate (pH 6.8). Arrows indicate cylindrical molecules. x 120 000. From Berg (1975), with the permission of Academic Press.

from the glycerol gradient for electron microscopic study by Berg would not contain these dissociated molecules, but might be selectively enriched with other contaminating molecules of molecular weight approximating to that of the 19S thyroglobulin. Examples of proteins in this category might be α_2-macroglobulin (molecular weight 725 000, sedimentation coefficient 19.6S) or the human erythrocyte cylindrin (molecular weight approximately 800 000, sedimentation coefficient 22.5S). The attractive theory was, nevetheless, advanced by Berg and Ekholm (1975), Berg et al. (1975) and Berg (1978) that the conversion of the cylindrical thyroglobulin molecule into a more ovoid shaped molecule might be concomitant with iodination, the claim being made that on incubating the cylindrical form with horseradish peroxidase, H_2O_2 and potassium iodide, a conformational change occurred, resulting in more than 50% of the molecules having an ovoid conformation. The compact cylindrical thyroglobulin closely resembles the human erythrocyte cylindrin (Fig. 22) although the latter has slightly smaller dimensions (i.e., length 17 nm and diameter 12 nm), and the more porous cylindrical thyroglobulin is extremely similar to α_2-macroglobulin (see Fig. 23 and cf. Figs 20 and 21). Immunodiffusion or immunoelectrophoretic analysis of the purified low iodinated thyroglobulin would readily reveal the presence of more than one antigenic species. If fusion of immunoprecipitin lines occurred, evidence would be provided to further support the thyroglobulin conformational change hypothesis, whereas is the arcs crossed one another the presence of contaminatory proteins would be indicated. SDS-PAGE analysis of the polypeptide molecular weights would also provide useful information. From the first hand experience of the author using sugrose density gradient centrifugation, which

Fig. 22: Purified human erythrocyte cylindrin, negatively stained with 2% sodium phosphotungstate (pH 7.0). Note the similarity between cylindrin and the compact cylinder structures shown in the thyroglobulin samples, Figs. 20 and 21. x 300 000.

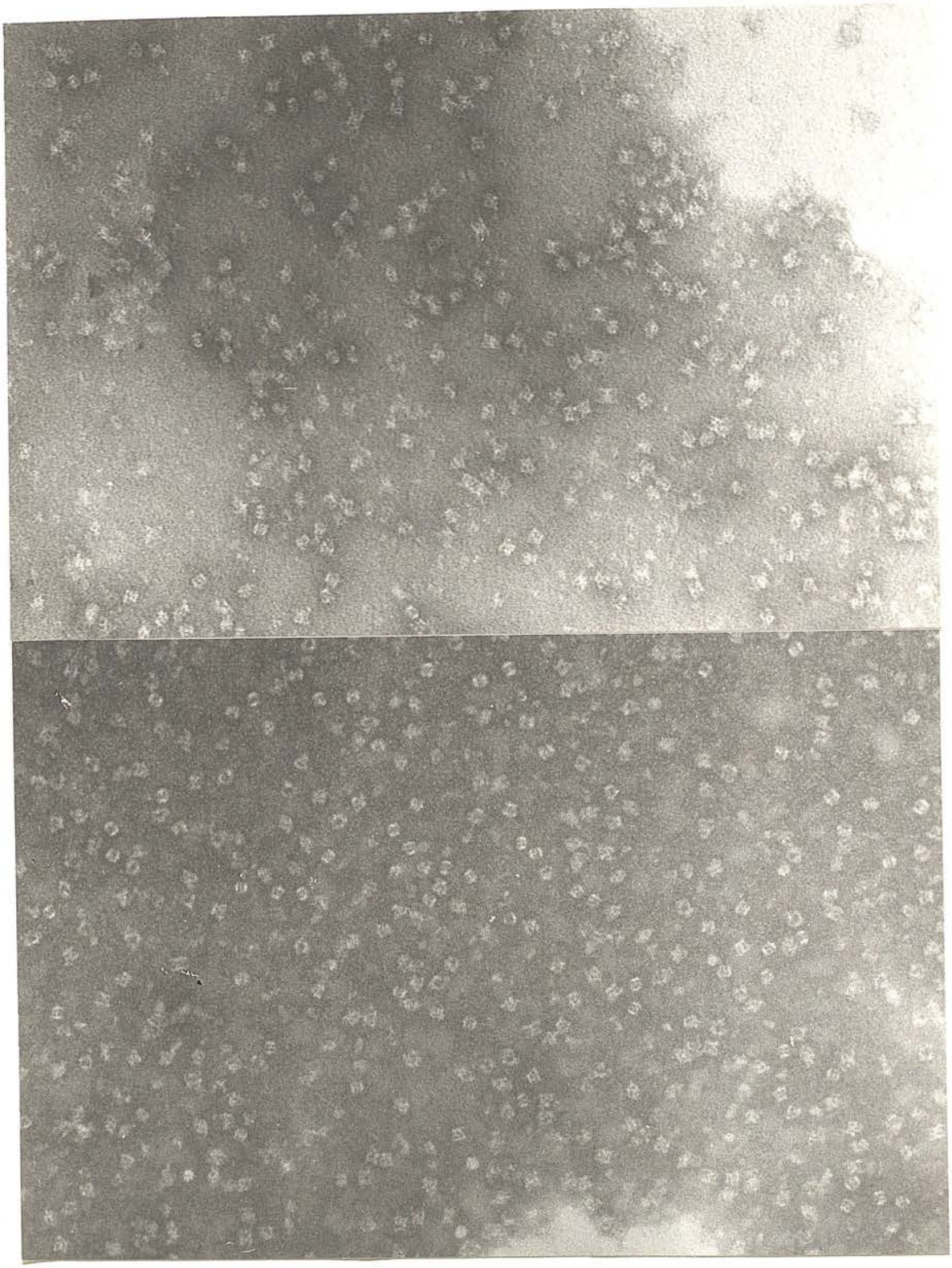

Fig. 23: Purified human α_2-macroglobulin, negatively stained with 2% ammonium molybdate (pH 7.0). Note the similarity between the images of this molecule and the more porus cylindrical image of low iodinated thyroglobulin, shown in Figs. 20 and 21.
x 198 000.

is directly equivalent to glycerol gradient centrifugation used by Berg to purify thyroglobulin, it is considered that homogeneity would probably not be achieved by a single centrifugation, as indeed indicated by the presence of the hexagonal protein complex in Fig. 18 (arrowed), which has been shown to be a plasma protein by Bloth et al. (1975). It must be acknowledged that Berg and Ekholm (1975) do state that the iodine content alone may not necessarily determine the shape of thyroglobulin, but that independent or secondary factors such as the formation of disulphide bonds are also likely to be of importance.

IV. Insect Vitellogenins

The insect female-specific proteins, termed vitellogenins, which circulate in the haemolymph and are incorporated into the maturing oocytes, have been shown to be of high molecular weight and of lipoprotein composition. For the silkwork Philosamia cynthia, Chino et al., (1969)(1976) presented polyacrylamide gel electrophoretic data to show that the yellow pigmented vitellogenin isolated from the oocytes and from the haemolymph were co-migratory. Other supporting evidence was also obtained from negative staining transmission electron microscopy using uranyl acetate (Fig. 24), the mean diameter of the oocyte lipoprotein being 13.0 $\pm$ 0.8 nm and the haemolymph lipoprotein 12.6 $\pm$ 0.8 nm. The amino acid composition of the two lipoproteins was very similar, as was their ability to bind phospholipids, diacyl-glycerol and cholesterol .

Another example is the vitellogenin of the cockroach Nauphoeta cinerea (Buhlman, 1976), which can likewise be obtained from both the hamolymph and the oocytes. Samples of this lipoprotein, negatively

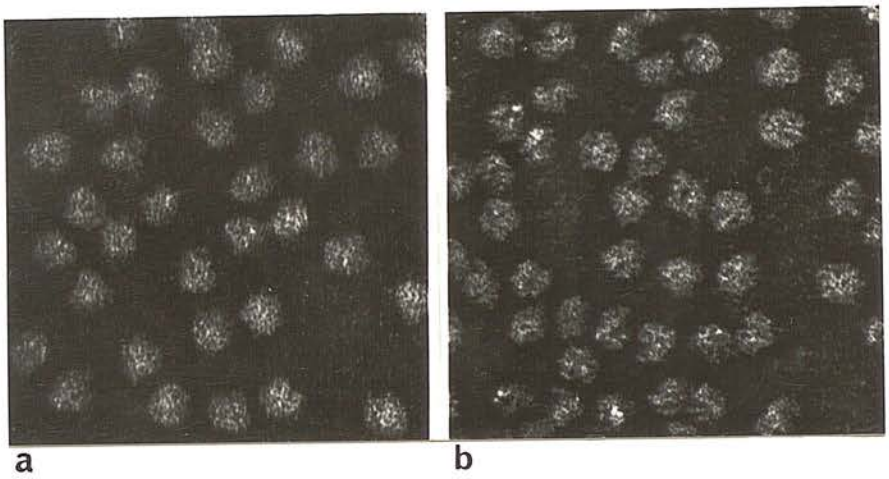

Fig. 24: Silkworm Philosamia cynthia oocyte lipoprotein-I (a) and haemolymph lipoprotein-II (b), negatively stained with uranyl acetate (pH 4.5). x 440 000. From Chino et al. (1976), with the permission of Elsevier North Holland Biomedical Press.

stained with sodium phosphotungstate and uranyl acetate are shown in Fig. 25. There appears to be little indication of structural symmetry within either the silkworm or coackroach vitellogenin, but in both cases there is some penetration of stain into the centre of the molecules.

V. Contortin

An interesting extracellular polymeric protein, termed contortin, has been found in the intestine of the parasitic nematode Haemonchus contortus (Munn, 1976; Munn, 1977). This protein, which coats the microvillar glycocalyx (Fig. 26), has a conformation resembling helical filaments, approximately 40 nm in diameter with a variable pitch, aligned lengthwise along the microvilli. The polymeric protein has been isolated and partly purified (Fig. 27), and it is thought to be composed of a monomeric subunit of molecular weight approximately 60 000. This monomer appears from negative staining to be Y-shaped, with arms about 4.5 nm long and 2.5 nm wide, which may polymerize as pairs, possibly thereby accounting for the 'double' image of the helix (arrows in Fig. 27). although other nematodes have material coating their intestinal microvilli (see Munn, 1977), contortin-like protein has been detected only in Ostertagia circumcincta, and it is also thought to be present in Haemonchus placei. The suggestion has been advanced that contortin might be an anticoagulant and therefore be of benefit to the survival of the nematode.

VI. α-Crystalin

One of the principal proteins of the eye lens is α-crystalin. This protein, isolated from bovine lens, has been shown to exhibit three size populations. The smallest population, termed low molecular

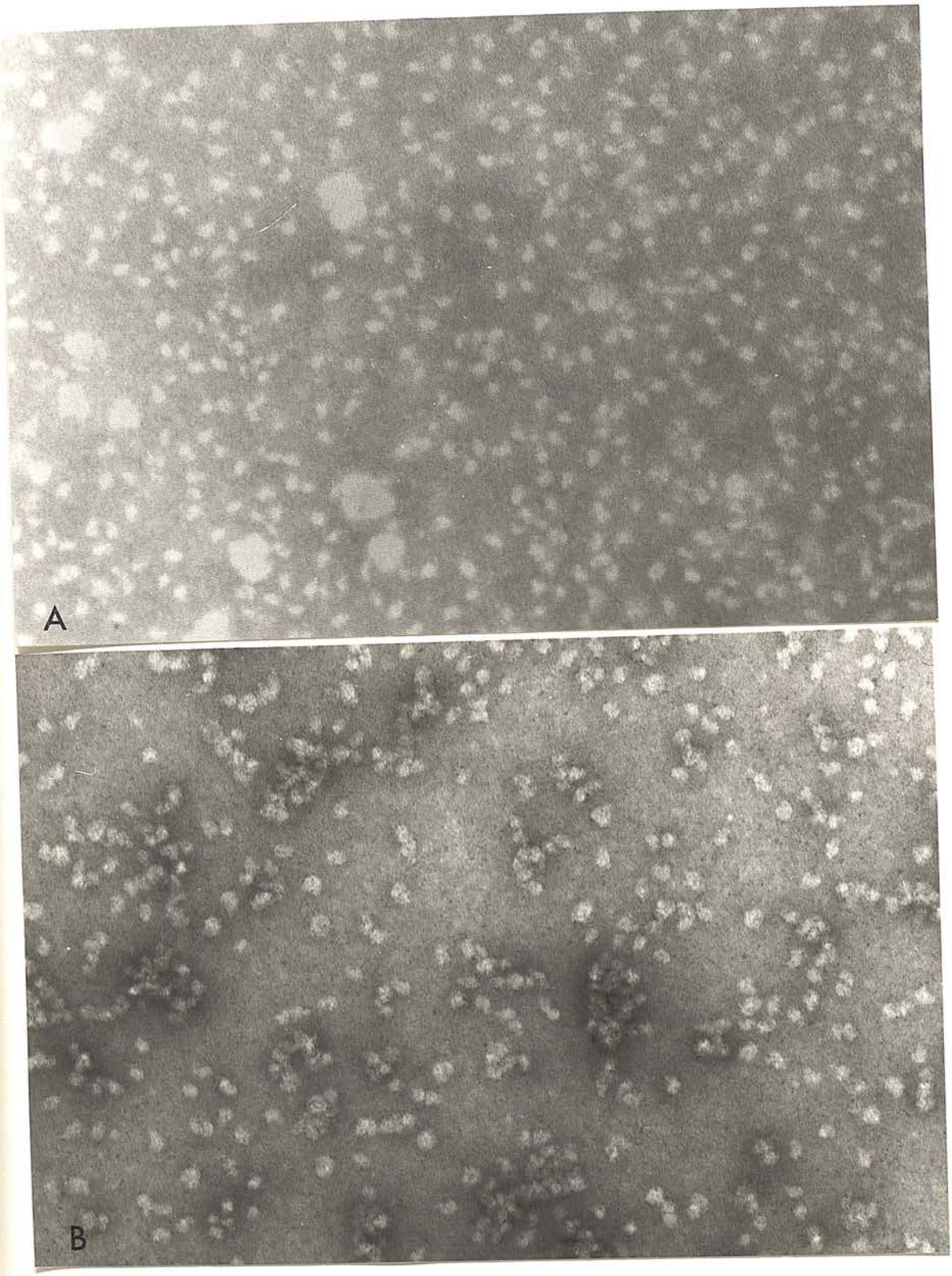

Fig. 25: Purified vitellogenin from oocytes of the cockroach Nauphoeta cinerea (by courtesy of G. Buhlman). (A) negatively stained with 2% sodium phosphotungstate and (B) with 2% uranyl acetate, showing some aggregation of molecules. x 240 000.

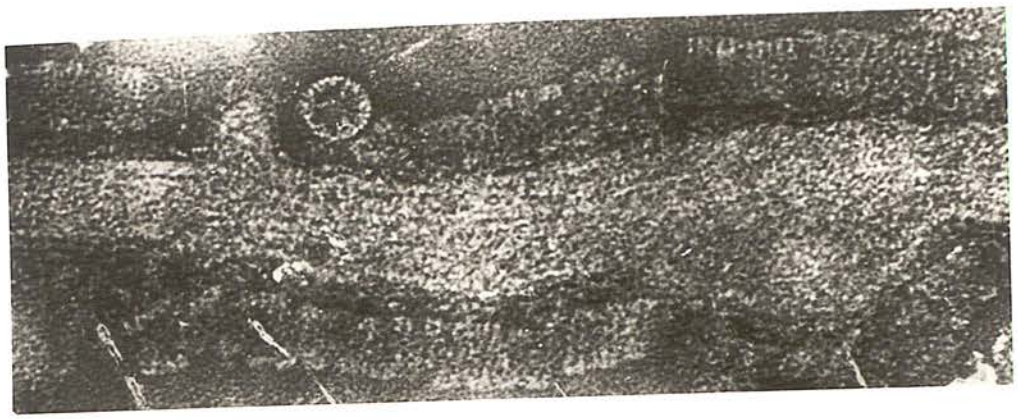

Fig. 26: A portion of an intestinal microvillus of Haemonchus contortus coated with helical arrays of contortin. The surface glycocalyx of the microvillus is clearly seen to be located between the contortin and the microvillar plasma membrane. Negatively stained with ammonium molybdate (pH 6.9). x 231 000.
By the courtesy of E.A. Munn.

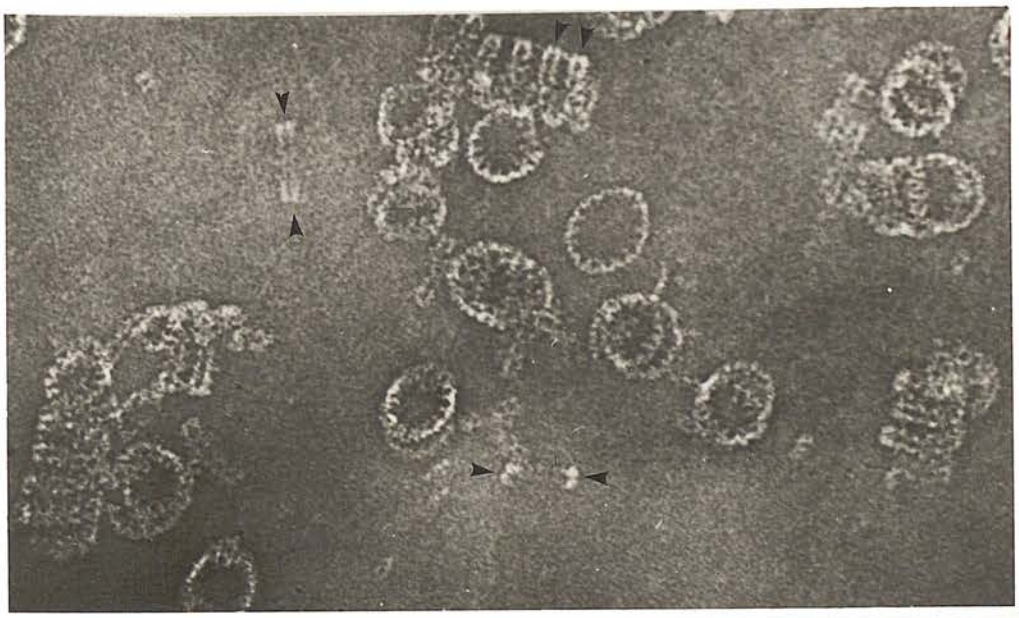

Fig. 27: Partly purified contortin obtained by differential centrifugation of a Haemonchus contortus homogenate prepared in phosphate buffered saline. Negatively stained with ammonium molybdate (pH 6.9). Arrows indicate the 'double'image of the contortin helix. x 244 000. By courtesy of E.A. Munn.

weight α-crystalin (LMWα) predominates in calf lens cortex. LMWα is an approximately spherical protein 13.5 to 16.0 nm in diameter, molecular weight 0.7 to 1.0 x 10^6 and sedimentation coefficient 17 to 23 S (Siezen et al., 1978). Electron micrographs of negatively stained LMWα, isolated by Ultragel AcA 22 column chromatography, are shown in Fig. 28. The molecules can be dissociated by treatment with urea and dithioerythritol, and reassociated by dialysis against a saline-EDTA buffer. Electron microscopy of the reassociated LMWα has revealed that the particle size diminishes to 8.5 to 12.5 nm (Fig. 29). Protein isolated from the lens nucleus contains groups of LMWα molecules, which have been classed by Siezen et al. (1979) as "oligometric" α-crystalin (predominantly dimers, trimers and tetramers, as shown in Fig. 30), and "polymeric" α-crystalin (predominantly very high molecular weight aggregates of 10 to 15 x 10^6, as shown in Fig. 31). These elegant studies emphasise the contribution that electron microscopy can make to the interpretation of biochemical data of macromolecules, particularly that obtained from column chromatography, isoelectric focusing, preparative and analytical ultracentrifugation, and concur with the forementioned studies of the author on apoferritin and its oligomers (Section II).

VII. Bacterial Proteins

The E. coli terminating factor "rho", which is thought to function by binding to specific sites on the DNA template and thereby terminate RNA chain elongation, has been studied electron microscopically by Oda and Takanami (1972). The molecule "rho" (Fig. 32) has an approximately circular profile of external diameter 11.5 nm, a

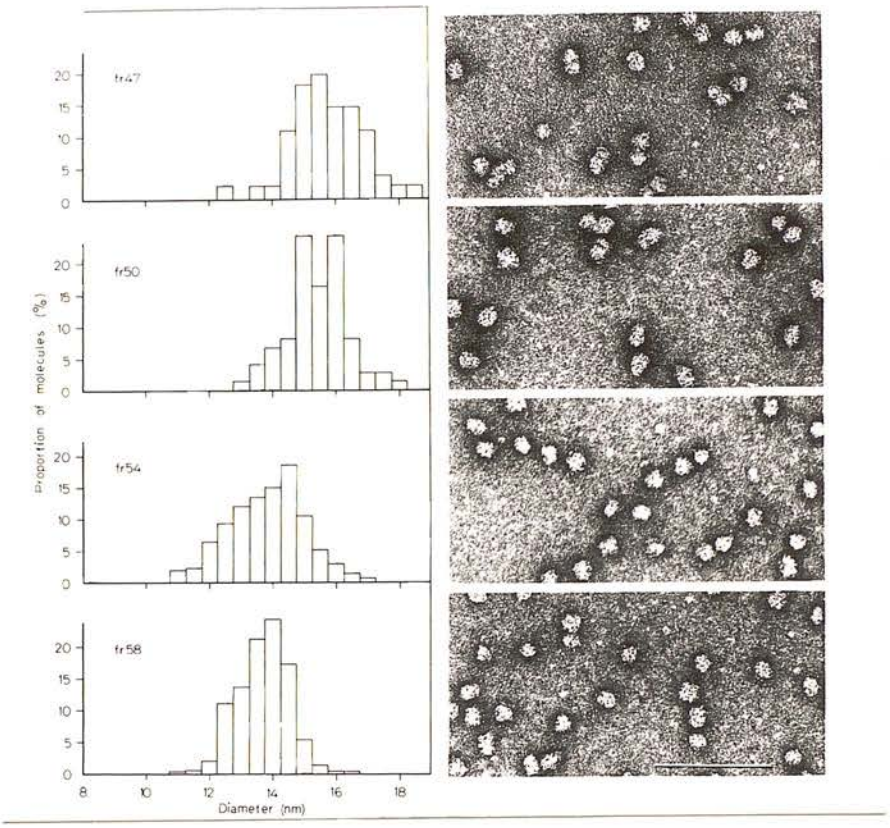

Fig. 28: Native calf lens α-crystalin molecules obtained by gel filtration on Ultrogel AcA 22, showing fractions 47, 50, 54 and 58 of the column effluent. The histograms represent the size distributions of the molecules present in the respective fractions. Negatively stained with 1% uranyl acetate (pH 4.5). The scale marker indicates 100 nm. From Siezen et al. (1978), with the permission of Springer-Verlag.

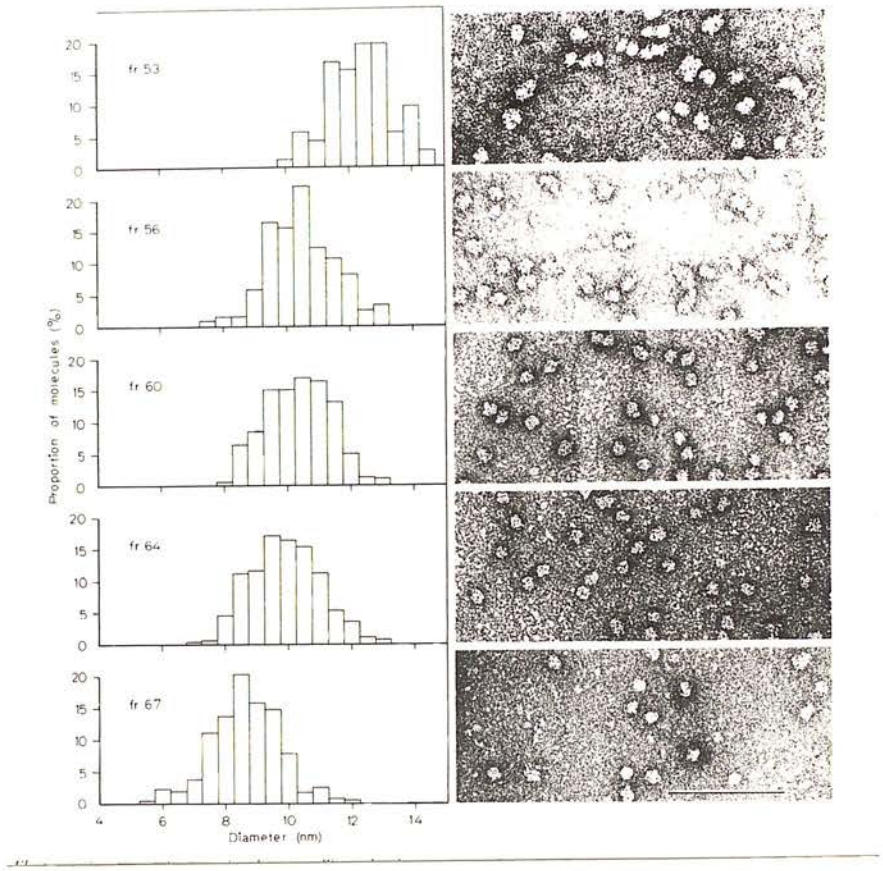

Fig. 29: Reassociated calf lens ∝-crystalin molecules present in Ultrogel AcA 22 column fractions 53, 56, 60, 64 and 67. The histograms represent the size distributions of the particles present. Negatively stained with 1% uranyl acetate (pH 4.5). The scale marker indicates 100 nm. The reassociated protein particles are significantly smaller than the native protein (Fig. 28). From Siezen et al. (1978) with the permission of Springer-Verlag.

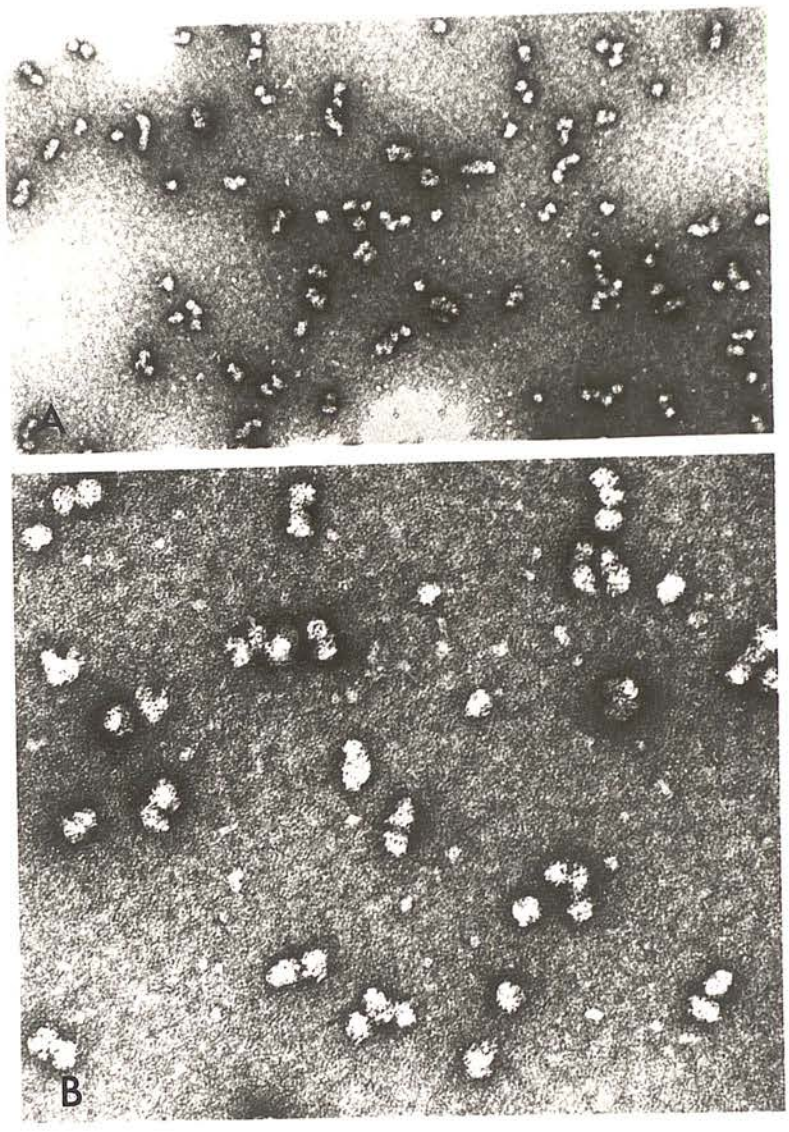

Fig. 30: (A) Calf lens nuclear oligomeric α-crystalin. This preparation is a mixture of predominantly mono-, di-, tri- and tetramers. (B), as in (A), but at a higher magnification. The diameter of the spherical units in the oligomers is 15.4 ± 1.4 nm (S.D.: n=56). Negatively stained with 1% uranyl acetate (pH 4.5). (A) x 115 000 and (B) x 250 000. From Siezen et al.(1979), with the permission of Academic Press.

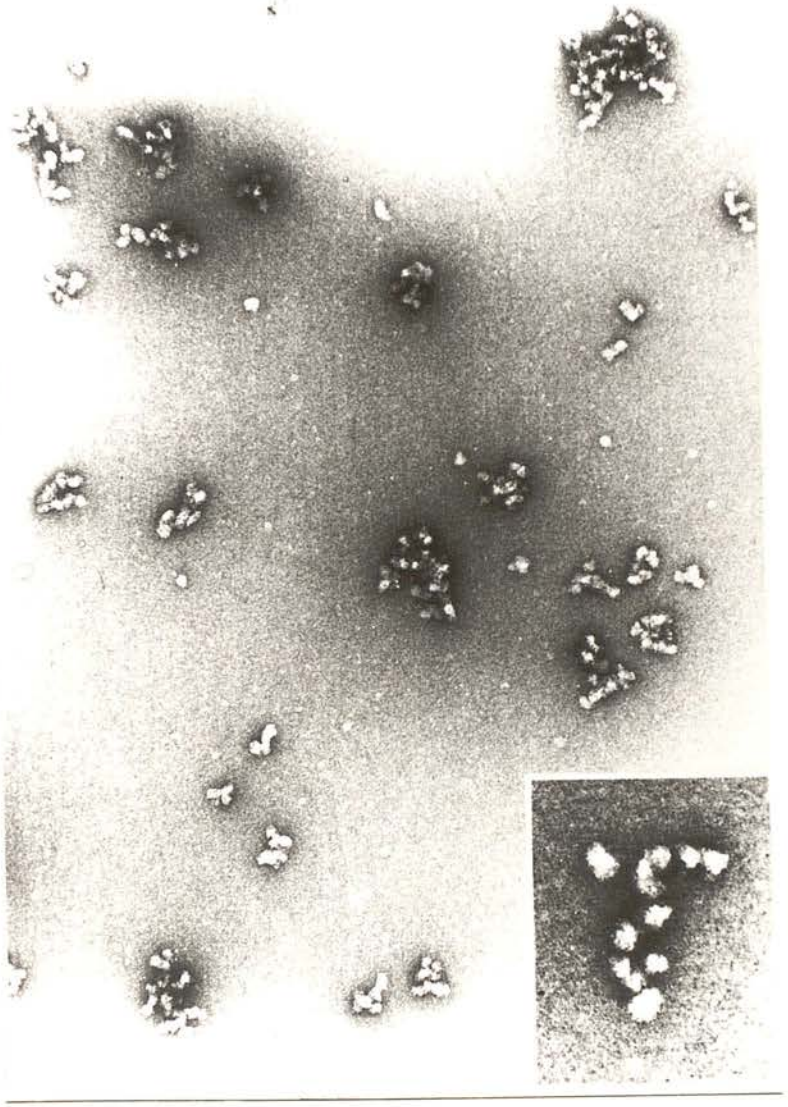

Fig. 31: Nuclear polymeric ∝-crystalin. This preparation is a heterogeneous mixture of monomeric spherical units to very high polymers, which are irregularly shaped and have dimensions up to 200 nm. Negatively stained with 1% uranyl acetate (pH 4.5). x 115 000 (insert x 250 000). From Siezen et al. (1979), with the permission of Academic Press.

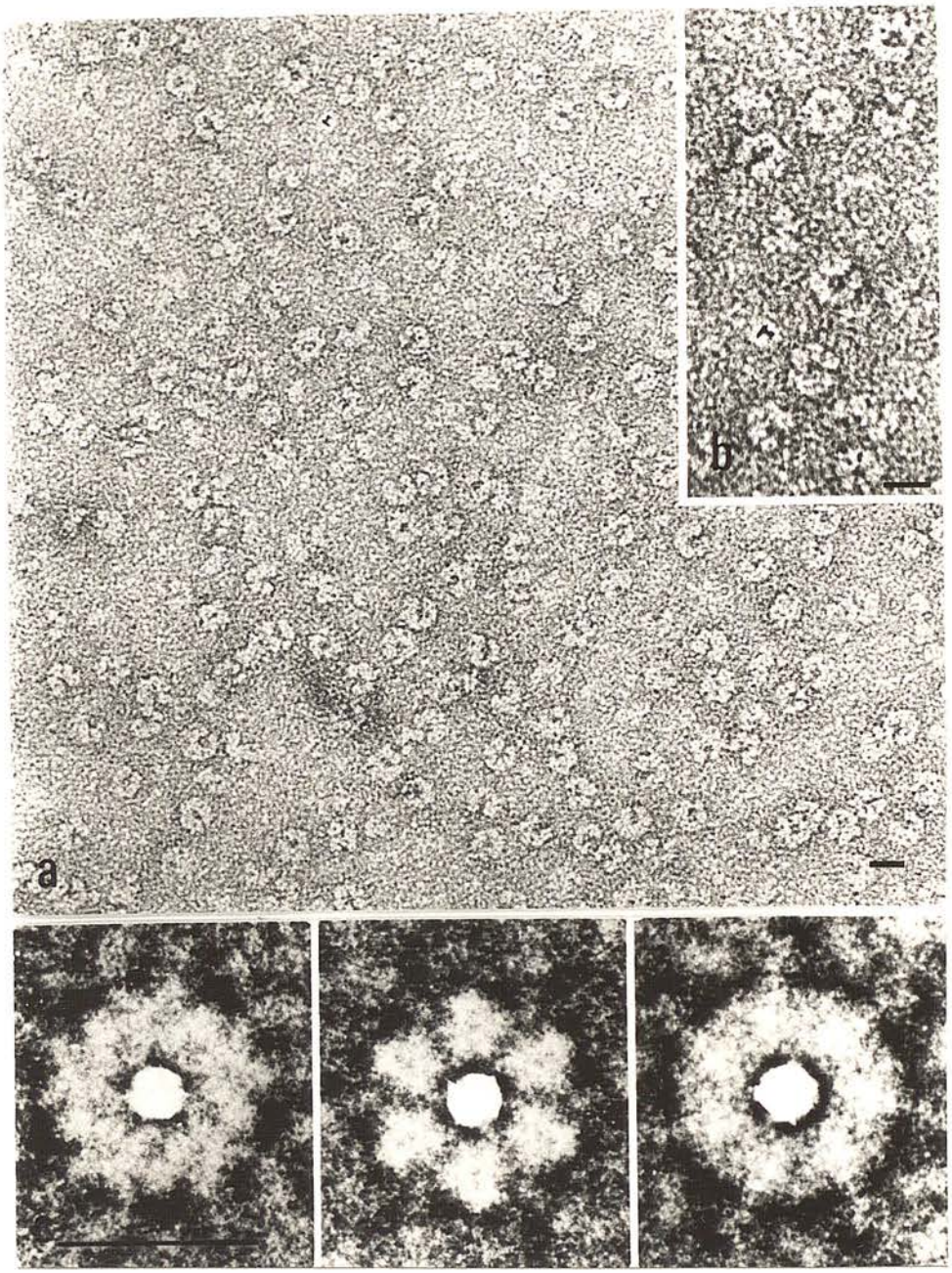

Fig. 32: (a) The rho preparation, negatively stained with 1% uranyl acetate. (b) The same as (a), but at higher magnification. (c) The rho particle printed by the rotational enhancement method of Markham et al. (1963), at n= 5, 6 and 7 (left to right). The scale markers indicate 10 nm. From Oda and Takanami (1972), with the permission of Academic Press.

sedimentation coefficient of 9.0S at pH 7.4 and 7.8, and by SDS-PAGE after dissociation has been shown to have a single subunit of molecular weight approximately 50 000. Image enhancement by the rotational method of Markham et al. (1969) has indicated the presence of six subunits with in the intact molecule (Fig. 32), suggesting a native molecular weight of approximately 300 000, which is compatible with a sedimentation coefficient of 9.0S. Despite the apparent underlying symmetry, most of the "rho" molecules appear as slightly open rings, or more precisely rings of proteins subunits in which there is a single narrow gap (arrows Fig. 32). It is interesting to speculate as to whether or not this gap in the molecule might be of significance in relation to the functional attachment of "rho" to the doubly closed replicative form of DNA.

Another high molecular weight bacterial proteins that has received the attention of electron microscopists is the "22S antigen" from Bordetella pertussis , initially documented by Sato and Nagase (1967), which MacLennan et al. (1977) claim to be present in many other bacteria, there being considerable antigenic cross-reactivity of this protein between organisms. Fig. 33 shows a negatively stained electron micrograph of the "22S antigen" from Bordetella pertussis (protein sample by courtesy of Dr. A.P. MacLennan). This molecule has a conformation resembling a hollow cylinder approximately 12 nm in length and 12 nm in diameter, composed of four rings of subunits. All four rings are likely to contain the same subunits and it appears that there are seven subunits in each ring. The physiological function of this protein is not yet known, and its presence in organisms from different genera is extremely intriguing. There is a remarkable similarity

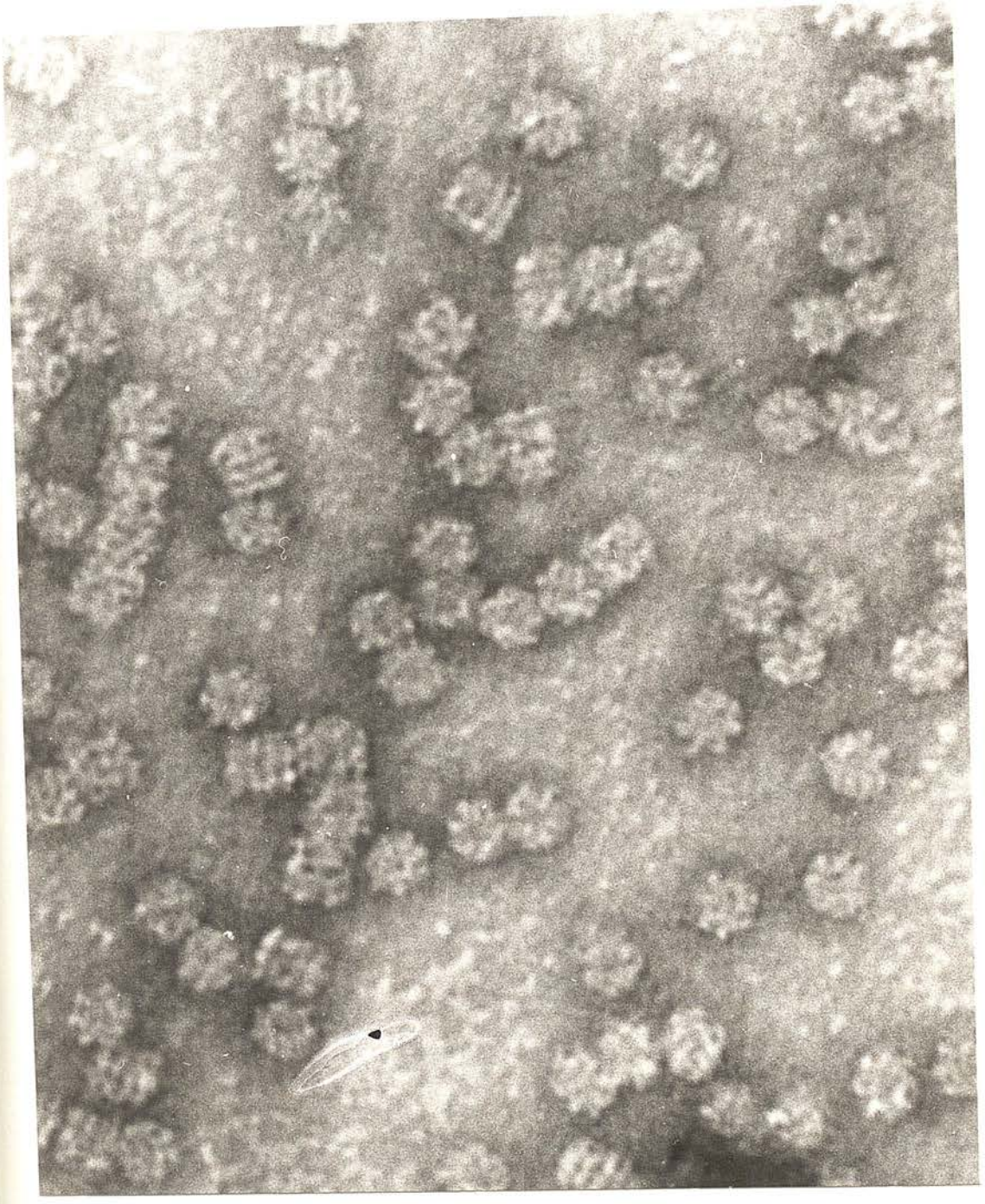

Fig. 33: Purified '22S antigen' from Bordetella pertussis (By the courtesy of A.P. MacLennan), negatively stained with 2% ammonium molybdate (pH 7.0). This micrograph was exposed with the image very close to focus. x 640 000.

between the "22S antigen" and the 900 000 molecular weight protein complex termed groE, from E. coli (Hohn et al., 1978), which is thought to be related to bacteriophage proteins (cf. Bradley, 1966), as shown in Fig. 34. The molecule is clearly cylindrical in conformation and was shown by Hohn et al. (1978) to have a seven-fold rotational symmetry. These workers maintained that dark field scanning transmission electron microscopy provided a superior detail of the apparently globular subunits of the groE complex than did conventional bright field transmission electron microscopy (cf. Fig. 34a and 34b). When spread on freshly cleaved mica in the presence of 1% ammonium molybdate, coated with a thin layer of carbon and floated off onto 2% uranyl acetate (Horne and Pasquali-Ronchetti, 1974), the "22S antigen" from Bordetella pertussis was found to produce random monomolecular arrays of molecules and also regions containing quasi-regular monolayer arrays of molecules (Fig. 35). The reason for this apparent regularity is because the length and diameter of the molecule are almost equal (i.e., 12 nm), which enables a reasonably regular packing of molecules to be produced with molecules orientated both on their sides and on their ends. To date it has not been possible to produce monolayer arrays with molecules orientated totally on their ends or totally on their sides, thereby giving truly paracrystalline arrays (Harris, 1978). With the protein cylindrin (hollow cylinder protein complex) from human or cattle erythrocyte ghosts the problems encountered are even more severe, because the molecule has a length of approximately 17 nm and a diameter of approximately 12.5 nm, which results in the production of almost completely non-regular monolayer arrays by the carbon-flim negative staining technique (Fig. 36). In addition, there is a strong tendency for cylindrin molecules to associate together in groups of

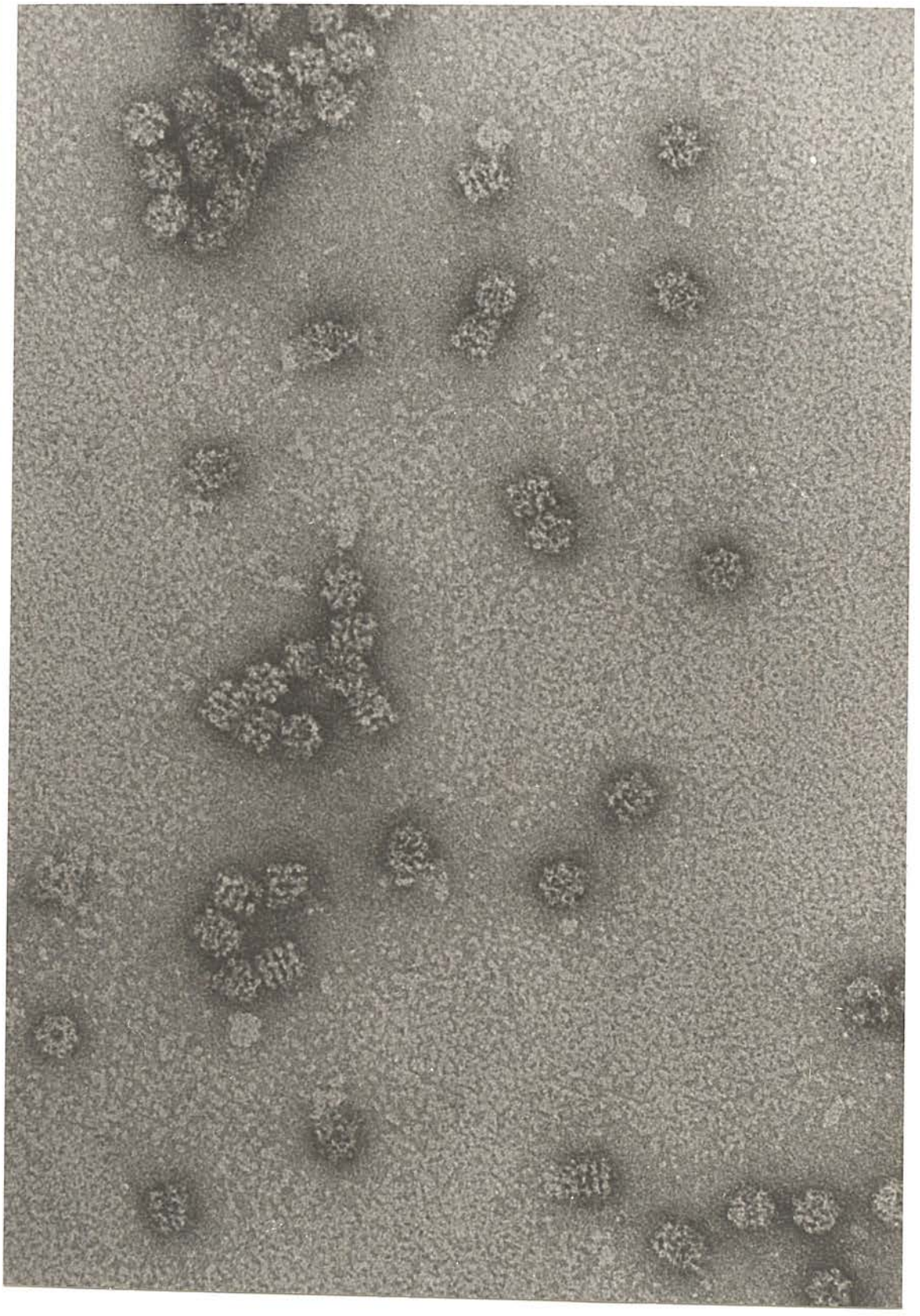

Fig. 34a:

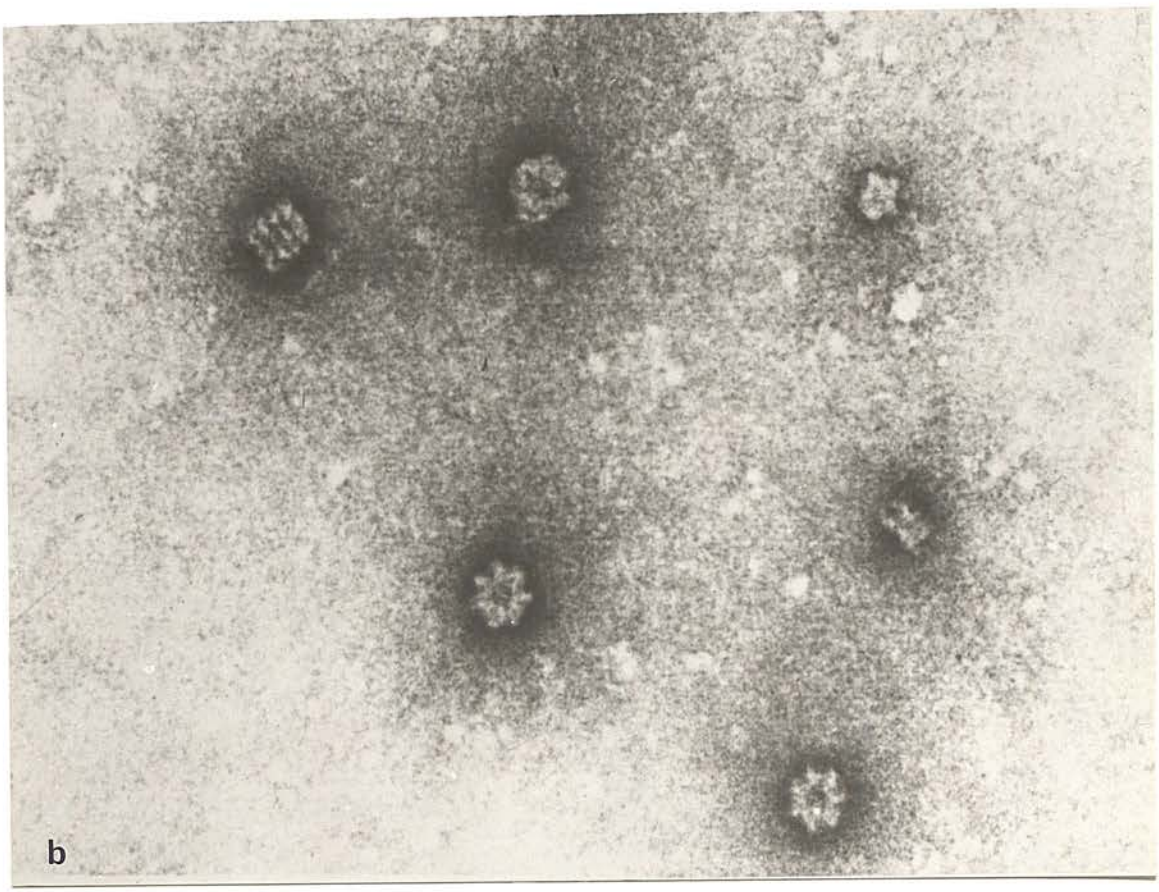

Fig. 34: (a) A conventional bright field electron micrograph of the gp groE complex, indicating side and end orientations (cf. Fig. 33). Negatively stained with uranyl acetate.
(b) A scanning transmission dark field electron micrograph of the gp groE complex, showing side and end orientations. Previously unpublished micrographs of T. Hohn. x 600 000 (approx.).

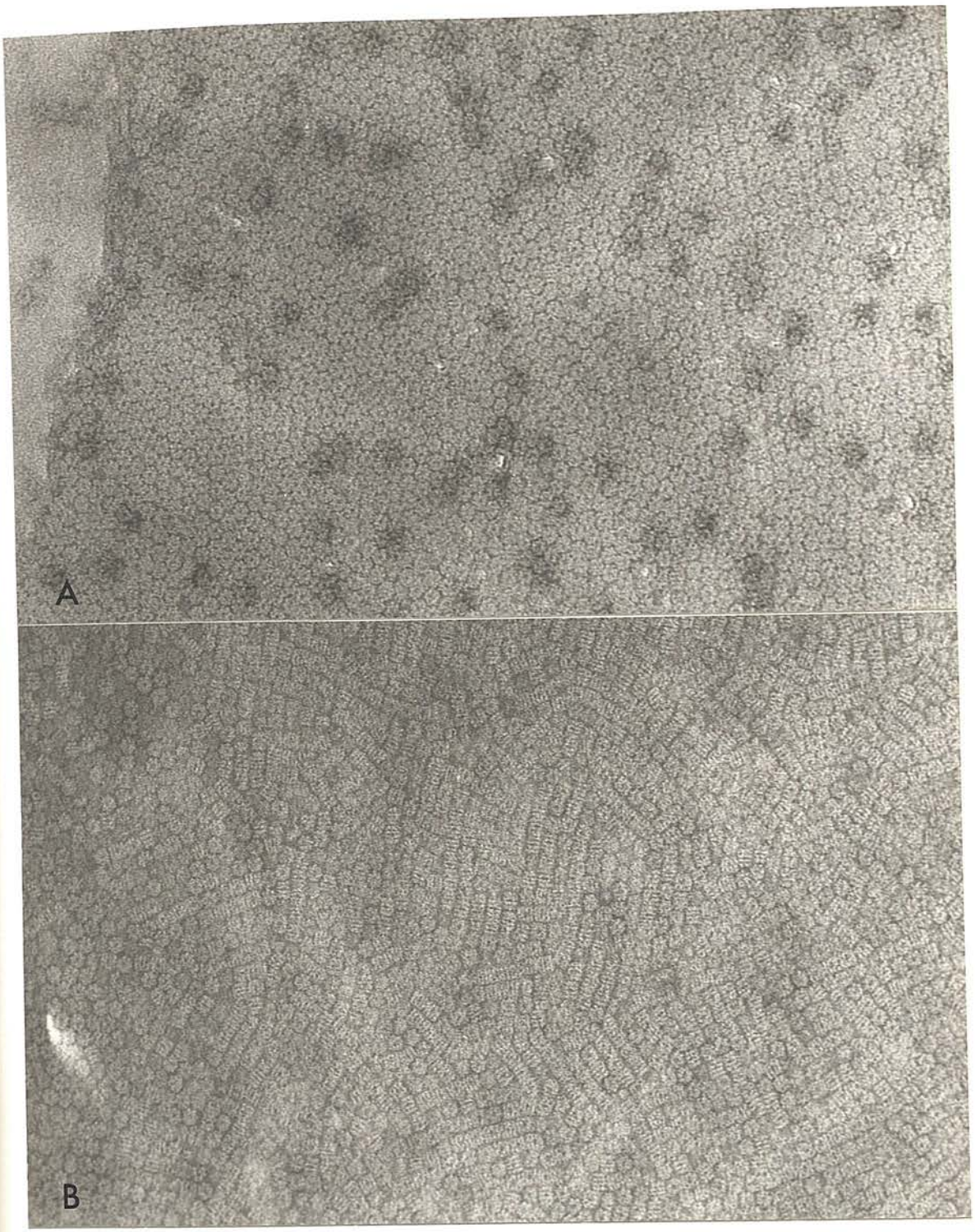

Fig. 35: The '22S antigen' from Bordetella pertussis, prepared using the negative staining-carbon film technique. In (A) a region of quasi regularity is shown, in which most of the molecules are orientated on their ends. In (B) there is again some regularity of molecular packing, with a high proportion of the molecules orientated on their sides. x 198 000.

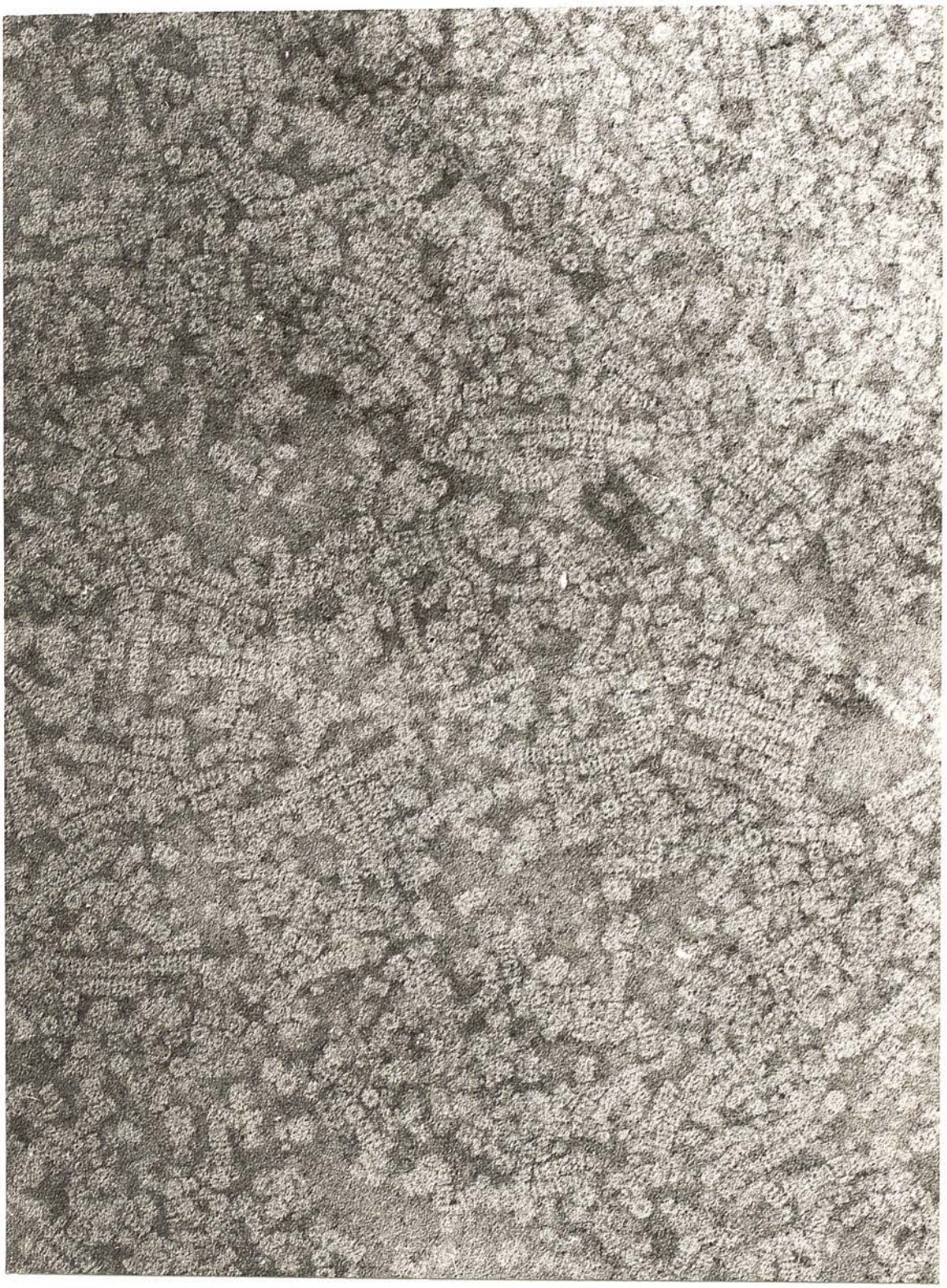

Fig. 36: Human erythrocyte cylindrin, specimen prepared using the negative staining-carbon film technique(with ammonium molybdate followed by uranyl acetate). The molecules are spreadin a predominantly random manner, although some short linear arrays are present. x 186 000.

four off-set molecules (Fig. 37), such that the 'seeding' of a paracrystalline monomolecular array is effectively prevented.

Application of single sideband phase contrast interference (Harris and Kerr, 1976) to the bacterial "22S antigen" again provides contrast enhancement (Fig. 38), as has been shown above for apoferritin (Fig. 14) and for erythrocyte membrane cylindrin (Fig. 39), from Harris and Kerr, (1976). Although this electron optical shadowing technique does impart contrast enhancement and an impression of three dimensional structure within the image, it is likely that in fundamental terms the image should be considered an electron optical artifact, which will probably not be of value for high resolution studies.

VIII. Lectins

The term lectin will be used in the broad sense to refer to proteins of plant, animal and bacterial origin which have the ability to bind to cell surfaces and produce agglutination, usually by a specific glycosidic interaction which can be inhibited by the presence of the appropriate sugar.

A protein from Limulus polyphemus, which produces haemagglutination by its affinity for available surface neuraminic acid groups, has been studied electron microscopically by Fernández Morán et al. (1968). This protein, of molecular weight approximately 400 000, has a conformation resembling a double disc or ring of protein (Fig. 40), which tends to orientate itself preferentially on its side (cf. Harris, 1969). The The molecule also orientates itself vertically on its edge to a lesser extent (arrows, Fig. 40), the image in this instance appears as two closely associated pairs of electron transparent 'double-dots'.

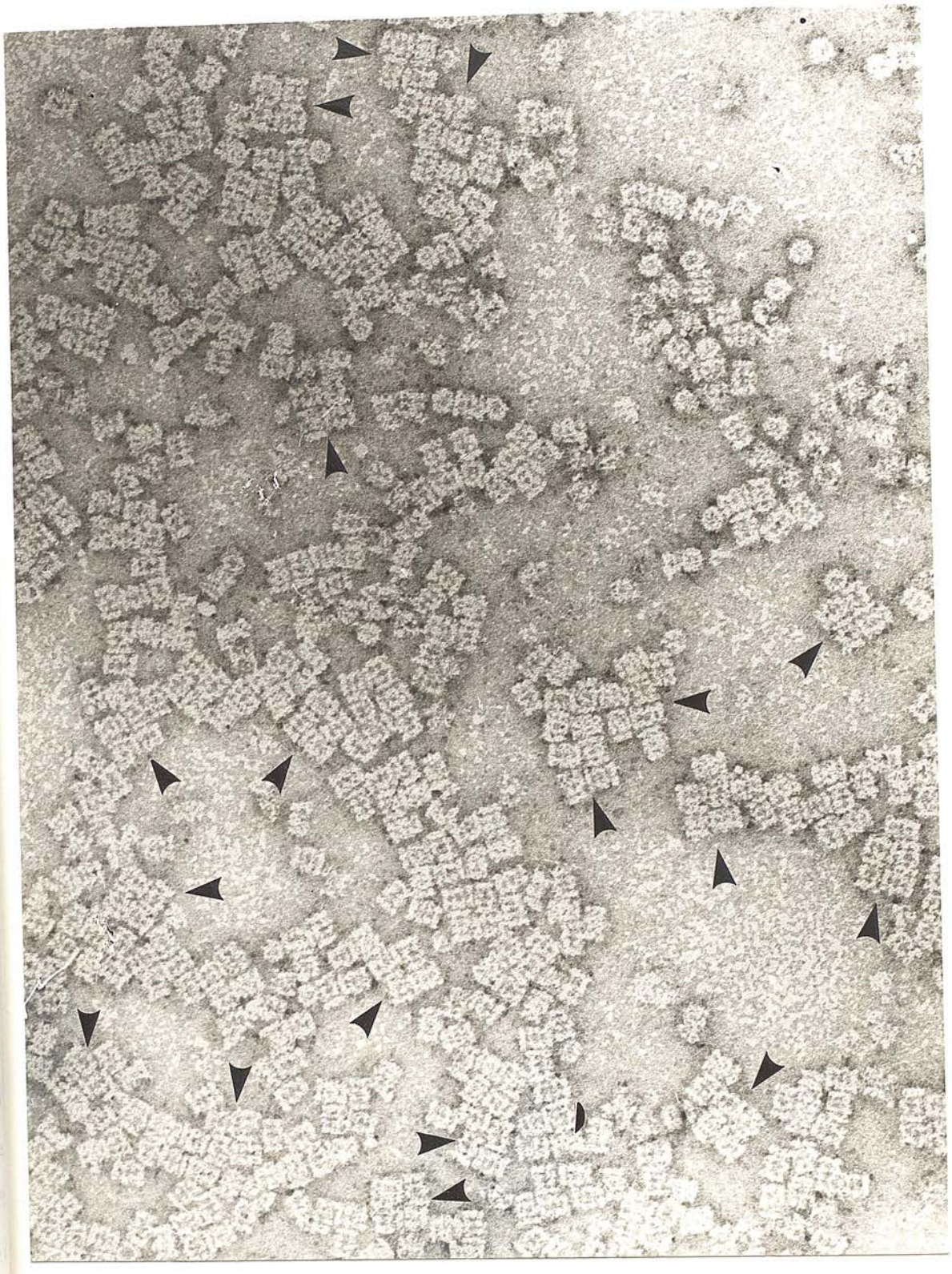

Fig. 37: Human erythrocyte cylindrin, specimen prepared by the negative staining-carbon film technique. In this region groups of four off-set sideways-orientated molecules are indicated (arrows), which prevent subsequent nucleation or the build up of a regular monolayer arred, as does the presence of molecules orientated on their ends. x 320 000.

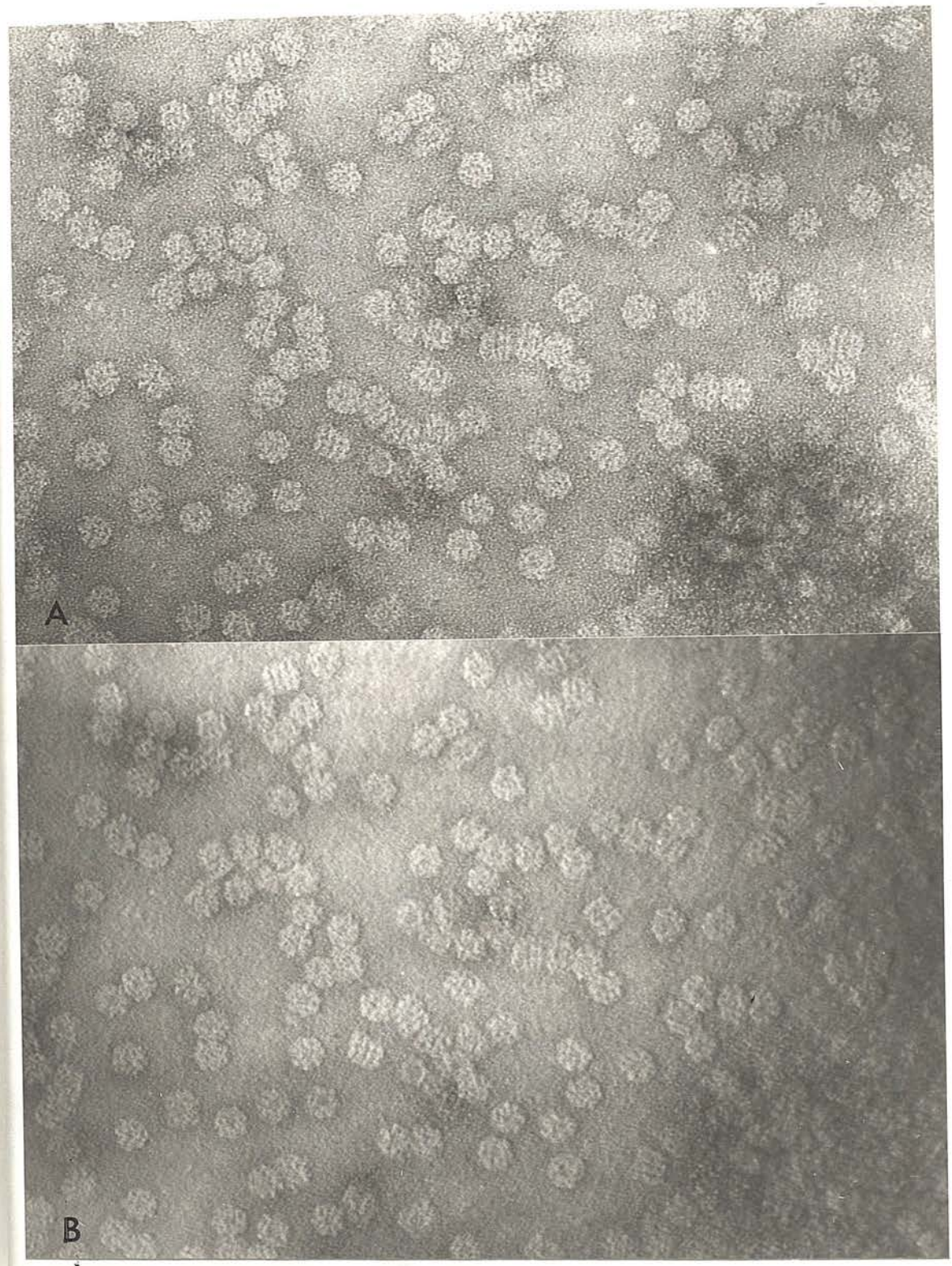

Fig. 38: The '22S antigen' from Bordetella pertussis, (A) revealed by conventional bright field electron optics, and (B) by single sideband phase contrast interference (Harris and Kerr, 1977). Specimen prepared by the negative staining-carbon film technique. Note the 3-D shadowed profiles of the molecules in (B). By coutresy of the Philips Electron Optics Applications Laboratory, Pye Unicam, Cambridge. x 390 000.

Fig. 39(A): Human erythrocyte cylindrin revealed by conventional bright field electron optics. x 186 000.

Fig. 39 (B): Human erythrocyte cylindrin revealed by single sideband phase contrast interference electron optics. Compare with Fig. 39(A). x 186 000.

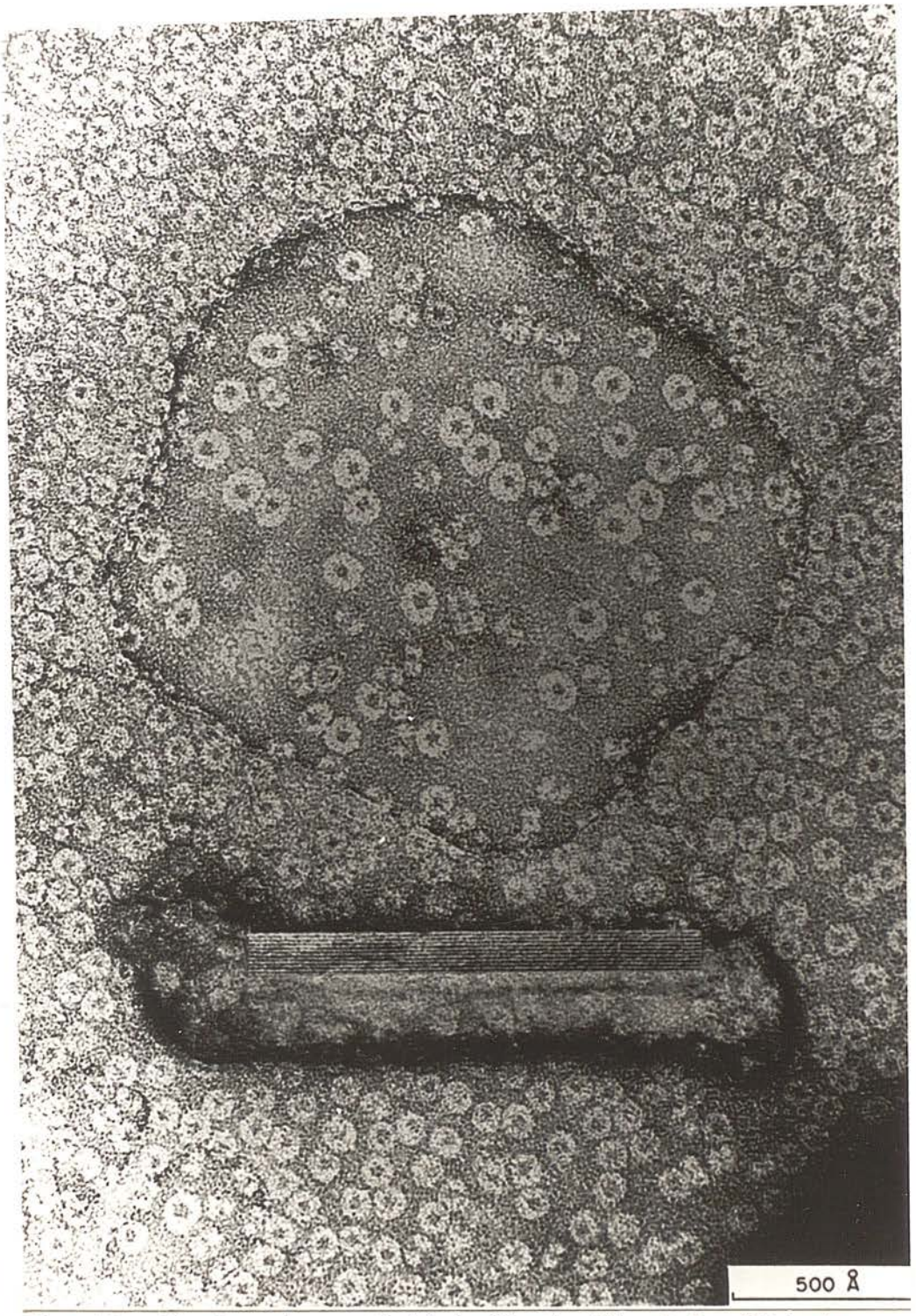

Fig. 40: Limulus haemagglutinin fixed with glutaraldehyde (1.5%), stained and embedded in an ultrathin film of uranyl formate extending unsupported over a hole in a fenestrated carbon film. In the central area the ring-shaped molecules are often distended, displaying their fine structure in various orientations. The arrows indicate molecules orientated on their edges. The asbestos filament (Insert) exhibits a lattice periodicity of 0.73 nm. The scale marker indicates 50 nm. From Fernandez Morán et al. (1968), with the permission of Academic Press.

Although the agglutinin from Helix pomiatia, of molecular weight approximately 79 000 with an affinity for N-acetyl-α-D galactosamine groups, has been studied electron microscopically (Schnitzler et al., 1971), the protein particles do not present any regular quaternary conformation, undoubtedly because of the inherent limitations due to the small molecular dimensions. On the other hand, the phytohaemagglutinin from Phaseolus vulgaris, of molecular weight approximately 100 000, which has the same sugar affinity, has been shown by Höglund and Dahlgren (1970) to be an extremely regular rectangular protein of dimensions 7.7 nm by 4.3 nm, there being some indication of two subunits within the molecules (Fig. 41). From biochemical evidence it is, however, thought that there are four subunits per molecule. Purification of this protein, which has a pronounced affinity for leucocytes, has indicated that its mitogenic activity and agglutinating activity are determined by varying the combination of subunits. Thus, molecules with a high erythro-agglutinating activity can be separated from those with a high mitogenic and leucoagglutinating activity.

The bacterium Bordetella pertussis produces two haemagglutinins, termed the fimbrial-haemagglutinin and the lymphocytosis promoting factor-haemagglutinin (LPF-haemagglutinin), (Irons and MacLennan, 1979). These molecules, which have molecular weights of approximately 200 000 and 80 000, respectively, are shown in Figs. 42 and 43. The fimbrial-haemagglutinin is filamentous, with a diameter approximately 2 nm and has a length varying between 40 to 100 nm, and is thought to be identical to the bacterial surface fimbriae. This agglutinin apparently binds to cholesterol, the hydroxyl and phospholipid head groups both possibly being involved (Irons, 1979). The LPF-haemagglutinin, which

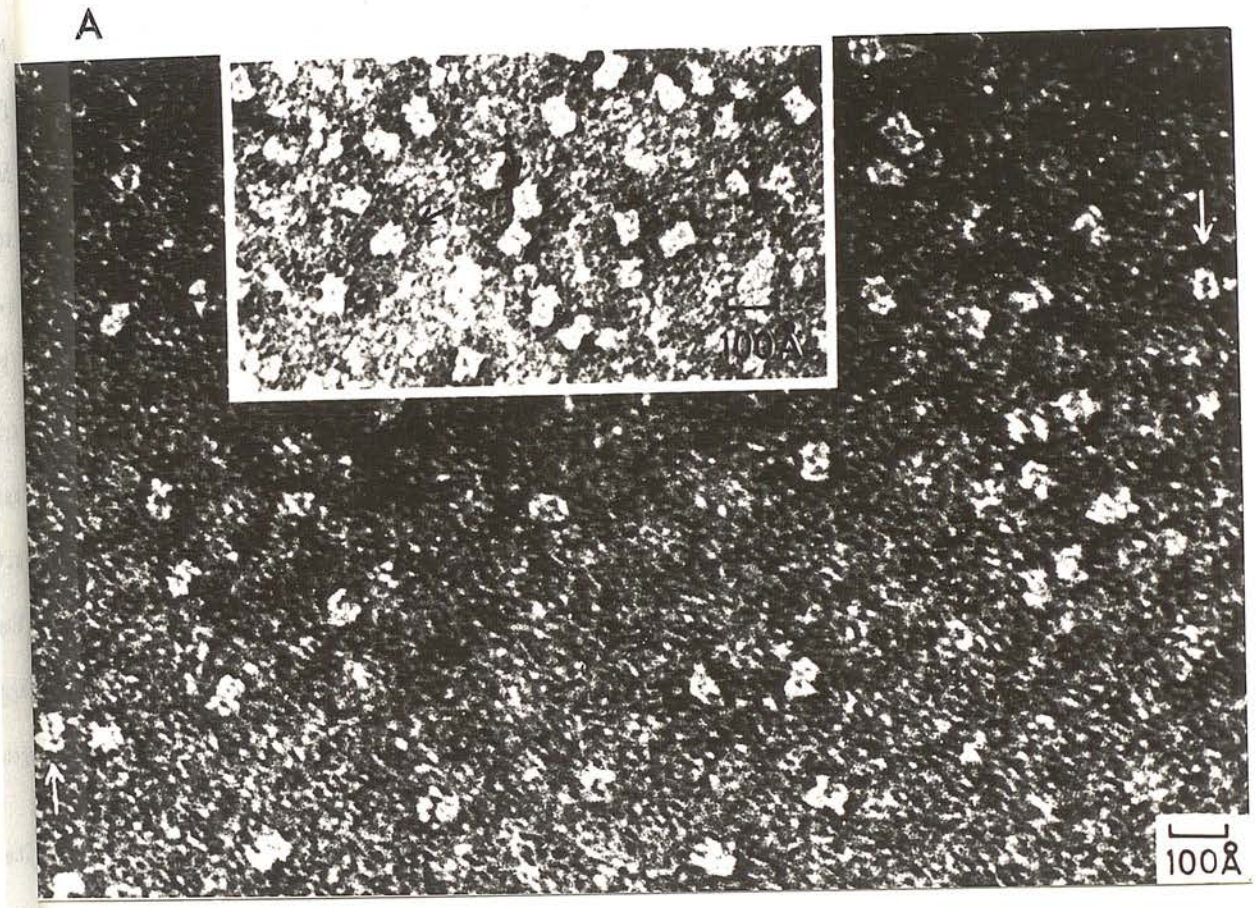

Fig. 41: Phytohaemagglutinin (A) negatively stained with uranyl acetate (Höglund and Dahlgren, 1970; with the permission of Springer-Verlag), (B) negatively stained with 2% sodium phosphotungstate (pH 7.0) and (C) after additon to human erythrocyte ghosts, negatively stained with 2% ammonium molybdate. (B) and (C) x 300 000 and x 150 000, respectively

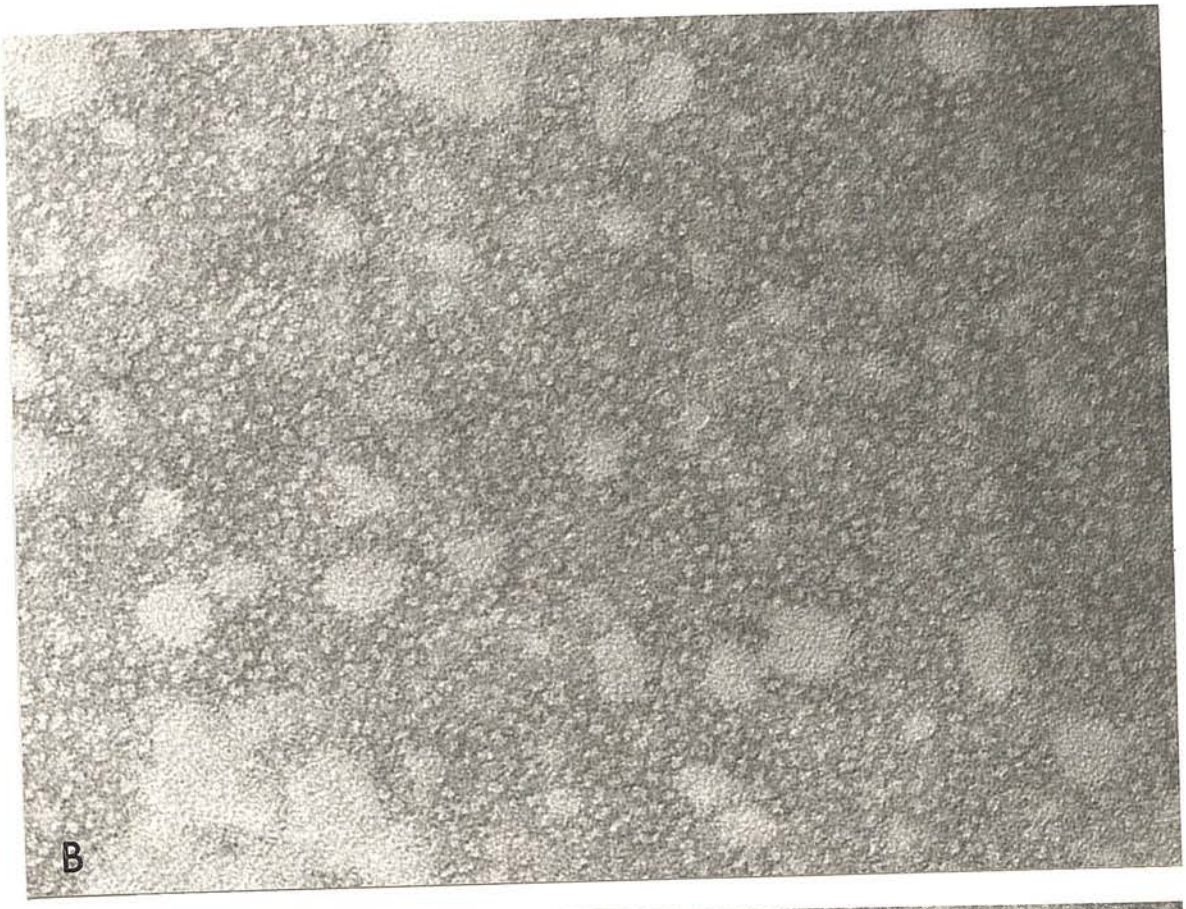

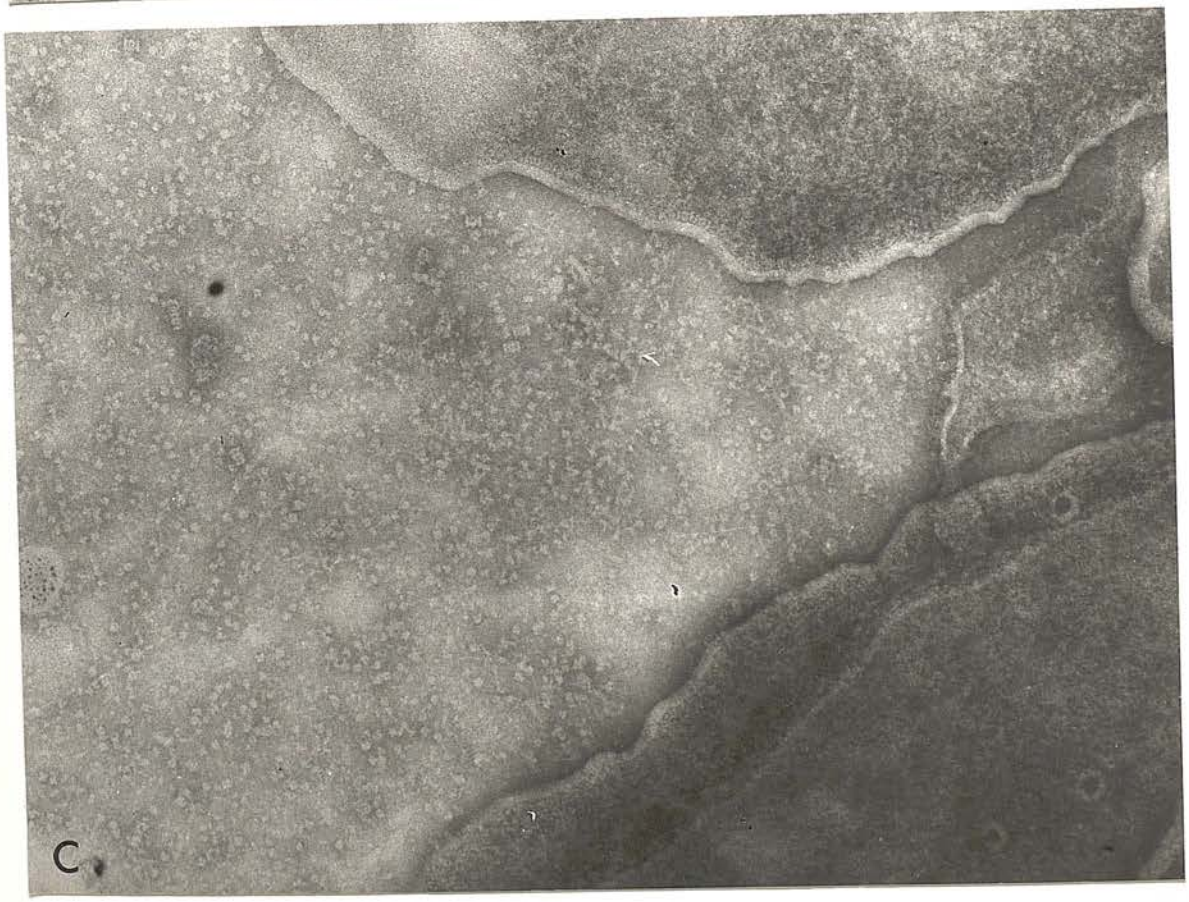

Fig. 41 (B) & (C):

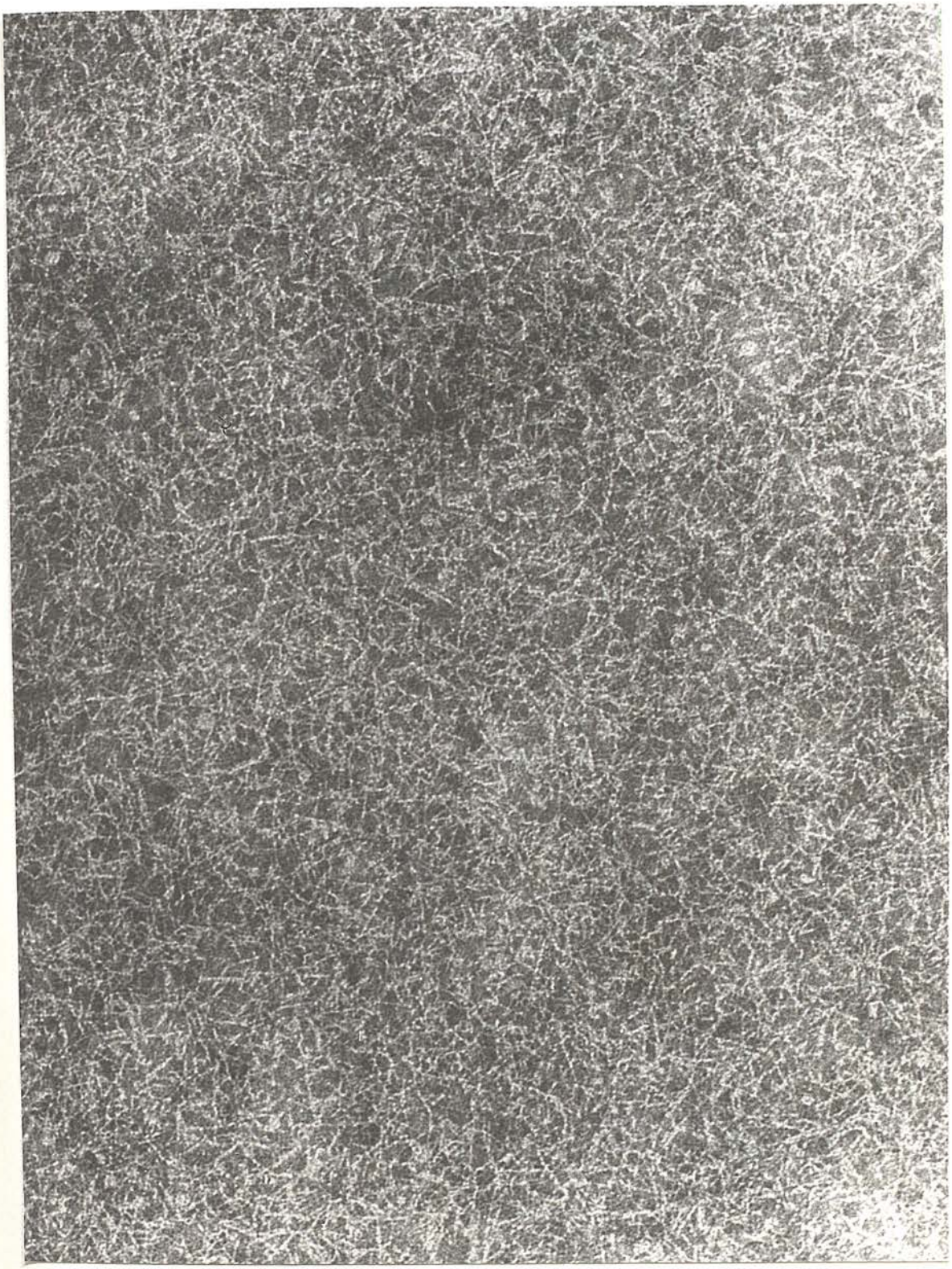

Fig. 42: The fimbrial haemagglutinin from Bordetella pertussis, negatively stained with 2% sodium phosphotungstate (pH 7.0). The filaments are of variable length, with average dimensions 2.0 x 40.0 nm. By courtesy of L. I. Irons and A.B. Dowsett. x 160 000.

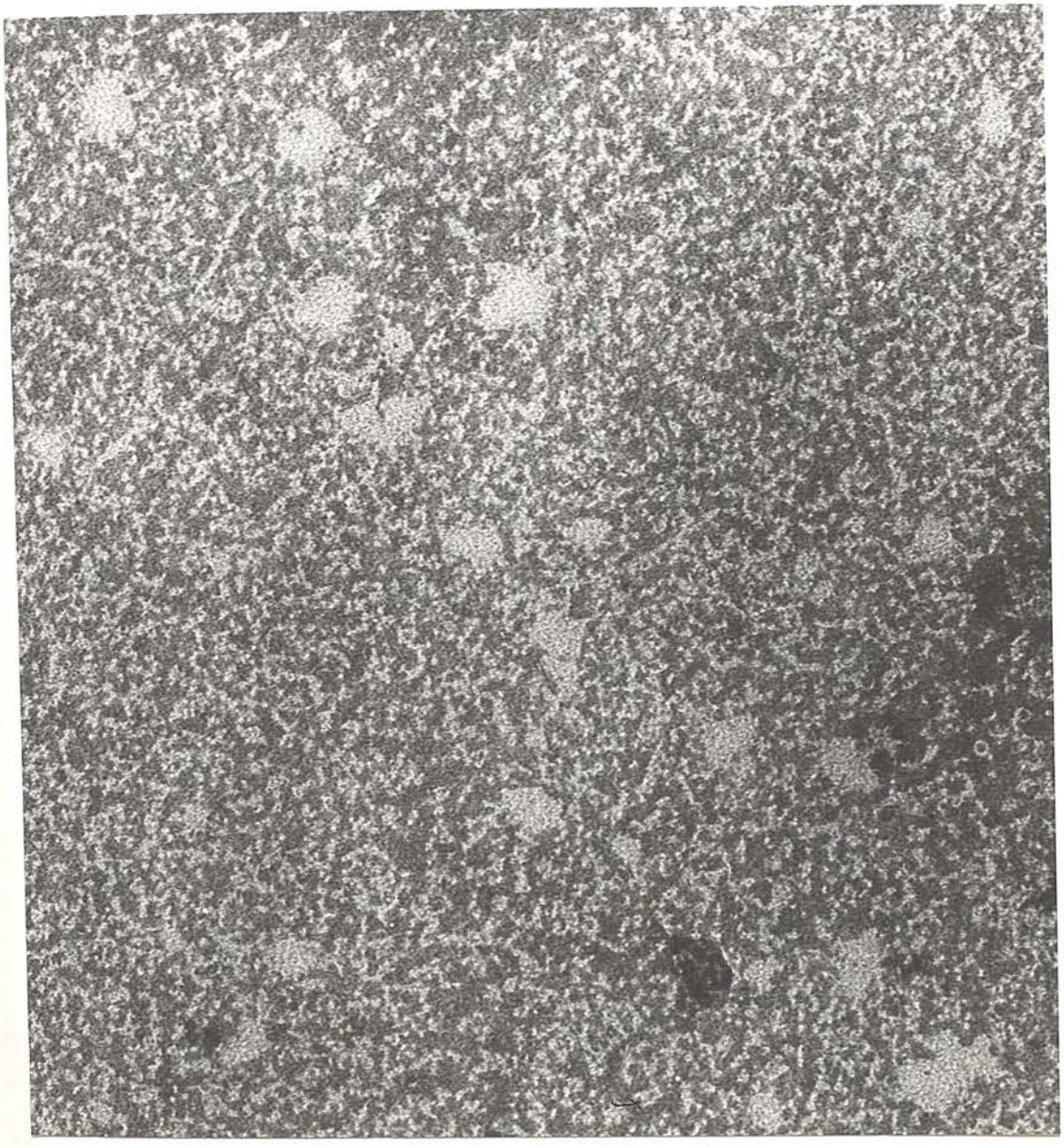

Fig. 43: The lymphocytosis-promoting factor haemagglutinin from Bordetella pertussis purified by affinity chromatography. Negatively stained with 2% sodium phosphotungstate (pH 7.0). From Irons and MacLennan (1979), with the permission of Elsevier North Holland Biomedical Press. x 160 000.

appears to be a spherical particle approximately 6 to 8 nm in diameter, has an affinity for neuraminic acid residues, probably in combination with an as yet unknown sugar residue. Biochemical evidence from SDS-PAGE suggests that the LPF-haemagglutinin has four or five subunits, but it is not at the moment possible to resolve these subunits by electron microscopy.

Although not in the lectin category, the seed storage or reserve proteins, some of which are high molecular weight proteins, have not been studied extensively by electron microscopy. One example, arachin from the pea nut Arachis hypogoea, has been characterized as a globular protein of molecular weight approximately 400 000 and sedimentation coefficient 14.6 S, which has a tendency to dissociate into two 9.5S components (Johnson and Shooter, 1950). Fig. 44 showns partly purified arachin, at pH 8.0, negatively stained with sodium phosphotungstate. Although treatment at a slightly acidic pH (4.0) is thought to dissociate the 14.6S molecule into the 9.5S form, no pronounced change of the electron optical images was detected (Fig. 45)., so it is possible that the molecules were already dissociated or that reassociation occurred rapidly in the presence of neutral sodium phosphotungstate.

IX. High Resolution Studies On Individual Proteins

Attempts to obtain information on the tertiary conformation of small molecular weight proteins by bright field transmission electron microscopy have been fraught with difficulties (Levin, 1963a and 1963b; Mellema et al., 1968), undoubtedly because of inadequate staining technique and gross irradiation damage. More recently Ottensmeyer and

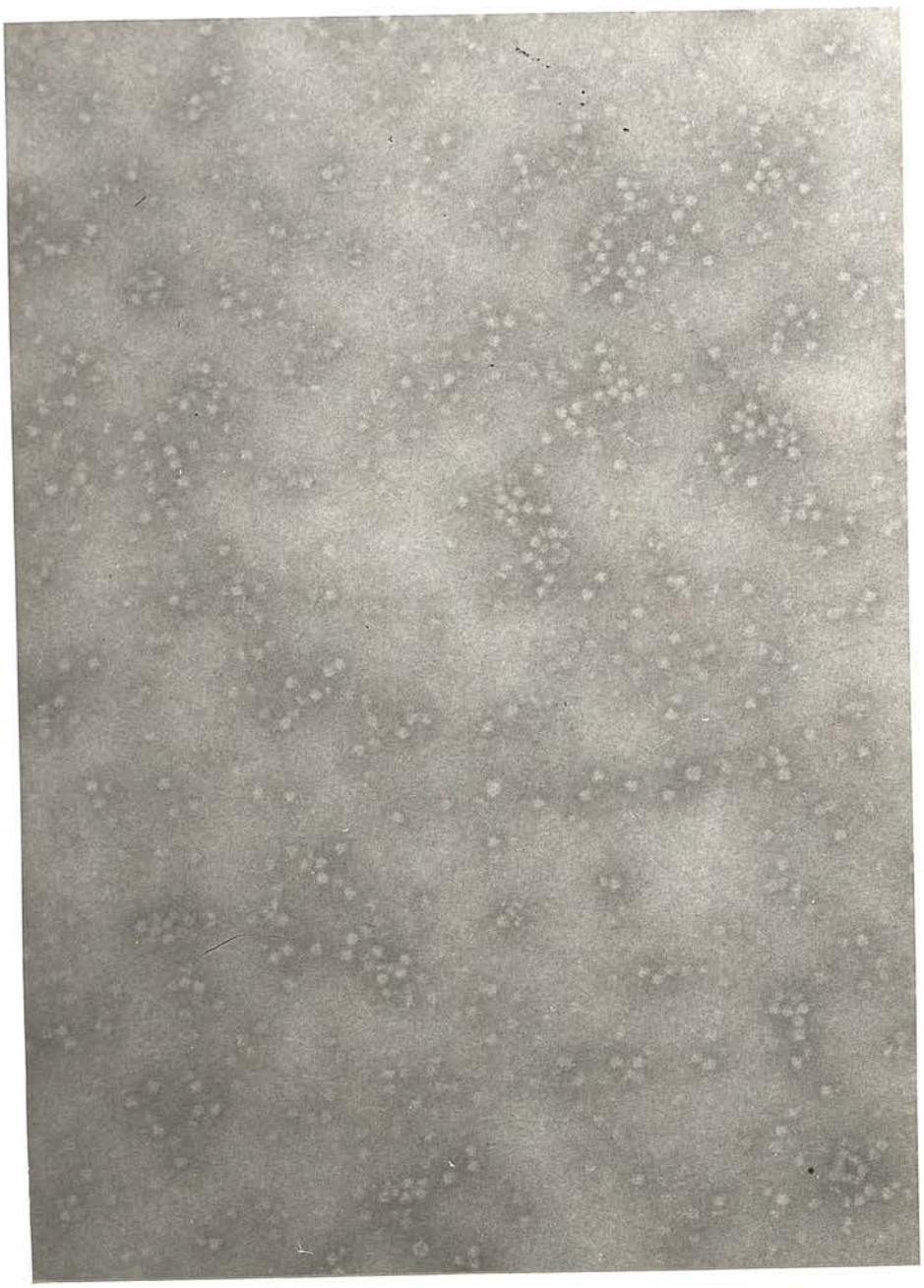

Fig. 44: Partly purified arachin from the peanut Arachis hypogea, negatively stained with 2% sodium phosphotungstate (pH 7.0). x 183 000.

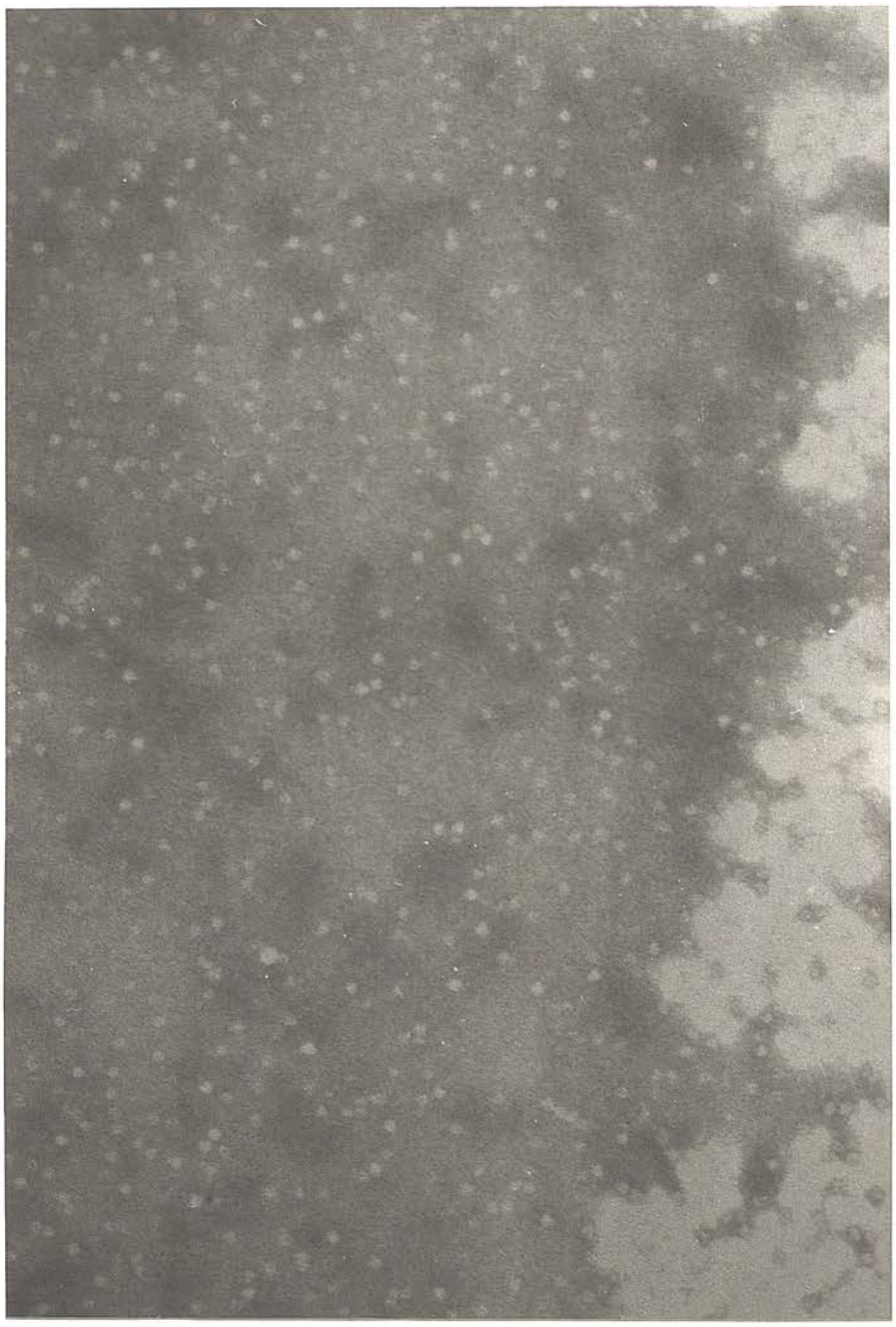

Fig. 45: Partly purified arachin, after treatment at pH 4.0 and subsequent neutralization. Negatively stained with 2% sodium phosphotungstate (pH 7.0). x 183 000.

his colleagues have approached the problem from a slightly different stand point, in that they have used dark field transmisssion electron microscopy in conjunction with minimal exposure of the specimen to the electron beam, the unstained material being supported on very thin carbon films (Ottensmeyer et al., 1975; Bazett-Jones and Ottensmeyer, 1979). From this work a model for the tertiary conformation of fish nucleoprotamine (molecular weight approximately 4 000) and protamine-DNA complexes was presented (Figs 46 and 47). It was claimed that nucleoprotamine was an ellipsoid molecule with a comb- or star-shaped profile around which the DNA double helix is organized, possibly one supercoil turn per protamine molecule. In an attempt to take their studies to even lower molecular weight material, Ottensmeyer and his colleagues have selected for investigation the cyclic peptides vasopressin-8-lysine (molecular weight 1 056), valinomycin (molecular weight 1 111) and bacitracin (molecular weight 1 411), all of which have a tendency to orientate themselves flat on the carbon support film, thereby reducing the number of possible orientations of the molecule relative to the electron beam (Ottensmeyer et al., 1977 and 1978). When dark field minimal exposure transmission electron microscopy was combined with the selection of individual images for manual reconstruction of regular monomolecular layer arrays and the production of optically averaged and filtered images as shown in Figs 48 and 49, (cf. Unwin and Henderson, 1975), it was claimed that the images of the polypeptides contained genuine structural features. For instance, the position of the iodinated tyrosine of vasopressin was shown to be clearly indicated (Fig. 49) and the bound potassium ion of valinomycin was claimed to be at the centre of an approximately triangular polypeptide. In addition, it was shown (Ottensmeyer et al., 1978a) that bacitracin

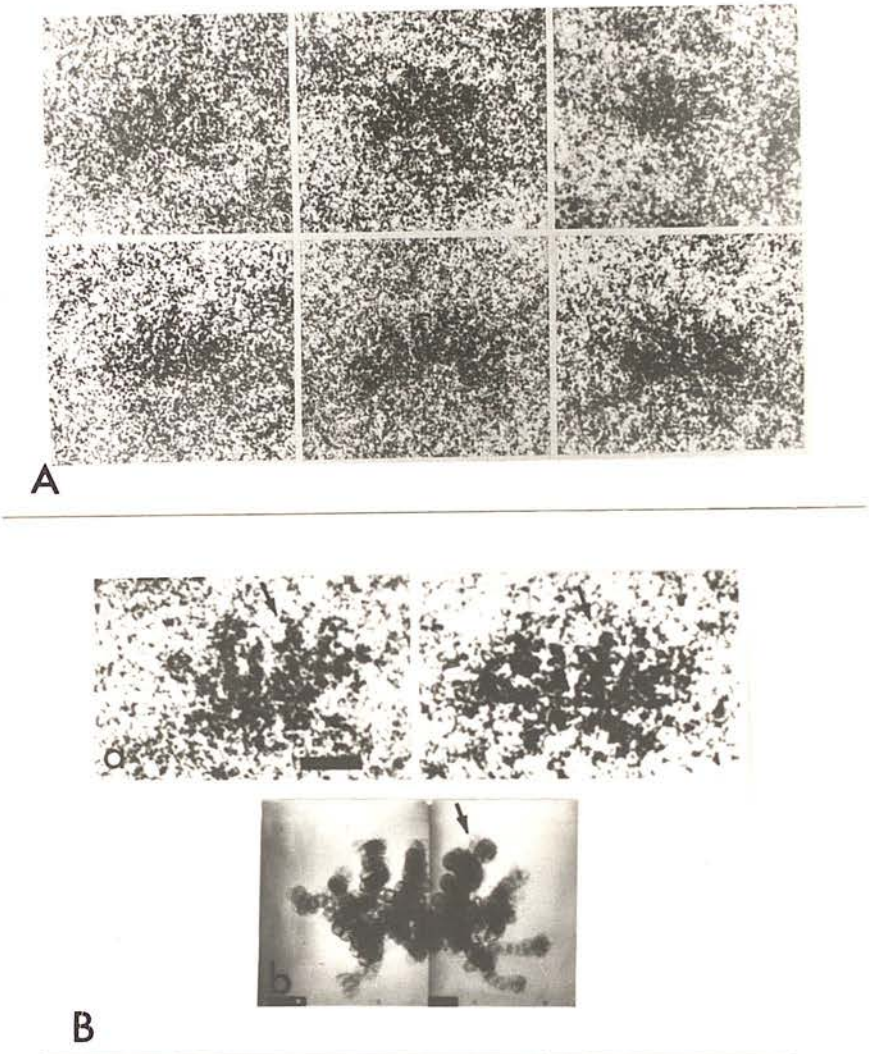

Fig. 46: (A) Representative dark field unstained electron micrographs of triphosphrylated trout sperm protamine. The scale markers indicates 5 nm. From Bazett-Jones and Ottensmeyer (1979), with the permission of Academic Press. (B) Molecules of herring sperm protamine clupeine Y-I. A comparison of dark field electron micrographs (a) with the roentgenogram (b) of a space filling model of clupeine Y-I constructed from the dark field electron optical images. From Ottensmeyer et al. (1975), with permission. The scale marker indicates 1.0 nm.

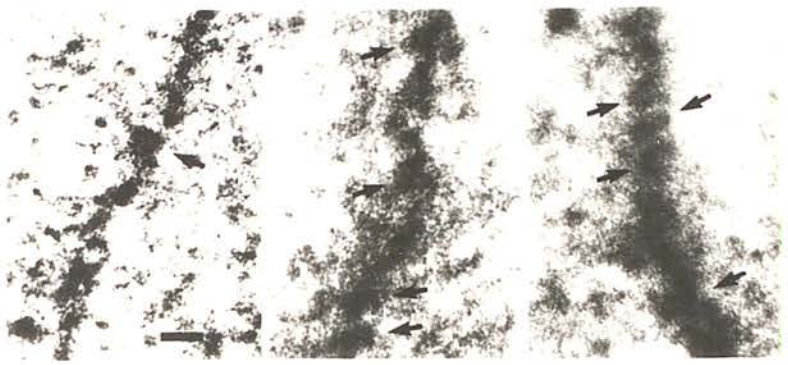

Fig. 47: Dark field electron micrographs of unstained complexes of DNA and trout sperm protamine, suggesting a supercoiling of the DNA. The left hand micrograph shows a loop structure. In the middle and right hand micrographs, the arrows on the left sides of the fibrils point out striations across the fibrils. The scale markers indicates 6.0 nm. From Bazett-Jones and Ottensmeyer (1979), with the permission of Academic Press.

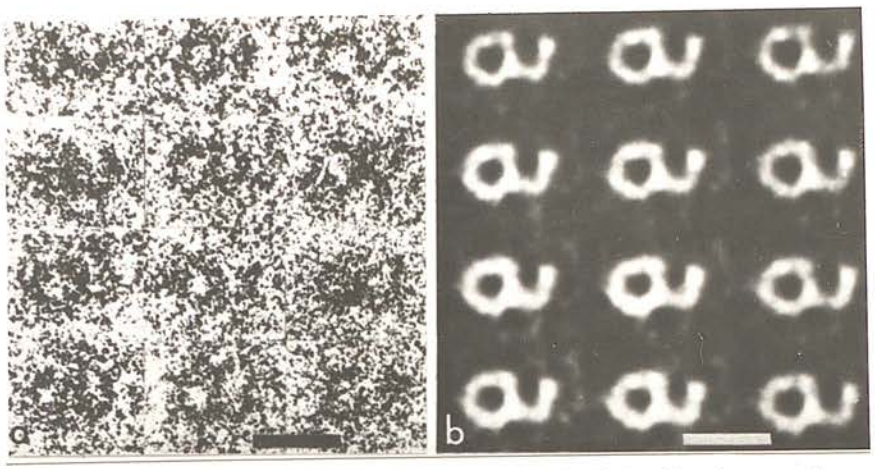

Fig. 48: A set of twelve unstained dark field electron micrographs of vasopressin, manually selected and orientated (a), from which and optical diffraction pattern was obtained, filtered and used to produce the reconstructed images (b). The scale marker indicates 1.5 nm. From Ottensmeyer et al. (1977), with the permission of Blackwell Scientific Publications.

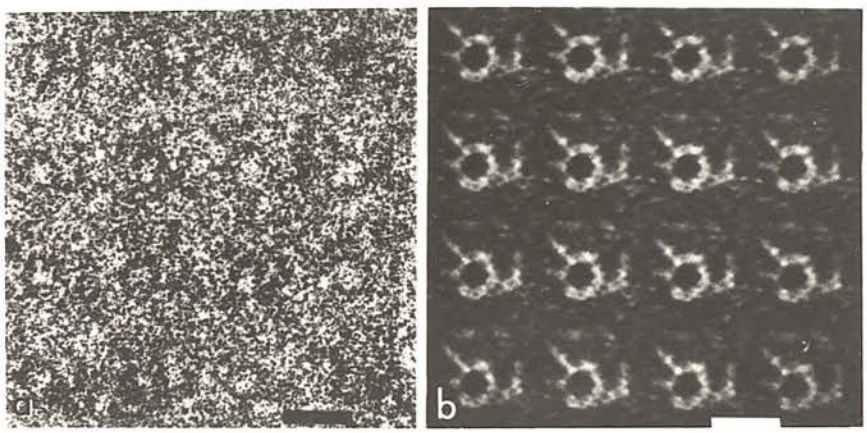

Fig. 49: (a) Sixteen dark field images of unstained vasopressin molecules iodinated at the ring tyrosine residue, manually selected and orientated. (b) Reduction of noise by the 'Filtering of Arrays of Images in Reciprocal Space' (FAIRS) technique, produces in a clear delineation the position of the marker iodine atoms which indicate that the tyrosine is located near the top of the ring structure. The scale marker indicates 1.5 nm. From Ottensmeyer et al. (1977), with the permission of Blackwell Scientific Publications.

appears as a double ring structure, one ring being slightly larger than the other. A resolution of 0.5 nm or better was claimed from this study. Despite the fact that this work has been reviewed fairly extensively (Ottensmeyer, 1979; Ottensmeyer et al., 1978b), others have not generally accepted the claims made (Klug, 1979). Considerable scepticism has been expressed regarding both the survival of the polypeptide chain at the electron doses employed in the studies of Ottensmeyer and his colleagues, and also the use of subjective selection and orientation of the electron optical images of the molecules for the construction of regular two dimensional arrays has likewise been criticised. Until other groups are able to confirm and extend these high resolution studies, doubts as to their validity will surely remain.

X. Conclusions and Future Prospects

It has been the aim of this chapter to demonstrate the current range of application of negative staining electron microscopy to the study of predominantly high molecular weight proteins. The examples selected are by no means exhaustive and the omission of other work in no way detracts from its possible value. While in many cases electron microscopic data has been gained on the subunit composition of proteins, which can be correlated successfully with that obtained from the varous biochemical approaches, the studies cannot in general be considered to be in the truly high resolution category of the type performed by Unwin and Henderson (1975). This is because they have mostly been performed by conventional bright field transmission electron microscopy without minimum exposure techniques, and as a result

little or no information has been forthcoming on the folding of the polypeptide chain within any one subunit.

With the availability of electron microscopes offering an instrumental resolution of 0.2 nm or better, it is likely that in the future increasing numbers of proteins will be studied and indeed discovered by electron microscopy. There appear to be few recorded examples of electron microscopic studies that indicate qualitatively that protein purity has been achieved, by showing the presence of a single well defined particle, revealed by established staining techniques, which do not also receive support on purity from immunochemical and electrophoretic data. This does not extend to the level of being able to distinguish between molecules with small amino acid differences, although such molecules may exhibit different quaternary conformations and crystallization properties, for instance haemoglobin-S (Dykes et al., 1978) and haemoglobin-C (Houston et al., 1979). There must always be the possibility that owing to the hydrated nature of a particular protein, extensive penetration of the polypeptide chain occurs, such that the negative stain is unable to reveal the polypeptide chain, but this does not appear to be a major problem.

The forementioned studies of Ottensmeyer and his colleagues and also those of Dubochet (1973) claim and increased signal to noise ratio from dark field transmission electron microscopy and indicate that this procedure may be of benefit to future studies on single molecules. Another approach is the low-dose averaging technique of Frank and his colleagues (see Frank, 1979), which is applicable to proteins that, like the polypeptides studied by Ottensmeyer, have a unique plane of attachment to the carbon support film. The enzyme glutamine synthetase has

received particular attention, as it has a pronounced tendency to orientate itself on its side, revealing ring-like molecular images composed of two superimposed rings of subunits, but the technique is unlikely to be of value for the study of molecules which have random orientations. If, ordered two dimensional arrays of molecules that are a single polypeptide thick can be produced (e.g. Harris, 1978 and see Fig. 50), and studied by minimum exposure techniques, possibly in conjunction with low temperature techniques (Knapek and Dubochet, 1980), it is possible that radiation-induced molecular damage may be dramatically reduced. On processing the electron micrographs by image averaging of a large number of unit cells to decrease quantum noise, it may be possible that further three dimensional reconstructions of the tertiary conformation of proteins will be achieved (vis. Unwin and Henderson, 1975; Henderson et al., 1977; Baker and Amos, 1978).

Recently, Kam (1980) has applied the "spatial correlation" technique to the problem of image information enhancement from electron micrographs of randomly spread macromolecules. Convincing three demensional reconstructions of the enzyme glutamic dehydrogenase were achieved. This approach is limited by preferential orientation of protein molecules on the support film, which would indicate inherent molecular asymmetry, and also the extent to which protein molecules collapseonto the support film during specimen preparation is likely to be variable.

The aim of most biochemically orientated electron microscopists is to correlate protein structure and function. Although this may be possible in some instances, in the main this is not yet possible for most of the examples cited above. One area in which it may be possible to perform meaningful structural studies that relate to protein function is the interaction of cell surfaces with lectins,

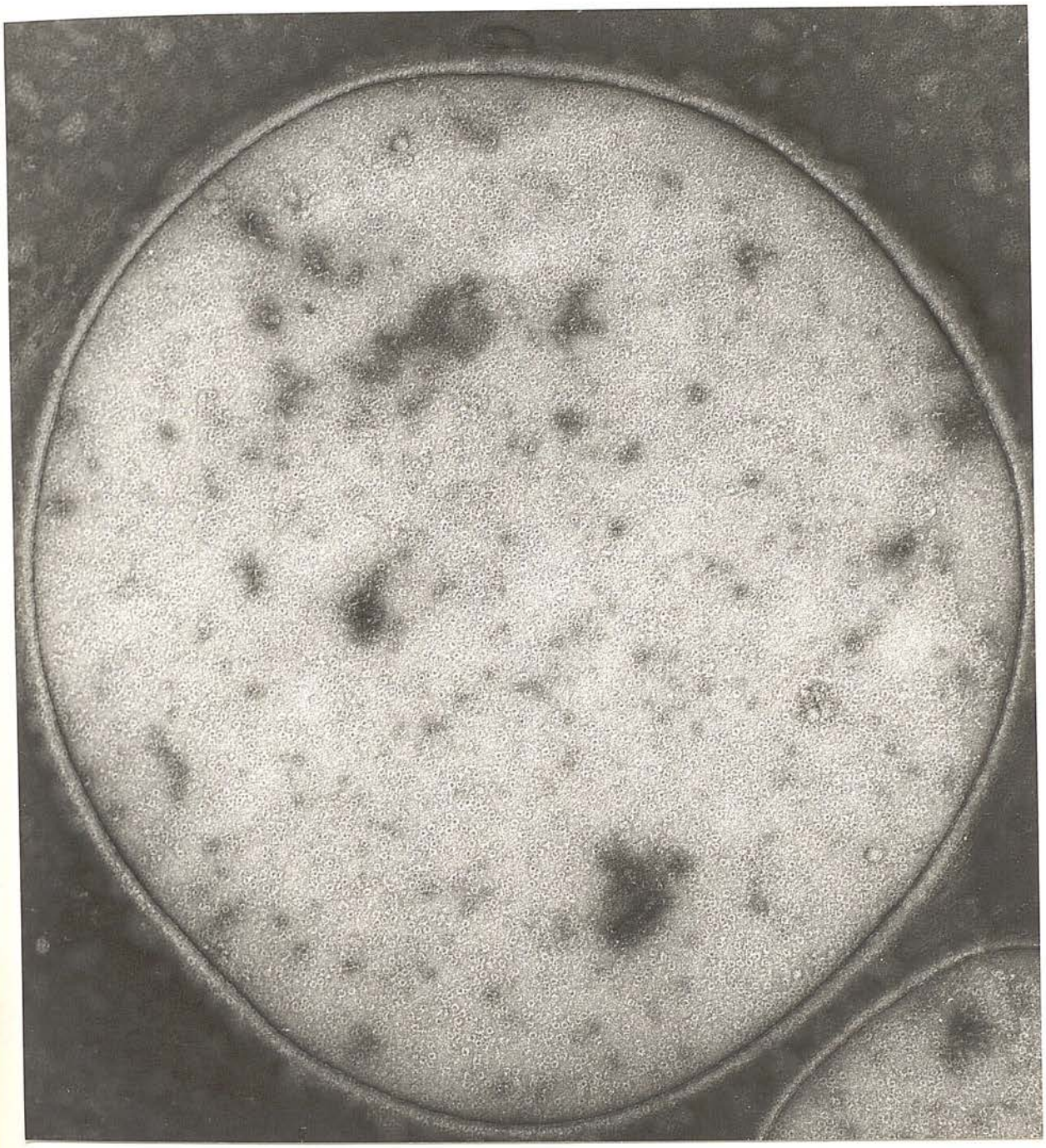

Fig. 50: The molecule 'torin' from human erythrocytes, which is a single ring structure (M.W. approx. 200 000, with 10 subunits). Specimen prepared by the negative stain-carbon film technique, using ammonium molybdate followed by uranyl acetate. Most of the molecules are orientated on their sides, and groups of molecules appear to be starting to form ordered monomolecular layer arrays (arrows). x 100 000.

bacterial and viral proteins. As mentioned previously, the fimbrial haemagglutinin from Bordetella pertussis binds to cholesterol, which opens up the possibility for electron microscopic studies of agglutinin-liposome interactions. If isolated membrane glycoproteins are incorporated into liposomes it should also be possible to determine the selective binding of lectins, together with the inhibition of binding and displacement by addition of the appropriate sugar or oligosaccharide. Similarly, the direct interaction of lectins with isolated cell surface membrane vesicles, or indeed purified glycoproteins, will probably, in the future, be investigated electron microscopically.

XI. References

Baker, T.S. and Amos, L.A. (1978). J. Mol. Biol. 123, 89-108.

Bazett-Jones, D.P. and Ottensmeyer, F.P. (1979). J. Ultrastruct. Res. 67, 255-266.

Berg, G. (1973). J. Ultrastruct. Res. 42, 324-336.

Berg, G. (1975). J. Ultrastruct. Res. 55, 113-118.

Berg, G. and Ekholm, R. (1975). Biochim. Biophys. Acta 886, 422-431.

Berg, G., Bjorkman, U. and Ekholm, R. (1975) in Exerpta Medica Int. Cong. Series No. 378, Thyroid Research, p 169, Elsevier.

Berg, G. (1978). In "Principles and Techniques of Electron Microscopy" (M.A. Hayat, ed) Vol. 9, pp. 246-261. Van Nostrand Reinhold.

Bjork, I. (1973) Eur. J. Biochem. 36, 178-184.

Bloth, B., Utter, G. and Svehag, S.-E. (1975). Experientia 31, 760-762.

Bradley, D.E. (1966). In 6th Int. Cong. Electron Microscopy, Kyoto, p 115.

Brown, J.N. and Harris, J.R. (1970). J. Ultrastruct. Res. 32, 405-416.

Buhlman, G. (1976). J. Insect. Physiol. 22, 1101-1110.

Chino, H. , Marakani, S. and Harashima, K. (1969). Biochim. Biophys. Acta 176, 1-26.

Chino, H., Yamagata, M. and Takahashi, K. (1976). Biochim. Biophys. Acta 441, 349-353.

Dubochet, J. (1973). J. Microscopy 98, 334-344.

Dykes, G., Crepeau, R.H. and Edelstein, S.J. (1978). Nature 272, 506-510.

Fernández Morán, H., Marchalonis, J.J. and Edelman, G.M. (1968). J. Mol. Biol. 32, 467-469.

Frank, J. (1979). J. Microscopy 117, 25-38.

Fromherz, P. (1971). Nature 231, 267-268.

Haggis, G.H. (1965). J. Mol. Biol. 14, 598-602.

Harris, J.R. (1969). J. Mol. Biol. 46, 329-335.

Harris, J.R. and Kerr, J. (1976). J. Microscopy 108, 51-59.

Harris, J.R. (1978). Proc. Roy. Mic. Soc. 13, Pt.4, 29.

Henderson, R.,Capaldi,R.A. and Leigh, J.S. (1977). J. Mol. Biol. 112, 631-648.

Höglund, S. and Dahlgren, K. (1970). Eur. J. Biochem. 17, 23-26.

Hohn, T., Wurz, M. and Engel, A. (1978). J. Ultrastruct. Res. 65, 90-93.

Horne, R.W. and Pasquali-Ronchetti, I. (1974). J. Ultrastruct. Res. 47, 361-383.

Houston,T.E., Girling, K.L., Amma, E.L. and Huisman, T.H.J. (1979). Biochim. Biophys.Acta 576, 497-501.

Irons, L.I. and MacLennan, A.P. (1979) Biochim. Biophys. Acta 580, 175-185.

Irons, L.I. (1979). In Int. Symp. on Pertussis (C.R. Manclark and J.C.Hill, eds), U.S. Dept. Health Education and Welfare, pp 338-349.

Johnson, P. and Shooter, E.M. (1950). Biochim. Biophys. Acta 5, 361-375.

Kam, Z. (1980). J. Theor. Biol. 82, 15-39.

Knapek, E. and Dubochet, J. (1980). J. Mol. Biol. 141, 147-161.

Klug, A. (1978-79) Chemical Scripta 14, 291-293.

Levin, O. (1963a). J. Mol. Biol. 6, 137-140.

Levin, O. (1963b). J. Mol. Biol. 6, 158-163.

MacLennan, A.P., Hawkins, D.C., Ekersley, B. and Blake, J. (1977). Proc. Soc. Gen. Microbiol. 4, 81.

Markham, R., Frey, S. and Hills, G.J. (1963). Virology 20, 88-102.

Massover, W.H. (1978a). In 9th Int.Cong. on Electron Microscopy, Toronto. Vol 11, pp 182-183, Microscopical Society of Canada.

Massover, W.H. (1978b). J. Mol. Biol. 123, 721-726.

Massover, W.H. and Cowley, J.M. (1975). In Proteins of Iron Storage and Transport in Biochemistry andd Medicine (R.R.Crighton, ed) pp 237-244, North Holland.

Mellema, J.E., van Bruggen, E.F.J. and Gruber, M. (1968). J. Mol. Biol. 31, 75-82.

Munn, E.A. (1976). In 6th Europ.Cong. on Electron Microscopy, pp 515-516.

Munn, E.A. (1977). Tiss.Cell 9, 23-34.

Oda, T. and Takanami, M. (1972). J. Mol. Biol. 71, 799-802.

Ottensmeyer, F.P.,Whilings, R.F. and Korn, A.P. (1975). Proc. Nat. Acad.Sci. USA 72, 4953-4955.

Ottensmeyer, F.P., Andrew, J.W.,Bazett-Jones, D.P, Chan, A.S.K. and Hewitt, J. (1977). J. Microscopy, 109, 259-268.

Ottensmeyer, F.P., Bazett-Jones, D.P., Hewitt, J. and Price, O.B. (1978a). Ultramicroscopy 3, 303-313.

Ottensmeyer, F.P., Bazett-Jones, D.P. and Korn, A.P. (1978b). 9th Int Cong. on Electron Microscopy, Toronto, Vol 111, pp 147-159, Microscopical Society of Canada.

Ottensmeyer, F.P. (1979). Ann.Rev. Biophys. Bioeng. 8, 129-144.

Sato, Y. and Nagase, K. (1967). Biochem. Biophys. Res. Commun. 27, 195-201.

Schnitzler, St., Uerlings, I. and David, H. (1971). Acta biol. germ. 26, 193-203.

Siezen, R., Bindels, J.G. and Hoenders, H.J. (1978). Eur. J. Biochem. 91, 387-396.

Siezen, R.J., Bindels, G. and Hoenders, H.J. (1979). Exp. Eye Res. 28, 551-567.

Unwin, P.N.T. and Henderson,R. (1975). J. Mol. Biol. 94, 425-440.

Williams, M.A. andHarrison, P.M. (1968). Biochem. J. 110, 265-280.

The Production of Paracrystalline Monolayers of Purified Protein Molecules

INTRODUCTION

The production of ordered monomolecular arrays of purified protein molecules for electron microscopic investigation has presented itself as a distinct possibility following the development of the negative staining-carbon film technique of Horne and his colleagues (Horne and Pasquali Ronchetti, 1974; Horne et al. 1975a and 1975b), which has been found to be widely applicable to icosahedral and filamentous viral particles. The main value of this approach is that in providing ordered paracrystalline monomolecular arrays of protein molecules, image analysis by optical diffractometry, filtering and image reconstruction can be performed. This, in many instances within the field of viral structure, has been shown to result in a greater quantitative understanding of the molecular structures under investigation (Horne, 1978; Klug and Berger, 1964; De Rosier and Klug, 1968; Horne and Markham, 1972). Despite the fact that the negative staining-carbon film techniques was established a number of years ago, few attempts have been made to extend its application to isolated macromolecules of non-viral origin. In a preliminary communication (Harris, 1978) presented a brief account of the studies which are presented below in greater detail and which have been extended to include the enzyme glutamine synthetase from *E. coli* in addition to horse spleen apoferritin, *Bordetella pertussis* and *E. coli* '22S antigen', and the proteins cylindrin and torin from human erythrocytes.

In the negative staining-carbon film technique it is clear that charge interactions between the mica surface the stain and the protein are of considerable importance. It is therefore, interesting to note that Fromherz (1971) was able to produce an ordered array of ferritin molecules by absorption of the protein onto a positively charged lipid monolayer. It is known that the surface of mica carries bound potassium ions, which will similarly be responsible for a net positive charge and may influence the ordering of negatively charged protein molecules as the aqueous solution of stain plus protein dries onto the mica.

MATERIALS AND METHODS

Proteins: Human erythrocyte cylindrin and torin were purified by established procedures (Harris and Naeem, 1978). Horse spleen apoferritin was purchased from Cal. Biochem. Ltd and Sigma (London) Chemical Company Ltd. Both products consist of approximately 90% apoferritin monomer, with significant amounts of dimer, trimer and higher oligomers. The monomer of apoferritin was purified by preparative electrophoresis using the apparatus manufactured by Quickfit Instrumentation. Highly purified Bordetella pertussis and E. coli. '22S antigen' and E. coli glutamine synthetase were donated by the PHLS Centre for Applied Microbiology and Research, Porton Down, by courtesy of Dr. A. P. MacLennan.

Negative Staining Procedure: The original procedure of Horne and Pasquali-Ronchetti (1974) for the negative staining-carbon film technique has been applied throughout this study. Single droplets of protein solution (concentration of protein varying between approximately 1 mg/ml to 10 mg/ml) were placed on a clean parafilm surface and mixed with an equal volume of 2% ammonium molybdate (pH 7.0 to 9.0), adjusted with sodium hydroxide. A small quantity of this mixture was applied to the surfaces of freshly cleaved mica and allowed to drain onto the edge of a filter paper. After drying at room temperature the mica strips were coated with a thin layer of carbon layer plus adhering protein was floated off on the surface of 2% uranyl acetate (pH 4.5) and portions picked up on specimen grids coated with perforated carbon films.

Electron Microscopy: Specimens were screened at relatively low electron optical magnifications (x 25,000) for regions containing ordered arrays of protein molecules. Specimens have been studied in the following instruments: the Philips EM 301, the Jeol EM 100C and 100CX, and the AEI Corinth 275, under conventional high electron dose imaging conditions. Images were recorded primarily at electron optical magnifications between 60,000 and 130,000 diameters.

Optical Diffractometry: Optical diffraction patterns of ordered regions on electron-micrographs were obtained through the courtesy of Professor R. W. Horne, John Innes Institute, Norwich, and Dr. M.J.Dickens, Department of Biophysics, King's College, University of London.

RESULTS AND DISCUSSION

1) Apoferritin

From a priori consideration of symmetry it would be expected that the protein apoferritin (molecular weight approximately 450,000, sedimentation coefficient 17S) with its 24 apparently identical subunits, would behave in a somewhat similar manner to the icosahedral viral particles initially studied by the negative staining-carbon film technique. Specimens of apoferritin have, in fact, revealed regions containing completely randomly spread molecules as well as more ordered regions in which close-packed or paracrystalline monolayer arrays are present (Figs 1 to 3). In addition, regions containing multi-layer random and regular arrays can also be detected, which produce more complex images, as shown in Figs. 4 to 6. It is clear that in principle, the negative staining-carbon film technique does work for apoferritin, as even with the arrays of viral particles specimen regions containing random and complex ordered arrays were present, the regular monolayer regions suitable for optical diffraction analysis being selected manually.

2) Cylindrin and Torin

The proteins cylindrin and torin (Harris, 1968, 1974 and 1980) from human erythrocytes immediately present a more difficult technical problem for the production of paracrystalline monolayer arrays than does apoferritin, because of their molecular asymmetry. This results in the production of an increased number of favourable stable orientations for the molecules within the negative stain, which will reduce the possibility of regular molecular close-packing, but need not necessarily prevent a true crystallization process forming a paracrystalline monolayer.

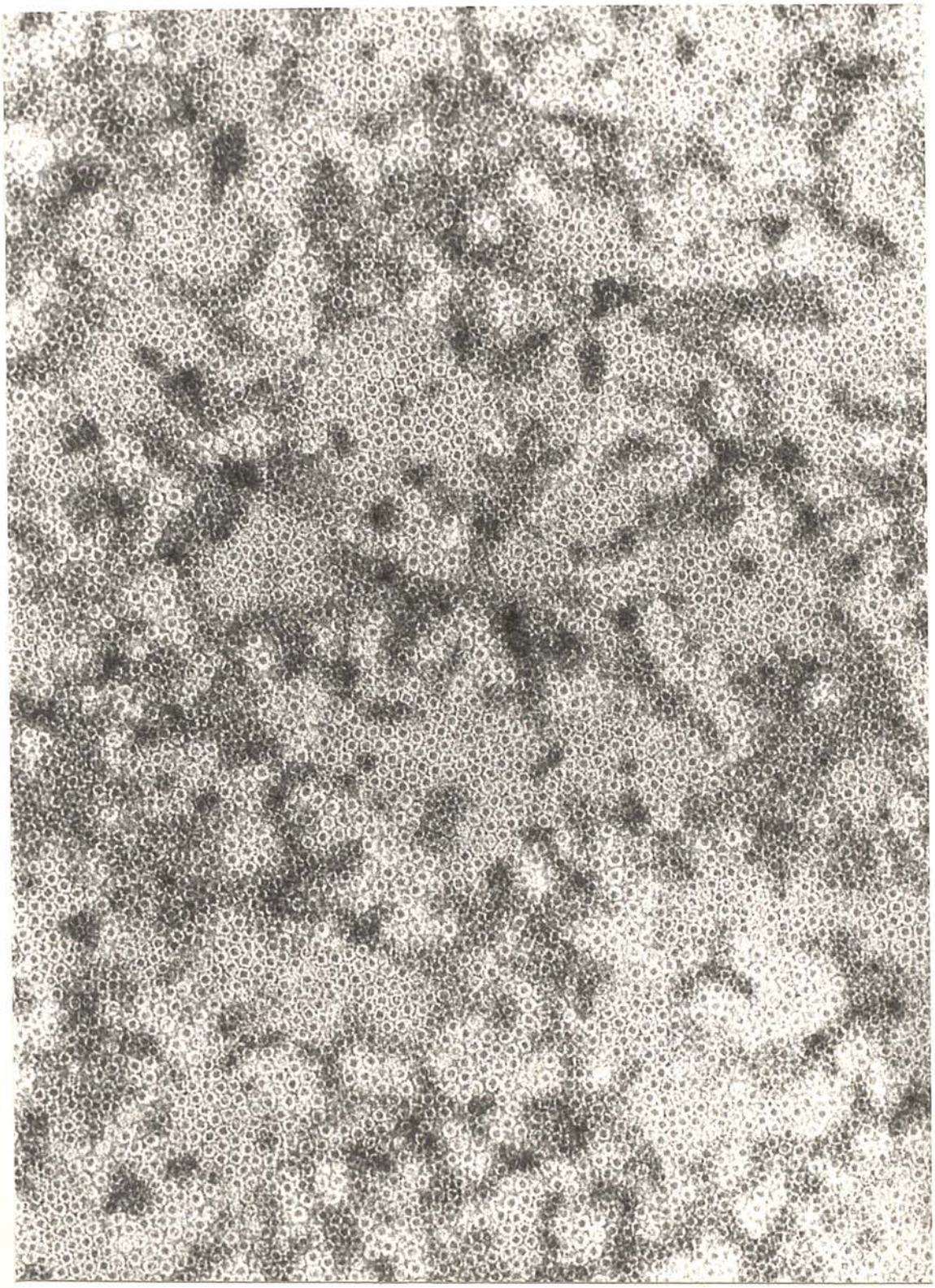

Fig. 1: Apoferrtin spread by the negative staining-carbon film technique, showing a predominantly random monomolecular layer. Some irregular multi-layer regions are present. x 198 000.

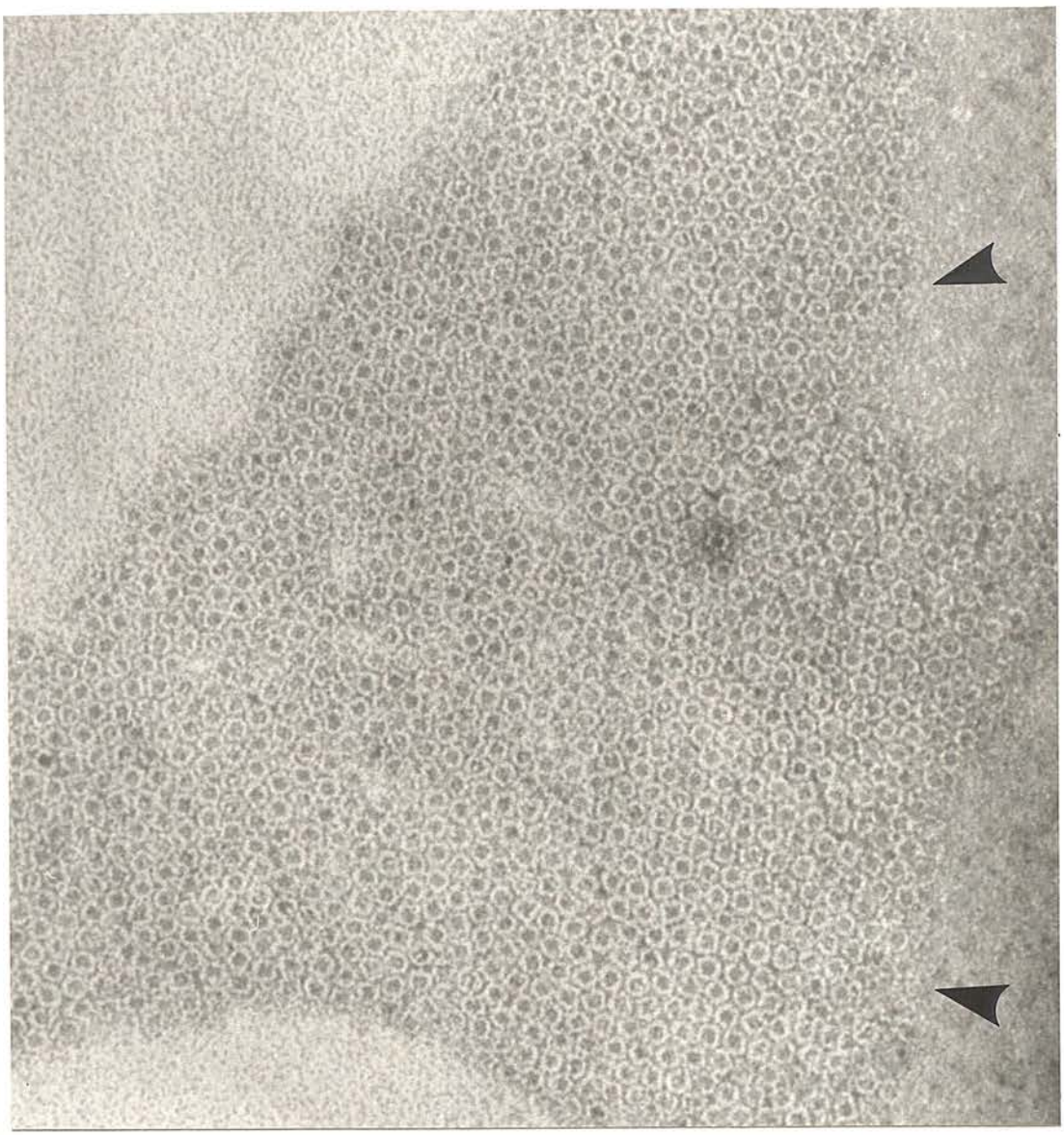

Fig. 2: A small pool of apoferritin molecules, spread by the negative staining-carbon film technique, showing regions of regular monomolecular layer packing. (arrowed). x 300 000.

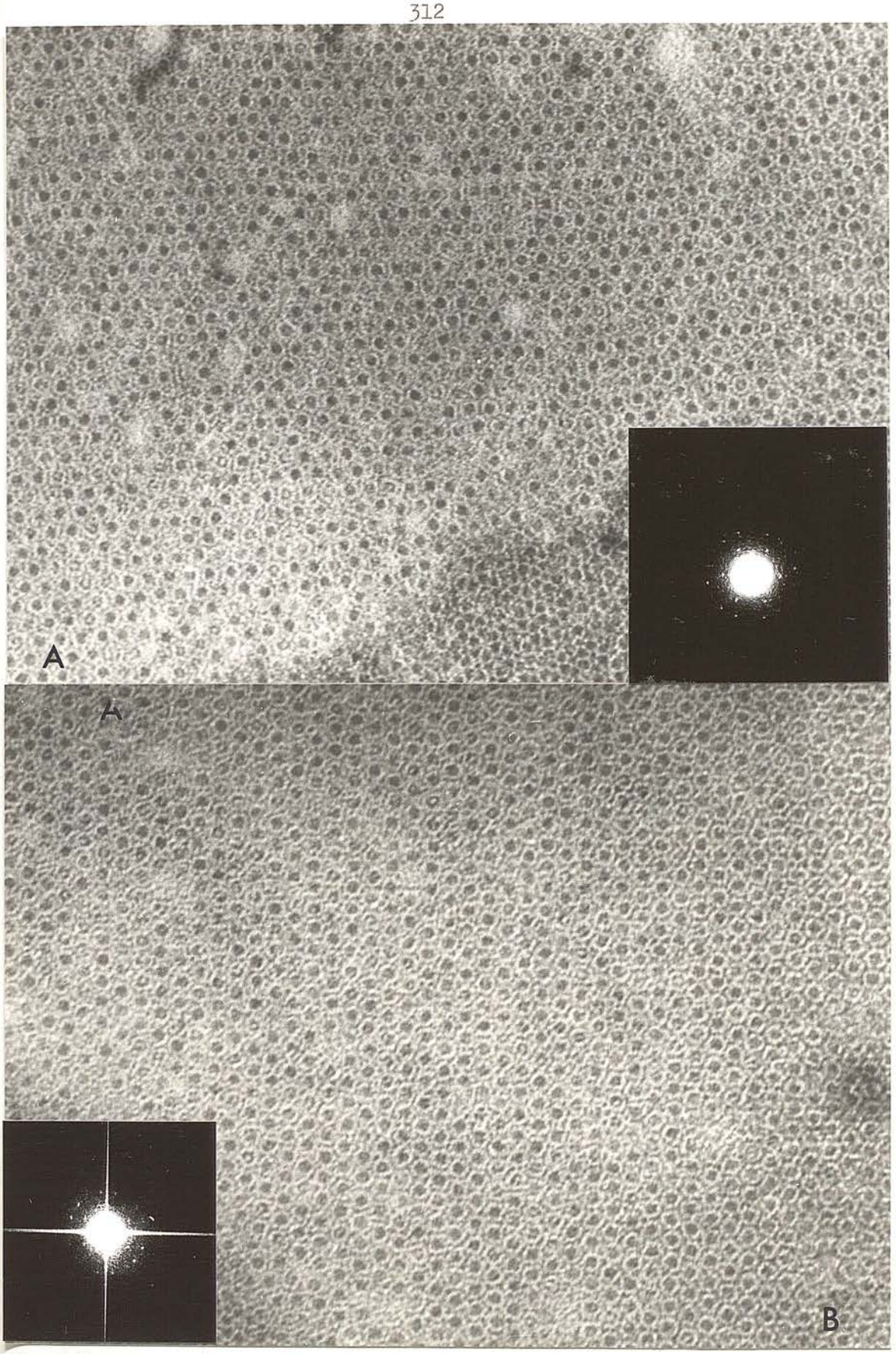

Fig. 3 (A, B, & C): Regions showing large pools of apoferritin exhibiting regular monomolecular layer arrays, spread by the negative staining-carbon film technique. Inserts show optical transforms. x 300 000.

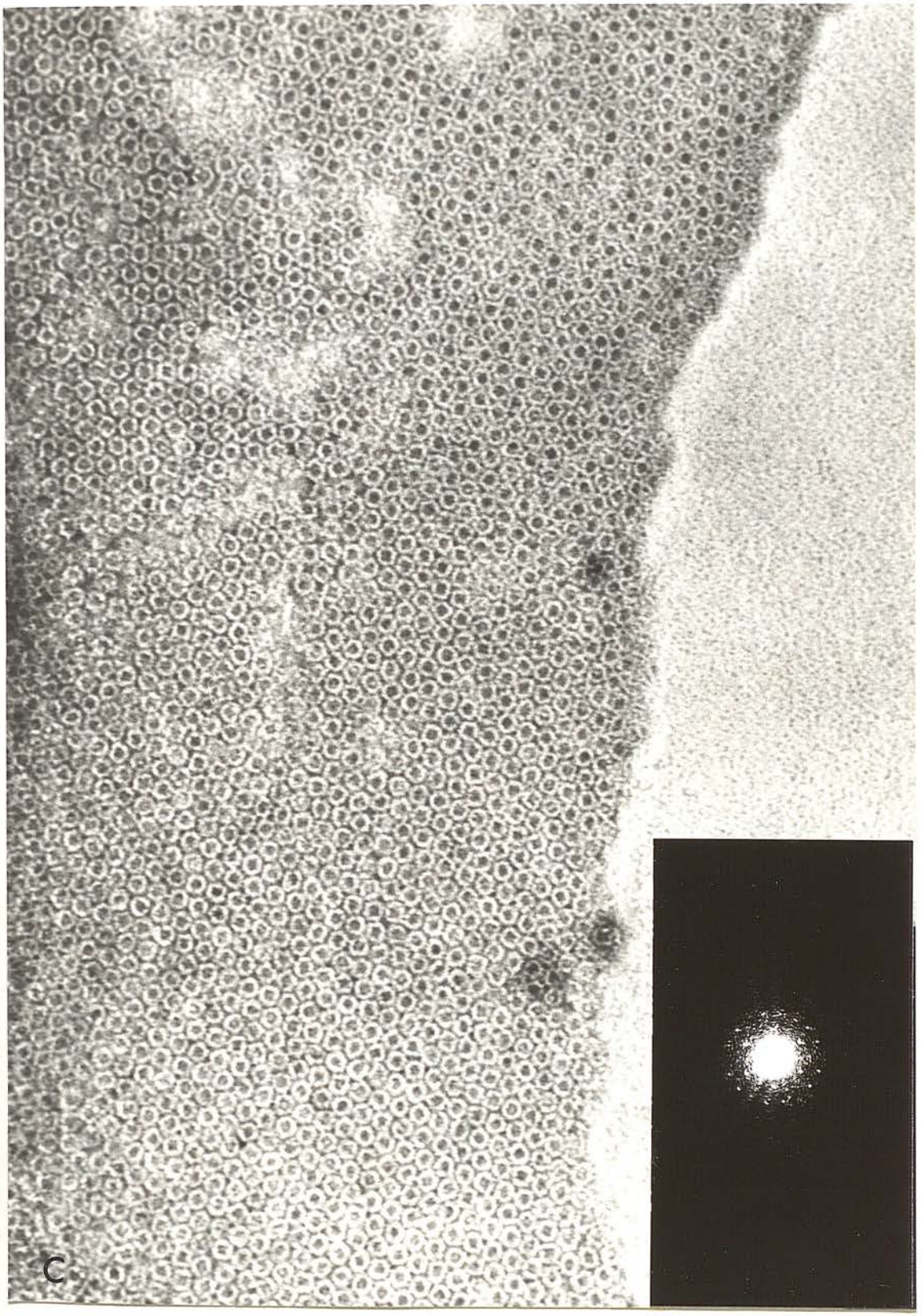

Fig. 3 C:

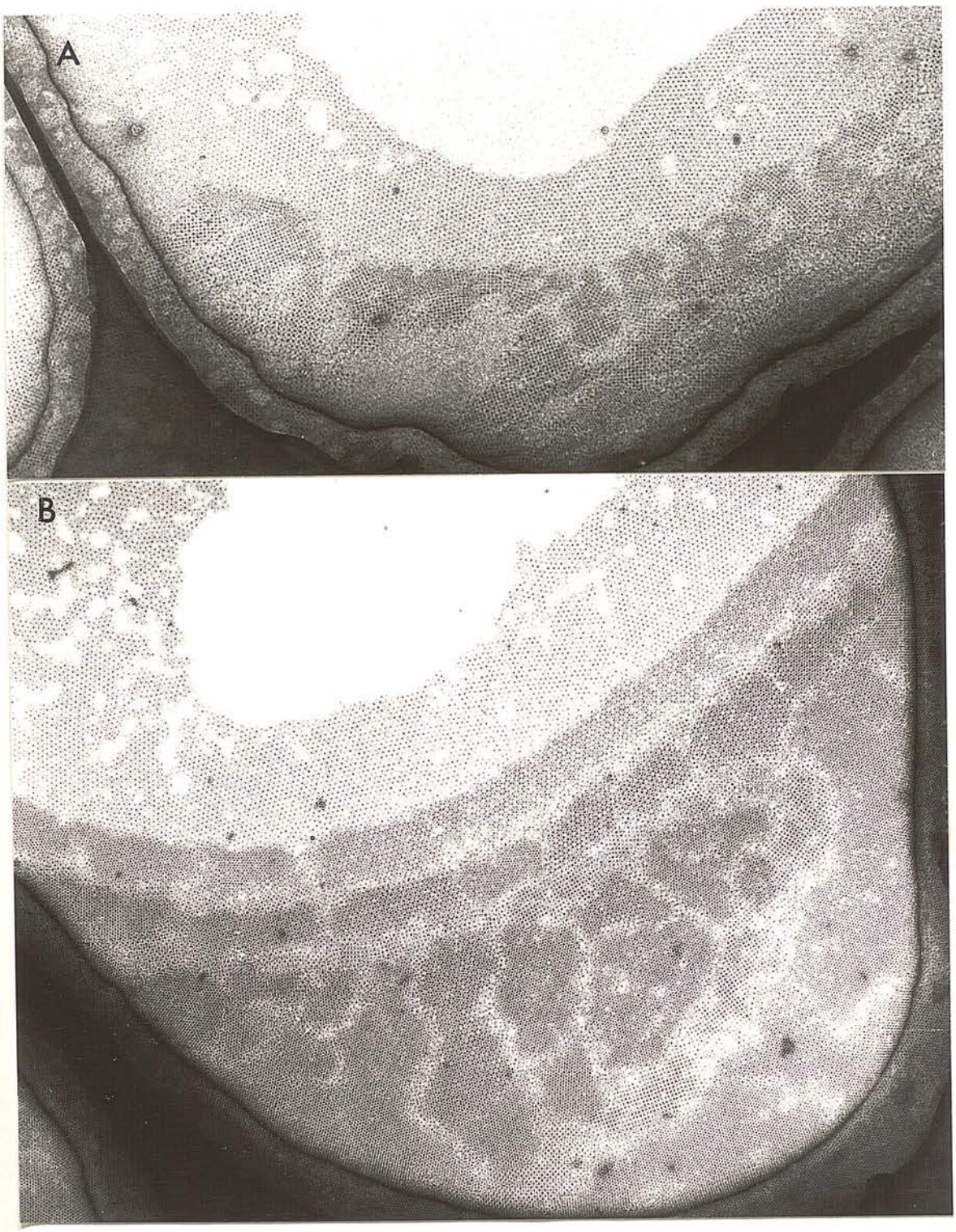

Fig. 4 (A & B): Survey regions showing a hole of a perforated carbon support film, across which the apoferritin on its thinner carbon support is extended. Towards the edge of the hole multi-molecular layer, regular and random arrays can be seen. Both, x 75 000.

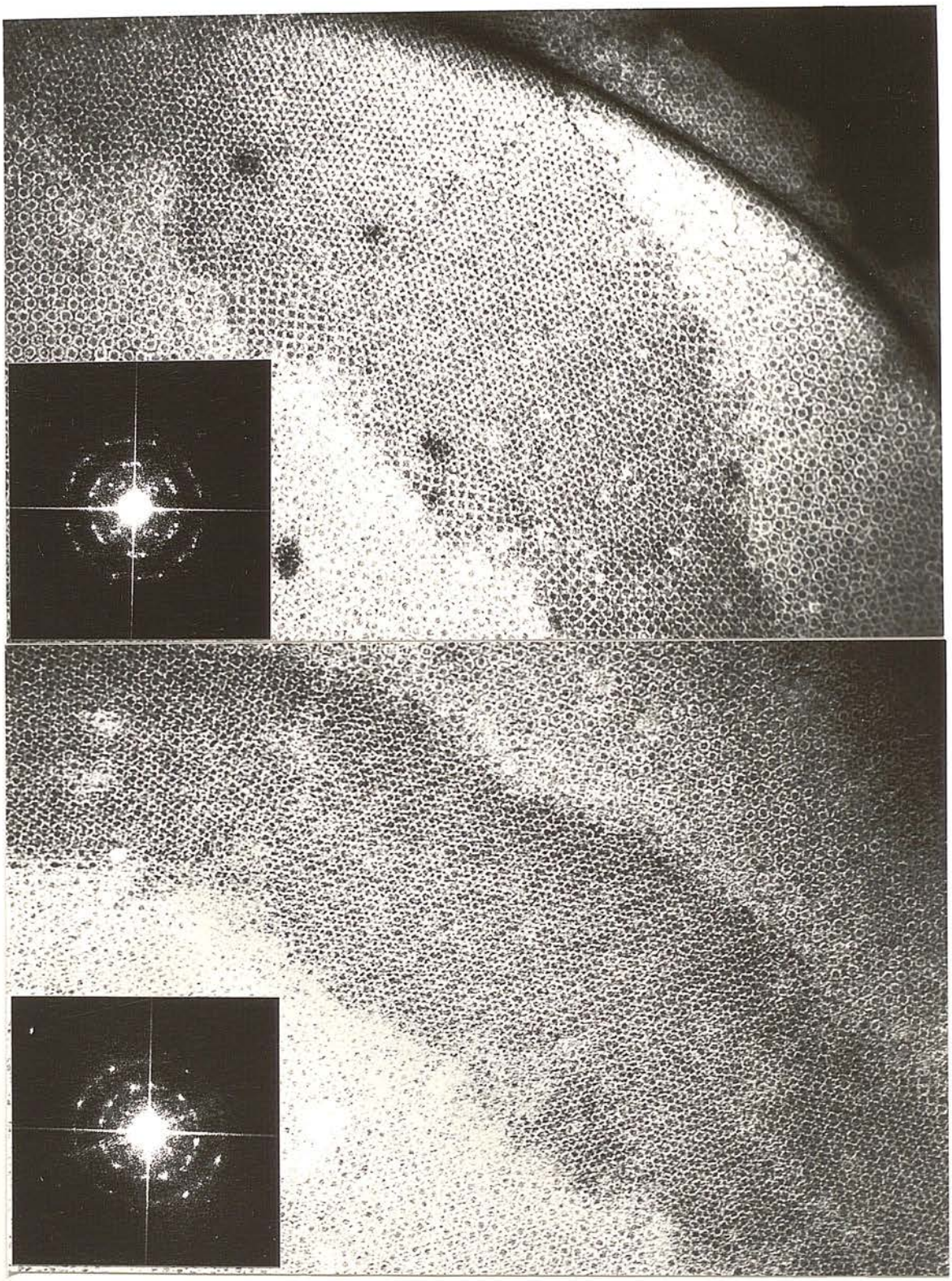

Fig. 5: Two regions showing multi-molecular layer regular arrays of apoferritin spread by the negative staining-carbon film technique. Inserts show optical transforms. Note that the multi-layer regions are surrounded by regular mono-molecular layer arrays in both cases. x 180 000.

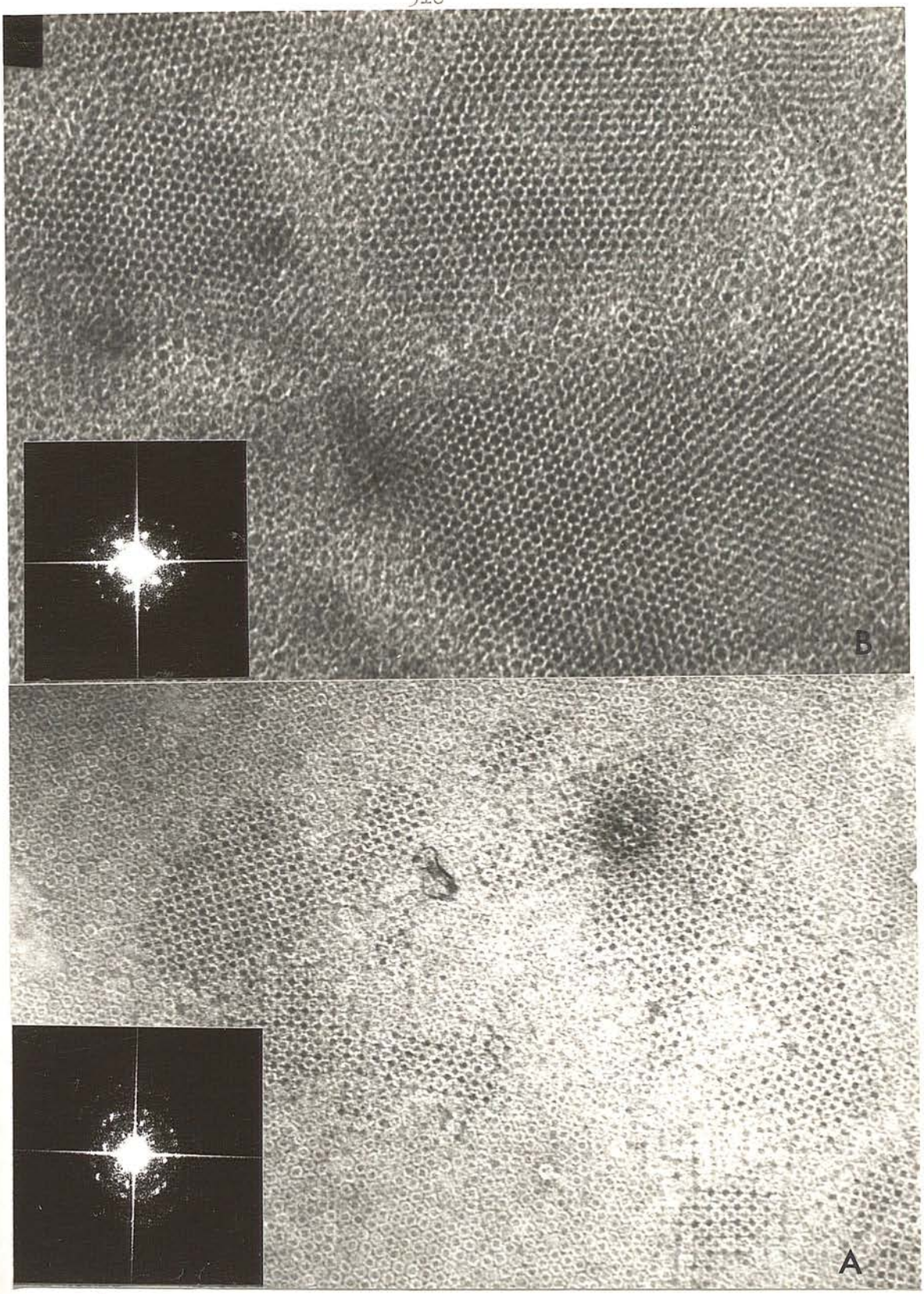

Fig. 6 (A & B): Regions showing multi-molecular layer arrays of apoferritin spread by the negative staining-carbon film technique, which are clearly distinguishable from those shown in Fig. 5, and also one from another. This is reflected in the different optical transforms.
A, x 180 000; B, x 300 000.

a) Cylindrin: This molecule, which has a molecular weight of approximately 800,000 and a sedimentation coefficient of 22.5S, is a hollow cylindrical structure of length approximately 17 nm and external diameter 11 nm. Cylindrin has been found to have a pronounced tendency to aggregate during the negative staining, carbon film technique to produce groups of four off-set molecules, as shown in Fig. 7, which have a marked disrupting influence which results in the production of completely randomly organised monolayer arrays (Fig. 8). Extremely limited regions have, nevertheless, been detected which contain ordered arrays of cylindrin, in both the end-on (Fig. 9) and sideways-on orientations (Fig. 10) have been observed.

b) Torin: This ring-like molecule from human erythrocytes has an external diameter of approximately 12 nm, a sedimentation coefficient of 9.0S and an approximate molecular weight of 200,000. Under conventional negative staining conditions torin has been shown to orientate itself predominantly on its side in shallow stain, giving the ring-like profile, but in deeper stain it can be trapped at varying orientations relative to the electron beam, the characteristic paired-dot image being given by the vertically orientated molecule (Harris, 1969). When spread on mica for the negative staining-carbon film technique, it is very likely that torin will be located in varying orientations, together with the possibility that there will be overlapping of horizontally orientated molecules. Figures 11 to 13 show representative regions of specimens containing torin which depict these problems. In Fig. 13 there is a monolayer of close packed torin molecules orientated horizontally, but the molecules have not ordered themselves into a hexagonal or square array, as might be predicted to occur from the viral studies and from the work on apoferritin. It is probable that a precise amount of protein is required, just enough to produce a single complete monolayer, of horizontally orientated protein, before the drying forces and charge interactions can so organise the torin molecules into a regular array. This does not appear to be readily achieved.

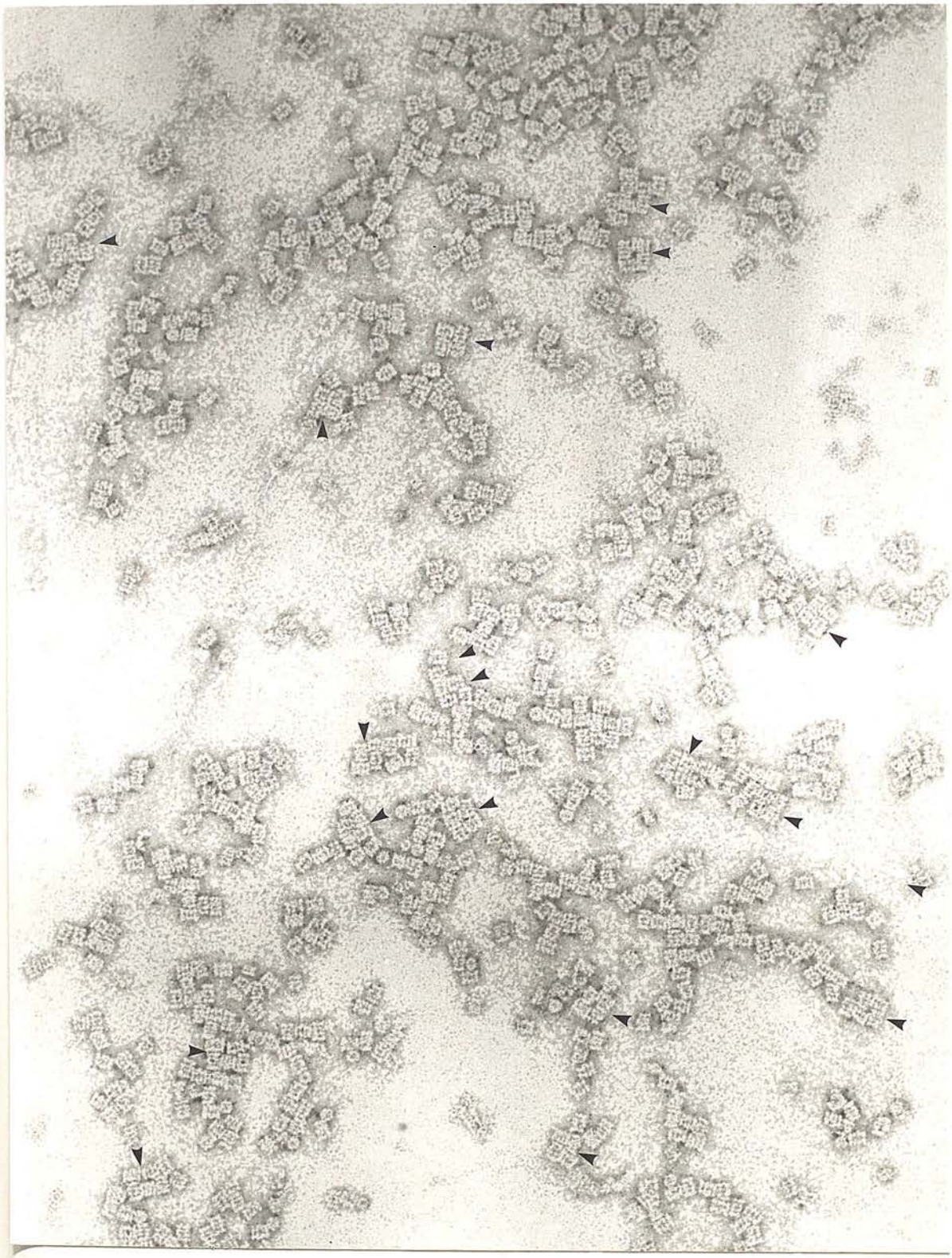

Fig. 7: Cylindrin molecules spread by the negative staining-carbon film technique, showing individual molecules and small groups. Arrows indicate groups of four offset molecules, which would sterically prevent the formation of larger regular or paracrystalline mono-molecular layer arrays. x 183 000.

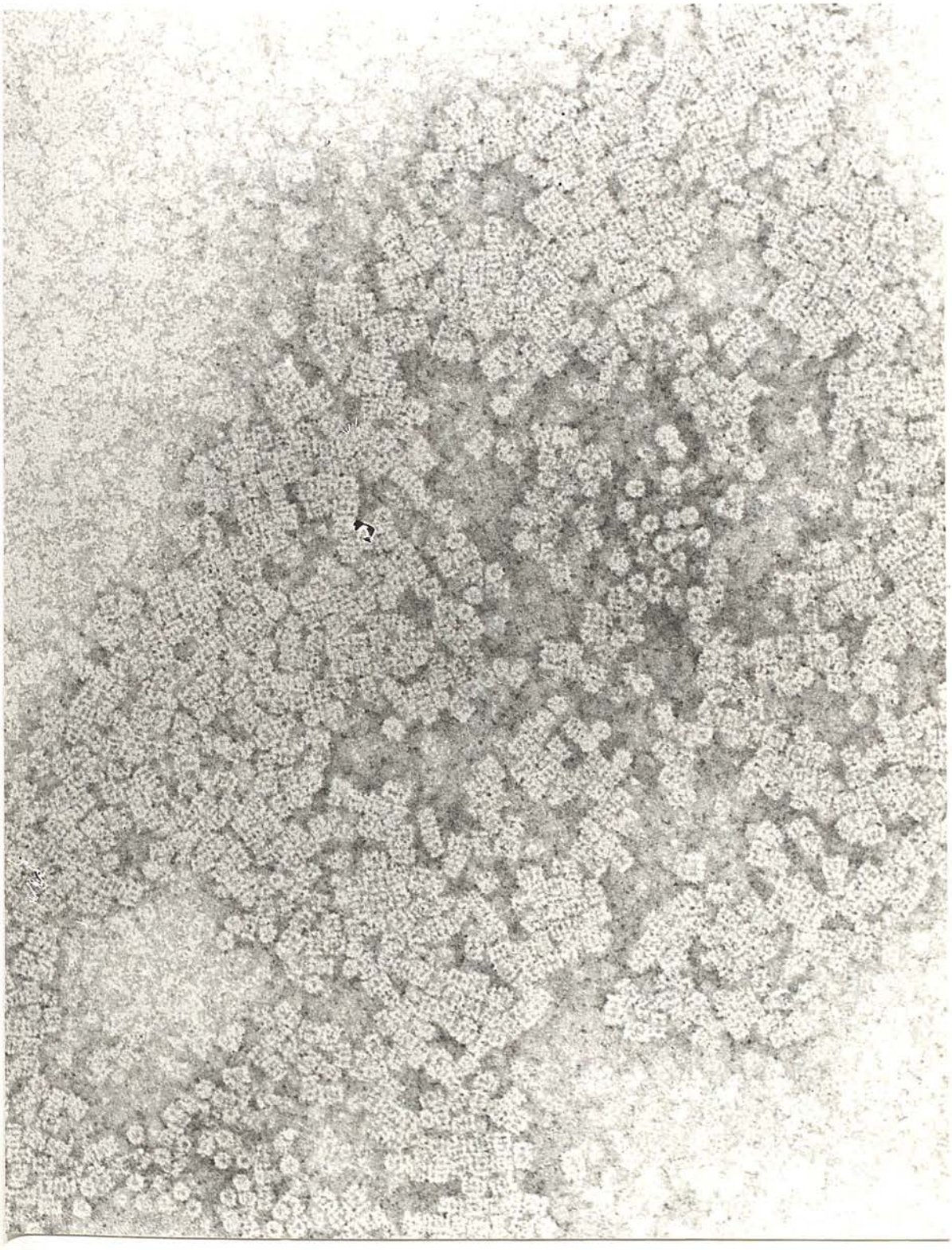

Fig. 8: A close-packed monomolecular layer array of cylindrin, spread by the negative staining-carbon film technique, showing how the offset association of molecules effectively prevents regular monomolecular layer formation. x 240 000.

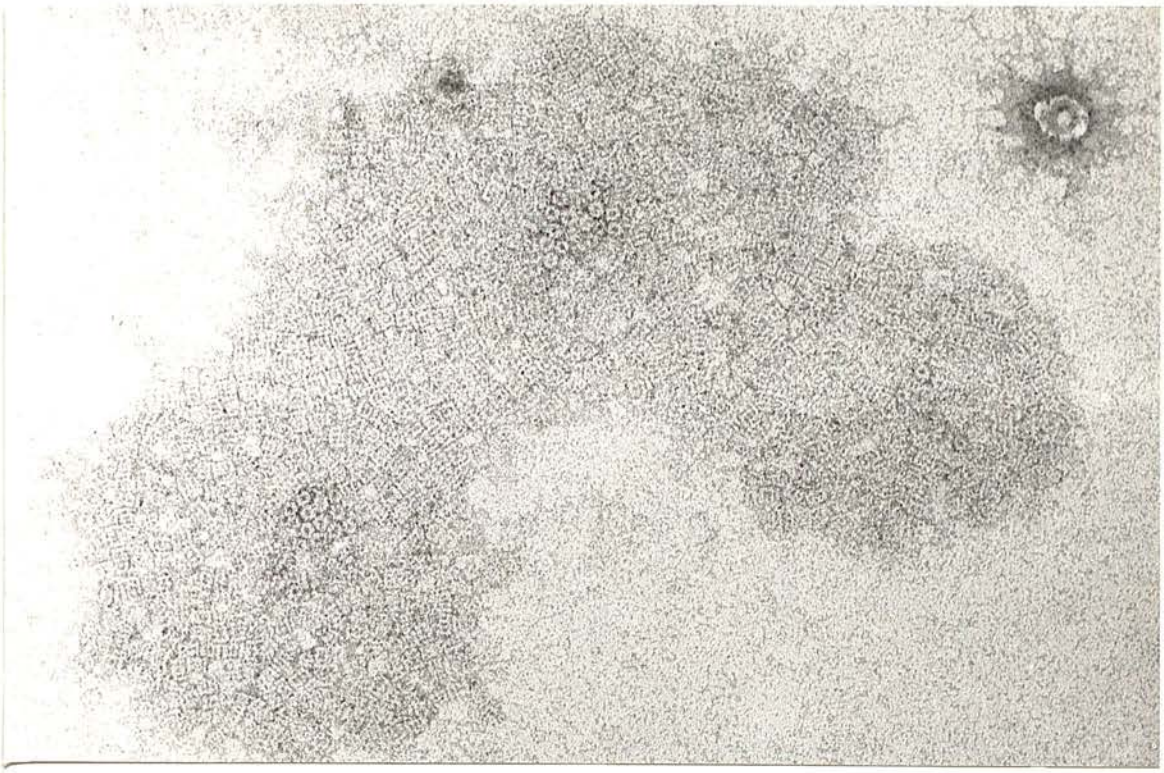

Fig. 9: Cylindrin spread by the negative staining-carbon film technique, showing limited regions containing vertically (end-on) orientated molecules with regular packing. x 183 000.

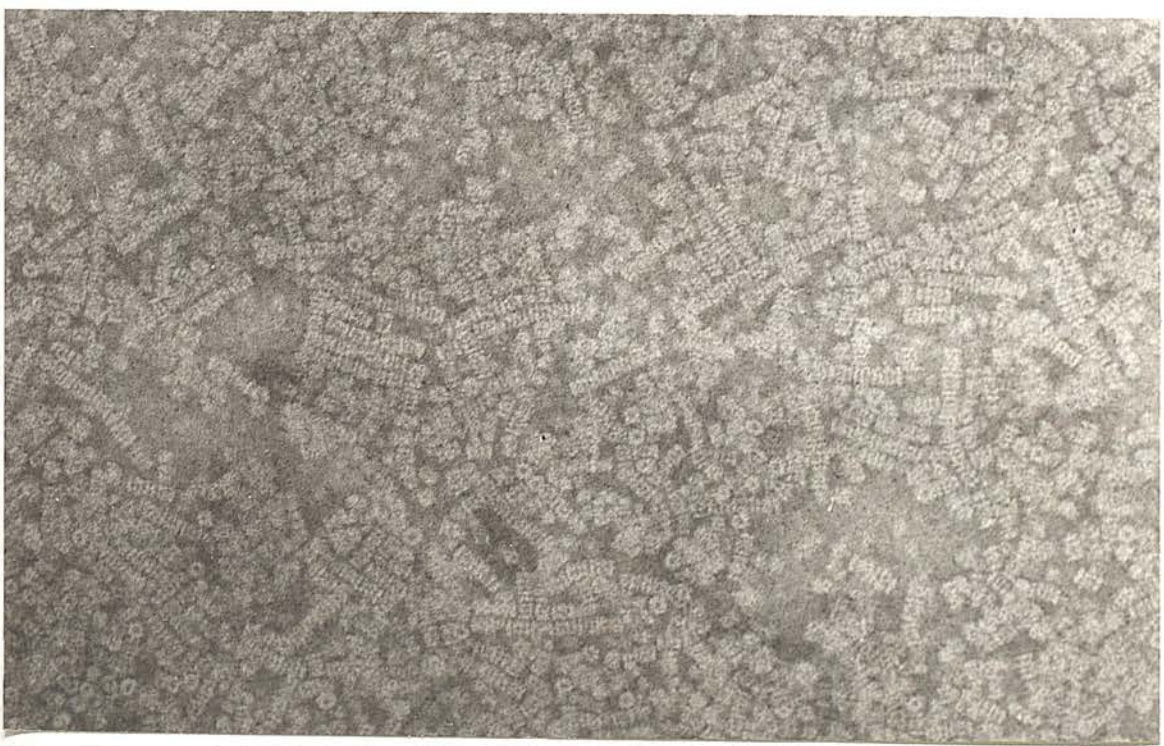

Fig. 10: Cylindrin spread by the negative staining-carbon film technique, showing regions with regular horizontal (side-on) molecular packing. x 183 000.

Fig. 11 (A & B): Torin molecules spread by the negative staining-carbon film technique. Individual molecules and small clusters or aggregates are clearly defined. Almost all of the molecules are horizontally orientated, exhibiting the torus profile; arrows indicate the few vertically orientated molecules exhibiting the characteristic paired-dot profile. A, x 198 000; B, x 180 000.

Fig. 12: Torin molecules spread by the negative staining-carbon film technique. The region shown contains considerable overlapping of molecules. x 198 000.

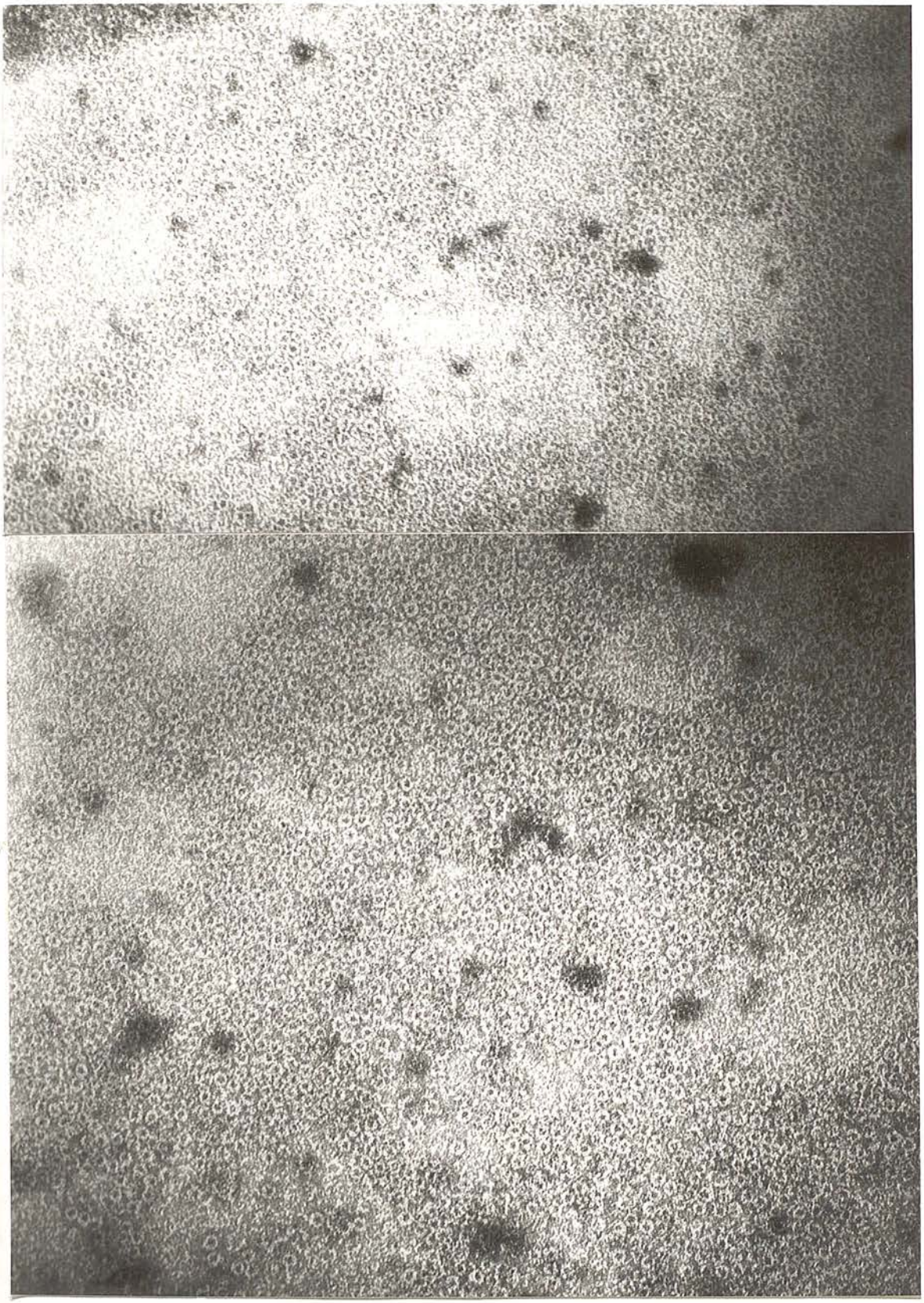

Fig. 13: Torin molecules spread by the negative staining-carbon film technique. The regions shown contain mono-molecular layer arrays of randomly orientated molecules. x 180 000.

3) The Bordetella pertussis '22S Antigen':

The B. pertussis '22S antigen' of Sato & Nagase (1967) may prove to be the same protein as the one termed groE from E. coli (Hohn et al., 1978 and 1979), as MacLennan et al., (1977) have shown this high molecular weight protein to be present in many bacterial genera. The molecule has a cylindrical conformation, both the length and diameter being approximately 12 nm. It appears that the molecule is composed of four rings each containing seven subunits, (Fig. 14). Specimens prepared by the negative staining-carbon film technique contain regions of partial regularity with monolayers of molecules orientated on their ends and on their sides (Fig. 15). Because the length and external diameter of the '22S antigen' are almost equal, the presence within the momomolecular array of molecules on their sides which are off-set and also molecules orientated on their ends, does not per se introduce complete disruption of the overall regularity of molecular packing (Fig. 15), although the information content under these conditions is probably too complex for interpretation by optical diffractometry. With the '22S antigen' both large sheet-like monomolecular arrays and smaller pool-like arrays have been detected (Figs. 16 and 17). The latter may well be organised primarily by surface tension forces rather than a true crystallization, whereas the former, large arrays, are probably produced by true crystallization (Fig. 16).

4) Glutamine Synthetase:

The enzyme glutamine synthetase from E. coli, which is composed of a double disc of protein, each disc containing six subunits (Valentine et al., 1968; Frey et al., 1975; Rasulov et al., 1977; Tsuprun et al., 1980) tends to orientate itself in two stable orientations in conventional negative staining, (viz, on its side and on its end, in the same way as cylindrin and the '22S antigen'), see Fig. 18. The molecular weight of glutamine synthetase is approximately 600,000, its sedimentation coefficient is ≈20S and its molecular dimensions are approximately 14 nm for the diameter and 9 nm for the height of the double disc. When specimens are prepared by the negative

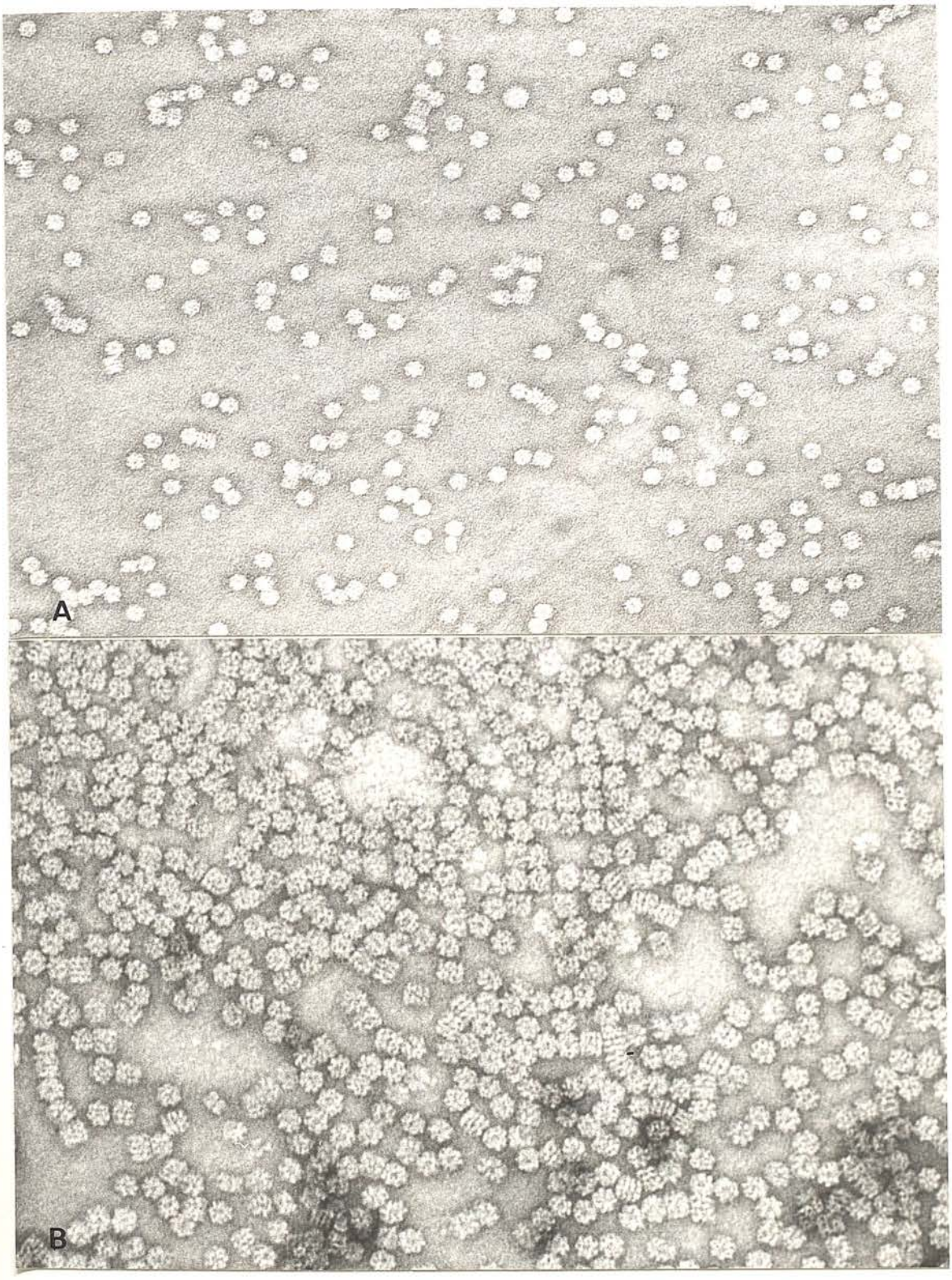

Fig. 14: (A & B): The Bordetella pertussis '22S antigen' spread by the negative staining-carbon film technique. In (A) the molecules are mostly spaced from one another, whereas in (B) the molecules are close packed as a random mono-molecular layer array. A, x 198 000; B, x 300 000.

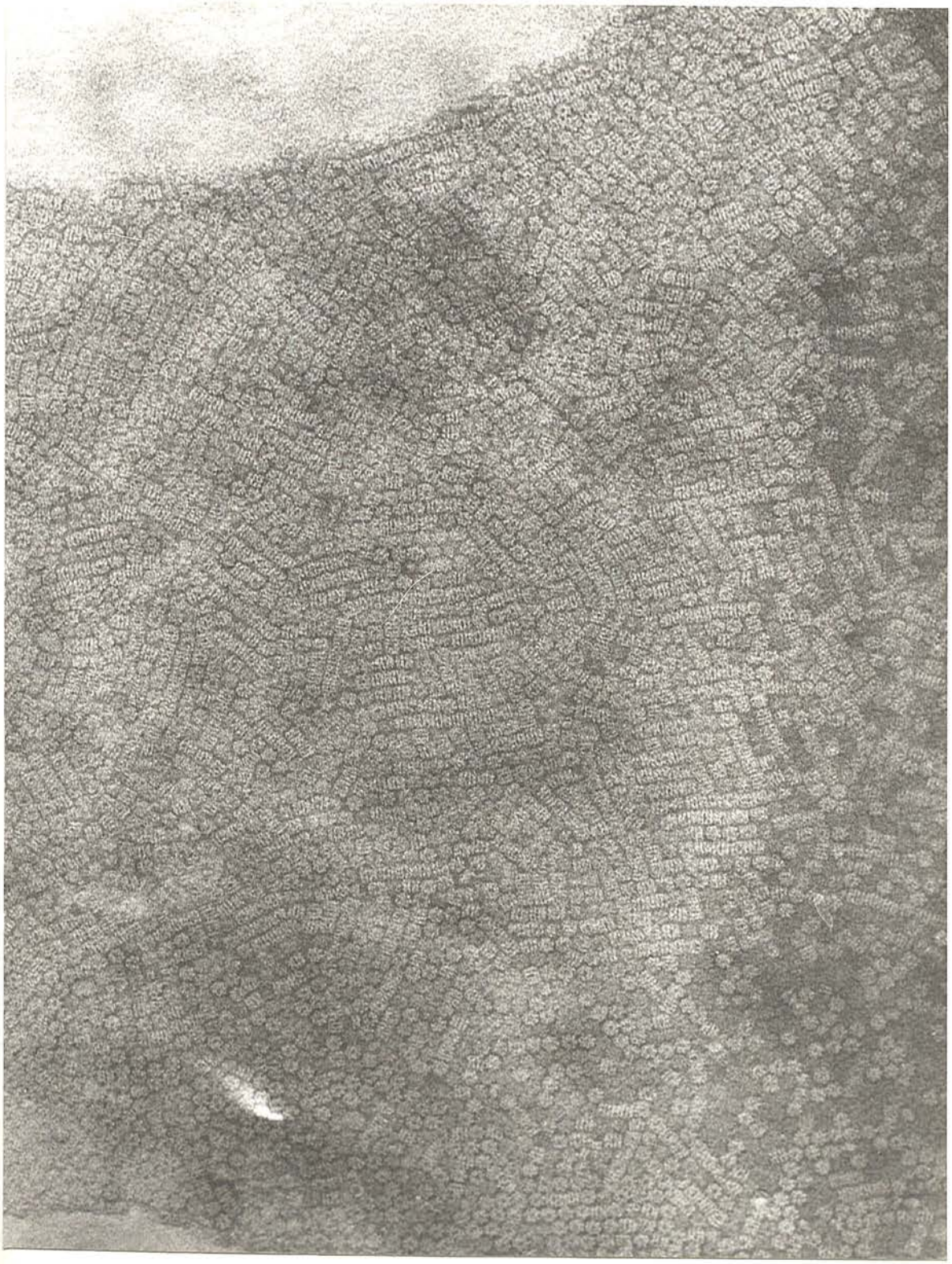

Fig. 15: The Bordetella pertussis '22S antigen', spread by the negative staining-carbon film techique. The region shown contains close packed molecules in a monolayer array. Molecules are orientated on their sides and on their ends, and pack intimately together because the length (13 nm) and diameter (12 nm) are approximately equal. x 198 000.

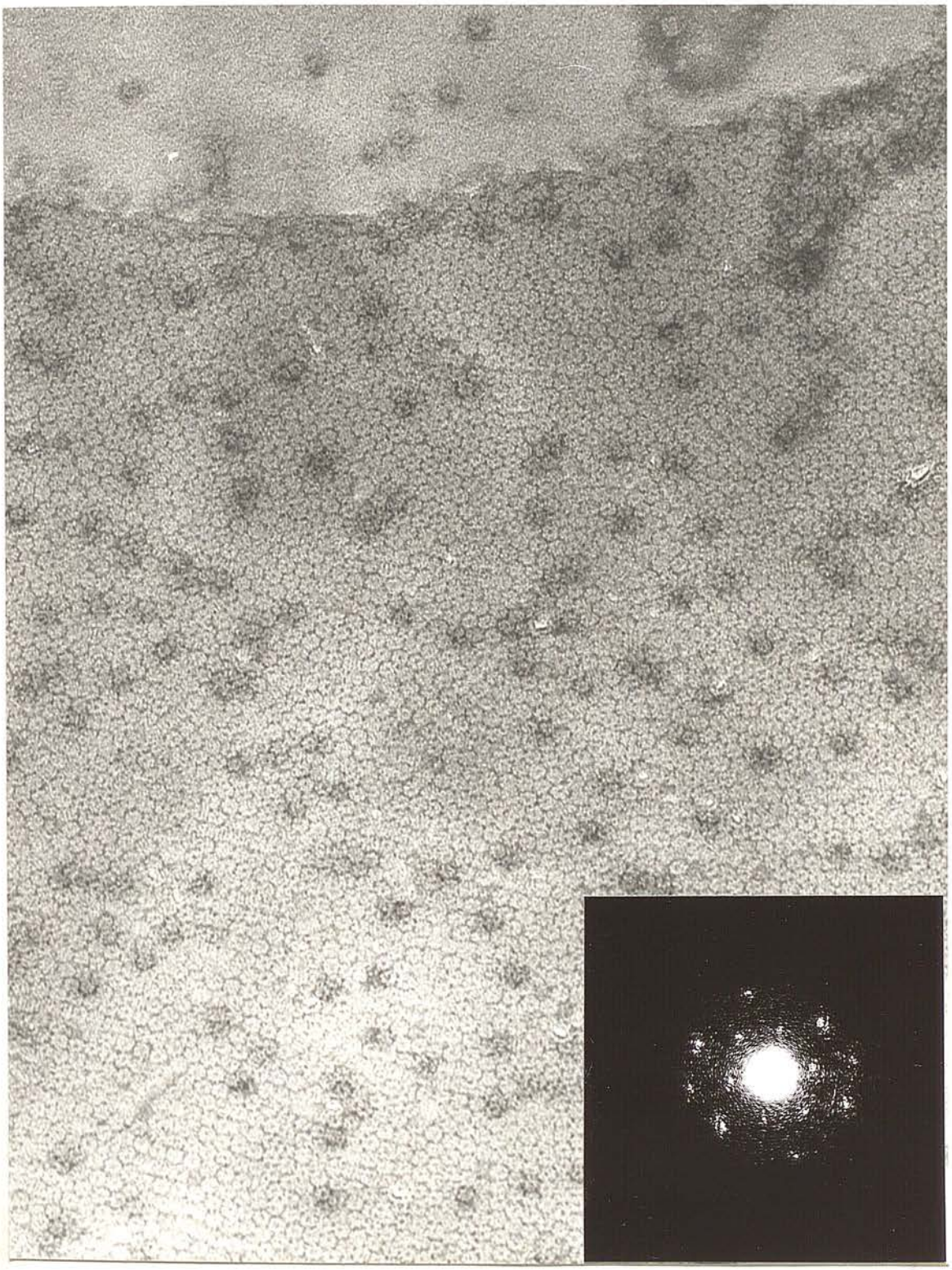

Fig. 16: The Bordetella pertussis '22S antigen', spread by the negative staining-carbon film technique. This region shows part of a large sheet-like array of molecules, orientated predominantly on-end. x 198 000. Insert shows the optical transform.

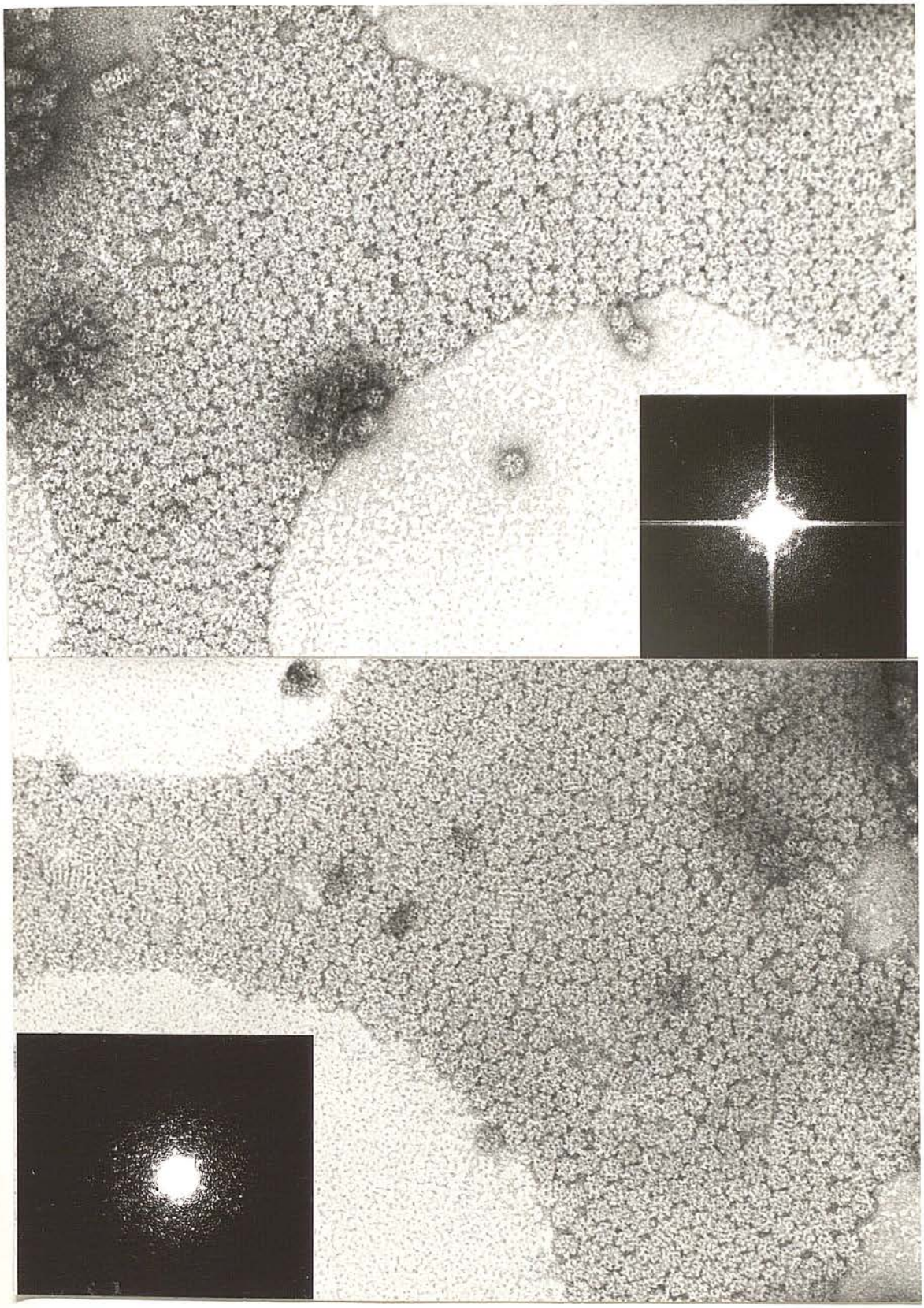

Fig. 17: The Bordetella pertussis '22S antigen' spread by the negative staining-carbon film technique. Both micrographs show small pool-like regular arrays of molecules, orientated predominantly on-end. x 198 000. Insert shows the optical transform.

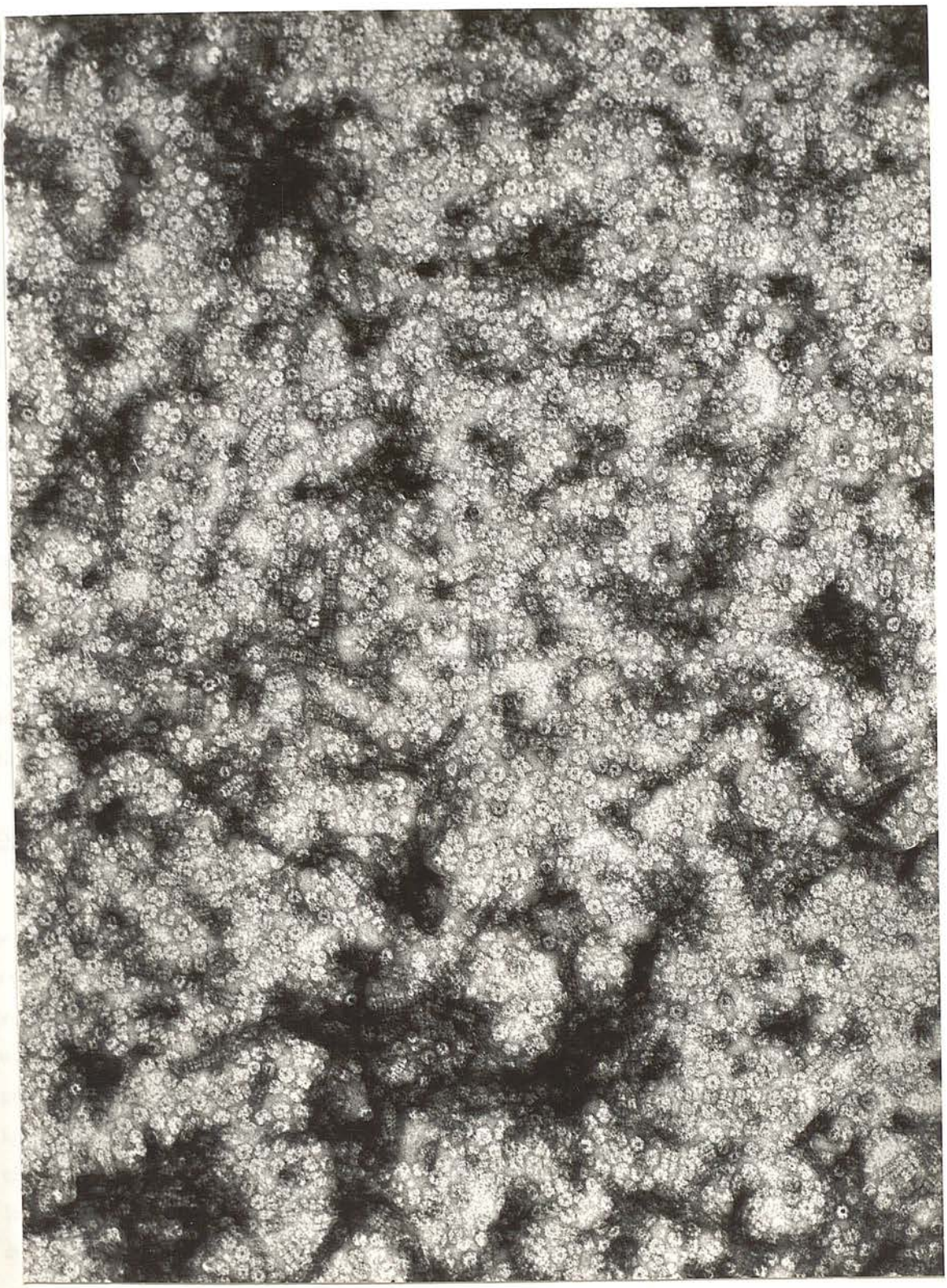

Fig. 18: E. coli glutamine synthetase, spread by the negative staining carbon film technique. This region contains individual molecules, orientated on their sides and on-end (some short stacks). x 150 000.

staining-carbon film technique, it might be predicted that the presence of molecules in both stable orientations would not be conducive to the production of ordered monomolecular arrays, and it was therefore hoped that one or other of the two orientations might predominate, giving rise to either hexagonal or square arrays of molecules orientated on their ends, or to rows of molecules orientated on their sides. In fact it has been the latter mode of organization that has been detected, but only somewhat limited regions of the specimen exhibit regularity, see Figs. 19 and 20. It would seem that a true crystallization process has, nevertheless, been occurring, in order to produce the type of molecular arrays shown in Figs. 19 and 20, rather than a random coming together of molecules due to surface tension forces during the drying of the stain.

Image analysis of glutamine synthetase 3 and 6+1 stranded cables has been performed by Frey et al. (1975) and Weiss et al. (1976), and on individual molecules by Frank et al. (1978a) and (1978b) using low dose imaging. It will be of interest to apply these techniques to glutamine synthetase paracrystals of the type shown in Fig. 20, and possibly also paracrystalline arrays of molecules orientated on their ends, exhibiting the ring-like profile.

CONCLUSIONS

The results presented above show that for several high molecular weight protein molecules it is possible to produce by the negative staining-carbon film technique, regular monolayer arrays, which are suitable for image analysis by optical diffractometry. The complexity of the molecular composition (i.e., subunit organization) in most cases prevents the production of detailed molecular information. This would apply even if low electron dose images of the specimens had been produced at varying angles of tilt relative to the electron beam, and in this study specimen damage would have been produced during the high dose irradiation conditions employed.

The ring-like molecule, torin, from human erythrocytes, with which it has not yet proved possible to form regular monolayer arrays, is the only molecule which is able to provide a single polypeptide thickness, when orientated on its side. It is considered, therefore,

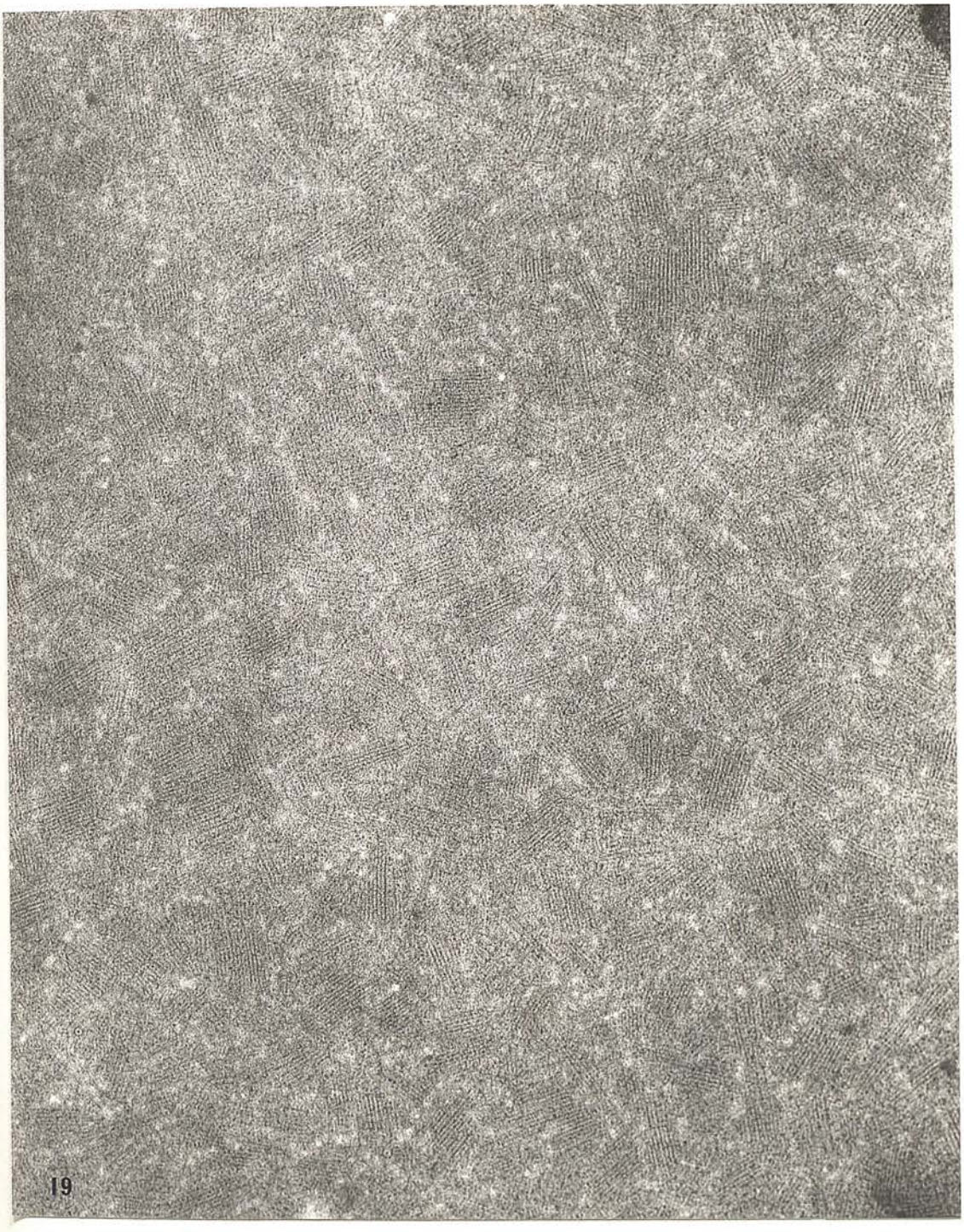

Figs 19 & 20: E. coli glutamine synthetase, spread by the negative staining carbon film technique. Discrete regions showing parallel rows of stacked molecules on their sides can be readily defined, as well as individual molecules on-end. x 78 000 and x 150 000

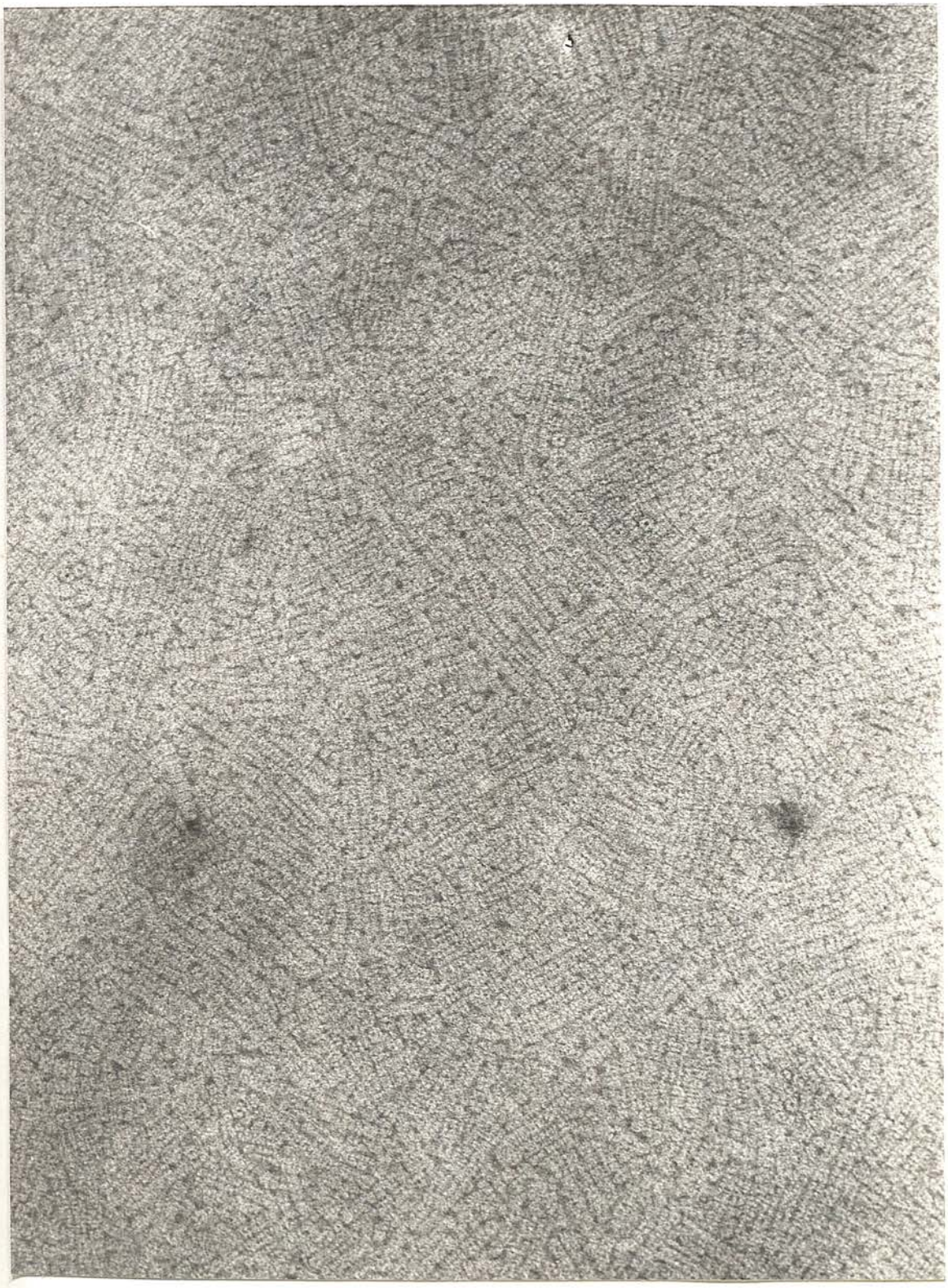

Fig. 20:

that this molecule is worthy of further effort, with the aim of producing regular arrays, from which molecular information may well be derived by low dose imaging and specimen tilting. The torin molecules would need to be in a truly paracrystalline organization rather than a regular close-packed array, in order to achieve this objective, since under conditions of close-packing, the molecules may not be in crystallographically identical orientations relative to one another. It would also be a requisite that all the torin molecules exhibit the same orientation with respect to their secondary and tertiary structure, which may not be truly so in a superficially regular quaternary structure array. The enzyme foraminotransferase-cyclodeaminase from porcine liver has been shown by Beaudet and Mackenzie (1976) to also be a ring-like molecule, from which thin crystals were also produced, so this enzyme complex would also be suitable for investigation by the negative staining-carbon film technique.

Despite the inherent difficulties in preparing paracrystalline monolayer arrays of proteins by the negative staining-carbon film technique, it is thought that by varying the protein concentration, the sample pH, the type and pH of the negative stain added during the mica spreading stage, the drying conditions, the type and pH of the second negative stain used at the floating off stage, the length of time the carbon layer + protein is left in contact with the second negative stain, it may be possible to influence the behaviour of the proteins and thereby determine the appropriate conditons for the formation of paracrystalline monolayers. The protein purity and stability with respect to dissociation of subunits during the procedure are of vital importance as any protein other than the intact native species will immediately tend to prevent the production of ordered arrays. For both apoferritin and glutamine synthetase regions containing multi-layer molecular arrays have been detected. While the presence of such regions is not desirable from the point of view of high resolution imaging, they do indicate that in all probability a true crystallization process has been occurring.

It is likely that in the future several proteins other than the ones mentioned above will be selected for investigation using the negative staining-carbon film technique, which may in due course prove to be a valuable technical contribution, if the conformation of the polypeptide chain can be determined at a resolution of approximately 0.7 nm, in a manner similar to bacteriorhodopsin in the purple membrane of Halobacterium halobium (Unwin and Henderson, 1975). From a comparative point of view it will certainly be of interest to use the technique for proteins that have already been studied by X-ray crystallography and whose conformations are already known, in order to test the validity of the electron microscopic approach.

REFERENCES

Beaudet, R. and Mackenzie, R.E. (1976). Biochim. Biophys. Acta 453, 151-161.

De Rosier, D.J. and Klug, A. (1968). Nature 217, 130- 134.

Frank, J., Goldfarb, W. and Kessel, M. (1978a).9th Int. Cong. Electron Microscopy, Toronto. Volume 11, pp 8-9.

Frank, J., Goldfarb, W., Eisenberg, D. and Baker, T.S. (1978b). Ultramicroscopy 3, 283-290.

Frey, T.G., Eisenberg, D. and Eiserling, F.A. (1975). Proc. Natl. Acad. Sci. USA 72, 3402-3406.

Fromherz, P. (1971). Nature 231, 267-268.

Harris, J.R. (1968). Biochim. Biophys. Acta 150, 534-537.

Harris, J.R. (1969). J. Mol. Biol. 46, 329-335.

Harris, J.R. (1974). In Methodological Developments in Biochemistry, (E. Reid, ed.) Volume 4, pp 393-404, Longmans.

Harris, J.R. (1978). Proc. Roy. Mic.Soc. 13 pt.4, 29.

Harris, J.R. (1980). Nouv. Rev. Franc. Hematol., **22, 411-448.**

Harris, J.R. and Naeem, I. (1978). Biochim. Biophys. Acta 537, 495-500.

Hohn, T., Wurtz, M. and Engel, A. (1978). J. Ultrastruct. Res. 65,, 90-93.

Hohn, T., Hohn, B., Engel, A., Wurtz, M. and Smith, P.R. (1979). J. Mol. Biol. 129, 359-373.

Horne, R.W. (1978). 9th Int. Cong. Electron Microscopy, Toronto, Volume 111, pp 470-482.

Horne, R.W., Hobart, J.M. and Pasquali-Ronchetti, I. (1975a). J. Ultrastruct. Res. 53, 361-393.

Horne, R.W. and Markham, R. (1973). In Practical Methods in Electron Microscopy, Vol. 1 (A.M. Glauert, ed.) pp 327-444, North-Holland.

Horne, R.W., and Pasquali-Ronchetti, I. (1974). J. Ultrastruct. Res. 47, 361-383.

Horne, R.W., Pasquali-Ronchetti, I. and Hobart, J.M. (1975b). J. Ultrastruct. Res. 51, 233-252.

Klug, A. and Berger, J.E. (1964). J. Mol. Biol. 10, 565-569.

MacLennan, A.P., Hawkins, D.S., Eckersley, B and Blake, J. (1977). Proc. Soc. Gen. Microbiol. 4, 81.

Rasulow, A.S., Evstigneeva, E.G., Kretovich, V.L., Stel'mashchuk, V. Ya., Samsonidze, T.G. and Kiselev, N.A. (1977). Biokhimiya 42, 350-358.

Sato, Y. and Nagase, K. (1967). Biochem. Biophys. Res. Commun. 27, 195-201.

Tsuprun, V.L., Samsonidze, T.G., Radukina, N.A., Pushkin, A.V., Evstigneeva, Z.G. and Kretovich, W.L. (1980). Biochimica et Biophysica Acta 626, 1-4.

Unwin, P.N.T. and Henderson, R. (1975). J. Mol. Biol. 94, 425-440.

Valentine, R.C., Shapiro, B.M. and Stadtman, E. R. (1968). Biochemistry 7, 2134-2152.

Weiss, R.M., Frey, T.G., Burton, Z., Eiserling, F.A. and Eisenberg, D. (1976). Proc. 6th Europ. Cong. Electron Microscopy, Volume 1, pp 20-23.

TORIN AND CYLINDRIN,

TWO EXTRINSIC PROTEINS OF THE ERYTHROCYTE MEMBRANE:

A REVIEW

(This Review article will appear, in a slightly modified form,

in the Journal 'Nouvelle Revue Française d'Hématologie')

CONTENTS

KEY WORDS: Erythrocyte, Membrane, Protein, Cylindrin, Torin.

INTRODUCTION

The two erythrocyte membrane proteins, previously termed the torus protein complex and hollow cylinder protein complex, will henceforth be termed torin and cylindrin, following the convention established by others in naming proteins, by using the suffix in. These proteins were discovered by negative staining electron microscopy of erythrocyte ghosts, fragmented by either prolonged distilled water dialysis or by direct treatment with 0.01% W/V sodium dodecyl sulphate (SDS), as documented by Harris (1968a) and (1968b).

In the absence of any known functional activity for these proteins, it was proposed to the author by Dr. G. Ralston, the University of Sydney, that it might be appropriate to introduce the concise names torin and cylindrin, which retain the conformational identities indicated by the former more cumbersome names. Should, in the future, enzymic activities be allocated to these proteins, it would then be natural for them to be specifically re-named, thereby superseding the present terminology.

In this review it is proposed that detailed coverage will be given to the procedures used for the isolation and purification of torin and cylindrin, with emphasis on the means by which they are separated from spectrin, which is also present in the initial low ionic strength extract from erythrocyte membranes. The biochemical characteristics of the proteins will be presented and some hitherto unpublished data will be included alongside previously published data of the author and others. The important contribution made by electron microscopy will be emphasised, and the recent attempts of the author to produce paracrystalline monolayers and the application of single sideband phase contrast interference electron microscopy will be presented. A survey of the relevant literature will lead on to a discussion of areas for future development. An attempt will be made to integrate the overall topic with current thinking about the structure and composition of the erythrocyte membrane, with emphasis on the complex organisation of extrinsic proteins on the cytoplasmic surface.

The Release of Torin and Cylindrin

The initial observation of the presence of torin and cylindrin was made with a sample of haemoglobin-free human erythrocyte ghosts, prepared by the procedure of Dodge et al. (1963), which had been exhaustively dialysed against distilled water (4 days at 4°C, with several changes of dialysate) to remove inorganic phosphates, prior to performing analysis for organic phosphate. An aliquot of this material taken for negative staining electron microscopy revealed that the formerly intact ghosts had fragmented and that alongside the membrane fragments could be seen many discrete molecular structures, with two predominant conformations resembling a ring and a banded rectangle (i.e., a cylinder on its side), as shown in Fig. 1. In regions of deeper negative stain alternative electron optical images of the two structures could be defined, namely a 'paired-dot' image for the ring (Fig. 2) and a compact ring (i.e., a hollow cylinder on its end), as shown in Fig. 3, which is readily distinguishable from the ring structures in Fig. 1. It was thus immediately apparent that two macromolecular species, now termed torin and cylindrin, were being released from the erythrocyte membranes. At the time of their discovery (Harris, 1968b) it was surmised that torin and cylindrin might be structurally related, a view which though not entirely disproven, is not currently thought to be correct. An alternative procedure for releasing the two molecules was found to be treatment of the haemoglobin-free erythrocyte ghosts with 0.01% SDS, which fragments the membranes, without producing significant solubilization (Fig. 4). This particular approach was not pursued further at the time owing to the difficulty of centrifugally removing the small membrane fragments and the problem of removing the SDS, which would be likely to produce protein dissociation on concentrating the extract. An interesting reproducible observation has been that cattle erythrocyte ghosts treated by either prolonged distilled water dialysis or with 0.01% SDS release only cylindrin (Harris and Maddy, 1974), and that in this species the protein appears to be less stable than cylindrin from human erythrocytes, (Fig. 5).

The release of torin and cylindrin was found to be more efficient if the distilled water dialysed ghosts were given a single

Fig. 1. The release of cylindrin and torin during the prolonged distilled water dialysis of human erythrocyte ghosts. Membrane fragments are also present. Negatively stained with 2% sodium phosphotungstate (pH 7.0). x 200 000.

Fig.2. The paired-dot image of torin (arrowed), as revealed in deep negative stain following release from fragmented human erytnrocyte ghosts. Negatively stained with 2% sodium phosphotungstate (pH 7.0) x 200 000.

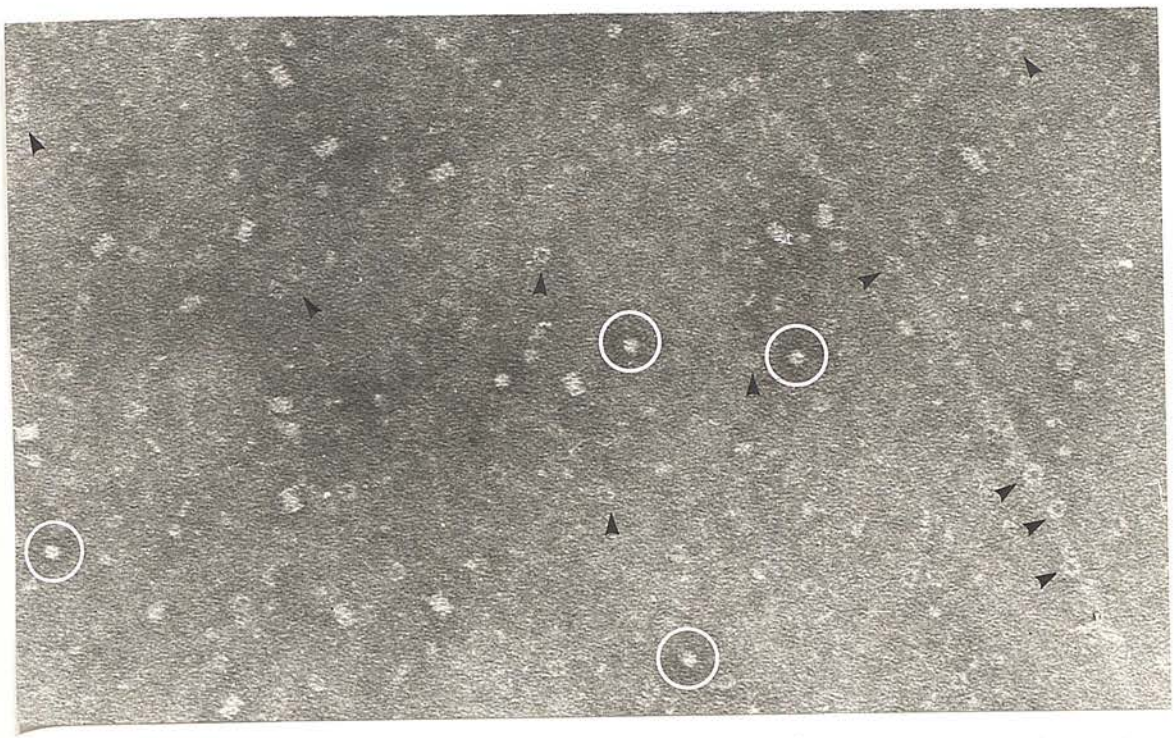

Fig. 3. The compact ring-like image given by cylindrin when orientated vertically on its end (encircled) for comparison with the more open ring-like image of torin (arrows). The central hollow core of cylindrin is not clearly revealed in this instance. Negatively stained with sodium phosphotungstate (pH 7.0). x 200 000

Fig. 4. Human erythrocyte ghosts following treatment with sodium dodecylsulphate (0.1 mg / ml). Negatively stained with 2% sodium phosphotungstate (pH 7.0). Both torin and cylindrin have been released (arrows). x 150 000

Fig. 5. Cattle erythrocyte ghosts treated with sodium dodecyl sulphate (0.1 mg/ ml). Cylindrin alone appears to have been release. Negatively stained with 2% soidium phosphotungstate (pH 7.0). x 200 000

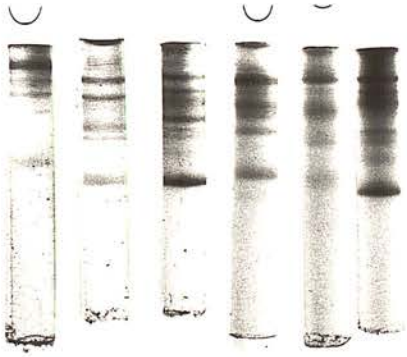

Fig. 6. Polyacrylamide gel electrophoresis in the absence of sodium dodecyl sulphate of the distilled water dialysis / freeze-thaw extract obtained from human erythrocyte ghosts, indicating the heterogeneity of this initial extract.

freeze-thaw treatment, which undoubtedly assists the fragmentation of the membranes. Only recently has the full significance of the prolonged distilled water dialysis been fully appreciated. On reducing the ionic strength, any residual haemoglobin tends to bind to the membrane fragments, as noted by Dodge et al. (1963), and this would be particularly so at the reduced pH produced by the slight acidity of distilled water (approximately pH 5). In addition, under these slightly acidic conditions, spectrin will also tend to remain bound to the membrane fragments, since it precipitates at a pH of less than approximately 5.5, as does cylindrin. The forementioned factors account for the apparent ease by which torin was obtained in a relatively highly purified state (Harris, 1969), when dialysis for up to four days was routinely employed. When the dialysis time was reduced to two days the initial extract obtained after centrifugally removing the membrane fragments was found to contain several proteins, including spectrin, cylindrin and torin, as well as traces of haemoglobin and other proteins, because the pH of the suspension was still near to neutrality (Harris, 1970 and 1974), as shown by the polyacrylamide gel electropherograms, run under non-dissociating conditions, in Fig. 6. Subsequent procedural modifications, include the direct adjustment of the pH of the low ionic strength extract of pH 5.2 and calcium precipitation (30mM) of spectrin (Kirkpatrick et al., 1976) have lead to a more standardised scheme for the purification of both torin and cylindrin (Harris and Naeem, 1978), which will be dealt with in further detail below.

It is of significance that the conventional 1mM EDTA (pH 8.0) extraction of erythrocyte ghosts for obtaining spectrin also releases torin and cylindrin, as does the extract termed soluble ghost protein (SGP) by Howe and Lee (1969), which was obtained by resuspending water washed and lyophilized ghosts in distilled water, extraction for 18 hr. and centrifugation for 2 hr. at 100,000 x g, see Figs. 7 and 8. This material, has an acid solubility curve very similar to our distilled water extract (Fig. 9a and 9b). The SDS gel electrophoresis of Kirkpatrick and LaCelle (1974) and Kirkpatrick et al. (1975) shows that the water soluble proteins from erythrocyte membranes have a predominant peptide in the 20,000 molecular weight

Fig. 7. The Soluble Ghost Protein (SGP) water extract from human erythrocyte ghosts produced by C. Howe. Both cylindrin and torin are present along with other proteins, among which is spectrin (see Fig. 8). Negatively stained with 2% sodium phosphotungstate (pH 7.0). x 250 000.

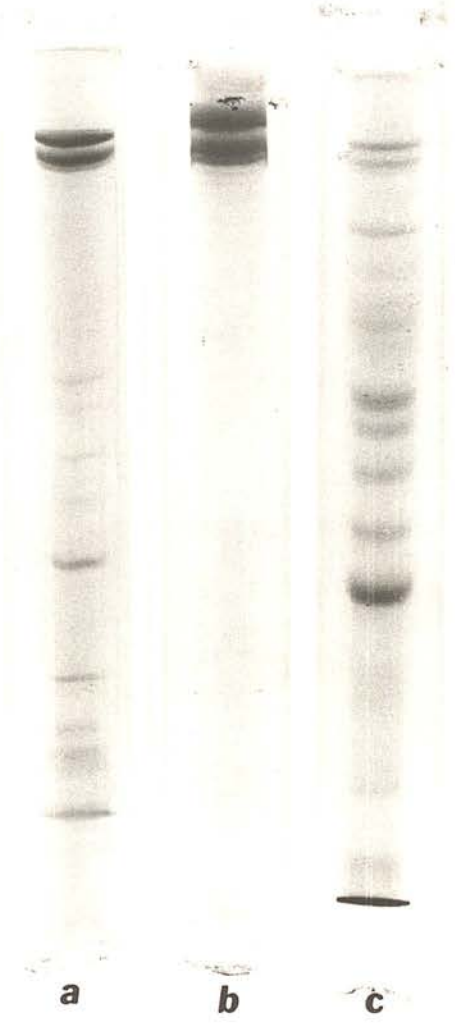

Fig. 8. SDS-polyacrylamide gel electrophoresis of crude spectrin (a), purified spectrin (b), and soluble ghost protein (SGP) (c), from Deas et al. (1978). Note the presence of the rapidly migrating polypeptide bands on gel (c) and also the faint spectrin bands. With the permission of the authors and Academic Press.

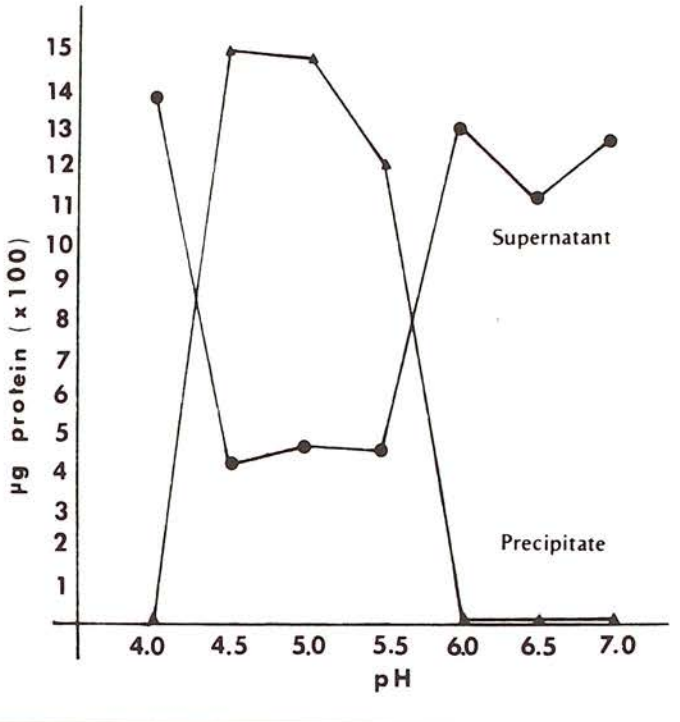

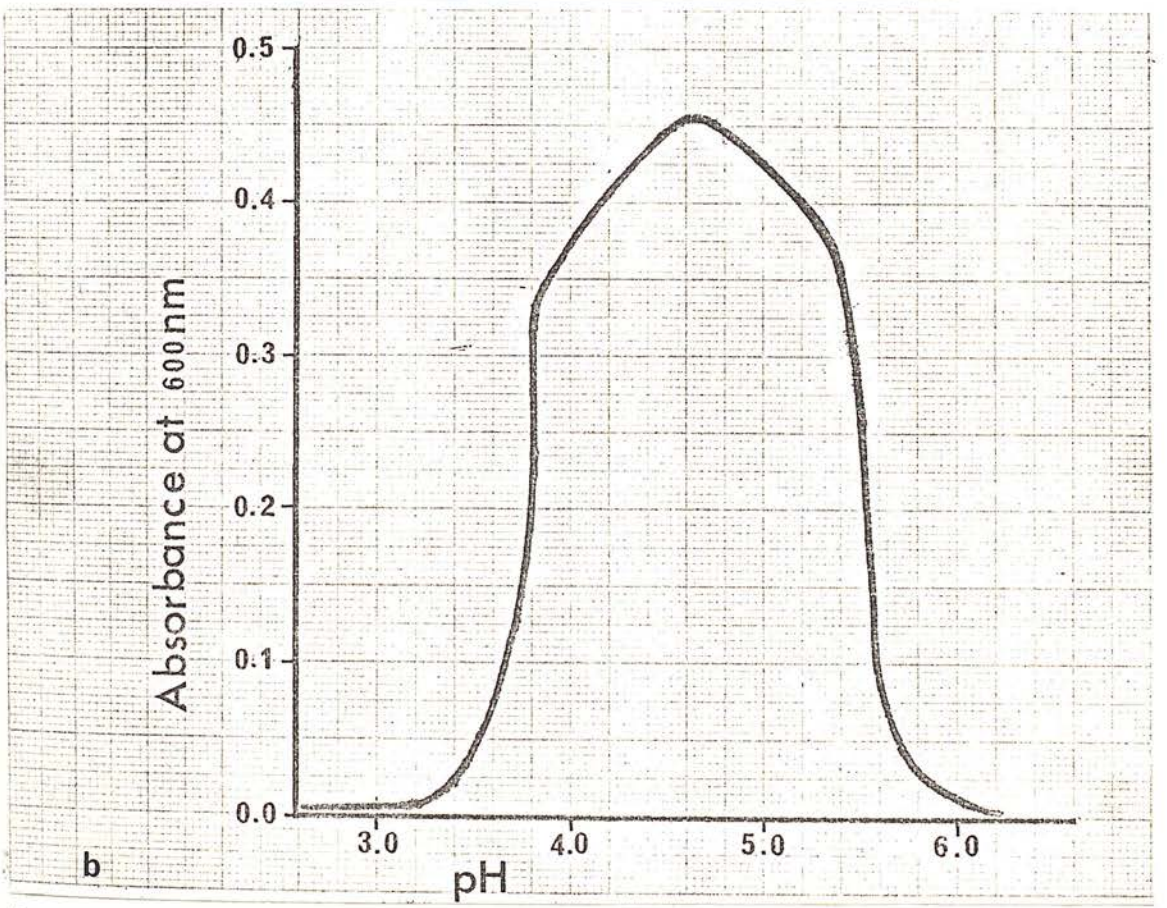

Fig. 9. The pH solubility curve, (a) of soluble ghost protein (SGP) from Deas et al. (1978), with the permission of Academic Press, and (b) the distilled water freeze-thaw extract from human erythrocyte ghosts.

range, which remains soluble on precipitating spectrin at a pH of 5.1, and is in all probability torin (Fig. 10).

Localization of Cylindrin and Torin

Because negative staining of intact erythrocyte ghosts does not reveal a surface coat of proteins (Harris and Agutter, 1970) as is the case for blood platelets, kidney tubule microvilli and intestinal microvilli, it is strongly implied that torin and cylindrin might well be located on the cytoplasmic surface. Evidence in support of this suggestion has come from two sources. Firstly, from the negative staining of erythrocyte ghosts where lesions in the membrane have been located, immediately adjacent to which torin and cylindrin can be seen on the carbon support film (Harris, 1971c), as shown in Figs. 11 and 12 of human and cattle erythrocyte ghosts, respectively. In addition, cylindrin can be located within the tube-like projections of cattle erythrocyte ghosts that have taken on the appearance of 'stromalytic forms' (Fig. 13). The interpretation is thereby advanced that torin and cylindrin must have remained attached to the cytoplasmic surface of the erythrocyte membrane throughout the centrifugal washing scheme used to remove haemoglobin and other cytosol proteins. Recent evidence has, however, indicated that cylindrin is also lost into the supernatant during the final centrifugal washes, from which it can be recovered by precipitation at pH 5.2. A second line of independent evidence for the location of torin and cylindrin has come from Howe and Bachi (1973), who raised rabbit anti sera against what they called T-protein (probably fairly pure cylindrin), which on immunoelectrophoresis gave a single precipitin arc against the mixture of antibodies produced by haemoglobin-free erythrocyte ghosts. Following conjugation with ferritin the antibody to T-protein was shown by thin sectioning electron microscopy to be localized predominantly on the cytoplasmic surface of the intact erythrocyte ghosts, which were, nevertheless, permeable to the ferritin-antibody conjugate, as shown in Fig. 14. More precisely, it might be stated that the conjugate is located within the 'fuzzy' layer on the membrane cytoplasmic surface, which is thought to be composed of spectrin, actin and other extrinsic erythrocyte membrane proteins (Lux, 1979), Ralston (1976).

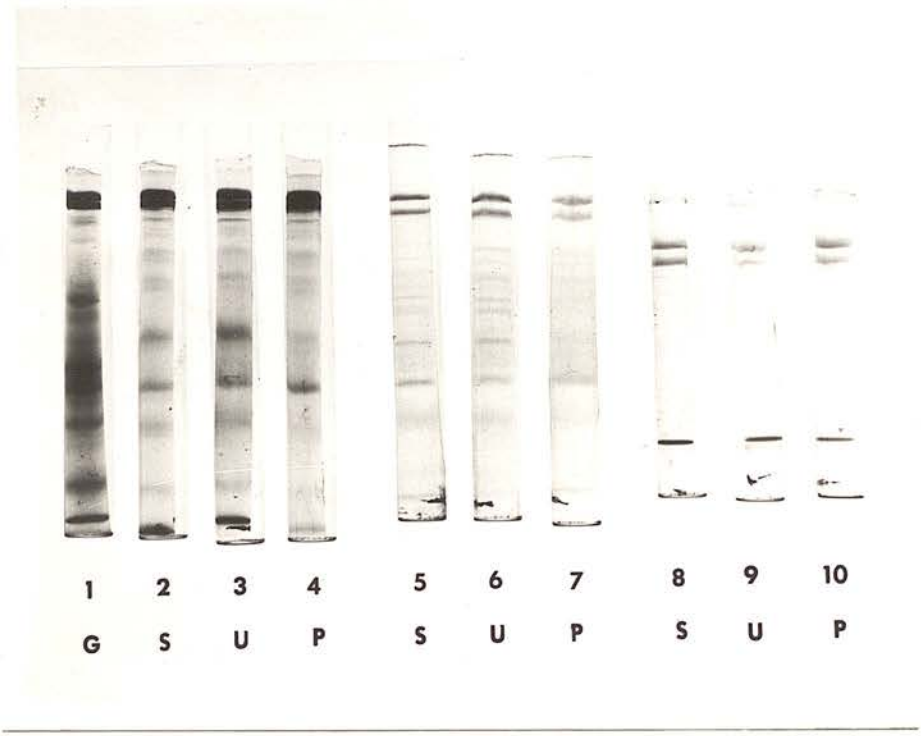

Fig. 10. SDS-polyacrylamide gel electrophoresis of spectrin, calcium precipitates and supernatants of human erythrocyte ghost extracts, from Kirkpatrick et al. (1976), with the permission of Academic Press. Gels 1 to 4 were 28% precipitated, gels 5 to 7 were 22% precipitated and gels 8 to 10 were 47% precipitated. G, ghosts; S, spectrin; U, supernatant after calcium treatment; P, pellet from calcium treatment.

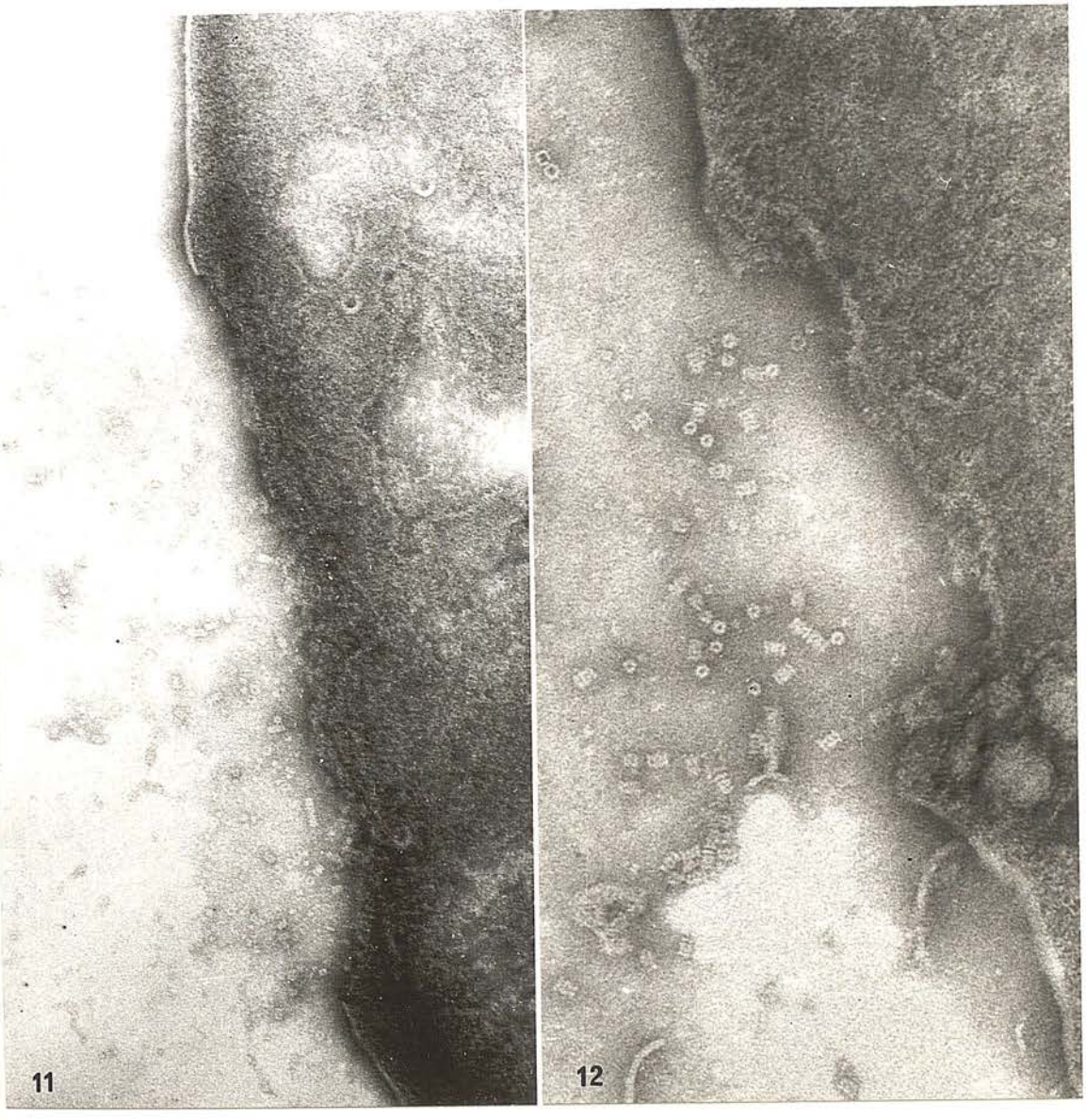

Figs. 11 and 12. Human and Cattle erythrocyte ghosts showing discrete lesions in the membrane from which torin and cylindrin have escaped and are located on the support film adjacent to the membrane. Negatively stained with 2% ammonium molybdate (pH 7.0). From Harris (1971c), with the permission of Academic Press. x 100 000 & x 200 000, respectively.

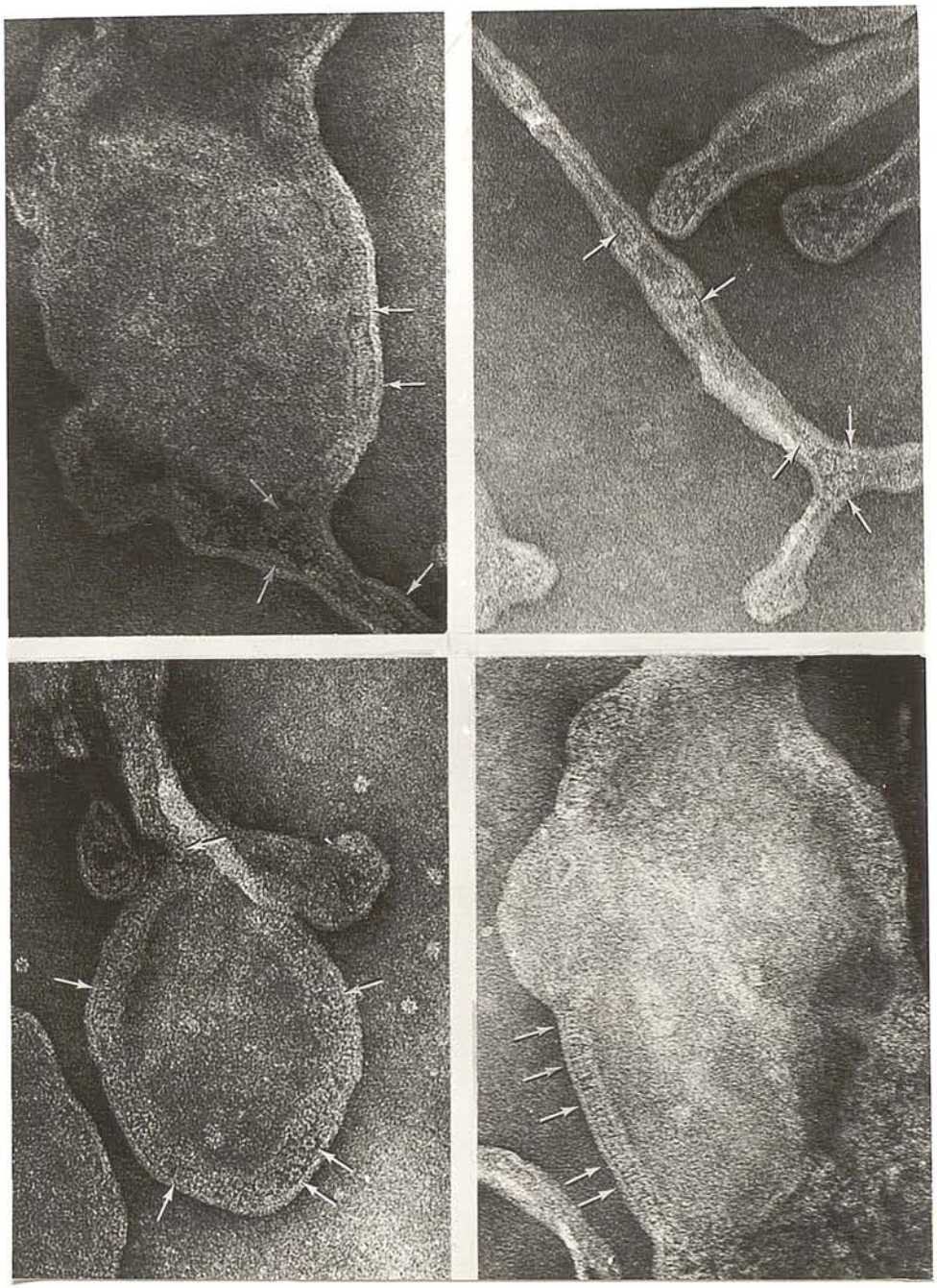

Fig. 13. Stromalytic tube-like projections from cattle erythrocyte ghosts, within which cylindrin molecules can be located (arrowed). Negatively stained with 2% ammonium molybdate (pH 7.0). x 200 000. From Harris (1971c), with the permission of Academic Press.

Fig. 14. Human erythrocyte ghosts after interaction with ferritin-labeled antibody to T protein. From Howe and Bächi (1973), with the permission of Academic Press. x 90 000.

Using an elegant freeze fracture-negative staining technique, Nermut (personal communication) has shown that the cytoplasmic face of sheep erythrocyte membranes in all probability contains both cylindrin and torin (see Fig. 15). In this technique, intact erythrocytes were attached to polylysine coated mica, lysed directly with distilled water and washed, leaving pieces of membrane attached to the mica with their cytoplasmic surfaces exposed. Following the positioning of a second piece of mica on the exposed cytoplasmic surfaces, the material was frozen and cleaved, negatively stained specimens then being prepared from the inner and outer fracture monolayers, or from the intact membrane if the fracture has passed along the cytoplasmic surface as apparently happens to a fairly high proportion of the membranes (Nermut and Williams, 1977).

It might be hoped that conventional freeze fracture-metal shadowing electron microscopy, in conjunction with deep etching would reveal cylindrin and torin on the cytoplasmic surface of erythrocyte ghosts, but this does not appear to be the case (D. Shotton, personal communication). Nevertheless, the published electron micrographs of Seeman and Iles (1972) do show particles on the etched cytoplasmic surface which resemble cylindrin, but the interpretation is not absolutely clear cut. It is possible that during etching the molecules collapse, even when high concentrations of glycerol are present, and in any case they would need to be raised above the surrounding spectrin-matrix before metal shadowing could resolve them.

The interesting negative staining results obtained by Moll (1973), (1974) from blood group A erythrocyte ghosts obtained by freeze lysis and distilled water washing, which depict 9.0 nm particles on or in the surface of the membrane (Fig. 16a) are difficult to correlate with the negative staining results of the author. Moll found both irregular distributions as well as regular arrays of particles (Fig. 16a) It is tempting to draw a comparison between these regular arrays and the arrays of torin which can be produced by drying on mica (see below), but this is probably not valid, especially as Moll considered the particles to be lipoproteins, possibly A antigen sites. Somewhat similar particles were detected by Haggis (1969) on erythrocyte ghost fragments stained at 37°C. with sodium phosphotungstate, and with ghost fragments produced by treatment with SDS at 0.1 mg / ml (Harris, 1968), as shown in Fig. 17.

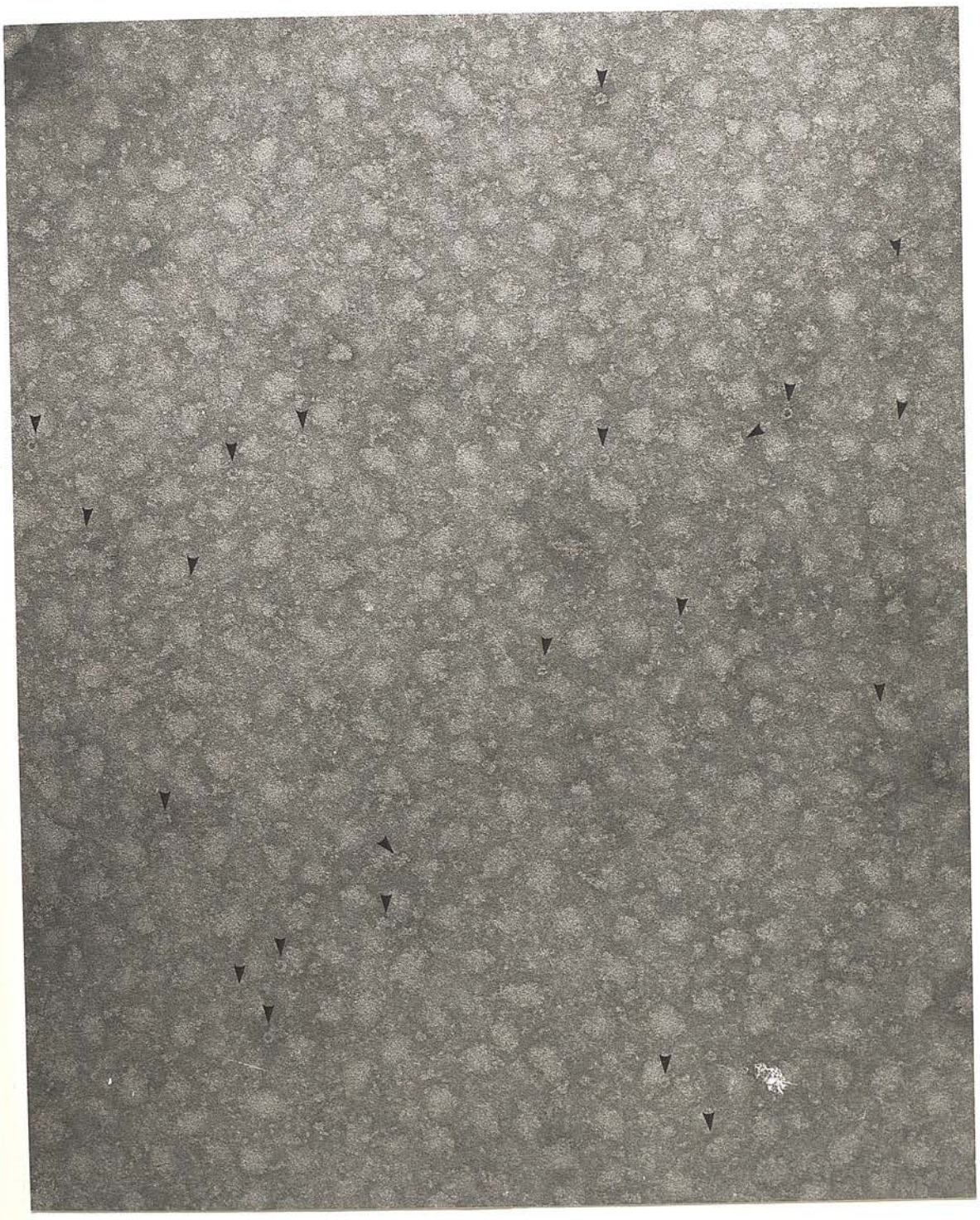

Fig. 15. Sheep erythrocyte membranes freeze-fractured and then negatively stained with ammonium molybdate (M.V. Nermut, previously unpublished data). Arrows indicate torin molecules and circles indicate cylindrin molecules. x 150 000

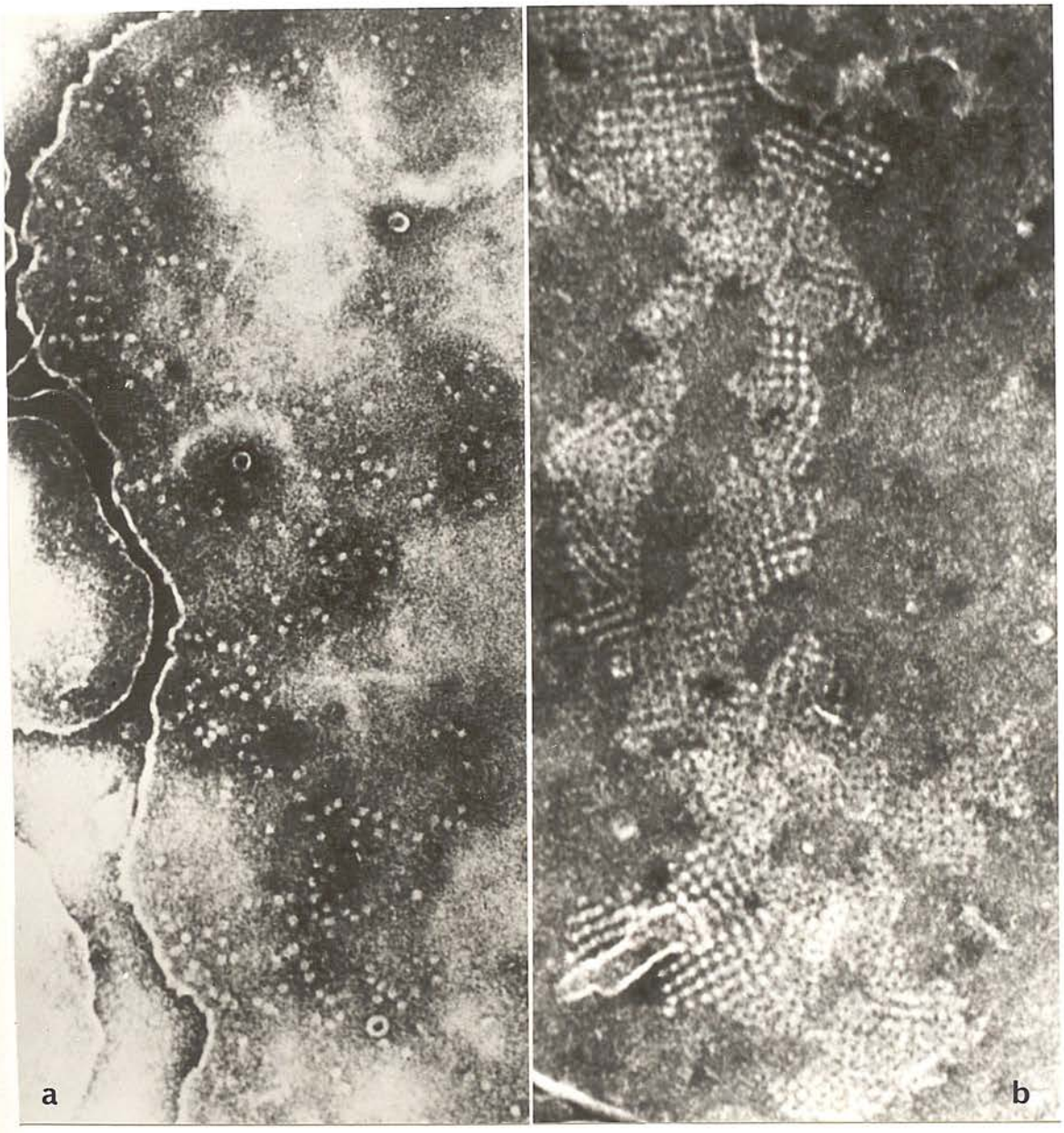

Fig. 16. Fragmented human erythrocyte ghosts from blood group A_1, showing 9 nm particles randomly distributed over the membrane surface (a), and a region showing regular arrays of the 9 nm particles (b). x 80 000. By coutesy of G. Moll.

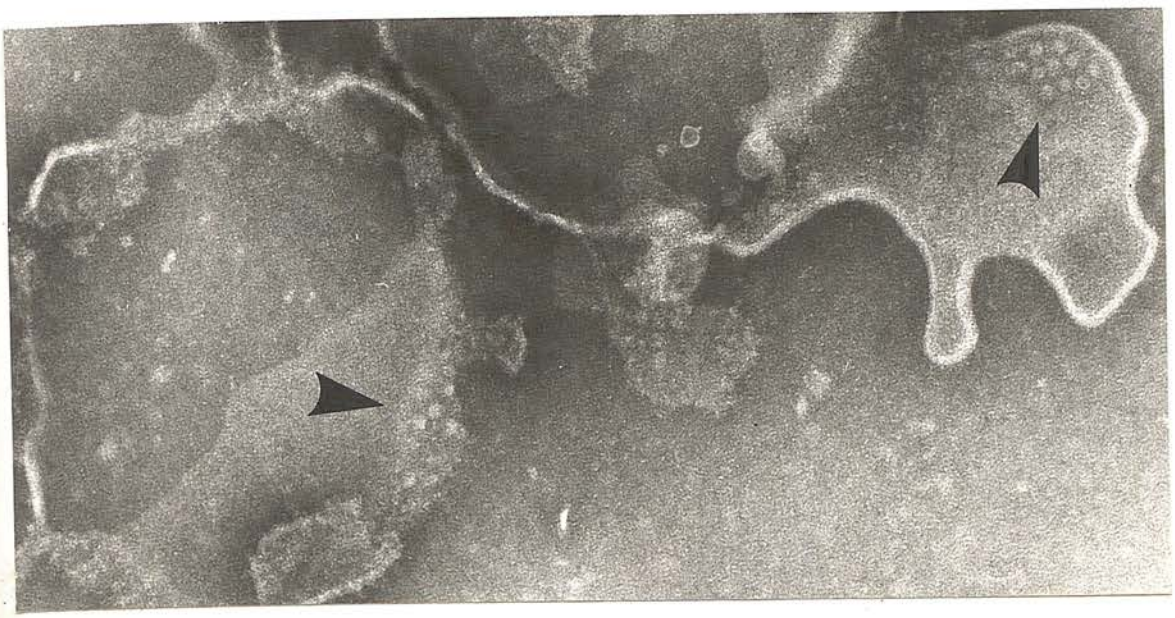

Fig. 17. Human erythrocyte ghosts following treatment with sodium dodecyl sulphate (0.1 mg/ml). Negatively stained with sodium phosphotungstate (pH 7.0). The arrows indicate particles similar to those shown in Fig. 16, but they also resemble cylindrin. x 150 000

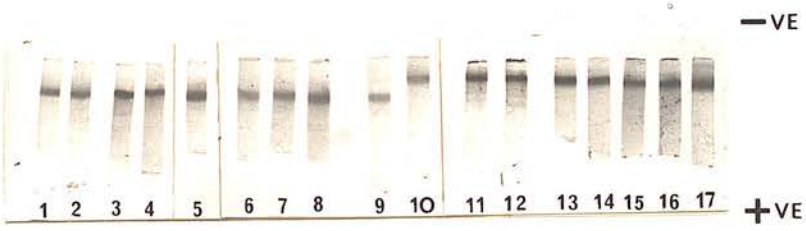

Fig. 18. Polyacrylamide gel electrophoresis of purified torin obtained by differential centrifugation and sucrose density gradient centrifugation (from Harris, 1969a). Gels 1 to 9 were electrophoresed in 20 mM Tris-HCl buffer (pH 8.0), and on gels 10 to 17 the protein sample had been treated with 8 M urea. In all cases there is a predominant band of migratory protein, which correlates with the presence of torin detected by electron microscopic study, see Fig. 19. With the permission of Elsevier North Holland Biomedical Press.

The Development of Isolation and Purification Procedures for Torin and Cylindrin

The original distilled water dialysis and freeze-thaw procedure (Harris, 1969a) produced an initial membrane-free extract from human erythrocyte ghosts which was rich in torin, and a further purification was achieved by either sucrose density gradient centrifugation or simply high speed differential centrifugation. The criterion for torin purity used was the presence of a single band of stained protein following polyacrylamide gel electrophoresis (PAGE) under non-dissociating conditions, together with the presence of torin as a single molecular species when studied by negative staining electron microscopy, (see Figs. 18 and 19). This overall procedure suffered from the disadvantage that cylindrin was not recovered, undoubtedly owing to the fall in pH during the prolonged water dialysis that allowed only torin to be extracted, spectrin, cylindrin and haemoglobin remaining bound to the membrane fragments (cf. Fig. 9 and see below for isoelectric precipitation of proteins). In addition, any cylindrin present would have been pelleted by the sucrose density gradient or differential centrifugation conditions employed at this time. Subsequently, the distilled water dialysis period was reduced to approximately 40 hours, the pH of the initial extract then being close to pH 7 and after concentration the material was dialysed against pH 8 buffer rather than distilled water (Harris, 1971a and 1974). This resulted in a far more heterogenous mixture of proteins in the extract (Figs. 6 and 20), from which both torin and cylindrin were purified. A sequential scheme was used which first of all removed any haemoglobin present by gel filtration chromatography through Biogel P 300, the excluded peak containing torin, cylindrin and any spectrin being taken for further processing. Sucrose density gradient centrifugation has been the most satisfactory procedure for purifying cylindrin, and is still used currently for this purpose (Figs. 21 and 22). Torin was purified by taking the upper region of the sucrose density gradient and subjecting it to preparative polyacrylamide gel electrophoresis, a procedure which proved to be extremely time consuming and appeared to give rise to considerable losses (Harris 1974). More recently a simplified purification procedure has been developed (Harris and Naeem, 1978),

Fig. 19. A sample of purified torin obtained by sucrose density gradient centrifugation which exhibited a single band of protein on polyacrylamide gel electrophoresis. Negatively stained with sodium phosphotungstate (pH 7.0). In this region there is relatively shallow negative stain and all the molecules are orientated on their sides, exhibiting the ring-like profile of the molecule. x 300 000

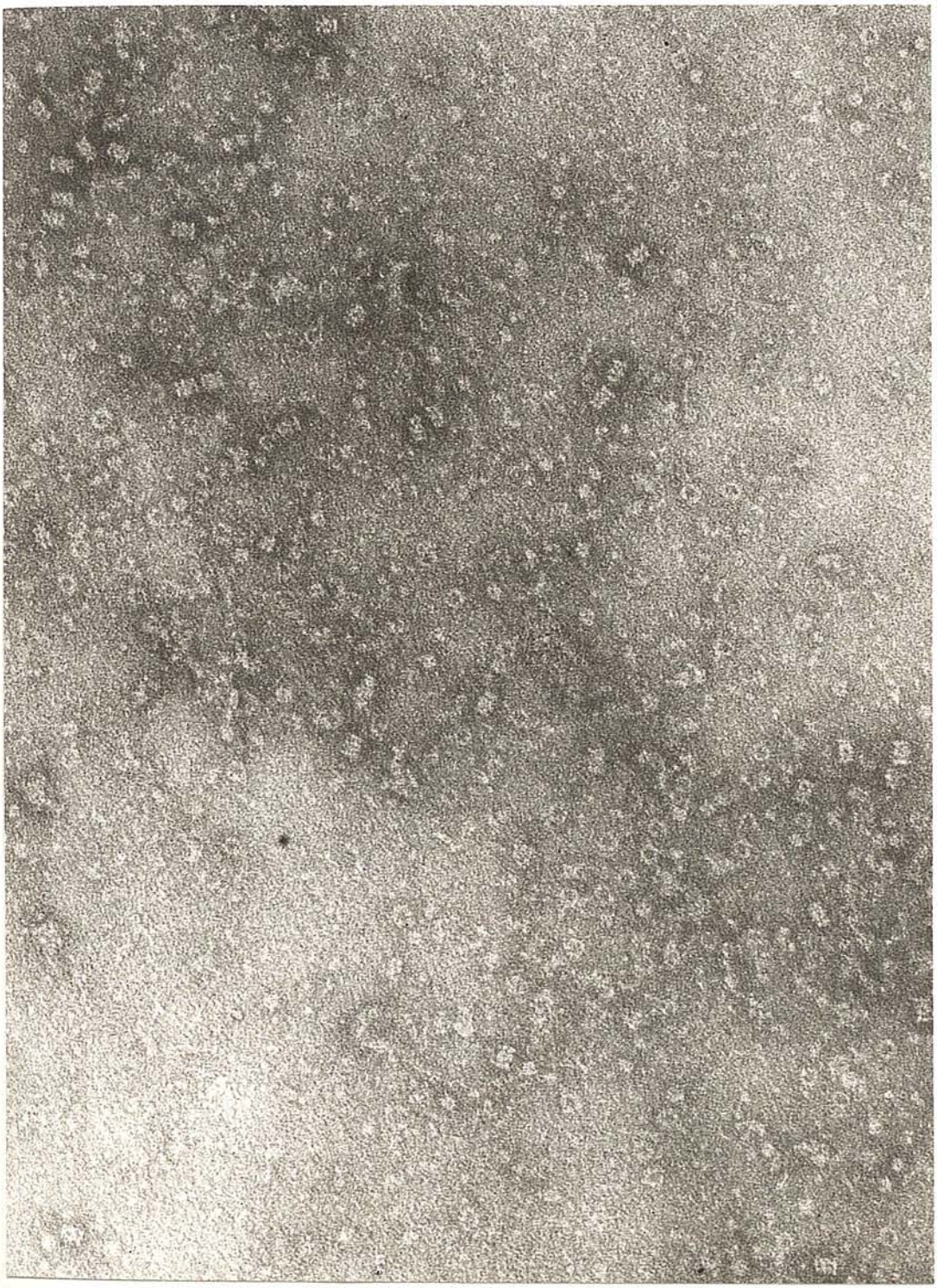

Fig. 20. The initial distilled water dialysis / freeze-thaw extract (at pH approx. 7.0) from human erythrocyte ghosts. Cylindrin, torin and other smaller particles are present (i.e., spectrin and haemoglobin). Negatively stained with sodium phosphotungstate (pH 7.0). x 200 000

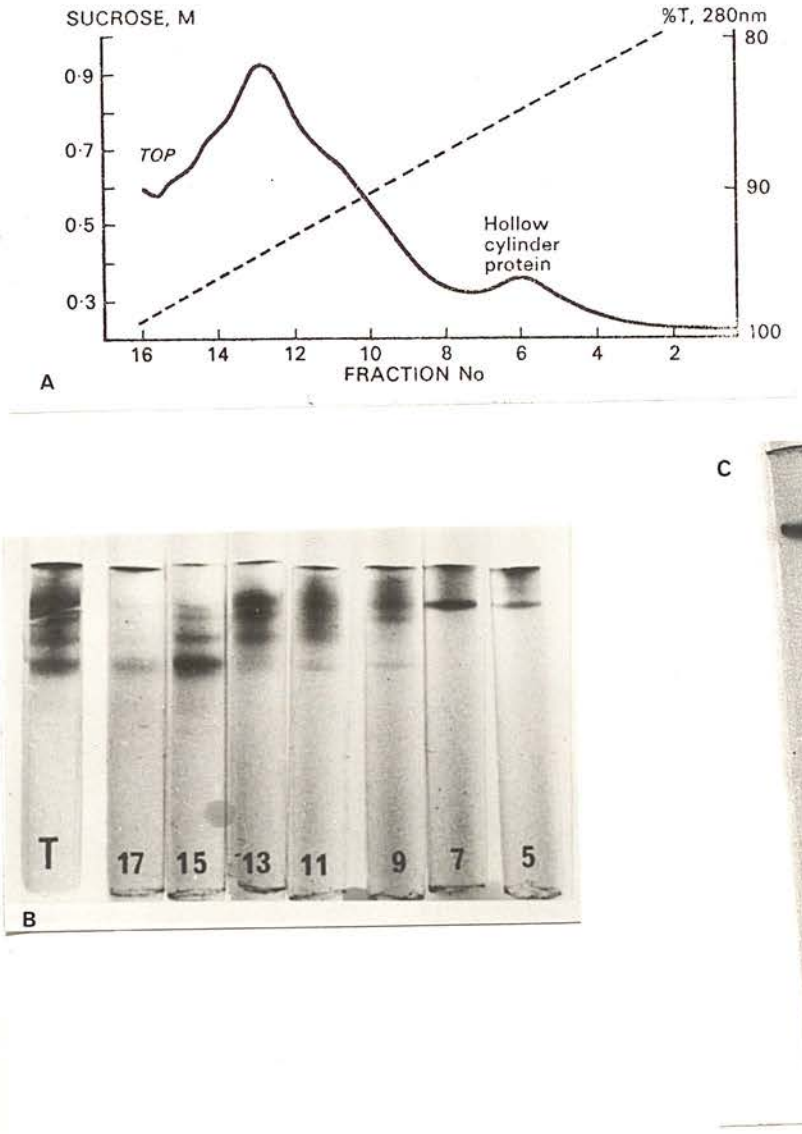

Fig. 21. The purification of cylindrin by sucrose density gradient centrifugation at 27 000 rev/min for 24h; (A) the % transmission at 280 nm of the tube effluent after centrifugation, and (B) the polyacrylamide gel electrophoresis of the gradient fractions. (C) More highly purified cylindrin obtained after re-centrifuging on a second sucrose density gradient. Modified from Harris (1974), with the permission of the Longman Group Ltd.

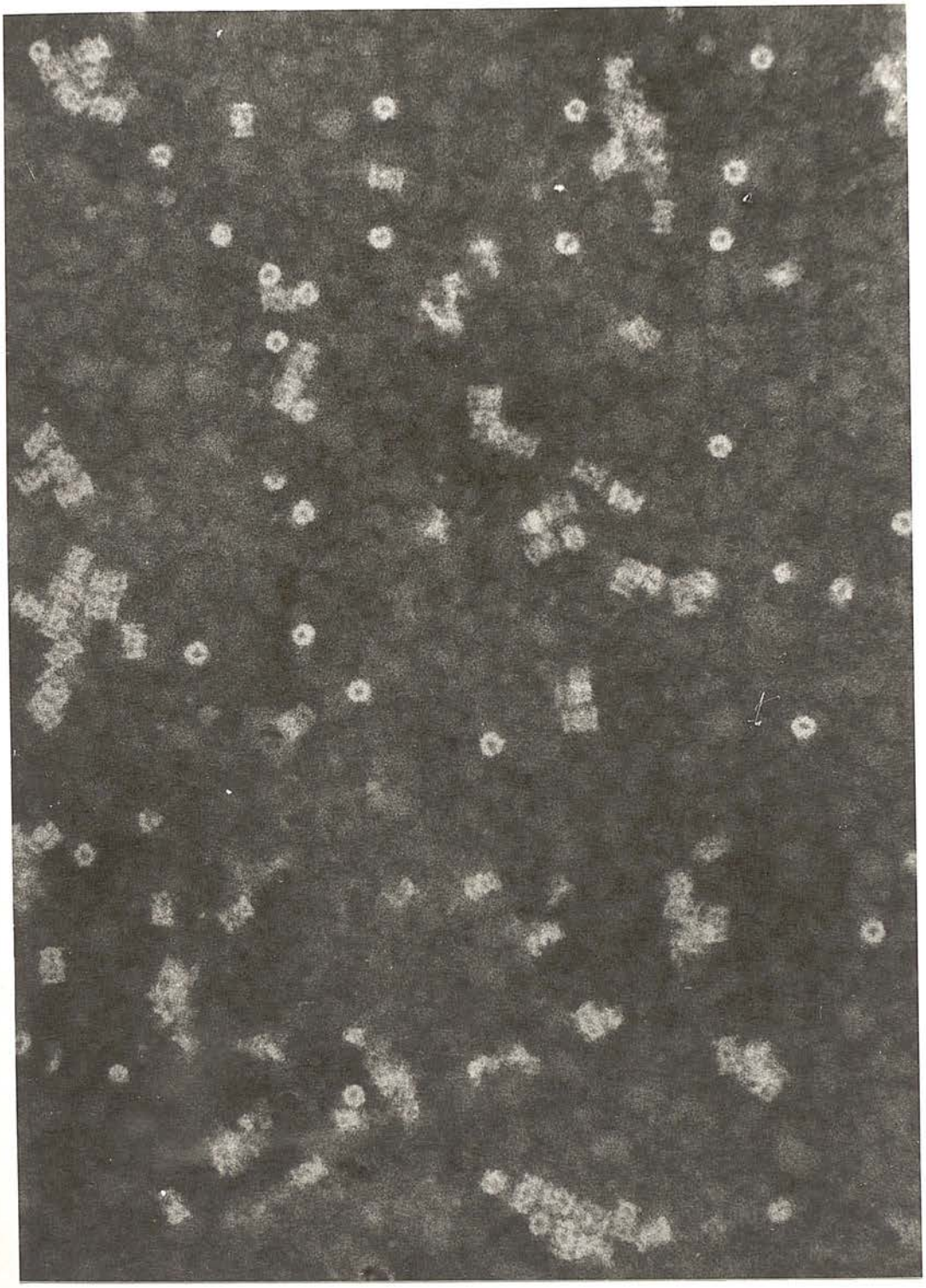

Fig. 22. Purified cylindrin obtained by sucrose density gradient centrifugation, as shown in Fig. 21(C). Negatively stained with sodium phosphotungstate (pH 7.0). x 360 000

see Chart 1, which makes use of the solubility of torin at pH 5.2 when cylindrin and spectrin are insoluble and of the fact that spectrin can be selectively precipitated by the addition of calcium (30mM) at pH 7.0 following solubilization of the pH 5.2 pellet. This calcium treatment was discovered by Kirkpatrick et al. (1976). The calcium supernatant obtained by Kirkpatrick et al. is shown in Fig. 23; arrows indicate the cylindrin molecules.

In our hands it has been found necessary to use gel filtration chromatography on Biogel P 300 or Ultragel AcA 34 as the final purification step for torin, and sucrose density gradient centrifugation for cylindrin (Figs. 21 and 22). The incorporation of other beneficial modifications in the future is not ruled out. For instance, precipitation of torin and cylindrin with 50% saturated ammonium sulphate is likely to be a useful treatment for removing contaminatory haemoglobin, and DEAE cellulose ion exchange chromatography has been shown by White and Ralston (1979) to be an alternative procedure for obtaining purified cylindrin (Fig 24).

The Characterization of Torin and Cylindrin

In this section a brief discussion will be presented dealing with several of the analytical approaches that are available for the biochemical characterization of torin and cylindrin. It must be stated at the outset that in most cases the data available is far from complete, in the main owing to the limited availability of the purified proteins.

Subunit Composition:

It is of interest to know whether torin and cylindrin are multimetric complexes of identical or different subunits and whether the subunit molecular weights of the two proteins are the same. The technique of SDS - PAGE is well established for determining the molecular weights of dissociated proteins and polypeptides, when used in conjunction with marker proteins of known molecular weight. In our hands (Harris and Naeem, 1978), using 7% polyacrylamide tube gels, it has been shown that torin contains a single polypeptide

Chart 1

Purification of Human Erythrocyte Ghost Cylindrin and Torin

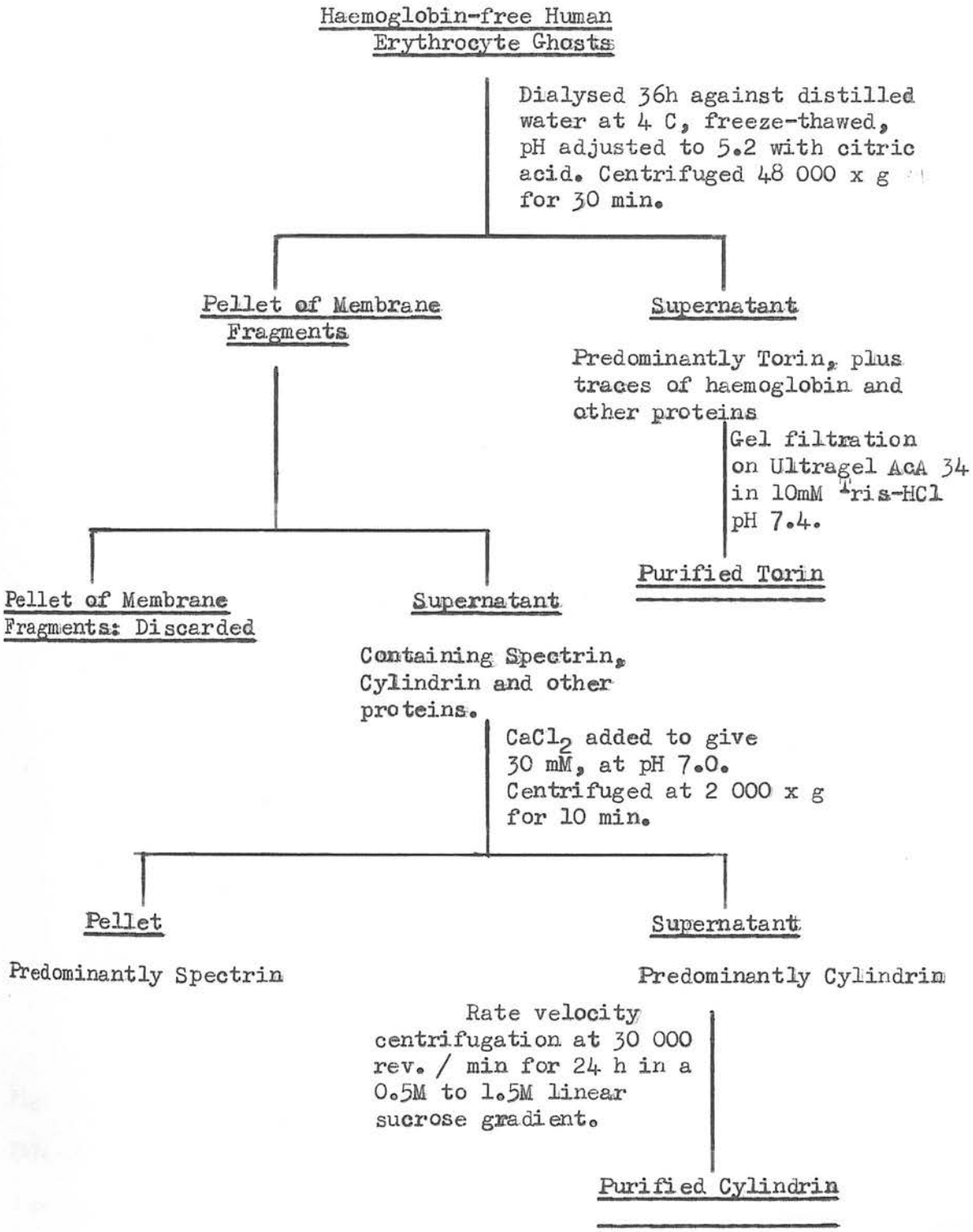

(Modified from Harris and Naeem, 1978)

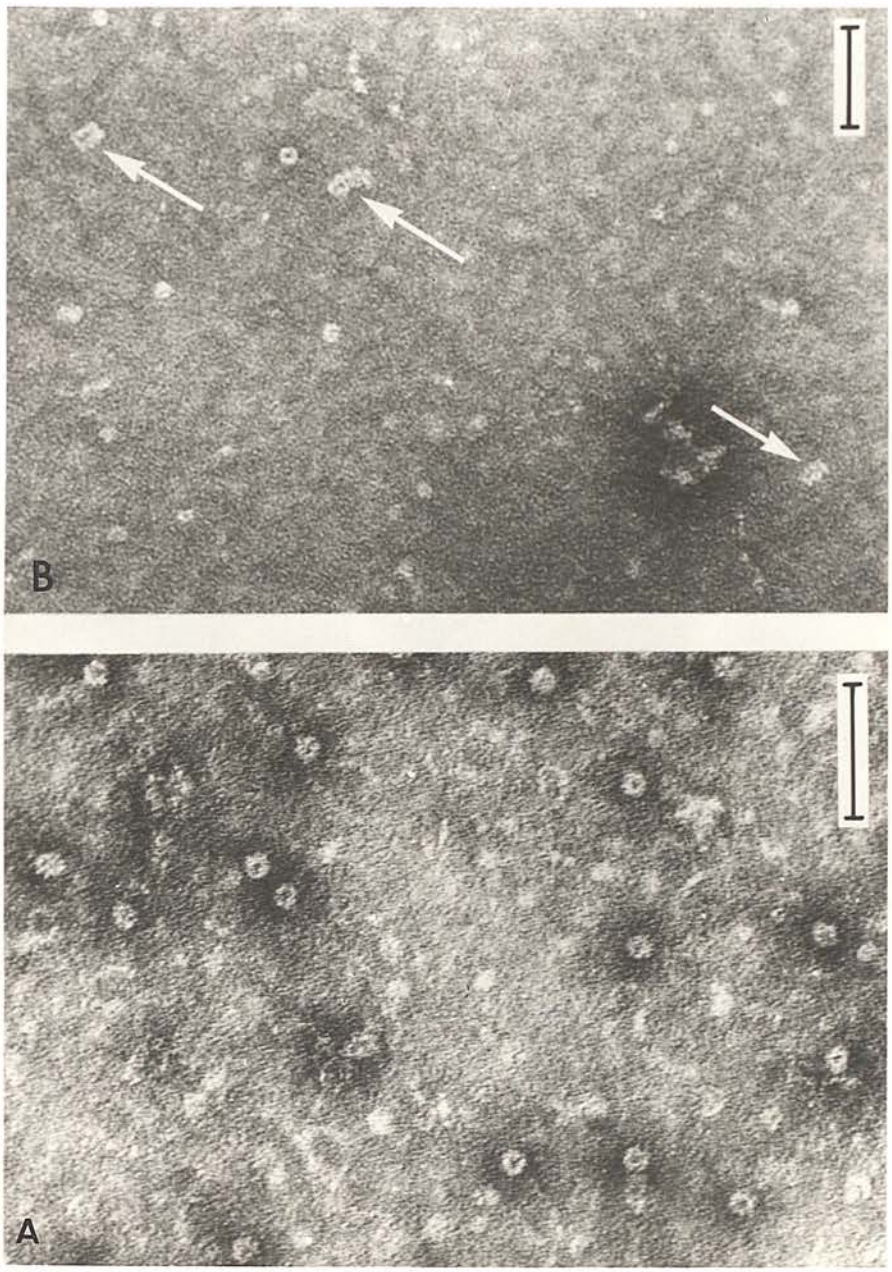

Fig. 23. The calcium supernatant from the human erythrocyte ghost EDTA extract prepared by Kirkpatrick et al. (1976). (A) retreated with 3 mM $CaCl_2$; (B) no further $CaCl_2$ treatment. The scale bar indicates 100 nm. With the permission of Academic Press.

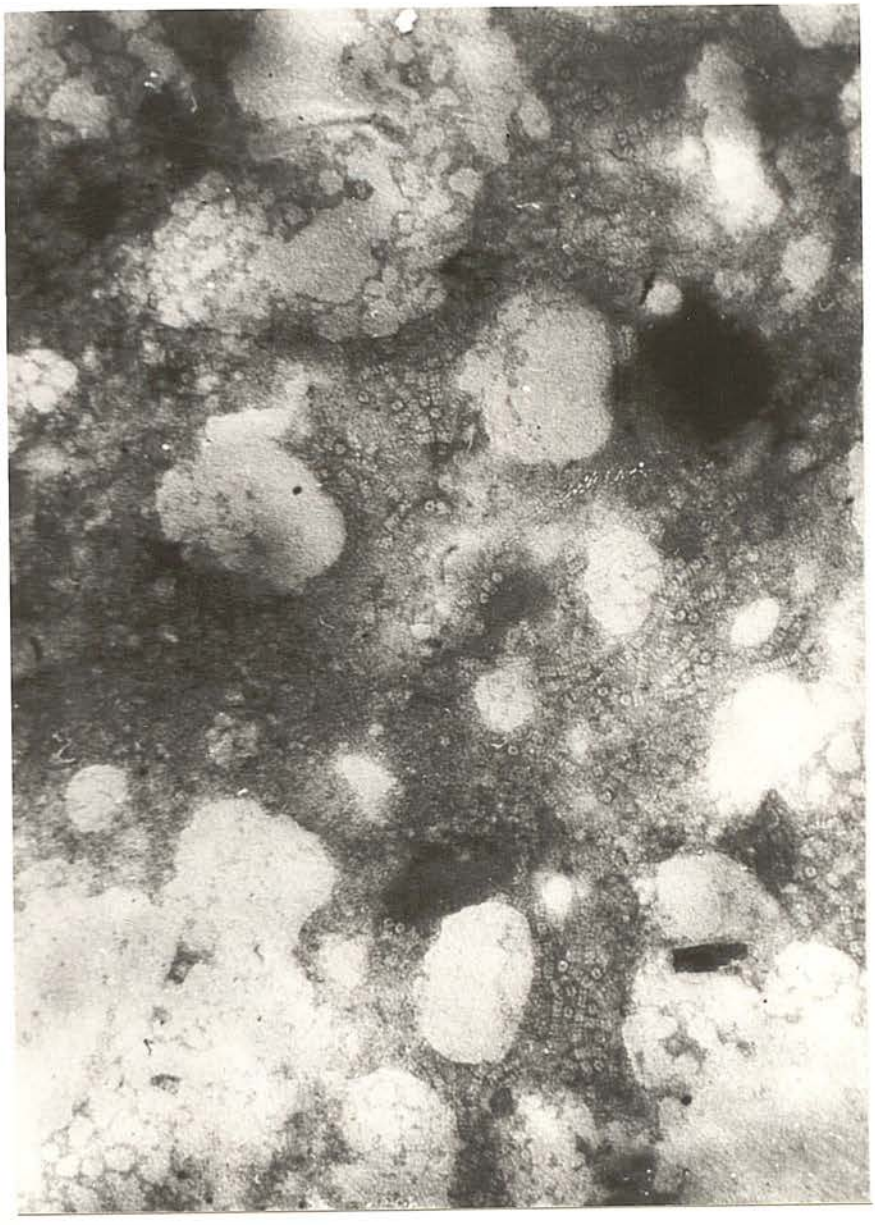

Fig. 24. Cylindrin purified by DEAE cellulose column chromatography by White and Ralston (1979). Negatively stained with sodium phosphotungstate (pH 7.0). x 200 000 approx. With the permission of Elsevier/North-Holland Biomedical Press.

of molecular weight approximately 20,000, and that cylindrin contains two predominant polypeptides of molecular weight only slightly greater than that of torin (see Fig. 25). White and Ralston (1979) have also performed SDS polyacrylamide gel electrophoresis with cylindrin, from which they detected two predominant polypeptides of molecular weight 22,500 and 28,000 with a smaller quantity of a 25,000 molecular weight band (Fig. 26). These polypeptides correspond to bands 7.1, 7.2 and 8 of the nomenclature of Fairbanks et al. (1971), and must be considered to be in reasonably good agreement with out own data. The claims that polyacrylamide gradient gels can reveal upwards of 35 polypeptide from erythrocyte membranes (Banga et al., 1979) and that two dimensional polyacrylamide gel electrophoresis can reveal over two hundred (Rubin and Milikowski, 1978), are likely to lead to a more detailed study of the subunits of torin and cylindrin. As with all studies on highly purified proteins, it is always desirable that data supporting the purity of the samples be available, such as may be obtained from polyacrylamide gel electrophoresis under non-dissociating conditions, isoelectric focusing, immunocelectrophoresis and electron microscopy prior to performing subunit determinations.

Analytical Ultracentrifugation:

The analytical ultracentrifuge has been used to determine the sedimentation coefficient of torin and cylindrin (Harris, 1971) and of cylindrin (White and Ralston, 1979). Figures of 22.5 S and 9.0 S were determined by Harris (1971) for cylindrin and torin on extrapolation to infinate dilution (see Fig. 27), whereas White and Ralston (1979) obtained a figure of 19.3 S for cylindrin at a protein concentration of approximately 0.5 mg/ml. By meniscus depletion sedimentation equilibrium White and Ralston (1979) obtained a value of 747,000 $\pm$ 38,000 (mean of three determinations) for the molecular weight of cylindrin, which is comparable with our own results (896,000 $\pm$ 19,000 and 725,000 $\pm$ 23,000, two determinations).

Amino Acid Analysis

The amino acid composition of cylindrin obtained from human

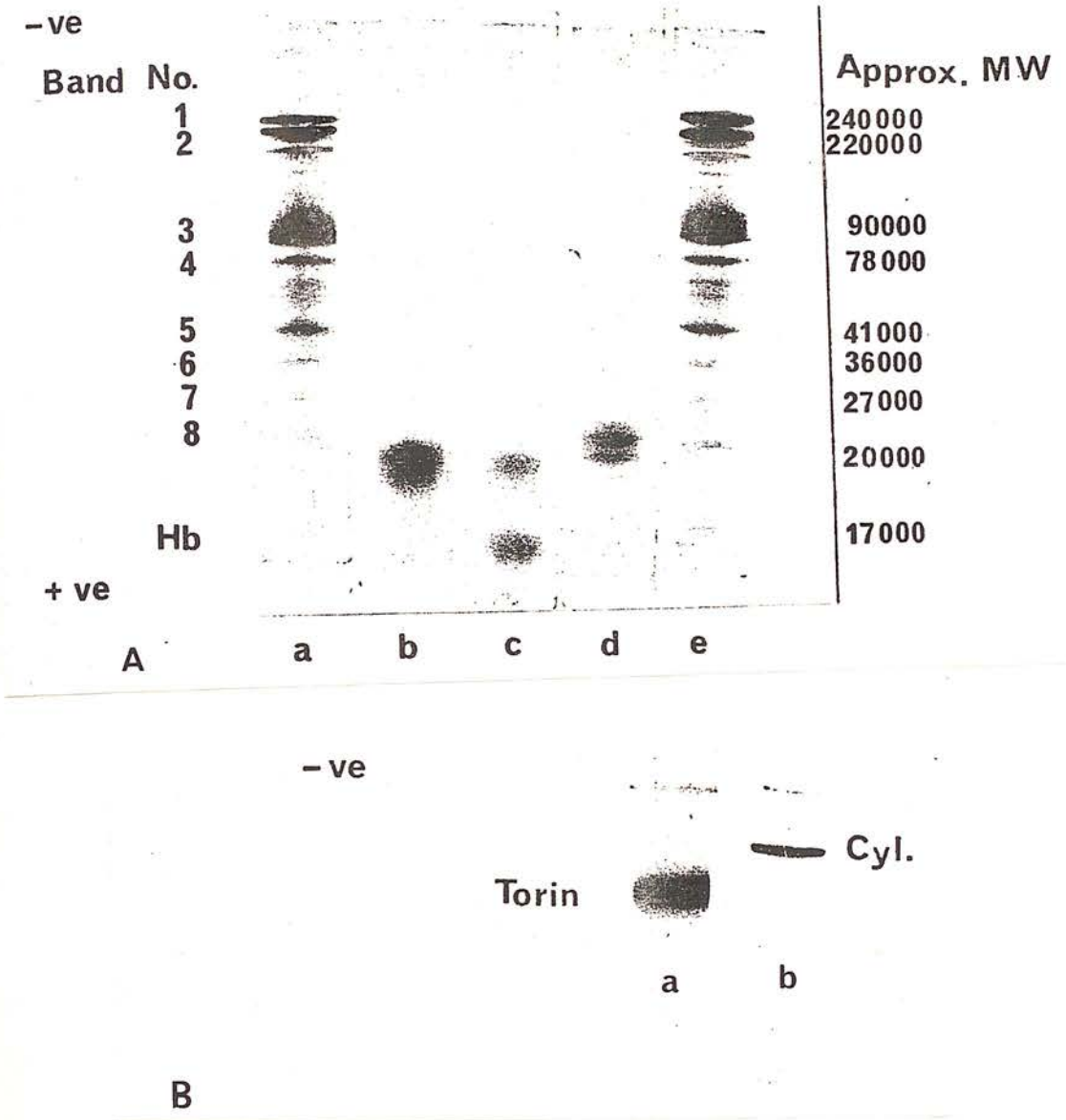

Fig. 25. (A) 7% polyacrylamide gel electrophoresis in a 0.1% SDS, 50mM Tris-HCl (pH 8.0) continuous buffer system; gels (a and e) show erythrocyte ghosts, (b) purified torin, (c) purified torin plus haemoglobin, (d) purified cylindrin. (B) 7% polyacrylamide gel electrophoresis in a non-dissociating 50 mM Tris-HCl (pH 8.0) continuous buffer system; gel (a) shows native torin, gel (b) native cylindrin. From Harris and Naeem (1978), with the permission of Elsevier/North-Holland Biomedical Press.

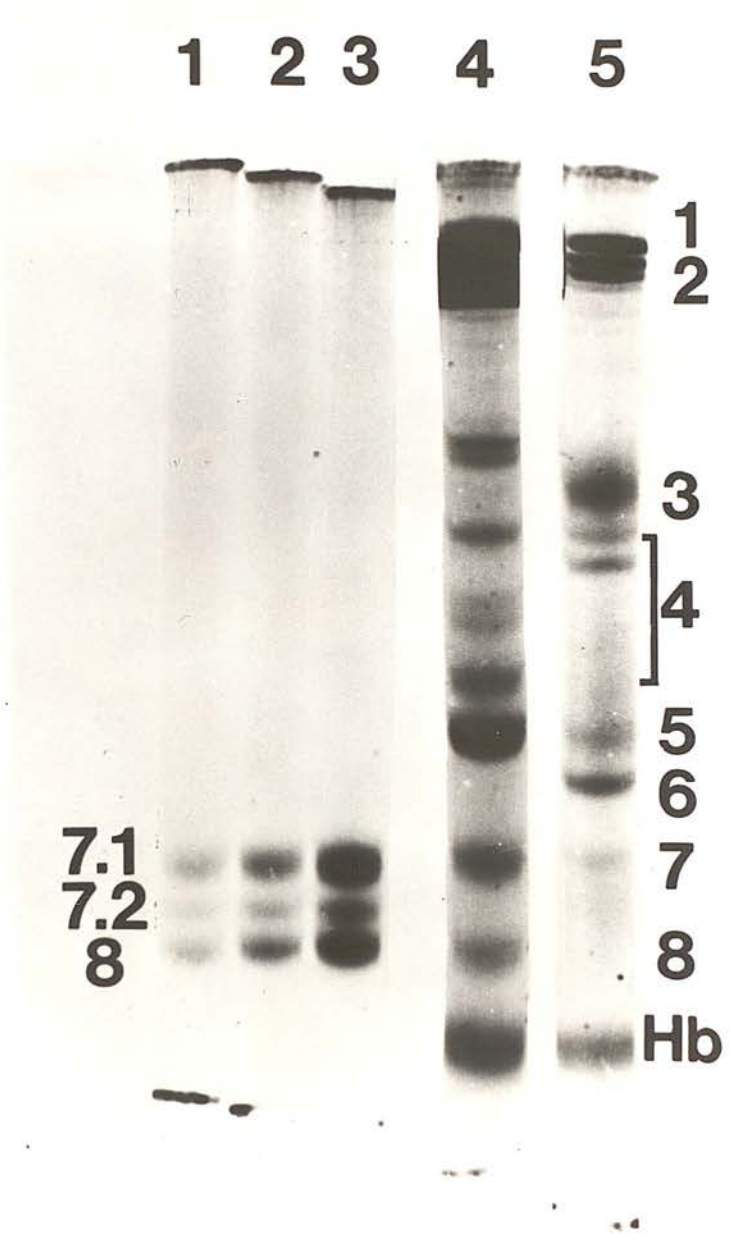

Fig. 26. SDS polyacrylamide gel electrophoresis, from White and Ralston (1979). Purified cylindrin was applied in increasing amounts to gels (1 to 3); gel (4) is of the crude water soluble proteins from human erythrocyte ghosts and gel (5) is of total erythrocyte ghosts. The polypeptide bands are numbered according to the scheme of Fairbanks.

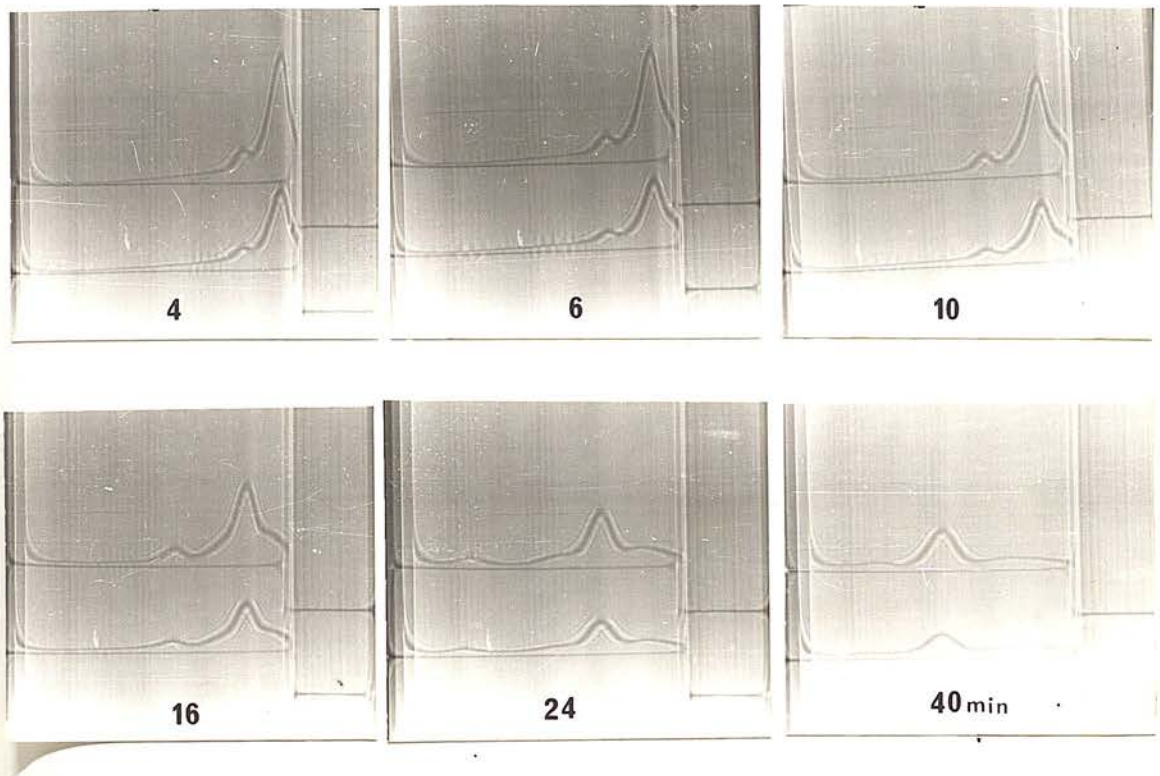

Fig. 27. Analytical ultracentrifugation Schlieren patterns of the concentrated water extract from human erythrocyte ghosts. The phase plate angle was 20° and the speed of rotation was 54 600 rev/min. The protein concentration was approx. 12 mg/ml (upper trace) and 8 mg/ml (lower trace). Note the similarity to the distribution of protein on the sucrose density gradient, Fig. 21(A). By extrapolation to infinite dilution the sedimentation coefficient of cylindrin was determined to be 22.5S and of torin 9.0S.

and cattle erythrocytes is shown in Chart 11. For comparison purposes the amino acid analysis of Spectrin (Tillack et al, 1970 and Shotton et al., 1979), the pH 4.5 precipitate of Hamaguchi and Cleve (1971) which is very heterogeneous and rich in spectrin, and the pH 4.5 supernatant of Hamaguchi and Cleve (1971), which contains one predominant polypeptide with two minor bands, are included. While there is a considerable degree of agreement between the composition of the human and cattle cylindrin, there are distinct differences between both cylindrins and human spectrin. The amino acid composition of cylindrin is not unlike that of other proteins which form multimeric structures, such as tubulin.

Isoelectric focusing:

Determination of the isoelectric point of human cylindrin and torin has been performed in 7% polyacrylamide tube gels containing 1% Ampholine (pH range 3 to 6). Cylindrin has an isoelectric point of approximately 4.6 and torin of 4.8, see Fig 28. These figures agree reasonably well with the determinations of Bhakdi et al., (1974), who obtained isoelectric points of pH 4.6 and 4.8 for polypeptide bands 7 and 8 of the erythrocyte membrane (by SDS polyacrylamide gel electrophoresis), which they maintained represented the most homogeneous proteins in the EDTA extract. The pH precipitation curve of soluble ghost protein (SGP of Deas et al., 1979 and Fig. 9), conforms with the cylindrin isoelectric point, although SGP does contain some spectrin which also precipitates in the pH 5 range. Why torin remains soluble at pH 5.1 is not clear, but it is a well established fact that not all proteins become insoluble at or close to their isoelectric points.

Immunochemical studies:

The immunoelectrophoresis studies of Howe and Lee (1969) revealed that their water soluble proteins from erythrocyte membranes (SGP) gave three predominant precipitin lines with antisera against haemoglobin-free ghosts. Apart from spectrin, Deas et al., (1979) maintain that catalase is a componenet of SGP, but their SDS-PAGE indicates the presence of several components,

Chart 11

Amino Acid Composition of Cylindrin and Spectrin

	A Human Cylindrin	B Cattle Cylindrin	C Human Spectrin	D Human Spectrin	E pH 4.5 ppt.	F pH 4.5 sup.
4Hypro	2.0	5.5	---	---	---	---
Asp	106.8	104.0	103.2	109.0	100.0	95.0
Thr	52.9	50.8	41.6	36.0	48.0	64.0
Ser	63.3	65.9	57.0	41.0	57.0	77.0
Glu	126.7	129.3	184.7	205.0	161.0	118.0
Pro	41.7	52.7	22.5	24.0	39.0	61.0
Gly	70.0	79.6	45.2	49.0	58.0	81.0
Ala	84.5	86.3	84.4	92.0	85.0	81.0
Val	59.2	64.5	49.9	47.0	53.0	71.0
Met	2.7	7.0	18.0	17.0	21.0	13.0
Isoleu	42.1	41.1	42.0	40.0	42.0	37.0
Leu	88.2	88.5	122.0	124.0	121.0	93.0
Tyr	27.4	26.0	20.7	20.0	26.0	28.0
Phe	31.1	34.6	31.5	30.0	37.0	35.0
Lys	63.2	71.3	66.5	67.0	60.0	60.0
His	20.9	27.5	28.2	26.0	27.0	27.0
Arg	72.0	53.9	59.0	58.0	59.0	42.0
Cys	---	---	5.4	---	9.0	11.0
Tryp	---	---	17.5	---	---	---
	Mean of 3 Detns.	Mean of 2 Detns.				

(Number of Residues / 1000 Residues)

A and B, previously unpublished data of JRH; C from Shotton et al. (1979); D from Tillack et al. (1970); E and F from Hamageuchi and Cleve (1971).

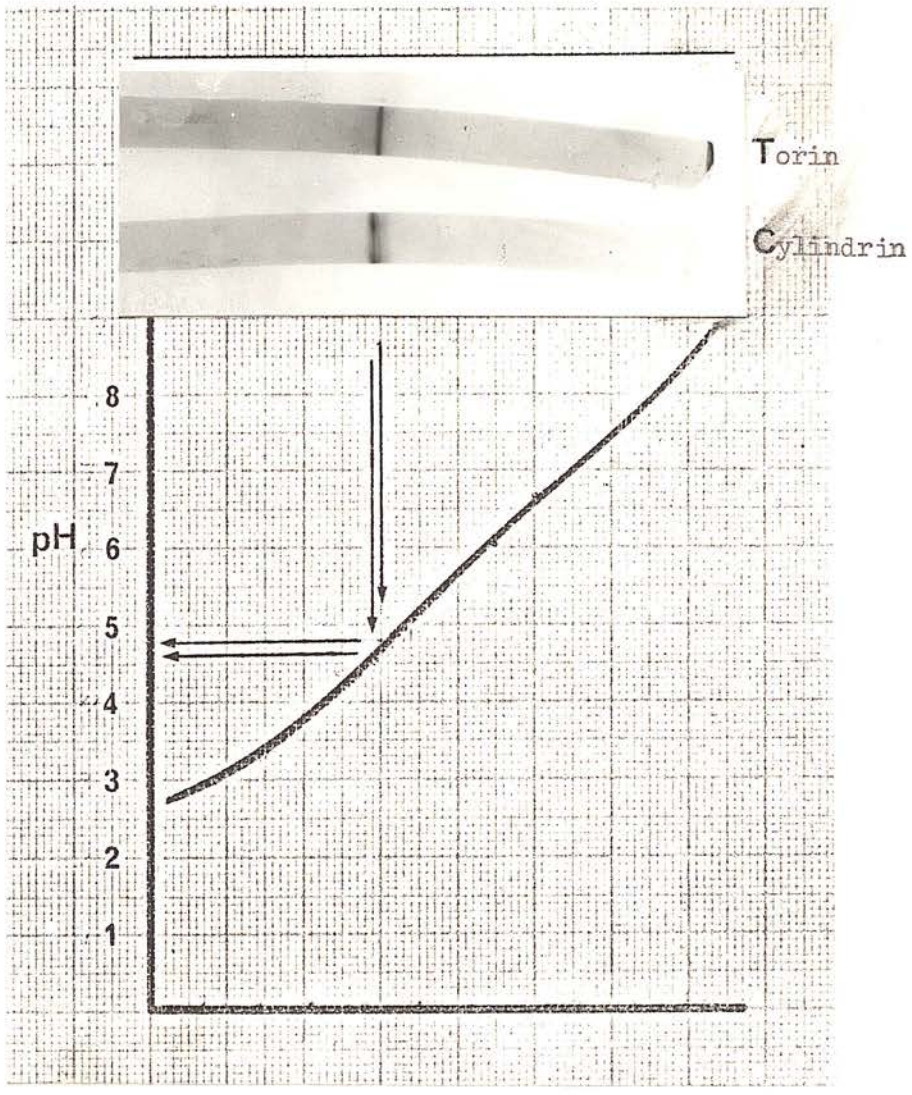

Fig. 28. Isoelectric focusing of cylindrin and torin on 7% polyacrylamide gel containing 1% ampholine (LKB), pH range 3 to 8. By extrapolation from a blank gel which was sliced for plotting a curve of pH versus gel length, the isoelectric points of cylindrin and torin were determined as approximately 4.6 and 4.8, respectively. The presence of a single band of stained protein provides further support for the assessment of purity obtained by polyacrylamide gel electrophoresis and electron microscopy.

among which are torin and cylindrin, see Figs. 7 and 8.

It is important that the antisera against T-protein (predominantly cylindrin, see Fig. 29) and the antisera against haemoglobin-free membranes both gave a single precipitin line in immunoelectrophoretic analysis of T-protein (Howe and Bachi, 1973), otherwise their immunoferritin labeling of the cytoplasmic surface of intact ghosts (Fig. 13), could be open to misinterpretation, particularly if there is the possibility of there being any spectrin present. Unfortunately no SDS-PAGE of T-protein was included in this study. The earlier Ouchterlony immunodiffusion studies of Hamaguchi and Cleve (1971) showed that the pH 4.5 supernatant of their water dissolved erythrocyte membrane proteins gave a single precipitin line, whereas SDS PAGE of the same material showed one predominant polypeptide (possibly band 5) together with two minor bands of lower molecular weight, one of which could be torin.

Our own immunodiffusion studies (Harris, 1974) indicate that the initial water extract contains several predominant antigens (Fig 30.). On separating cylindrin by sucrose density gradient centrifugation, the precipitin line closest to the antigen well is lost from the fractions taken from the sucrose gradient top, but appears as a single line against the sample of purified cylindrin. The pronounced precipitin line against the sucrose gradient top, which is rich in torin, appears to cross the line given by the purified cylindrin possibly indicating separate antigenicity of the two proteins. Nevertheless, more detailed immunoelectrophoretic studies are required to show conclusively that native and dissociated torin and cylindrin carry different antigenic determinants.

Electron Microscopy

Image Interpretation:

The two predominant electron optical images of cylindrin are readily appreciated because of the stable end-on and side-on orientations of the molecule with respect to the carbon support film (Fig. 31). With torin, the situation is not quite so simple.

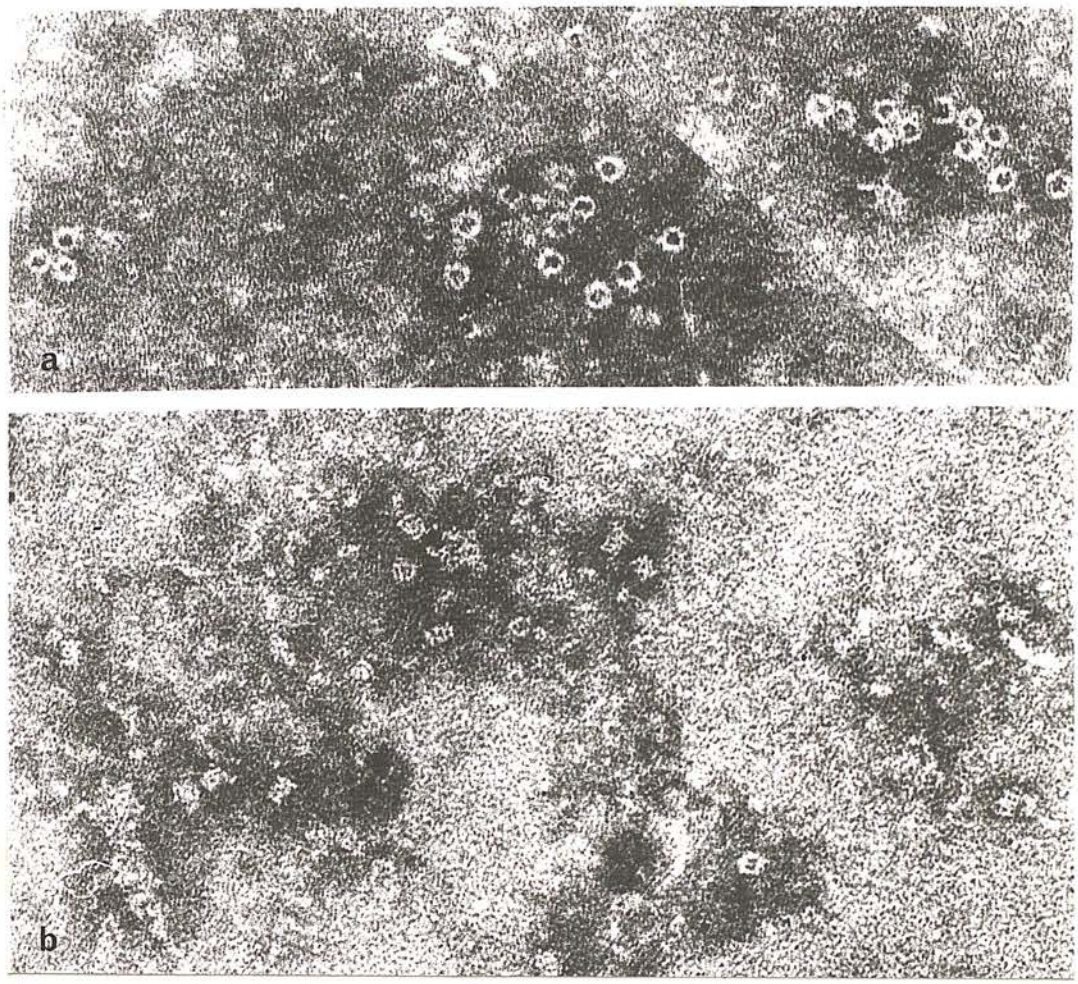

Fig. 29. Negatively stained (T) protein purified by Howe and Bächi (1973), using 2% sodium phophotungstate (pH 7.2). (a) shows pronounced ring-like molecules which may be either torin or cylindrin. (b) shows cylindrin molecules orientated on their sides together with a few ring-like profiles of torin and cylindrin. The scale markers indicate 100 nm. With the permission of Academic Press.

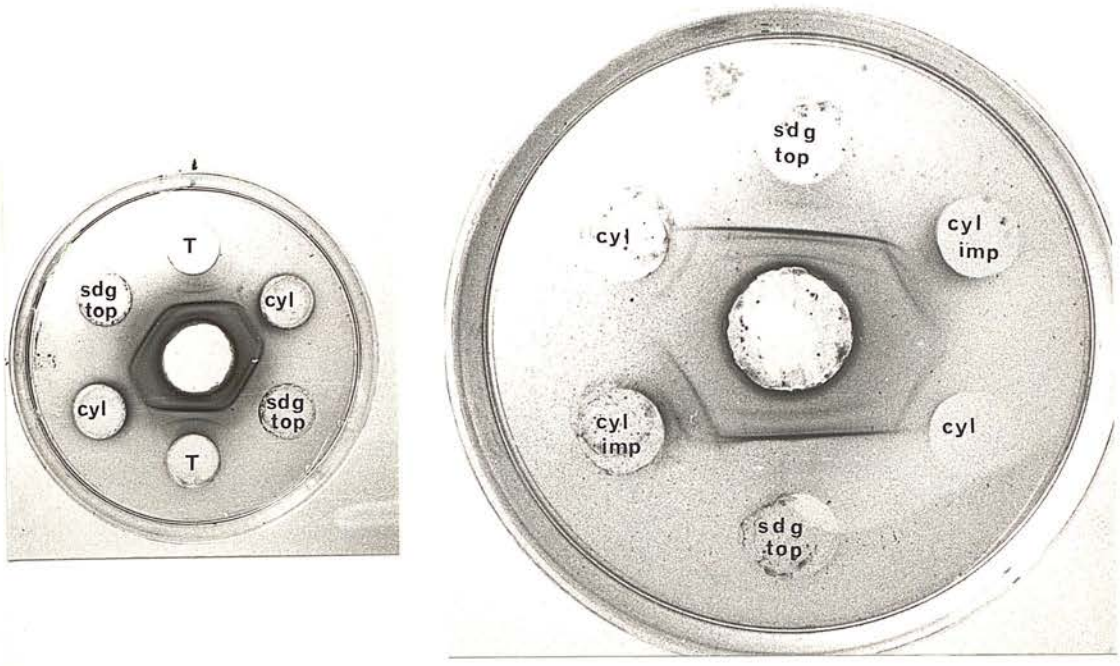

Fig. 30. Ouchterlony double diffusion analysis of the distilled water extract from human erythrocyte ghosts and sucrose density gradient (sdg) fractions. Note the presence of the precipitin arc close to the total extract (T) on plate (A), which fuses with the arc against purified cylindrin. This arc is absent from the sucrose density gradient top, plates (A and B), which contains a predominant arc, in all probability produced by torin. The cylindrin and torin precipitin arcs are seen to cross on plate (B).

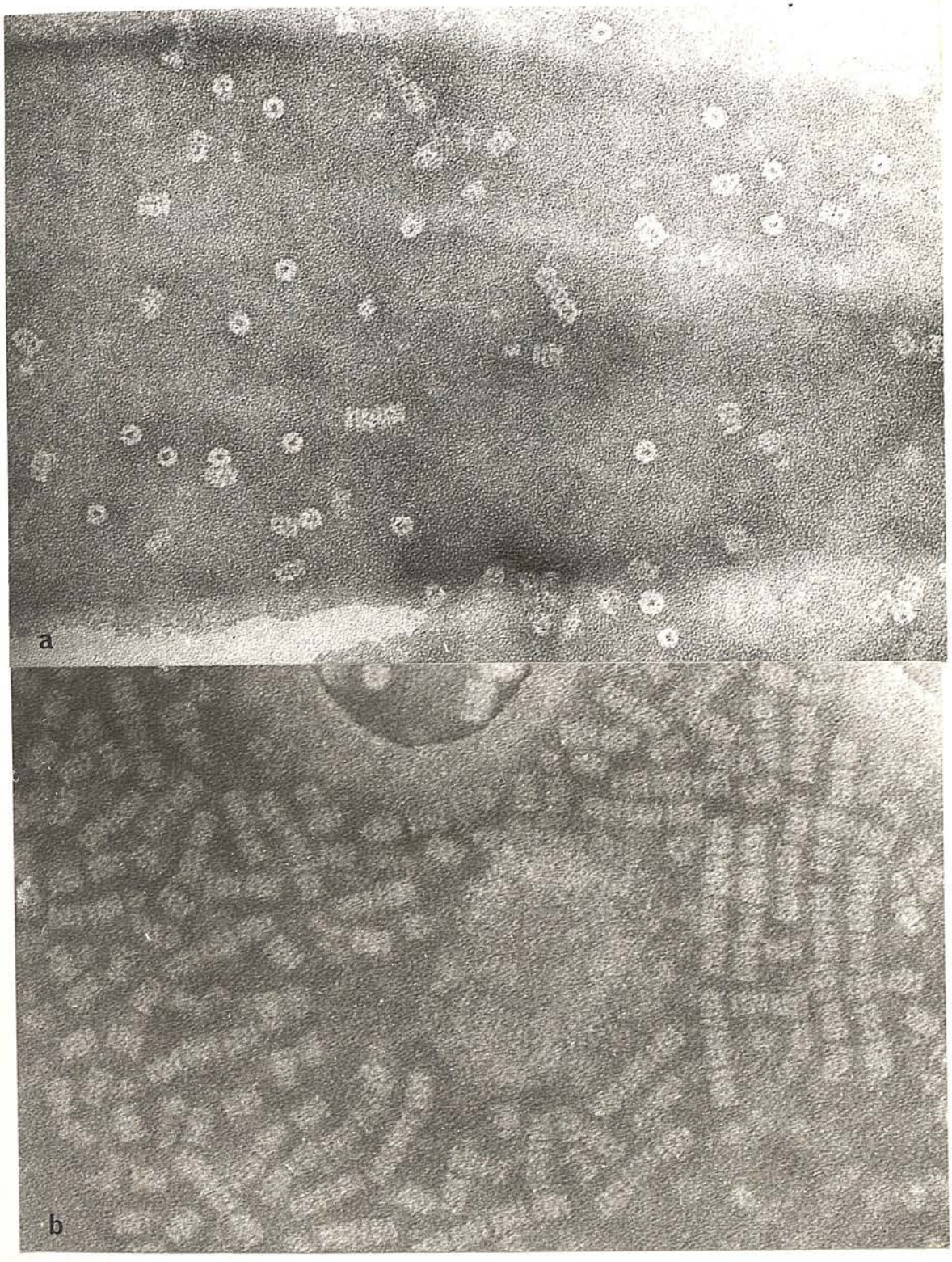

Fig. 31. Cylindrin purified by sucrose density gradient centrifugation;
(a) negatively stained with 2% uranyl acetate (pH 4.5), x 300 000,
(b) negatively stained with 2% sodium phosphotungstate (pH 7.0), x 400 000.
See also, Fig. 22.

In shallow negative stain the molecules of torin have a strong tendency to all orientate themselves on their sides, giving the pronounced ring-like image (Figs. 19 and 32), as long as there is no overlapping of molecules. In deeper stain, the molecules have the possibility of being trapped at various orientations relative to the carbon support film as the negative stain dries. This, in theory, will produce ring-like images, a variety of oval images and pronounced paired-dot images (Harris, 1969b), as shown in Figs. 2 and 33). The paired-dot image is readily comprehended if one summates the thickness of a vertically orientated torin molecule within a pool of surrounding negative stain, which thereby provides two maxima for the transmission of electrons. Exactly the same reasoning underlies the ring-like image of the spherical apoferritin molecule, a zone through the diameter of which would result in the paired-dot image (i.e., from a torus), and likewise, the rotation of the paired-dot image through 180° would produce the ring-like image from a hollow spherical structure, (i.e., apoferritin).

There is some evidence that negative stain is able to penetrate within the subunits of torin, producing an electron dense region with the centre of each of the electron transparent regions of the paired-dot image (Fig. 32), this being particularly apparent when uranyl acetate staining is used. Because of the complex summated nature of this electron optical image from the vertically orientated protein, great care must, nevertheless, be taken not to propound artifactual features of the protein structure. The penetration of negative stains between and within the polypeptides of a multimeric protein will undoubtedly be dependent upon the hydrated spaces available and also on the localized electrical charge on the peptide chain. From the negative staining results using sodium phosphotungstate, it is apparent that this stain does not have a tendency to reveal the side-on orientated cylindrin molecule as a row of four paired-dots, whereas uranyl acetate does indicate this image at least to some extent (see Fig. 35), possibly because of its greater ability to scatter electrons and because of charge attraction of the uranyl cation. The dimensions of torin and cylindrin shown in Chart 111

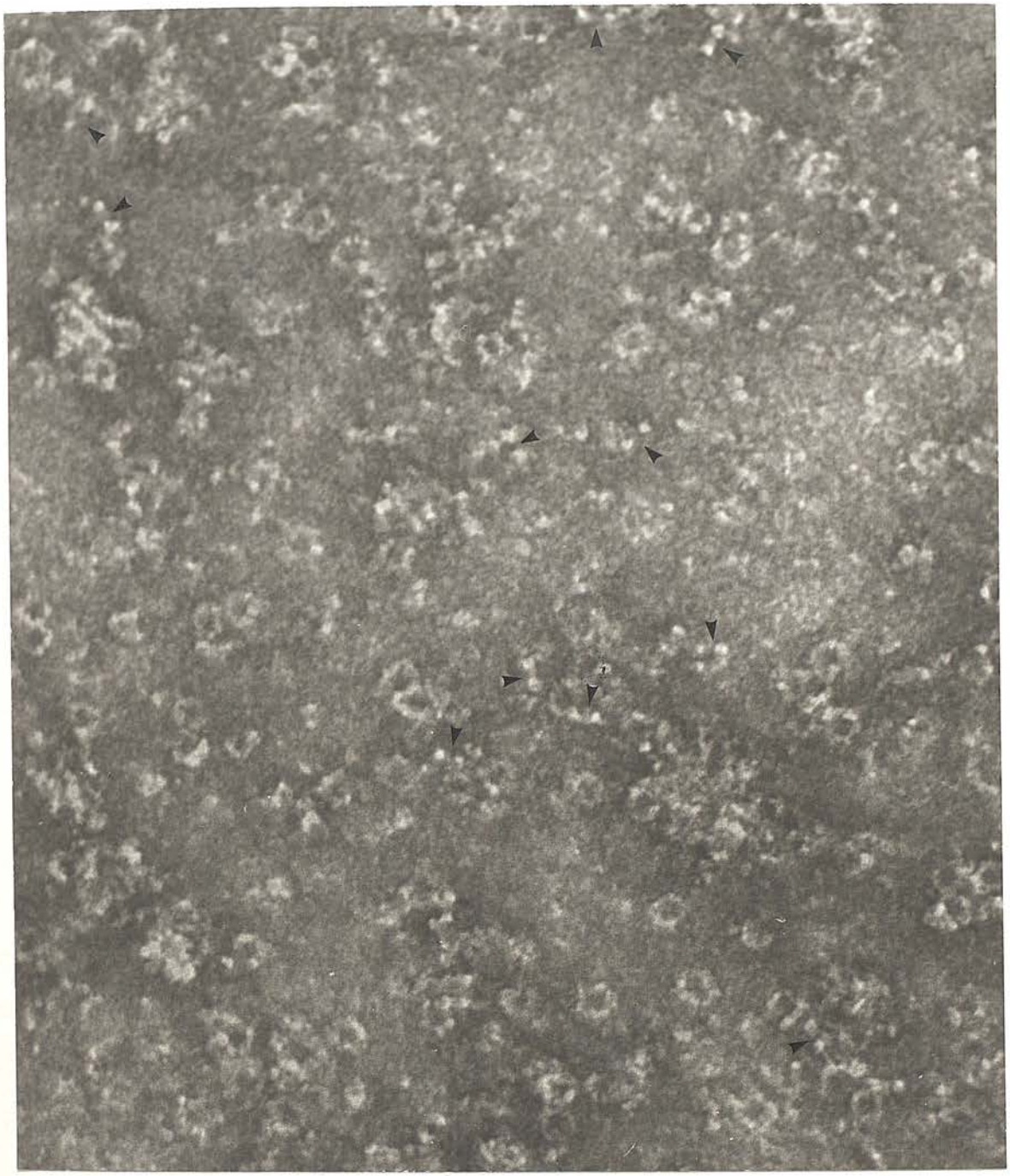

Fig. 32. Purified torin obtained by gel filtration chromatography Ultragel AcA34, negatively stained with 2% sodium phosphotungstate (pH 7.0). In the field shown there is relatively deep negative stain and the molecules are orientated at many different angles relative to the electron beam. The ring-like images are present (c.f. Fig. 19), and arrows indicate the paired-dot images. x 400 000.

Fig. 33. Purified torin at a slightly lower protein concentration than that in Fig. 32. In this field there is deep negative stain and the paired-dot image of torin predominates. Several faint oval and ring-like images are present (arrowed). Negatively stained with 2% sodium phosphotungstate (pH 7.0). x 400 000

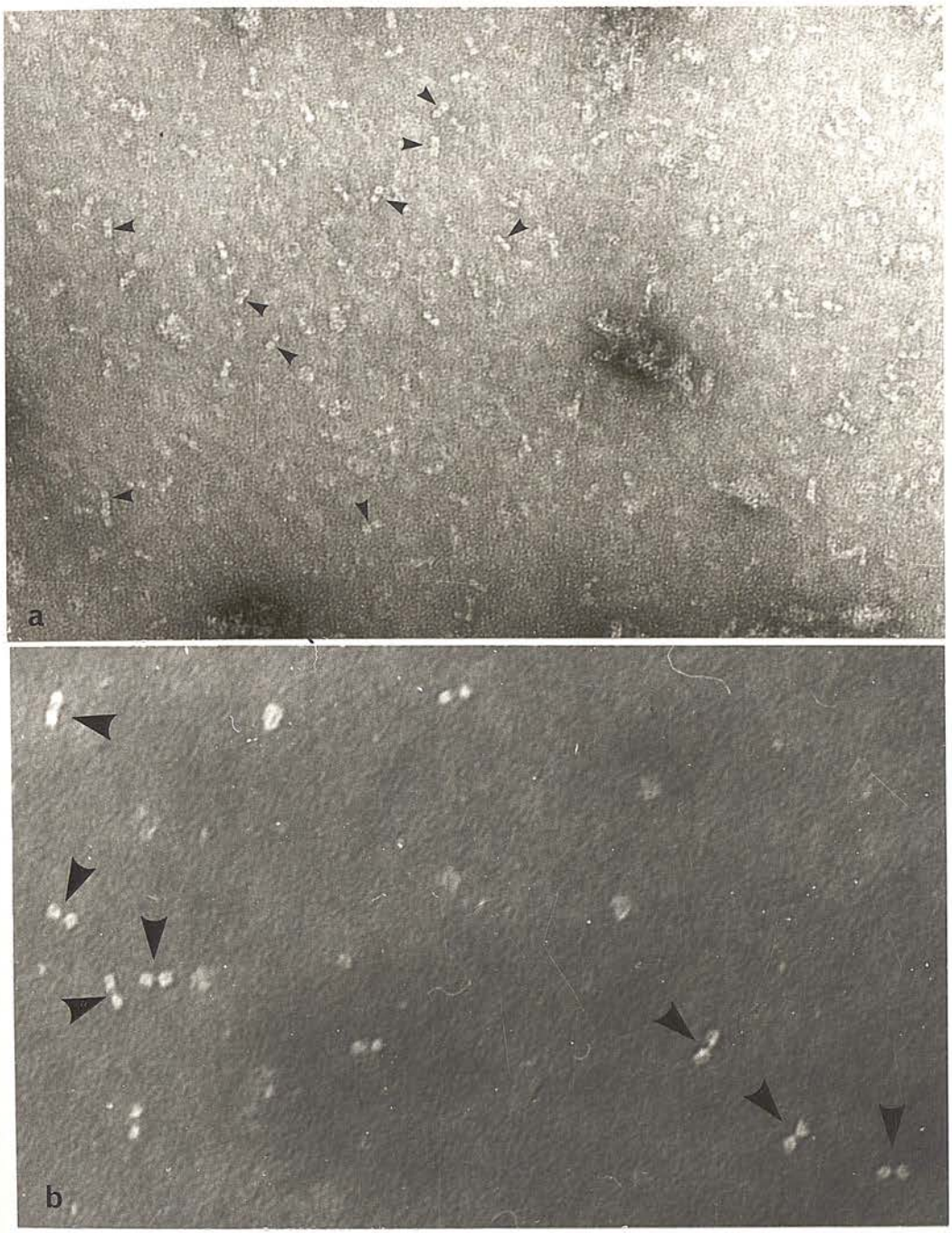

Fig. 34. The paired-dot image of torin showing an indication of stain penetration within the subunits, thereby producing electron dense centres to each of the 'dots'. (a) negatively stained with 2% uranyl acetate (pH 4.5); (b) negatively stained with 2% sodium phosphotungstate (pH 7.0). Arrows indicate molecules showing the feature described.
x 200 000 and x 400 000, respectively.

Fig. 35. Purified cylindrin indicating the penetration of negative stain into the hollow core of the molecule, thereby producing an image of the molecule on its side resembling four paired-dots (arrowed). Negatively stained with 2% uranyl acetate (pH 4.5). x 300 000

Chart 111

A. Dimensions of Negatively Stained Torin

(a) Horizontal Orientation of Ring-Like Image:

Inner diameter	6.0 ± 0.4 nm
Outer Diameter	13.1 ± 0.5 nm
Mean of inner and outer diameter	9.6 ± 0.5 nm

(b) Vertical Orientation 'Paired Dot' Image:

Dot inner edge-to-edge distance	2.7 ± 0.6 nm
Dot outer edge-to-edge distance	12.4 ± 0.5 nm
Dot centre-to-centre distance	8.0 ± 0.6 nm

B. Dimensions of Negatively Stained Cylindrin

(a) End-on Orientation:

Inner diameter	4.0 nm
Outer diameter	12.0 nm
Mean of inner and outer diameter	8.0 nm

(b) Side-on Orientation:

(i) The 'Striped' Rectangle:

Width of rectangle	12.5 ± 0.4 nm
Length of rectangle	17.0 ± 0.4 nm

(ii) The Tetramer of 'Paired dots':

Dot inner edge-to-edge distance	3.0 nm
Dot outer edge-to-edge distance	12.0 nm
Dot centre-to-centre distance	8.0 nm
Length of tetramer	17.0 nm

Dimensions were measured using a x5 micrometer (Graticules Ltd), on photographs printed at a final magnification of x 200 000. Standard deviations of the mean were calculated where possible from the dimensions of 50 molecules. Modified from Harris (1969b).

(from Harris, 1969b), do indicate fundamental differences between the internal and external diameters of the two molecules, which though not emphasised at the time, now appear to be significant and provide supportive evidence for the proposal that torin and cylindrin are unrelated molecules. The banded rectangular image of the side-on cylindrin molecule usually indicates that the central pair of protein rings are more closely fused than the peripheral ones (Harris, 1971b). In view of the fact that no groups of two and three rings are encountered, or indeed groups of five or more, it would appear that the subunits of the central pair of rings in cylindrin differ from those of the peripheral rings. Thus, if torin was in any way related to cylindrin, it might not be to the complete molecule, but only to the central or peripheral tori, and these possibilities cannot be ruled out at the moment.

Application of the photographic technique for rotational enhancement of structural symmetry within regular biological structures (Markham et al., 1963) had indicated that torin contains ten subunits (Fig. 36). As the molecular weight of the dissociated subunits is approximately 20,000 which is reasonable when compared with the figure of 18,500 for the subunit of apoferritin and the resultant native molecular weight of approximately 200,000 is acceptable, when correlated with the sedimentation coefficient of 9.0s. The more complex cylindrin molecule presents the additional difficulty that the number of subunits in its inner rings may not be the same as the peripheral rings. The rotational image enhancement technique generally indicates the presence of eight subunits (Fig. 37), which would suggest that the intact molecule contains approximately four times this number. The complex image summation of the four rings of subunits within cylindrin may be responsible for the fact that on occasions molecules appeared to have a nine-fold symmetry. Extrapolation on the basis of eight subunits of mean molecular weight approximately 25,000 would result in a native molecular weight of approximately 800,000, which is compatible with the figures obtained from analytical ultra-centrifugation (see above), and a sedimentation coefficient of 22.5 S.

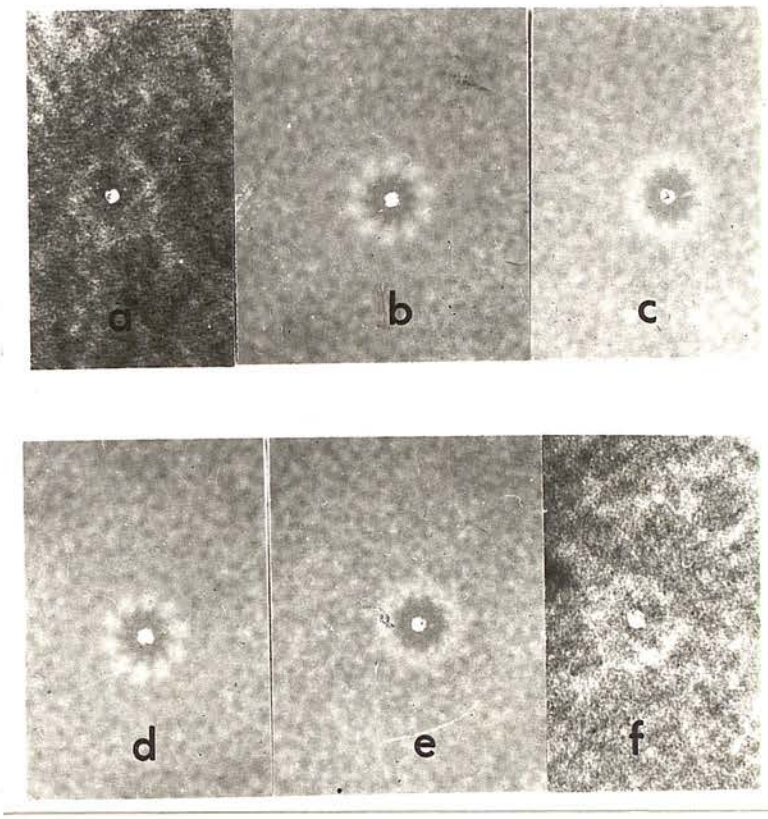

Fig. 36. Rotational image enhancement of torin, which indicates the probable presence of ten subunits. (a and f) unrotated molecules; (b and d), molecules rotated by 360°/10; (c) molecule rotated 360°/11; (e) molecule rotated 360°/9. x 500 000 approx. From Harris (1969b), with the permission of Academic Press.

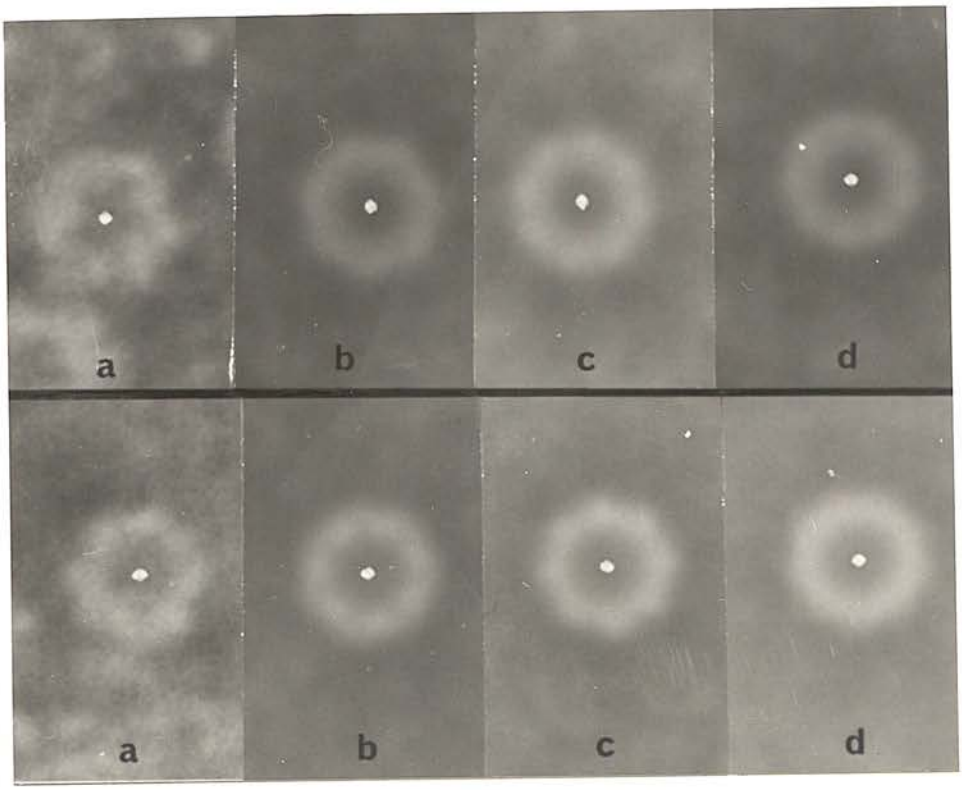

Fig. 37. Rotational image enhancement of cylindrin, indicating the probable presence of eight subunits in each of the four rings of protein. (a) unrotated; (b) rotated $360^{\circ}/7$; (c) rotated $360^{\circ}/8$; (d) rotated $360^{\circ}/9$. x 800 000.

Paracrystalline Arrays:

For high resolution electron microscopic studies on protein conformation which utilize optical diffraction analysis, it is necessary to have regular arrays of precisely orientated molecules, from which accurate averaging of molecular sub-structure can be obtained (Unwin and Henderson, 1975). A technique has recently been developed for the production of monolayer arrays of regular viruses (Horne and Pasquali-Ronchetti, 1974). This technique utilizes the affinity of the hydrophilic surface and net charge of freshly cleaved mica to produce paracrystalline monolayers of viruses mixed with negative stain, usually ammonium molybdate. The crystalization is influenced by the pH of the negative stain used on the mica and also during the second stage of the technique when the carbon coated layer of virus particles is floated off onto negative stain, usually uranyl acetate, prior to attachment to a holey carbon film. Attempts to produce paracrystalline monolayer arrays of torin and cylindrin using this technique have been only partly successful (Harris, 1978). A major problem appears to be the presence of either trace amounts of contaminatory proteins or partly dissociated proteins, which interfere with the packing of the molecules into ordered arrays. Fig. 38 shows representative results obtained with torin, using 2% ammonium molybdate pH 7.0 as the first negative stain and 2% uranyl acetate pH 4.5 as the second negative stain. There is some indication of molecular packing, but no regularity is present. The possibility that protein molecules lie at varying orientations to the electron beam and that they may lie on top of one another is bound to prevent paracrystal formation. With cylindrin, small regions of regularly packed molecules have been detected, with molecules on their sides and on their ends, see Fig. 39. Insufficiently large groups of ordered molecules have been detected to justify performing optical diffraction analysis. One fundamental problem is that cylindrin appears to have a strong tendency to dry down on the mica as discrete groups of four molecules which are so arranged (Fig. 40) as to prevent any subsequent build up into a regular array, because of the offset nature of the molecular interaction. Despite the limited success achieved to date, it is

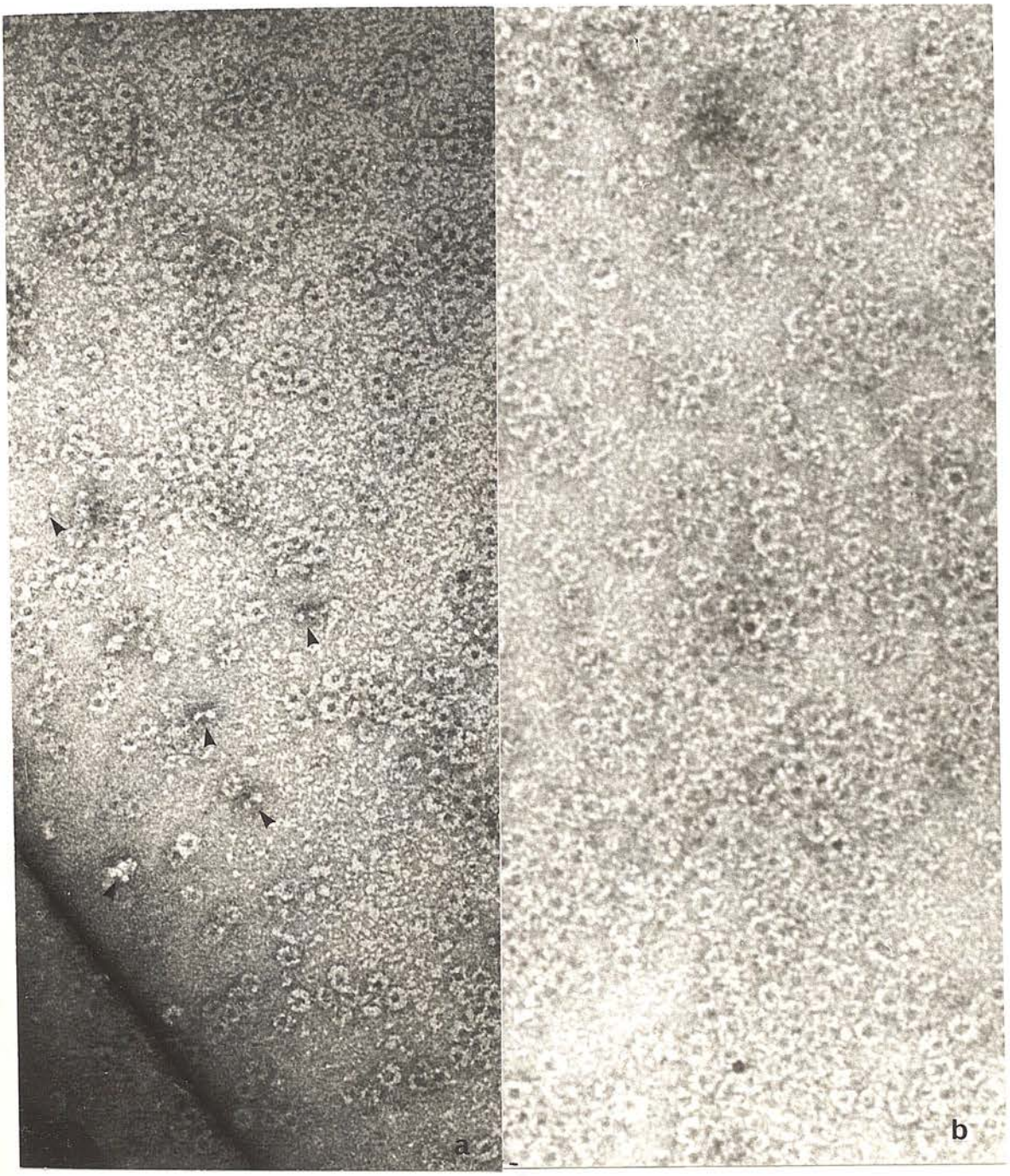

Fig. 38. Application of the carbon-film negative staining technique to purified torin. In (a) the molecules are well dispersed, but show a tendency to group toegether as random arrangements. Arrows indicate molecules in deeper stain exhibiting the paired dot image. In (b) there are more molecules spread as an almost continuous monolayer, which does not reveal any regularity of packing, possibly due to molecules overlapping. x 300 000

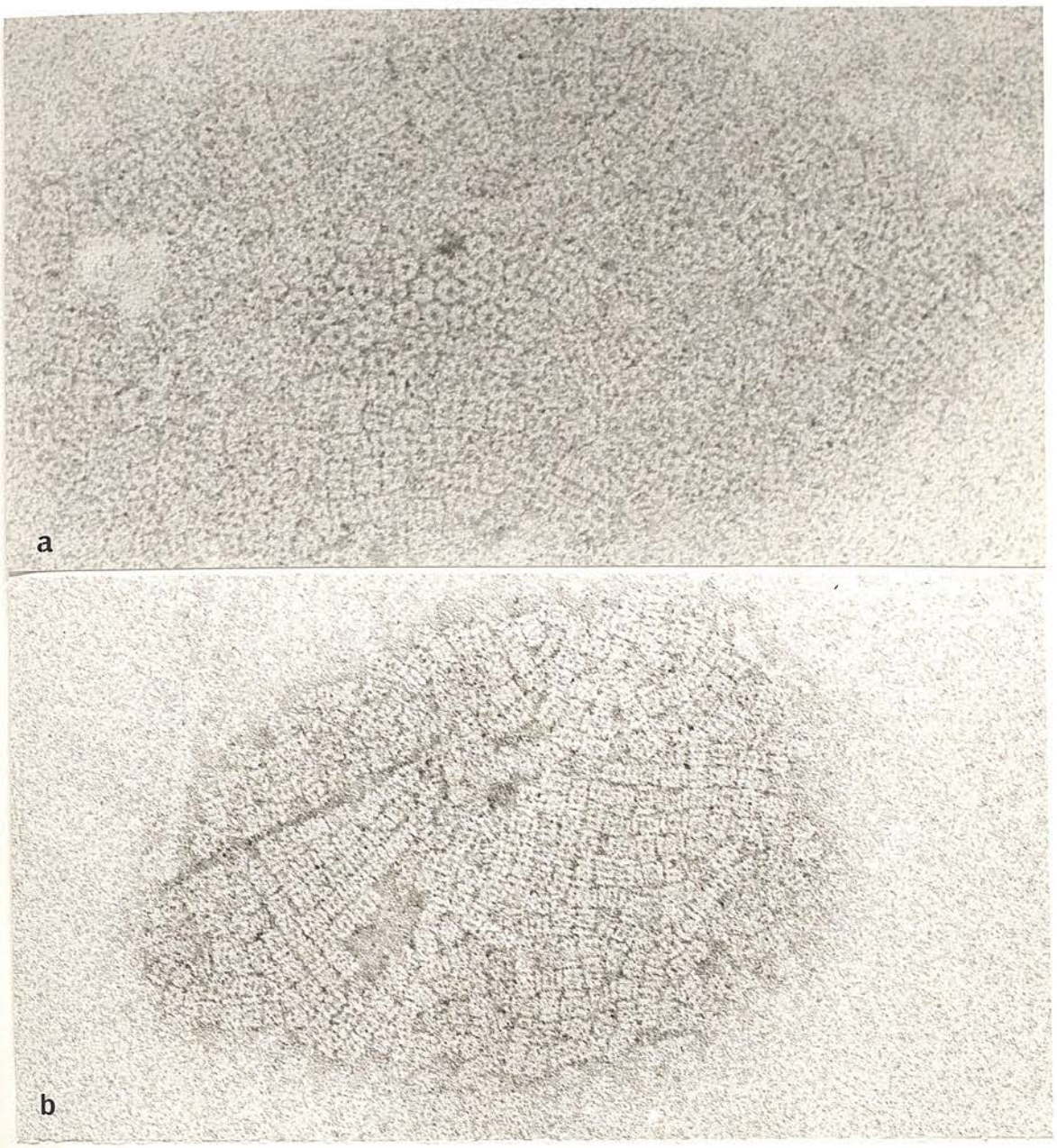

Fig. 39. Application of the carbon-film negative staining technique to purified cylindrin. (2% ammonium molybdate at pH 7.0 on the mica, followed by 2% uranyl acetate, pH 4.5). In (a) a group of molecules can be see which are orientated on their ends exhibiting hexagonal packing. In (b) most of the molecules are orientated on their sides as a randomly packed array. x 300 000.

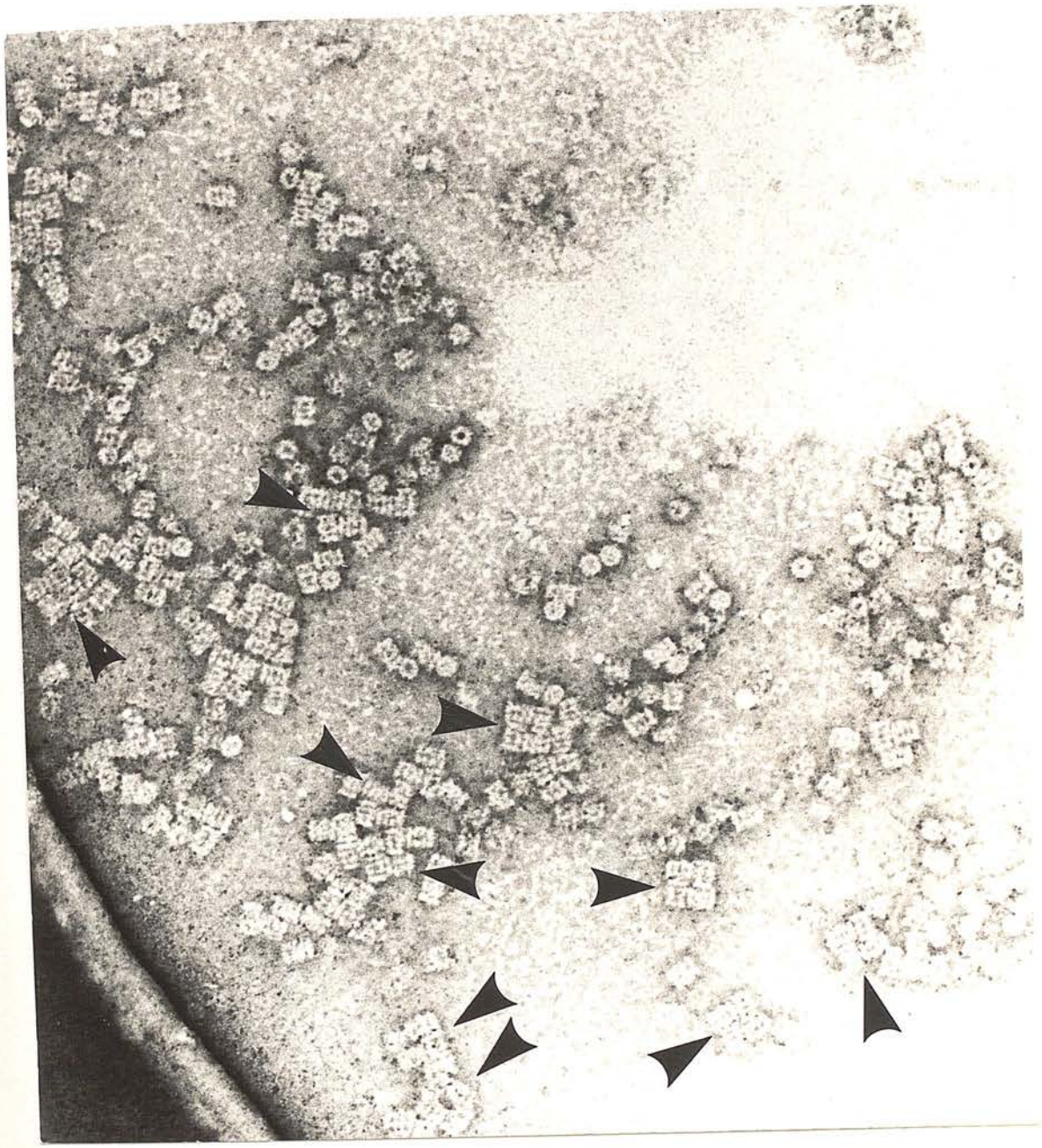

Fig. 40. Groups of four offset cylindrin molecules orientated on their sides (arrowed), in an arrangement that would prevent the subsequent nucleation of a regular monolayer array. Negatively stained by the carbon-film technique, as in Fig. 39. x 244 000.

quite possible that further effort might produce superior results, particularly if torin and cylindrin of high purity can be obtained, which could also be rendered more stable by intra-molecular crosslinking with glutaraldehyde or other agents.

Phase Contrast Studies

Cylindrin has been used in the electron microscope as a test material on which to apply the relatively new and little exploited technique of single sideband phase contrast interference (Harris and Kerr, 1976). This technique, which in practical terms is a type of electron optical shadowing (Haydon and Lemons, 1972 Haydon, 1974), is somewhat equivalent to the light microscopic Nomarski differential interference system in that it induces optically a three dimensional shadowed type of image. In our hands the optimal electron optical conditions were achieved by tilting the electron beam from pre-set dark field conditions obtained by hollow cone illumination. Fig. 41 shows a comparison of cylindrin illuminated under bright field and single sideband phase contrast interference conditions. It is seen that under the phase contrast conditions there is a superior image contrast as well as an apparent three dimensional nature to the profiles of the molecules. Scanning microdensitometry performed on individual molecules confirms the visual assessment of the contrast increase (Fig. 42).

General Discussion and Future Developments

Although no functional activities have been discovered for torin and cylindrin it must be highly probable that these proteins do possess as yet unknown enzymic activity. For instance, torin morphologically resembles the enzyme sucrose, isolated from rabbit intestinal epithelium by papain digestion (Nishi et al., 1968), and also the foraminotransferase-cyclodeaminase complex from pig liver (Beaudet and Mackenzie 1976). It has been claimed by Berg and Ekholm (1975) that mouse thyroglobulin produced under conditions of low iodination has the conformation of a cylinder 25 nm long and 13.5 nm in diameter, as well as more compact structures resembling α_2-macroglobulin. The sedimentation coeficient of 19S was given

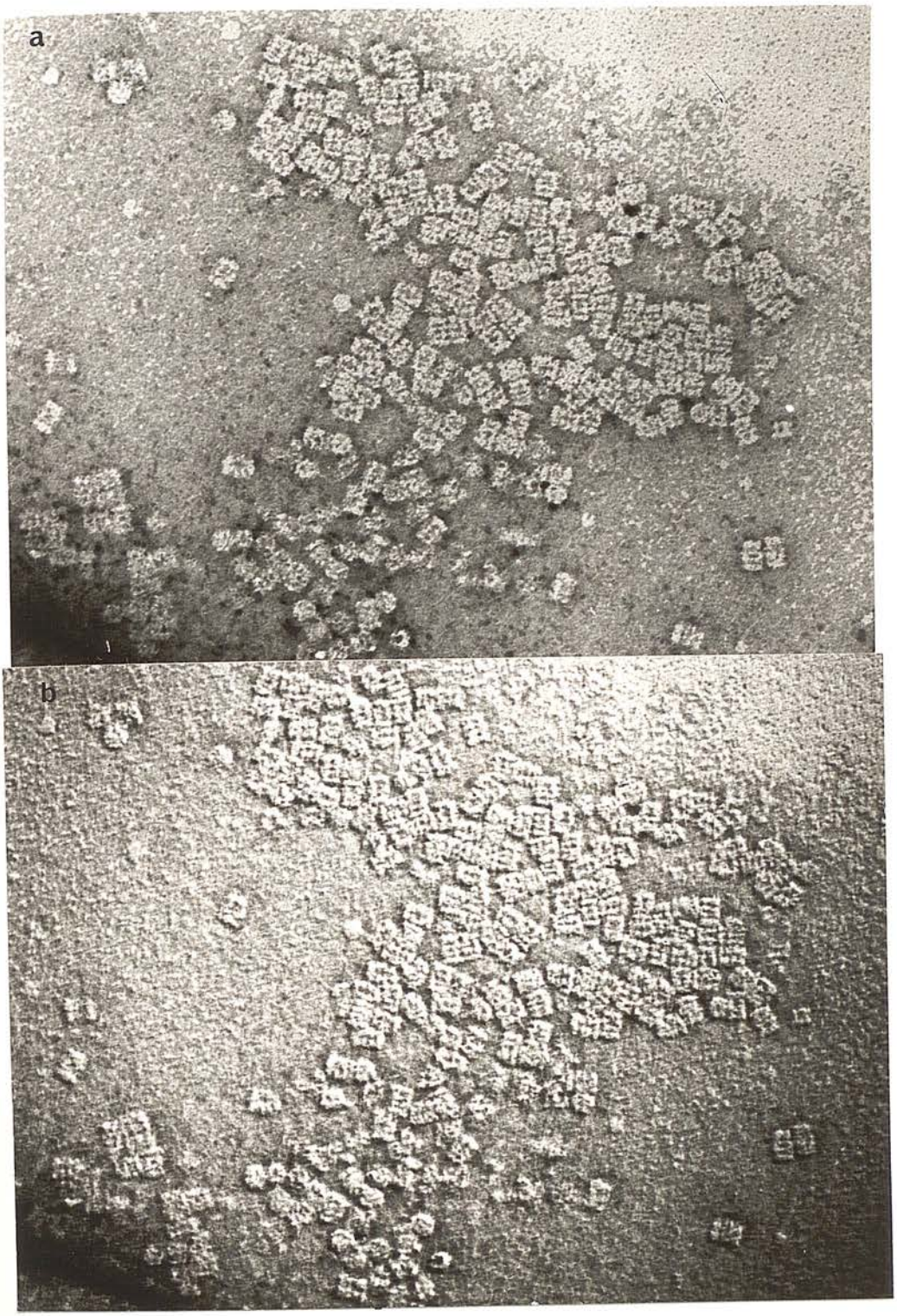

Fig. 41. The image of purified cylindrin molecules obtained by single sideband phase contrast interference (electron optical shadowing) (b), for comparison with conventional bright field electron optics (a). Three dimensional shadowing is induced by this technique, which also provides a superior image contrast. Negatively stained by the carbon-film technique, as for Fig. 39. x 244 000

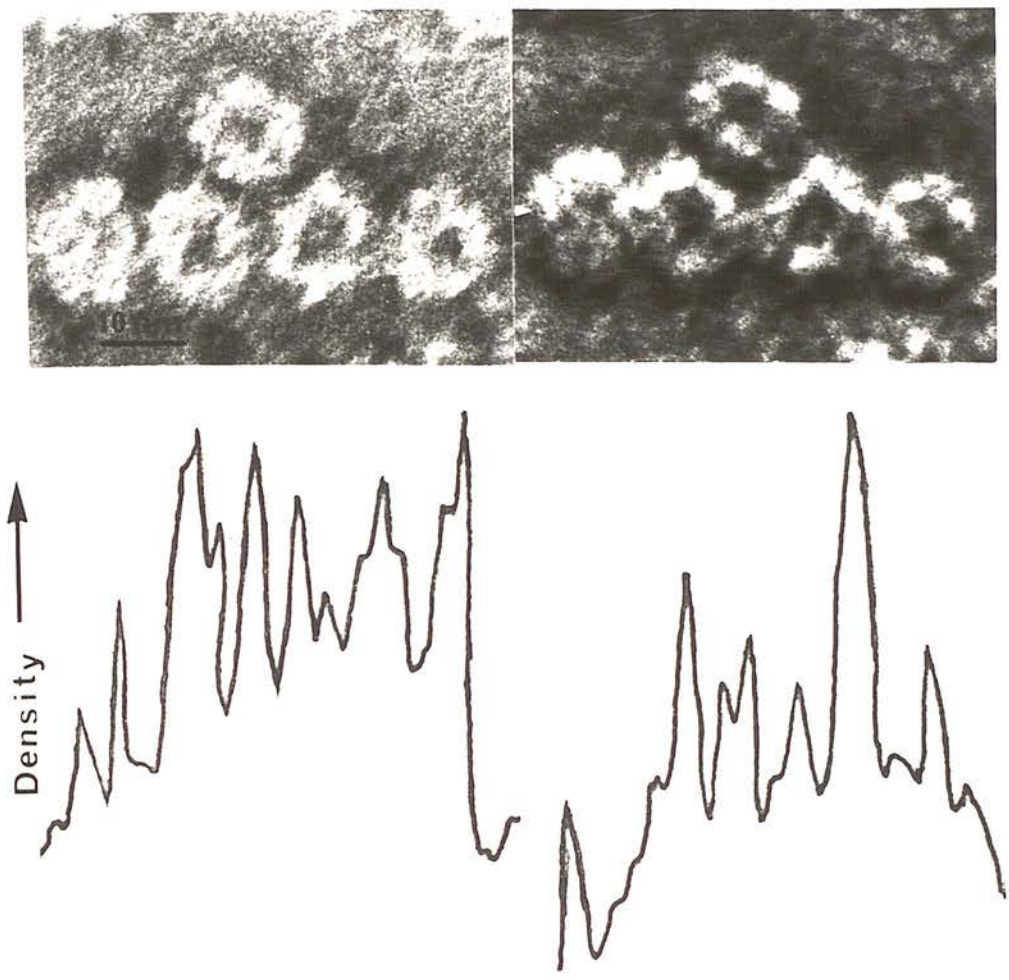

Fig. 42. Densitometry of cylindrin molecules on micrographs obtained by bright field and single sideband phase contrast interference confirms the subjective assessment of the increased contrast produced by single sideband phase contrast interference. x 1 107 000. From Harris and Kerr (1977) with permission of Blackwell Scientific Publications Ltd.

by Berg and Ekholm (1975) for their thyroglobulin, which is compatible with cylindrin and α_2-macroglobulin, so it is possible that these molecules were present as contaminants in the thyroglobulin. Two proteins which closely resemble cylindrin are the "22S antigen" from Bordetella pertussis (Sato and Nagase 1967) and groE from E. coli, (Hohn et al., 1978), both of which are of unknown function, but may be related to bacteriophage tail proteins.

Recent studies on the erythrocyte membrane cyclic AMP stimulated protein kinase (Boivin and Galand, 1978) indicate that this enzyme is soluble at pH 5.3 and can be precipitated by 50% ammonium sulphate, as is torin. The subunit composition of this enzyme, subsequently isolated from the cytosol (Boivin and Galand, 1979) indicates the presence of a regulatory subunit of about 48,000 and a catalytic subunit of about 30,000, which does not suggest an identity with torin.

Earlier studies (Boivin and Galand, 1977), do however, indicate that several of the low molecular weight polypeptides detected on SDS-PAGE that have been derived from a pH 5.3 soluble fraction of erythrocyte ghosts, do become phophorylated by the cyclic AMP-dependent protein kinase, so it is possible that torin could be among these. It is interesting that the recent study of Allen and Cadman (1979) has shown that in the presence of increased cellular calcium erythrocyte membranes tend to bind greater quantities of cytosol proteins, in particular catalase (band 45) and band 8 of the membrane SDS-PAGE polypeptides. Furthermore, they confirm that band 8 is EDTA extractable from the membranes, has a subunit molecular weight of approximately 24,000 and a pI of 5.35, figures which are compatible with torin.

Any confusion between torin and cylindrin, and spectrin and its oligomers is clearly no longer justified (Harris and Naeem, 1978; White and Ralston, 1979). As pointed out by Deas et al. (1979) proteins other than spectrin precipitate in the pH range 4.5 to 5.5, and indeed that others including catalase and torin which have their isoelectric points in the same range but do not precipitate, may interact with spectrin within the matrix on the cytoplasmic

surface of the membrane. The concept that one of these extrinsic proteins could serve as a co-factor for a contractile system remains to be proven. Certainly, band 7 (cylindrin?) is implicated along with spectrin, actin and other polypeptides (Yu et al., 1973, Liu and Palek, 1980), by being present in the membranous skeleton which remains after Triton X-100 extraction.

Despite the lack of functional information relating to torin and cylindrin and the possibility that such information may be forthcoming eventually, there are several biochemical studies which can be profitably pursued. For instance, it would be of great interest to know whether the two (or three) subunits of cylindrin have differing aminoacid compositions and whether they behave as different antigens, as is the case for the spectrin polypeptides (Kirkpatrick et al. 1978). Immunological cross-reactivity of the cylindrin subunits with that of torin is also worthy of investigation, as is the amino acid composition of torin. Studies along these lines would be assisted by further knowledge of the dissociation properties of the two proteins, for instance by urea, guanidine hydrochloride, acidic conditions and ultrasonication, as well as subsequent knowledge of their re-association properties. As intimated earlier, the difficulties of paracrystalline monolayer production could well be overcome by more rigorous assessment of protein purity, together with protein stabilization to prevent dissociation during the mica/carbon film negative stain procedure. Attempts to produce true crystals of torin and cylindrin would also be worth while, as X-ray diffraction and low angle electron diffraction studies could complement optical diffraction analysis performed on electron micrographs of paracrystalline monolayers.

The ability of torin and cylindrin to bind to cationically charged liposomes could possibly provide an artificial membrane system for the further investigation of the ionic conditions required for membrane-extrinsic protein binding, which could also be pursued using inside-out erythrocyte membrane vesicles (Steck et al., 1970), Perhaps one of the most exciting future prospects, which stems from the greatly increased resolution afforded by SDS-PAGE on gradient gels (i.e., 3 to 30%), is the distinct possibility of relating functional disorders of the erythrocyte membrane to the increase or deletion of specific polypeptides (Banga et al. 1979; Allen et al. 1977).

REFERENCES

Allen, D.W. and Cadman, S.: Calcium-induced erythrocyte membrane changes. The role of adsorption of cytosol proteins and proteases. Biochem. Biophys. Acta 551, 1-9, 1979.

Allen, D.W. Cadman, S., McCann, S.R., Finke, B.: Increased membrane binding of erythrocyte catalase in hereditary spherocytes and in metabolically stressed normal cells Blood 49, 113-123, 1977.

Banga, J.P. Pinder, J.C., Gratzer, W.B., Linch, D.C., Huehns, E.P.: An erythrocyte membrane protein anomaly in march haemoglobinuria. The Lancet Nov. 17th 1048-1049, 1979.

Beaudet, B. and Mackenzie, R.: Foraminotransferase-cyclodeaminase from procine liver. Biochem. Biophys. Acta 453, 151-161, 1976.

Berg, G. and Eckholm, R.: Electron microscopy of low iodinated thyroglobulin molecules. Biochem. Biophys. Acta 386, 422-431, 1975.

Bhakdi, C., Knufemann, H. and Wallach, D.F.H.: Separation of EDTA-extractable erythrocyte membrane proteins by isoelectric focussing linked to electrophresis in SDS. Biochem. Biophys. Acta 345, 448-457, 1974.

Boivin, P. and Galand, C.: Phosphorylation of proteins extracte from human erythrocyte membrane. FEBS Lett. 79, 91-95, 1977.

Boivin, P. and Galand, C: Purification and characterization of an adenosine cyclic 3':5' monophosphate-dependent protein kinase from human erythrocyte membrane. Biochem. Biophys. Res. Commun. 81, 473-480, 1978.

Boivin, P. and Galand, C.: Purification and Characterization of a casein kinase from human erythrocyte cytosol. Biochem. Biophys. Res. Commun. 89, 7-16, 1979.

Deas, J.E., Lee, L.T. and Howe, C.: Peripheral proteins of human erythrocytes. Biochem. Biophys. Res. Commun. 82, 296-304, 1978.

Dodge, J.T., Mitchell, C. and Hanahan, D.J.: The preparation and chemical characteristics of haemoglobin-free ghosts of human erythrocytes. Arch. Biochem. Biophys. 100, 119-130, 1963.

Fairbanks, G.,Steck, T.L. and Wallach, D.F.H.: Electrophretic Analysis of the major polypeptides of the human erythrocyte membrane. Biochemistry 10, 2606-2611, 1971.

Haggis, G.H.: Electron microscopic study of the disruption of red cell membranes. Biochem. Biophys. Acta 193, 237-246, 1969.

Hamaguchi, H. and Cleve, H.: Properties of water dissolved membrane proteins of human erythrocytes. Biochem. Biophys. Acta 233, 320-333, 1971.

Harris, J.R.: The structure of the red blood cell membrane using the electron microscope. Ph.D Thesis, University of Edinburgh, 1968a.

Harris, J.R.: Release of a macromolecular protein component from human erythrocyte ghosts. Biochem. Biophys. Acta 150, 534-537, 1968b.

Harris, J.R.: The isolation and purification of a macromolecular protein component from human erythrocyte ghosts. Biochem. Biophys. Acta 188, 31-42, 1969a.

Harris, J.R.: Some negative contrast staining features of a protein from erythrocyte ghosts. J. Mol. Biol. 46, 329-335, 1969b.

Harris, J.R. and Agutter, P.S.: A negative staining study of human erythrocyte ghosts and rat liver nuclear membranes. J. Ultrastruct. Res. 33, 219-232, 1970.

Harris, J.R.: Further studies on the proteins released from haemoglobin-free erythrocyte ghosts at low ionic strength. Biochem. Biophys. Acta 229, 761-770, 1971a.

Harris, J.R.: The proteins release from intact erythrocyte ghosts at low ionic strength, Biochem. J. 122m 38-40p, 1971b.

Harris, J.R.: The location of a membrane-associated protein complex in human and bovine erythrocyte ghosts. J. Ultrastuct. Res. 36, 587-591, 1971c.

Harris, J.R.: The prufication of some membrane-associated proteins from erythrocyte ghosts. In Methodological Developments in Biochemistry, Vol. 4: Subcellular studies. ed., Reid, E., Longmans 1974, p. 395-404.

Harris, J.R.: and Maddy, A.H.: An electron microscopic study of some protein fractions from bovine erythrocyte ghosts. J. Ultrastruct. Res. 48, 190-200, 1974.

Harris, J.R. and Kerr, J.: Contrast enhancement of negatively stained macromolecules and biomembranes by single sideband phase contrast interference. J. Microscopy, 108, 51-59, 1976.

Harris, J.R.: Some problems associated with the production of paracrystalline arrays of protein molecules. Proc. Roy. Mic. Soc. 13, 29, 1978.

Harris, J.R. and Naeem, I.: The subunit composition of two high molecular weight extrinsic proteins from human erythrocyte membranes. Biochem. Biophys Acta 537, 495-500, 1978.

Haydon, G.B. and Lemons, R.A.: Optical shadowing in the electron microscope. J. Microscopy 95, 483-491, 1972.

Haydon, G.B.: Optical shadowing. In: Hayat, M.A., ed., Principals and Techniques of Electron Microscopy, Vol. 3, Van Nostrand Reinhold, 1974, -p. 1-15.

Hohn, T., Wurtz, M. and Engel, A: Sevenfold Rotational Symmetry of a Protein Complex. J. Ultrastruct. Res. 65, 90-93 (1978).

Hoogeveen, J.Th, Juliano, R., Coleman, J. and Rothstein,A:Water-soluble proteins of the human red cell membrane. J. Memb. Biol. 3, 156-172 (1970).

Horne, R.W. and Pasquali-Ronchetti, I.: A negative staining-carbon film technique for studying viruses. I. Preparative procedure for studying icosahedral and filamentous viruses. J. Ultrastruct. Res. 47, 361-383, 1974.

Howe, C. and Bachi, T.: Localization of erythrocyte membrane antigens by immune electron microscopy. Exptl. Cell. Res. 76, 321-332, 1973.

Howe, C. and Lee, L.T.: Immunochemical study of haemoglobin-free human erythrocyte membranes. J. Immunol. 102, 573-592, 1969.

Howe, C. and Bachi, T.: Localization of erythrocyte membrane antigens by immune electron microscopy. Exptl. Cell Res. 76, 321-332, 1973.

Kirkpatrick, F.H and LaCelle, P.L.: Comparison of preparations of erythrocyte membrane proteins by SDS-gel electrophoresis. Experientia 30, 140-148, 1974.

Kirkpatrick, F.H., Woods, G.M., LaCelle, P.L. and Weed, R.I.: Calcium and magnesium ATPases of the spectrin fraction of human erythrocytes. J. Supramolec. Struct. 3, 415-425, 1975.

Kirkpatrick, F.H., Woods, G.M. Wee, R.I. and LaCelle, P.L.: Fractionation of spectrin by differential precipitation with calcium. Arch. Biochem. Biophys. 175, 367-372, 1976.

Kirkpatrick, F.H., Rose, D.J. and La Celle, P.: Spectrin Bands 1 and 2 are antigemically distinct and are not composed of subunits. Arch. Biochem. Biophys. 186, 1-8, 1978.

Liu, S. C. and Palek, J.: Spectrin Tetramer-dimer equilibrium and the stability of erythrocyte membrane skeletons. Nature 285, 586-588, 1980.

Lux, S.E.: Spectrin-actin membrane skeleton of normal and abnormal red blood cells. Semin. Haematol. 16, 21-51, 1979.

Markham, R., Frey, S. and Hills, G.J.: Methods for the enhancement of image detail and accentuation of structure in electron microscopy: Virology 20, 88-102, 1963.

Mitchell, C.D., Mitchell, W.B. and Hanahan, D.J.: Enzyme and haemoglobin retention in human erythrocyte stroma. Biochem. Biophys. Acta 104, 348-358, 1965.

Moll, G.: A simple method of releasing 90Å particles, networks and ring-like micelles from human erythrocyte membranes. Cytobiologie 8, 150-157, 1973.

Moll, G.: Two-dimensional arrays of particles in negative staining preparations of fragmented human erythrocyte ghosts. Bioenergetics 6, 41-44, 1974.

Nermut, M.V. and Williams, L.D.: Freeze-fracturing on monolayers (capillary layers) of cells, membranes and viruses: some technical considerations. J. Microscopy 110, 121-132, 1977.

Nishi, Y., Yoshida, J.O. and Takesue, Y.: Electron Microscope Studies on the Structure of Rabbit intestinal sucrase. J. Mol. Biol. 37, 441-444, 1968.

Ralston, G.B.: Physico-chemical characterization of the spectrin tetramer from bovine erythrocyte membranes. Biochem. Biophys. Acta 455, 163-172, 1976.

Rubin, R.W. and Milikowski, C.L Over two hundred polypeptides resolved from the human erythrocyte membrane. Biochem. Biophys. Acta 509, 100-110, 1978.

Sato, Y., Nagase, K.: Isolation of Protective Antigen from Bordetella Pertussis. Biochem. Biophys. Res. Commun. 27, 195-201, 1967.

Seeman, P. and Iles, G.H.: Pits in the freeze-cleavage plane of normal erythrocyte membranes and ultrastructure of membrane lesions in immune lysis. Nouv. Rev. Franc. Hematol. 12, 889-900, 1972.

Shotton, D., Burke, B.E. and Branton, D.: The molecular structure of Human Erythrocyte spectrin. J. Mol. Biol. 131, 303-329, 1979.

Steck, T.L., Weinstein, R.S., Straus, J.H. and Wallach, D.F.H.: Inside-out red cell membrane vesicles: preparation and purification. Science 168, 255-257, 1970.

Tillack, T.W., Marchesi, S.L., Marchesi, V.T., and Steers, L.: A comparative study of spectrin: a protein isolated from red blood cell membranes. Biochem. Biophys Acta 200, 125-131, 1970

Unwin, P.N.T. and Henderson, R.: Molecular structure determination by electron microscopy of unstained crystalline specimens. J. Mol. Biol. 94, 425-440, 1975.

White, M.D. and Ralston, G.B.: The 'hollow cylinder' protein of erythrocyte membranes. Biochem. Biophys. Acta 554, 469-478, 1979.

Yu, J., Fischman, D.A. and Steck, T.L.: Selective solubilization of proteins and phospholipids from red blood cell membranes by J. Supramolec Struct. 1, 232-248, 1973.

PUBLISHED WORK SUBMITTED

A) ON ERYTHROCYTE MEMBRANE, HEPATOMA AND CULTURED CELL PROTEINS

1. Release of a macromolecular protein component from human erythrocyte ghosts, by J.R.Harris. Biochim. Biophys. Acta 150 (1968) 534-537.
2. The isolation and purification of a macromolecular protein component from the human erythrocyte ghost, by J.R.Harris. Biochim. Biophys. Acta 188 (1969) 31-42.
3. Some negative contrast staining features of a protein from erythrocyte ghosts, by J.R.Harris. J. Mol. Biol. 64 (1969)329-335.
4. The entry of ferritin into haemoglobin-free human erythrocyte ghosts prepared under different conditions, by J.N.Brown and J.R.Harris. J. Ultrastruct. Res. 32 (1970) 405-416.
5. The proteins released from intact erythrocyte 'ghosts' at low ionic strength, by J.R.Harris. Biochem. J. 122 (1971) 38-40.
6. Further studies on the proteins released from haemoglobin-free erythrocyte ghosts at low ionic strength, by J.R.Harris. Biochim. Biophys. Acta 229 (1971) 761-770.
7. The location of a membrane-associated protein complex in human and bovine erythrocyte ghosts, by J.R.Harris. J. Ultrastruct. Res. 36 (1971) 587-594.
8. Fractionation of plasma membrane-associated tumour-specific antigen from an aminoazo-dye-induced rat hepatoma, by R.W. Baldwin, J.R.Harris and M.R.Price. Int. J. Cancer 11 (1973) 385-397.
9. The purification of membrane-associated tumour antigens by preparative polyacrylamide gel electrophoresis, by J.R.Harris, M.R. Price and R.W. Baldwin. Biochim. Biophys. Acta 311 (1973) 600-614.

10. The purification of some membrane-associated proteins from erythrocyte ghosts, by J.R.Harris. In 'Methodological Developments in Biochemistry', Vol. 4, edited by E. Reid, (1974), Longmans, pp 393-404.

11. An electron microscopic study of some protein fractions from bovine erythrocyte membranes, by J.R.Harris and A.H. Maddy. J. Ultrastruct. Res. 48 (1974) 190-200.

12. The high molecular weight proteins released from cultured cells, by J.R.Harris, K.D. Brown and J.F. Aiton. Biochim. Biophys. Acta 427 (1976) 727-737.

13. Contrast enhancement of negatively stained macromolecules and biological membranes by single sideband phase contrast interference, by J.R.Harris and J. Kerr. J. Microscopy 108 (1976) 51-59.

14. Shape changes of the human erythrocyte ghost, by J.R.Harris. Biochem. Soc. Trans. 4 (1976) 664-667.

15. The breakdown of spectrin produced by ultrasonication, by J.R.Harris, P. Marshall and I. Naeem. Biochim. Biophys. Acta 534 (1978) 173-178.

16. The subunit composition of two high molecular weight extrinsic proteins from human erythrocyte membranes, by J.R.Harris and I. Naeem. Biochim. Biophys. Acta 537 (1978) 495-500.

17. Some problems associated with the production of paracrystalline arrays of protein molecules, by J.R.Harris. Proc. Roy. Mic. Soc. 13 (1978) 29.

B) ON AVIAN ERYTHROCYTES

18. The preparation of nucleated erythrocyte ghosts from avian erythrocytes, by J.R.Harris and J.N. Brown. Br. Poult. Sci. 12 (1971) 95-99.

19. Fractionation of the avian erythrocyte: an ultrastructural study, by J.R.Harris and J.N. Brown. J. Ultrastruct. Res. 36 (1971) 8-23.

20. The ultrastructure of the erythrocyte, by J.R.Harris. In 'Physiology and Biochemistry of the Domestic Fowl', edited by D.J. Bell and B.M. Freeman, Academic Press (1971), pp 853-862.

21. Ultrastructural and biochemical studies on avian erythrocyte plasma membrane and nuclear envelope, by J.R.Harris, P.S. Agutter and J.F. Milne. Micron 9 (1978) 117-125.

22. The preparation and ultrastructure of avian erythrocyte nuclear envelope enclosed by the plasma membrane, by J.R.Harris. J. Cell Sci. 34 (1978) 81-90.

C) ON RAT LIVER NUCLEAR ENVELOPE

23. A negative staining study of human erythrocyte ghosts and rat liver nuclear membranes, by J.R.Harris and P.S. Agutter. J. Ultrastruct. Res. 33 (1970) 219-232.

24. A method for the isolation and purification of normal rat liver and hepatoma nuclear 'ghosts' by zonal centrifugation, by M.R.Price, J.R.Harris and R.W. Baldwin. J. Ultrastruct. Res. 40 (1972) 178-196.

25. A comparative study on nuclear membranes from rat liver and hepatoma, by J.R.Harris, M.R.Price and M. Willison. J. Ultrastruct. Res. 48 (1974) 17-32.

26. Some electron microscopic studies on nuclear 'ghosts' and nuclear membrane fragments, by J.R.Harris. Phil. Trans. Roy. Soc. (B) 268 (1974) 109-117.

27. A rapid procedure for the isolation and purification of rat liver nuclear envelope, by J.R.Harris and J.F. Milne. Trans. Biochem. Soc. 2 (1974) 1251-1253.

28. The isolation and characterization of nuclear envelope, by J.R.Harris and P.S. Agutter, In 'Biochemical Analysis of Membranes' edited by A.H. Maddy, Chapman and Hall Ltd, (1976), pp 132-173.

29. Fractionation of the nuclear envelope, by J.R.Harris. In 'Methodological Surveys, Vol. 6: Membranous Elements and Movement of Molecules: Techniques', edited by E. Reid, Horwood, (1977) pp 245-250.

30. Negative staining of fractionated nuclear envelope, by J.R.Harris and P. Marshall, Micron 8 (1977) 217-219.

31. Biochemistry and ultrastructure of the nuclear envelope, by J.R.Harris. Biochim. Biophys. Acta 515 (1978) 55-104.

32. Characterization of mammalian liver nuclear envelope, by J.F. Milne, P.S. Agutter, J.R.Harris and G. Stubbs. Trans. Biochem. Soc. 6 (1978) 271-273.

Reprinted from
Biochimica et Biophysica Acta
Elsevier Publishing Company
Amsterdam
Printed in The Netherlands

BBA 71020

Release of a macromolecular protein component from human erythrocyte ghosts

The method to be outlined below depends upon the fragmentation of intact erythrocyte ghosts. (The term *intact* refers to the electron microscopic appearance see below.) This fragmentation is done by the removal of the buffer in which the are suspended by dialysis against distilled water, or alternatively by the addition of sodium dodecyl sulphate to 0.1 mg/ml. Most previous attempts to disrupt or solubilize erythrocyte ghosts have employed more drastic treatments than these. Thus, MADDY and REGA *et al.*[2], used a two-phase *n*-butanol–water system to solubilize over 90% of the ghost protein, as did MORGAN AND HANAHAN[3], by the use of an ultrasonicated single-phase 10% *n*-butanol–water system. A sodium dodecyl sulphate treatment (50 mg/ml) was used by BAKERMAN AND WASEMILLER[4], and a pyridine treatment (33%, by vol.) by BLUMENFELD[5]. A dialysis system using β-mercaptoethanol and ATP was developed by MARCHESI AND STEERS[6], which solubilized a protein component that could be polymerized to give actin-like fibrils, visible in the electron microscope by negative contrast staining.

Haemoglobin-free erythrocyte ghosts are prepared as follows from fresh or 14-day-old human whole blood, in acid citrate dextrose, by a modification of the method of DODGE, MITCHELL AND HANAHAN[7]. The cells are first washed 3 times with isotonic phosphate buffer (pH 7.0), the buffy coat being removed at each wash. Haemolysis is then performed by the addition of approx. 5 vol. of 0.01 M phosphate or Tris–HCl buffer (pH 7.4). The ghosts are then washed in this buffer until haemoglobin free. Occasionally it is found that the phosphate-washed ghosts remain pink. Two further washings with the Tris–HCl buffer will release the bound haemoglobin. Ghosts of creamy white colouration were usually obtained, but a slight haemoglobin contamination does not appear to alter the extraction.

At this stage *intact* ghosts can be seen in the electron microscope (A.E.I. E.M.6B) using the negative contrast staining technique. Using uranyl acetate (pH 4.5) as the negative stain it is not necessary to fix the ghosts, but with sodium phosphotungstate (pH 7.0) it is essential to fix the ghosts with osmic acid or glutaraldehyde prior to negative contrast staining. When preparing the ghosts from 14-day-old blood it is desirable not to use the Tris–HCl buffer, otherwise fragmentation of the ghosts occurs.

To release the material under discussion, the intact ghosts in 0.01 M phosphate or Tris–HCl buffer (pH 7.4) are dialysed 1–4 days against glass-distilled water at 4°. To prevent bacterial growth during the longer dialyses, the antibiotic tetracycline hydrochloride (approx. 10 μg/ml) was used, and removed by distilled water dialysis for 12 h, before the electron microscope study. Samples taken for viewing in the electron microscope show that the ghosts have undergone fragmentation, together with the release of a considerable amount of fine material. This material can be seen all over the background in Fig. 1, two types of profile being revealed. The first type consists of ring or torus forms, having an external diameter of approx. 110 Å and an inner diameter of approx. 50 Å. The other profile to be seen has a rectangular shape, with dimensions of approx. 110 Å and 180 Å. These rectangles appear to repre-

sent a stacked aggregate of four single-ring structures; thus, they are in fact cylindrical. In Fig. 1 all the single-ring structures are lying in a horizontal plane on the carbon backing film and the cylinders on their sides. In areas of deeper negative stain, the single rings can also be found lying in a vertical plane and in this position they show up as pairs of dots approx. 50 Å apart (see Fig. 2). Likewise, the cylindrical structures are occasionally seen lying vertically in the negative stain, showing up as clear rings with a dense central hole (see Figs. 3 and 4). (Theoretically both the single rings and cylinders could also lie in any position between the vertical and horizontal, in a deep pool of stain.) To summarize the main features of Figs. 1–4, two particles can be seen, a single ring structure and a cylindrical four-ring structure. Each structure has been described lying in a vertical and a horizontal plane, thus resulting in four profiles.

Very often the two outer rings of the cylindrical structures (lying horizontally) show up more clearly than the central pair. This may be a staining artifact, but may indicate that the inner two rings have a different composition to the outer rings. One can thus speculate why no groups of two rings are observed in the electron microscope. When the cylindrical structures break down, the central pair of rings

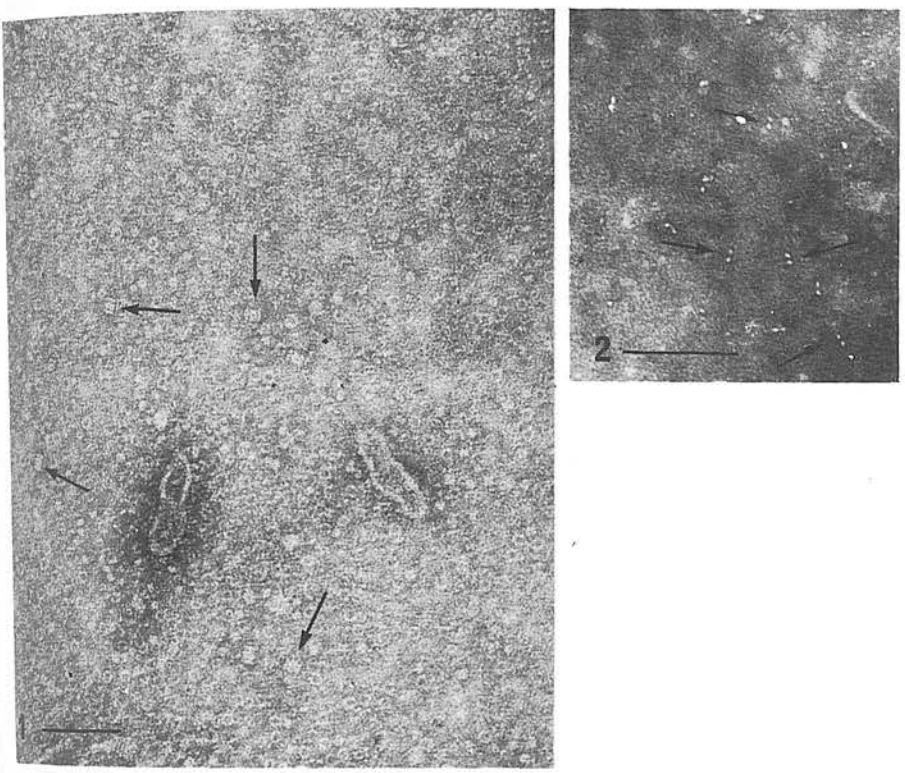

Fig. 1. Human erythrocyte ghosts after distilled water dialysis at 4° for 4 days. Negatively stained with 2% sodium phosphotungstate (pH 7.0). The line marker indicates 1000 Å. Arrows indicate the cylindrical structures. Membrane fragments and many single-ring structures are also visible.

Fig. 2. Human erythrocyte ghosts after distilled water dialysis at 4° for 4 days. Negatively stained with 2% sodium phosphotungstate (pH 7.0). The line marker indicates 1000 Å. In this deep pool of negative stain, the single-ring structures are lying in a vertical plane, being revealed as paired white dots (arrowed).

may be destroyed, leaving intact only the outer rings which do not tend to pack together. The fact that no groups of three, five, or more rings are observed is also evidence supporting the hypothesis that the centre pair of rings in the cylindrical four-ring structures are different from the outer rings. Nevertheless, all four rings in the cylindrical structures may be identical, this aggregate of four and the single-ring structure being the stable configurations.

Many of the single-ring structures in Fig. 1 give an indication of being composed of subunits. It is proposed to apply the photographic rotation technique for contrast enhancement of MARKHAM, FREY AND HILLS[8] to this structure.

The alternative procedure for releasing the structures described above from *intact* ghosts, is to cause fragmentation by the addition of sodium dodecyl sulphate to 0.1 mg/ml. When this is done with ghosts from fresh blood only the cylindrical structures are found by electron microscopy (see Fig. 3). However, when ghosts from 14-day-old blood are treated in this manner both single-ring and the cylindrical four-ring structures are found. This, together with the observations from the water dialysis treatment, suggests that when the ghosts fragment, the cylindrical structures are released, and that these tend to break down to give the single-ring structures and possibly other material 'invisible' in the electron microscope. It must also be stressed that an aggregation of the more fundamental subunit composing the ring structures could occur after removal from the ghosts.

Thus, no suggestion can yet be put forward with conviction as to the possible location of the structures described in the *intact* ghost. If cylindrical structures of the dimensions quoted above are located on or in the outer surface of the *intact* ghost membranes, one might expect to see them by negative contrast staining, but this is not the case. On the other hand, if they are located on or in the inner surface, they would be unlikely to be observed in the electron microscope. It is possible that the

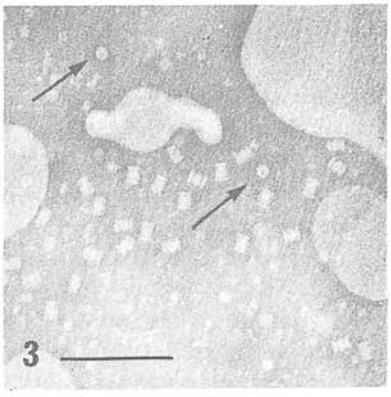

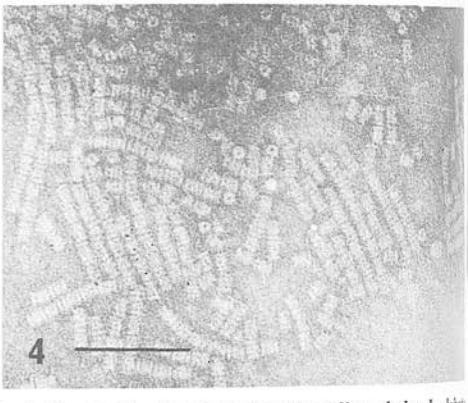

Fig. 3. Human erythrocyte ghosts from fresh blood after treatment with sodium dodecyl sulphate (0.1 mg/ml). Negatively stained with 2% sodium phosphotungstate (pH 7.0). The line marker indicates 1000 Å. Membrane fragments and cylindrical (four-ring) structures are visible. Arrows indicate cylinders lying in a vertical plane.

Fig. 4. Ox erythrocyte ghosts after distilled water dialysis at 4° for 2 days. Negatively stained with 2% sodium phosphotungstate (pH 7.0). The line marker indicates 1000 Å. Many cylindrical (four-ring) structures are visible, lying individually and in long columns, being arranged in this latter array by the forces of drying. (Membrane fragments are also present, but not included in this print.)

structures presented do not represent a membrane component and that they are intracellular structures that have been bound by the membrane during haemolysis and the subsequent washings.

Work is in progress regarding the purification and characterisation of this extractable material. Preliminary results indicate it is of protein composition and may represent up to 5 % of the protein of the *intact* ghost. Two preparations of ox erythrocyte ghosts have revealed a very similar release of material when fragmented by either of the treatments described (see Fig. 4). The significance of the results presented cannot be fully discussed at the present stage of the investigation. But it would appear that, as the material is so readily released not only by sodium dodecyl sulphate but by the mild treatment of water dialysis, it is unlikely that an artifact is being created.

I wish to acknowledge the financial assistance from the Medical Research Council of Great Britain throughout this study.

Department of Physiology, University of Edinburgh, Edinburgh (Great Britain) J. R. HARRIS

1 A. H. MADDY, *Biochim. Biophys. Acta*, 117 (1966) 193.
2 A. F. REGA, R. I. WEED, C. F. REED, G. G. BERG AND A. ROTHSTEIN, *Biochim. Biophys. Acta*, 147 (1967) 297.
3 E. MORGAN AND D. J. HANAHAN, *Biochemistry*, 5 (1966) 1050.
4 S. BAKERMAN AND G. WASEMILLER, *Biochemistry*, 6 (1967) 1100.
5 O. O. BLUMENFELD, *Biochem. Biophys. Res. Commun.*, 30 (1968) 200.
6 V. T. MARCHESI AND E. STEERS, JR., *Science*, 159 (1968) 203.
7 J.T. DODGE, C. MITCHELL AND D. J. HANAHAN, *Arch. Biochem. Biophys.*, 100 (1963) 119.
8 R. MARKHAM, S. FREY AND G. J. HILLS, *Virology*, 20 (1963) 88.

Received January 30th, 1968

Reprinted from
Biochimica et Biophysica Acta
Elsevier Publishing Company
Amsterdam
Printed in The Netherlands

(2)

BBA 35401

THE ISOLATION AND PURIFICATION OF A MACROMOLECULAR PROTEIN COMPONENT FROM THE HUMAN ERYTHROCYTE GHOST

J. R. HARRIS*
Department of Physiology, University of Edinburgh, Edinburgh, (Great Britain)

(Received April 2nd, 1969)

SUMMARY

1. A method is described for the isolation of a macromolecular protein component from intact human erythrocyte ghosts. This is done by the centrifugal removal of ghost fragments following distilled water dialysis and a freeze–thaw treatment. The protein is identified by electron microscopy using negative staining. It has the form of a hollow cylinder, which dissociates into torus structures.

2. The torus protein is purified by sucrose density gradient centrifugation and differential centrifugation. Purity is estimated by electron microscopy and polyacrylamide-gel electrophoresis.

3. The results are discussed in relation to the electron microscopic assessment of purity. It is considered that the hollow cylinder protein rather than the torus is the structure associated with the membrane of the intact ghost. The mild extraction procedure described releases only a small percentage of the ghost protein. It is less likely, however, to produce an alteration of the membrane proteins than the extraction methods that produce a high degree of protein solubilization.

INTRODUCTION

The erythrocyte membrane is known to contain a large number of different lipids, but very little precise information is available on the proteins which account for some 60% of the membrane by weight. It might be reasonable to consider that some of the proteins play a structural role within the membrane, but there must be many that have functional roles, *e.g.*, carrier, enzymic or antigenic. The methods for the separation of protein from the erythrocyte membrane, such as the *n*-butanol treatment of MADDY[1] and REGA *et al.*[2] and the pyridine treatment of BLUMENFELD[3], have stressed the difficulty of solubilizing the protein, which under physiological conditions is essentially 'insoluble'. These two treatments release protein which has a strong tendency to aggregate and has not readily undergone further fractionation,

* Present address: Department of Zoology, University of Edinburgh, West Mains Road, Edinburgh 9.

though the gel electrophoresis results of ZWALL AND VAN DEENEN[4] have indic
that the *n*-butanol extract contains a complex mixture of proteins. However,
precise conditions under which the protein solubilized by *n*-butanol can be
sociated are not yet clearly defined.

The work of DODGE *et al.*[5], and MITCHELL *et al.*[6], indicated a considerable
of non-haemoglobin protein from erythrocyte ghosts at pH's around 8.0 and follo
distilled water washing. The same conclusion was drawn by REGA *et al.*[2] follo
washing with distilled water, freeze–thawing and high salt treatment. The erythro
ghost appears to undergo fragmentation when subjected to high pH, low
strength, high ionic strength or freeze–thawing, with a parallel release of
haemoglobin protein.

The method for the isolation of the protein under discussion is an extensio
the distilled water dialysis treatment presented previously, HARRIS[7], which
probably not unlike distilled water washing in its action on the erythrocyte gho
This treatment was shown to cause fragmentation of intact human erythro
ghosts, with the release of a macromolecular protein component, which was dete
using the electron microscope. This component has the form of a hollow cylin
composed of four torus structures aggregated side by side; it undergoes spontane
dissociation into single torus structures under the conditions of isolation. The pres
publication outlines a method for the isolation and subsequent purification of
macromolecular component from intact human erythrocyte ghosts.

It cannot be claimed without reservation that the protein under considera
is a true component of the erythrocyte membrane. There is a possibility that it co
be an adsorbed contaminant from the intracellular fluid or from the serum. T
distinction between true membrane components, which are bound with vary
degrees of firmness and adsorbed contaminants, is often extremely difficult to defi
For instance, it is now generally assumed that haemoglobin is not a component
the erythrocyte membrane, but until fairly recently this was not accepted as work
were unable to obtain erythrocyte ghosts free from haemoglobin. The possibi
remains that other protein contaminants could be present with 'haemoglobin-fre
erythrocyte ghost preparations and that they could be released alone or toget
with true membrane components when solubilization procedures are applied.

METHODS

The preparation of intact human erythrocyte ghosts

Fresh or 14-day-old human whole blood in acid–citrate–dextrose (from th
Blood Transfusion Unit of the Royal Infirmary, Edinburgh), was washed 3 times
isotonic phosphate buffer (pH 7.0) at 4°, the supernatant and buffy coat being re
moved by aspiration. The erythrocytes were then haemolysed in 5 vol. of 0.01 M
phosphate or Tris–HCl buffer (pH 7.4) at 4°. The ghosts were then collected by
centrifugation at 21 000 rev./min (in the M.S.E. 10 × 100 ml angle rotor) for 30 min
and washed 6–7 times in the same buffer, until estimated to be haemoglobin-free by
visual observation. The Tris–HCl buffer was found to release the haemoglobin more
readily than the phosphate buffer. Ghosts of creamy white colouration were obtained
which appeared intact in the electron microscope by negative contrast staining, see
Fig. 1.

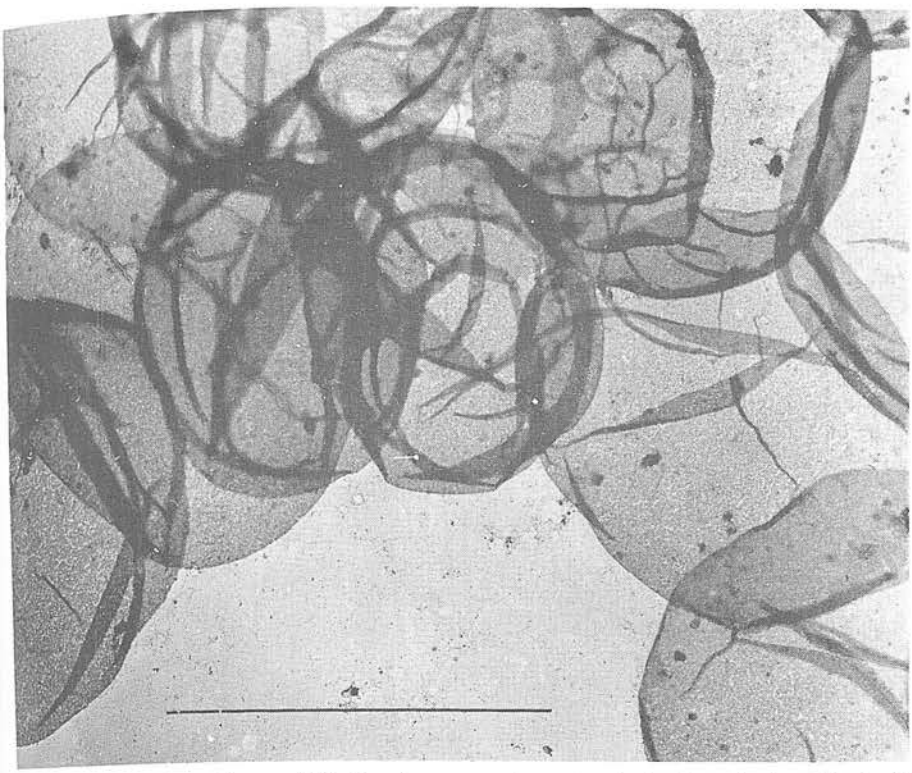

Fig. 1. A sample of intact haemoglobin-free human erythrocyte ghosts. Negatively stained with 2% uranyl acetate (pH 4.5) without prior fixation. The scale marker indicates 50 000 Å. (5 μ).

The repeated use of Tris–HCl buffer for washing the ghosts from 14-day-old blood was not considered desirable as some fragmentation was observed in the electron microscope. However, two final washes in the Tris–HCl buffer following the series of phosphate buffer washes always gave intact ghosts from the 14-day-old blood. Owing to the difficulty of obtaining regular supplies of fresh blood, the 14-day-old blood was used most frequently. No differences were observed regarding the extraction of the protein under DISCUSSION, whether the fresh or the 14-day-old blood was used. Experiments currently in progress are making use of 7-day-old packed erythrocytes, which can be obtained in larger quantities than the whole blood, from the Blood Transfusion Unit.

Protein estimation

Protein was estimated by the method of LOWRY *et al.*[8], using a bovine serum albumin (Koch-Light) standard.

Concentration methods

Protein extracts were concentrated using solid sucrose (British Drug Houses), or Aquacide II (Cal. Biochem.), and concentration was followed by distilled water dialysis to remove the sucrose or dialysable impurities from the Aquacide II.

Density gradient centrifugation

4.0-ml linear sucrose density gradients, 5.0–40.0%, were prepared using a mixing apparatus following that of BRITTEN AND ROBERTS[9]. Protein samples (0.2–

0.5 ml) were applied to the top of such gradients which were centrifuged at 40 rev./min for 16 h at 4° (using the M.S.E. 3 × 5 ml swing-out rotor). Nine equ fractions were then taken from the tops of the gradients using a syringe and we dialysed against distilled water at 4° to remove the sucrose prior to protein estimat and electron microscopic study.

Polyacrylamide-gel electrophoresis

Disc electrophoresis of the protein extracts was performed on 7.0% polyacry amide gel in 0.02 M Tris–HCl buffer (pH 8.0), at 8 mA per tube for 30 min. The ge were fixed and stained with saturated amido black in water–methyl alcohol–acet acid (5:5:1, by vol.) and destained by washing in the same solvent mixture.

Electron microscopy

Samples of the erythrocyte ghost suspensions were negatively stained with 2% uranyl acetate (pH 4.2) without prior fixation, or with 2% sodium phosphotungsta (pH 7.0) after fixation with 0.5% glutaraldehyde or osmic acid. Samples of the protei extracts (non-fixed) from erythrocyte ghosts were negatively stained with 2% sodium phosphotungstate. Uranyl acetate tended to cause aggregation of the protein.

Viewing was done on an A.E.I., E.M. 6B, at routine electron optical magnifi cations of 50 000 and 100 000 diameters. The electron microscopic magnificatio scale was found to be correct by calibration using a standard containing 2160 lines/mm Photographs were taken on Ilford 3.25 inch plates, 'Special Lantern Contrast'.

RESULTS

Isolation of the macromolecular component

Intact human erythrocyte ghosts in either 0.01 M phosphate or Tris–HCl buffe (pH 7.4) were dialysed against distilled water at 4° for 1–4 days. 1.25 inch Visking Tubing which had been soaked for 30 min in distilled water was used. The ghosts (approx. 3 mg protein per ml) were dialysed against approx. 100 vol. of distilled water which was changed at intervals of approx. 12 h. The antibiotic tetracycline·HCl (10 μg/ml) was present throughout the longer dialyses to prevent the growth of bacteria and was itself removed by dialysis against distilled water alone for the final 12 h. Experience has shown that dialysis for 2 days is sufficient and that it is not necessary to use the antibiotic for this length of dialysis. Samples taken for electron microscopy at this stage, using negative staining, indicated that the ghosts had undergone fragmentation, with the release of many torus and hollow cylinder structures, in agreement with preliminary observations[7].

Following centrifugation of the dialysed ghosts at 21 000 rev./min for 30 min the torus and hollow cylinder structures were found to be bound with the membrane fragments which had sedimented to give a firm pad. However, a freeze-thaw treatment applied prior to centrifugation allowed the torus and hollow cylinder structures to remain in the clear supernatant. Traces of haemoglobin were found to bind preferentially with the membrane fragments. Freezing was routinely performed in a deep-freeze at −20°, and thawing in a 40° water bath. For experiments currently in progress a more rapid freezing using a dry ice–methanol mixture is being used.

The above extraction method has been successfully performed on eight preparations of erythrocyte ghosts from fresh whole blood and on thirteen preparations of

Fig. 2. A sample from a 21 000 rev./min supernatant of a preparation of intact human erythrocyte ghosts following distilled water dialysis and freeze–thawing. Negatively stained with 2% sodium phosphotungstate (pH 7.0). The scale marker indicates 1000 Å.

ghosts from 14-day-old whole blood. The quantity of protein released was within the range 10.0–20.0% of the total protein of the intact ghosts.

Fig. 2 shows a representative negatively stained electron microscope field of a 21 000 rev./min ghost supernatant after the distilled water dialysis and freeze–thaw treatment. Many torus and hollow cylinder structures can be seen, together with irregular material. Few membrane fragments were observed, having mostly been removed by the centrifugation.

Purification

(A) By sucrose density gradient centrifugation: With electron microscopic support. The 21 000 rev./min ghost supernatant after distilled water dialysis and freeze-thawing, was concentrated using solid sucrose, and then dialysed for 24 h against distilled water at 4° to remove the sucrose. The trace of precipitate was

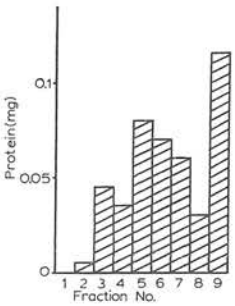

Fig. 3. The histogram shows the distribution of protein from a concentrated 21 000 rev./ghost supernatant, after centrifugation at 40 000 rev./min for 16 h at 4° on a 5.0–40.0% sucr density gradient.

removed by low-speed centrifugation. 0.2–0.5-ml quantities of the low-speed supernatant were applied to a 4.0-ml 5.0–40.0% sucrose density gradient, which was centrifuged at 40 000 rev./min for 16 h. The distribution of protein on the gradient after centrifugation is shown in Fig. 3. The protein peak spread over Fractions 5–7 was shown by electron microscopic study to contain large numbers of the torus structures. Figs. 4 and 5 show samples taken from Fraction 6 following removal of the sucrose by dialysis against distilled water for approx. 24 h. In Fig. 4 there is deep negative stain (> 100 Å), and the torus proteins are orientated at all possible angles relative to the carbon backing film. In Fig. 5 there is shallow negative stain (< 50 Å

Fig. 4. A sample from Fraction 6 of the sucrose density gradient centrifugation shown in Fig. 3. Negatively stained with 2% sodium phosphotungstate (pH 7.0). There is deep negative stain (approx. 150 Å) in the field shown. The torus proteins are orientated at all possible angles relative to the carbon backing film. The scale marker indicates 1000 Å.

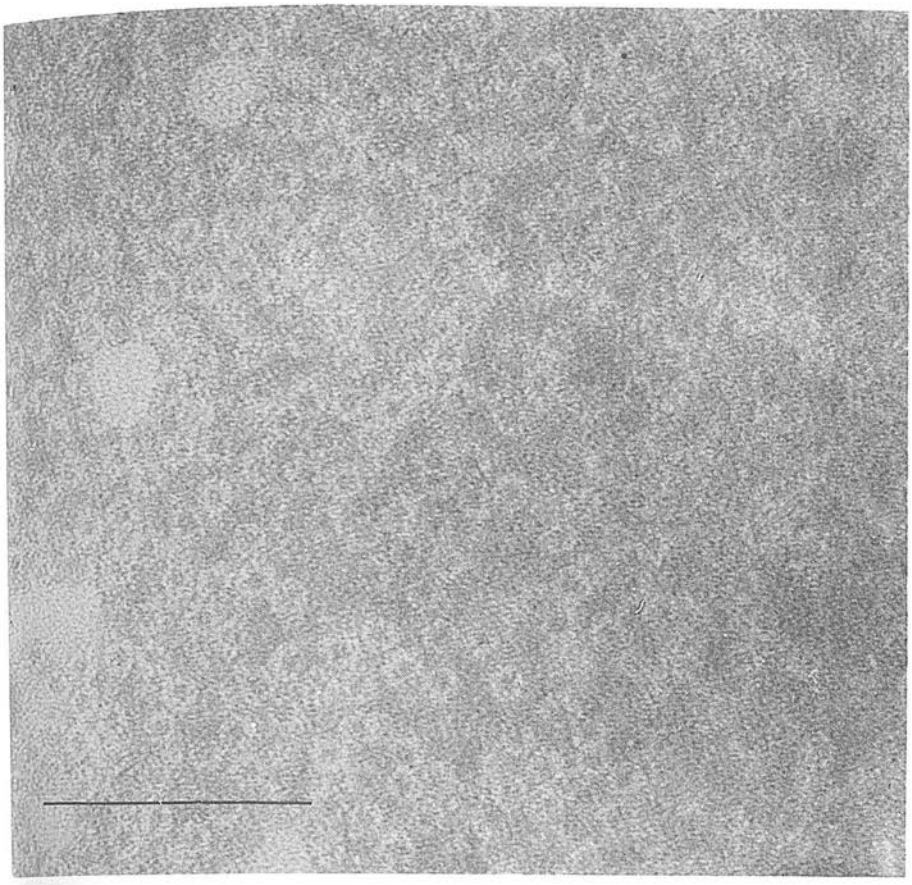

Fig. 5. A sample from Fraction 6 of the sucrose density gradient centrifugation shown in Fig. 3. Negatively stained with 2% sodium phosphotungstate (pH 7.0). There is shallow negative stain (<50 Å) in the field shown, and all the torus proteins are orientated horizontally on the carbon backing film. The scale marker indicates 1000 Å.

and all the torus proteins are lying horizontally. The clarity of the background in Figs. 4 and 5 is much greater than that in Fig. 2, in the sense that there is no irregular material revealed. It is therefore thought reasonable to consider Fractions 5–7 from the density gradient as purified solutions of the torus protein. The protein peak in Fraction 9 of Fig. 3 was shown to contain irregular aggregated material by electron microscopy. No hollow cylinder (tetramer) proteins were detected, which is suggestive of their having dissociated into the single torus proteins.

(B) By direct differential centrifugation: With electron microscopic and electrophoretic support. The 21 000 rev./min ghost supernatant was concentrated by either solid sucrose or Aquacide II, and was followed by distilled water dialysis for 24 h at 4°. The solution was then centrifuged at 40 000 rev./min for 15 min. The supernatant from this centrifugation was found by negative staining to contain the single torus protein, see Fig. 6. The background is very clean, which suggests that the torus protein is the only detectable material in solution. Scheme I summarizes the treat-

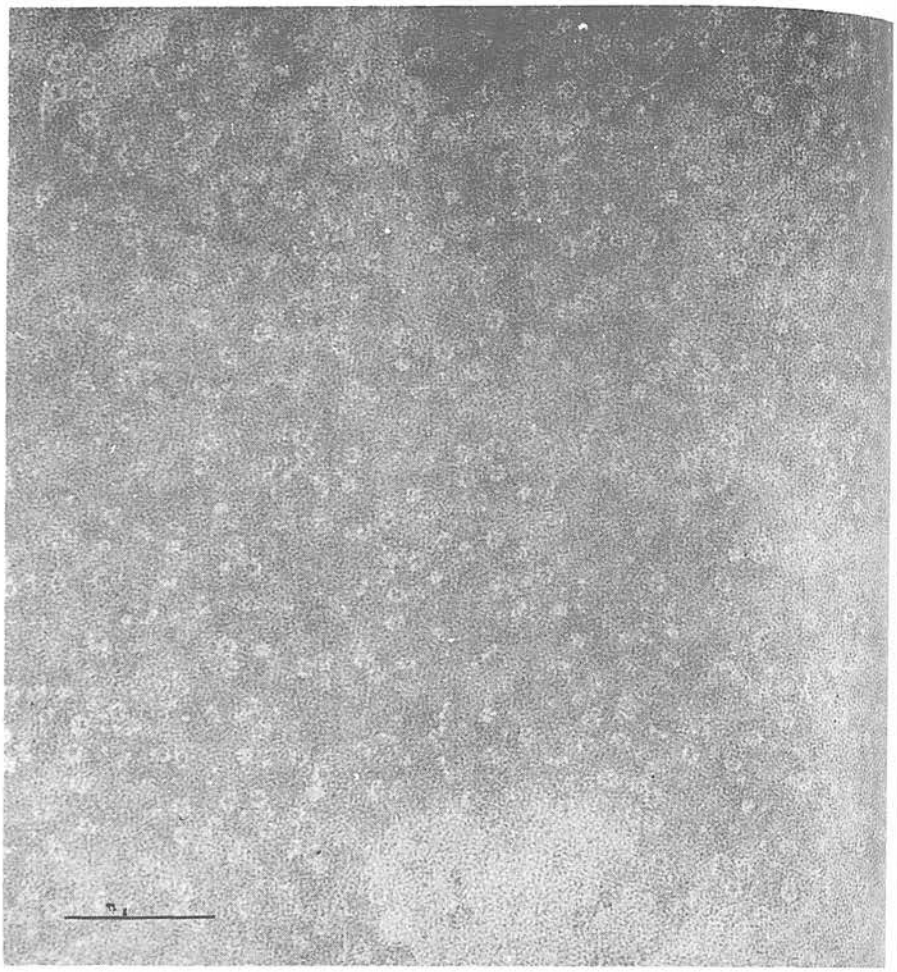

Fig. 6. A sample of a purified torus protein solution, following the differential centrifugation procedure. Negatively stained with 2% sodium phosphotungstate (pH 7.0). The scale marker indicates 1000 Å.

ments applied to the erythrocytes throughout the extraction and purification procedures described in the previous sections.

Disc electrophoresis of the protein purified by differential centrifugation, on 7.0% polyacrylamide gel at pH 8.0 with or without the presence of 8 M urea, revealed a single band of protein migrating towards the anode, see Fig. 7. This electrophoretic evidence for purity supports the electron microscopic evidence. The electron microscopic evidence alone is not satisfactory, since small protein molecules might not be resolved if the negative stain penetrates the protein, as has been suggested for bovine serum albumin by GLAUERT[10]. Traces of impurity were occasionally detected by disc electrophoresis, in the form of nonmigratory material at the origin of the gels (see Fig. 7). On such occasions irregular aggregated material was usually detected in the electron microscope.

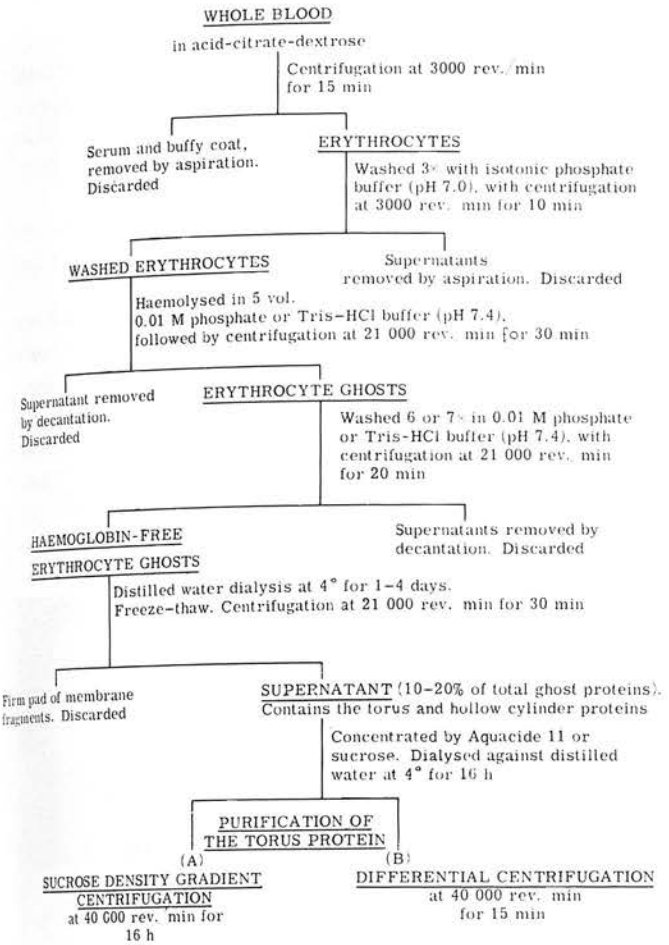

Scheme 1. Summary of the total treatment procedure for the preparation of erythrocyte ghosts, the isolation of the torus and hollow cylinder proteins and the purification of the torus proteins.

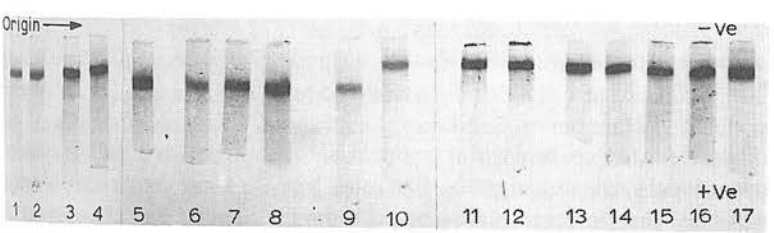

Fig. 7. Polyacrylamide-gel electrophoresis results. (7.0% gel in 0.02 M Tris–HCl buffer at pH 8.0). Gels 1, 2, 5 and 17 are of the torus protein solution shown in Fig. 6. Gels 1, 2 and 5 were electrophoresed in the absence of urea and Gel 17 in the presence of 8 M urea. Gels 3–9 are of a different sample of purified torus protein solution, electrophoresed in the absence of urea. Gels 10, 13 and 14 show this sample when electrophoresed in the presence of 8 M urea. Gels 11, 12, 15 and 16 show a sample of impure material ,electrophoresed in the presence of 8 M urea. There are clear indications of nonmigratory material at the origins for the impure material, though there is a single band of material which has migrated the same distance as the band given by the pure torus protein solutions.

It has been possible to remove the protein from the single migratory band in polyacrylamide gels and then to perform electron microscopy. The band containing protein was sliced out of nonstained frozen gels, when lying beside stained gels, and suspended in distilled water for 4 to 6 h during which time the protein diffused from the gel. Samples of the suspending fluid taken for electron microscopy revealed only the torus protein.

The differential centrifugation method for purifying the torus protein has been found to be more satisfactory than the sucrose density gradient method, since larger quantities of purified material could be obtained.

A typical absorbtion spectrum of the purified torus protein in distilled water is shown in Fig. 8. Significantly, there is no absorbtion peak in the region of 410 mμ, which would have indicated contamination with haemoglobin. The quantity of purified torus protein obtained following the differential centrifugation procedure ranged from approx. 1.0–4.0% of the total protein of the intact ghosts. A considerable loss of protein is likely to occur during the purification, and it is probable that an incomplete release of protein from the ghosts occurs following the distilled water dialysis and single freeze-thaw treatment, therefore 4.0% is probably a conservative estimate.

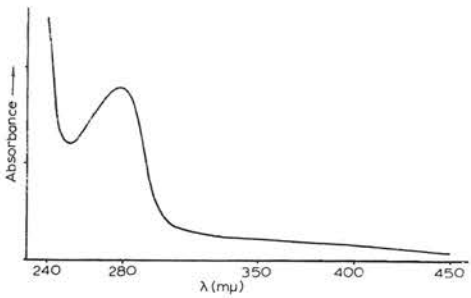

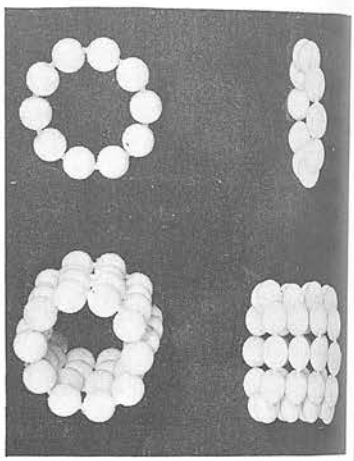

Fig. 8. A typical absorbtion spectrum of the purified torus protein solution in distilled water.

Fig. 9. Suggested molecular models for the torus and hollow cylinder proteins. These models are are not strictly to scale.

Fig. 9 shows tentative molecular models for the torus and hollow cylinder proteins. These models are not strictly to scale, but they do emphasize the main features revealed by the electron microscopic study.

DISCUSSION

Most techniques applied to erythrocyte ghosts to solubilize membrane protein have undoubtedly resulted in the extraction of a number of different proteins, which have nevertheless presented considerable difficulties when attempts were made to perform further fractionation. The isolation method described above probably releases

a relatively small number of proteins, among which are the torus and hollow cylinder proteins. The purification methods developed apply only to the torus protein. Work is in progress regarding the purification of the hollow cylinder protein (tetramer), its controlled dissociation into the torus protein, and reaggregation. Electron microscopy has indicated that the torus protein is composed of ten more fundamental subunits[11]. The dissociation–reaggregation properties of the torus protein are also under investigation, as are the enzymic properties and molecular weights of the hollow cylinder, the torus and its fundamental subunit.

The hollow cylinder structure rather than the torus is thought to be associated with the intact erythrocyte ghost. Electron microscopic evidence in support of this statement is that the hollow cylinder is released in larger quantities than the torus following the sodium dodecyl sulphate treatment[7] and that the use of either the distilled water dialysis or sodium dodecyl sulphate treatments with ox erythrocyte ghosts released only the hollow cylinder structures. At the moment it cannot be claimed that the hollow cylinder protein is composed of four identical tori. Previous electron microscopy[7] suggested that the centre pair of tori had a different stability from the outer tori, but this could be a staining artifact. The purified single torus proteins could thus be derived from the outer tori of the tetramer, the centre pair having been destroyed, and removed by centrifugation.

The electron microscopic criterion of purity for the torus protein, which is based on a qualitative assessment of clarity of the negatively stained fields obtained, may be reasonably accurate when applied following the sucrose density gradient purification. However, proteins with a similar sedimentation coefficient could be present, yet might not be revealed by electron microscopy if completely penetrated by negative stain. The same comments apply following the differential centrifugation procedure when other soluble proteins might be present.

Polyacrylamide-gel electrophoresis has supported the electron microscopic observations, for the purification by differential centrifugation, which is now used routinely in preference to density gradient centrifugation. Gel electrophoresis and electron microscopy are together thought to provide a good, though qualitative, estimation of purity for the torus protein. It is unlikely that the presence of proteins other than the torus would be undetected using both these techniques.

It is proposed that extraction methods such as the one described above which produces the solubilization of a small percentage of the erythrocyte ghost protein might nevertheless contribute significantly to the understanding of the membrane proteins. If mild extraction procedures are used there is a reduction of the possibility that the membrane material is drastically modified on extraction. Such modification has undoubtedly occurred in the past, for example the elenin of MOSKOWITZ AND CALVIN[12] and even in the *n*-butanol method of MADDY[1] one cannot completely rule out the possibility that the membrane protein is seriously altered relative to its state when in the ghost.

No claims can yet be made as to the significance of the hollow cylinder or torus proteins in relation to the intact erythrocyte ghost, but it might be reasonable to consider that they will have functional rather than structural properties.

ACKNOWLEDGMENTS

The author wishes to acknowledge the financial support made available by the Medical Research Council. Thanks are given to Dr. G. H. Haggis (Department of Physiology, University of Edinburgh) for introducing the author to the subject of the erythrocyte ghost and for the continual source of guidance he has been throughout this study. The critically helpful comments made by Mr. P. Kelly and Mr. P. Agutter (Department of Zoology, University of Edinburgh) throughout the preparation of the manuscript are gratefully acknowledged.

REFERENCES

1 A. H. MADDY, *Biochim. Biophys. Acta*, 117 (1966) 193.
2 A. F. REGA, R. I. WEED, C. F. REED, G. G. BERG AND A. ROTHSTEIN, *Biochim. Biophys. Acta*, 147 (1967) 297.
3 O. O. BLUMENFELD, *Biochem. Biophys. Res. Commun.*, 30 (1968) 200.
4 R. F. A. ZWALL AND L. L. M. VAN DEENEN, *Biochim. Biophys. Acta*, 163 (1968) 44.
5 J. T. DODGE, C. D. MITCHELL AND D. J. HANAHAN, *Arch. Biochem. Biophys.*, 100 (1963) 119.
6 C. D. MITCHELL, W. B. MITCHELL AND D. J. HANAHAN, *Biochim. Biophys. Acta*, 104 (1965) 348.
7 J. R. HARRIS, *Biochim. Biophys. Acta*, 150 (1968) 534.
8 O. H. LOWRY, N. J. ROSEBROUGH, A. L. FARR AND R. J. RANDALL, *J. Biol. Chem.*, 193 (1951) 265.
9 R. J. BRITTEN AND R. B. ROBERTS, *Science*, 131 (1960) 32.
10 A. M. GLAUERT, *Lab. Invest.*, 14 (1965) 331.
11 J. R. HARRIS, in preparation.
12 M. MOSKOWITZ AND M. CALVIN, *Exptl. Cell. Res.*, 3 (1952) 33.

Reprinted from *J. Mol. Biol.* (1969) **46**, 329–335

(3)

Some Negative Contrast Staining Features of a Protein from Erythrocyte Ghosts

J. R. Harris

J. Mol. Biol. (1969) **46**, 329–335

Some Negative Contrast Staining Features of a Protein from Erythrocyte Ghosts

J. R. Harris

Department of Zoology
University of Edinburgh, Scotland

(*Received 28 April 1969, and in revised form 11 July 1969*)

Negative contrast staining has been used to study a protein from erythrocyte ghosts. This protein has a quaternary conformation resembling a hollow cylinder built from a stack of four rings of protein subunits. The outer diameter of the hollow cylinder (tetramer) is estimated to be approximately 125 Å and the height approximately 170 Å. The hollow cylinder is thought to dissociate into single ring or torus structures, which show a tenfold rotational symmetry. The outer diameter of these tori is estimated to be approximately 130 Å and the thickness approximately 35 Å.

The different electron images which the tetramer and single torus proteins produce in the electron microscope are presented. Negative contrast staining was carried out using both sodium phosphotungstate and uranyl acetate. A theoretical interpretation of the electron images produced by the side-on orientation of these molecules is put forward.

The results are discussed, and compared with those from other protein molecules which show cylindrical shapes in the electron microscope. A general postulate is made that the hollow cylindrical protein assembly, composed of rings of subunits, is a thermodynamically stable quaternary conformation for the subunits of some proteins.

1. Introduction

Methods for the release, and subsequent isolation and purification, of a macromolecular protein component from *intact* human and ox erythrocyte ghosts have been described previously (Harris, 1968,1969). This component has the form of a hollow cylinder approximately 170 Å in height and approximately 125 Å in external diameter, with a hole approximately 50 Å in diameter down the middle. Electron microscopic evidence suggested that the hollow cylinders were composed of four stacked tori. Under the conditions of isolation, the hollow cylinder (tetramer) protein from human erythrocyte ghosts appears to undergo dissociation into single tori, approximately 130 Å in external diameter and approximately 35 Å thick, with a hole approximately 60 Å in diameter. No single tori have been observed in the extracts made from ox ghosts.

The aim of this paper is to present some features revealed by the electron microscopic study of this protein, which have not been fully described previously, and to put the discussion of the electron microscopic images obtained during this study on a more sound theoretical footing.

Negative contrast staining has found general usage in recent years for revealing protein molecules in the electron microscope (Horne, 1965). It was thought desirable to study the protein under discussion using both anionic and cationic negative stains.

Uranyl acetate and sodium phosphotungstate were used as negative stains throughout this investigation.

2. Materials and Methods

(a) *Preparation of intact erythrocyte ghosts*

Intact haemoglobin-free erythrocyte ghosts were prepared from fresh or 14-day old human whole blood in acid–citrate–dextrose, or from fresh, defibrinated ox whole blood following the method of Dodge, Mitchell & Hanahan (1963). The erythrocytes were washed three times in isotonic phosphate buffer (pH 7·0). Haemolysis was brought about by adding 5 vol. of 0·01 M-phosphate buffer (pH 7·4). The ghosts were sedimented at 59,000 *g* for 20 min and washed six or seven times in the same buffer to remove the haemoglobin. Ghosts of creamy-white coloration were obtained. Traces of haemoglobin did not interfere with the extraction of the protein under consideration.

The ghosts were sometimes given two final washes in 0·01 M-Tris–HCl buffer (pH 7·4) which aided the release of haemoglobin. Both the phosphate and Tris buffer ghosts appeared as discrete intact entities in the electron microscope using uranyl acetate negative staining. With sodium phosphotungstate as the negative stain, it was necessary to fix the ghosts beforehand with 0·5% glutaraldehyde or osmic acid.

(b) *Release, isolation and purification of the protein component*

The protein under discussion was released from intact erythrocyte ghosts by distilled water dialysis or by the addition of sodium dodecyl sulphate to 0·1 mg/ml. (Harris, 1968). The former method has been developed for the isolation of the protein component (Harris, 1969). Following the distilled water dialysis treatment (1 to 2 days at 4°C), the ghosts were freeze–thawed and centrifuged at 59,000 *g* for 30 min. The membrane fragments formed a firm pad during this centrifugation and the clear supernatant fraction was readily decanted. Traces of residual haemoglobin were found to remain with the membrane fragments at this stage. The supernatant fraction was shown to contain 10 to 20% of the protein present in the erythrocyte ghosts (using the method of Lowry, Rosebrough, Farr & Randall, 1951). the hollow-cylinder (tetramer) and single-torus proteins were shown to be present by electron microscopy, together with irregular material.

Purification of the single-torus protein was performed by sucrose density-gradient centrifugation or differential centrifugation, following concentration of the above supernatant fraction by Aquacide 11 (Calbiochem. Ltd.) or solid sucrose (B.D.H.). Disc electrophoresis on polyacrylamide gel revealed a single band of protein migrating towards the anode at pH 8·0 in the purified preparations of the single-torus protein (Harris, 1969). The controlled dissociation of the hollow cylinder (tetramer) protein is now under investigation. Experiments so far have indicated that, by speeding up the isolation and concentration procedures, an extract can be obtained containing the tetramer but very little single-torus protein. The tetramer has been purified by density-gradient centrifugation.

(c) *Electron microscopy*

Electron microscope observations were made using the A.E.I. E.M.6B. Samples of the protein extracts from erythrocyte ghosts were negatively stained with unbuffered 2% sodium phosphotungstate (pH 7·0) or 2% uranyl acetate (pH 4·5). The routine use of electron optical magnifications of 50,000 and 100,000 diameters was found to be most convenient for the study of the extracted protein molecules. The magnification scale of the electron microscope was calibrated with a standard carbon grating containing 2160 lines/mm. Electron micrographs were taken on Ilford $3\frac{1}{4}$ in. × $3\frac{1}{4}$ in. plates (Special Lantern Contrasty).

3. Results

(a) *The intact erythrocyte ghosts*

A representative sample of negatively stained haemoglobin-free human erythrocyte ghosts is shown in Plate I. Ghosts in this condition have been the starting material for the extraction of the protein under consideration.

PLATE I. Intact human erythrocyte ghosts after fixation with 0·5% osmic acid in Palade–sucrose buffer. Negatively stained with 2% sodium phosphotungstate (pH 7·0). The scale marker indicates 10,000 Å.

[*facing p. 330*

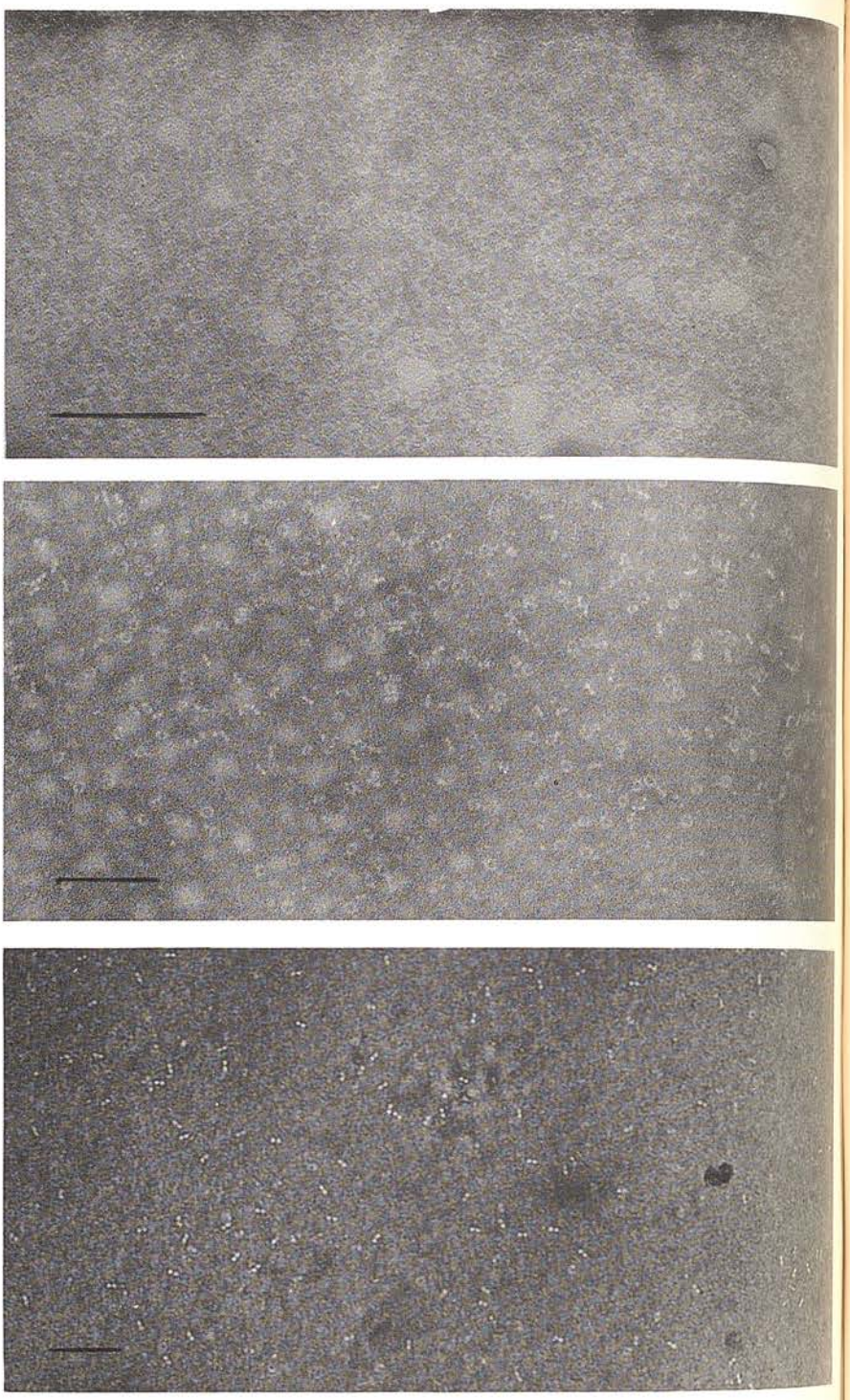

PLATE II. Purified preparations of the single-torus protein negatively stained with 2% sodium phosphotungstate (pH 7·0).

(a) A region of shallow negative stain within which all the single-torus proteins are lying horizontally, giving ring-like images.

(b) A region containing deeper negative stain. The torus proteins are orientated at all angles relative to the carbon backing film, giving paired-dot, dumb-bell and ring-like images.

(c) A region containing even deeper negative stain. Only the paired-dot images of the torus proteins are visible (see text). The scale markers indicate 1000 Å.

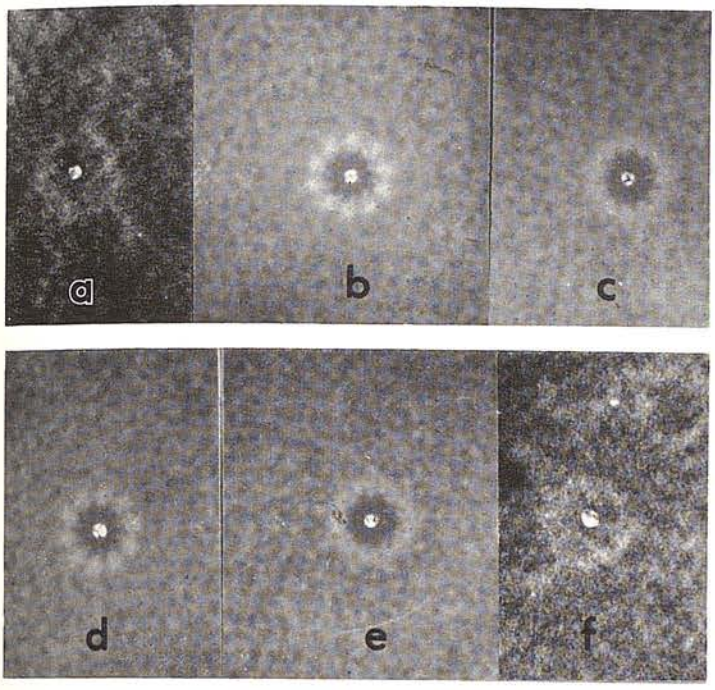

PLATE III. The photographic rotation technique for contrast enhancement applied to the single-torus protein lying in a horizontal plane. Images (a) and (f) have not been rotated. Images (b) and (d) have been rotated by steps of 360/10 degrees; image (c) by steps of 36/11 degrees and image (e) by steps of 360/9 degrees.

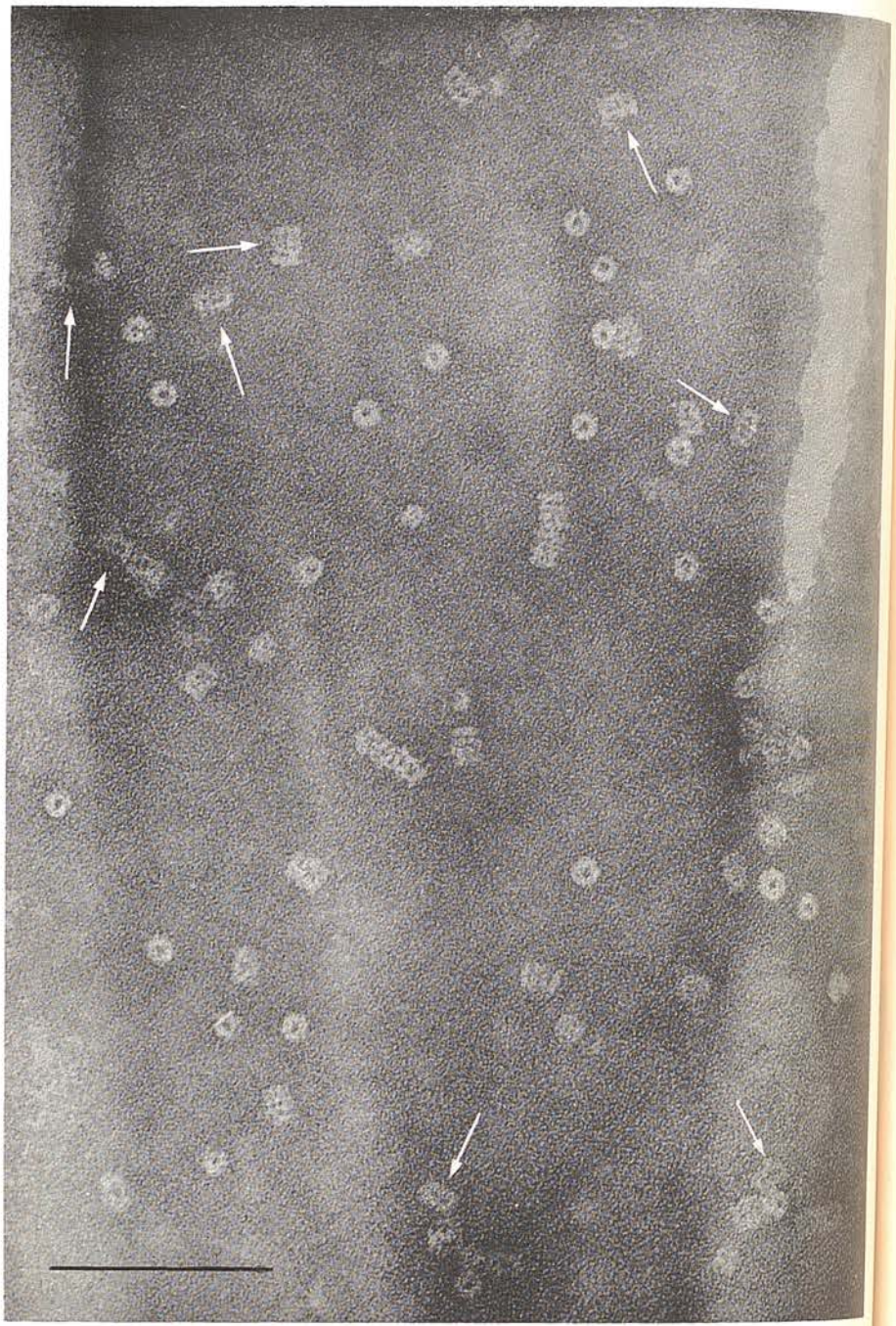

PLATE IV. A purified preparation of the hollow-cylinder (tetramer) protein, negatively stained with 2% uranyl acetate (pH 4·5). The arrows indicate molecules which are orientated on their sides and appear as four parallel dumb-bells or four double dots (see text). The scale marker indicates 1000 Å.

(b) *The single-torus protein*

The single-torus protein has been found to give rise to a number of different negatively stained images in the electron microscope, depending first on whether it is orientated horizontally or vertically on the carbon film of the viewing grid, and secondly, on the depth of the surrounding stain. Plate II shows samples of purified torus protein negatively stained with sodium phosphotungstate. In Plate II(a), there is a shallow negative stain and all the tori are lying horizontally. Plate II(b) shows a region containing a deeper pool of negative stain. The tori can be orientated at any angle relative to the backing film. Ring-like images of horizontal tori are present, together with some elliptical images which are probably given by tori orientated at angles between the horizontal and vertical. Also present are many dumb-bell and double-dot images which probably are given by vertically orientated tori. Plate II(c) shows an even deeper region of stain in which only the double-dot images due to vertically orientated tori can be observed. Horizontal tori must be present, but the deep stain masks their presence in the electron microscope. When negatively stained with uranyl acetate, the torus protein gave the same orientation-dependant images, but some aggregation of the protein was observed to occur.

From direct observation of the horizontally orientated torus protein, it has very often been possible to follow five or six consecutive subunits, it being found that they encompassed approximately half the torus. Application of the photographic rotation technique for contrast enhancement (Markham, Frey & Hills, 1963), indicated that the tori were composed of ten subunits (Plate III).

The electron images given by the vertically orientated single-torus protein are described diagrammatically in Figure 1. The electron-opaque stain surrounding the torus gives rise to the paired dot image in regions of deep stain. In shallower stain there appears to be a line connecting the two dots, giving a dumb-bell image. In even shallower stain, if it could maintain a vertical position, the torus protein would be revealed as a straight rod, but this presumably never happens and the structure appears to fall on to its side if it is not supported by stain. The rod image is observed, however, in the hollow cylinder (tetramer) protein (see below).

The diagrammatic explanation put forward for the paired-dot image of the vertically orientated torus (Fig. 1) is not strictly accurate, since the dimensions of the horizontal

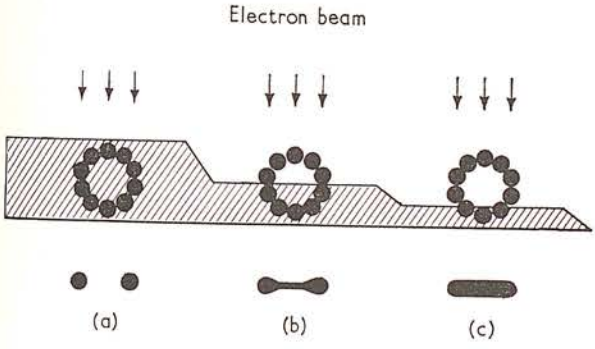

FIG. 1. A diagrammatic explanation for the paired-dot and dumb-bell electron images of the vertically orientated torus protein. The cross-hatching represents varying depths of negative stain.

torus and the paired dots are not in precise agreement (see Table 1). After a more careful consideration of the electron microscopic images, it was realised that this discrepancy is in fact expected. Figure 2 shows two tori composed of ten subunits; one with a subunit centre at 0° and the other with subunit centred at 90°. The thickness of protein summed vertically through each torus is plotted graphically above. It is seen that the maximum thickness of protein occurs at distances of approximately 40 Å from the centres of the tori. The subunit tori depicted in Figure 2 are not an accurate representation of the torus protein, since the degree to which each subunit is in contact with the two adjacent subunits is not known. However, they are probably a more accurate representation than a solid circular ring, for which the points of maximum protein thickness would correspond to the inner radius of the ring.

The shape and varying thickness of protein on negatively stained electron microscope specimens are primarily responsible for the image obtained. In a depth of negative stain sufficient for the vertically orientated tori to be completely immersed,

TABLE 1

Dimensions of the negatively stained single-torus protein

(a)	*Horizontal orientation*	
	Inner diameter	60 ± 4 Å
	Outer diameter	131 ± 5 Å
	Mean of inner and outer diameters	96 ± 5 Å
(b)	*Vertical orientation*	
	Dot inner edge-to-edge distance	27 ± 6 Å
	Dot outer edge-to-edge distance	124 ± 5 Å
	Dot centre-to-centre distance	80 ± 6 Å

Dimensions were measured by eye using a ×5 micrometer (Graticules Ltd.), on photographs printed at a final magnification of 200,000. Standard deviations of the mean were calculated from the dimensions of 50 molecules. All the above figures were obtained from molecules on a single electron micrograph.

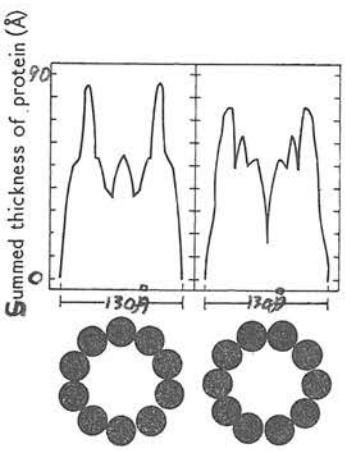

FIG. 2. Graphical representations of the vertical summed thickness of protein for vertically orientated torus proteins which are composed of 10 subunits.

the density distribution in their images will have very strong contrast and will be characterized by two peaks corresponding to the two peaks of the torus-protein thickness curves (Fig. 2) where minimum electron scattering occurs.

From the curves in Figure 2, it is seen that the distances between the maxima are approximately 80 Å, and that the distances between the two inner and the two outer lines of the peaks, at a protein thickness of 55 Å, are approximately 45 Å and 100 Å respectively. These figures compare favourably with those obtained by direct measurement on electron micrographs containing the paired-dot electron image (Table 1).

(c) *The hollow cylinder (tetramer) protein*

Negatively stained specimens of the hollow cylinder (tetramer) protein component give rise to two types of image, depending on whether the protein is orientated 'end-on' or 'side-on', on the carbon film of the viewing grid.

TABLE 2

Dimensions of the hollow cylinder (tetramer) protein

(a)	*End-on orientation*	
	Inner diameter	40 Å
	Outer diameter	120 Å
	Mean of inner and outer diameter	80 Å
(b)	*Side-on orientation*	
	(1) The 'striped' rectangle	
	Width of rectangle	125 ± 4 Å
	Length of rectangle	170 ± 4 Å
	(2) The tetramer of double dots	
	Length	170 Å
	Dot inner edge-to-edge	30 Å
	Dot outer edge-to-edge distance	120 Å
	Dot centre-to-centre distance	80 Å

Dimensions were measured as in Table 1. Insufficient molecules could be found on a single electron micrograph to calculate the standard deviations of the mean for sections (a) and (b) (2).

When lying side-on, the tetramer protein gives a rectangular image with either sodium phosphotungstate or uranyl acetate. The longer dimension of the rectangle shows four cross-striations or rods, which are interpreted as being four vertically orientated tori. The phosphotungstate stain does not appear to penetrate significantly into the hollow core of the protein, since even in deep stain few electron images have been observed resembling two lines each composed of four dots, or four parallel dumbbells. With uranyl acetate, on the other hand, some of the tetramers have been observed to give this electron image (Plate IV). This indicates the penetration of uranyl stain within the hollow core of the protein.

The vertically orientated (end-on) tetramer protein gives a negatively stained electron image resembling a ring (Plate IV). This image is observed with both sodium phosphotungstate and uranyl acetate negative staining. The ring-like image of the end-on tetramer protein is easily distinguishable from that of the single torus lying flat, owing to the greater change in electron contrast between the embedded protein and the surrounding stain, for the tetramer.

The dimensions of the hollow cylinder protein are given in Table 2. These dimensions are similar to those obtained for the single-torus protein (Table 1). This supports the suggestion that the single-torus proteins are formed by the dissociation of the tetramers. The slight difference in the apparent diameter of the horizontal torus (Table 1) and the tetramer end-on (Table 2) are thought to be insufficient to suggest that the two structures are not closely related. The accuracy of the dimensions measured depends very much upon the clarity of the electron images of these molecules, which in turn depends upon the efficiency of the negative staining.

4. Discussion

The hollow-cylinder (tetramer) and single-torus protein molecules released from *intact* erythrocyte ghosts have been observed electron microscopically by negative contrast staining with uranyl acetate and sodium phosphotungstate. The electron images revealed by the two stains are in general agreement with one another, which supports the proposition that the images are not electron artifacts.

The proteins are known from electrophoretic studies to carry a net negative charge at neutral pH and would be expected to repel the phosphotungstate anion. The uranyl cation would be expected to be attracted towards the protein molecules, as long as they carried a negative charge. This binding of stain and protein may be responsible for some of the observed aggregation, but the acidity of the uranyl solution is thought to be the major factor since the proteins have their isoelectric points in the pH range 4 to 5. Despite the aggregation with uranyl acetate, many individual molecules were always found. No aggregation was observed with the phosphotungstate stain, which might therefore be considered to fulfil the criterion of satisfactory negative staining (i.e. no stain–material interaction) more successfully than the uranyl stain. Disruptive effects produced by the phosphotungstate stain, however, cannot be ruled out.

The slight disparity of the electron images of the tetramer protein viewed side-on and the single-torus protein viewed edge-on can be satisfactorily explained in terms of the variable penetration of the negative stain within the hollow cores of the molecules. The images also depend to some extent on the depth of the negative stain surrounding the molecules (Plate II). The diagrammatic explanations put forward for the images given by the edge-on torus (Fig. 1) are substantiated by the results presented, except for the rod-like image (section (c) of Fig. 1). The side-on hollow cylinders were, however, clearly shown to give rectangular images consisting of four rods aligned parallel to one another. The fact that the hollow cylinders seldom gave clear images resembling four pairs of dots is thought to be due to the imperfections of the staining method.

Many groups of workers have made electron microscopic studies of protein molecules having quarternary structures resembling hollow cylinders (Bradley, 1966; Colvill, van Bruggen & Fernández-Moran, 1966; Fernández-Moran, van Bruggen & Ohtsuki, 1966; Fernández-Moran, Marchalonis & Edelman, 1968; Finch, Leberman, Yu-Shang & Klug, 1966; Lauffer & Stevens, 1968; Lubin, 1969; Roche, 1965; Sato & Nagase, 1967; Valentine, Thang & Grunberg-Manago, 1969; Zillig, Fuchs, Walter, Millette & Priess, 1967). Of these workers Roche, and Lauffer & Stevens, showed clearly that a negatively stained hollow cylindrical protein molecule could give a multiple paired-dot image when orientated on its side. Electron microscopic observations have also been made on protein molecules composed of a single ring of subunits (Nishi, Yoshida & Takesue, 1968; Boeker & Snell, 1968). These groups did not comment on the possible electron

images that such molecules would give if orientated at varying angles relative to the carbon backing film of the specimen.

It is apparent from these papers and from the results presented earlier, that the images of protein molecules observed in the electron microscope by negative staining must be very dependent upon the electron scattering properties and degree of penetration of the negative stain within the quaternary arrangement of the protein subunits, as well as upon the orientation of the protein on the specimen grid.

From the number of protein molecules now isolated which show the general conformation demonstrated in this paper (i.e. the hollow cylinder composed of a number of tori each of which is formed by an ordered arrangement of subunits), it might be postulated that this conformation provides a thermodynamically stable arrangement for the subunits of many proteins, in a similar manner to the spherical shell of subunits found for the ferritin molecule and many virus particles, and the helices of repeating subunits found for fibrous proteins such as actin and for many rod-shaped viruses.

I wish to acknowledge the guidance given by Drs A. H. Maddy and G. H. Haggis throughout the preparation of this manuscript. Electron microscope facilities were made available by Professor W. E. Watson, Department of Physiology, University of Edinburgh. The financial support of the Medical Research Council is gratefully acknowledged.

REFERENCES

Boeker, E. A. & Snell, E. E. (1968). *J. Biol. Chem.* **243**, 1678.
Bradley, D. E. (1966). *Proc. Int. Conf. Electron Microscopy*, 6th Kyoto, vol. 2, p. 115.
Colville, A. J. E., van Bruggen, E. F. J. & Fernández-Moran, H. (1966). *J. Mol. Biol.* **17**, 302.
Dodge, J. T., Mitchell, C. & Hanahan, D. J. (1963). *Arch. Biochem. Biophys.* **100**, 119.
Fernández-Moran, H., van Bruggen, E. F. J. & Ohtsuki, M. (1966). *J. Mol. Biol.* **16**, 191.
Fernández-Moran, H., Marchalonis, J. J. & Edelman, G. M. (1968). *J. Mol. Biol.* **32**, 467.
Finch, J. T., Leberman, R., Yu-Shang, C. & Klug, A. (1966). *Nature*, **212**, 349.
Harris, J. R. (1968). *Biochim. biophys. Acta*, **150**, 534.
Harris, J. R. (1969). *Biochim. biophys. Acta*, **188**, 31.
Horne, R. W. (1965). In *Techniques for Electron Microscopy*, ed. by W. H. Kay, p. 346. Oxford: Blackwell.
Lauffer, M. A. & Stevens, C. L. (1968). *Advanc. Virus Res.* **13**, 1.
Lowry, O. H., Rosebrough, N. J., Farr, A. L. & Randall, R. J. (1951). *J. Biol. Chem.* **193**, 265.
Lubin, M. (1969). *J. Mol. Biol.* **17**, 302.
Markham, R., Frey, S. & Hills, G. J. (1963). *Virology*, **20**, 88.
Nishi, Y., Yoshida, T. O. & Takesue, Y. (1968). *J. Mol. Biol.* **37**, 441.
Roche, J. (1965). In *Studies in Comparative Biochemistry*, vol. 23, p. 62. Oxford: Pergamon Press.
Sato, Y. & Nagase, K. (1967). *Biochem. Biophys. Res. Comm.* **27**, 195.
Valentine, R. C., Thang, M. N. & Grunberg-Manago, M. (1969). *J. Mol. Biol.* **39**, 389.
Zillig, W., Fuchs, E., Walter, G., Millette, R. L. & Priess, H. (1967). *Proc. Fed. European Biochem. Socs*, p. 37. Oslo: Universitets forlaget.

J. ULTRASTRUCTURE RESEARCH 32, 405–416 (1970)

The Entry of Ferritin into Hemoglobin-Free Human Erythrocyte Ghosts Prepared under Different Conditions

J. N. BROWN AND J. R. HARRIS[1]

Department of Physiology, University Medical School, Edinburgh, EH8 9AG, Scotland

Received October 9, 1969, and in revised form January 5, 1970

Erythrocyte ghosts, with low residual hemoglobin content, can be prepared from human blood by hemolysis and subsequent washings in 0.01 *M* phosphate buffer (pH 7.4). By using 0.01 *M* Tris-HCl buffer (pH 7.4) for the final washings, rather than phosphate buffer, the residual hemoglobin can be more readily released. The differing capacity of the two buffers to preserve the intact state of the erythrocyte ghost was investigated by the addition of ferritin. Lesions in the erythrocyte membranes were indicated by the entry of ferritin. Ghosts prepared throughout in phosphate buffer were generally found to be impermeable to ferritin whereas ghosts washed in Tris-HCl buffer, although morphologically intact, were all permeable to ferritin. It is suggested that although Tris-HCl buffer facilitates the release of hemoglobin, it produces in human erythrocyte ghosts permanent lesions that are not found in ghosts prepared in phosphate buffer.

In the preparation of hemoglobin-free erythrocyte ghosts from the blood of different mammalian species, most recent workers have followed the preparative method of Dodge *et al.* (*1*), who showed that human erythrocyte ghosts can be isolated containing a very low hemoglobin content and with only a small loss of nonhemoglobin protein by hemolysis and subsequent washing in 0.01 *M* phosphate buffer at pH 7.4. Other workers have made use of Tris-HCl buffer for preparing their ghosts (*5. 6. 9, 11*). It has been observed by Harris (*3. 4*), that washing in Tris-HCl buffer tends to release hemoglobin from human erythrocyte ghosts more readily than phosphate buffer. Repeated washing in Tris-HCl buffer was shown to have a disruptive effect on the ghosts, in that it caused some fragmentation. However, two final washes given in Tris-HCl buffer following a series of phosphate buffer washes always gave intact ghosts, as judged by electron microscope examination using negative staining.

The present communication reports a further investigation on the differing capacities of the two buffers to preserve the intact state of human erythrocyte ghosts. The entry of ferritin has been used as an indication of the presence of holes in the

[1] Present address: Department of Zoology, University of Edinburgh.

CHART I

THE PREPARATION OF ERYTHROCYTE GHOSTS FROM HUMAN BLOOD

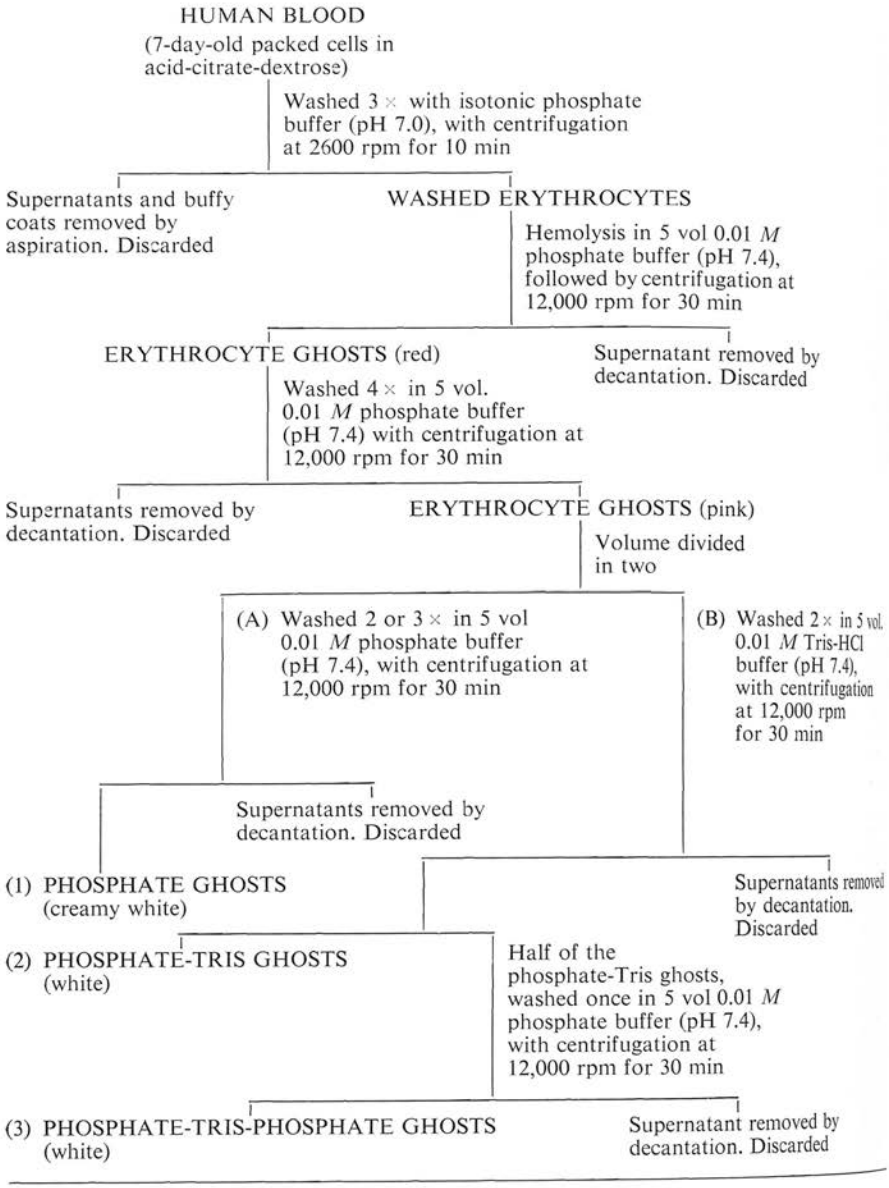

erythrocyte membranes. Seeman (*10*), has shown that ferritin and colloidal gold can permeate human erythrocytes only from about 15 to 25 seconds after the onset of hemolysis in hypotonic phosphate buffer. This result was explained by the demonstration of holes 200–500 Å in diameter in the membranes in thin-section electron micrographs when glutaraldehyde fixation was performed between 10 and 20 seconds after the start of hemolysis. Fixation before 10 seconds revealed continuous membranes not containing ferritin, and fixation after 25 seconds revealed continuous membranes containing ferritin.

From Seeman's results it might be expected that, when erythrocyte ghosts are repeatedly washed in phosphate buffer, there is at each wash a transient opening of holes in the membrane, thus allowing the escape of hemoglobin, until the intracellular osmotic pressure falls to that of 0.01 *M* phosphate buffer. The more rapid depletion of hemoglobin by washing in Tris-HCl buffer might indicate the presence of larger or more permanent holes in the membranes. In the work to be presented, hemoglobin-free human erythrocyte ghosts were prepared in phosphate and Tris-HCl buffers. Ferritin was added to the ghosts, which were subsequently fixed with glutaraldehyde. Following OsO_4 staining, embedding and thin sectioning, the preparations were examined electron microscopically to find whether or not ferritin had entered the ghosts.

MATERIALS AND METHODS

The preparation of human erythrocyte ghosts. Seven-day-old packed erythrocytes (0 + ve) in acid-citrate-dextrose were obtained from the Blood Transfusion Unit of the Royal Infirmary, Edinburgh. These cells were washed three times in isotonic phosphate buffer (pH 7.0) at 4°C, the supernatants and buffy coats being removed by aspiration following centrifugation at 2600 rpm for 10 minutes. The erythrocytes were then hemolyzed with 5 volumes of 0.01 *M* phosphate buffer (pH 7.4) at 4°. The ghosts were collected by centrifugation at

---

FIG. 1. Intact phosphate-ghost. Negatively stained with 2 % uranyl acetate (pH 4.5) without prior fixation. × 8000.

FIG. 2. Surface of phosphate-ghost. Negatively stained with 2 % uranyl acetate (pH 4.5) without prior fixation. × 90,000.

FIG. 3. Intact phosphate-Tris-ghost. Negatively stained with 2 % uranyl acetate (pH 4.5) without prior fixation. × 8000.

FIG. 4. Surface of phosphate-Tris-ghost. Negatively stained with 2 % uranyl acetate (pH 4.5) without prior fixation. × 90,000.

FIG. 5. Phosphate-ghosts with added ferritin (black dots). The symbol (*I*) indicates the intracellular compartment and the symbol (*E*) the extracellular compartment. No ferritin molecules have penetrated the cell membranes. (Some aggregates of ferritin are present in the extracellular compartment, appearing as dense particles.) × 25,000.

FIG. 6. Phosphate-ghosts with added ferritin. The typical unit membrane structure of the membrane is visible (arrowed). The ferritin molecules are clearly visible along the outer surface of the membrane. × 90,000.

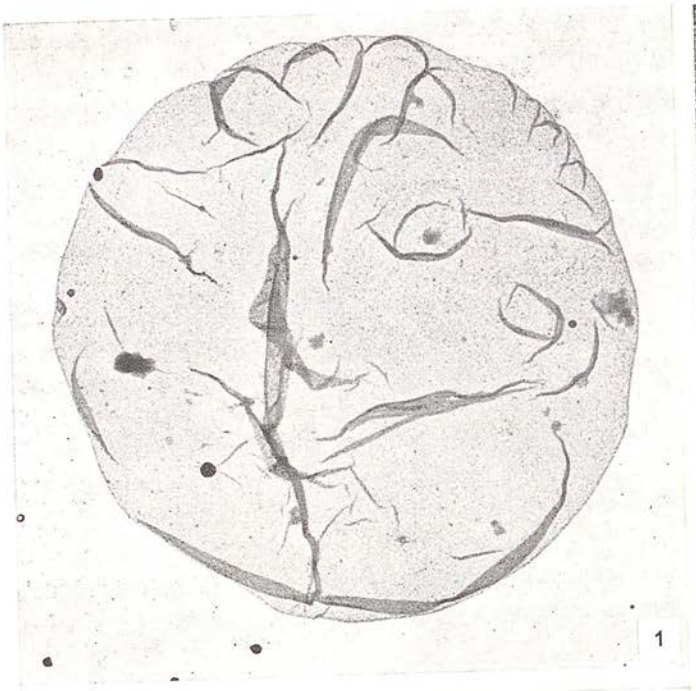

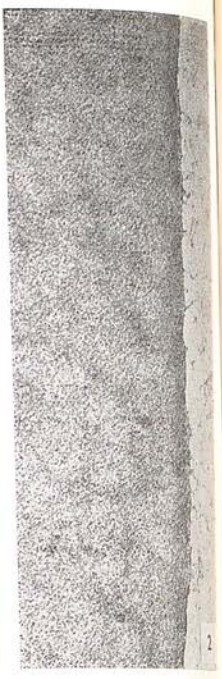

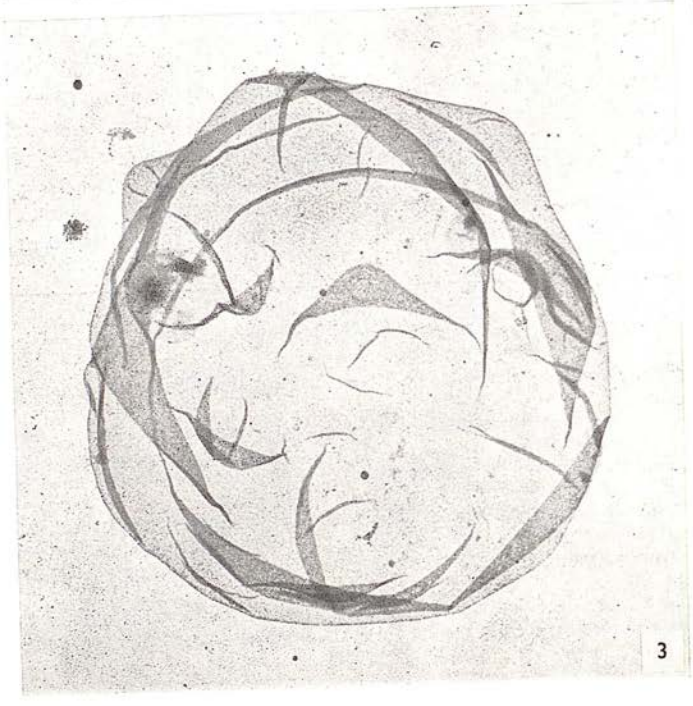

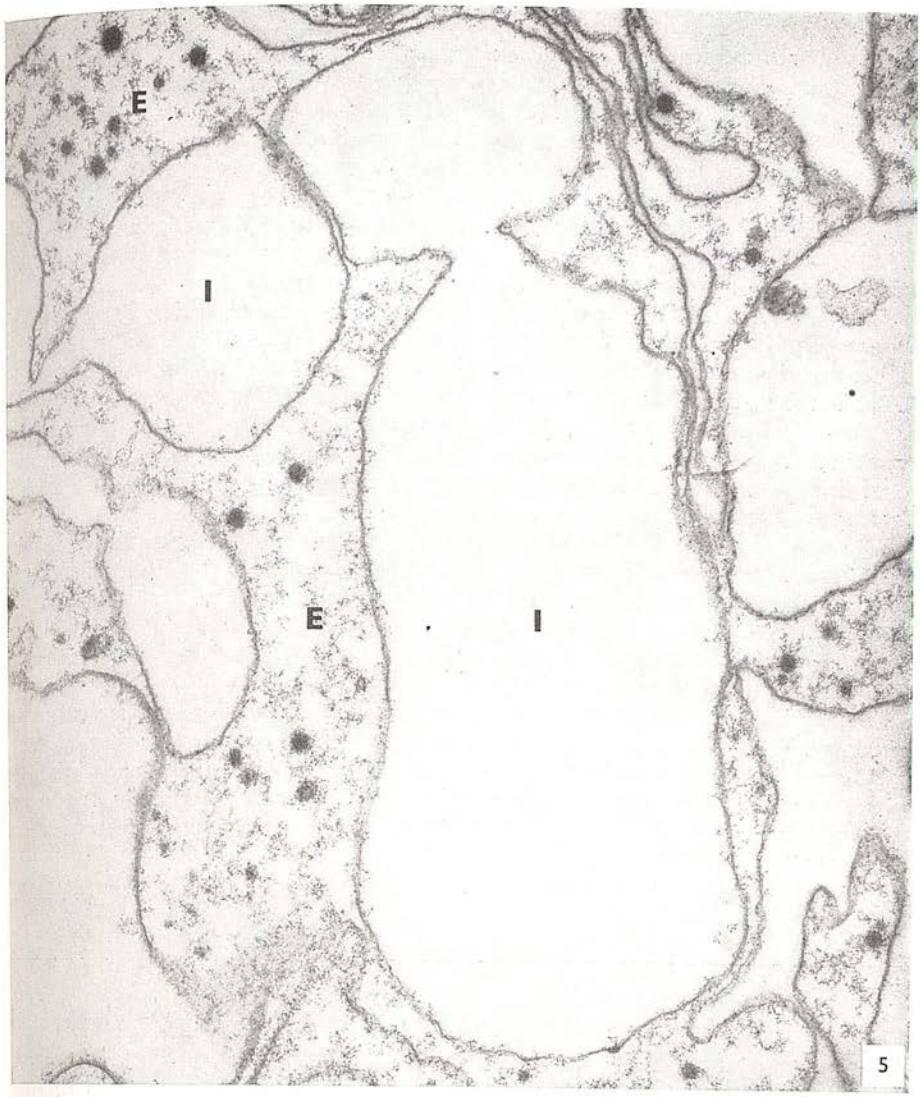
E
I
E
I
5

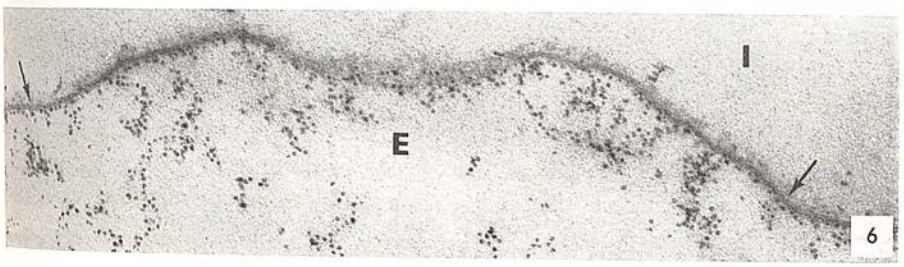
I
E
6

12,000 rpm for 30 minutes. Four washes were then given in 5 volumes of the same phosphate buffer and the ghosts were halved for further washing as follows: (a) Two or three washes in 5 volumes of phosphate buffer were given, resulting in the phosphate-ghosts (see Chart I) which were creamy-white. (b) Two washes in 5 volumes of 0.01 *M* Tris-HCl buffer (pH 7.4) were given, resulting in pure white phosphate-Tris-ghosts. Half of these ghosts were given a single wash in 5 volumes 0.01 *M* phosphate buffer (pH 7.4) and were then termed phosphate-Tris-phosphate-ghosts.

Ferritin treatment and embedding. Ghost samples for thin sectioning were treated with ferritin. Ferritin, 0.25 ml (Koch-Light, horse spleen ferritin, 100 mg/ml), was added to 0.25 ml of erythrocyte ghosts; the suspension was mixed and allowed to stand for 30 seconds. Calcium chloride (1–6 m*M*) was added to samples of the phosphate-tris-ghosts and (1 m*M*) to samples of the phosphate-tris-phosphate-ghosts before the addition of the ferritin in some of the experiments. Fixation was performed by the addition of 2.0 ml of glutaraldehyde, 2.0 % in Palade buffer (7), at pH 7.4. The preparation was left overnight at 4°, then stained for 1 hour by the addition of 2.0 ml OsO_4, 1.0 % in Palade buffer (pH 7.4). The ghosts were then firmly pelleted by centrifugation at 38,000 rpm for 20 minutes, dehydrated by passing them through graded ethanols and finally epoxy propane (B.D.H.), before embedding in TAAB epoxy resin.

Thin sectioning. Thin sections were cut with a Porter-Blum MT-2 ultramicrotome, using glass knives. Silver-white sections were mounted on LKB Type 400 grids without a supporting membrane. Poststaining was performed using uranyl acetate in 50 % ethanol.

Negative staining. Samples of the various ghost preparations, without prior fixation, were studied by negative staining with 2 % uranyl acetate (pH 4.5). This provided a rapid check on the condition of the ghosts in a given preparation.

Electron microscopy. Electron microscopic examination of the ghost preparations was performed in an A.E.I., E.M. 6B. The instrument had an accelerating voltage of 60 kV, a 250 μ condenser aperture, and a 50 μ objective aperture. The magnification scale of the microscope was found to have an error of less than 2 % by calibration with a replica containing 2160 lines/mm. Photographs were taken on Ilford $3\frac{1}{4}'' \times 3\frac{1}{4}''$ plates, "Special Lantern Contrasty."

RESULTS

Negative staining

When viewed in the electron microscope after negative staining, samples of the different ghost preparations revealed discrete membrane sacs (Figs. 1 and 3). At higher magnification the surface of the phosphate-ghosts and phosphate-Tris-ghosts have a similar appearance (Figs. 2 and 4). Lesions thought to be produced by the Tris-HCl buffer were not observed by the negative staining. The only apparent difference between the samples was that, whereas the majority of the phosphate-ghosts appeared intact, a small number of the phosphate-Tris-ghosts appeared fragmented. This fragmentation (*2*) was probably produced by the spreading forces applied to the ghosts during preparation of the specimens, but may also suggest an increased fragility of the phosphate-Tris-ghosts.

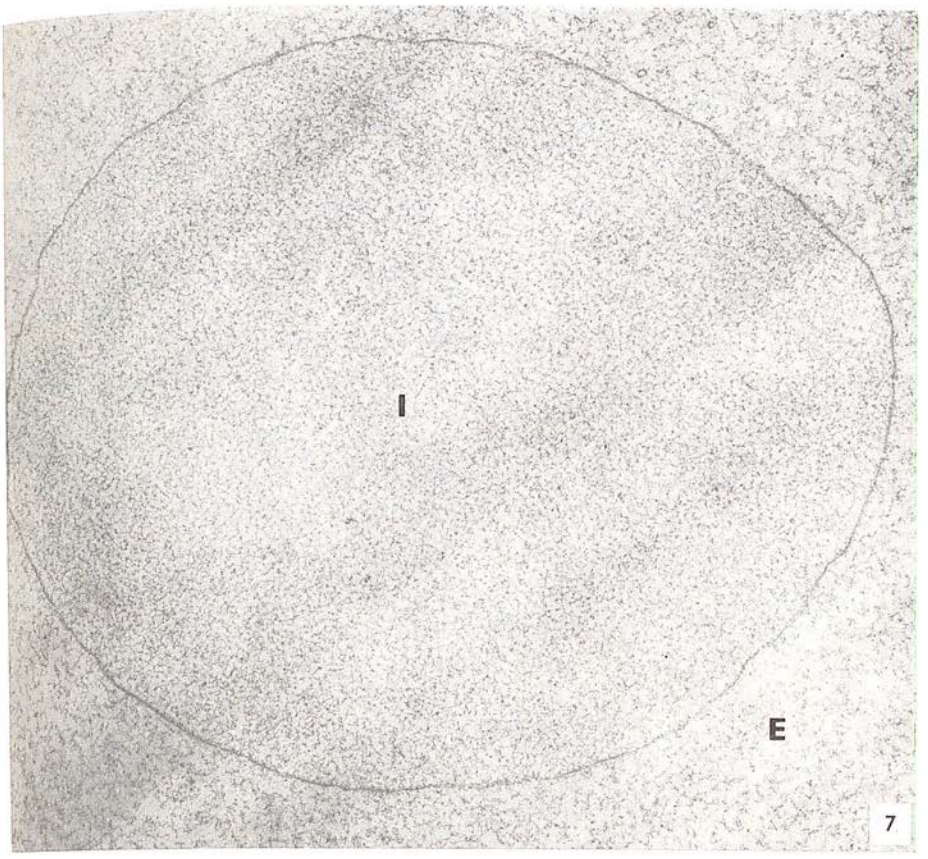

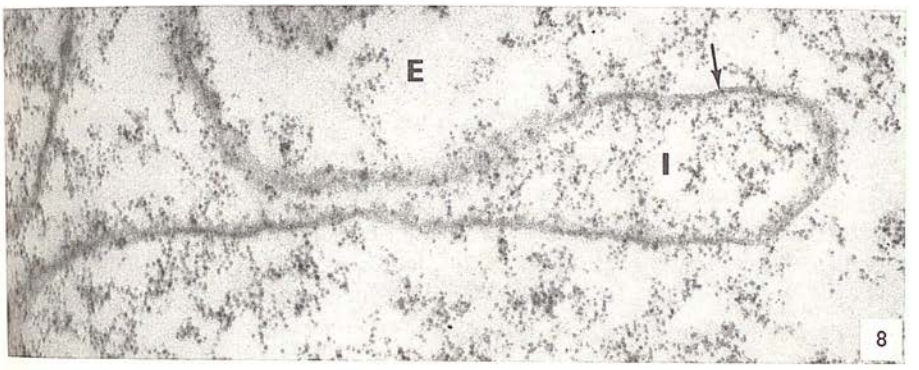

FIG. 7. Phosphate-Tris-ghosts with added ferritin. The ferritin molecules are present in both the intracellular (*I*) and extracellular (*E*) compartments. × 20,000.

FIG. 8. A higher magnification region of phosphate-Tris-ghosts with added ferritin. The unit membrane can be seen (arrowed) with ferritin molecules on both sides. × 90,000.

Thin sectioning

The permeability of the ghost preparations to ferritin has been qualitatively estimated by thin sectioning. Nearly all the phosphate-ghosts appear as intact empty sacs surrounded by ferritin molecules (Fig. 5). The typical "unit membrane" structure (*8*), is clearly visible at higher magnification, with the ferritin molecules aligned along the outer surface (Fig. 6). A few of the phosphate-ghosts did contain a small number of ferritin molecules. The fact that the ghosts are made from a population of erythrocytes of varying age means that some of the ghosts will be derived from the older and possibly more fragile cells. This may explain why some of the phosphate-ghosts are permeable to ferritin, whereas the majority are impermeable.

All the phosphate-Tris-ghosts, on the other hand, appeared to be permeable to ferritin (Figs. 7 and 8), though they still retained the continuous "unit membrane" appearance. The majority of the phosphate-Tris-ghosts were still permeable to ferritin when calcium chloride (1–6 m*M*) was added prior to the ferritin treatment (Fig. 9).

The phosphate-Tris-phosphate-ghosts were also permeable to ferritin (Fig. 10). Addition of calcium chloride (1 m*M*) to the phosphate-Tris-phosphate-ghosts prior to the ferritin treatment prevented the entry of ferritin (Figs. 11 and 12).

Chart II summarizes the above results.

DISCUSSION

The results presented indicate that Tris-HCl buffer produces permanent lesions in human erythrocyte ghosts, thus permitting the entry of ferritin molecules. Phosphate buffer, on the other hand, does not produce permanent lesions since ferritin does not enter the erythrocyte ghosts. It must, however, be assumed that the repeated washing in 0.01 *M* phosphate buffer does open holes in the membrane at each wash to permit the escape of hemoglobin. These holes must reseal fairly rapidly, in agreement with the observations of Seeman (*10*). The existence of permanent holes produced in erythrocyte ghosts by Tris-HCl buffer could account for the more rapid release of hemoglobin compared to phosphate buffer (*3*, *4*).

Tris-HCl is known to be a weak chelating agent and may remove divalent cations from erythrocyte membranes thus leaving them in weakened condition. In this state membrane holes may be unable to reseal themselves even when the ghosts have been returned to phosphate buffer. The addition of calcium chloride (1 m*M*), does, however, produce a resealing of the phosphate-Tris-phosphate-ghosts though only a few of the phosphate-Tris-ghosts reseal with 1–6 m*M* calcium chloride.

The removal of membrane components other than divalent cations by Tris-HCl buffer cannot be ruled out, though the appearance of the membrane in thin sectioning is normal, i.e., they have the usual continuous "unit membrane" structure. It is

CHART II

SUMMARY OF RESULTS

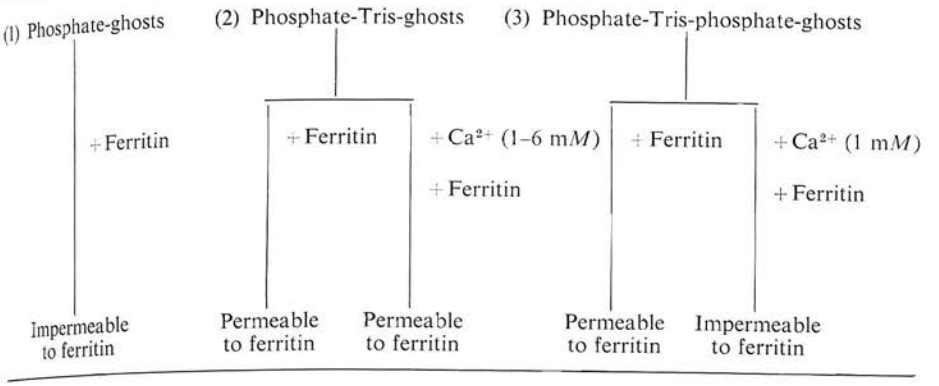

interesting to note that very few holes were seen in the phosphate-Tris-ghosts in the electron microscope in thin sections. But if the holes have diameters in order of 200-500 Å, as suggested by Seeman (*10*), it is unlikely that thay would be revealed very often in thin sections. By negative staining no small lesions or large breaks were observed in these ghosts. However, the fact that ferritin entry occurs indicates that holes (at least 120 Å in diameter) must be present.

It can be concluded that though Tris-HCl buffer does facilitate the release of hemoglobin from human erythrocyte ghosts, it does so with a loss of membrane stability, possibly with a loss of some membrane components, such as divalent cations, or even membrane proteins. The use of phosphate buffer for preparing hemoglobin-free ghosts from human erythrocytes is thus considered to be more desirable than Tris-HCl buffer.

The authors are greatly indebted to Dr. G. H. Haggis (Cell Biology Research Institute, Central Experimental Farm, Ottawa) for the helpful advice and criticism received throughout the preparation of the manuscript.

FIG. 9. Phosphate-Tris-ghosts with ferritin added in the presence of Ca^{2+} (1 mM). The ferritin molecules are present in both the intracellular (*I*) and extracellular (*E*) compartments. × 20,000.

FIG. 10. Phosphate-Tris-phosphate-ghosts with added ferritin. The ferritin molecules are present in both the intracellular (*I*) and extracellular (*E*) compartments. × 20,000.

FIG. 11. Phosphate-Tris-phosphate-ghosts with ferritin added in the presence of Ca^{2+} (1 mM). The ferritin is located only in the extracellular (*E*) compartment. × 25,000.

FIG. 12. Phosphate-Tris-phosphate-ghosts with ferritin added in the presence of Ca^{2+} (1 mM). The unit membrane structure of the ghosts is visible (arrowed). The ferritin molecules are located only in the extracellular compartment. × 90,000.

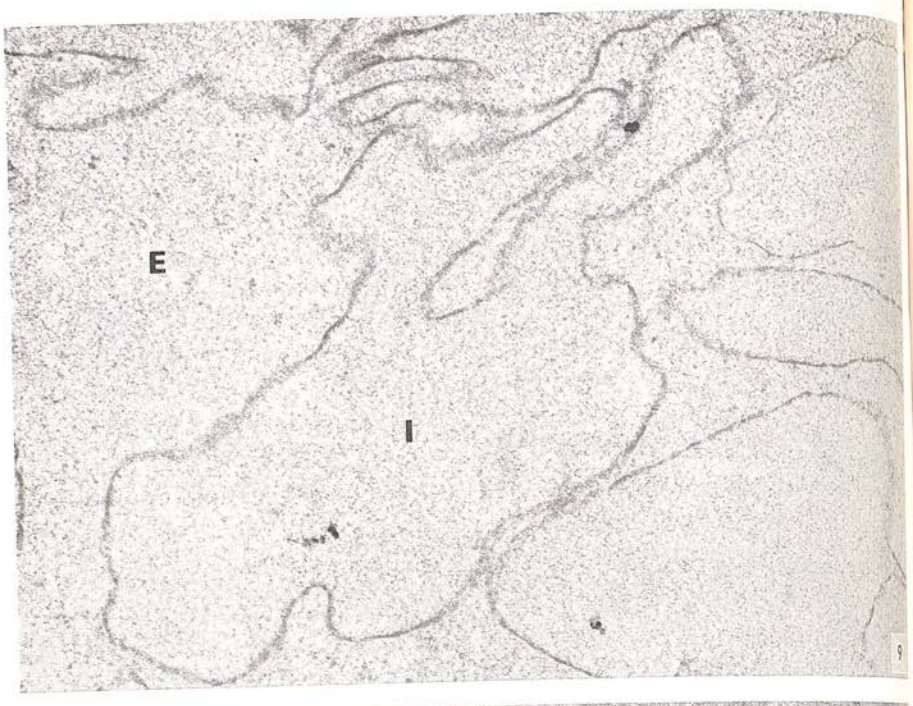
E
I
9

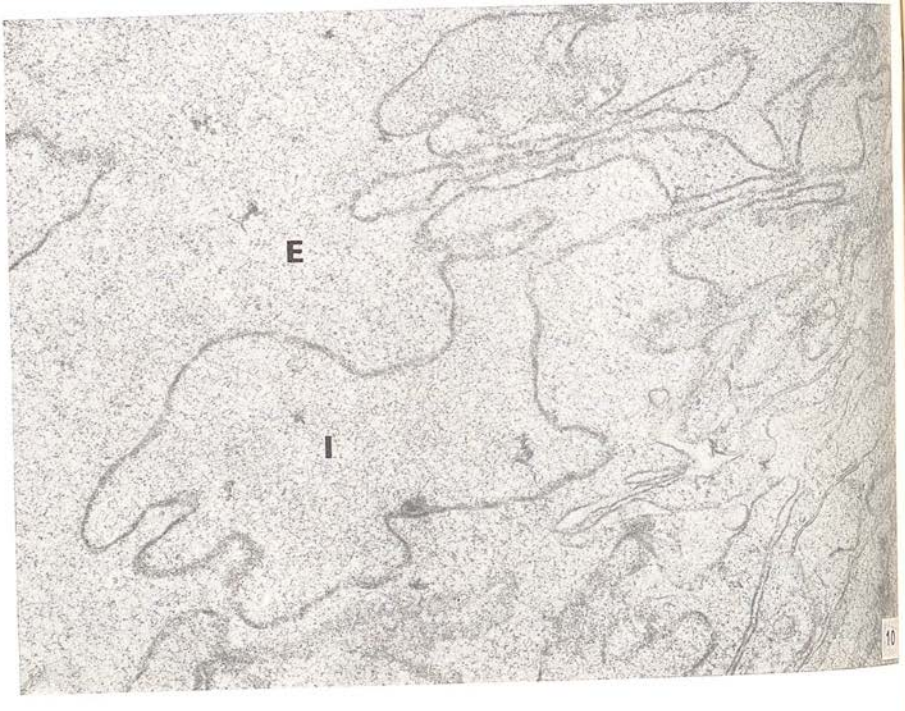
E
I
10

11

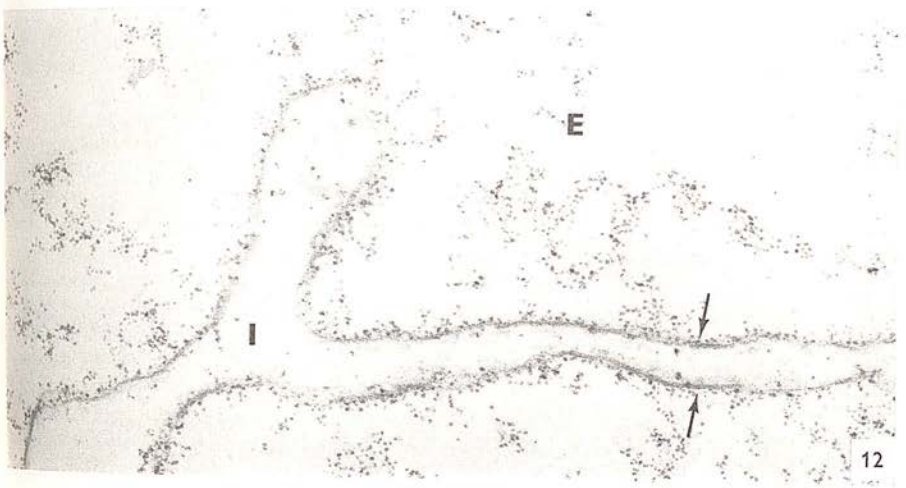

12

REFERENCES

1. DODGE, J. T., MITCHELL, C. and HANAHAN, D. J., *Arch. Biochem. Biophys.* **100**, 119 (1963).
2. HAGGIS, G. H. and HARRIS, J. R., *Proc. 4th European Regional Conf. Electron Microscopy, Rome*, Vol. 2, p. 21 (1968).
3. HARRIS, J. R., *Biochim. Biophys. Acta* **150**, 534 (1968).
4. —— *ibid.* **188**, 31 (1969).
5. MARCHESI, V. T. and PALADE, G. E., *J. Cell Biol.* **35**, 385 (1967).
6. MORGAN, T. E. and HANAHAN, D. J., *Biochemistry* **5**, 1050 (1966).
7. PALADE, G. E., *J. Exptl. Med.* **95**, 285 (1952).
8. ROBERTSON, J. D., *Progr. Biophys. Biophys. Chem.* **10**, 343 (1960).
9. SCHNEIDERMAN, L. J., *Biochem. Biophys. Res. Commun.* **20**, 763 (1965).
10. SEEMAN, P., *J. Cell Biol.* **32**, 55 (1967).
11. WEED, R. I., REED, C. F. and BERG, G., *J. Clin. Invest.* **42**, 581 (1963).

[*Reprinted from the Proceedings of the Biochemical Society*, 19 *February* 1971.
Biochem. J., 1971, Vol. 122, No. 5, 38–40 P.]

The Proteins Released from Intact Erythrocyte 'Ghosts' at low Ionic Strength

By JAMES R. HARRIS. (*Department of Cancer Research, University of Nottingham, Nottingham NG7 2RD, U.K.*)

The methods currently in use for the preparation of haemoglobin-free mammalian erythrocyte 'ghosts' by different research groups vary considerably. This may explain to some extent the overall lack of agreement and co-ordination that exists in the field of erythrocyte membrane proteins. Even though haemoglobin-free erythrocyte 'ghosts' can reasonably be considered as a homogeneous membrane preparation, there can be little doubt that every research group is dealing with a slightly different product from which their protein extracts are made. The preparation method employed by the present author closely follows the procedure developed by Dodge, Mitchell & Hanahan (1963). The incorporation of a single wash with tris-HCl buffer has been found to aid the release of haemoglobin from human erythrocyte 'ghosts', but phosphate buffer alone has been found successful for the preparation of bovine erythrocyte 'ghosts'. These 'ghosts' are intact as judged by phase-contrast and electron microscopy, though the bovine 'ghosts' do tend to show some stromalytic forms (Burger, Fujii & Hanahan, 1968).

In a series of publications the present author has developed a method for the release of several proteins from haemoglobin-free erythrocyte 'ghosts' by causing membrane fragmentation to take place as a result of exhaustive dialysis against distilled water followed by freeze-thawing (Harris, 1968, 1969*a*, 1971). Two of these proteins have been characterized by gel electrophoresis, ultracentrifugation and electron microscopy. A molecule with a quaternary conformation resembling a hollow cylinder, approx. 170 Å long, 125 Å external diameter and 40 Å internal diameter, with a sedimentation coefficient of 22.5 S, has been isolated from both human and bovine erythrocyte 'ghosts'. Another component has a quaternary conformation resembling a torus or ring, approx. 130 Å external diameter, 60 Å internal diameter and 40 Å thick, and has a sedimentation coefficient of 9.0 S. This second protein, which photographic rotation suggests has ten subunits (Harris, 1969*b*), has only been isolated from human erythrocyte 'ghosts'. At the moment it is not possible to say whether or not the single-torus protein is a dissociated form of the hollow-cylinder protein, though the electron-microscopic results may indicate this. Purified preparations of each protein are very stable at pH 8.0. As yet no function can be ascribed to these proteins.

The main method used for the purification of the above-mentioned proteins has been sucrose-density-gradient centrifugation, which avoided the problem of protein aggregation that was generally encountered when the protein extracts were applied to Bio-Gel or Sepharose columns. Samples were taken directly from the sucrose gradients for polyacrylamide-gel electrophoresis at pH 8.0 in the absence of dissociating agents. After dialysis samples were studied electron microscopically by negative staining.

The electron-microscopic images given by the single-torus and hollow-cylinder proteins are meaningful with respect to protein symmetry. Even though the electron-microscopic image of a protein is a two-dimensional representation of a three-dimensional structure, it has been shown that for the proteins under discussion it is possible to interpret these images in three-dimensional terms (Harris, 1969*b*). For proteins that do not have such a geometrical quaternary conformation this may not be possible, since the number of orientations of the protein on the carbon backing film might then be very large, resulting in a large number of slightly different electron images. The single-torus protein exhibits simple cyclic symmetry, whereas the hollow-cylinder protein appears to have a rather complex dihedral and cyclic symmetry. In the electron microscope the hollow-cylinder protein oriented on its side is seen to be composed of four stacked rings. Careful examination of this image suggests that the inner pair of rings are fused more closely than each of the inner rings is to its adjacent outer ring. This might indicate that all four rings are not of identical composition or that steric hindrance is playing a significant role. The inner pair of rings might be identical and also the outer pair. As no aggregates of two, three, five or more protein rings are found, this might support the above suggestion. The binding affinities between the subunits or adjacent protein rings must determine the possible number of rings that can stack together. The inner rings may possess an affinity for each other on one side and an affinity for the outer ring on the opposite side. The outer rings may have no affinity for each other but possess on one side an affinity for the surface of the inner-ring

dimer. Proposals such as this are purely speculative, but are thought to be reasonable in terms of the molecular symmetry observed in the electron microscope.

Recent studies have suggested that the hollow-cylinder and single-torus proteins may be located on the inner surface of the erythrocyte membrane. As mentioned above, bovine 'ghosts' prepared in phosphate buffer tend to give rise to stromalytic forms. Inside some of the stromalytic projections the hollow-cylinder protein has clearly been seen by negative staining with ammonium molybdate. In the case of the hollow-cylinder protein situated on a large area of membrane (Harris & Agutter, 1970) it is not possible to say for certain whether the molecule is located on the inner or the outer surface of the collapsed membrane. The interpretation applicable to the electron image of the stromalytic tube is more precise and there can be little doubt that the molecules are located inside the membrane projections. The assumption is implied that the inner surface of the stromalytic projection is continuous with the inner surface of the normal membrane, and, though likely, this cannot be accepted as fact. A further result that is indicative of the single-torus and hollow-cylinder proteins being loosely bound to the inner surface of the membrane is that small membrane lesions, probably produced at the time of preparation of the negatively stained specimens, often have large numbers of these molecules located on the adjacent carbon backing film. It is reasoned that the trauma that produced the membrane lesion permitted the escape of the molecules.

The tentative conclusions drawn from the above observations are supported by the immunological approach of C. Howe, who has shown that antibodies prepared against the single-torus protein do not agglutinate intact erythrocyte (personal communication). Also, Hoogeveen, Juliano, Coleman & Rothstein (1970), using intact human erythrocytes and erythrocyte 'ghosts' that had been labelled with a fluorescent stilbene compound, have shown that on extraction at low ionic strength all the fluorescence remained with the residual membrane fragments. Both these observations suggest that the proteins that are released when the intact erythrocyte 'ghost' undergoes fragmentation at low ionic strength come from the inner surface of the membrane.

The possibility remains that the proteins under discussion are predominantly adsorbed cytoplasmic contaminants. Hoogeveen *et al.* (1970) present a calculation that argues very much against this being the case. The present author considers that, as the proteins have bound to the 'ghosts' through the extensive washings during which the haemoglobin is released, it is unlikely that other cytoplasmic proteins would remain bound. Even if in the intact erythrocyte an equilibrium exists between membrane-bound and cytoplasmic protein, it is reasonable to consider the proteins to be membrane-associated, though not membrane 'structural' proteins.

Burger, S., Fujii, T. & Hanahan, D. J. (1968). *Biochemistry, Easton*, **7**, 3682.

Dodge, J. T., Mitchell, C. & Hanahan, D. J. (1963). *Archs Biochem. Biophys.* **100**, 119.

Harris, J. R. (1968). *Biochim. biophys. Acta*, **150**, 534.

Harris, J. R. (1969*a*). *Biochim. biophys. Acta*, **188**, 31.

Harris, J. R. (1969*b*). *J. molec. Biol.* **46**, 329.

Harris, J. R. (1971). *Biochim. biophys. Acta* (in the Press).

Harris, J. R. & Agutter, P. (1970). *J. Ultrastruct. Res.* **33**, 219.

Hoogeveen, J. Th., Juliano, R., Coleman, J. & Rothstein, A. (1970). *J. Membrane Biol.* **3**, 156.

PRINTED IN GREAT BRITAIN BY WILLIAM CLOWES AND SONS LIMITED, LONDON, COLCHESTER AND BECCLES

Reprinted from

(6)

Biochimica et Biophysica Acta
Elsevier Publishing Company, Amsterdam - Printed in The Netherlands

BBA 35761

FURTHER STUDIES ON THE PROTEINS RELEASED FROM HAEMOGLOBIN-FREE ERYTHROCYTE GHOSTS AT LOW IONIC STRENGTH

J. R. HARRIS*
Department of Zoology, University of Edinburgh, Edinburgh (Scotland)

(Received October 16th, 1970)

SUMMARY

1. A number of different proteins are solubilized from intact haemoglobin-free human and bovine erythrocyte ghosts by dialysis against distilled water followed by a freeze–thaw treatment.

2. The heterogeneity of the extract is revealed by polyacrylamide gel electrophoresis at pH 8.0, in the absence of dissociating agents. Among the proteins in solution are ones which have quaternary conformations resembling hollow cylinders and single tori. These proteins are identified by electron microscopy.

3. By analytical ultracentrifugation the sedimentation coefficients of the hollow cylinder and single torus proteins are calculated at 22.5 S and 9.0 S, respectively, at infinite dilution.

4. The soluble proteins are separated by sucrose density gradient centrifugation. Fractions taken for electrophoresis and electron microscopic study indicate the positioning of the hollow cylinder and torus proteins on the gradient.

5. The results presented are discussed in relation to those of other workers in the field of erythrocyte membrane proteins.

INTRODUCTION

In a recent series of papers[1–3] it was shown that a class of proteins with characteristic quaternary conformations resembling hollow cylinders and single tori, could be released from intact haemoglobin-free human and bovine erythrocyte ghosts. The treatment applied amounted to dialysis against distilled water followed by freeze–thawing. A purification method for the single torus protein from human erythrocyte ghosts was developed[2]. This method depended primarily upon the selective aggregation and sedimentation of other proteins present in the original extract. In the present communication attempts have been made to show that the low ionic strength extraction of both human and bovine erythrocyte ghosts does in fact release a number of

* Present address: Department of Cancer Research, University of Nottingham, Nottingham, England.

different proteins. Following concentration procedures, these proteins are kept in solution by dialysis against 10 mM Tris buffer (pH 8.0). Previously, this dialysis was done against distilled water, which resulted in the aggregation of some of the proteins leaving only the single torus protein in solution[2].

METHODS

The preparation of intact erythrocyte ghosts

Haemoglobin-free human and bovine erythrocyte ghosts were prepared in 10 mM phosphate buffer (pH 7.4) by previously published methods[2,4], which are themselves modifications of the method of DODGE *et al.*[5]. By phase contrast microscopy human erythrocyte ghosts showed the typical biconcave-disc shape of the intact erythrocyte, whereas quite a large proportion of the bovine erythrocyte ghosts exhibited stromalytic forms[6,7].

The extraction procedure

Basically, the original method developed for the extraction of human erythrocyte ghosts[2] has been followed throughout this study. The distilled-water dialysis was, however, performed for 40 h at 4° with two changes of the dialysate. The ratio of erythrocyte ghosts, packed at 23 000 × *g* for 30 min, to dialysate was 1:50. Freezing was done with a dry ice–methanol mixture and thawing in a 37° shaking water bath. The supernatant obtained following centrifugation at 58 000 × *g* for 30 min, which contained 10–20% of the ghost protein[2], was concentrated to approx. 12 mg/ml. Precipitation with 50% saturated $(NH_4)_2SO_4$ at 4°, rapid pervaporation at room temperature and removal of water with Aquacide II at 4°, were the principal concentration methods employed. Following concentration, the solution was dialysed overnight against 10 mM Tris–HCl buffer (pH 8.0) at 4°. The material was then centrifuged at 150 000 × *g* for 20 min to pellet any aggregated protein and the supernatant taken for further investigation by gel electrophoresis, ultracentrifugation and electron microscopy.

Electron microscopy

Samples of the protein extracts (diluted to approx. 0.1 mg protein/ml) were negatively stained with 2.0% sodium phosphotungstate (pH 7.0). Electron microscopic study was performed with an A.E.I. E.M. 6B. Routine electron optical magnifications of 50 000 and 100 000 diameters were employed. The electron microscope magnification scale had less than 2.0% error, by calibration using a standard grid containing 2160 lines/mm. Photographs were taken on Ilford 3.25-inch plates, "Special Lantern Contrasty".

Polyacrylamide gel electrophoresis

Disc electrophoresis of the crude protein extracts and of sucrose gradient fractions was performed on 7.0% polyacrylamide gel in 0.02 M Tris–HCl buffer (pH 8.0). Gels 7 cm long and 4 mm diameter were pre-run for 30 min before the application of protein samples. Electrophoresis was performed at 7 mA per tube until the bromophenol blue tracer dye reached the bottom of the tubes. The gels were stained in

0.1% Coomassie Blue in 10% acetic acid–10% methanol and destained by washing in the same solvent mixture.

Sucrose density gradient centrifugation

5.0–20% sucrose density gradients were prepared using a mixing apparatus following that of BRITTEN AND ROBERTS[8], for use with the M.S.E. 3 × 23 ml swing-out rotor. 1.0–1.5-ml samples of the concentrated protein extract from human and bovine erythrocyte ghosts were layered over the gradients, which were centrifuged at 25 000 rev./min (65 000 × g_{av}) for 16 h. The contents of the tubes were then displaced from the bottom by 40.0% sucrose and passed through the flow cell of an ISCO Model 222 ultraviolet analyser. Fractions were taken manually on following the absorbance at 280 mμ as the gradients were displaced. Samples for electron microscope study were dialysed against 2 mM Tris–HCl (pH 8.0) to remove the sucrose. The material from the gradients was applied directly to the polyacrylamide gels without prior dialysis.

Analytical ultracentrifugation

Samples of the concentrated protein extracts from human and bovine erythrocyte ghosts were studied using the M.S.E. analytical ultracentrifuge. Runs were performed in 0.1 M KCl at 20° and the sedimentation coefficients extrapolated to infinite dilution.

Column chromatography

Chromatographic columns of Biogel P300 and Sepharose 6B were employed for gel filtration studies of the proteins extracted from human and bovine erythrocyte ghosts. Columns were pre-run overnight with 10 mM Tris–HCl buffer (pH 8.0), prior to the application of protein samples. The effluent from the columns was monitored at 280 mμ with an ISCO Model 222 ultraviolet analyser.

RESULTS

Heterogeneity of the protein extracts

The low ionic strength extraction procedure applied to haemoglobin-free human and bovine erythrocyte ghosts releases several protein species (Figs. 1 and 2). Among

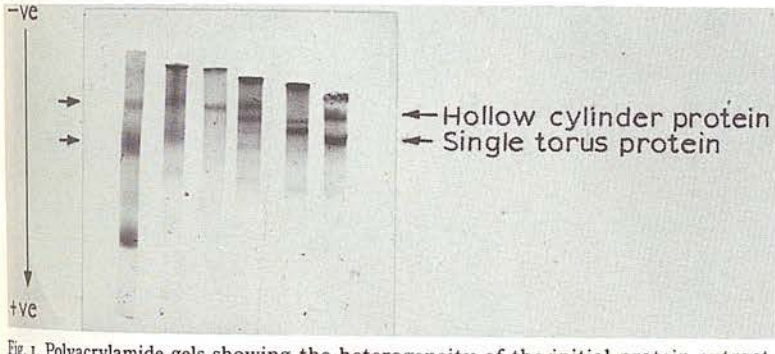

Fig. 1. Polyacrylamide gels showing the heterogeneity of the initial protein extract from human erythrocyte ghosts. The two gels on the left hand side have been electrophoresed longer than those on the righthand side. Material at the origin tends to interfere with the migration rates of the soluble proteins.

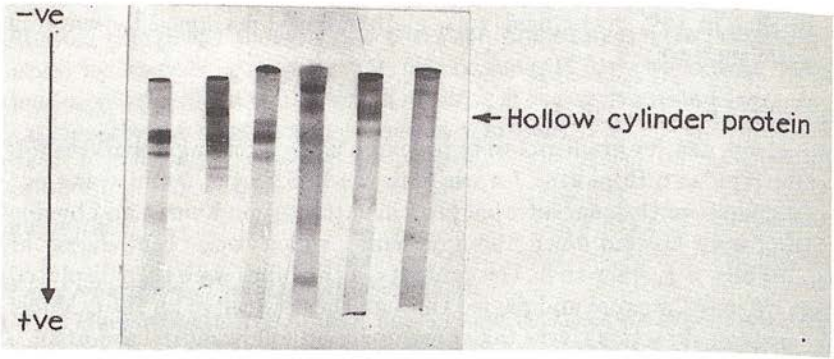

Fig. 2. Polyacrylamide gels showing the heterogeneity of the initial protein extract from bovine erythrocyte ghosts. Material at the origin has caused anomalous protein migration rates on some of the gels.

these are the hollow cylinder and single torus proteins[1–3], which were initially detected by electron microscopy. By gel slicing it has been possible to determine the position of these proteins on polyacrylamide gels after electrophoresis[2]. Figs. 3 and 4 show representative negatively stained electron microscope fields of the initial protein extract from bovine and human erythrocyte ghosts. The hollow cylinder protein complex can be seen in both Fig. 3 and Fig. 4, whereas the single torus protein is only present in Fig. 4 (the extract from human erythrocyte ghosts). Apart from these morphologically recognisable proteins there is also much fine material with no defin

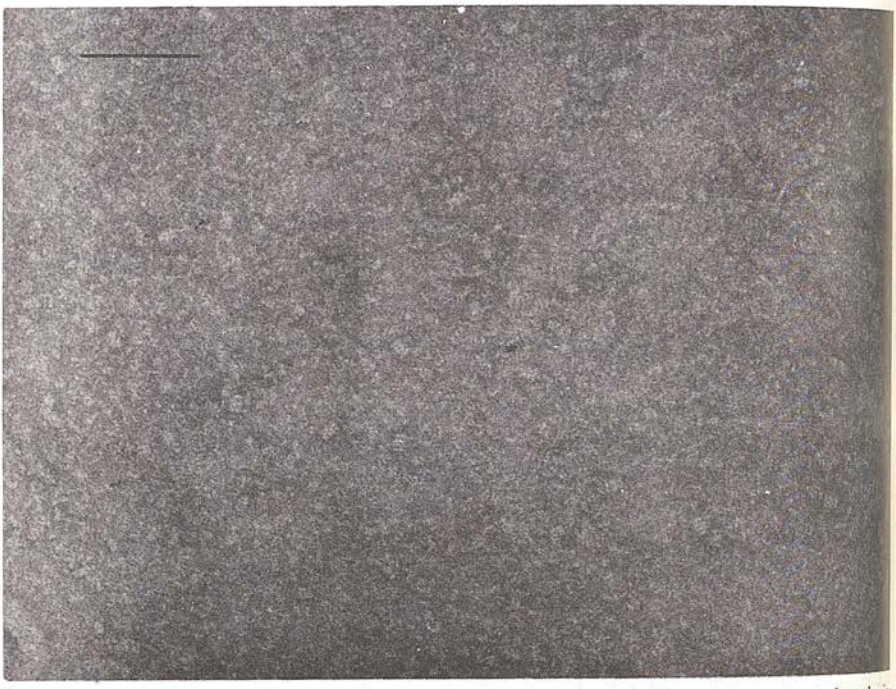

Fig. 3. A representative electron micrograph showing the initial protein extract from bovine erythrocyte ghosts. Negatively stained with 2% sodium phosphotungstate (pH 7.0). The scale marker indicates 1000 Å.

Fig. 4. A representative electron micrograph showing the initial protein extract from human erythrocyte ghosts. Negatively stained with 2% sodium phosphotungstate. The scale marker indicates 1000 Å.

able shape on the background. This background should be compared with the "clean" negatively stained background obtained from purified solutions of the single torus[2] and hollow cylinder[3] proteins (see below).

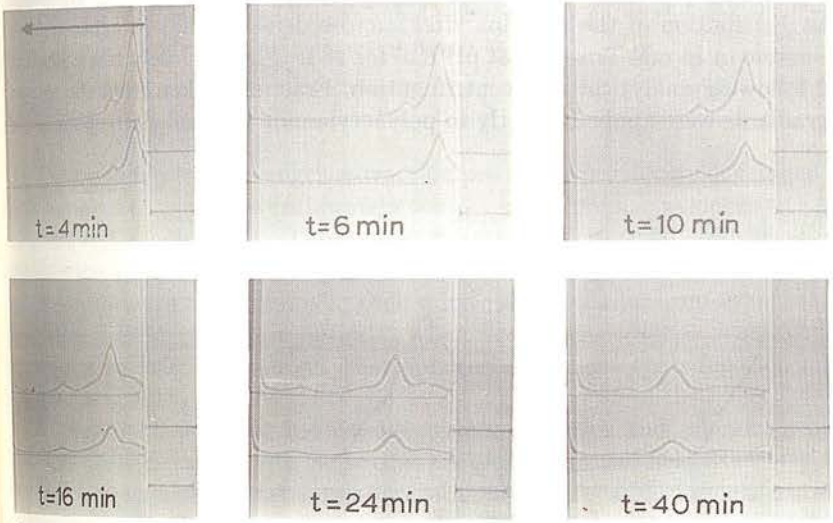

Fig. 5. Analytical ultracentrifugation Schlieren patterns of the concentrated protein extract from human erythrocyte ghosts. The phase plate angle was 20°, and the speed of rotation 54 600 rev./min. The protein concentration was approx. 12 mg/ml (upper trace) and 8 mg/ml (lower trace).

Ultracentrifugation

The concentrated protein extracts from human and bovine erythrocyte ghosts have been studied in the M.S.E. analytical ultracentrifuge and also by sucrose density gradient centrifugation. Fractions taken from the density gradients have been further studied by gel electrophoresis and electron microscopy. Fig. 5 shows the Schlieren pattern given by an extract from human erythrocyte ghosts, in which the single torus protein was shown by electron microscopy to be the main species in solution. The

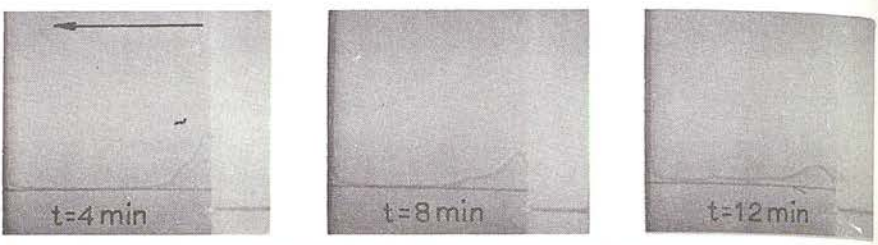

Fig. 6. Analytical ultracentrifugation Schlieren patterns of the concentrated protein extract from bovine erythrocyte ghosts. The phase plate angle was 25° and the speed of rotation 45 200 rev./min. The protein concentration was approx. 8 mg/ml.

sedimentation coefficients of the main Schlieren peak (the single torus) and the small fast moving peak (the hollow cylinder) have been calculated as 9.0 and 22.5 S, respectively, at infinite dilution. The broad shoulders leading up to the main Schlieren peak indicate the presence of other material. The Schlieren patterns obtained with the extracts from bovine erythrocyte ghosts (Fig. 6) were more difficult to interpret, as the peaks were all rather broad. This does in fact agree with the greater heterogeneity of the gel electrophoresis pattern exhibited by the extract from bovine erythrocyte ghosts (Fig. 2), compared with that from human erythrocyte ghosts (Fig. 1).

The distribution of the proteins after sucrose density gradient centrifugation (5–20% sucrose in 10 mM Tris–HCl at pH 8.0) for 16 h (Fig. 7) closely resembles that observed following analytical ultracentrifugation. Fractions taken from the sucrose density gradients were applied directly to polyacrylamide gels and electrophoresed in

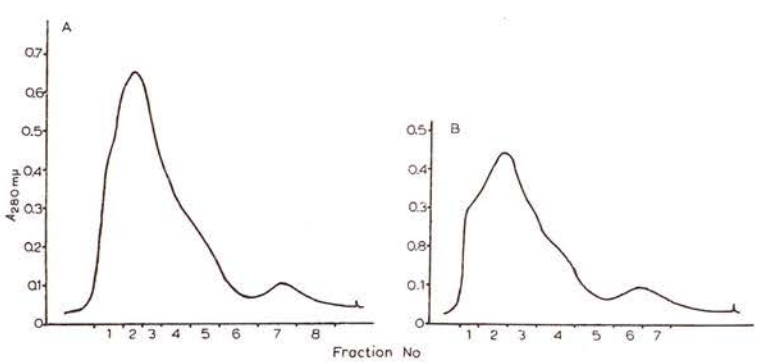

Fig. 7. The distribution of protein on sucrose density gradients (5–20%) after 16 h at 25 000 rev./min. A, the concentrated protein extract from human erythrocyte ghosts; B, the concentrated protein extract from bovine erythrocyte ghosts.

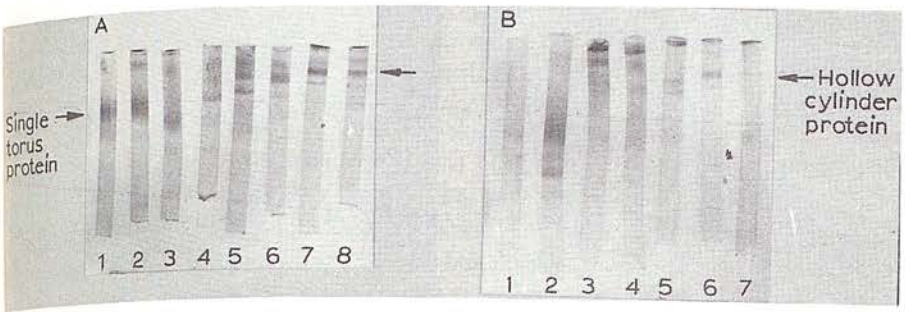

Fig. 8. Polyacrylamide gel electrophoresis of fractions taken directly from sucrose density gradients. A, the extract from human erythrocyte ghosts; and B, the extract from bovine erythrocyte ghosts.

the usual manner (Fig. 8). The two sets of gels in Fig. 8 correspond to the protein distribution curves shown in Fig. 7. By electron microscopic study of the gradient fractions following dialysis, the positions of the hollow cylinder and single torus protein complexes were determined. Fig. 9 shows a sample of the single torus protein region of a sucrose density gradient run of the human erythrocyte ghost extract and Fig. 10 a sample of the hollow cylinder protein region of a gradient run of the bovine erythrocyte ghost extract.

Column chromatography

Gel filtration chromatography of the human and bovine erythrocyte ghost extracts on Biogel P300 revealed that both the single torus and hollow cylinder proteins were present in the excluded volume. Work currently in progress has shown both proteins to be retarded by Sepharose 6B. Some difficulty has been encountered owing to the aggregation of proteins other than the hollow cylinder and single torus on passing down the P300 columns. Thus, the excluded protein peak generally did not represent purified hollow cylinder or single torus protein.

DISCUSSION

The simple low ionic strength extraction procedure previously developed[1,2], has now been shown to release several protein components from haemoglobin-free human and bovine erythrocyte ghosts. Throughout the studies performed on the proteins extracted by this system, the use of agents such as urea and detergents has been avoided, in the hope of leaving the proteins in their native undissociated conformations. Also, the presence of these agents is undesirable when electron microscopic studies are to be performed in conjunction with gel electrophoresis, gradient centrifugation and column chromatography.

It might be hoped that the results presented in this and previous papers[1–4], would agree to some extent with those of other workers in this field. Recently, HOWE AND LEE[9] have obtained a water-soluble fraction (S.G.P.) from human erythrocyte ghosts following lyophilization. Immunologically, this fraction appears to be very similar to that obtained by distilled-water dialysis followed by freeze–thawing, (C. HOWE, personal communication), and the hollow cylinder protein has been shown by

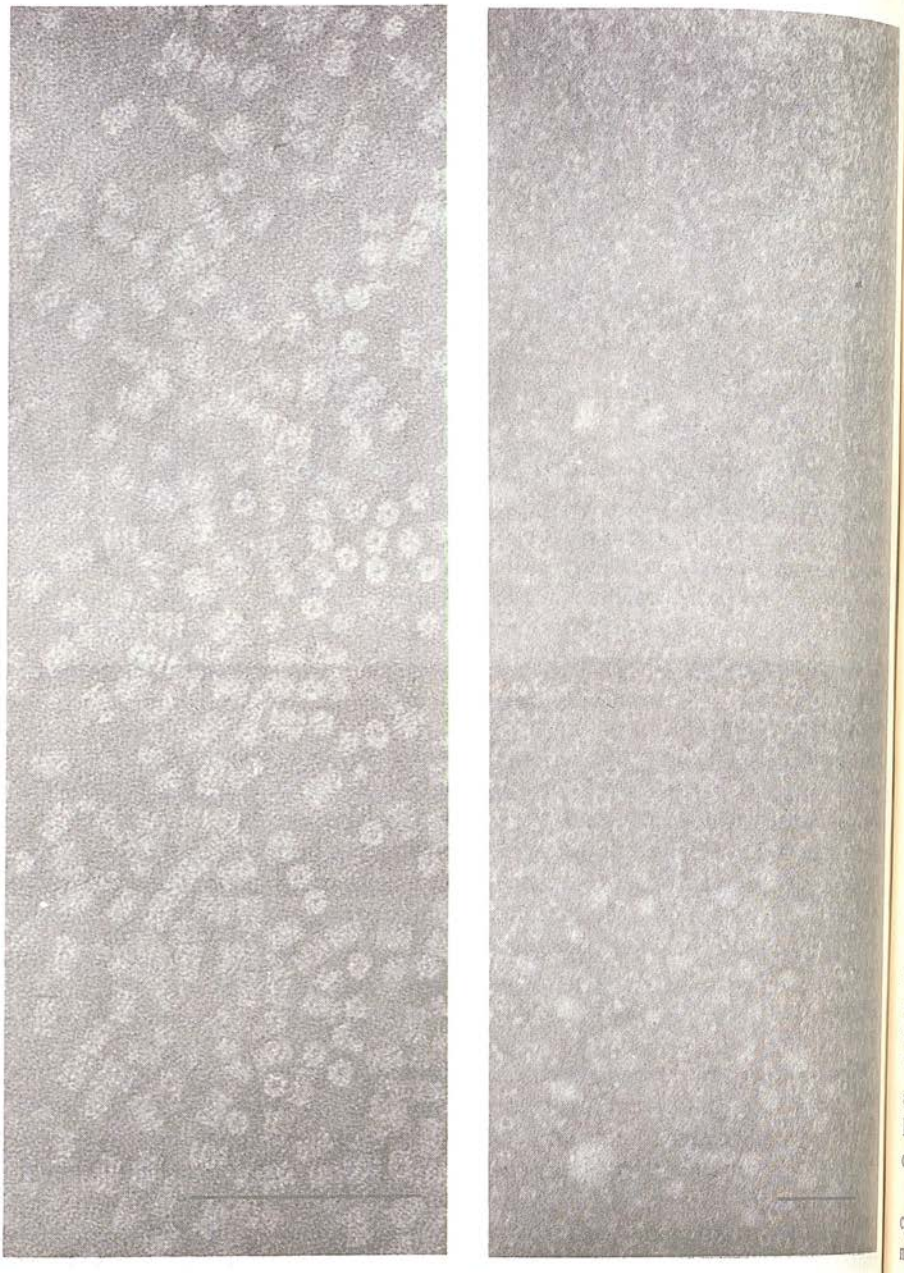

Fig. 9. A representative electron microscope field showing a sample from the single torus region of a sucrose density gradient run done with an extract from human erythrocyte ghosts. Negatively stained with 2% sodium phosphotungstate (pH 7.0). The scale marker indicates 1000 Å.

Fig. 10. A representative electron microscope field showing a sample from the hollow cylinder protein region of a sucrose density gradient run done with an extract from bovine erythrocyte ghosts. Negatively stained with 2% sodium phosphatungstate (pH 7.0). The scale marker indicates 1000 Å.

electron microscopy to be one of the components released by lyophilization (J. R. HARRIS, unpublished results). The ferritin-labeled antibody to HOWE's S.G.P. binds to the surface of intact erythrocytes and erythrocyte ghosts (see ref. 10). This result does not seriously conflict with the recent suggestion of HARRIS[7], that the single torus and hollow cylinder proteins are probably binding to the inner surface of the erythrocyte membrane, since the ferritin-labeled antibodies to other membrane components might be responsible for the observed labeling.

Extensive washing of erythrocyte ghosts in distilled water causes them to undergo fragmentation, and this procedure alone has been found to release the hollow cylinder and single torus proteins from human erythrocyte ghosts (J. R. HARRIS, Ph. D. thesis, University of Edinburgh). HAGGIS[11] has shown that some of the proteins released from human erythrocyte ghosts by distilled-water washing have a tendency to form fibrous bundles in the presence of divalent cations. His published electron micrographs do, however, also show the hollow cylinder and single torus proteins. In this context it might be mentioned that MARCHESI[12] has stated that the protein which he terms "spectrin" can be extracted with distilled water alone, as well as by his more usual EDTA extraction. Neither MARCHESI and his coworkers[13–15] nor ROSENTHAL and his[16], have commented on the presence of the protein components I have detected, though the latter group has stated that EDTA extraction releases several membrane proteins. Both these groups have been more concerned with the proteins from the erythrocyte ghosts which give rise to fibres in the presence of divalent cations than with solubilized proteins which do not give fibres. When negatively stained electron microscope specimens are made under the fibre-forming conditions, the soluble hollow cylinder and single torus proteins tend to be hidden by the larger aggregates of fibrous material[17]. This may explain why the forementioned groups were unable to detect the hollow cylinder and single torus proteins. The state of fragmentation of the erythrocyte ghosts prior to extraction might also be important since it is likely that the hollow cylinder and single torus proteins are readily lost owing to their loosely binding properties.

Recently HOOGEVEEN *et al.*[18] presented data on the proteins liberated from human erythrocyte ghosts at low ionic strength and commented on the varying binding properties of membrane proteins and the problems of interpretation that these phenomena might incur. The statement by this group to the effect that MARCHESI's "spectrin" (see ref. 12), and the hollow cylinder and single torus proteins are different aggregation states of the same protein cannot at the moment be accepted as proven. However, their conclusion that water washing releases proteins from the inner surface of the erythrocyte ghost is in agreement with the author's current views.

As mentioned above, it has been shown directly[7] that the single torus and hollow cylinder proteins are almost certainly situated on the inner surface of the erythrocyte membrane rather than the outer surface. The possibility remains, however, that the proteins could be loosly absorbed cytoplasmic components rather than true membrane components. The discussion of membrane proteins which are bound with varying degrees of firmness is not at the moment very meaningful, yet it is hoped that it will be eventually. Likewise, the discussion of membrane structural and functional proteins will eventually contribute to the overall understanding of membrane physiology.

To date there has been very little attempt to integrate the results of the different research groups working on cell membrane proteins. This somewhat unsatisfactory sit-

uation will have to be changed before an accurate concept of membrane structure and function can be obtained.

ACKNOWLEDGEMENTS

The author wishes to thank Dr. A. H. Maddy (Department of Zoology, University of Edinburgh) for the guidance he has given throughout this study. The help provided by Mr. P. Kelly, during the use of the analytical ultracentrifuge is gratefully acknowledged. Electron microscope facilities were provided by Professor W. E. Watson (Department of Physiology, University of Edinburgh).

REFERENCES

1 J. R. HARRIS, *Biochim. Biophys. Acta*, 150 (1968) 534.
2 J. R. HARRIS, *Biochim. Biophys. Acta*, 188 (1969) 31.
3 J. R. HARRIS, *J. Mol. Biol.*, 46 (1969) 329.
4 J. R. HARRIS AND P. S. AGUTTER, *J. Ultrastruct. Res.*, in the press.
5 J. T. DODGE, C. D. MITCHELL AND D. J. HANAHAN, *Arch. Biochem. Biophys.*, 100 (1963) 119.
6 S. BURGER, T. FUJII AND D. J. HANAHAN, *Biochemistry*, 7 (1968) 3682.
7 J. R. HARRIS, *J. Ultrastruct. Res.*, submitted for publication.
8 R. J. BRITTEN AND R. B. ROBERTS, *Science*, 131 (1960) 32.
9 C. HOWE AND L. T. LEE, *J. Immunol.*, 102 (1969) 573.
10 C. HOWE, H. SPIELE, F. MINIO AND K. C. HSU, *J. Immunol.*, 104 (1970) 1406.
11 G. H. HAGGIS, *Biochim. Biophys. Acta*, 193 (1969) 237.
12 V. T. MARCHESI, in JAMIESON AND GREENWALT, *Red Cell Membrane*, Lippincott Co., Philadelphia, Pa., 1969, p. 156.
13 V. T. MARCHESI AND E. STEERS, *Science*, 159 (1968) 203.
14 S. L. MARCHESI, E. STEERS, V. T. MARCHESI AND T. W. TILLACK, *Biochemistry*, 9 (1969) 50.
15 T. W. TILLACK, S. L. MARCHESI, V. T. MARCHESI AND E. STEERS, *Biochim. Biophys. Acta*, 211 (1970) 125.
16 A. S. ROSENTHAL, F. M. KREGENOV AND H. L. MOSES, *Biochim. Biophys. Acta*, 196 (1970) 254.
17 A. H. MADDY AND J. R. HARRIS, manuscript in preparation.
18 J. TH. HOOGEVEEN, R. JULIANO, J. COLEMAN AND A. ROTHSTEIN, *J. Memb. Biol.*, 3 (1970) 191.

J. ULTRASTRUCTURE RESEARCH 36, 587–594 (1971)

The Location of a Membrane-Associated Protein Complex in Human and Bovine Erythrocyte Ghosts

JAMES R. HARRIS[1]

Department of Zoology, University of Edinburgh, Edinburgh, Scotland

Received July 13, 1970, and in revised form December 15, 1970

A more precise explanation is advanced for the location of two protein complexes in the hemoglobin-free mammalian erythrocyte ghost. It is shown directly by negative staining that the protein complexes are released from membrane lesions, probably produced at the time of preparing the negatively stained specimens. Also, that one of the proteins can be seen inside the stromalytic projections of bovine erythrocyte ghosts. The suggestion is therefore put forward that the proteins are binding loosely to the inner surface of the erythrocyte membrane. The proteins may in fact be adsorbed cytoplasmic contaminants, but in the present state of knowledge it is thought reasonable to consider them as a membrane-associated proteins if not as membrane "structural" proteins. Recent biochemical, immunological, and electron microscopic results that relate to the results presented are discussed.

In a recent series of papers (*4–7*) the extraction and properties of certain proteins from human and bovine erythrocyte ghosts have been presented. Two of these proteins have been shown by electron microscopy to have quaternary conformations resembling single tori and hollow cylinders, respectively. To date it has not been possible to suggest with any degree of precision a location for these molecules within the intact erythrocyte ghost. It was recently shown that the hollow cylinder protein could be observed on the surface of intact erythrocyte ghosts by negative staining (*8*). The author now reinterprets these results in the light of further experience. It is not possible to say from the negatively stained electron microscope image whether the molecules are located on the outside surface of the upper or lower of the two membrane layers of the collapsed ghosts or are in fact on the inner surfaces of the membranes. Also, the possibility that the molecules are actually situated within the overall membrane matrix, though unlikely, cannot be ruled out.

The results to be presented below give further evidence on the possible location of the torus and hollow cylinder protein molecules in the intact erythrocyte ghost.

[1] Present address: Department of Cancer Research, University of Nottingham, University Park, Nottingham, England.

The suggestion is made that the molecules are binding loosely to the inner surface of the membrane.

MATERIALS AND METHODS

The intact erythrocyte ghost

The preparation of haemoglobin-free erythrocyte ghosts. Human and bovine erythrocyte ghosts were prepared in 10 m*M* phosphate buffer (pH 7.4) by previously published procedures (*5*, *8*). The human erythrocyte ghosts are *intact* and stable in this suspending medium, whereas the bovine erythrocyte ghosts are unstable giving rise to many stromalytic forms (*1*).

Negative staining. Samples of the erythrocyte ghost suspensions were negatively stained with 2% ammonium molybdate (pH 7.0), without prior fixation.

Fixation and embedding. Fixation was performed by the addition of 4 volumes of 2% glutaraldehyde in Palade buffer to 1 volume of erythrocyte ghosts. The material was left at room temperature for 1 hour and then pelleted by centrifugation at 1 000 *g* for 10 minutes. The pellets were postosmicated in 1% osmic acid in Palade buffer for 1 hour, dehydrated by passing through graded ethanols and finally epoxypropane, before embedding in TAAB epoxy resin.

Thin sectioning. Thin sections were cut with a Porter-Blum MT-2 ultramicrotome equipped with glass knives. Sections showing a silver-white interference color were mounted on LKB Type 400 grids without a supporting membrane. Post staining was performed using uranyl acetate in 50% ethanol.

Electron microscopy. Electron microscopic examination of the erythrocyte ghost preparations was performed with an A.E.I., E.M. 6B. The instrument had an accelerating voltage of 60 kV, a 250 μ condenser aperture, and a 50 μ objective aperture. Electron optical magnifications of 25 000 and 50 000 diameters were routinely employed. Photographs were taken on Ilford $3\frac{3}{4}'' \times 3\frac{3}{4}''$ plates, Special Lantern Contrasty.

RESULTS

Specimens negatively stained with ammonium molybdate (pH 7.0) generally reveal intact erythrocyte ghosts which have collapsed down onto the carbon film of the viewing grid. A few of these ghosts do, however, show small membrane lesions which are probably produced by the spreading forces applied at the time of preparing the specimen grids, see Figs. 1 and 2. On the background adjacent to these lesions many free single torus and hollow cylinder protein molecules can be seen. It is thus reasoned that the molecules might have escaped during the staining process in order to be confined only to the background region beside the membrane lesion. These protein

FIG. 1. Part of a hemoglobin-free human erythrocyte ghost where a membrane lesion can be seen (between the arrows). Many protein molecules can be seen on the background adjacent to this lesion. Negatively stained with 2% ammonium molybdate, pH 7.0. × 100 000.

FIG. 2. Part of a hemoglobin-free bovine erythrocyte ghost where a membrane lesion has permitted the escape of protein molecules. Negatively stained with 2% ammonium molybdate, pH 7.0. × 150 000.

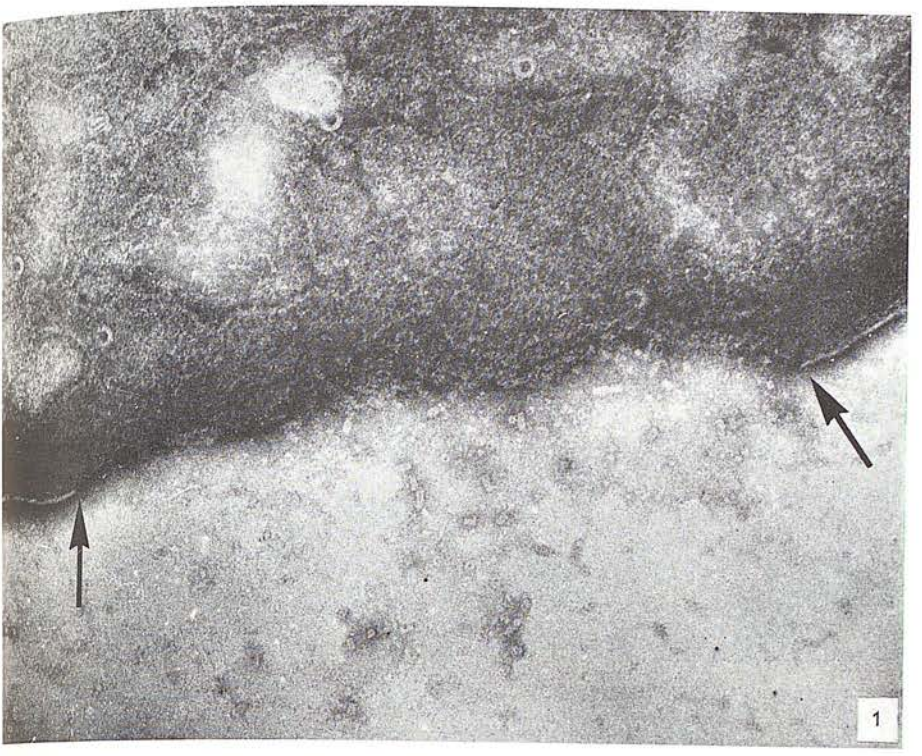

1

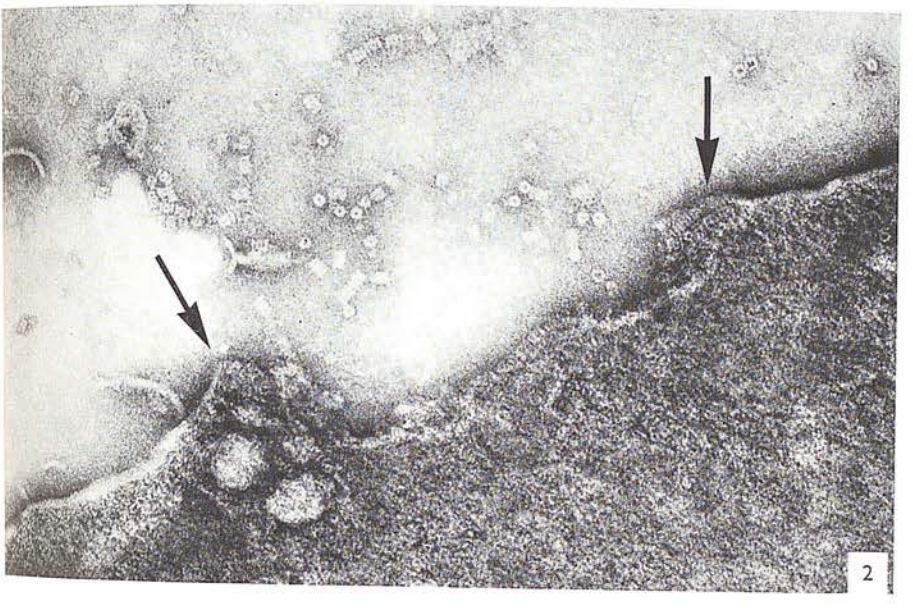

2

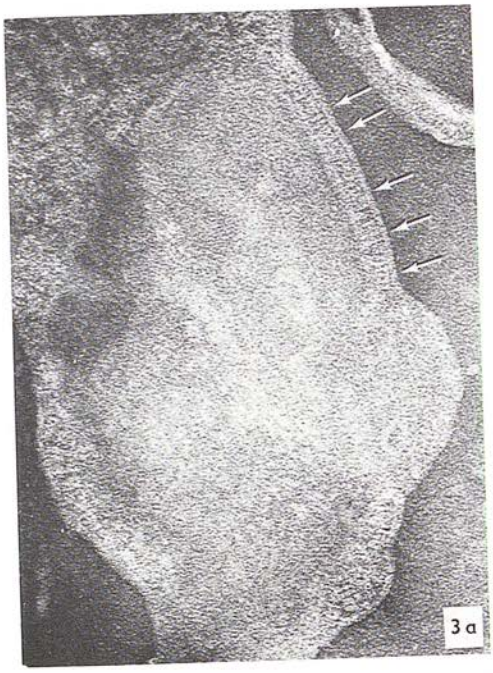
3a

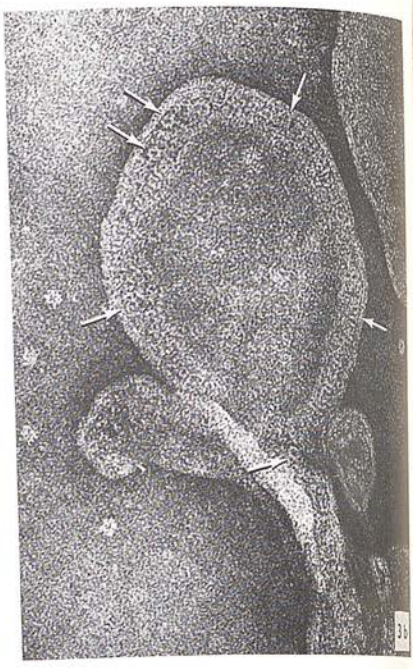
3b

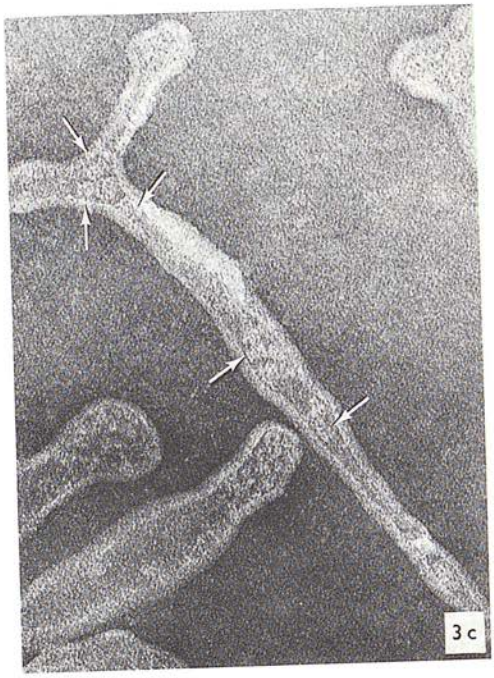
3c

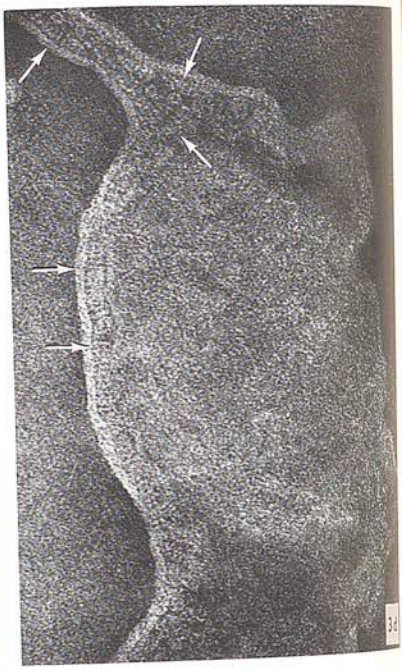
3d

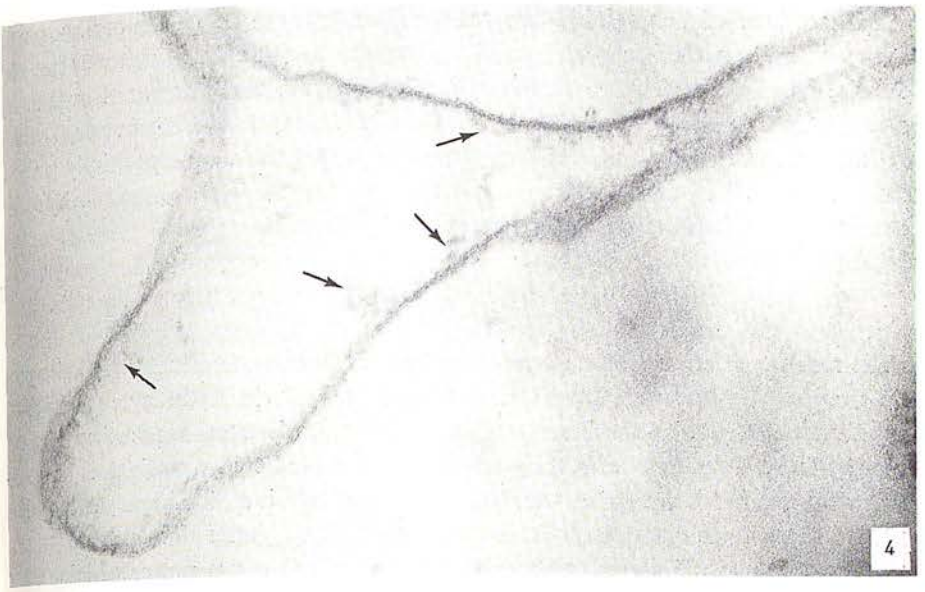

FIG. 4. Part of a thin-sectioned hemoglobin-free bovine erythrocyte ghost. Arrows indicate the "fuzz" associated with the inner surface of the membrane. × 100 000.

molecules could have escaped from the inner or outer surfaces of the membrane, the overall membrane matrix, or from the cytoplasmic compartment of the ghosts (see below).

The stromalytic erythrocyte ghost

When prepared in 10 m*M* phosphate buffer at pH 7.4, bovine erythrocyte ghosts give rise to stromalytic forms much more readily than human erythrocyte ghosts (*1*). These stromalytic forms can be observed by phase contrast microscopy, which rules out the possibility of their being produced by negative staining with ammonium molybdate. It has, however, been shown that staining with sodium phosphotungstate does tend to produce stromalytic forms from human erythrocyte ghosts (*3*), though ammonium molybdate does not have this tendency (*8*). Figure 3 shows selected regions from several bovine erythrocyte ghosts where detail can be seen within the stromalytic forms (arrowed). This detail is immediately seen to resemble the cylindrical protein complex, shown previously to be liberated from ox ghosts when the intact membrane is made to undergo disruption (*4*).

FIG. 3. Selected regions of bovine erythrocyte ghosts which show stromalytic projections. Arrows indicate the cylindrical protein complex within these stromalytic projections. In 3b several free molecules can also be seen. Negatively stained with 2 % ammonium molybdate pH 7.0. × 200 000.

Thin sections of hemoglobin-free mammalian erythrocyte ghosts are known to show a "fuzz" on the inner surface of the membrane (Fig. 4). Whether or not this material can be correlated with the cylindrical protein complex is not certain. If, as suggested by the above results, this protein is binding to the inner surface of the erythrocyte membrane, one would expect it to contribute to the positively stained electron image. Most discussion on this feature has, however, centred around the consideration of it being a fibrous protein (see below).

DISCUSSION

The results presented above suggest that the single torus and hollow cylinder protein complexes previously isolated from human and bovine erythrocyte ghosts (*4–7*) may be associated with the inner surface of the red cell membrane rather than the outer surface. Recently two other groups have obtained evidence which is in agreement with this proposal. Howe (*12*) has shown that rabbit antibody prepared against purified single torus protein from human erythrocyte ghosts does not agglutinate intact erythrocytes. This indicates that the antigenic sites are not accessible to the antibodies and that they are therefore probably located on the inside of the membrane. Hoogeveen et al. (*11*) have labeled the proteins on the outer surface of human erythrocytes and erythrocyte ghosts with a fluorescent stilbene compound and have found that all the fluorescence stayed with the membrane fragment fraction after releasing nonhemoglobin proteins by a low ionic strength treatment similar to that developed by the author. This result was interpreted as indicating that as erythrocyte ghosts break up under low ionic conditions there is a loss of protein from the inner surface of the membrane.

It can be nervertheless be argued that the proteins might have initially been present in the cytoplasm of the erythrocyte and have become adsorbed to the membrane during the preparation of the erythrocyte ghosts. Hoogeveen et al. (*11*) mention the not unreasonable possibility that an equilibrium might exist between membrane bound and soluble protein inside the intact erythrocyte. They do, however, calculate that relative to hemoglobin the nonhemoglobin water-soluble proteins from human erythrocyte ghosts must have a selective binding factor as high as 1 500:1. The author considers that as the single torus and hollow cylinder proteins fall within the category discussed by Hoogeveen et al. (*11*), that it is reasonable to consider them as membrane-associated proteins, although probably not as membrane "structural" proteins.

The stromalytic forms shown in Fig. 3 clearly have the hollow cylinder protein within their tubular membranes. In the case of the intact erythrocyte ghost (*8*) or of large membrane fragments it is not always possible to say whether such molecules

are located on the exterior of the upper or lower layers of membrane or are for instance situated on the interior surfaces or merely trapped between the two membrane layers. At the moment one cannot say for certain that the inner surface of the erythrocyte ghost stromalytic projections is continuous with the inner surface of the normal erythrocyte membrane, though in the present discussion the postulation is made that it probably is.

The presence of large numbers of the single torus and hollow cylinder protein molecules in the vicinity of small membrane lesions at the edges of negatively stained erythrocyte ghosts (Figs. 1 and 2), strongly suggests that the molecules have been released from the ghost interior or the inner surface of the membrane. They could also have been released from the overall membrane matrix or from the outer surface, but from the evidence of Howe (*12*) and Hoogeveen et al. (*11*) it seems unlikely that they are situated on the outer surface.

If the above suggestions are correct, one might hope to be able to detect these molecules by thin sectioning. Several groups of workers have in fact observed a "fuzz" on the inner surface of hemoglobin-free mammalian erythrocyte ghosts (*13*, *14*, *18*), as shown in Fig. 4. This has generally been expressed in terms of a membrane fibrous protein, but compared with the fibrils seen on the inner surface of avian erythrocyte ghosts (*9*, *10*) this "fuzz" cannot truly be considered to have a fibrous nature. It could equally well be the image given by positively stained protein molecules that are binding to the inner surface of the membranes. Recent freeze-cleaving and etching studies (*2*, *15*, *16*, *17*) have indicated that 85 Å particles are located within the membrane matrix and may even penetrate through to the inner surface. Some of these particles could be compatible with the cylindrical protein complex. Freeze-etching has not yet given any positive indication of the presence of fibers on the inner surface of the mammalian erythrocyte membrane.

The author wishes to acknowledge the fact that electron microscope facilities were made available by Professor W. E. Watson, Department of Physiology, University of Edinburgh. The embedding and thin sectioning was skillfully performed by Mr J. N. Brown, Department of Physiology, University of Edinburgh.

REFERENCES

1. BURGER, S., FUJII, T. and HANAHAN, D. J., *Biochemistry* **7**, 3682 (1968).
2. DA SILVA, P. P. and BRANTON, D. J., *J. Cell Biol.* **45**, 598 (1970).
3. HAGGIS, G. H. and HARRIS, J. R., *Proc. Eur. Reg. Conf. Electron Microsc. 4th, Rome*, p. 21 (1968).
4. HARRIS, J. R., *Biochim. Biophys. Acta* **150**, 534 (1968).
5. — *ibid.* **188**, 31 (1969).
6. — *J. Mol. Biol.* **46**, 329 (1969).

7. —— *Biochim. Biophys. Acta* **229**, 761 (1971).
8. HARRIS, J. R. and AGUTTER, P., *J. Ultrastruct. Res.* **33**, 219 (1970).
9. HARRIS, J. R. and BROWN, J. N., *Brit. Poultry Sci.* **12**, 95 (1971).
10. —— *J. Ultrastruct. Res.* in press.
11. HOOGEVEEN, J. T., JULIANO, R., COLEMAN, J. and ROTHSTEIN, A., *J. Memb. Biol.* 3, 156 (1970).
12. HOWE, C., personal communication.
13. MARCHESI, V. T. and PALADE, G. E., *J. Cell Biol.* **35**, 385 (1967).
14. ROSENTHAL, A. S., KREGENOW, F. M. and MOSES, H. C., *Biochim. Biophys. Acta* 196, 254 (1970).
15. TILLACK, W. T. and MARCHESI, V. T., *J. Cell Biol.* **45**, 649 (1970).
16. WEINSTEIN, R. S. and KOO, V. M., *Proc. Soc. Exp. Biol. Med.* **128**, 353 (1968).
17. WEINSTEIN, R. S., CLOWES, A. W. and MCNUTT, N. S., *Proc. Soc. Exp. Biol. Med.* **134**, 1195 (1970).
18. ZELANDER, T. and ERICSSON, L., *J. Ultrastruct. Res.* **12**, 240 (1965).

Int. J. Cancer: **11**, 385-397 (1973)

(8)

FRACTIONATION OF PLASMA MEMBRANE-ASSOCIATED TUMOUR-SPECIFIC ANTIGEN FROM AN AMINOAZO DYE-INDUCED RAT HEPATOMA

by

R. W. BALDWIN, J. R. HARRIS [1] and M. R. PRICE

Cancer Research Campaign Laboratory, The University of Nottingham, University Park, Nottingham, NG7 2RD, England

Tumour-specific antigens from an aminoazo dye-induced rat hepatoma were liberated in a soluble form following limited papain digestion of tumour cell membrane preparations. Fractionation of the soluble extract by DEAE-cellulose chromatography, gradient centrifugation and preparative electrophoresis yielded a major antigenic fraction, with an approximate molecular weight of 55,000, together with a range of other minor antigenic components of larger molecular weight. All preparations retained the capacity to inhibit the reaction of antibody in tumour-immune sera with the plasma membrane of viable hepatoma target cells in the indirect immunofluorescence test. It is considered that the defined antigen fractions isolated provide material suitable for analysing the nature of tumour antigen expression in chemical carcinogenesis and for evaluating the involvement of antigen-antibody interaction in tumour immunity.

Tumour-specific antigens expressed at the cell surface of carcinogen-induced rat hepatomas and fibrosarcomas are held to be new, discrete components of the transformed cell plasma membrane (Baldwin *et al.*, 1971*a*,*c*). It has been established that these antigenic determinants represent specific products of individual tumours and that they have the capacity to evoke an immune response which may lead to tumour rejection (Baldwin and Barker, 1967*a*; Baldwin, 1970). In order to evaluate more precisely the nature of tumour-specific antigen expression in chemical carcinogenesis, and to determine the involvement of antigen-antibody interactions in tumour immunity, methods are required for the isolation and purification of these membrane-associated components.

Previous studies have indicated that plasma membrane fractions, from aminoazo dye-induced rat hepatomas (Baldwin and Moore, 1969*a*), 3-methylcholanthrene-induced rat sarcomas (Baldwin and Pimm, unpublished findings) and a spontaneously arising rat mammary carcinoma (Baldwin and Embleton, 1970), retain tumour-specific antigenic activity and the immunogenicity of hepatoma and sarcoma membrane preparations has been demonstrated by their capacity to elicit tumour-specific antibody responses in syngeneic rats. Limited papain digestion of membrane preparations from one aminoazo-dye induced hepatoma (D23) has been shown to liberate a soluble antigenic fraction (Baldwin and Glaves, 1972). Ion exchange chromatography allowed partial purification of the components displaying antigenic activity, although the fraction isolated was heterogeneous as indicated by analytical polyacrylamide gel electrophoresis. The present communication reports studies concerned with the further fractionation and characterization of hepatoma D23 specific antigen.

Received: October 9, 1972.

[1] Present address: Department of Physiology, Bute Medical Buildings, St. Andrews, Fife, Scotland.

MATERIAL AND METHODS

Rats and tumour

Hepatoma D23, originally induced in a male Wistar rat by oral administration of 4-dimethylaminoazobenzene, was maintained by serial transplantation in syngeneic male recipients. Tumour tissue, harvested from the peritoneal cavity and dissected free from capsular connective and necrotic tissues, was finely chopped. All subsequent operations were performed at 0° to 5° C unless otherwise stated.

Homogenization and membrane preparation

Hepatoma D23 tissue, resuspended in 1 mM $NaHCO_3$, 2 mM $CaCl_2$, 2 mM $MgCl_2$, pH 7.6 (4 volumes of medium per g of tissue) was reduced to a suspension of single cells and free nuclei using an Ultraturrax homogenizer operated at approximately 1/3 maximum output. Remaining connective tissue debris was removed by filtration through 60-mesh stainless steel screens and approximately 90% cellular disruption was finally effected using a Potter-Elvehjem homogenizer. The total homogenate was filtered through 120-mesh stainless steel screens and centrifuged at $600 \times g$ for 10 min. Nuclear pellets were washed with homogenization medium three times by centrifugation at $600 \times g$ for 10 min to release occluded membrane material. A crude " extra-nuclear " membrane preparation was sedimented from the combined $600 \times g$ supernatants by centrifugation at $78{,}00 \times g$ for 45 min.

Papain solubilization

" Extra-nuclear " membranes were dispersed in 5 mM Tris-PO_4, pH 7.8 containing 5 mM L-cysteine, at 30 mg of membrane protein per ml. Papain (Sigma Chemical Co., Kingston-upon-Thames, England) was added at a concentration of 1 mg per 30 mg of membrane protein and the suspension was stirred for 60 min at 37° C. Undegraded membrane material was removed by centrifugation at $78{,}000 \times g$ for 90 min and the combined supernatants were dialysed against 5 mM Tris-PO_4, pH 7.8, concentrated by dialysis against Aquacide II (Calbiochem.) and further dialysed against 5 mM Tris-PO_4 for 16 h. The solution was then centrifuged at $165{,}000 \times g$ for 15 min to remove denatured protein aggregates.

Column chromatography

The papain-solubilized extract of hepatoma D23 " extra-nuclear " membranes was applied to a DEAE-cellulose column (2.5×40 cm). The anion exchanger (Whatman DE52) was equilibrated with 5 mM Tris-PO_4, pH 7.8. Fractions (18 ml), eluted from the column with a concave concentration gradient from 5 mM Tris-PO_4, pH 7.8 to 0.5 M Tris-PO_4, pH 4.5, were dialysed against PBS (phosphate buffered saline, pH 7.2), concentrated against Aquacide II to approximately 4 ml and redialysed against PBS for 16 h. All fractions were stored at −20° C.

Sucrose density gradient centrifugation

Fractions eluted from the DEAE-cellulose column and exhibiting antigenic activity, were pooled, dialysed against 5mM Tris-HCl, pH 8.0, concentrated and further dialysed against 5 mM Tris-HCl, pH 8.0. The solution was centrifuged at $165{,}000 \times g$ for 15 min and then subjected to sucrose density gradient centrifugation using either the Spinco S.W.25.1 swing-out rotor (Beckman Instruments Inc., Croydon, England) or the M.S.E. B-XIV zonal rotor. All sucrose solutions were prepared in 5 mM Tris-HCl, pH 8.0.

For centrifugation in the swing-out rotor, 1.0 ml aliquots of the antigenic protein solution were layered upon 25 ml linear 5 to 20% (w/w) sucrose gradients and centrifugation was carried out in the S.W.25.1 rotor for 16 h at 64,000 rpm. Fifteen drop fractions were then collected from the bottom of each centrifuge tube.

For centrifugation in the B-XIV zonal rotor, a 490 ml sucrose gradient (5 to 20% w/w, linear with respect to volume) was pumped to the periphery of the rotor followed by sufficient 25% (w/w) sucrose until the light end of the gradient began to emerge from the centre feed line. An aliquot (16 ml) of the antigenic protein solution, obtained by DEAE-cellulose column chromatography, was introduced into the rotor via the centre feed line followed by an overlay of 90 ml of 5 mM Tris-HCl, pH 8.0. The rotor was accelerated to $115{,}000 \times g$ for 5.5 h. After reduction of the rotor speed to 2,000 rpm, the contents were unloaded by displacement with 30% (w/w) sucrose, and fractions were collected in 25-ml aliquots.

The sucrose concentration of each fraction was determined by measurement of refractive

using an Abbé refractometer. Sucrose was then removed by dialysis against PBS and the fractions were concentrated and redialysed against PBS for 16 h before storing at −20° C.

Preparative polyacrylamide gel electrophoresis

Preparative electrophoresis was performed at room temperature using the Quickfit Instrumentation prep-PAGE apparatus. A 30 ml gel was formed by polymerizing 7.0% acrylamide (Kodak) and 0.1% N,N′methylenebisacrylamide (B.D.H.) in 0.05 M Tris-HCl, pH 8.0, with 10% N,N,N′,N′-tetramethylethylene-diamine (Koch Light) and 0.05% ammonium persulphate. The buffer in both electrode compartments and the elution system was 0.05 M Tris-HCl, pH 8.0. After being left overnight to polymerize, the gel was pre-run until a sample of bromophenol blue dye had been eluted.

An aliquot (3.0 ml) of antigenic protein solution (in 5 mM Tris-HCl, pH 8.0) was applied to the surface of the gel and electrophoresis was performed at 50 mA after gradually increasing the current from an initial value of 10 mA. Fractions (approximately 1.5 ml), eluted from the gel were dialysed against PBS and stored at −20° C.

Antigen assay

Membrane immunofluorescence. The membrane immunofluorescence test was performed with viable hepatoma D23 cells in suspension as previously described (Baldwin and Barker, 1967*b*) using sera from syngeneic rats sensitized to hepatoma D23 cells. Fluorescence indices were calculated for test serum samples by determining the percentage of cells unstained with control normal rat serum minus the percentage of cells unstained with the test serum divided by the former figure.

Individual or pooled soluble fractions, dialysed against PBS, were assayed for antigenic activity by determining their capacity to neutralize the reaction of antibody in hepatoma D23-specific immune serum with tumor-specific cell surface antigens on viable hepatoma D23 cells as assessed using the membrane immunofluorescence test (Baldwin and Moore, 1969*a*; Baldwin and Glaves, 1972). Thus, antigenic activity associated with soluble fractions was denoted by a reduction of fluorescent staining with absorbed immune serum as compared with immune serum diluted with equivalent volumes of PBS. The percentage inhibition of the fluorescence index with absorbed serum was defined as a measure of antigenic activity.

Immunodiffusion. Antiserum against hepatoma D23 cells was prepared in rabbits by weekly intramuscular injections of 1×10^8 cells for a period of 8 weeks. The serum was absorbed with normal rat liver cells (5×10^6 per ml) and normal rat serum (1.0 ml per ml) and stored at −20° C before testing against isolated antigen fractions on standard agar immunodiffusion plates.

Analytical polyacrylamide gel electrophoresis

7.0% acrylamide gels, 7.0 cm in length and 0.5 cm in diameter, were prepared in a manner identical to that described for the preparative electrophoretic procedures. Protein samples were routinely dialysed against 5 mM Tris-HCl, pH 8.0 before application to the gels. Electrophoresis was performed at 3 mA per tube until bromophenol blue, added as tracker dye, had passed to the bottom of the gel. Gels were stained for protein with Coomassie Blue.

Sedimentation coefficient and molecular weight estimations

Sedimentation coefficients were estimated and molecular weights were calculated according to the methods of Martin and Ames (1961). Sucrose density gradients were calibrated using the following standard proteins: egg albumin (3.66*s*), human haemoglobin (4.48*s*), human γ globulin (7.0*s*), catalase (11.3*s*) and thyroglobulin (19.2*s*).

Electron microscopy

Negatively stained specimens of purified or semi-purified hepatoma D23 specific antigens were prepared using 2.0% uranyl acetate, pH 4.5. Specimens were studied using a Phillips E.M. 300 electron microscope. Photographs were taken on Ilford 3.25 × 4 inch E.M.6 plates.

Protein analysis

Protein concentration was determined by the method of Lowry *et al* (1951).

RESULTS

DEAE-cellulose column chromatography

Three large-scale papain extractions of hepatoma D23 " extra-nuclear " membranes were

performed. In each case the concentrated soluble extract was applied to a DEAE-cellulose column and eluted with a concave Tris-PO_4 concentration gradient using the method of Baldwin and Glaves (1972). Details of the initial materials and recoveries are summarized in Table I. Figure 1 shows a representative O.D. 280 nm profile given by the column eluant. In one experiment, the material located in fractions 55 to 65 (Fig. 1) was collected following elution of the column with the Tris-PO_4 gradient by further application of 200 ml of 0.5 M Tris-PO_4 to the column. However, since no antigenic activity was associated with the proteins found in this region, this procedure was subsequently considered unnecessary.

Hepatoma D23 specific antigen activity was detected by the capacity of isolated fractions to neutralize the membrane immunofluorescence staining of antibody in hepatoma D23 immune rat serum and by this assay, antigen was found to be associated with fractions 36 to 46 (Fig. 1). As a means of rapidly monitoring antigen, column fractions were also assayed by immunodiffusion analysis with a rabbit antiserum prepared against hepatoma D23 cells and preabsorbed with normal liver cells and normal rabbit serum (Fig. 2). In agreement with the membrane immunofluorescence assays for tumour-specific antigen, a major precipitin band was obtained with fractions 36 to 46. The antiserum was not monospecific, however, even after absorption with normal tissues and a second component was detectable in fractions 26 to 40.

Analysis of the column fractions by polyacrylamide gel electrophoresis indicated that all fractions were complex, giving multiple bands of stained protein on the gel (Fig. 3). The recovery of the heterogeneous material from the pooled fractions which retained antigenic activity was within the range 10 to 13 mg protein per 100 g of hepatoma tissue (Table I).

TABLE I

PAPAIN SOLUBILIZATION OF HEPATOMA D23 ANTIGEN—INITIAL MATERIALS AND RECOVERIES

Experiment	Wet weight of hepatoma D23 tissue (g)	"Extra nuclear" membrane protein (g)	Protein displaying antigenic activity recovered from the DEAE-cellulose column (mg)
1	315	8.0	30
2	540	9.6 [1]	56
3	475	13.5	61

[1] 600 × g pellets from homogenates were not washed by further centrifugation.

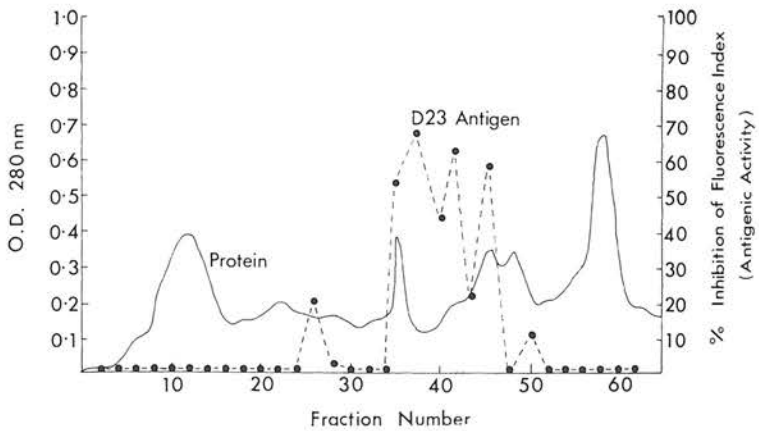

FIGURE 1

DEAE-cellulose column chromatography of papain-solubilized hepatoma D23 "extra-nuclear" membranes. Tumour antigen was determined from the capacity of fractions to neutralize antibody in a standard antiserum from syngeneic rats immunized against hepatoma D23 cells. This was expressed as the percentage inhibition of serum fluorescence index compared with appropriately diluted untreated serum when tested against hepatoma D23 cells (see "Material and Methods").

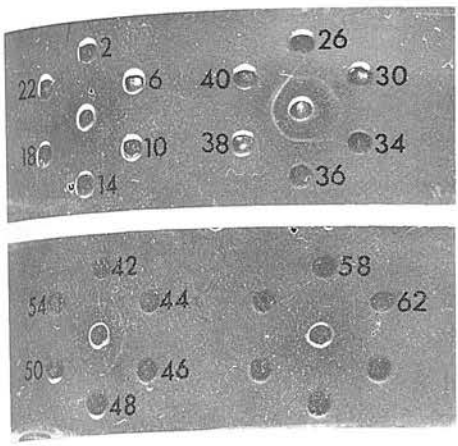

FIGURE 2

Immunodiffusion analysis of fractions isolated by DEAE-cellulose chromatography of papain-solubilized hepatoma D23 " extra-nuclear " membrane (Figure 1). Outer wells contain sequential fractions and centre wells rabbit anti-hepatoma D23 antiserum absorbed with normal rat liver and serum. The major precipitin line is associated with fractions 36 to 46. A second component is also detectable in fractions 26 to 40.

Sucrose density gradient centrifugation

Sucrose density gradient centrifugation using either the S.W.25.1 swing-out rotor or B-XIV zonal rotor was employed to fractionate any large molecular components from the antigenic material isolated by column chromatography. Figure 4 illustrates the separation achieved following centrifugation of 46 mg of antigenic protein in the B-XIV zonal rotor. Since the loading capacity of this rotor is considerably greater than the S.W.25.1 swing-out rotor, a more complete characterization of trace high molecular weight components was obtained by this procedure. Fractions from five regions of the gradient (regions " A " to " E ") were pooled as shown in Figure 4. The majority of the protein applied to the gradient did not sediment far into the gradient and was confined to the region " A " (Fig. 4). By analytical polyacrylamide gel electrophoresis the proteins in this region were heterogeneous (Fig. 5) and this fraction was retained for further fractionation. Similarly the material in region " B " was heterogeneous, although the pooled regions " C ", " D " and " E " contained predominantly single molecular species as judged by gel electrophoresis (Fig. 5). This view was confirmed by an electron microscopic study of the pooled regions " B " to " E ". Representative fields of negatively stained proteins present in regions " B " to " E " are shown in Figures 6 to 9 respectively. Although there was some aggregation caused by the cationic negative stain employed, most of the protein was spread as a dispersed monolayer on the carbon support of the viewing grid.

Each of the fractions " A " to " E " exhibited hepatoma D23-specific antigenic activity as assessed by the immunofluorescence antigen assay (Table II). The fractions " A ", " C " and " D " gave significant reductions of the fluores-

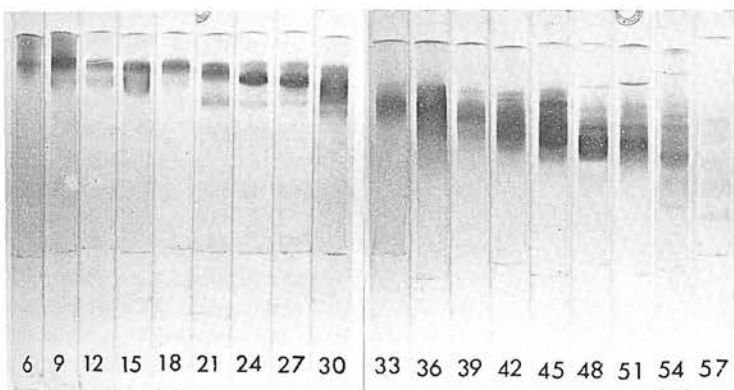

FIGURE 3

Analytical polyacrylamide gel electrophoresis of fractions isolated by DEAE-cellulose column chromatography of papain-solubilized hepatoma D23 " extra-nuclear " membranes (Figure 1).

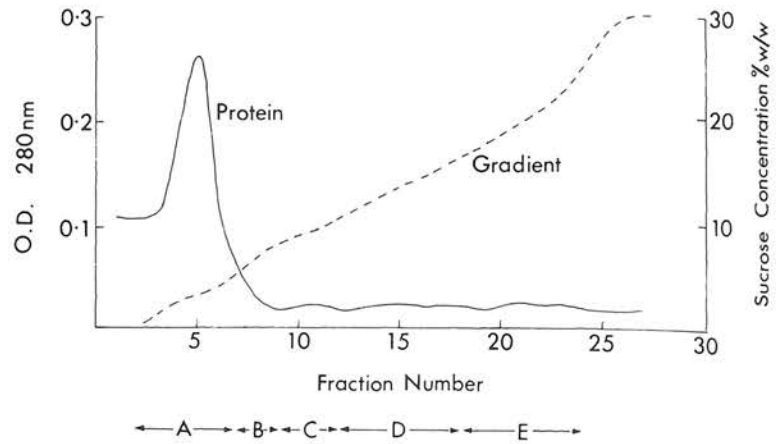

FIGURE 4

Sucrose density gradient centrifugation in a B-XIV zonal rotor (115,000 $\times g$ for 5.5h) of pooled antigen fraction isolated by DEAE-cellulose column chromatography of papain-solubilized hepatoma D23 extra-nuclear membrane (Tubes 36 to 46, Figure 1). Pooled fractions designated A to E were analysed for tumour-specific antigen by their capacity to neutralize syngeneic tumour-immune rat serum (Table II).

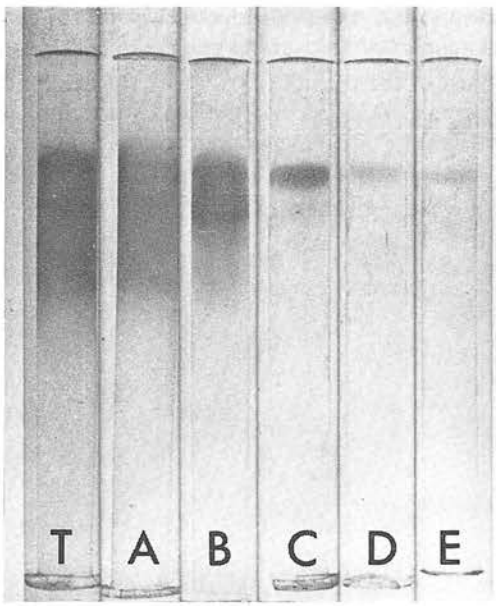

FIGURE 5

Analytical polyacrylamide gel electrophoresis of the pooled antigenic fractions A to E isolated by B-XIV zonal sucrose density gradient centrifugation (Figure 4). T represents the total extract before fractionation.

cence index below the level of 0.3 whereas fractions " B " and " E " were less consistent in this respect. Reactions given on immunodiffusion against absorbed rabbit anti-hepatoma D23 antiserum were strong with material from region " A ", but considerably weaker with the large molecular weight components in regions "B" to " E ".

The total recovery of protein in the region " B " to " E " was between 1 to 2 mg per 500 g of hepatoma tissue. This yield precluded extensive studies upon these fractions. However, using the technique of Martin and Ames (1961), it was determined that the proteins from regions "C" and " D " had sedimentation coefficients of approximately 12*s* and 22*s* respectively.

Preparative polyacrylamide gel electrophoresis

The heterogeneous, low molecular weight proteins (region A) prepared by sucrose density gradient centrifugation were subjected to preparative polyacrylamide gel electrophoresis. Fig. 10 shows the O.D. 280 nm profile of the eluant from the gel following electrophoresis of the protein sample (24 mg). Hepatoma D23 specific antigen content of the fractions, assayed

TABLE II

ABSORPTION OF HEPATOMA D23 IMMUNE SERUM BY SOLUBLE ANTIGENIC FRACTIONS ISOLATED FOLLOWING DEAE-CELLULOSE COLUMN CHROMATOGRAPHY AND B-XIV ZONAL CENTRIFUGATION OF PAPAIN-SOLUBILIZED HEPATOMA D23 "EXTRA-NUCLEAR" MEMBRANES

Absorption conditions		Fluorescence index	
Fraction[1]	mg of protein per ml of antiserum	Unabsorbed	Absorbed
A	1.0	0.49, 0.51	0.04, 0.15
B	1.0	0.47, 0.47, 0.61	0.30, 0.40, 0.22
C	0.4	0.47, 0.47, 0.61	0.20, 0.10, 0.09
D	0.2	0.47, 0.47, 0.61	0.19, 0.11, 0.00
E	0.2	0.47, 0.47, 0.61	0.35, 0.18, 0.12

[1] See Figure 4.

by specific inhibition of membrane immunofluorescence staining of a standard syngeneic rat immune serum with viable hepatoma cells, indicated that activity was confined to fractions 20 to 36 (Fig. 10). When these fractions were analysed by immunodiffusion against the absorbed rabbit anti-hepatoma D23 serum, a major component was detected in samples from tubes 16 to 32 (Fig. 11). It is evident, however, that other minor components are detectable in some of these fractions.

In this experiment fractions 23 to 32 were pooled since only these reduced the fluorescence index of the standard syngeneic immune rat serum to below the value (0.30) taken as positive (Baldwin and Moore, 1969*a*). Analytical polyacrylamide electrophoretic gels corresponding to the fractions isolated by preparative gel electrophoresis (Fig. 10) are illustrated in Figure 12. Fractions 24 to 32, displaying significant antigenic activity, gave single diffuse bands of stained protein. Figure 13 illustrates the final fractionation achieved, by comparing analytical polyacrylamide gels of the initial soluble papain extract (1), the antigenically active region taken following DEAE-cellulose column chromatography (2), and the purified hepatoma D23 antigen fraction isolated by preparative gel electrophoresis (3). No further protein bands were revealed when larger amounts (up to 250 µg protein) were applied to the gels.

Estimation of the sedimentation coefficient of the hepatoma D23 antigen fraction isolated by preparative polyacrylamide gel electrophoresis was obtained by sucrose density gradient centrifugation according to the method of Martin and Ames (1961). The antigenic fraction migrated in linear sucrose gradients as a single peak and by calibration of the gradients with standard proteins, a molecular weight of 55,000±5,000 was calculated.

The major preparative procedures employed for the isolation and fractionation of hepatoma D23 antigen are summarized in Table III.

In each of the three experiments, the yield of purified hepatoma D23 antigen obtained from the preparative electrophoresis apparatus was low. At each stage in the preparation, a significant proportion of the fractions isolated was used for antigen assay such that following the final fractionation procedure only a few milligrams of purified protein were available for further analysis. This recovery was estimated to be of the order of 5 mg of antigenic protein per 500 g of original hepatoma D23 tissue.

DISCUSSION

The present studies demonstrate that a membrane-associated tumour-specific antigen on hepatoma D23 may be rendered water-soluble by limited papain digestion of cell membranes so that further purification may be achieved. Sequential fractionation of the soluble extract by ion exchange chromatography, gradient centrifugation and preparative gel electrophoresis allowed the recovery of an essentially homogeneous antigenic fraction with an approximate molecular weight of 55,000. Other proteins of larger molecular weight were isolated and these retained tumour-specific antigen determinants. It is not known whether these products reflect a true physiological state of the antigen as a membrane constituent or whether they arise as a result of aggregation, this being a common phenomenon associated with solubilized membrane proteins. This may be viewed as a disadvantage in the use of papain for solubilizing membrane-associated tumour-specific antigen. It is possible, however, that the size heterogeneity of liberated proteins from hepatoma D23 membrane is not due to enzymic fragmentation by papain,

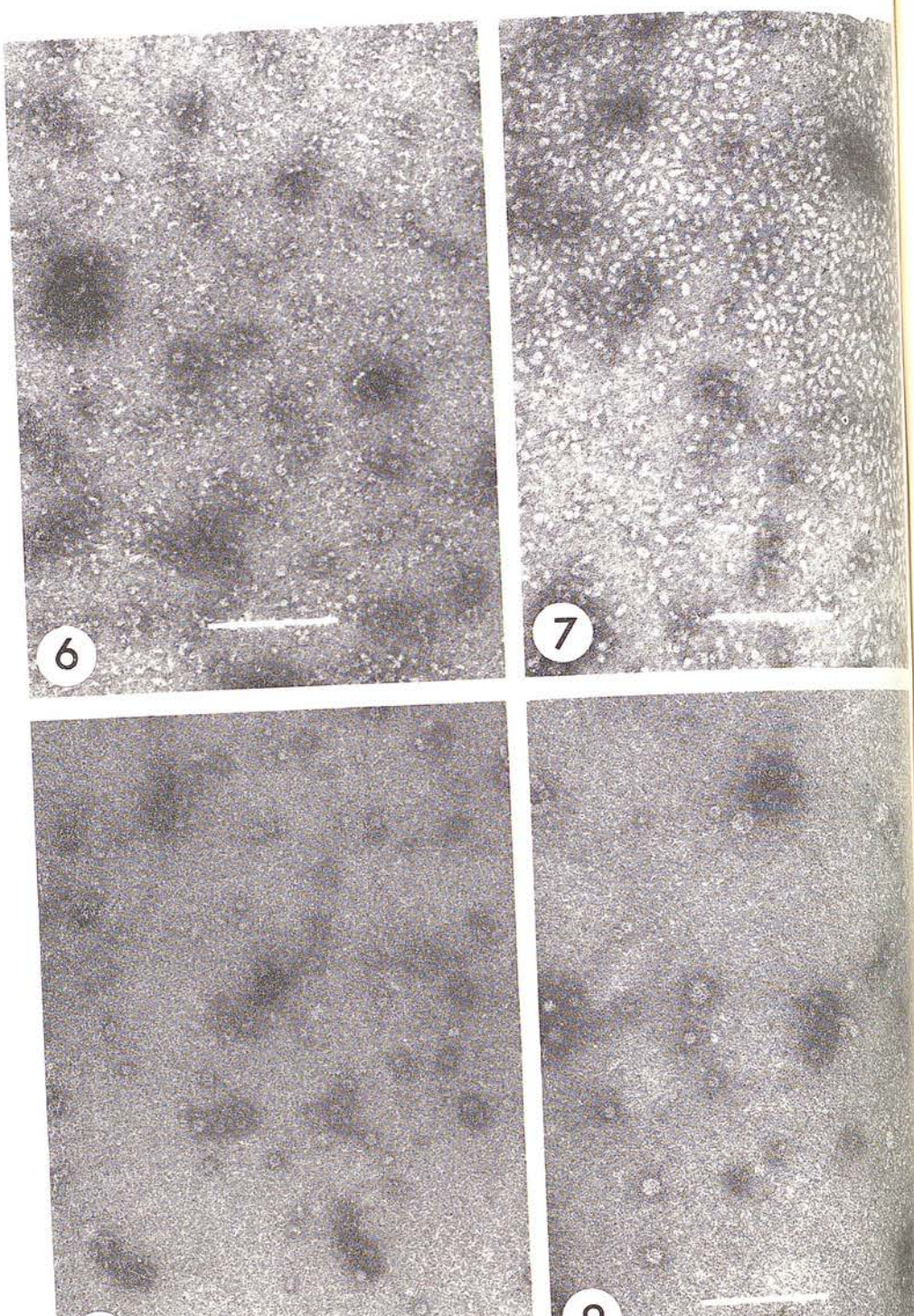
6
7
8
9

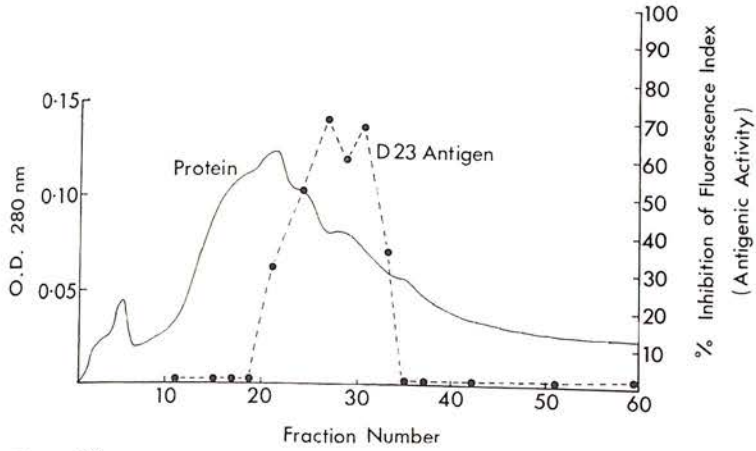

FIGURE 10

Preparative polyacrylamide gel electrophoresis of the low molecular weight fraction A isolated by B-XIV zonal centrifugation of papain-solubilized hepatoma D23 membrane (Figure 4). See Figure 1 for description of tumour antigen assay.

since soluble antigens released from chemically-induced guinea-pig sarcomas by extraction with isotonic saline were also associated with several molecular species (Suter *et al.*, 1972). A number of alternative solubilization techniques have also been tested on hepatoma D23 cells and plasma membrane fractions including extraction with 3 M KCl or EDTA, or sonication, but none of these was as effective as limited papain digestion. It has recently been established, however, that tumour antigen release from hepatoma D23 plasma membrane can be effected with β-glucosidase (Baldwin *et al.*, 1971*b*) and this warrants investigation as an alternative method for antigen isolation.

An important feature contributing to the success of the separative methods employed has been the reproducible and defined behaviour of the antigenic components upon DEAE-cellulose

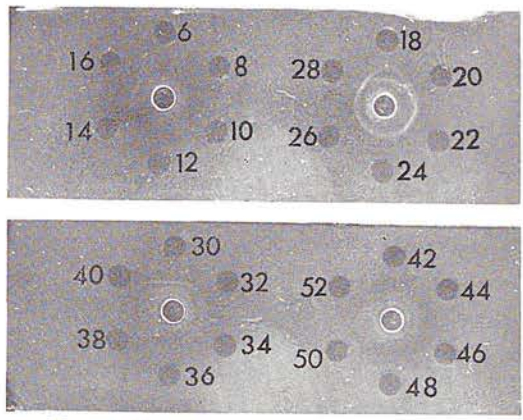

▲ FIGURE 11

Immunodiffusion analysis of fractions isolated by preparative polyacrylamide gel electrophoresis (Figure 10). Outer wells contain sequential fractions eluted from the gel and centre wells absorbed rabbit anti-hepatoma D23 antiserum.

◀ FIGURES 6 TO 9

Electron microscopic analysis of the protein present in the pooled antigenic fractions B to E isolated following DEAE-cellulose column chromatography and B-XIV zonal centrifugation of papain-solubilized hepatoma D23 " extra-nuclear " membranes. Negatively stained with uranyl acetate (PH 4.5). Proteins present in region B (Figure 6) were of variable shape and ranged in size from less than 10 nm up to approximately 20 nm. In region C (Figure 7), the proteins exhibited a regular rod shape, approximately 20 nm in length and 10 nm in breadth. Many of these rod profiles, in fact, appeared as though they might represent dimers composed of two 10 nm particles side by side. The proteins present in region D (Figure 8) exhibited a regular spherical shape with a diameter of approximately 20 nm. Region E also contained many of the 20 nm spherical proteins together with some larger components which were up to 30 nm in diameter (Figure 9). (Scale marker in Figures 6 to 9 represents 200 nm.)

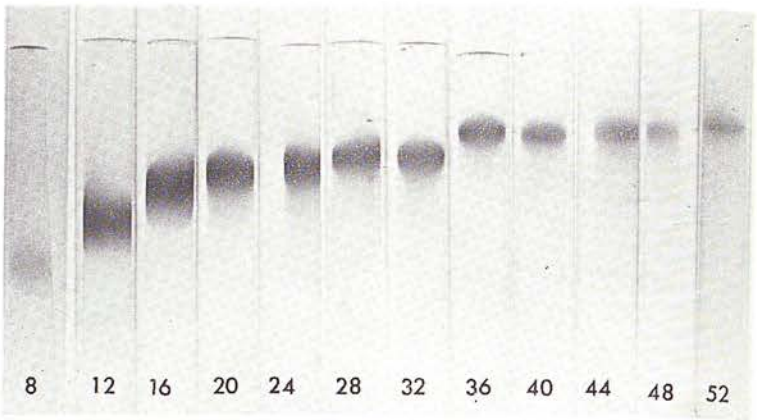

FIGURE 12

Analytical polyacrylamide gel electrophoresis of fractions isolated by preparative polyacrylamide gel electrophoresis (Figure 10).

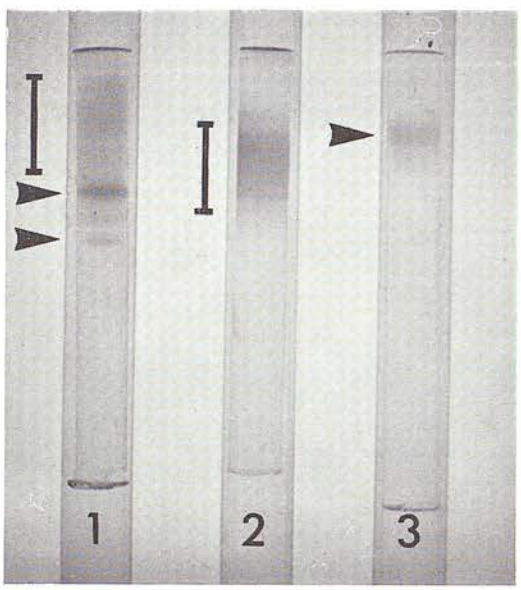

FIGURE 13

Analytical polyacrylamide gel eletrophoresis of the major antigenic fractions isolated. Gel 1: unfractionated papain-solubilized hepatoma D23 " extra-nuclear " membranes. Gel 2: pooled antigenic fractions isolated following DEAE-cellulose column chromatography of papain-solubilized hepatoma D23 " extra-nuclear " membranes. Gel 3: purified hepatoma D23 antigen, of molecular weight 55,000 ± 5,000 isolated following DEAE-cellulose column chromatography, gradient centrifugation and preparative polyacrylamide gel electrophoresis. Arrows indicate major, well-resolved bands of stained protein and bars show regions of the gel where multiple protein bands are unresolved.

TABLE III

SUMMARY OF HEPATOMA D23 ANTIGEN ISOLATION AND FRACTIONATION PROCEDURE

Hepatoma D23 tissue

1) Controlled cellular disruption using Ultra-turrax and Potter-Elvehjem homogenizers.
2) Centrifuge at 600 × *g* for 10 min; pellet washed × 3 by centrifugation at 600 × *g* for 10 min.
3) 600 × *g* supernatants pooled and centrifuged at 78,000 × *g* for 45 min. Supernatants discarded.

Crude " extra-nuclear " membrane fraction

1) Papain digestion at 37° C for 60 min.
2) Centrifuge at 78,000 × *g* for 90 min. Pellet discarded.

Crude soluble extract

1) DEAE-cellulose column chromatography, column eluted with a concave concentration gradient from 0.005 M Tris-PO_4 (pH 7.8) to 0.5 M Tris-PO_4 (pH 4.5).

Semi-purified soluble extract

1) Sucrose density gradient centrifugation using either an S.W.25.1 swing-out rotor or a B-XIV zonal rotor.

Main antigenic fraction

1) Preparative polyacrylamide gel electrophoresis. — a range of large molecular weight proteins containing antigenic activity.

Purified hepatoma D23 antigen

(molecular weight approximately 55,000)

column chromatography and preparative gel electrophoresis, both of which are operative on a molecular charge basis. Concordant with these observations, it was determined, by analytical polyacrylamide gel electrophoresis, that the major antigenic fraction was within at least a limited molecular charge range as visualized by a single but diffuse band of stained protein on the electrophoresis gels. Velocity sedimentation indicated a comparable homogeneity with respect to the weight estimations of 55,000±5,000. It remains to be elucidated whether the antigen preparation represents a homogeneous molecular species, or a restricted group of proteins produced artefactually by proteolysis, but retaining hepatoma D23-specific antigen determinants. The final yield of the protein fraction retaining hepatoma D23 was of the order of 5 mg of protein per 500 g of wet weight of hepatoma tissue. Although this recovery is low, hepatoma D23 specific antigen is a minor component of the plasma membrane since tumour-specific immune reactions elicited by hepatoma D23 cells are considerably weaker than those produced against Wistar alloantigens. Furthermore, previous studies (Baldwin and Moore, 1969*a*,*b*) showed that the process of tumour-cell rupture led to a considerable loss of tumour-specific antigen, whereas almost total recoveries of Wistar alloantigen were obtained, suggesting a particular liability of the tumour component.

The approximate value of 55,000 for the molecular weight of hepatoma D23 antigen is within the broad range of 40,000 to 75,000 obtained for papain-solubilized murine H-2 and human HL-A histocompatibility antigens (reviewed by Reisfeld and Kahan, 1970). The values are, however, lower than the molecular weight range of 75,000 to 150,000 estimated for tumour-specific antigens solubilized by 3 M KCl extraction of diethylnitrosamine-induced guinea-pig hepatoma cells (Meltzer *et al.*, 1971). Extraction of guinea-pig sarcomas with isotonic saline also yielded soluble tumour-specific antigen which could be separated into two fractions by ammonium sulphate precipitation, one having a molecular weight of about 50,000, the other being in excess of 10^6 (Suter *et al.*, 1972). This is in accord with present studies indicating the liberation of large molecular weight fractions as well as the 55,000 component which retain tumour-specific antigen activity.

A major factor limiting more precise characterization of solubilized hepatoma D23 antigen is the lack of sensitive *in vitro* assay methods for its detection and quantitation. An inherent quality of the membrane immunofluorescence assay used as the primary test in this investigation is that it measures interaction of tumour-specific antibody with antigens expressed at the surface of viable target tumour cells in suspension. The technique is relatively insensitive, however, requiring antigen equivalent to approximately 10^7 hepatoma cells per ml serum for significant absorption of tumour-specific antibody (Baldwin and Moore, 1969*a*). The test is also laborious in that antigen can only be measured by its capacity to absorb antibody which is then assayed in a secondary reaction by showing loss of staining with viable target hepatoma cells. For these reasons an attempt was made in this study to use immunodiffusion reactions with heterologous antisera prepared against intact hepatoma D23 cells as a rapid method for screening fractions retaining tumour-specific antigen. The results (Fig. 2 and 11) show that these antisera have some value for this purpose even though, after absorption with normal liver and serum, they were not monospecific. Nevertheless, it is clear that heterologous antisera are of limited secondary use in controlling tumour antigen fractionation and ultimately the validity of antigen isolation has to be assayed using tumour-specific immune reagents prepared in autochthonous or syngeneic hosts.

One of the objectives of the present studies has been the development of techniques for the isolation of purified tumour-specific antigen to permit investigation of the nature of the antigenic determinant, which in the case of chemically-induced tumours is an individually distinct component of the tumour cell. These studies are relevant to chemical carcinogenesis in that it may ultimately be possible to distinguish at the chemical level unique antigen determinants of individual tumours which may be viewed as products arising from direct or indirect action of the carcinogen on the cell genome (Baldwin *et al.*, 1971*c*). The tumour antigen fractions so far prepared from hepatoma D23 are probably still not sufficiently purified for this stage. Further purification of hepatoma D23 antigen may be feasible, but dependent, as already indicated, upon more sophisticated immunological assays. An alternative approach, however, in comparing

the reactive antigenic species from two immunologically distinct rat hepatomas, may be to resort to partial degradation to polypeptides, retaining antigenic activity.

In terms of tumour immunobiology, the isolation of defined antigen fractions from hepatoma D23 makes possible a study of the significance of antigen interactions in tumour immunity. In this context, *in vitro* tests have shown that papain-solubilized hepatoma D23 antigen has the capacity to form complexes with tumour-specific antibody which effectively block lymphocyte-mediated cytotoxic reactions against plated hepatoma D23 cells in a manner analogous to the blocking of target tumour cells with serum from tumour-bearing rats (Baldwin *et al.*, 1972, 1973). It has also been established that soluble hepatoma D23 antigen can specifically block lymphocyte cytotoxicity for plated hepatoma D23 cells when added to the effector cells (Baldwin, Price and Robins, to be published). Based upon these *in vitro* studies with soluble hepatoma D23 antigen it is now possible to determine the contribution of lymphocyte blocking by free antigen and/or immune complexes and target cell blocking by immune complexes in the overall blocking observed in the serum of tumour-bearing animals.

ACKNOWLEDGEMENTS

This study was supported by the Cancer Research Campaign and Medical Research Council and also by a Government Equipment Grant through the Royal Society. Thanks are expressed to Professor H. K. Weinbren (Department of Pathology, Medical School, University of Nottingham) for making available the electron microscope facilities which were provided by the Medical Research Council. The authors wish to acknowledge the skilful technical assistance of Mrs. M. E. Marshall and Mrs. C. Wright.

FRACTIONNEMENT D'UN ANTIGÈNE SPÉCIFIQUE D'UNE TUMEUR, ASSOCIÉ A LA MEMBRANE PLASMATIQUE ET PROVENANT D'UN HÉPATOME INDUIT CHEZ LE RAT PAR UN COLORANT AMINO-AZOÏQUE

Les antigènes spécifiques de la tumeur, provenant d'un hépatome induit chez le rat par un colorant amino-azoïque, ont été libérés sous forme soluble à la suite d'une action limitée de la papaïne sur des préparations de membrane de cellules tumorales. Le fractionnement de l'extrait soluble par chromatographie en colonne de DEAE-cellulose, centrifugation en gradient et électrophorèse préparative a donné une grande fraction antigénique d'un poids moléculaire approximatif de 55,000, ainsi qu'une série d'autres éléments antigéniques mineurs dont le poids moléculaire était plus élevé. Toutes les préparations conservent leur aptitude à inhiber la réaction de l'anticorps, dans le sérum immunisé contre la tumeur, avec la membrane plasmatique des cellules-cibles d'hépatome viables, ce qui a été mis en évidence par immunofluorescence indirecte. Nous estimons que les fractions antigéniques ainsi isolées constituent un matériel approprié pour analyser la nature de l'expression de l'antigène tumoral dans la carcinogénèse chimique et pour évaluer le rôle de l'interaction anticorps-antigène dans l'immunité antitumorale.

REFERENCES

BALDWIN, R. W., Tumour specific antigens associated with chemically induced tumours. *Europ. J. clin. biol. Res.*, **15**, 593-598 (1970).

BALDWIN, R. W., and BARKER, C. R., Tumour-specific antigenicity of aminoazo dye-induced rat hepatomas. *Int. J. Cancer*, **2**, 355-364 (1967*a*).

BALDWIN, R. W., and BARKER, C. R., Demonstration of tumour-specific humoral antibody against aminoazo dye-induced rat hepatomata. *Brit. J. Cancer*, **21**, 793-800 (1967*b*).

BALDWIN, R. W., BARKER, C. R., EMBLETON, M. J., GLAVES, D., MOORE, M., and PIMM, M. V.

Demonstration of cell surface antigens on chemically induced tumours. *Ann. N.Y. Acad. Sci.*, **177**, 268-278 (1971*a*).

BALDWIN, R. W., and EMBLETON, M. J., Detection and isolation of tumour-specific antigen associated with a spontaneously arising rat mammary carcinoma. *Int. J. Cancer*, **6**, 372-382 (1970).

BALDWIN, R. W., EMBLETON, M. J., and ROBINS, R. A., Cellular and humoral immunity to rat hepatoma-specific antigens correlated with tumour status. *Int. J. Cancer*, **11**, 1-10 (1973).

BALDWIN, R. W., and GLAVES, D., Solubilization of tumour-specific antigen from plasma membrane of an aminoazo-dye-induced rat hepatoma. *Clin. exp. Immunol.*, **11**, 51-56 (1972).

BALDWIN, R. W., GLAVES, D., HARRIS, J. R., and PRICE, M. R., Tumour-specific antigens associated with aminoazo-dye-induced rat hepatomas. *Transplant. Proc.*, **3**, 1189-1190 (1971*b*).

BALDWIN, R. W., GLAVES, D., and PIMM, M. V., Tumour-associated antigens as expressions of chemically induced neoplasia and their involvement in tumour-host interactions. *In:* D. B. Amos (ed.) *Progress in immunology*, p. 907-920, Academic Press, New York (1971*c*).

BALDWIN, R. W., and MOORE, M., Isolation of membrane-associated tumour-specific antigen from an aminoazo-dye-induced rat hepatoma. *Int. J. Cancer*, 4, 753-760 (1969*a*).

BALDWIN, R. W., and MOORE, M., Rat hepatoma cell surface antigens: Demonstration and isolation of membrane-associated isoantigens. *Europ. J. Cancer*, **5**, 475-483 (1969*b*).

BALDWIN, R. W., PRICE, M. R., and ROBINS, R. A., Blocking of lymphocyte-mediated cytotoxicity for rat hepatoma cells by tumour-specific antigen-antibody complexes. *Nature New Biol.*, **238**, 185-187 (1972).

LOWRY, O. H., ROSEBROUGH, N. L., FARR, A. L., and RANDALL, R. J., Protein measurement with the Folin phenol reagent. *J. biol. Chem.*, **193**, 265-275 (1951).

MARTIN, R. G., and AMES, B. N., A method for determining the sedimentation behaviour of enzymes: application to protein mixtures. *J. biol. Chem.*, **236**, 1372-1379 (1961).

MELTZER, M. S., LEONARD, E. J., RAPP, H. J., and BORSOS, T., Tumour-specific antigen solubilized by hypertonic potassium chloride. *J. nat. Cancer Inst.*, **47**, 703-709 (1971).

REISFELD, R. A., and KAHAN, B. D., Transplantation antigens. *Advanc. Immunol.*, **12**, 117-200 (1970).

SUTER, L., BLOOM, B. R., WADSWORTH, E. M., and OETTGEN, H. F., Use of the macrophage migration inhibition test to monitor fractionation of soluble antigens of chemically induced sarcomas of inbred guinea pigs. *J. Immunol.*, **109**, 766-775 (1972).

Reprinted from
Biochimica et Biophysica Acta, 311 (1973) 600–614

(9)

BBA 76384

THE PURIFICATION OF MEMBRANE-ASSOCIATED TUMOUR ANTIGENS BY PREPARATIVE POLYACRYLAMIDE GEL ELECTROPHORESIS

J. R. HARRIS*, M. R. PRICE and R. W. BALDWIN

Cancer Research Campaign Laboratory, The University of Nottingham, University Park, Nottingham, NG7 2RD (Great Britain)

(Received February 27th, 1973)

SUMMARY

The technique of preparative polyacrylamide gel electrophoresis has been employed to purify solubilized membrane-associated tumour antigens from two aminoazo dye-induced rat hepatomas.

Limited papain digestion and EDTA treatment of subcellular membrane fractions or viable ascites hepatoma cells was found to liberate soluble antigenic material suitable for further fractionation. The heterogeneity of initial extracts was revealed by analytical polyacrylamide gel electrophoresis. This technique was used to monitor fractions obtained throughout the preparative electrophoresis in order to assess the purification obtained.

The value of preparative polyacrylamide gel electrophoresis is discussed in relation to other methods currently available for the purification of solubilized membrane-associated antigens.

INTRODUCTION

The isolation of tumour-specific antigens has, in the main, followed closely the concepts developed for the study of mouse H-2 and human HL-A histocompatibility antigens. The proteolytic enzyme papain has been used by several groups to release cell surface antigens from a variety of normal and neoplastic cell types (Mann *et al.*[1], Shimada and Nathenson[2], Yamane and Nathenson[3]) and has recently been employed to release tumour-specific antigen from rat hepatoma D_{23} by Baldwin and Glaves[4]. Fractionation of the extracted antigens was performed by DEAE-cellulose column chromatography and a single hepatoma D_{23} antigenic region was defined in the effluent. Analytical polyacrylamide gel electrophoresis has shown this region to be heterogeneous (Baldwin *et al.*[5]) and further purification was therefore attempted by rate zonal centrifugation followed by preparative polyacrylamide gel electrophoresis.

To avoid this overall lengthy procedure efforts have been made to perform

* Present address: Department of Physiology, Bute Medical Buildings, St. Andrews, Fife, Scotland.

a single step purification of hepatoma-specific antigen by preparative polyacrylamide gel electrophoresis. The results of this study are to be described and will be compared with those obtained when partially purified hepatoma-specific antigen from DEAE-cellulose chromatography and rate zonal centrifugation was used as the starting material for the preparative electrophoresis. Because of the sensitivity of the analytical polyacrylamide gel electrophoresis procedure in resolving the initially very complex papain extract from rat hepatoma D_{23} and its ability to reveal the heterogeneity of the partially purified antigen obtained following DEAE-cellulose chromatography, it can reasonably be concluded that when put onto a preparative scale the technique might have the ability to separate the many components in the initial papain extract directly. The method has in fact been successfully used to purify prolactin and growth hormone by Groves and Sells[6], and to purify HL-A antigens by Reisfeld and Kahan[7].

Throughout this study hepatoma-specific antigen was extracted by limited papain digestion from suspensions of rat ascites hepatoma cells (D_{23} and D_{31}) and also from an 'extranuclear' membrane fraction obtained following homogenization of rat hepatoma D_{23} tissue. Preliminary experiments have also been performed with protein extracted by EDTA treatment of the membrane fraction. Tumour-specific antigenicity was detected throughout the purification schemes (a) by the capacity of fractions to neutralise antibody in syngeneic immune serum, thereby preventing the reaction of this antibody with tumour-specific antigen at the surface of viable hepatoma cells, as detected by the indirect membrane immunofluorescence test (Baldwin and Barker[8]), and (b) by a simple immunodiffusion system using rabbit anti-rat hepatoma serum that has been absorbed with normal liver cells and normal rat serum to remove antibodies directed against normal tissue and serum antigens.

The results presented will be discussed in relation to current concepts of the meaning of 'homogeneity' with regard to solubilized membrane antigens. The technique of preparative polyacrylamide gel electrophoresis will be critically evaluated and compared with other purification methods.

MATERIALS AND METHODS

Rats and tumours

Rat hepatomas D_{23} and D_{31} were originally induced by oral administration of 4-dimethylaminoazobenzene and have been maintained by serial transplantation in syngeneic Wistar rats. The ascites variants of hepatomas D_{23} and D_{31} were established by intraperitoneal injection of single cell suspensions obtained from solid tumour mince by trypsin digestion. Ascites hepatoma D_{23} was grown for 9 or 10 days and D_{31} for 7 days; $2 \cdot 10^8$–$3 \cdot 10^8$ D_{31} cells and $1 \cdot 10^8$–$2 \cdot 10^8$ D_{23} cells were harvested per rat.

Homogenization of hepatoma D_{23} tissue

Hepatoma D_{23} tissue was homogenized by controlled mechanical disruption using an Ultraturrax homogenizer and a crude 'extranuclear' subcellular membrane fraction (the $78\,000 \times g$ sediment of the $600 \times g$ supernatant from the homogenate) was prepared according to previously reported methods (Baldwin and Glaves[4], Baldwin *et al.*[5]).

Papain extraction of hepatoma D_{23} 'extranuclear' membrane

Crude hepatoma D_{23} membrane in 5 mM Tris–HCl buffer, pH 8.0, prepared as above, was incubated with papain (Sigma) at a concentration of approximately 1 mg enzyme per 30 mg membrane suspension. The papain was activated by the addition of L-cysteine to give a concentration of 5 mM. The stirred suspension was then incubated at 37 °C for 60 min and the membrane fragments sedimented at 78 000 × *g* for 90 min. The supernatant was then dialysed overnight against 5 mM Tris–HCl buffer (pH 8.0) at 4 °C to remove the L-cysteine and thereby inactivate the papain. This dialysis was followed by concentration using either rapid pervaporation or Aquacide II (Calbiochem.) and the solution was then redialysed against 5 mM Tris–HCl buffer (pH 8.0) at 4 °C. The solution was finally clarified by centrifugation at 165 000 × *g* for 10 min and the small pellet discarded. The supernatant was used immediately for the fractionation procedures or was stored at 4 °C with 0.01% sodium azide present until required.

EDTA extraction of hepatoma D_{23} 'extranuclear' membrane

Crude hepatoma D_{23} membranes prepared as above were stirred at 4 °C for 60 min following the addition of EDTA solution (pH 9.0) to give a final concentration of 20 mM EDTA. The suspension was then centrifuged at 78 000 × *g* for 30 min and the supernatant removed, concentrated as above, dialysed overnight against 5 mM Tris–HCl buffer (pH 8.0) at 4 °C and finally clarified by centrifugation at 165 000 × *g* for 10 min. The solution was used immediately or stored at 4 °C with 0.01% sodium azide present.

Papain extraction of ascites hepatoma cells

Ascites hepatoma D_{23} and D_{31} cells were collected in heparinised medium 199 and washed in Tris–NH_4Cl buffer (pH 7.2) to haemolyse and remove the red blood cells. The ascites hepatoma cells were then washed three times with medium 199. D_{23} cells were then washed three times with calcium-free Lockes solution. This step was omitted with the D_{31} cells owing to the fact that the cells clumped extensively if it was included. L-Cysteine was then added to the cells following suspension in medium 199 to give a 5 mM concentration. A measured volume of papain suspension (Sigma) was then added (1 mg papain/$5 \cdot 10^8$ cells) and the cells incubated at 37 °C for 60 min with stirring. Following the incubation the cells were sedimented at 3000 rev./min for 10 min, the supernatant decanted and recentrifuged at 78 000 × *g* for 30 min. The supernatant from this centrifugation was then dialysed overnight at 4 °C against deionized water to reduce the salt concentration and then reduced in volume by rapid pervaporation. This was followed by overnight dialysis against 5 mM Tris–HCl buffer (pH 8.0) and the solution finally clarified by centrifugation at 165 000 × *g* for 10 min.

Analytical polyacrylamide gel electrophoresis

Analytical polyacrylamide gel electrophoresis was performed on gels composed of 7.0% acrylamide (Kodak), 0.1% *N*,*N*′-methylenebisacrylamide (B.D.H.) in 0.05 M Tris–HCl buffer (pH 8.0), polymerized by 0.1% *N*, *N*, *N*′, *N*′-tetramethylethylenediamine (Koch-Light) and 0.05% $(NH_4)_2S_2O_8$ (B.D.H.). Gels 7.0 cm in length and 0.5 cm in diameter were formed and left overnight before use. 0.05 M

Tris–HCl buffer (pH 8.0) was used in both the anode and cathode compartments. Gels were routinely pre-run before application of protein samples to remove possible impurities from the system and the electrolysis buffer replaced.

Electrophoresis was performed using approximately 50-μl quantities of the protein solutions per tube, at a current of 3 mA per tube. Current was passed until bromophenol blue, added as a tracked dye, had passed to the bottom of the gels. Gels were then removed from their tubes and stained in 0.01% Coomassie blue in acetic acid–methanol–water (10:20:70, by vol.) and destained by washing in the same solvent mixture, in which the gels were stored without appreciable fading of the stained bands of protein. Photography was performed using Kodak Tri-X Pan 35 mm film with gels positioned over a Shandon Illuminated Viewer.

Preparative polyacrylamide gel electrophoresis

Preparative polyacrylamide gel electrophoresis was performed using the Quickfit Instrumentation apparatus with tap water cooling. 30-ml gels were formed using the same acrylamide composition as for the analytical polyacrylamide gel electrophoresis system, above. The gel was left overnight before use and was pre-run until a sample of bromophenol blue had been eluted before the protein sample was applied. The electrolysis buffers were replaced at this stage. Samples of approximately 3.0 ml containing up to 90 mg of protein were applied to the region just above the gel surface. The current was gradually increased from 10 mA to the running current of 80 mA. The eluant buffer (0.05 M Tris–HCl, pH 8.0) was monitored at 280 nm. Fractions of 1.5 ml were taken and the material thus collected was used immediately or stored at −20 °C.

Immunodiffusion analysis of tumour antigen

Antiserum against ascites hepatomas D_{23} and D_{31} were prepared in rabbits by weekly injecting subcutaneously $1 \cdot 10^8$ cells in Freunds Complete Adjuvant, over a period of 8 weeks. After preliminary immunodiffusion testing had been performed the rabbits were bled out and the serum stored at −20 °C. This serum was absorbed with $5 \cdot 10^6$ normal liver cells per ml and also with 1.0 ml normal rat serum per ml to produce an antiserum reacting primarily with tumour antigens.

Agar immunodiffusion plates were prepared on 3 inches × 1 inch microscope slides and wells cut in the conventional hexagonal pattern. The centre wells were filled with the absorbed rabbit anti-hepatoma antiserum and the outer wells with sequential fractions from preparative polyacrylamide gel electrophoretic tumour antigen purifications. In this way the fractions exhibiting tumour (specific) antigenic activity were rapidly located, following overnight development of precipitin lines.

Membrane immunofluorescence assay of tumour specific antigen

The indirect membrane immunofluorescence test was performed with viable hepatoma D_{23} cells in suspension as previously described[8], using sera from syngeneic rats sensitised to hepatoma D_{23} cells. Fluorescence indices were calculated for test serum samples by determining the percentage of cells unstained with control normal rat serum *minus* the percentage of cells unstained with the test serum divided by the former figure.

Individual or pooled soluble fractions, dialysed against phosphate-buffered saline, pH 7.3, were assayed for antigenic activity by determining their capacity to neutralise the reaction of antibody in hepatoma D_{23} immune serum with tumour-specific antigens on viable hepatoma D_{23} cells as assessed using membrane immunofluorescence (Baldwin and Glaves[4], Baldwin *et al.*[5]). Thus, antigenic activity associated with soluble fractions was denoted by a reduction of fluorescent staining with absorbed immune serum as compared with immune serum diluted with equivalent volumes of phosphate-buffered saline. The percentage inhibition of the fluorescence index with absorbed serum was defined as a measure of antigenic activity.

Electron microscopy

Electron microscopic studies of rat ascites hepatoma D_{23} and D_{31}, and hepatoma D_{23} tissue employed conventional procedures. Fixation was performed in phosphate-buffered 2.0% glutaraldehyde solutions at room temperature overnight and was followed by staining with 1.0% osmic acid in phosphate buffer for 2 h. Samples were then dehydrated by taking them through a series of graded ethanol solutions at 4 °C and finally epoxy propane before embedding in TAAB epoxy resin. Thin sections were cut with an LKB Ultratome 111 using glass knives and were mounted on Micron Type 400 grids. Post staining was performed using 2.0% uranyl acetate in 50% ethanol. Specimens were viewed in a Philips E.M. 300 and photographs were taken on Ilford E.M. 6 plates.

RESULTS

The purification of extracts from cell suspensions of ascites hepatoma D_{23} and D_{31}

Electron microscopy of the cells. Figs 1 and 2 show representative electron

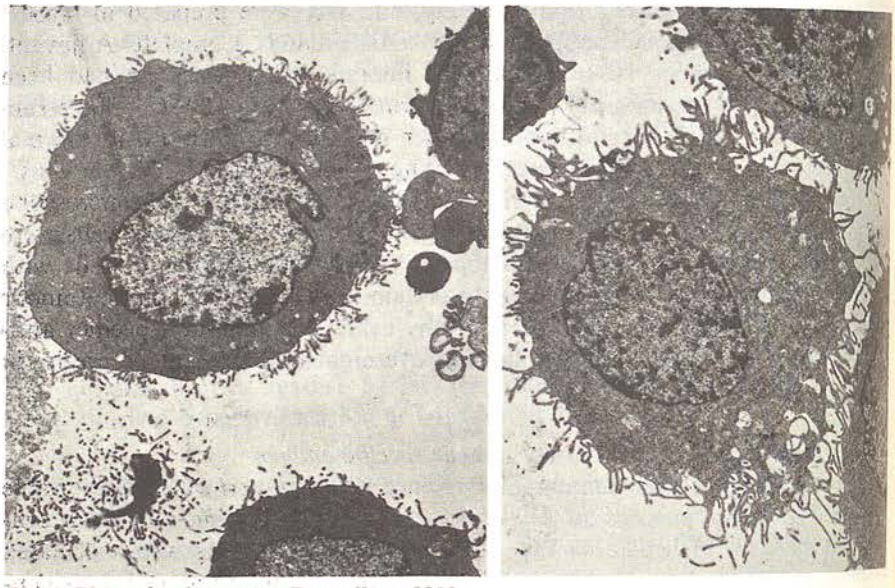

Fig. 1. Rat ascites hepatoma D_{23} cells. × 2800.

Fig. 2. Rat ascites hepatoma D_{31} cells. × 4000.

micrographs of ascites hepatoma D_{23} and D_{31}, respectively. The cells in both cases are coated with microvilli and have extensive endoplasmic reticulum. The two cell types are easily distinguished as ascites hepatoma D_{31} has a larger number of lipid containing vesicles within the cytoplasm. Following papain digestion for 60 min at 37 °C the cells remain viable as judged by their exlusion of methylene blue, but in the electron microscope it has been found that the microvilli are less pronounced, indicating the possibility that they have been broken off and that the cell surface has resealed during the incubation, see Fig. 3.

Analytical polyacrylamide gel electrophoresis of ascites hepatoma extracts. The release of protein from ascites hepatoma cells by papain digestion was as follows: D_{23} ascites; 0.6 mg protein per 10^8 cells (mean of 11 extractions). D_{31} ascites; 0.8 mg protein per 10^8 cells (mean of 16 extractions). These extracts showed tumour-specific antigenicity when tested by the indirect membrane immunofluorescence technique and by the production of precipitin lines when analysed by immuno-diffusion. Representative analytical polyacrylamide gel electrophoresis runs performed with ascites hepatoma D_{23} and D_{31} papain extracts are shown in Fig. 4. The complexity of the protein solutions is immediately apparent. It should be mentioned at this stage that papain itself is electropositive at the pH at which the electrophoresis is performed (pH 8.0), and therefore it can be concluded that all the protein bands seen on the gels are derived from the ascites hepatoma cells.

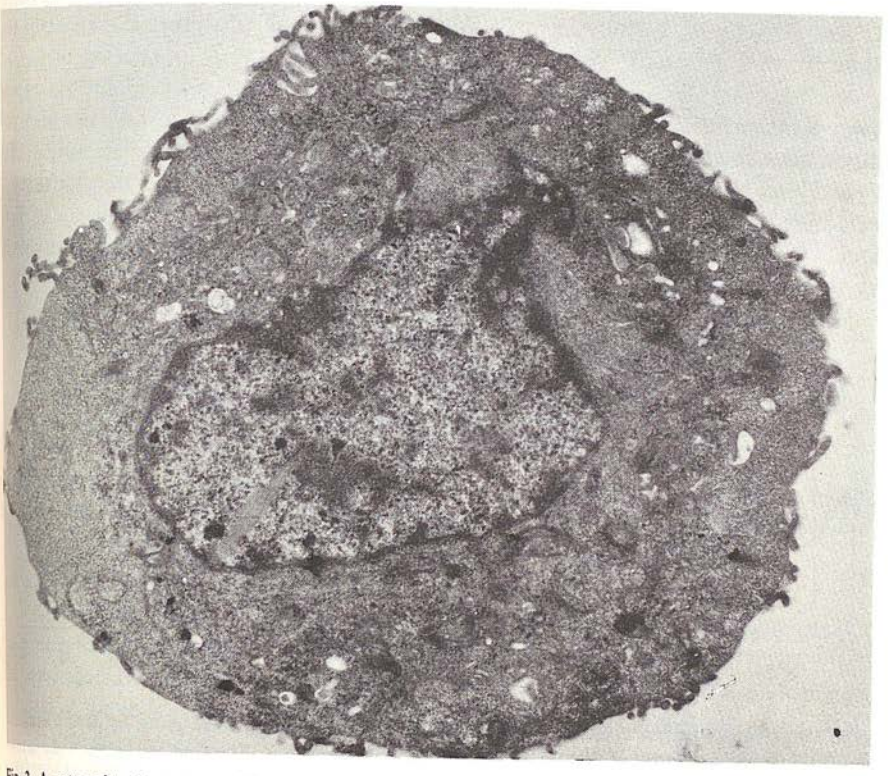

Fig. 3. A rat ascites hepatoma D_{23} cell following proteolytic digestion with papain for 60 min at 37 °C. Many of the surface microvilli appear to have been lost. × 6000.

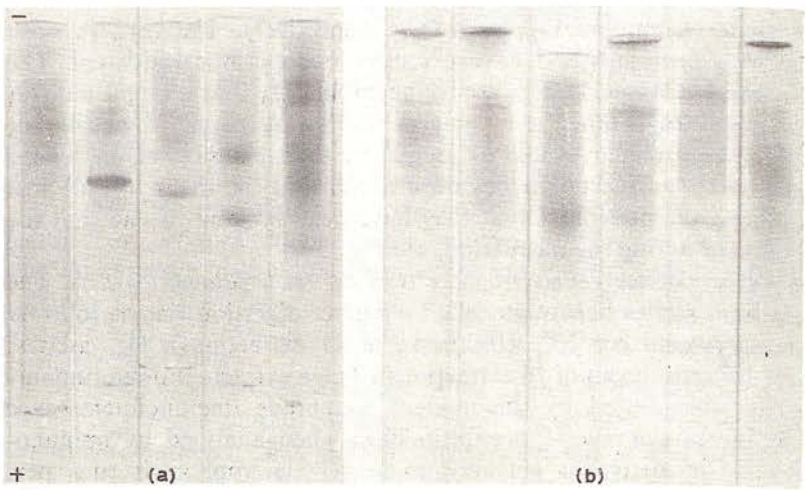

Fig. 4. Analytical polyacrylamide gel electrophoresis of the papain-extracted protein obtained from rat ascites hepatoma; (a) D_{23} cells. (b) D_{31} cells.

Preparative polyacrylamide gel electrophoresis of extracts from ascites hepatoma D_{23} and D_{31}. Fig. 5 shows representative profiles of the protein content of the eluant from preparative polyacrylamide gel electrophoresic separation performed on papain extracts from rat ascites hepatoma D_{23} and D_{31}, respectively. The region between the arrows indicates the range of fractions containing tumour-associated antigen, as assessed by the production of immunodiffusion precipitin lines. Analytical polyacrylamide gel electrophoresis performed with samples of the preparative polyacrylamide gel electrophoresis fractions reveals the separation obtained, see Figs 6 and 7. In the case of the D_{31} extract the purification obtained was not very good over the range where the antigenic activity was detected.

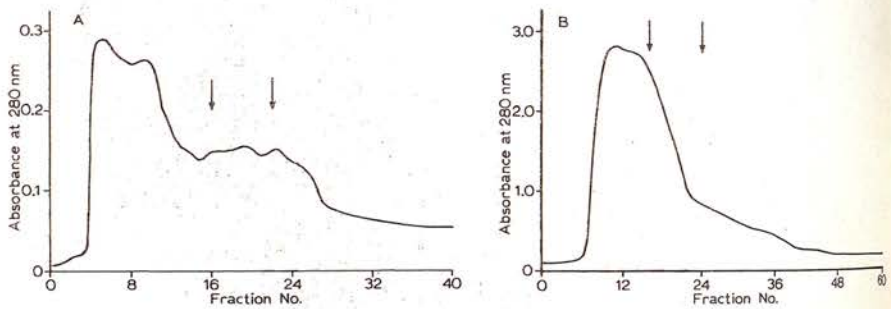

Fig. 5. Preparative polyacrylamide gel electrophoresis elution profiles given by papain extracted protein from rat ascites hepatomas D_{23} and D_{31}, respectively. The region between the arrows indicates in each case the fractions containing tumour-associated antigen, detected by immunodiffusion.

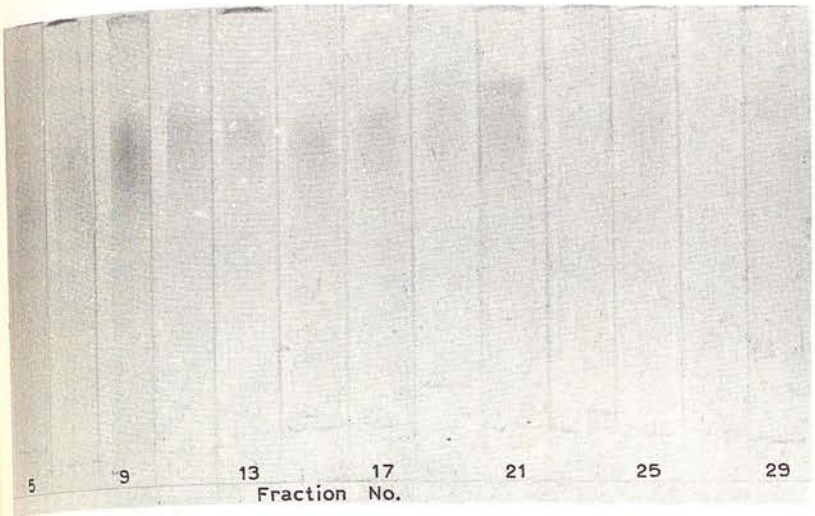

Fig. 6. Analytical polyacrylamide gel electrophoresis corresponding with the preparative electrophoretic separation of rat ascites hepatoma D_{23} papain extracted protein shown in Fig. 5A.

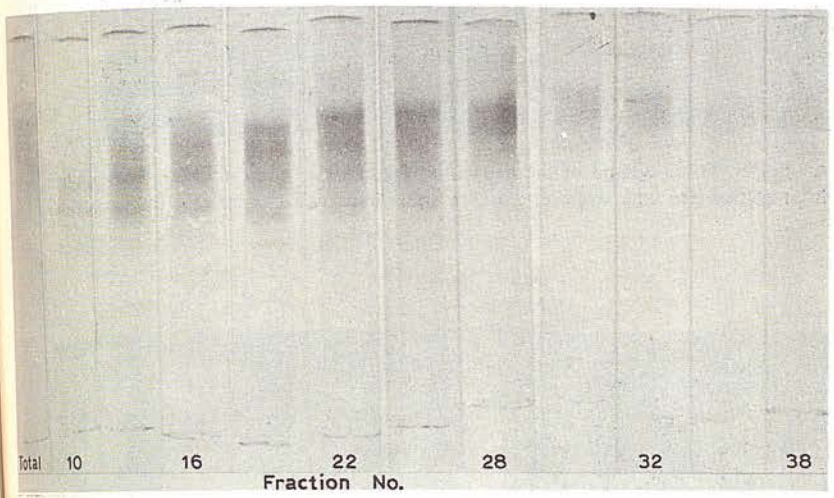

Fig. 7. Analytical polyacrylamide gel electrophoresis corresponding with the preparative electrophoretic separation of rat ascites hepatoma D_{31} papain extracted protein shown in Fig. 5B.

Extracts from rat hepatoma D_{23} 'extranuclear' membrane

Electron microscopy of the intact tissue. The cells within rat hepatoma D_{23} tissue are extremely irregular in shape and many show surface microvilli, see Fig. 8. The tissue abounds with collagen and as with the ascitic hepatoma, the endoplasmic reticulum of the cells is very well developed, as expected in rapidly growing tissue.

Analytical polyacrylamide gel electrophoresis of hepatoma D_{23} 'extranuclear' membrane extracts. Figs 9 and 10 show representative analytical polyacrylamide gel electrophoretic separations of papain and EDTA extracts obtained from

Fig. 8. An electron micrograph of rat hepatoma D_{23} tissue. The bundles of collagen lying in the extracellular spaces are very apparent as are the varied cell chapes and the microvilli. ×4200.

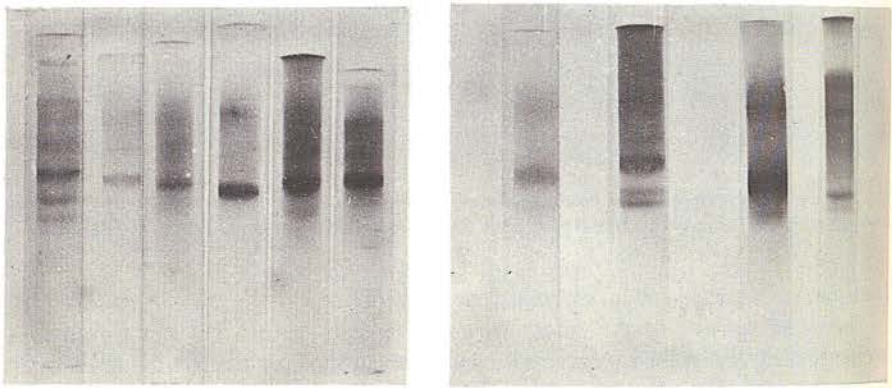

Fig. 9. Analytical polyacrylamide gel electrophoresis of extracts obtained from rat hepatoma D_{23} 'extranuclear' membrane by papain digestion.

Fig. 10. Analytical polyacrylamide gel electrophoresis of extracts obtained from rat hepatoma D_{23} 'extranuclear' membrane by EDTA treatment (20 mM at pH 9.0).

hepatoma D_{23} 'extranuclear' membrane. Both types of extract exhibit hepatoma-specific antigenicity when tested by indirect membrane immunofluorescence and immunodiffusion.

Preparative polyacrylamide gel electrophoresis of papain and EDTA extracts from hepatoma D_{23} 'extranuclear' membrane. Representative profiles of the preparative polyacrylamide gel electrophoretic purifications of hepatoma D_{23} papain and EDTA extracts are shown in Figs 11 and 12. Included in Fig. 11 is a curve showing the results of the indirect membrane immunofluorescence test, which compares favourably with the immunodiffusion analysis for the localisation of fractions

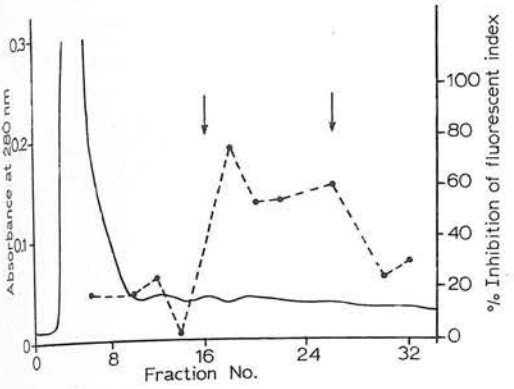

Fig. 11. A preparative polyacrylamide gel electrophoretic elution profile given by papain extracted protein from rat hepatoma D_{23} 'extranuclear' membrane. The broken line indicates the presence of tumour-specific antigen as assessed by indirect membrane immunofluorescence and the region between the arrows indicates the presence of tumour-associated antigen as detected by immunodiffusion.

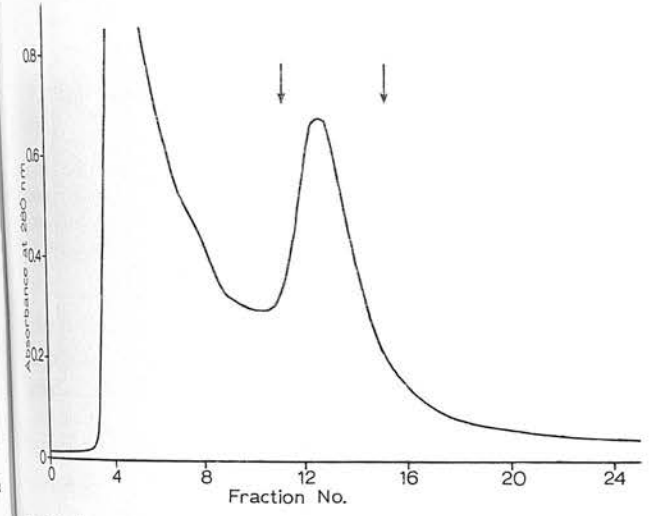

Fig. 12. A preparative polyacrylamide gel electrophoretic elution profile given by EDTA-extracted protein from rat hepatoma D_{23} 'extranuclear' membrane. The region between the arrows indicated the presence of tumour-associated antigen as detected by immunodiffusion.

containing tumour-specific antigen. Analytical polyacrylamide gel electrophoretic separations of the purified fractions from the two preparative polyacrylamide gel electrophoretic runs are shown in Figs 13 and 14.

Preparative polyacrylamide gel electrophoresis of partially purified hepatoma D_{23} specific antigen. Pooled fractions from DEAE-cellulose chromatography and rate zonal centrifugation, which showed hepatoma D_{23} specific antigenicity[5], located by both the detection methods, were applied as the starting sample in the preparative polyacrylamide gel electrophoresis apparatus. The protein elution

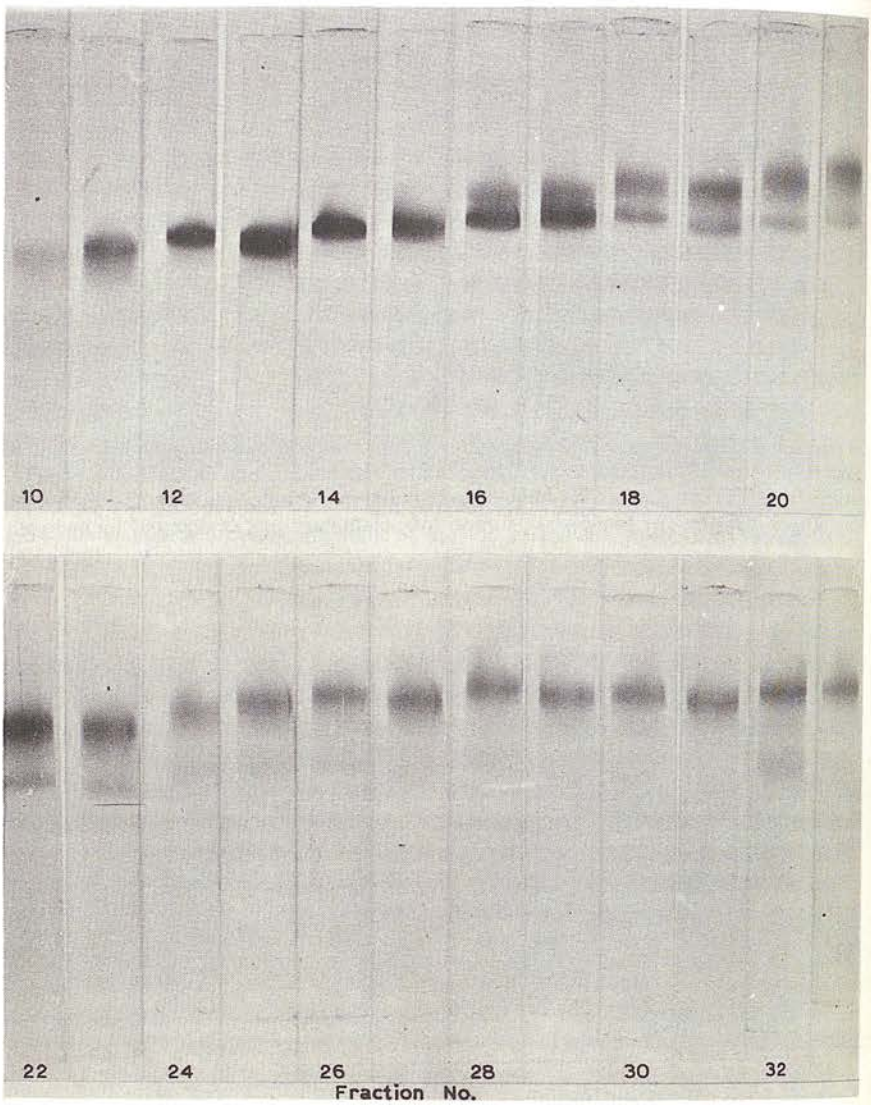

Fig. 13. Analytical polyacrylamide gel electrophoresis of the fractions obtained following preparative electrophoresis of the proteins released from rat hepatoma D_{23} 'extranuclear' membrane by papain digestion, shown in Fig. 11.

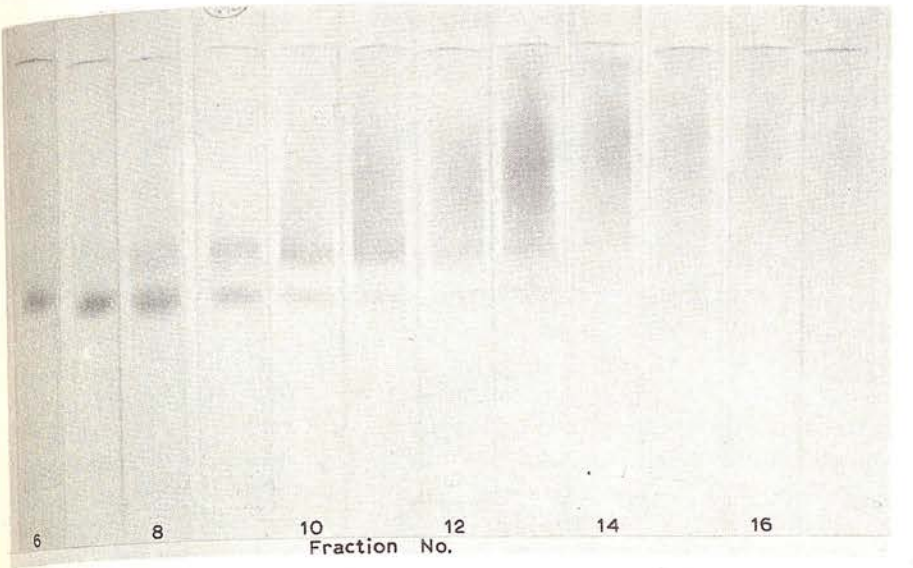

Fig. 14. Analytical polyacrylamide gel electrophoresis of the fractions obtained following preparative electrophoresis of the protein released from rat hepatoma D_{23} 'extranuclear' membrane by EDTA treatment, shown in Fig. 12.

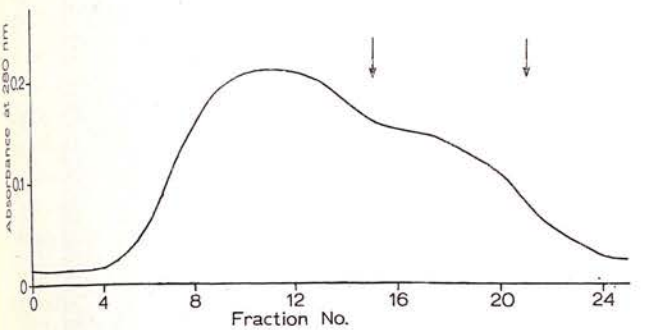

Fig. 15. A preparative polyacrylamide gel electrophoretic elution profile given by hepatoma D_{23} tumour-specific antigen that had been partially purified by DEAE-cellulose column chromatography. The region between the arrows indicates the fractions containing purified tumour-associated antigen as detected by immunodiffusion.

profile from a representative separation is shown in Fig. 15. The corresponding analytical polyacrylamide gel electrophoretic and immunodiffusion analysis performed in the purified fractions are shown in Figs 16 and 17.

DISCUSSION

The results presented indicate that the technique of preparative polyacrylamide gel electrophoresis has the ability to separate purified fractions containing tumour-specific antigen from the many components present in the initial extracts

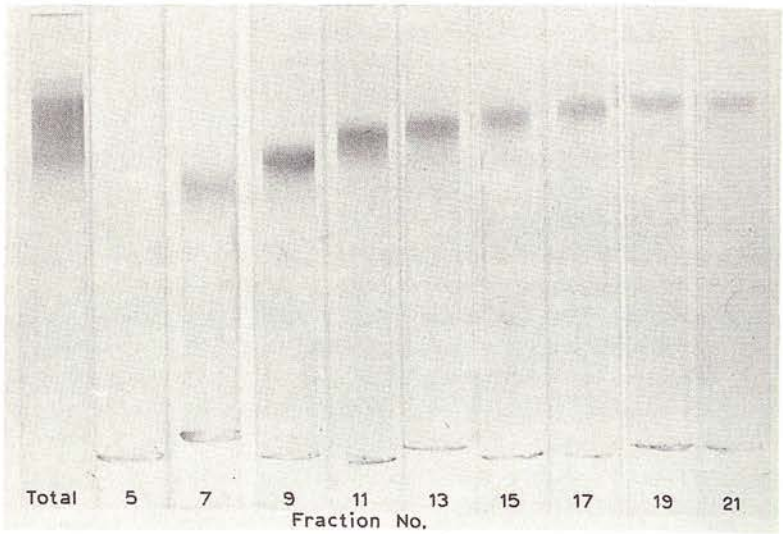

Fig. 16. Analytical polyacrylamide gel electrophoresis of the fractions obtained following preparative electrophoresis of hepatoma D_{23} tumour-specific antigen that had previously been partially purified by DEAE-cellulose chromatography, as shown in Fig. 15.

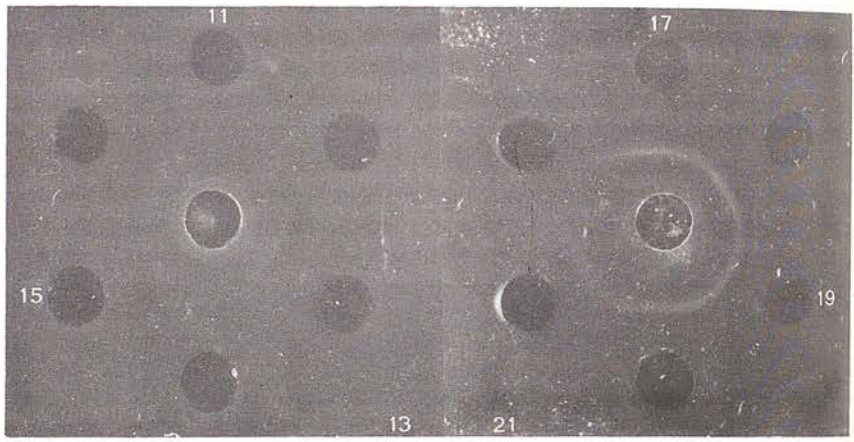

Fig. 17. Immunodiffusion analysis of the fractions obtained following preparative electrophoresis of rat hepatoma D_{23} tumour-specific antigen that had previously been partially purified by DEAE-cellulose chromatography, as shown in Fig. 15.

made from ascites hepatoma cells and hepatoma cell membrane. The major limitation of the method is that the upper limit to the amount of protein that can conveniently be applied to the electrophoresis apparatus is in the region of 200 mg. This immediately indicates that a preliminary purification prior to preparative electrophoresis is highly desirable to remove some of the non-tumour-specific components of the protein extracts. Thus, the most successful preparative polyacrylamide gel electrophoretic purifications have been obtained when material from DEAE-cellulose chromatography was taken for preparative electrophoresis[5].

Nevertheless, it is also shown that a very significant purification can be obtained directly from the initially complex extracts by the single step preparative electrophoresis procedure.

There has recently been much discussion and criticism of the use of papain as a solubilisation agent for membrane antigens (Reisfeld and Kahan[7]). This is directed firstly at the low percentage release of antigens by papain digestion, together with the fact that many non-antigenic components are released. Secondly, there is the possibility that destruction of the antigens might occur and thirdly, since papain is a proteolytic enzyme of broad specificity, antigenic fragments of varying molecular weight might be obtained. The concept of antigenic 'homogeneity' thus becomes rather vague if fragmentation of the true antigenic molecule has occurred, though it is likely that the part of the molecule acting as the antigenic determinant remains the same in the fragments of varying size.

Along with the possible loss of antigenic activity during the papain extraction, it must be borne in mind that the antigen purification methods may themselves inactivate the antigen under investigation. There is evidence that ion-exchange chromatography does lead to a large loss of membrane antigen (Reisfeld and Pellegrino[9]), but the situation with regard to preparative electrophoresis appears to be less worrying. With the tumour-specific antigens under investigation it has not been possible to quantify the loss of antigenicity throughout the extraction and purification schemes owing to the essentially qualitative nature of the antigen-assay methods employed (indirect membrane immunofluorescence and immunodiffusion). It must be stated that the rabbit antisera to rat hepatomas D_{23} and D_{31} are not absolutely monospecific after the absorption with normal rat serum and normal rat liver cells. They probably detect a range of components which are expressed on hepatoma and not on normal liver; these components being immunogenic in the rabbit. However, on the basis of the inhibition of membrane immunofluorescence data, it can reasonably be said that one of these components is the tumour-specific antigen. Quantitative information would be extremely valuable and it is hoped that by developing a radioimmunoassay system for hepatoma D_{23}-specific antigen a more precise determination of antigenicity will be possible in the future.

The preliminary experiments performed using material extracted from hepatoma D_{23} 'extranuclear' membrane by EDTA treatment in general follow a similar pattern to the papain extract when purified by preparative polyacrylamide gel electrophoresis. With EDTA antigenic degradation is less likely to occur than with papain, since it has been used by several groups of workers to solubilise membrane proteins (Tillack *et al.*[10]; Tanner and Gray[11]), without producing any denaturation, though dissociation due to the removal of calcium is likely.

Analytical polyacrylamide gel electrophoresis is considered to be a very sensitive method for detecting heterogeneity in a protein solution, but with regard to the purified hepatoma-specific antigen it has always been found that a rather diffuse band of stained protein was detected on the gels[5]. This could be because the material consists of a range of almost identical molecules rather than a homogeneous solution, due to the degradative effects of papain action of the antigen, as mentioned above. On the other hand, the purified antigen extracted initially by EDTA likewise gave a rather broad band, as did the H-LA antigen extracted

by KCl and purified by preparative electrophoresis by Reisfeld and Kahan[7], so it may be that on the cell surface there is a spectrum of similar molecules all carrying the same antigenic determinant.

Recently the technique of isoelectric focusing in polyacrylamide gel has been developed which increases still further the resolution obtainable with the analytical polyacrylamide gel system. Preliminary results have indicated that the purified material which gives a single diffuse band on the simple analytical polyacrylamide gel electrophoresis system does in fact give rise to more than one band of protein when ampholines are incorporated into the gel. Preparative isoelectric focusing may be of use for purifying membrane antigens, though in preliminary experiments it has been found that the antigenic material underwent severe aggregation in the electrofocusing column. In this context it should be mentioned that O'Neil and Davies[12] considered that ordinary electrophoresis was superior to isoelectric focusing for separating mouse H-2 specificities.

The importance of obtaining tumour-specific antigen in a highly purified form for molecular characterisation studies is considered to be paramount in relation to the understanding of the changes that occur at the cell surface during carcinogenesis. These studies may also contribute to the development of cancer immunotherapy and to the understanding of the fundamental genetic lesions which are responsible for cancerous changes. Progress along this line will require a detailed comparison of normal tissue antigens with tumour specific antigens at the molecular level.

ACKNOWLEDGEMENTS

This work was supported by the Cancer Research Campaign and the Medical Research Council. Electron microscope facilities were made available by Professor H. K. Weinbren (Department of Pathology, Medical School, University of Nottingham). The authors also wish to acknowledge the skilful technical assistance provided by Mrs C. Wright and Miss B. Smith.

REFERENCES

1 Mann, D. L., Rogentine, G. N., Fahey, J. L. and Nathenson, S. G. (1969) *J. Immunol.* 103, 282–292
2 Shimada, A. and Nathenson, S. G. (1969) *Biochemistry* 8, 4048–4062
3 Yamane, K. and Nathenson, S. G. (1970) *Biochemistry* 9, 4743–4750
4 Baldwin, R. W. and Glaves, D. (1972) *Clin. Exp. Immunol.* 11, 51–56
5 Baldwin, R. W., Harris, J. R. and Price, M. R. (1973) *Int. J. Cancer* 11, 385–397
6 Groves, W. E. and Sells, B. H. (1968) *Biochim. Biophys. Acta* 168, 113–121
7 Reisfeld, R. A. and Kahan, B. D. (1971) *Transplant. Rev.* 6, 81–112
8 Baldwin, R. W. and Barker, C. R. (1967) *Br. J. Cancer* 21, 793–800
9 Reisfeld, R. A. and Pellegrino, M. in *Immunology: An International Series*, (Kahan, B. D. and Reisfeld, R. A., eds), Vol. 2, Academic Press, New York, in the press
10 Tillack, T. W., Marchesi, S. L., Marchesi, V. T. and Steers, Jr, E. (1970) *Biochim. Biophys. Acta* 200, 125–131
11 Tanner, M. J. A. and Gray, W. R. (1971) *Biochem. J.* 125, 1109–1117
12 O'Neil, J. and Davies, D. A. L. (1971) *Biochim. Biophys. Acta* 243, 337–342

Reprinted from

METHODOLOGICAL DEVELOPMENTS IN BIOCHEMISTRY

Vol. 4: SUBCELLULAR STUDIES

Edited by Eric Reid

U.K. net price £5.25

Other volumes in the series (Editor: Eric Reid)

SEPARATIONS WITH ZONAL ROTORS (Vol. 1)

1971 Wolfson Bioanalytical Centre, University of Surrey, Guildford, U.K.
(available from the University of Surrey Bookshop. U.K. net price £2.40; net price abroad £2.90)

Vol. 2: PREPARATIVE TECHNIQUES

1973 Longman Group Limited, London
U.K. net price £3.00

Vol. 3: ADVANCES WITH ZONAL ROTORS

1973 Longman Group Limited, London
U.K. net price £3.00

38 THE PURIFICATION OF SOME MEMBRANE-ASSOCIATED PROTEINS FROM ERYTHROCYTE 'GHOSTS'

James R. Harris
Department of Physiology
University of St. Andrews
Bute Medical Buildings
St. Andrews, Fife, U.K.

The proteins under investigation are released from mammalian erythrocyte 'ghosts' when intact haemoglobin-free membranes are made to undergo fragmentation in a low ionic strength solution. This fragmentation is produced by overnight dialysis against distilled water followed by freezing and thawing. The initial extract is obtained as the supernatant following the centrifugal pelleting of the membrane fragments. This extract contains several proteins, two of which have been characterized by electron microscopic and electrophoretic studies. For further studies which require larger quantities of purified material, a scheme has been developed to separate the extracted proteins, with monitoring by analytical polyacrylamide gel electrophoresis, Ouchterlony immunodiffusion and electron microscopy. A preliminary fractionation by column chromatography using Biogel P300 removes traces of haemoglobin, if present. The fractions under the excluded peak from the P300 column contain a mixture of high molecular weight proteins. These fractions are pooled for the next stage of the purification. Sucrose density-gradient centrifugation very effectively separates the larger of the two proteins (the hollow cylinder protein, 22.5 S; m.wt. ∿ 900,000). Preparative electrophoresis on polyacrylamide gel has been employed to purify the second protein (the torus protein, 9.0 S; m.wt. ∿ 225,000) from the heterogeneous region taken from the top of the gradient. The overall scheme is discussed and proposed characterization studies are briefly described.

Electron microscopic studies and preliminary biochemical investigations have been performed on a class of high molecular weight multi-subunit proteins that are released when haemoglobin-free mammalian erythrocyte 'ghosts' undergo a fragmentation which is brought about by distilled water dialysis followed by freeze-thawing [1, 2, 3]. From electron microscopic observations of the protein molecules escaping from lesions in intact 'ghosts' and of molecules situated inside stromalytic tubules [4], it has been suggested that the proteins may be associated with the inner surface of the erythrocyte membrane. Additional support for this interpretation comes from the immunoferritin studies of Howe and Bächi [5] who have shown that the ferritin

antibody directed against the torus protein will bind to the inner surface of erythrocyte ghosts. The experiments of Hoogeveen *et al.* [6] using a fluorescent label for the outer surface of the erythrocyte membrane indicated the absence of fluorescence on the proteins released from labelled 'ghosts' by low ionic strength solutions, thus suggesting that these proteins came from the inner surface.

Recently, work has commenced on the characterization of the hollow cylinder and torus proteins. These studies need milligram quantities of the purified proteins, and to this end a more comprehensive purification scheme has been developed for the separation of the various proteins present in the initial extract obtained from the erythrocyte 'ghosts'.

MATERIALS AND METHODS

Preparation of erythrocyte 'ghosts'

Out-dated human blood (group O, +ve) was obtained from the Blood Transfusion Service at Victoria Hospital, Kirkcaldy. Fresh, defibrinated cattle blood was obtained direct from the St. Andrews slaughter-house. The methods employed for washing the erythrocytes and for producing their 'ghosts' by osmotic haemolysis and repeated washing are as previously published [2, 3], except that the Beckman J-21 centrifuge with the JA-10 (3 l capacity) angle rotor was used throughout. Up to 1 l of packed erythrocytes can be converted to haemoglobin-free erythrocyte 'ghosts' within one working day, as the J-21 centrifuge has extremely rapid acceleration and deceleration.

Preparation of the initial protein extract

Intact erythrocyte 'ghosts' are made to undergo fragmentation by overnight dialysis followed by freeze-thawing [1, 2, 3]. The membrane fragments are then pelleted at 21,000 rev/min (48,000 × *g*) for 1 h and the supernatant taken as the crude extract. Prior to any of the fractionation procedures the protein extract is concentrated by rotary film evaporation at 35° and pervaporation, and dialyzed against 5mM Tris-HCl buffer (pH 8.0) at 4. The solution is then clarified by centrifugation at 50,000 rev/min (165,000 × *g*) for 10 min and the small pellet discarded.

Electron microscopy

Negatively stained specimens of the various protein solutions are prepared on carbon-coated grids (Type 400) using 2.0% sodium phosphotungstate (pH 7.0). The 'single-drop' technique is used to apply the protein and stain to the grid [7]. Specimens are routinely studied at electron optical magnifications in excess of 50,000 diameters. The Phillips EM 300 and EM 301, and also the AEI EM 6B, have been used to study the specimens. Photographic recording has been done on Ilford EM6 and Special Lantern Contrasty glass plates.

Analytical polyacrylamide gel electrophoresis

A simple system employing 7.0% polyacrylamide gels in 50 mM Tris-HCl buffer (pH 8.0) has been used. Gels 6.0 cm in length and 0.5 cm in diameter are prepared in the tubes provided with the Quickfit Instrumentation analytical polacrylamide gel electrophoresis modules. A solution of 7.0% acrylamide (BDH) and 0.1% *N,N'*-methylene *bis*acrylamide (BDH) in 50 mM Tris-HCl buffer (pH 8.0) is polymerized by the addition of *N,N,N',N'*-tetramethylethylenediamine to 0.1% and ammonium persulphate to 0.05%.

Gels are left at least 24 h at room temperature before use. In both the electrode compartments of the electrophoresis module, 50 mM Tris-HCl buffer (pH 8.0) is used. The gels are pre-run at 6 mA per tube until a sample of bromophenol blue has passed through. The electrode buffers are then replaced before applying the protein samples. Approximately 50 µl quantities of protein solution mixed with an equal quantity of 10% glycerol in 5 mM Tris-HCl buffer (pH 8.0) containing 0.01% bromophenol blue, are applied to each tube. The current is passed initially at 1 mA per tube for 5 min and then increased to 5 mA per tube. The completion of the electrophoretic separation is indicated by the emergence of the tracker dye from the bottom of the tubes. Gels are stained with Coomassie Blue dye in 10% acetic acid-20% methanol-70% water.

Immunodiffusion

Immunodiffusion plates are prepared from 1% agar solution in phosphate-buffered saline containing 0.1% sodium azide on microscope slides and 5 cm plastic Petri dishes. Outer-wells are cut in the conventional hexagonal pattern around a central well. Protein samples are put in the outer wells and antiserum prepared by injecting rabbits with human and cattle erythrocyte ghosts is put in the central well. Precipitin lines form over a period of 48 h at 4°. The gel is then exhaustively washed in phosphate-buffered saline and stained with Coomassie Blue dye.

RESULTS

Fractionating the protein extract from erythrocyte 'ghosts'

The complexity of the initial protein extract is indicated by the stained bands of protein revealed on analytical polyacrylamide gels (Fig. 1) and also by the multiple precipitin lines produced on the immunodiffusion plates. In the electron microscope the extract is seen (Fig. 2) to contain the hollow cylinder and the single ring or torus protein, along with smaller particles.

Column chromatography

This is the first step of the purification scheme, and is included only if significant quantities of haemoglobin have been carried over from the 'ghosts'

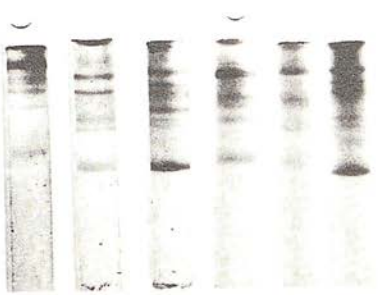

Fig. 1. Analytical polyacrylamide gels, showing the electrophoretic separation of the proteins in extracts made from several separate human erythrocyte 'ghost' preparations. *Note the overall similarity of the pattern of bands on the gels.*

into the protein extract and require to be removed before separating the other proteins. Gel filtration chromatography on Biogel P300 (Biorad Laboratories) with 10 mM Tris-HCl buffer (pH 8.0) has been used to separate haemoglobin as a retarded fraction, whereas the higher molecular weight proteins are eluted in the excluded peak (Fig. 3). Analytical polyacrlamide gels corresponding to the Biogel P300 separation are shown in Fig. 4. It is important to note that all the fractions under the excluded peak are heterogeneous; these excluded fractions are pooled for further separation.

The second step in the purification scheme is separation of the proteins by rate-dependant sedimentation through a sucrose density gradient. This technique is excellent for separating the high molecular weight hollow cylinder protein from the other proteins. Linear 0.25 M to 1.0 M sucrose gradients in 10 mM Tris-HCl buffer (pH 8.0) are used in the 40 ml tubes of the Beckman S.W. 27.1 rotor. Centrifugation is performed at 27,000 rev/min for 24 h. A typical sedimentation profile of the protein in the tube following centrifugation is shown in Fig. 5, and the corresponding analytical polyacrylamide gels in Fig. 6. The fractions under the small fast moving peak are taken as the partially purified hollow cylinder protein. Higher up the gradient the fractions are all heterogeneous and these are pooled for separation by the third stage, preparative polyacrylamide gel electrophoresis.

The partially purified hollow cylinder protein can be readily obtained in a more highly purified state by concentrating the pooled fractions from the first sucrose gradient run and reapplying it as the sample for a second identical sucrose gradient. A typical sedimentation profile is shown in Fig. 7, and an analytical polyacrylamide gel from the pooled fractions under the main protein peak is shown in Fig. 8. Electron microscopy of this material (Fig. 9) reveals that there is only one molecular species present and that the background is very clean, supporting the homogeneity indicated by Fig. 8. In addition, immunodiffusion analysis supports this claim for homogeneity, as shown in Fig. 10.

The more slowly sedimenting proteins on the first sucrose gradient run cannot be purified by applying them to a second gradient; accordingly,

Fig. 2. erythroc arrows i protein.

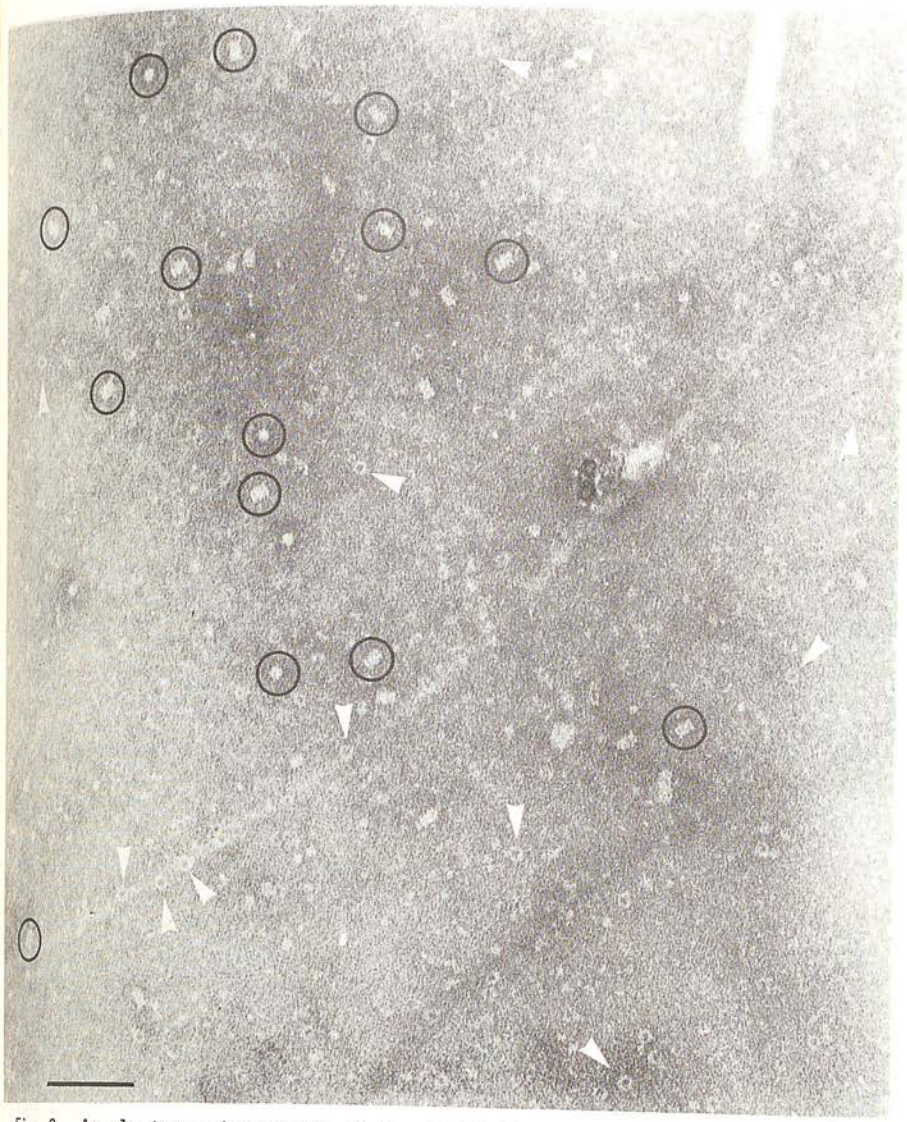

Fig. 2. An electron micrograph of the initial protein extract from human erythrocyte 'ghosts', negatively stained with Na phosphotungstate. White arrows indicate the torus protein and black circles the hollow cylinder protein. *The line represents 0.1 μm.*

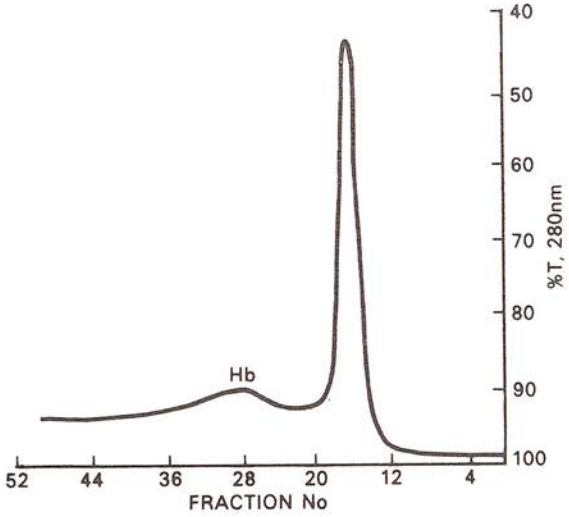

Fig. 3. The 280 nm absorption profile given by the effluent on passing the human erythrocyte 'ghost' extract through a Biogel P300 column.

Fig. 4 *(below, left)*. The analytical polyacrylamide gels corresponding to the P300 fractions indicated in Fig. 3.

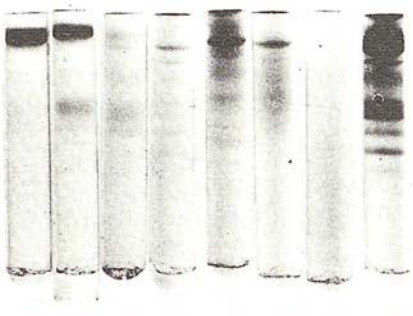

as mentioned above, preparative polyacrylamide gel electrophoresis has been employed

The apparatus manufactured by Quickfit Instrumentation Ltd. has been used, with the same gel and buffer system that was employed for the analytical polyacrylamide gel electrophoresis. The gels (30 ml) are prepared 24 h before use. The apparatus is pre-run to remove traces of contaminating material which absorbs at 280 nm, prior to the application of the protein sample (∿2 ml), which is dialyzed against 5 mM Tris-HCl buffer (pH 8.0) before application and is mixed with a small quantity of the bromophenol blue tracker dye. A typical 280 nm absorption profile obtained from the preparative electrophoretic separation of a sample containing approximately 30 mg of protein is shown in Fig.11, and the corresponding analytical gels are shown in Fig. 12. By electron microscopy (Fig.13) Fractions 13 to 15 were shown to contain the torus protein. Immunodiffusion analysis supports the electrophoretic and electron microscopic assessment of the homogeneity of the torus protein (Fig. 14). For comparison purposes, analytical gels of the purified hollow cylinder and torus proteins are shown beside the initial extract (Fig. 15).

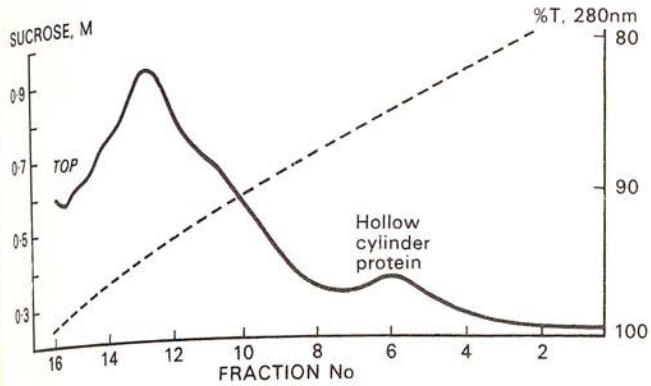

Fig. 5. The 280 nm adsorption profile given by the Biogel P300-excluded proteins on a 0.25 M to 1.0 M sucrose density gradient after centrifugation for 24 h at 27,000 rev/min.

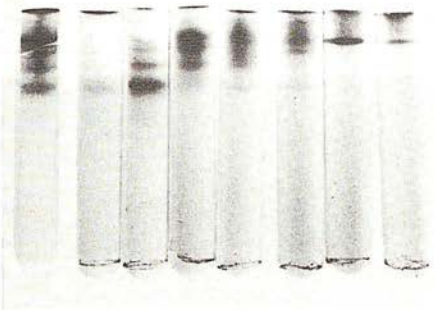

Fig. 6. The analytical polyacrylamide gels corresponding with the density gradient fractions shown in Fig. 5.

DISCUSSION

The purification scheme presented above for the separation of the loosely associated erythrocyte membrane proteins release by freeze-thawing following distilled water dialysis successfully isolated the two proteins under consideration, along with several others, for which no morphological characteristics of enzymic functions have yet been assigned. The scheme is in fact a further development of that described previously [3] in which sucrose density gradient centrifugation was the main technique employed. Preparative polyacrylamide gel electrophoresis was recently used successfully by the author to purify tumour-specific antigen from rat hepatoma [8] by the same method as described above, which was therefore transferred directly to the erythrocyte membrane proteins. In an early publication [2] it was mentioned that by slicing analytical polyacrylamide gels the torus protein could be detected by electron microscopy, so the preparative electrophoretic system naturally presented a hopeful separating method.

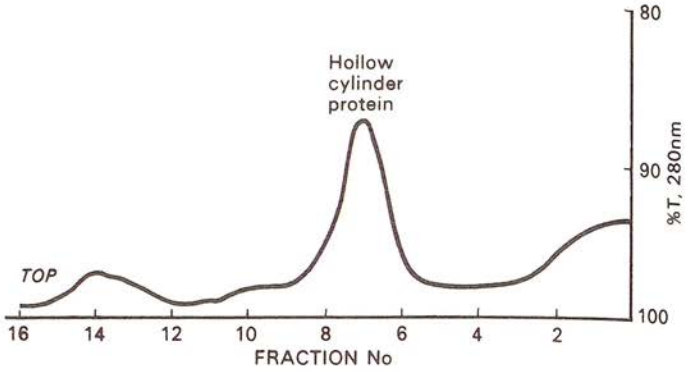

Fig. 7. The 280 nm absorption profile given by the partially purified human erythrocyte 'ghost' hollow cylinder protein on sedimenting through a 0.25→1.0M sucrose density gradient for 24 h at 27,000 rev/min.

Fig. 8. An analytical polyacrylamide gel corresponding to the main peak shown in Fig. 7.

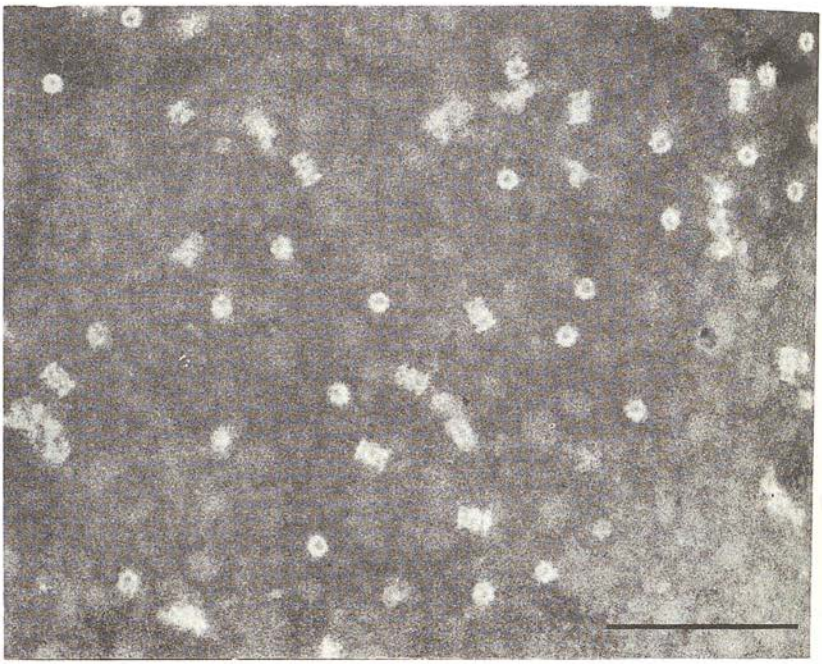

Fig. 9. *Legend opposite.*

The step-by-step separation of the hollow cylinder and torus proteins, though time-consuming, does enable highly purified fractions to be obtained more easily than if a one-step separation with preparative electrophoresis is attempted. The very slow electrophoretic migration of the hollow cylinder is not compatible with the easy use of the preparative electrophoresis, and the fact that the migration of haemoglobin is only slightly greater than that of the hollow cylinder would be a further complication in this instance.

Having obtained reasonable quantities of the purified hollow cylinder and torus proteins, one can now characterize them by the many standard biochemical and physical procedures currently available. Preliminary results obtained by several approaches will later be presented elsewhere in detail. In brief, molecular weight studies are in progress using meniscus-depletion sedimentation equilibrium in the analytical ultracentrifuge and sodium dodecylsulphate gel electrophoresis. These studies supplement the preliminary

---

Fig. 9 *(left, below)*. Electron micrograph of the highly purified human erythrocyte 'ghost' hollow cylinder protein obtained from a second sucrose density gradient run, as in Fig. 7. Negatively stained with phosphotungstate. *[The line represents 0.1* μm.

Fig. 10 *(below)*. Ouchterlony immunodiffusion plates using the human erythrocyte 'ghost' extract and the hollow cylinder protein at various stages of purification.

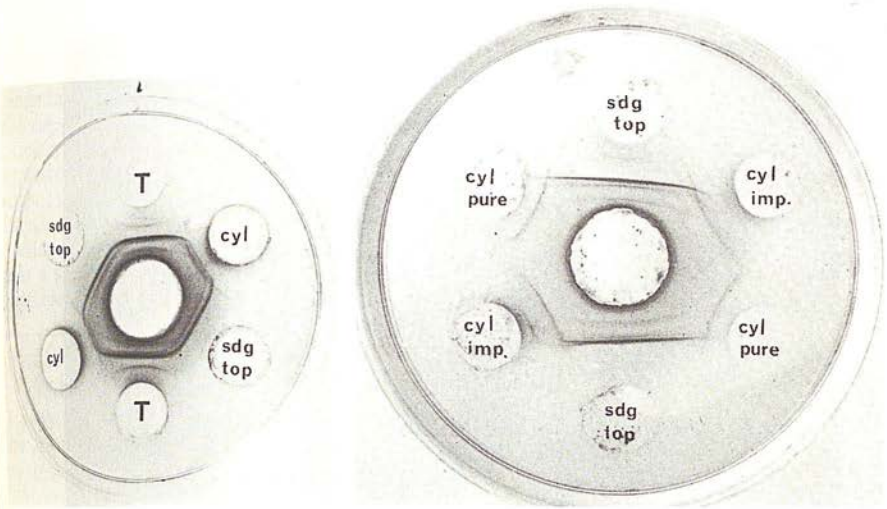

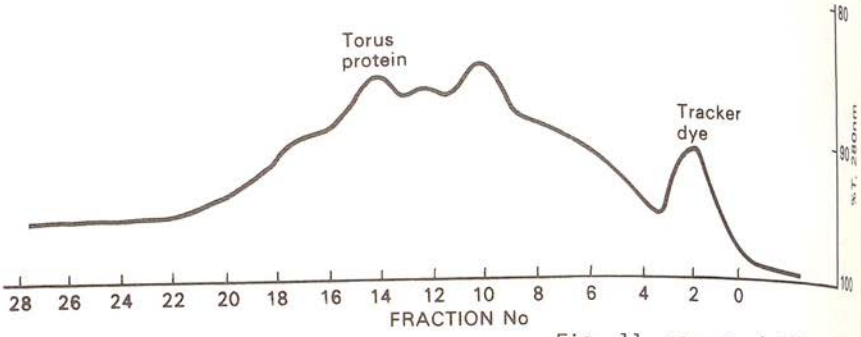

Fig. 11 *(above)*. A 280 nm absorption profile given by the eluate from the preparative polyacrylamide gel electrophoresis apparatus after application of the proteins in the pooled sucrose density gradient top fractions as the sample.

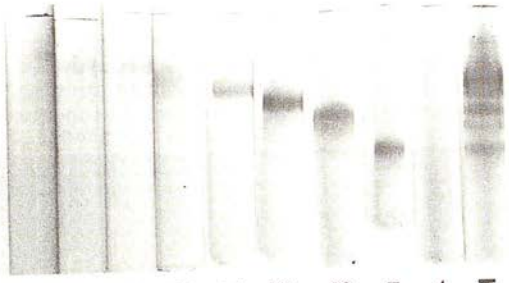

Fig. 12 *(left)* & Fig. 13 *(below)* *LEGENDS OPPOSITE*

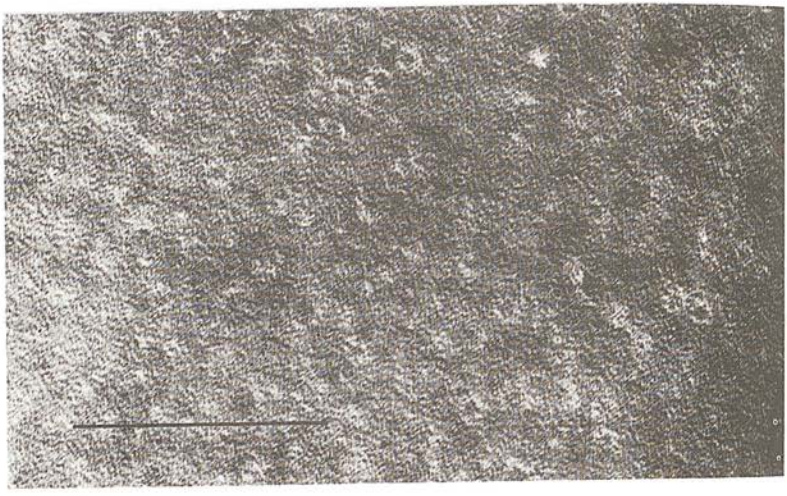

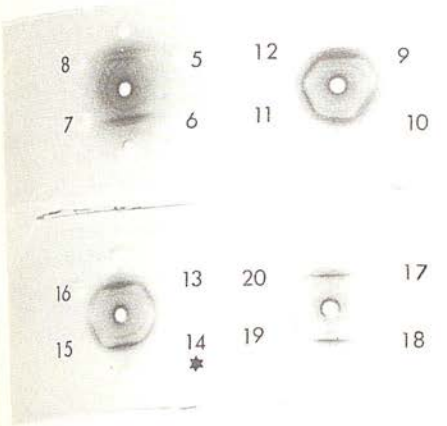

Fig. 14. Ouchterlony immunodiffusion plates of the preparative electrophoresis purification of the torus protein, corresponding with Fig. 11.

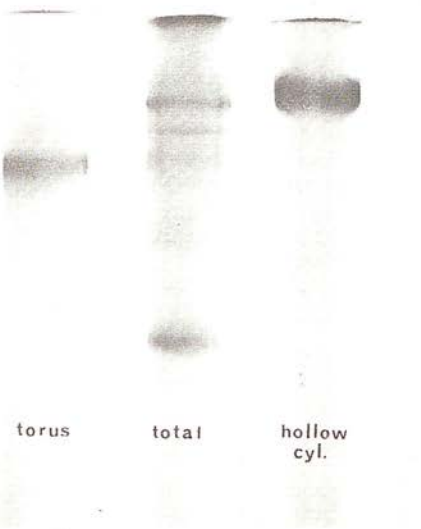

Fig. 15. Analytical polyacrylamide gels comparing the purified hollow cylinder and torus proteins with the initial protein extract from human erythrocyte 'ghosts'.

sedimentation-coefficient determinations already performed [3], which are also due to be amplified. Studies on the amino acid composition of the hollow cylinder protein from human and cattle erythrocyte 'ghosts' has so far indicated a close similarity of composition. In both cases the composition is compatible with that of other associating proteins. *N*-terminal analysis is to be undertaken in the near future. Isoelectric point determination is also of interest, and is relevant to the amino acid composition, as is a study of the absorption spectra of the proteins under different conditions.

Fig. 12 *(opposite, centre)*. Analytical polyacrylamide gels corresponding to the preparative electrophoretic separation shown in Fig. 11.

Fig. 13 *(opposite, below)*. Electron micrograph of fraction no. 14 from the preparative electrophoretic separation shown in Fig. 11. *The line represents 0.1 μm.*

Antigenic analysis is to be performed using the native and dissociated proteins to see if the subunits are antigenically identical or different. Antigenic cross-reactivity of the proteins and their subunits from different mammalian species is also a point of interest. In conjunction with a further high-resolution electron microscopic study of the two proteins, the interaction of antibody will be investigated using monospecific antiserum directly and following ferritin labelling. This latter complex will be used in an attempt to repeat and extend the studies of Howe and Bächi [5], i.e. to label the hollow cylinder and torus proteins when still associated with the inner surface of the erythrocyte membrane. High-resolution negative-contrast staining studies may elucidate the subunit interactions and the dissociation/association properties of the proteins and also their crystallization properties. Finally, enzyme screening has been commenced in an attempt to assign some function(s) to the proteins under investigation, so far with negative results.

References

1. Harris, J.R., *Biochim. Biophys. Acta 150* (1968) 534-537.
2. Harris, J.R., *Biochim. Biophys. Acta 188* (1969) 31-42.
3. Harris, J.R., *Biochim. Biophys. Acta 229* (1971) 761-770.
4. Harris, J.R., *J. Ultrastruct. Res. 36* (1971) 587-594.
5. Howe, C. & Bächi, T., *Exp. Cell Res. 76* (1973) 321-332.
6. Hoogeveen, J.Th., Juliano, R., Coleman, J. & Rothstein, A., *J. Memb. Biol. 3* (1970) 156-172.
7. Harris, J.R. & Agutter, P., *J. Ultrastruct. Res. 33* (1970) 219-232.
8. Harris, J.R., Price, M.R. & Baldwin, R.W., *Biochim. Biophys. Acta 311* (1973) 600-614.

An Electron Microscopic Study of Some Protein Fractions from Bovine Erythrocyte Ghosts

J. R. HARRIS and A. H. MADDY[1]

Department of Physiology, University of St. Andrews and [1]*Department of Zoology, University of Edinburgh, Scotland*

Received August 31, 1973, and in revised form March 4, 1974

Several different methods have been devised in recent years for solubilising proteins from bovine erythrocyte ghosts. An electron microscopic study of some of these extracts is presented, in which the technique of negative contrast staining has been employed. Most of the material studied is extremely heterogeneous with respect to the number of protein molecules in solution. The larger molecular weight proteins, by their very nature, tend to be revealed more easily by electron microscopy than do those of smaller molecular weight. The various protein extracts can, nevertheless, be distinguished from one another.

Electron microscopy can also make a contribution to the study of fibrous proteins or other more random aggregates of protein, which may be difficult to study by more conventional biochemical techniques. Emphasis is put upon the desirability of obtaining purified membrane proteins for study by electron microscopy, from which information on quaternary conformations may be obtained by high resolution studies.

The electron microscope has made a significant contribution to the study of cell membrane proteins over the last few years. In the main, electron microscopic results have correlated very well with those derived by the standard biochemical techniques. The discovery that some erythrocyte membrane proteins have a tendency to form fibrous aggregates (*9*) is an instance of information that could not have been readily obtained by means other than electron microscopy.

The aim of the present publication is to show that when a variety of different protein extracts are studied by electron microscopy, the electron optical images of the proteins revealed by negative contrast staining accord with the properties of these molecules when studied by methods such as ultracentrifugation, gel electrophoresis, and column chromatography. When conditions are present under which protein aggregation occurs, the results from the biochemical techniques tend to be more difficult to correlate with those from electron microscopy. The material to be presented has been obtained over a period of several years during which time the authors have

been investigating several methods for extracting erythrocyte membrane proteins (*1, 2, 6–8*).

For the preparation of electron microscope specimens sodium phosphotungstate (2% of pH 7.0) has been employed to a greater extent than the other negative stains currently available. This is because no aggregation of the protein has been found to occur during staining with sodium phosphotungstate, owing to the pH and the electronegativity of both the protein molecules in solution and the complex staining anion. There is always a danger that protein molecules will not be revealed by a negative stain because of the penetration of the stain within the polypeptide chains, resulting in complete electron scattering and the loss of the "negative" image of the protein under consideration. In practice this does not appear to be a problem, the major limitation being the rather high protein molecular weight that is required before the electron microscope can reveal details of the protein structure. Although claims have been made that the electron microscope will show the folding of the polypeptide chain within protein molecules (*10*), most information gained to date has dealt with the subunit organization (quaternary structure). Nevertheless, with the advent of new approaches to high resolution electron microscopy, such as striosscopy (darkfield electron microscopy) and "phase-type" techniques, it is hoped that in the future information may be gained which is relevant to the tertiary and secondary structure of protein molecules.

METHODS

The various protein extracts from bovine erythrocyte ghosts have been obtained by the previously published methods of the authors (*1, 2, 6–8*).

Analytical polyacrylamide gel electrophoresis was performed using either a Tris HCl (*2*) or a Tris-glycine system (pH 8.0) (*7*), and also a 0.26 M acetic acid system (*8*).

Electron microscopy was performed using negatively stained specimens. 2.0% solutions of sodium phosphotungstate (pH 7.0) were used for staining all the protein extracts except the one obtained by 1.5% acetic acid treatment, for which a 2.0% solution of uranyl acetate was employed. Electron microscopic study was routinely performed at electron optical magnifications of 50 000 or 60 000 diameters, using the Philips EM300. Photographs were taken on Ilford EM6 plates.

RESULTS

Extraction with distilled water

The distilled water extract from intact bovine erythrocyte ghosts prepared in 10 mM phosphate buffer (pH 7.4) was obtained by distilled water dialysis for 24 hours followed by freeze-thawing and centrifugal removal of the membrane fragments. This extract has been shown to contain several different proteins by analytical polyacrylamide gel electrophoresis (*2*). In the electron microscope this heterogeneity

is clearly apparent, see Fig. 1. A large molecular weight component with a quaternary conformation resembling a hollow cylinder is present (arrowed) along with a background spread of smaller proteins whose conformations cannot be described, and some membrane fragments.

Extraction with EDTA

The 5 mM EDTA (pH 8.0) extract from intact bovine erythrocyte ghosts contains even more components than the distilled water extract (*7*). Some of these components appear to be the same as those released by the distilled water treatment, as judged by electrophoretic mobilities and the fusion of immunodiffusion precipitin lines in the agar gel double diffusion technique. This is confirmed by electron microscopy, which again reveals the presence of the hollow cylinder protein, together with much smaller molecular weight material (see Fig. 2).

If the EDTA present in the protein extract is removed by dialysis against a phosphate buffer, with or without the presence of magnesium ions, an aggregation of some of the proteins occurs. In the electron microscope these aggregates appear as bundles of parallel fibrils approximately 40 Å in diameter, see Fig. 3. On the background beside the fibrils the cylindrical proteins are visible as well as other smaller proteins which have not taken part in the polymerization.

Evidence suggesting that the hollow cylinder protein is the largest component in the initial EDTA extract is as follows: if the solution is centrifuged at 145 000 g for 30 minutes, a small gelatinous pellet forms, which can readily be redispersed in 10 mM Tris HCl buffer (pH 8.0). By gel electrophoresis it is found that this redissolved pellet consists chiefly of the slowly migrating proteins, particularly the band nearest the origin. On studying this protein solution in the electron microscope it was found to be rich in the hollow cylinder protein (Fig. 4). These observations are in close agreement with those made previously (*2*) on the distilled water extract, from which the hollow cylinder protein was purified by sucrose density gradient centrifugation.

Extraction with n-butanol

The proteins released from centrifugally water washed bovine erythrocyte ghost fragments, or from the pelleted membrane fragments following EDTA extraction, by the original *n*-butanol system developed by Maddy (*6*, *7*) appear in the electron microscope to have no definable shape, see Fig. 5. Nevertheless, very discrete particles

---

FIG. 1. The distilled water extract from bovine erythrocyte ghosts. Negatively stained with 2% sodium phosphotungstate (pH 7.0). Arrows indicate the hollow cylinder protein. × 150 000.

FIG. 2. The EDTA extract from bovine erythrocyte ghosts. Negatively stained with 2% sodium phosphotungstate (pH 7.0). Arrows indicate the hollow cylinder protein, which is surrounded by a greater quantity of smaller MW protein than in Fig. 1. × 84 000.

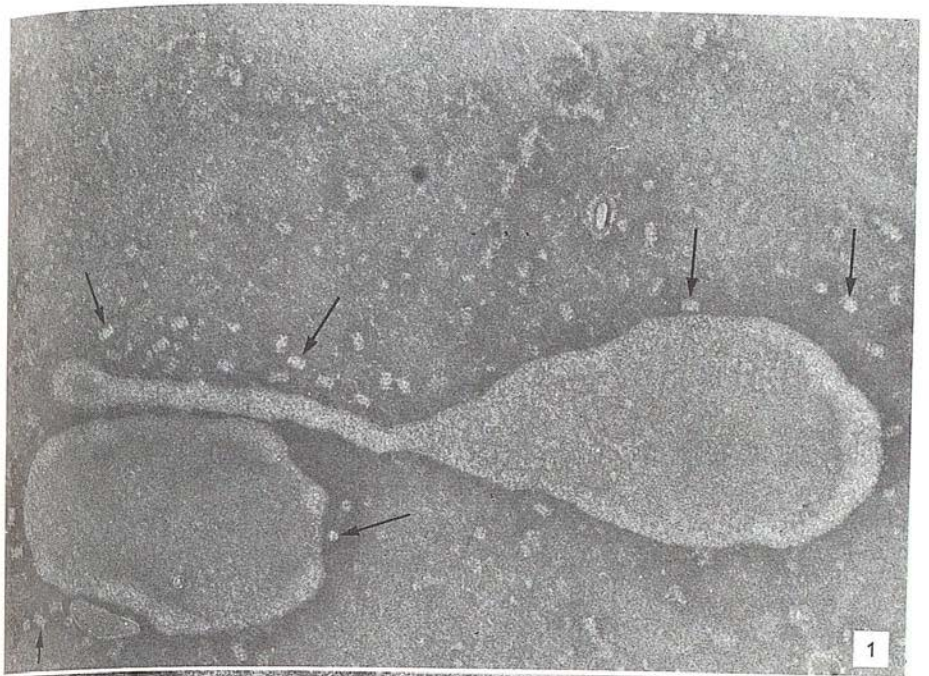
1


2

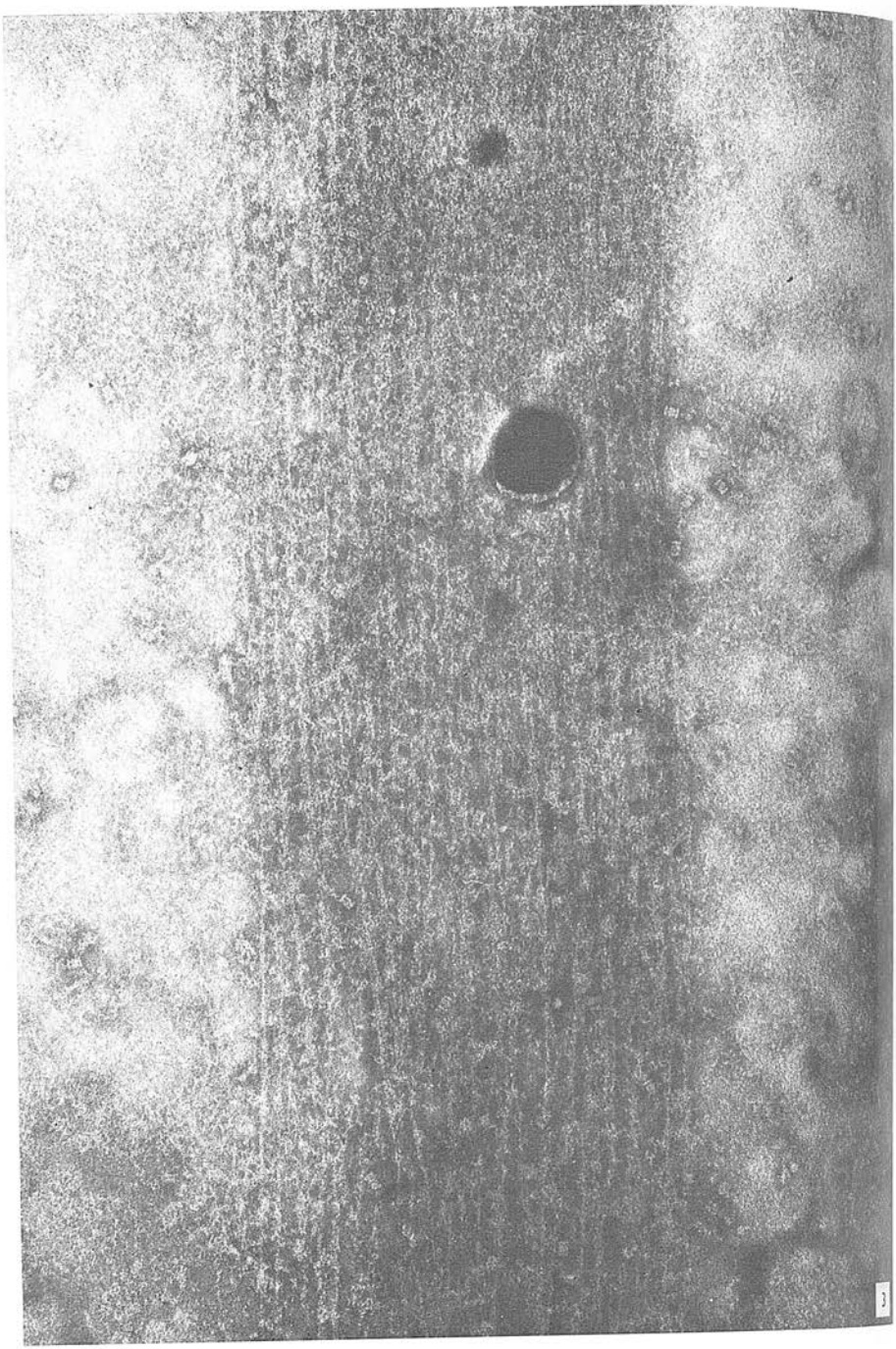

FIG. 4. The 145 000 *g* (30 minutes) pellet from the bovine erythrocyte ghost EDTA extract. Negatively stained with 2% sodium phosphotungstate (pH 7.0). The main protein present is clearly seen to be the hollow cylinder. × 159 000.

FIG. 3. The fibrous aggregates produced by dialysing the EDTA extract from bovine erythrocyte ghosts against phosphate buffer containing 5 mM $MgCl_2$. Note that on the background there is a spread of unpolymerised protein, among which the hollow cylinder can be seen. Negatively stained with 2% sodium phosphotungstate (pH 7.0). × 105 000.

are revealed which have a very clean background stain, suggesting the absence of smaller molecular weight particles. If, on the other hand, the *n*-butanol extract is made directly from intact erythrocyte ghosts to which EDTA has also been added (*7*), then the background is seen to contain many smaller molecular weight particles together with the hollow cylinder proteins, see Fig. 6. Fibre formation is also possible in this solution (see above) but the fibres are heavily contaminated with other proteins and therefore difficult to demonstrate. The differences between the extract shown in Fig. 5 and Fig. 6 confirm the biochemical analyses of the two extracts (*7*). The proteins in Fig. 5 cannot be fractionated, but those in Fig. 6 separate into several components, including some with the same properties as the proteins in the EDTA extract.

Centrifugation of the butanol-EDTA extract at 122 000 *g* for 3 hours has been shown by biochemical methods to remove the large components and this finding is confirmed by electron microscopy. The large *n*-butanol + EDTA particles and the hollow cylinder protein are absent from the supernatant (Fig. 7).

Extraction with acetic acid

The proteins which may be extracted with EDTA are also released from the membrane by 1.5 % acetic acid, but the more vigorous conditions have a deleterious effect on the proteins. When studied by negative staining the extract obtained from bovine erythrocyte ghosts by treatment with 1.5 % acetic acid (*8*) is revealed as a dispersion of very small particles, see Fig. 8, and the hollow cylinder protein is absent. This is likely to be because the hollow cylinders have been dissociated by the acidic treatment and are then not significantly larger than the other proteins in solution. Treatment of the purified hollow cylinder with 1.5 % acetic acid has been shown to break up this protein (J. R. Harris, unpublished observations). Fibrous structures cannot be formed from the acetic acid extract.

DISCUSSION

The results presented above show that the various protein extracts from bovine erythrocyte ghosts which have been dealt with can be distinguished by electron microscopy. The greater the heterogeneity of the protein solution under investigation the less precise electron optical information becomes. This statement might, never-

FIG. 5. The *n*-butanol extract obtained from bovine erythrocyte ghosts following extraction with EDTA. Negatively stained with 2 % sodium phosphotungstate (pH 7.0). Note the cleanliness of the background around the large protein particles, which indicates the absence of small MW proteins. × 105 000.

FIG. 6. The *n*-butanol-EDTA extract obtained from intact bovine erythrocyte ghosts. Negatively stained with 2 % sodium phosphotungstate (pH 7.0). Note the presence of the hollow cylinder protein (arrowed) together with much small MW material which surrounds the larger particles. × 159 000.

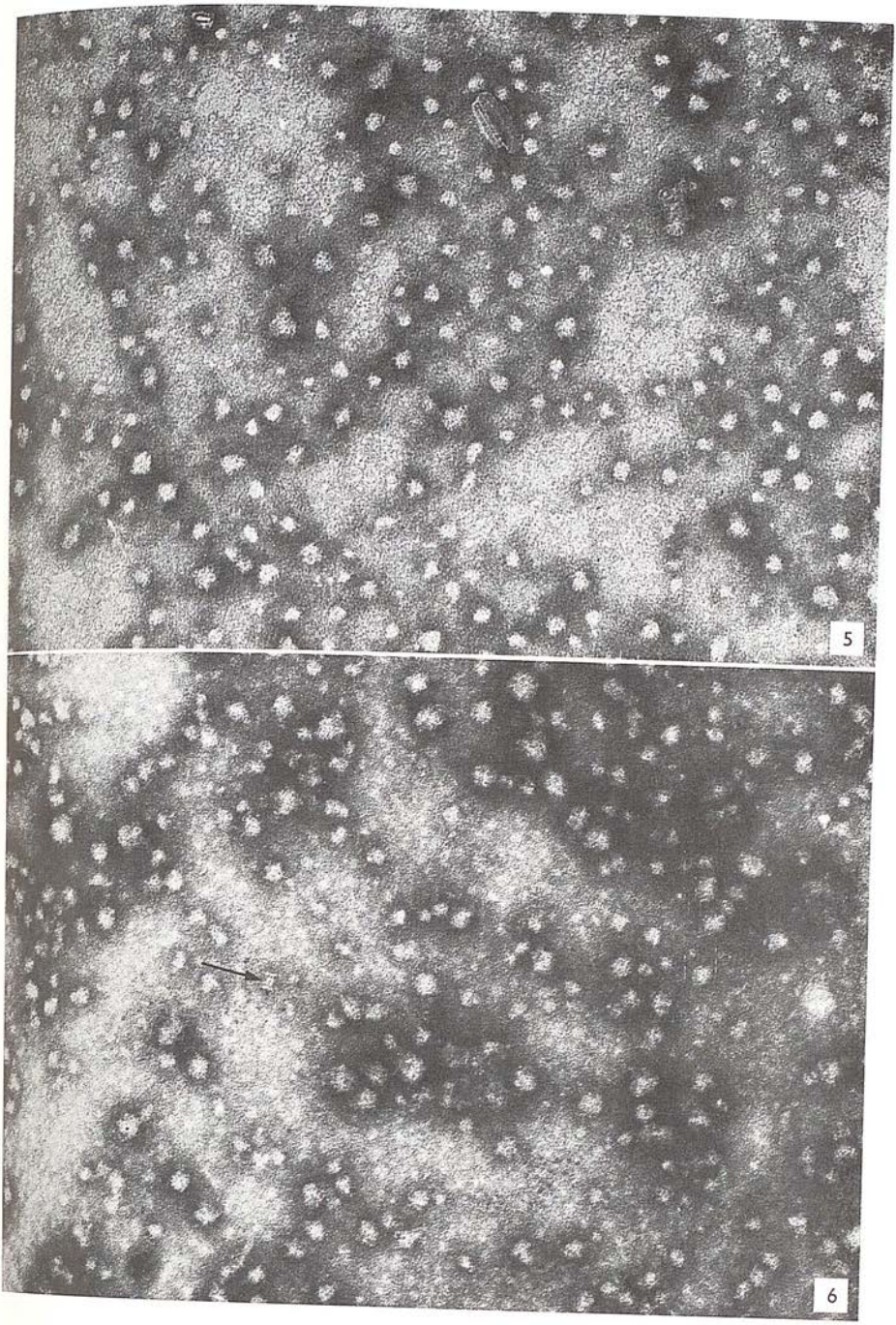
5
6

theless, be said to apply equally well to the biochemical methods available for the characterization of proteins. In the main, the conclusions drawn from the electron microscopic results fit in well with those obtained by electrophoretic and centrifugation studies (*2*, *7*, *8*) in relation to the range of molecular weights present, and they jointly emphasise the importance of obtaining the separation and purification of the components in solution prior to further characterisation studies.

It is significant that the hollow cylinder protein has been detected in only three of the extracts studied (the distilled water extract, the EDTA extract and the total *n*-butanol-EDTA extract). The fact that the cylinder protein is absent from the *n*-butanol-EDTA extract made from the EDTA extraction residue is in accord with the concept that this protein is relatively loosely associated with the inner surface of the erythrocyte membrane (*4*).

One interesting fact which has general implications for membrane protein solubilization studies is that significant quantities of the hollow cylinder protein (22.5 S, MW approx. 900 000) will pellet during a 30-minute centrifugation at 145 000 *g*. Similar or even greater gravitational forces and times are routinely used to remove small lipoprotein membrane fragments following solubilization treatments. It is thus suggested that caution should be observed to monitor the possible loss of high molecular weight proteins from protein extracts when clarification by high speed centrifugation is part of the procedure. The research of other groups employing EDTA treatment of erythrocyte ghosts (*12*) has very often employed a long high speed centrifugation, which may account for the fact that these workers failed to observe the hollow cylinder protein in their final extracts.

The formation of fibrous aggregates by some of the proteins released from erythrocyte ghosts by EDTA has been known for several years (*9*, *11*). From the results presented in this communication it is clear that the hollow cylinder protein does not participate in this fibre formation and is therefore likely to be different to Marchesi's Spectrin (*9*), contrary to the suggestion of Hoogeveen et al. (*5*). The individual fibrils are of very regular diameter (approximately 40 Å), but they are most often found to lie parallel to one another as large bundles. It appears that along any one fibril there are thicker regions, similar to those shown by Rosenthal et al. (*11*), which may represent sites of nucleation where monomers are binding around an existing fibril in the

---

FIG. 7. *The Ms protein*, obtained by centrifuging the total *n*-butanol-EDTA extract at 122 000 *g* for 3 hours. Negatively stained with 2 % sodium phosphotungstate (pH 7.0). Note the smallness of the protein particles compared with those in Figs. 5 and 6, and also the absence of the hollow cylinder protein. × 150 000.

FIG. 8. The 1.5 % acetic acid extract from bovine erythrocyte ghosts. Negatively stained with 2 % uranyl acetate (pH 4.5). Note, in general, the smallness of the protein particles. Some aggregation of the particles appears to be occurring, owing to the staining solution. × 150 000.


7

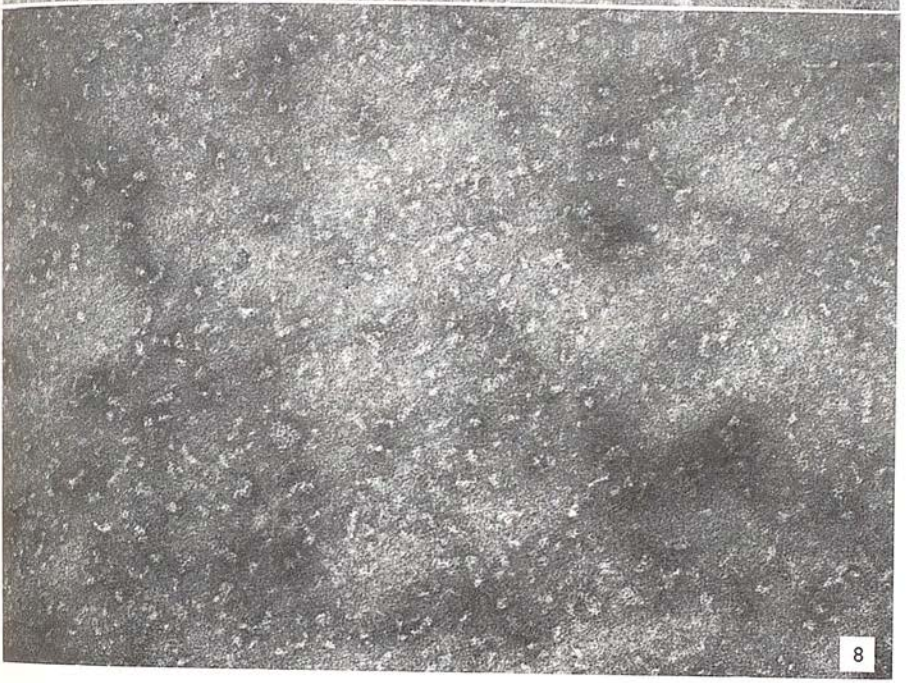
8

polymerisation process, or merely the sites where larger proteins are adsorbed to the fibrils.

Although the results obtained by electron microscopy must be considered to make a significant contribution only in relation to the larger molecular weight components released or the multimolecular aggregates produced by the various extraction procedures under discussion, it must nevertheless be stated that current electron optical advancements are likely to enable meaningful information to be gained from some of the smaller molecular weight proteins in the future. Before progress can be made at this high resolution level it will be necessary to prepare homogeneous protein fractions from the erythrocyte membrane. In the case of the hollow cylinder protein, by considering a restricted number of orientations of the protein relative to the electron beam a satisfactory interpretation of the electron optical images has been obtained (*3*). With other purified proteins which do not have such an easily recognisable and definable quaternary conformation, the interpretation of the electron optical images becomes more difficult, but here too methods for the analysis of electron optical images, such as by diffractometry, are undergoing rapid development and further progress can be expected in the future.

REFERENCES

1. HARRIS, J. R., *Biochim. Biophys. Acta* **150**, 534 (1968).
2. —— *ibid.* **229**, 761 (1971).
3. —— *J. Mol. Biol.* **46**, 329 (1969).
4. —— *J. Ultrastruct. Res.* **36**, 587 (1971).
5. HOOGEVEEN, J. Th., JULIANO, R., COLEMAN, J. and ROTHSTEIN, A., *J. Memb. Biol.* 3, 156 (1970).
6. MADDY, A. H., *Biochim. Biophys. Acta* **117**, 193 (1966).
7. MADDY, A. H., DUNN, M. J. and KELLY, P. G., *Biochim. Biophys. Acta* **288**, 263 (1972).
8. MADDY, A. H. and KELLY, P. G., *Biochim. Biophys. Acta* **241**, 290 (1971).
9. MARCHESI, V. T. and STEERS, E., *Science* **159**, 203 (1968).
10. MISRA, D. N. and GANGULY, P., *Arch. Biochem. Biophys.* **124**, 349 (1968).
11. ROSENTHAL, A. S., KREGENOW, F. M. and MOSES, H. L., *Biochim. Biophys. Acta* **196**, 254 (1970).
12. TILLACK, T. W., MARCHESI, S. L., MARCHESI, V. T. and STEERS, E., JR., *Biochim. Biophys. Acta* **200**, 125 (1970).

Reprinted from
Biochimica et Biophysica Acta, 427 (1976) 727–737

BBA 37282

THE HIGH MOLECULAR WEIGHT PROTEINS RELEASED FROM CULTURED CELLS

J. R. HARRIS*, K. D. BROWN and J. F. AITON
Department of Physiology, University of St. Andrews, Bute Medical Buildings, St. Andrews, Fife (U.K.)

SUMMARY

Studies have been performed with the serum-free culture medium taken from several fibroblast monolayer culture lines. A high molecular weight protein fraction was separated from the concentrated medium by sucrose density gradient centrifugation. Polyacrylamide gel electrophoresis was used to assess the degree of purification obtained. In the electron microscope the negatively stained high molecular weight proteins were found to closely resemble the α_2-macroglobulins. The suggestion that these proteins from cultured cells resemble the cylindrical protein complex isolated from mammalian erythrocyte ghosts is not supported by this study. The results are discussed in the light of the extensive literature now available on the electron microscopy of high molecular weight proteins.

INTRODUCTION

In a recent publication Narayan and Rounds [1] have shown that several different proteins are released from monolayer cultures of three cell lines of malignant origin (CMP, HeLa, and KB). A preliminary separation of the higher molecular weight proteins was obtained by taking the 105 000 × *g* pellet from the serum-free growth medium following an initial clarification at 25 000 × *g*. This pelleted protein was studied by polyacrylamide gel electrophoresis, which revealed several bands of protein. Electron microscopy using negative staining likewise revealed heterogeneity. Although an array of large molecular weight particles was observed, many of which exhibited ring-shaped and rectangular profiles other irregular particles were also present. It was suggested that the particles morphologically resembled the cylindrical protein complex released from erythrocyte ghosts by Harris [2–5], but it was claimed that the presence of nucleic acid was an underlying difference.

The present investigation was undertaken in an attempt to determine more precisely, using purified material, whether or not the erythrocyte membrane protein is the same as the ones released into the growth medium by cultured cells. Several fibroblast cell lines have been employed (HeLa, 3T3, Py3T3 and SV 3T3) and in all cases the proteins released into the serum-free growth medium have been purified using rate velocity separation on a linear sucrose density gradient, in a manner identical to that previously used for the erythrocyte membrane hollow cylinder pro-

* Present address: Dept. of Biological Science, North-East London Polytechnic, Romford Rd., London E15 4LZ (U.K.).

tein, Harris [4, 5]. Polyacrylamide gel electrophoresis has been used to assess purity and the material studied directly in the electron microscope by negative staining with sodium phosphotungstate following the removal of sucrose by dialysis.

Several publications have appeared in recent years on proteins (factors) released from cultured cells into the growth medium [1, 6–10]. Fundamental studies on the characterization of these proteins are necessary along with functional investigations of the effects the proteins have on growth and other cellular changes. In addition, there is an extensive literature on the various serum components which have growth-stimulating properties [11–13] some of which may be related to those produced by cultured cells.

MATERIALS AND METHODS

(1) Extraction of proteins. The hollow cylinder protein from human erythrocyte ghosts was obtained and purified by previously published methods [4, 5]. Fibroblast cell lines were cultured as monolayers in Roux bottles. Eagles basal medium supplemented with 10% calf serum was used for the HeLa cells and Dulbecco's modified Eagle medium, likewise supplemented, was used for the 3T3, Py3T3 and SV 3T3 cell lines. Preconfluent layers of cells, approx. $40 \cdot 10^6$ per Roux, were carefully washed two times with serum-free culture medium and incubation was then continued in the absence of serum. The culture medium was collected and replaced with fresh serum-free medium at approx. 12-h intervals, up to 48 h, pooled and stored at 4 °C. Immediately following the final collection, the medium was centrifuged at 10 000 rev./min (11 000 × *g*) for 30 min to remove any intact cells and cellular debris. The medium (usually 200–300 ml) was then exhaustively dialysed against distilled water at 4 °C for 24 h, with three changes of the dialysate. The salt-depleted fluid was then concentrated by rotary film evaporation at 30 °C to a volume of approx. 2.0 ml, which was then dialysed against 5 mM Tris·HCl buffer (pH 8.0). Traces of aggregated material were removed finally by centrifugation at 50 000 rev./min (198 000 × *g*) for 5 min. The quantity of protein released from the washed cells into the serum-free growth medium was approx. 0.1 mg per 10^6 cells over a 48-h period.

(2) Fractionation of the proteins released by cultured cells. Rate velocity separation of the concentrated and dialysed material released from cultured cells was performed on linear sucrose density gradients (0.25–1.0 M sucrose in 10 mM Tris·HCl, pH 7.0) in the 40-ml tubes of the Beckman SW 27.1 rotor. Centrifugation was performed for 24 h at 27 000 rev./min (100 000 × *g*). The content of the tubes was analysed by passing it through an LKB Uvicord 11 ultraviolet absorptiometer connected to a Bryans model 27000 chart recorder. Fractions of 40 drops were taken using an LKB Ultrorac fraction collector.

(3) Analytical polyacrylamide gel electrophoresis. Polyacrylamide gel electrophoresis was performed using the Quickfit Instrumentation PAGE apparatus. A simple Tris·HCl buffer system at pH 8.0 was employed with 7.0% polyacrylamide gels [4, 5]. Samples of approx. 50 µl were applied to the gels. Sucrose gradient fractions were monitored using this technique following the centrifugal separation of the protein extracts. Samples were also electrophoresed in the presence of 0.1% sodium dodecyl sulphate following incubation in 1.0% sodium dodecyl sulphate/β-mercaptoethanol at 100 °C for 1 min, to bring about dissociation of the polypeptide chains.

(4) Electron microscopy. Samples of the gradient fractions were freed from sucrose by dialysing overnight at 4 °C against 5 mM Tris·HCl buffer (pH 8.0). Negatively stained specimens were then prepared using the "single droplet" procedure, whereby a spread of the protein solution is applied to a carbon-coated electron microscope grid, followed by a spread of negative stain. 2.0% sodium phosphotungstate (pH 7.0) has been used throughout as the negative stain. Specimens were studied in a Philips EM 301 electron microscope at an accelerating voltage of 80 kV. Electron micrographs were taken at instrumental magnifications of 57 000 and 71 000 diameters using Ilford plates (type EM 6).

(5) Immunodiffusion. Double diffusion analysis was performed using the Ouchterlony technique. Antisera against human and bovine serum proteins were purchased from Miles Laboratories.

RESULTS

(1) Heterogeneity of the proteins released from cultured cells

The conditioned culture medium obtained from the fibroblast cell lines was subjected to analytical polyacrylamide gel electrophoresis to determine the number of protein species in solution. Fig. 1 shows a comparison of the various extracts. All

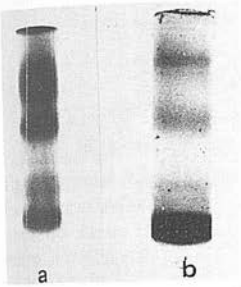

Fig. 1. Analytical polyacrylamide gel electrophoresis of the proteins released from HeLa cells (a) and Py3T3 cells (b).

the extracts contain a complex mixture of proteins. A major leading band of migration rate similar to serum albumin is present in all cases, but owing to the complexity it is not possible to distinguish differences between the extracts at this level of analysis. The higher molecular weight proteins, which in general migrate a short distance from the origin, represents only a small proportion of the total.

Separation of the high molecular weight proteins by high speed centrifugation (198 000 × *g* for 1 h) of the extract, as described by Narayan and Rounds [1] yielded a transluscent pellet which on resuspension was found to be enriched in the higher molecular weight proteins (see Fig. 2). This material is still extremely heterogeneous and is not considered suitable for accurate electron microscopic study or biochemical analysis.

(2) Purification of the high molecular weight proteins

Fractionation of the proteins present in the concentrated cell extracts was per-

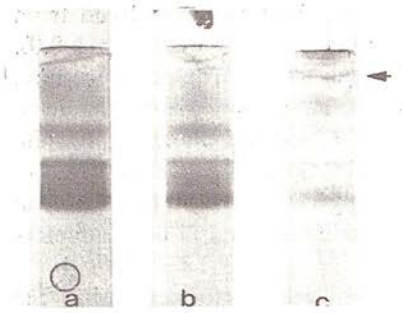

Fig. 2. Analytical polyacrylamide gel electrophoresis of the proteins released from HeLa cells (a), the 198 000 × *g* (60 min) supernatant (b), and the pellet (c). The presence of high molecular weight proteins on gel c is indicated by the arrow.

formed by centrifugation of the molecules through a 0.25–1.0 M sucrose density gradient for 24 h at 27 000 rev./min (100 000 × *g*). Typical sedimentation profiles of the proteins after centrifugation are shown in Fig. 3, and the corresponding analytical

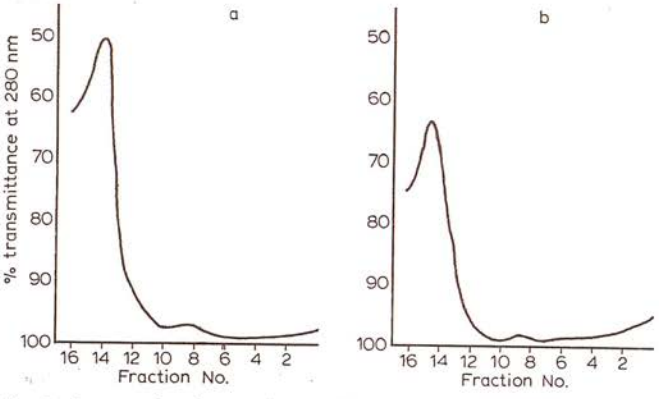

Fig. 3. Sucrose density gradient sedimentation profiles of the proteins released from HeLa cells (a) and Py3T3 cells (b). Note the small peak of high molecular weight protein spread over fractions 8–10.

polyacrylamide gel electrophoretic separation of the proteins in the gradient fractions is shown in Fig. 4. In the examples shown here it is to be noted that there is a small peak of faster sedimenting protein (high molecular weight) visible on the scans of the sucrose gradient tubes. This correlates well with the appearance of one or two discrete bands of protein on the polyacrylamide gels of the gradient fractions [8–10] under the small peak. With HeLa there is only one band of protein, but with 3T3 and its transformed lines there are always two bands of high molecular weight protein. On re-running the high molecular weight proteins from Py3T3 on an identical sucrose gradient, the two bands of protein were still found in the same position on the gradient. This strongly indicates that there are two discrete high molecular weight proteins. The lower molecular weight proteins under the main peak of the initial sucrose gradient separation are not obtained in a purified state and further attempts have not been made to date to obtain complete purification.

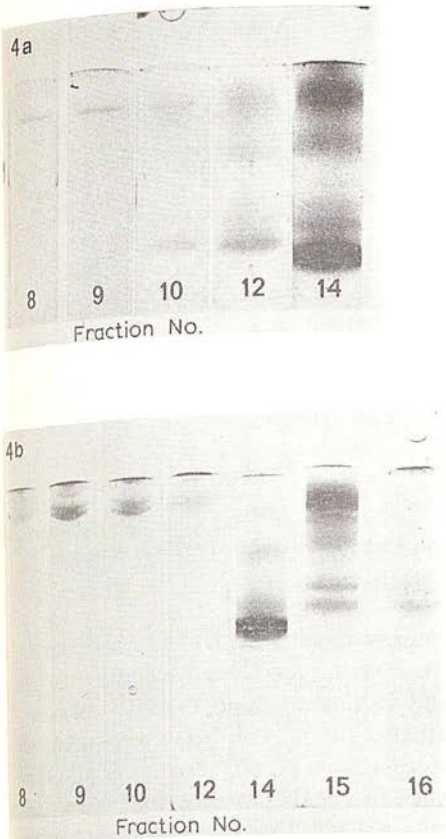

Fig. 4. Analytical polyacrylamide gels corresponding to the sucrose gradients shown in Fig. 3. The fractionated proteins from HeLa cells are shown on gels a, and those from Py3T3 cells on gels b. Arrows indicate the location on the gels of the high molecular weight protein, which is predominantly present in fractions 8–10.

On the Tris·HCl polyacrylamide gels the position of the high molecular weight proteins from the cultured cells is very similar to that of the cylindrical protein complex from human erythrocytes. When the proteins have been completely dissociated with 1.0% sodium dodecyl sulphate/β-mercaptoethanol the gel patterns are very different, indicating the presence of different polypeptide chains in the proteins. Fig. 5 shows this comparison, using the Py3T3 protein and the cylindrical protein from human erythrocyte ghosts.

The absorption spectra of the purified high molecular weight protein from HeLa and the hollow cylinder protein from human erythrocyte ghosts have a peak around 270 nm. This is typical of high molecular weight proteins. The absence of a peak at 260 nm indicates that nucleic acids are not present in the molecules.

(3) Electron microscope studies

Following the removal of sucrose by extensive dialysis against 5 mM Tris·HCl (pH 8.0) the protein in the fractions under the small peak of high molecular weight material, obtained from the sucrose gradient, was studied by negative staining. For

Fig. 5. Sodium dodecyl sulphate analytical polyacrylamide gels of the human erythrocyte hollow cylinder protein (a) and the Py3T3 high molecular weight protein (b). The positions of the polypeptide bands are very different, indicating the non-similarity of the subunits of the native proteins.

comparison purposes specimens were also prepared using the hollow cylinder protein from human erythrocyte ghosts. Figs. 6 and 7 show representative areas of the high molecular weight proteins from Py3T3 and HeLa cells, and Fig. 8 of the hollow cylinder protein. It is immediately apparent that the protein from the cultured cells has a different quaternary conformation to that from the erythrocyte ghosts. There appears to be no detectable difference between the HeLa protein, which gave a single band on gel electrophoresis and the 3T3 protein which gave two bands. The particles shown in Figs. 6 and 7 do not have an easily definable quaternary conformation. Several different electron optical images are visible, which are almost certainly due to the molecules orientating themselves randomly at different positions relative to the electron beam. Thus, different summated thicknesses of protein are present through which the transmitted electrons pass and thereby determine the appearance of the final image [3]. The depth of the negative stain is also an important factor in determining the electron optical image, since varying degrees of penetration and quantities of stain are likely to be present between the polypeptide chains. A composite figure to emphasise the various images of the high molecular weight proteins from cultured cells is shown in Fig. 9. Treatment of the human erythrocyte ghost hollow cylinder protein and the high molecular weight protein from cultured cells with deoxyribonuclease 1 and ribonuclease does not destroy the quaternary conformation of these macromolecules, as judged by negative staining.

Experiments performed using the Ouchterlony double diffusion technique have indicated that the proteins released from HeLa cells form precipitin lines with antiserum bovine serum proteins and to a lesser extent with antiserum against human serum proteins. Mono-specific antiserum against human α_2-macroglobulin interacts to give a single precipitin line, whereas the antiserum against human α_1-macroglobulin (α_1-trypsin inhibitor) does not form a precipitin line. The single precipitin line formed by the antiserum against human α_2-macroglobulin fuses with one of the

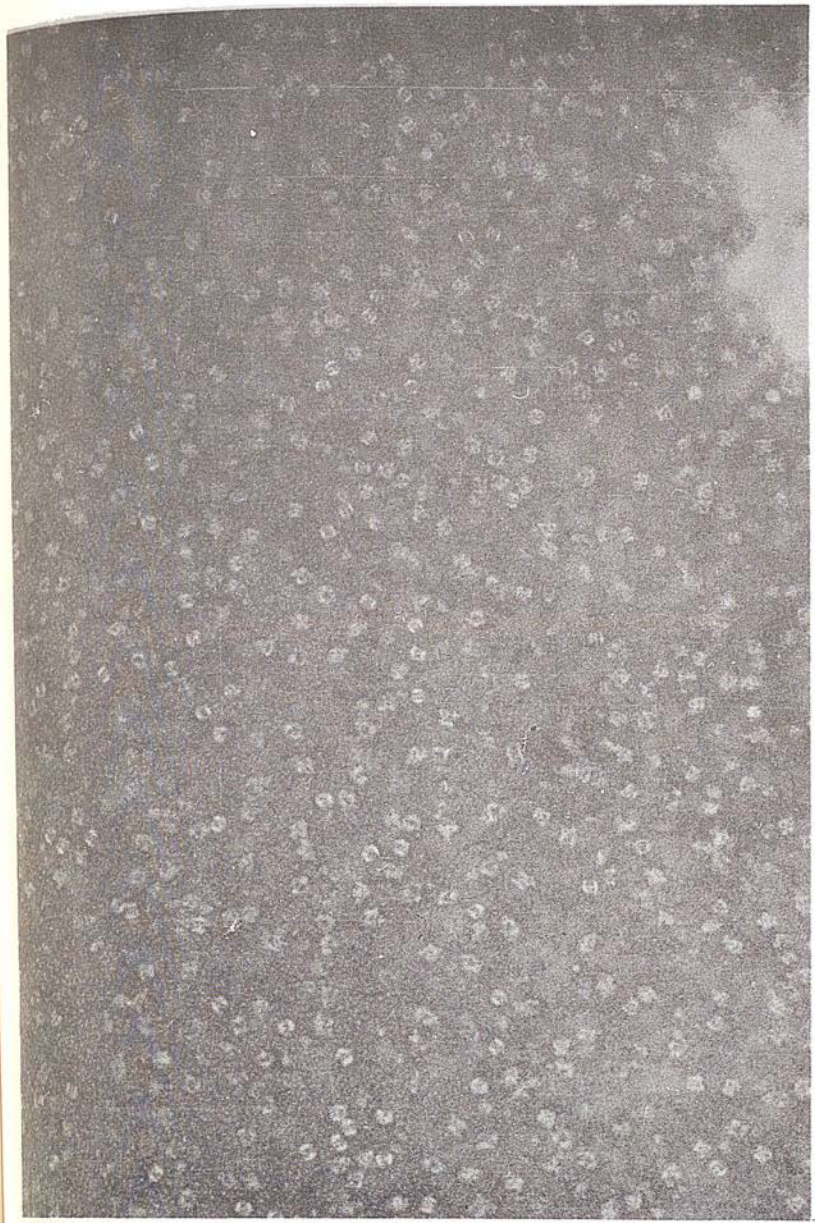

Fig. 6. The high molecular weight protein from Py3T3 cells. Negatively stained with 2% sodium phosphotungstate (pH 7.0). ×184 000.

lines given by the antiserum against human and bovine serum proteins. It thus appears that there is cross-reactivity between the human and bovine antiserum with respect to the α_2-macroglobulins. Thus, it is not possible by immunodiffusion to decide whether the α_2-macroglobulin under investigation is of human or bovine origin although the latter appears to be likely since the mono-specific antiserum against

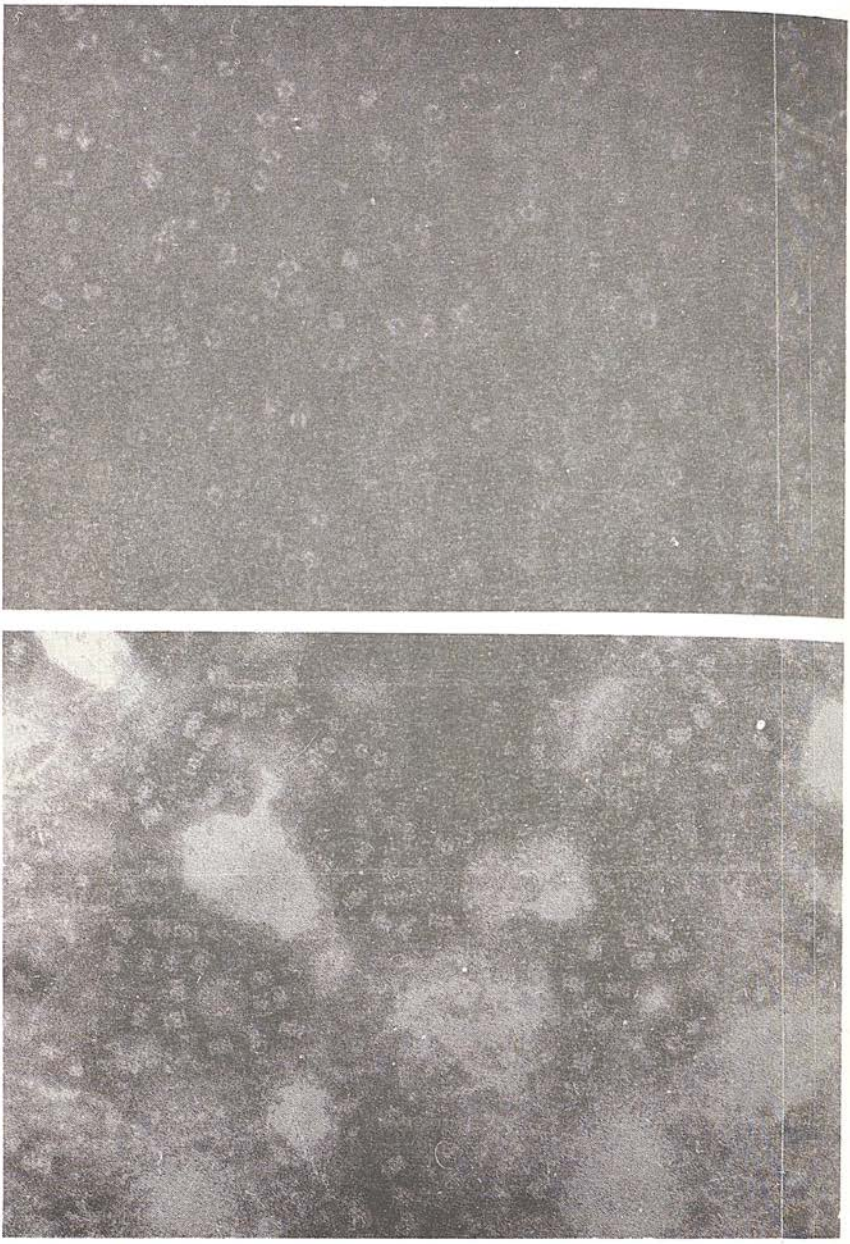

Fig. 7. The high molecular weight protein from HeLa cells. Negatively stained with 2% sodium phosphotungstate (pH 7.0). ×184 000.

Fig. 8. The purified hollow cylinder protein from human erythrocyte ghosts. Negatively stained with 2% sodium phosphotungstate (pH 7.0). ×184 000.

human α_2-macroglobulin gives a single precipitin line with calf serum.

DISCUSSION

The studies described in this paper have been restricted to a comparative

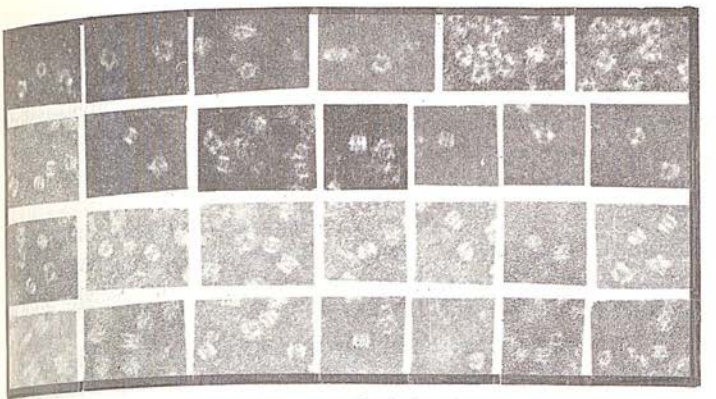

Fig. 9. A composite figure showing several of the electron optical images of the high molecular weight protein from cultured fibroblasts. ×184 000.

investigation of the high molecular weight proteins released from several tissue culture cell lines with the cylindrical protein complex released from human erythrocyte ghosts [2–5]. Further studies on the lower molecular weight proteins are proposed in relation to "conditioning factors" which effect growth and transport systems of cultured cells, since it has been suggested that the high molecular weight fraction does not appear to be a conditioning factor [9].

Narayan and Rounds [1], as previously mentioned, claimed that the predominant high molecular weight protein released from their cell lines (CMP, HeLa and KB) closely resembled the human erythrocyte ghost cylinder protein. Their published electron micrographs indicate that this interpretation is correct, but on both the electron micrographs and polyacrylamide gels there is clear evidence of the presence of other large and small molecular weight proteins. This is to be expected since the only purification that was applied was to prepare the 105 000 × g pellet from the conditioned medium after clarification at 25 000 × g. In our hands only trace amounts of the high molecular weight protein from the cultured cells was found to have a cylindrical conformation. The protein that is released, has nevertheless, a sedimentation coefficient similar to that of the human erythrocyte ghost cylindrical protein (22.5 S), on the basis of its position on the sucrose density gradients.

Narayan and Rounds [1] also suggested that the macromolecules they isolated contained nucleic acids. This conclusion was drawn from the destruction of the molecules, assessed electron microscopically, following incubation with DNAase and RNAase. Our spectral evidence suggests that the proteins liberated from HeLa and the 3T3 cell lines do not contain significant amounts of nucleic acid, and this is supported by the lack of any destruction of the molecules by DNAase and RNAase in our hands. In the electron micrographs of Narayan and Rounds [1] obtained following enzymic treatment many intact molecules can, nevertheless, be observed. There is also gross aggregation of protein which is probably because of the fact that uranyl acetate was used as the negative stain.

As expected when any multisubunit protein is trapped within a pool of negative staining salt as it dries onto the carbon support film, the molecules will tend to be orientated in several different positions relative to the support film. Thus, the production of several different electron optical images from one protein molecule (Fig. 9)

is acceptable, when other supportive evidence on the purity of the protein, such as gel electrophoresis, is available. The apparent complexity of the quaternary conformation of the high molecular weight protein released from cultured fibroblasts does not at the moment permit a molecular model of the subunit arrangement to be produced. Further studies are in progress using specimen tilting within the electron beam, which may assist with the interpretation of the electron optical images.

There is available an extensive literature dealing with the electron microscopy of multisubunit proteins and enzymes [2–5, 14–21], from which information on complex quaternary conformations is available. The high molecular weight protein released from the cultured cells bears some resemblance to the enzyme aspartate transcarbamylase [13]. An even closer resemblance is apparent between the α-macroglobulins [20, 21] which have a sedimentation coefficient in the order of 18 S and the proteins from the cultured cell lines used in this study. It is concluded that the high molecular weight proteins described in this publication are not the same as the cylindrical protein complex released from erythrocyte ghosts [2–5] although trace quantities of a cylindrical protein were repeatedly detected in the serum-free washes from cultured cells. Narayan and Rounds [1] performed most of their studies with washes from the CMP cell line, and it is possible that this line releases the high molecular weight proteins in varying proportions to HeLa and the 3T3 lines, so that there is a relatively greater quantity of the cylinder complex to the α-macroglobulin-like protein.

It is known that the α-macroglobulins act as growth-stimulating proteins [11-13]. In the experiments described in this publication it is possible that the high molecular weight proteins from the cultured cells were taken up onto the cell surface from the calf serum-complemented growth medium and then released into the serum-free medium, despite the thorough washing of the monolayer of cells. It has been shown by James et al. [22] that an increased quantity of α_2-macroglobulin is associated with the surfaces of lymphocytes in chronic lymphocytic leukaemia and other disorders. Previous ideas on the function of the α_2-macroglobulins have, however, centred on its inhibition of plasmin activity [23].

An alternative to the release of proteins adsorbed from the serum, is that they may be actively produced and secreted by the cultured cells. Our studies indicate that most of the proteins are of bovine origin, and therefore must have been bound onto the cell surface. Further work is in progress using radioactive amino acid incorporation into proteins in an attempt to clarify this issue, and also the apparent discrepancy between the proteins released by the CMP cell line [1] and the cell lines used in this investigation.

ACKNOWLEDGEMENTS

The technical assistance provided by Mr. J. Murdock throughout this study is gratefully acknowledged. K. D. Brown is supported by a Cancer Research Campaign Scholarship.

REFERENCES

1 Narayan, K. S. and Rounds, D. E. (1973) Nat. New Biol. 243, 146–150

2 Harris, J. R. (1968) Biochim. Biophys. Acta 150, 534–537
3 Harris, J. R. (1969) J. Mol. Biol. 46, 329–335
4 Harris, J. R. (1971) Biochim. Biophys. Acta 229, 761–770
5 Harris, J. R. (1974) Methodological Developments in Biochemistry (Reid, E., ed.), Vol. 4, pp. 394–404, Longmans, London
6 Austin, P. E., McCullock, E. A. and Till, J. E. (1971) J. Cell. Physiol. 77, 121–134
7 Nose, K., Nitta, K., Takaoka, T. and Katsuta, H. (1974) J. Cell. Physiol. 84, 269–274
8 Unkeless, J., Dano, K., Kellerman, G. M. and Reich, E. (1974) J. Biol. Chem. 249, 4295–4305
9 Brown, K. D., Hume, S. P., Lamb, J. F. and Weingart, R. (1974) J. Physiol. Lond. 244, 88P
10 Halpern, M. and Rubin, H. (1970) Exp. Cell Res. 60, 86–95
11 Hoffman, R. W., Ristow, H. J., Veser, J. and Frank, W. (1973) Exp. Cell Res. 80, 275–280
12 Renner, R., Hepp, K. D., Veser, J. and Frank, W. (1974) Exp. Cell Res. 84, 426–430
13 Michl, J. and Spurna, V. (1974) Exp. Cell Res. 84, 56–62
14 Haschemeyer, R. H. (1974) Annu. Rev. Biochem. 43, 279–301
15 Kretschmer, K. (1968) Hoppe-Seyler's Z. Physiol. Chem. 349, 715–718
16 Richards, K. E. and Williams, R. C. (1972) Biochemistry 11, 3393–3395
17 Junger, E. and Reinauer, H. (1972) Biochim. Biophys. Acta 250, 478–490
18 Marchesi, S. L., Steers, E. and Shifrin, S. (1969) Biochim. Biophys. Acta 181, 20–34
19 Greem, N. M., Valentine, R. C. and Wrigley, N. G. (1972) J. Biol. Chem. 247, 6284–6298
20 Bloth, B., Chesbro, B. and Svehag, S.-E. (1968) J. Exp. Med. 127, 749–756
21 Gauthier, F. and Mouray, H. (1975) Int. J. Biochem. 6, 95–98
22 James, K., Tunstall, A. M., Parker, A. C. and McCormick, J. N. (1975) Clin. Exp. Immunol. 19, 237–249
23 Ganrot, P. O. (1967) Clin. Chim. Acta 16, 328–329

© *Journal of Microscopy, Vol.* 108, *Pt* 1, *September* 1976, *pp.* 51–59.
Revision accepted 3 *June* 1976

Contrast enhancement of negatively stained macromolecules and biomembranes by single sideband phase contrast interference

by J. R. HARRIS* *and* J. KERR, *Department of Physiology, Bute Medical Buildings, University of St Andrews, St Andrews, Fife*

SUMMARY

A straightforward procedure is described for the production of contrast enhancement of negatively stained macromolecules and biological membranes by single sideband phase contrast interference (electron optical shadowing). The instrumental adjustment required to produce this type of phase contrast illumination is readily achieved by beam deflection from the strioscopic (dark field) mode. Part of the hollow cone of electrons from the annular condenser aperture that are unscattered by the specimen are permitted to pass through the objective aperture and interfere with the scattered beam. The electron optical shadowing effect is produced because only one side of the unscattered beam is used. Careful adjustment of the beam tilt control, with the ability to tilt in any azimuth, allows optimal illumination conditions to be achieved. The results presented show the increased image contrast obtained using as specimens the purified cylindrical macromolecule from human erythrocyte membranes, purified nuclear envelopes and collagen fibres.

INTRODUCTION

The use of phase contrast techniques for the enhancement of image contrast in the electron microscope has been investigated by several authors. Haydon *et al.* (1971) and Haydon & Lemons (1972) have produced optical shadowing by allowing the central electron beam to strike the objective aperture. In general, little biological emphasis has been put on this technique to date (Haydon, 1974). Using a more elaborate system employing an electrostatic absorbing phase plate consisting of a gold plated spider's thread positioned across a diaphragm mounted in the diffraction aperture holder, Unwin (1971) and (1973) showed a shadowed type of image with increased contrast and signal to noise ratio. Theoretical aspects of optical shadowing have been dealt with by Andersen (1972) and Scales (1974), both of whom used Fourier analysis. An essentially similar contrast enhancement has been obtained by Markham *et al.* (1963) using a different procedure.

* Correspondence: Dr J. R. Harris, Department of Biological Science, North East London Polytechnic, Romford Road, London E15 4LZ.

A preliminary report on this work was presented at the Edinburgh Electron Microscope Discussion Group, 2 November 1974, and a brief account appears in the *Philips Electron Optics Bulletin Electron Microscope*, February 1976.

The following procedure outlines a simple method for producing single sideband phase contrast interference, making use of magnetic beam tilt, to allow some of the unscattered electrons from one side of the direct beam to interfere with the scattered electrons which produce a pre-set strioscopic image.

Owing to the complexity of this imaging system, using a tilted hollow cone of electrons, no attempt has been made to deal with the more detailed theoretical aspects of the subject. Emphasis is placed on the possible benefits the technique provides for studying biological materials.

MATERIALS AND METHODS

Electron microscopy

The studies undertaken for this publication were performed using a Philips EM 301S electron microscope (EM) with high resolution specimen stage. The instrument was initially adjusted for strioscopy using hollow cone illumination produced by a 0·2 mm ring diaphragm with a central stop 1·7 mm in diameter held by three narrow supports. A 25 μ thin foil objective aperture was used in the objective diaphragm holder and the fixed aperture in the condenser 1 position was bored out to 2·0 mm. Having obtained satisfactory dark field illumination, the instrument was returned to bright field by removing the annular aperture and a suitable area of the negatively stained specimen was selected. On returning to dark field, no clear images of the biological macromolecules or membranes were visible. However, on activating the beam tilt device to give a slight deflection (less than 0·5°) of the beam, some of the unscattered electrons were allowed to interfere with those producing the dark field image and a clear image is produced.

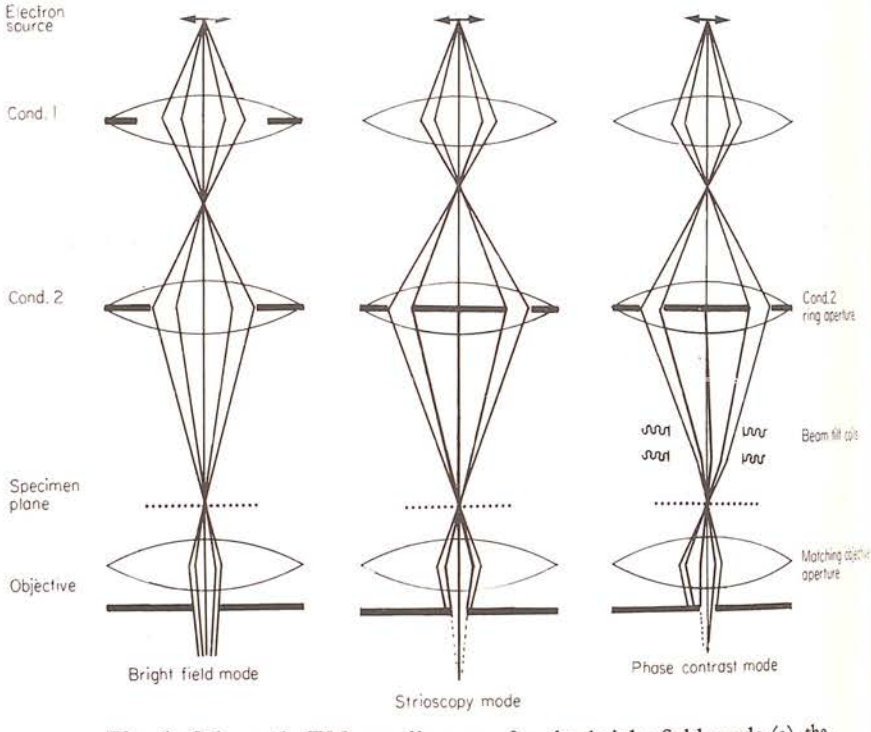

Fig. 1. Schematic EM ray diagrams for the bright field mode (a), the strioscopic mode (b) and the single sideband phase contrast mode (c).

The beam tilt device is a coil system which was embedded in araldite and is located in the upper bore of the objective lens. It was used to deflect the electron beam by operation of the beam tilt control, which has ten settings. The electron beam can be tilted to a maximum of 5° in any azimuth. To accomplish this the coil system produces four magnetic fields; two fields are arranged one above the other and produce a tilt of the beam in the X direction of azimuth; the other two fields are similarly arranged to produce a tilt of the beam in the Y direction of azimuth. If a beam tilt greater than approximately 0·5° is applied, the relative contrast of the single sideband phase contrast interference is reduced, as more unscattered electrons are transmitted, and a predominantly bright field image is gradually obtained. Figure 1 shows schematic ray diagrams for the bright field, strioscopic and single sideband phase contrast modes.

Electron microscopy was performed at an accelerating voltage of 80 kV. Electron micrographs were taken on Ilford 82·35 × 101·6 mm plates, type EM 6. Electron micrographs of any one region were taken by bright field and single sideband phase contrast illumination. Instrumental magnifications were corrected by the use of calibration specimens (Agar Aids).

Microdensitometry

Microdensitometry of individual hollow cylinder protein molecules was performed using a Vickers M85 scanning microdensitometer, with the density output connected to a chart recorder. Densitometric traces of individual molecules lying on their sides and ends were obtained in graphical form. Spot readings of maximum and minimum density from any one molecule were taken for the determination of contrast, which is defined as the maximum difference in density between the molecule and the background divided by the background density.

Biological materials

The cylindrical protein complex of molecular weight approximately 800,000, was isolated by previously published procedures (Harris, 1969, and 1974). Negatively stained specimens were prepared by the mica spreading and carbon coating method of Horne & Pasquali Ronchetti (1975), using a protein concentration of approximately 1·0 mg per ml in 2·0% ammonium molybdate (pH 7·0). The thin film of carbon plus absorbed protein molecules was floated off onto the surface of a 2·0% solution of uranyl acetate (pH 4·5) and picked up on holey carbons. Regions of specimens spanning the holes of the support film were selected for study.

Nuclear envelopes were prepared from rat liver nuclei by the procedure of Harris & Milne (1974). Negatively stained specimens were prepared using ammonium molybdate (pH 7·0) using the single droplet procedure (Harris & Agutter, 1970, Harris *et al.*, 1974).

RESULTS

A representative region containing the hollow cylinder protein (17 × 12 nm) from human erythrocyte membranes is shown in Figs. 2 and 3, by bright field and single sideband phase contrast illumination, respectively. The macromolecules are randomly positioned, some orientated on their sides and some on their ends. It is apparent the macromolecules illuminated by the single sideband phase contrast mode appear to project from the background in a three-dimensional manner (i.e. they are shadowed), and also that there is a superior contrast compared to that present in the bright field mode. In Figs. 4 and 5 illuminated by bright field and single sideband phase contrast, respectively, selected molecules are indicated,

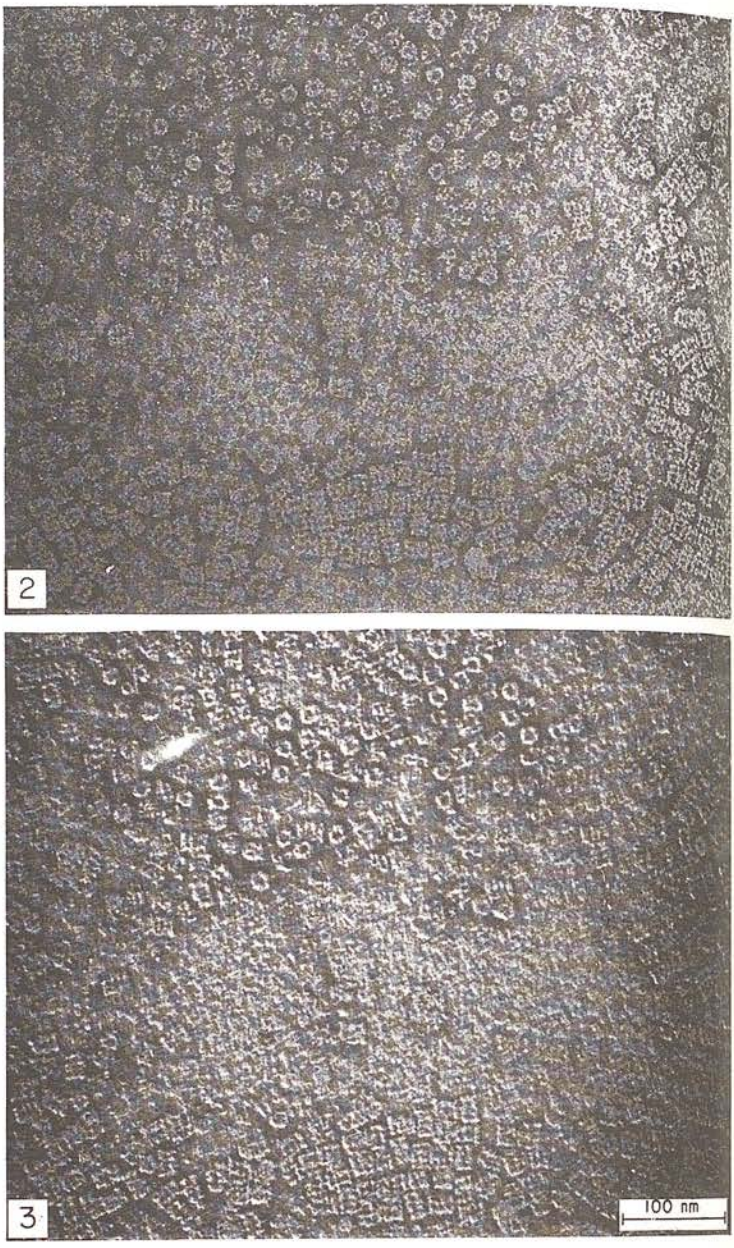

Figs. 2 and 3. Electron micrographs of negatively stained hollow cylinder protein molecules from human erythrocyte membranes, illuminated by the bright field and single sideband phase contrast modes, respectively. The macromolecules are orientated on their sides and on their ends. × 196,800.

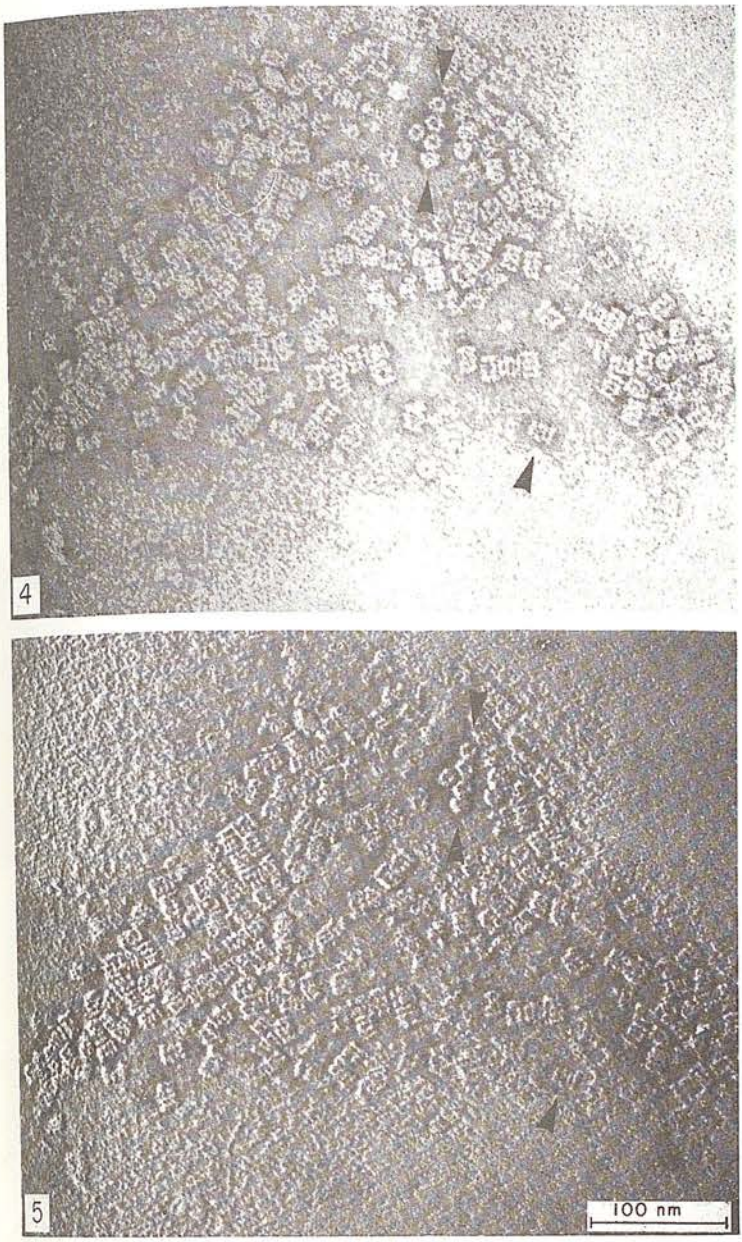

Figs. 4 and 5. The hollow cylinder macromolecules, as in Figs. 2 and 3, illuminated by the bright field and single sideband phase contrast modes, respectively. The molecules arrowed have been used for microdensitometric measurements, as shown in Figs. 6 to 9. × 196,800.

from which scanning microdensitometer traces have been obtained as shown in Figs. 6–9. The contrast calculated from the maximum and minimum density figures for the molecules in Figs. 6 and 7 are 0·69 and 0·74 and for Figs. 8 and 9, 0·71 and 0·81, respectively. This instrumental determination of overall contrast agrees with the assessment of contrast enhancement made by eye.

A negatively stained region containing rat liver nuclear envelope is shown in Figs. 10 and 11. by bright field and single sideband phase contrast illumination, respectively. Some enhancement of image contrast is apparent in Fig. 11, but it appears to be less than with the individual macromolecules shown earlier. It is likely that the increased overall specimen thickness reduces the contrast enhancement induced by single sideband phase contrast interference. This has also been found to occur with collagen fibres, as shown in Figs. 12 and 13.

DISCUSSION

Electron optical techniques which provide enhancement of image contrast are likely to be useful for the study of biological macromolecules. It must be emphasized that any such technique should be critically evaluated by comparing the electron

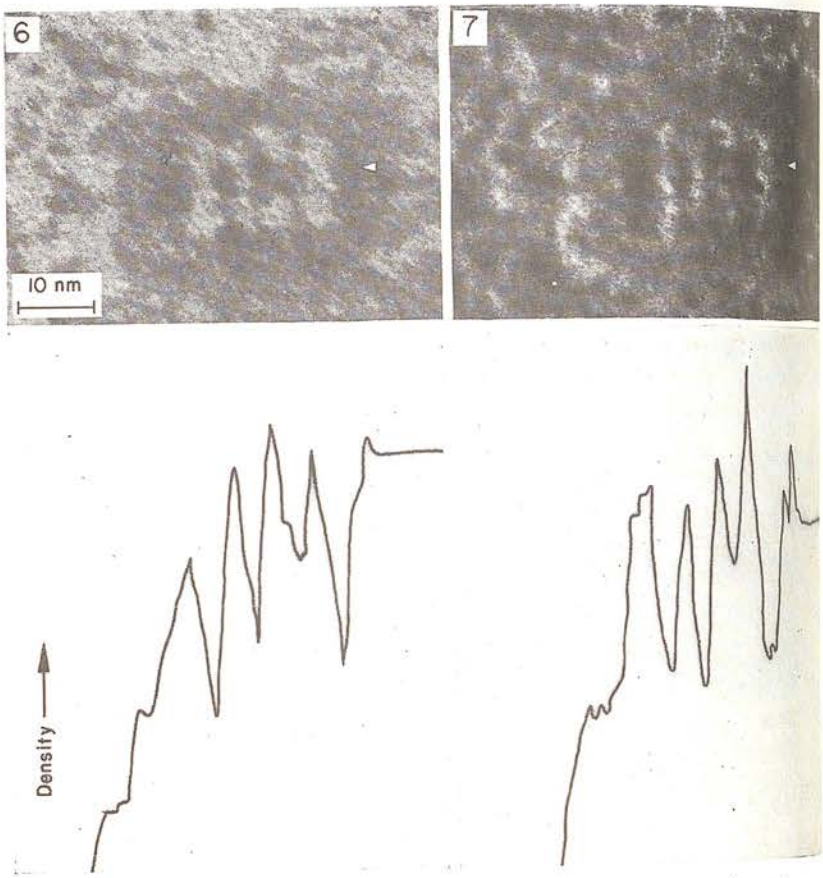

Figs. 6 and 7. Individual hollow cylinder macromolecules orientated on their sides, illuminated by bright field and single sideband phase contrast, respectively. Beneath each macromolecule is positioned the corresponding microddensitometer trace. × 1,107,000.

optical images obtained with those from conventional bright field illumination. The results described above, which were obtained using single sideband phase contrast interference produced by electronic beam tilt from the strioscopic mode, are compared throughout with identical bright field images. In all cases, enhancement of contrast in the single sideband phase contrast interference images is apparent. The background granularity in these phase contrast images, due to unevenness of stain, dissociated protein molecules or very small membrane fragments, appears to be increased compared with bright field images.

A similar increase in background granularity was observed by Haydon *et al.* (1971) and Unwin (1971, 1973). The three-dimensional shadowed image provided by single sideband phase contrast interference is very similar to that produced by high resolution scanning electron microscopy (Crewe & Wall, 1970).

The results obtained by electron optical shadowing must be clearly distinguished from those given by conventional bright field transmission electron microscopy of metal shadowed specimens. In the latter example, the amount of deposited metal and length of the shadow indicates the height and shape of the particles on the specimen grid, whereas with electron optical shadowing the apparent shadow

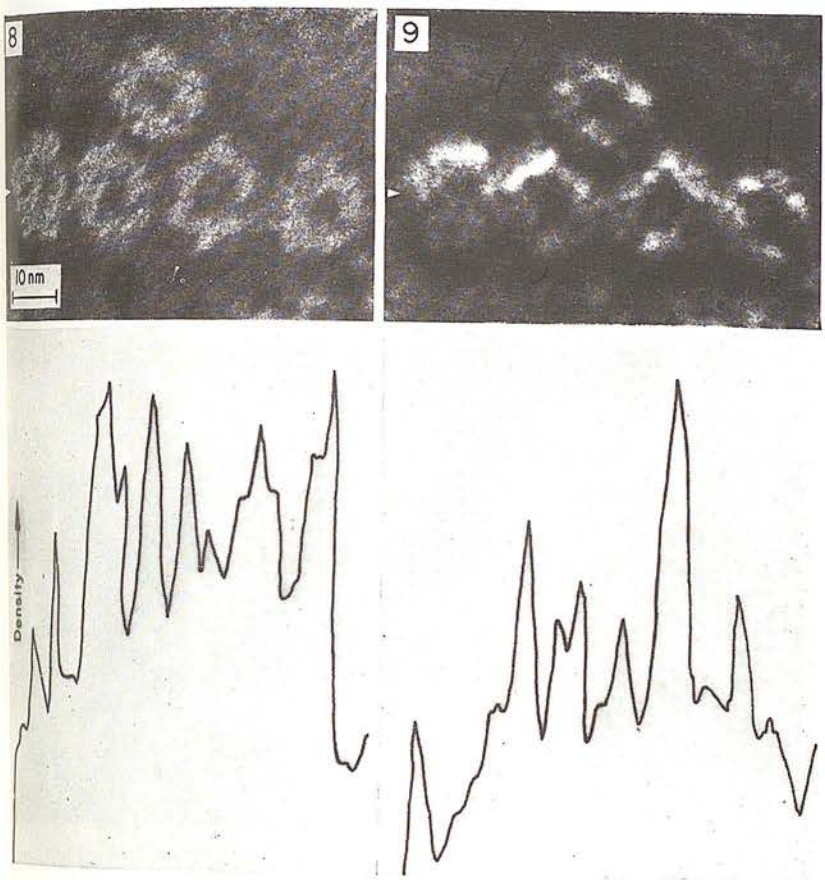

Figs. 8 and 9. A group of hollow cylinder macromolecules orientated on their ends, illuminated by bright field and single sideband phase contrast, respectively, together with their corresponding microdensitometer traces. × 1,107,000.

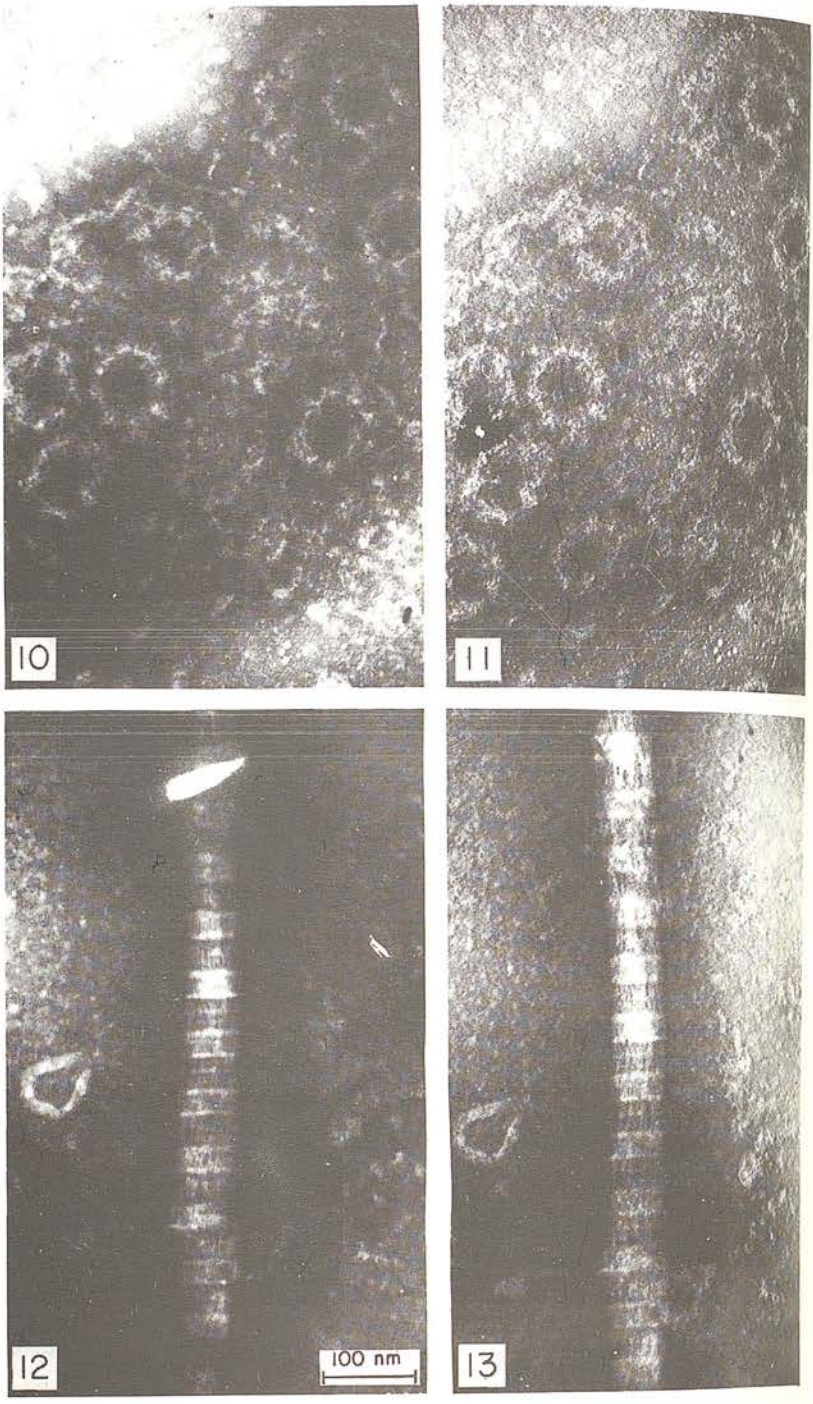

Figs. 10 and 11. A negatively stained piece of rat liver nuclear envelope, illuminated by bright field and single sideband phase contrast, respectively. × 138,600.

Figs. 12 and 13. A negatively stained collagen fibre, illuminated by bright field and single sideband phase contrast, respectively. × 138,600.

length is controlled by the amount of phase contrast interference induced by activating the beam tilt coils. Further experiments are currently in progress to see if there is any relationship between shadow length and particle height when the imaging system is carefully adjusted for maximal phase contrast interference.

The presence of only slight contrast enhancement observed with the relatively thick nuclear envelope and collagen fibres underlines the desirability of evaluating single sideband phase contrast interference by studying individual negatively stained macromolecules. The contrast enhancement is even less effective when thin sectioned specimens are studied (Haydon, 1974), and it is unlikely that the technique will be of any value for the study of freeze-etched or shadow cast specimens.

It can be concluded that the major benefit offered by single sideband phase contrast interference is for the study of purified macromolecules by negative staining. It should also be useful for the study of membrane-associated proteins and for virus particles, in conjunction with conventional bright field studies. The method can be applied using the manufacturer's attachments for strioscopy, without additional special equipment for phase contrast.

ACKNOWLEDGMENTS

This work is supported by the Medical Research Council. The support and guidance provided by Mr F. Sheldon, Pye-Unicam, Cambridge, is gratefully acknowledged.

References

Andersen, W.H.J. (1972) Phase contrast enhancement by single sideband modulation transfer. *Proc. 5th Europ. Congr. Electron Microsc.* p. 396.

Crewe, A.V. & Wall, J. (1970). A scanning microscope with 5A resolution. *J. molec. Biol.* **48**, 375.

Harris, J.R. (1969) Some negative contrast staining features of a protein from erythrocyte ghosts. *J. molec. Biol.* **46**, 329.

Harris, J.R. (1974) Purification of some membrane-associated proteins from erythrocyte ghosts. In: *Methodological Developments in Biochemistry* (Ed. by E. Reid), pp. 393. Longmans, London.

Harris, J.R. & Agutter, P.S. (1970) A negative staining study of human erythrocyte ghosts and rat liver nuclear membranes. *J. Ultrastruct. Res.* **33**, 219.

Harris, J.R. & Milne, J.F. (1974) A rapid procedure for the isolation and purification of rat liver nuclear envelope. *Trans. biochem. Soc.* **2**, 1251.

Harris, J.R., Price, M.R. & Willison, M. (1974) A comparative study on nuclear membranes from rat liver and hepatoma. *J. Ultrastruct. Res.* **48**, 17.

Haydon, G.B. & Lemons, R.A. (1972) Optical shadowing in the electron microscope. *J. Microsc.* **95**, 483.

Haydon, G.B., Hill, B.C. & Lemons, R.A. (1971) Optical shadowing of macromolecules. *Proc. 29th Ann. EMSA Meet.* p. 438.

Haydon, G.B. (1974) Optical shadowing. In: *Principles and Techniques of Electron Microscopy* (Ed. by M. A. Hayat), Vol. 3, p. 1. Van Nostrand Reinhold, New York.

Horne, R.W. & Pasquali Ronchetti, I. (1975) A negative staining-carbon film technique for studying viruses in the electron microscope. *J. Ultrastruct. Res.* **47**, 361.

Markham, R., Frey, S. & Hills, G.J. (1963) Methods for the enhancement of image detail and accentuation of structure in electron microscopy. *Virology* **20**, 88.

Scales, J.D. (1974) A Fourier approach to optical shadowing with a transmission electron microscope. *J. Microsc.* **102**, 49.

Unwin, P.N.T. (1971) Phase contrast and interference microscopy with the electron microscope. *Phil. Trans. R. Soc.* (B), **261**, 95.

Unwin, P.N.T. (1973) Phase contrast electron microscopy of biological materials. *J. Microsc.* **98**, 299.

PTO

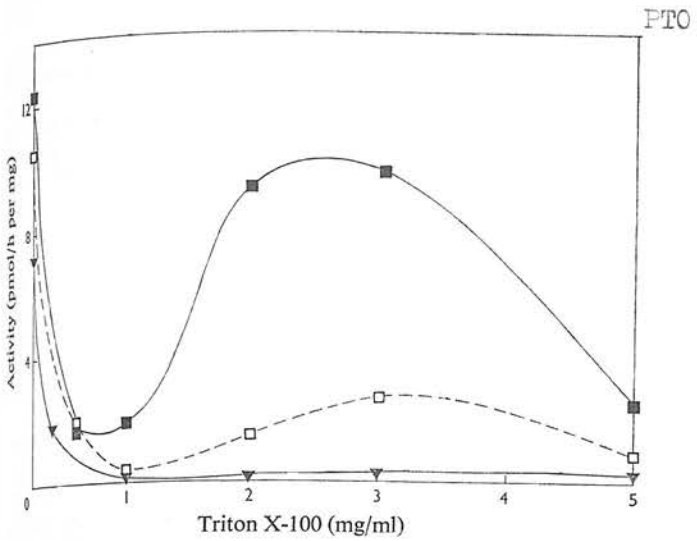

Fig. 1. *Effect of Triton X-100 on UDP-galactose–lactosylceramide galactosyltransferase activity in NIL 2E (Clone 8) cell homogenates*

Enzyme activity was determined by measuring the incorporation of [^{14}C]galactose into ceramide trihexoside by the method of Kijimoto & Hakomori (1971). The incubation medium consisted of 7 μmol of sodium phosphate buffer, pH 6.1, 0.1 μmol of $MnCl_2$, approx. 1 mg of enzyme protein and 0.025 μmol of UDP-[^{14}C]galactose, containing 0.2 μCi of ^{14}C, in a final volume of 0.2 ml. Assays were in the presence of 20 μg of lactosylceramide (□), or in the presence of 20 μg of lactosylceramide and 200 μg of phosphatidylinositol (■), or in the absence of added substrate, but in the presence of 200 μg of phosphatidylinositol (▼).

1971; Mookherjea & Yung, 1974), to glycosphingolipids (Constantino-Ceccarini & Suzuki, 1975; Shah, 1973; Neskovic *et al.*, 1974; Ishibashi *et al.*, 1975) and to retinol phosphate (Rosso *et al.*, 1975). In the present communication we show that the transfer of galactose to lactosylceramide is very sensitive to detergent action and that under certain conditions it is stimulated by phospholipids.

The assay for the enzyme *in vitro* is normally carried out in the presence of high detergent concentrations, owing to the lipid nature of the acceptor substrate. However, as shown in Fig. 1, there was considerable activity in the absence of any detergent. This activity was mainly contributed by the endogenous substrate, but there was some glycosylation of exogenous substrate, particularly when this was stabilized by the presence of added phospholipid. All activity was inhibited by low concentrations of the detergent, Triton X-100, with half-maximal inhibition occurring at a concentration of 0.0075% (w/v) (0.12mM). Since this concentration is considerably below the reported critical micelle concentration of the detergent in aqueous solution (Clarke, 1975), it is reasonable to assume that it is the monomer that is the inhibitory form of the detergent.

At higher detergent concentrations, activity is again observed in those preparations to which exogenous lipid substrate has been added, but still further increases in detergent concentration cause inhibition of the enzyme activity. Phosphatidylinositol, in the presence of detergent, caused a stimulation of activity of between two- and eight-fold in different experiments. This was not a specific effect, however, since several phospholipids had a stimulating effect. Phospholipids that increased enzyme activity were, in order of decreasing effectiveness, phosphatidylserine, phosphatidylinositol, phos-

phatidylethanolamine, cardiolipin, phosphatidic acid and phosphatidylcholine. Sphingomyelin and lysophosphatidylcholine were inhibitory. Control experiments showed that the phospholipid activation was not due to prevention of further metabolism of the ceramide trihexoside, nor was it the result of a protective effect on the nucleotide substrate, UDP-galactose. In fact there was greater hydrolysis of UDP-galactose to galactose 1-phosphate, suggesting that under our assay conditions phospholipids also stimulated nucleotide pyrophosphatase activity. The concentration of Triton X-100 that yielded maximum activity (3 mg/ml) did not solubilize the enzyme, since under these conditions 95% of the activity was still sedimentable by centrifugation at 100000*g* for 1 h.

Other detergents, including deoxycholate, acetyltrimethylammonium bromide, lysophosphatidylcholine, sarcosyl (sodium *N*-dodecylsarcosinate), Lubrol WX, Tween 80 and sphingosine, inhibited the enzyme at low concentrations and did not give an activation peak when assayed at higher concentrations. However, Triton X-114 and Cemulsol NP-12 (Neskovic *et al.*, 1974), both of which are quite similar to Triton X-100 in structure and in physical properties, behaved similarly to this detergent.

The mechanism by which phospholipids activate the enzyme in the presence of detergents is not very clear as yet. It is likely that phospholipid may provide a suitable environment for the lipid substrate to be acted on by the enzyme. However, an additional effect of the phospholipid on the enzyme protein cannot be ruled out, although the lack of specificity, and the fact that in these experiments, the enzyme was situated in a membrane in the presence of endogenous phospholipids, makes this unlikely.

We have also analysed the effect of detergents and phospholipids on the enzyme from a virally transformed line derived from the same clone (NIL 2E, Clone 8, HSV6). In agreement with previous reports, the enzyme activity was greatly diminished in the transformed line in comparison with the normal line. However, the response of this diminished enzyme activity to detergents and phospholipids was similar to that of the enzyme from the untransformed cell line, suggesting that the effect of transformation on the enzyme is not related to the effect of detergents and phospholipids on the enzyme activity.

We are grateful to Dr. Ian Macpherson, ICRF Laboratories, London, who provided the cell lines, and to the Cancer Research Campaign for financial support.

Brady, R. O. & Fishman, P. H. (1974) *Biochim. Biophys. Acta* **355**, 121–148
Clarke, S. (1975) *J. Biol. Chem.* **250**, 5459–5469
Constantino-Ceccarini, E. & Suzuki, K. (1975) *Arch. Biochem. Biophys.* **167**, 646–654
Critchley, D. R. & Macpherson, I. (1973) *Biochim. Biophys. Acta* **296**, 145–159
Critchley, D. R., Chandrabose, K. A., Graham, J. M. & Macpherson, I. (1974) *Cold Spring Harbor Conf. Cell Proliferation* **1**, 481–493
Den, H., Schultz, A. M., Basu. M. & Roseman, S. (1971) *J. Biol. Chem.* **246**, 2721–2723
Ishibashi, T., Atsuta, T. & Makita, A. (1975) *J. Natl. Cancer Inst.* **55**, 1433–1436
Kijimoto, S. & Hakomori, S. (1971) *Biochem. Biophys. Res. Commun.* **44**, 557–563
Mookherjea, S. & Yung, J. W. M. (1974) *Can. J. Biochem.* **52**, 1053–1066
Neskovic, N. M., Sarlieve, L. L. & Mandel, P. (1974) *Biochem. Biophys. Acta* **334**, 309–315
Rosso, G., De Luca, L., Warren, C. D. & Wolf, G. (1975) *J. Lipid Res.* **16**, 235–243
Shah, S. N. (1973) *Arch. Biochem. Biophys.* **159**, 143–150
Stoker, M. (1974) *Cold Spring Harbor Conf. Cell Proliferation* **1**, 1009–1013

Shape Changes of the Human Erythrocyte 'Ghost'

JAMES R. HARRIS

Department of Biological Science, North East London Polytechnic, Romford Road, London E15 4LZ, U.K.

It has been known for some considerable time that chemically treated erythrocytes and erythrocyte 'ghosts' produced by osmotic lysis are able to assume a variety of abnormal shapes (Furchegott, 1940; Baker, 1964; Watson *et al.*, 1950; Marikovsky & Danon, 1967; Harris, 1971), which have been termed hematexodies, myelin bodies and stroma-

lytic forms. The term stromalytic forms is used in the present communication to describe the shape of erythrocyte 'ghosts' that show by light- and electron-microscopy the presence of finger-like projections, of variable number and length, extending from their surfaces. These stromalytic forms are clearly distinguishable in the electron microscope from the smooth-surfaced erythrocyte 'ghosts', most of which retain the normal biconcave discoid shape of the intact cell when in aqueous suspension. Hoffman (1973) has stated that it is unlikely that metabolic energy is required for disc-sphere transformation of intact erythrocytes, in view of the observation that haemoglobin-free erythrocyte 'ghosts' obtained by freeze–thawing are mostly biconcave discs, and can be made to sphere by chemical treatment. The experiments described below tend to support the view of Hoffman (1973), in that some shape changes of the erythrocyte membrane may be independent of the metabolic state of the cell.

Erythrocyte 'ghosts' were prepared from freshly drawn heparinized blood by using the repeated centrifugal washing procedure of Dodge *et al.* (1963), as modified by Harris (1969). This modification includes, after the series of washes at 4°C with 10mM-phosphate buffer, pH7.4, one or two washes with cold 10mM-Tris/HCl buffer, pH7.4, which releases the final traces of haemoglobin and allows white, haemoglobin-free, erythrocyte 'ghosts' to be produced. Samples of 'ghosts' were taken after each successive wash so that a range of haemoglobin content was obtained. Preliminary experiments involving the use of phase-contrast light-microscopy indicated that on increasing the temperature of the suspension the proportion of 'ghosts' showing finger-like projections could be diminished, and that at the higher temperatures (30–40°C) most of the 'ghosts' tended to assume biconcave shapes. A quantitative electron-microscopic study with the use of 2% ammonium molybdate negative staining at pH7.0 was undertaken, as at

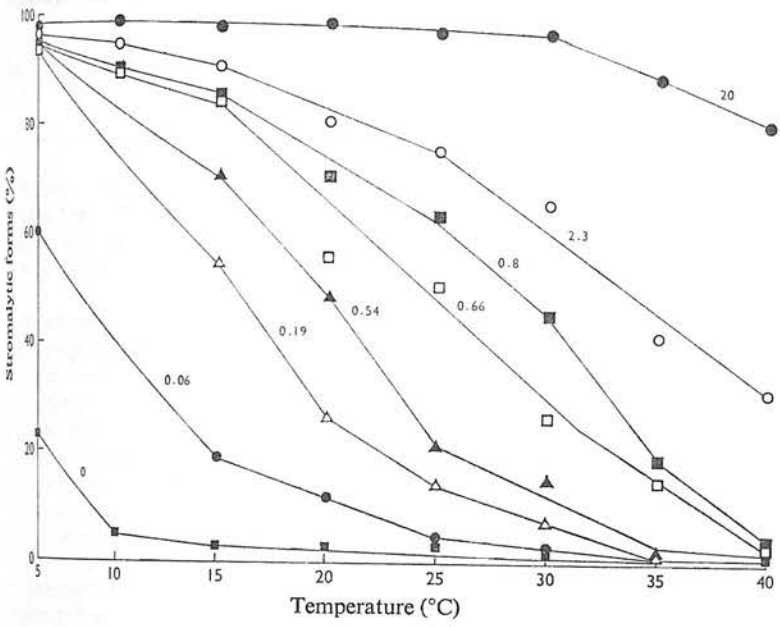

Fig. 1. *Percentage of stromalytic forms plotted against the temperature of the membrane suspension*

Details are given in the text. The ratio of haemoglobin to membrane protein is indicated beside each curve.

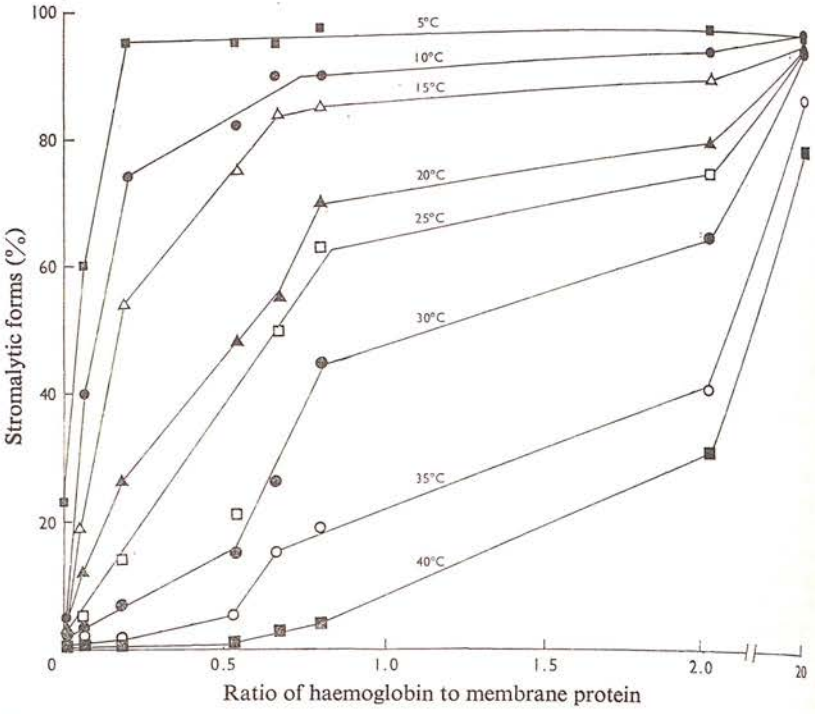

Fig. 2. *Percentage of stromalytic forms plotted against the ratio of haemoglobin to membrane protein*

Details are given in the text. The temperature of the membrane suspension is indicated beside each curve.

---

the higher magnifications provided by the electron microscope a clearer distinction between stromalytic forms and smooth membranes can be obtained (Marikovsky & Danon, 1967) than is possible by light-microscopy. Ammonium molybdate has been shown by Harris & Agutter (1970) to cause minimal disruption of erythrocyte 'ghosts', when used as the negative stain.

The erythrocyte 'ghost' samples, with gradually decreasing haemoglobin, were incubated in a water bath at 5°C, and samples were taken for the rapid preparation of negatively stained specimens, the stain being used at the same temperature as the membrane suspension. This was repeated at 5°C intervals up to 40°C, as the water-bath temperature was very slowly raised. The negatively stained specimens were viewed at low electron-optical magnifications, and a count of 200 erythrocyte 'ghosts' was made to determine the percentage present as stromalytic forms rather than smooth-surfaced membranes. The curves in Fig. 1 show the percentage of stromalytic forms plotted against the temperature of the suspension, for each of the membrane samples. The ratio of haemoglobin to membrane protein is indicated beside each curve. It is readily apparent that there is a higher percentage of stromalytic forms at the lower temperatures and also that the presence of haemoglobin gives rise to a greater proportion of stromalytic forms at all temperatures. The stromalytic forms containing large amounts of haemoglobin have large numbers of long finger-like projections, whereas when there is little or no haemoglobin present the projections tend to be broader and shorter. Fig. 2 shows the percentage of stromalytic forms plotted against the ratio of haemoglobin to membrane protein for the series of membrane samples, each curve representing a different

temperature. These curves emphasize the fact that the presence of haemoglobin causes a very marked increase in the percentage of stromalytic forms at lower temperatures, whereas the effect is much less marked at 35° and 40°C, at ratios of haemoglobin to membrane protein up to approx. 0.5.

The results described above are in general agreement with the observations made by Baker (1964), who stated that the finger- or tube-like projections visible on stromalytic forms contained haemoglobin. As the erythrocyte 'ghosts' are permeable to haemoglobin throughout the repeated washing scheme, it is probable that there will be some haemoglobin in the extracellular fluid. Thus haemoglobin will have access to both the inner and the outer surface of the membrane, and may be absorbed in either case to produce an alteration of the surface charge. Whether or not considerations such as this can account for the alteration of the erythrocyte 'ghost' shape is not clear, since lowering the temperature has also been shown to have a marked effect even in the absence of haemoglobin. An increase in membrane rigidity is likely to be produced at the lower temperatures owing to a decrease in the microviscosity of the lipoprotein, but no evidence is available to relate such changes (Aloni *et al.*, 1974) to cell shape.

Results similar to those described above have been obtained with erythrocyte 'ghosts' from outdated blood, in which the cellular ATP concentration is very low. In addition, the ATP concentration in the erythrocyte 'ghosts' from fresh blood is likely to be very low after the haemolysis and repeated washing, unless there is a fraction of the ATP bound to the membrane. Katsumata & Asai (1972) have claimed to obtain endocytocis of erythrocyte 'ghosts' that is independent of ATP. It is likely that the change of shape from biconcave disc to stromalytic form, which is at least partially reversible, is not energy-dependent.

Aloni, B., Shinitzhi, M. & Linvne, A. (1974) *Biochim. Biophys. Acta* **348**, 438–441
Baker, F. R. (1964) *J. Ultrastruct. Res.* **11**, 494–507
Dodge, J. T., Mitchell, C. & Hanahan, D. J. (1963) *Arch. Biochem. Biophys.* **100**, 119–134
Furchegott, R. F. (1940) *Cold Spring Harbor Symp. Quant. Biol.* **8**, 224–232
Harris, J. R. (1969) *Biochim. Biophys. Acta* **188**, 31–42
Harris, J. R. (1971) *J. Ultrastruct. Res.* **36**, 587–594
Harris, J. R. & Agutter, P. S. (1970) *J. Ultrastruct. Res.* **33**, 219–232
Hoffman, J. F. (1973) in *Red Cell Shape* (Bessis, M., Weed, R. I. & LeBlond, P. F., eds.), pp. 51–54, Springer-Verlag, Berlin.
Katsumata, Y. & Asia, J. (1972) *Arch. Biochem. Biophys.* **150**, 330–332
Marikovsky, Y. & Danon, D. (1967) *J. Ultrastruct. Res.* **20**, 83–90
Watson, J. H. L., Angulo, J. & Olarte, J. (1950) *Proc. Soc. Exp. Biol. Med.* **75**, 134–139

The Reconstitution of Photosystem 1 in Barley Plastids lacking Pigment P700

NEIL L. MORGAN and W. TREVOR GRIFFITHS

Department of Biochemistry, Medical School, University of Bristol, Bristol BS8 1TD, U.K.

Dark-grown etiolated plants contain a number of the components involved in photosynthetic electron transport, with the notable exception of chlorophyll (Plesnicar & Bendall, 1973). Illumination of such plants results in chlorophyll synthesis and the acquisition of photosynthetic activity. We have shown that if etiolated barley plants are pre-treated in the dark for 5 h with the antibiotic D-*threo*-chloramphenicol at 250 μg/ml, then on subsequent illumination such plants fail to develop photosynthetic electron transport even though chlorophyll formation is only partially (40%) inhibited. No such effects were found when the plants were treated with L-*threo*-chloramphenicol, even at 500 μg/ml (Morgan & Griffiths, 1975). One explanation for the lack of photosynthesis in such plants is the complete absence of any measurable Photosystem 1

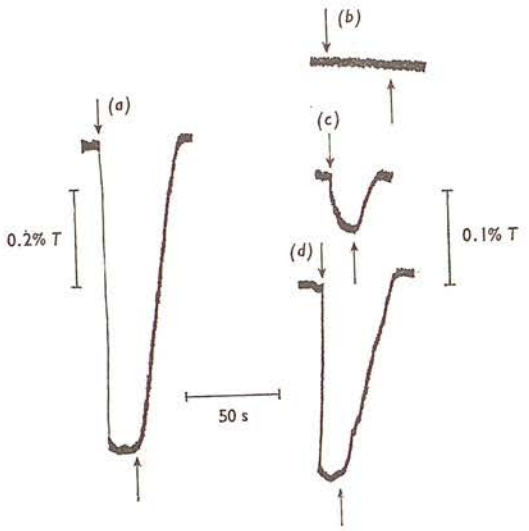

Fig. 1. *Cytochrome f photo-oxidation in chloramphenicol-treated and reconstituted membranes of barley plastids*

Cytochrome *f* photo-oxidation ($\Delta E_{554-540}$) was measured by the method of Bendall *et al.* (1971) with actinic side illumination of $\lambda > 660$ nm, intensity 16.6 mW·cm^{-2} switched on at (↓) and off at (↑). Trace (*a*), control membranes of plastids from leaves treated with L-*threo*-chloramphenicol (500 μg/ml); trace (*b*), membranes from leaves treated with D-*threo*-chloramphenicol (250 μg/ml); trace (*c*), membranes as in (*b*) reconstituted with purified reaction centres; trace (*d*), reconstituted membranes as in (*c*) plus 0.2 μM-plastocyanin. Abbreviation: *T*, transmission.

---

activity. Thus whole leaves and isolated plastids from such plants are unable to photo-oxidize their endogenous cytochrome *f*, and no pigment P700 or sodium dodecyl sulphate-solubilized pigment-protein complex I could be detected in the plastids. This has led us to try and reconstitute Photosystem 1-dependent cytochrome *f* photo-oxidation in such plastids by incorporating isolated reaction centres into deficient membranes.

Reaction centres were purified from chloroplasts isolated from 7-day-old light-grown barley. The chloroplasts, in 0.4 M-sucrose/10 mM-Tris/HCl (pH 8.0)/10 mM-NaCl/5 mM-$MgCl_2$ (Nelson & Bengis, 1975), were washed twice in 50 mM-Tris/HCl, pH 8.0, and once in 1 mM-EDTA (Anderson & Levine, 1974) to produce membranes essentially free of soluble proteins. Triton X-100-solubilized reaction centres were isolated from these membranes by the technique of Nelson & Bengis (1975) and purified on DEAE-cellulose (DE 23) with a linear NaCl gradient, 0–0.4 M, in 0.2% Triton X-100/50 mM-Tris/HCl, pH 8.0 (Malkin, 1975). A series of 1 ml fractions was collected and their absorption spectra were recorded. The fractions exhibiting a chlorophyll absorption at room temperature at 677 nm were found to contain pigment P700. These fractions were pooled and designated purified reaction centres. The preparation migrated as a single chlorophyll–protein complex of mol.wt. 100000 during electrophoresis on sodium dodecyl sulphate/polyacrylamide gels. Acetone extraction of the preparation gives four separate bands on electrophoresis, with mol.wts. of 16000, 18000, 25000 and 60000, the latter being the major component. Our preparation, which gives a chlorophyll/P700 ratio of 75:1 (w/w), contains no detectable cytochromes and is completely stable at 0°C.

Reprinted from

Biochimica et Biophysica Acta, 534 (1978) 173—178

BBA Report

BBA 31253

THE BREAKDOWN OF SPECTRIN PRODUCED BY ULTRASONICATION

J.R. HARRIS, P. MARSHALL and I. NAEEM

Biomembrane Unit, Division of Biochemistry, Faculty of Science, North East London Polytechnic, Romford Road, London, E15 4LZ (U.K.)

(Received March 6th, 1978)

Summary

The application of carefully controlled ultrasonication to human erythrocyte membranes (ghosts) has been found to produce a selective breakdown of the two spectrin polypeptides. This breakdown increases with the time and the intensity of ultrasonication. The 240 000 molecular weight spectrin polypeptide is slightly more susceptible to ultrasonication than the 220 000 molecular weight polypeptide. Isolated spectrin behaves in an identical manner when ultrasonicated. When highly purified samples of spectrin are ultrasonicated the progressive reduction of the molecular weight of the products with increasing time is clearly apparent.

The polypeptide composition of the mammalian erythrocyte membrane, as revealed by sodium dodecyl sulphate (SDS) polyacrylamide gel electrophoresis, has been found to be extremely reproducible in the hands of different investigators. The polypeptide numbering sequence introduced by Fairbanks [1] has been adopted by most workers and will be adhered to in this paper. SDS polyacrylamide gel electrophoresis of solubilized membrane polypeptides can be a quantitative study if scanning densitometry is performed on the gels in conjunction with integration of the area under each polypeptide peak. Thus, relative changes in the amount of any polypeptide in the membrane under varying experimental conditions can be readily determined.

The extrinsic erythrocyte membrane protein spectrin, which was discovered by Marchesi and his colleagues [2], has subsequently been studied by many workers. It is now accepted that spectrin amounts to approximately 30% of the erythrocyte membrane protein and that it is revealed as the first two polypeptide bands on SDS polyacrylamide gels. The molecular weights of these polypeptide bands are put at approximately 240 000 and 220 000 respectively. Single polypeptide chains of this size are very uncom-

of discretely spaced molecules to regions containing single brane so that no

mon in proteins and it has been suggested by several investigators [3–5] that spectrin may be composed of multiple subunits that are not dissociated by the conventional protein dissociation treatments (i.e. SDS, urea, SDS-urea and guanidine hydrochloride). There is evidence, however, to suggest that spectrin may dissociate in acetic acid at pH 3 [6], although this is now thought to be due to the activation of contaminating proteases [7]. The physical, biochemical and functional properties of spectrin have recently been reviewed by Kirkpatrick [8].

Outdated human blood (group O + ve) was obtained from the Pathology Department, Queen Mary's Hospital, Stratford, London. Haemoglobin-free erythrocyte ghosts were prepared by the conventional haemolysis and washing procedure of Dodge et al. [9] as modified by Harris [10]. Spectrin was isolated from erythrocyte ghosts by incubation of the distilled water extracted membrane fragments [11] with 1 mM NaEDTA at pH 8.0 for 60 min at 22° C. The extract was acidified with HCl to pH 5.2 [12] and the precipitate of partly purified spectrin redissolved at alkaline pH and dialysed overnight against 5 mM Tris/chloride pH 8.0. This impure spectrin was further purified by sedimentation through a linear 0.25 to 1.0 M sucrose density gradient for 20 h at 30 000 rev./min in the MSE 3 × 23 ml swing out rotor. Fractions containing dimers and trimers of native spectrin, which contained very little contamination with low molecular weight protein, were pooled. The main contaminant remaining is the polypeptide band 5 of the numbering sequence of Fairbanks. 2-ml samples of erythrocyte ghosts (protein concentration 1.6 mg/ml) and spectrin (protein concentration 3.5 mg/ml) were ultrasonicated using a MSE 150 watt Ultrasonic Disintegrator Mk. II, fitted with a 9.5 mm diameter titanium probe of transmission factor 5.5 to 1. Ultrasonication was carried out at peak to peak amplitudes of 3, 6, 9 and 12 μm, with a nominal frequency of 20 kHz. The probe and the MSE sample tube containing the sample were precooled, and an ice-water bath was used to keep the sample cool during the subsequent ultrasonication. Ultrasonication was applied as 10 s bursts followed by 10 s periods of cooling, which maintained the sample temperature at 6° C.

Polyacrylamide gels were prepared using 7% (w/v) acrylamide, 0.05% (w/v) *N*,*N*′-methylenebisacrylamide in 50 mM Tris·HCl buffer (pH 8.0), polymerized with 0.05% (v/v) *N*,*N*,*N*′,*N*′-tetramethylethylene diamine and 0.1% (w/v) ammonium persulphate. Samples were dissociated in 2% (w/v) sodium dodecyl sulphate, 1% (v/v) 2-mercaptoethanol buffered in 5 mM Tris·HCl (pH 8.0) by heating for 2 min at 100° C. After cooling, an equal volume of Bromophenol Blue tracker dye made up on 10% glycerol buffered by 5 mM Tris·HCl (pH 8.0) was added, and the samples layered directly onto the gels. 0.1% (w/v) sodium dodecyl sulphate in 50 mM Tris·HCl (pH 8.0) was used as the cathode buffer and 50 mM Tris·HCl (pH 8.0) as the anode buffer; gels were prephoresed at 1 mA per tube for 10 min prior to application of the samples, which were then run at 3 mA per tube. On completion of the electrophoresis gels were stained in 0.05% (w/v) Coomassie Brilliant Blue R250 in methanol/acetic acid/water (50:10:40, v/v) and unbound dye

subsequently removed by washing in methanol/acetic acid/water (20:10:70, v/v). Gels were photographed on Ilford FP4 35mm film and scanned at 540nm using a Joyce-Loebl Chromoscan to obtain densitometric profiles and integration of the areas under the peaks.

It has been found that ultrasonication of human erythrocyte ghosts and samples of partially purified spectrin, at intensities of 3, 6, 9 and 12 μm peak to peak amplitude resulted in the selective breakdown of the spectrin band 1 ($M_r \approx 240\,000$) and spectrin band 2 ($M_r \approx 220\,000$), with little or no breakdown of the other polypeptides present. Fig. 1 shows SDS gel electrophoresis patterns of erythrocyte ghosts ultrasonicated at 12 μm, and shows clearly the disappearance of bands 1 and 2 with increasing ultrasonication time. Partly purified samples of isolated spectrin behaved in a similar manner to the erythrocyte ghosts when treated with ultrasonication, as shown in Fig. 2.

Fig. 3 shows that the greater the intensity of ultrasonication the more rapid is the initial breakdown of both spectrin bands. It also appears that spectrin band 1 is slightly more susceptible to breakdown than band 2. When the more highly purified spectrin is subjected to ultrasonication at 3 μm (Fig. 4) it is clearly apparent that a range of breakdown products are initially produced, which progressively decrease in molecular weight with prolonged treatment. Significantly, the contaminating polypeptide band 5 (arrowed on Fig. 4) does not undergo any detectable breakdown even when the ultrasonication is applied at an intensity of 12 μm.

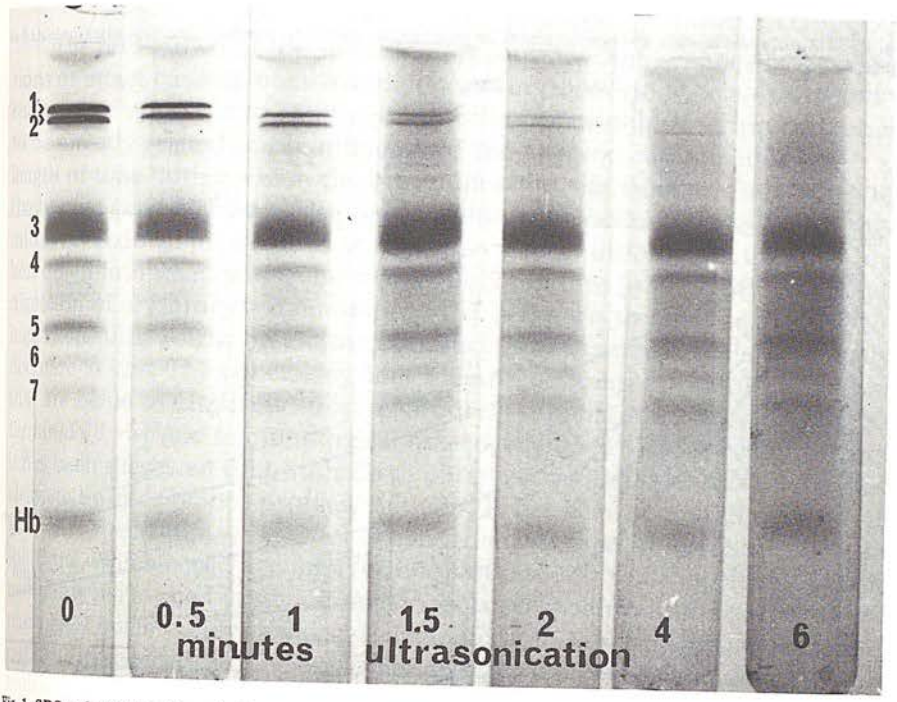

Fig. 1. SDS polyacrylamide gel electrophoresis patterns of erythrocyte ghosts ultrasonicated at 12 μm. The main polypeptide bands are numbered 1 to 7, and the leading band of haemoglobin is indicated by Hb.

of discretely spaced molecules to regions containing single

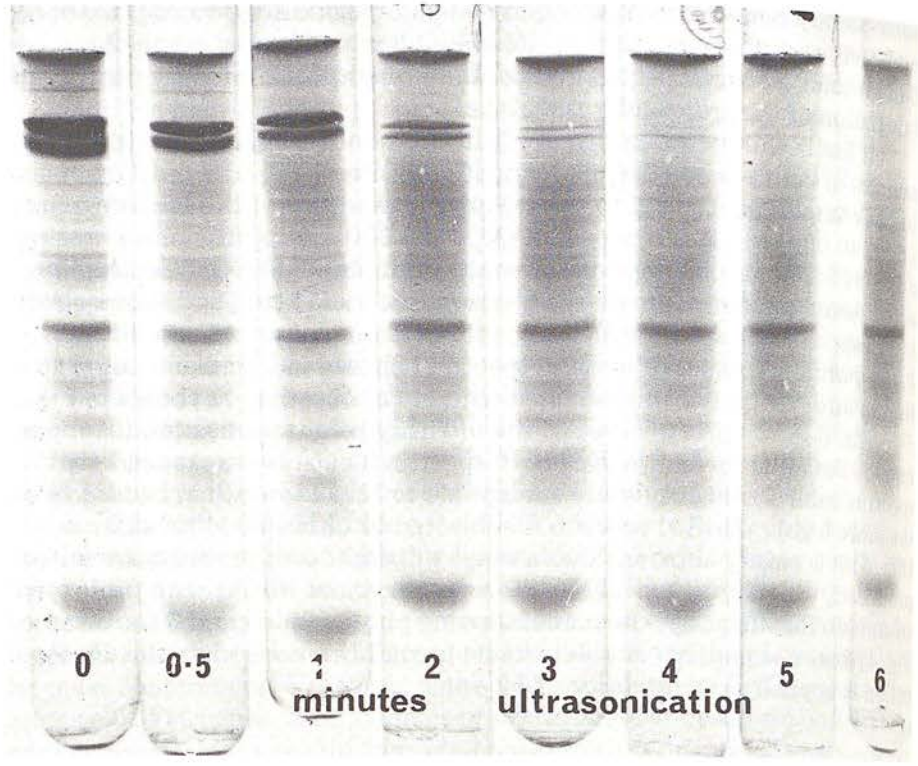

Fig. 2. SDS polyacrylamide gel electrophoresis patterns of partially purified spectrin ultrasonicated at 3 μm.

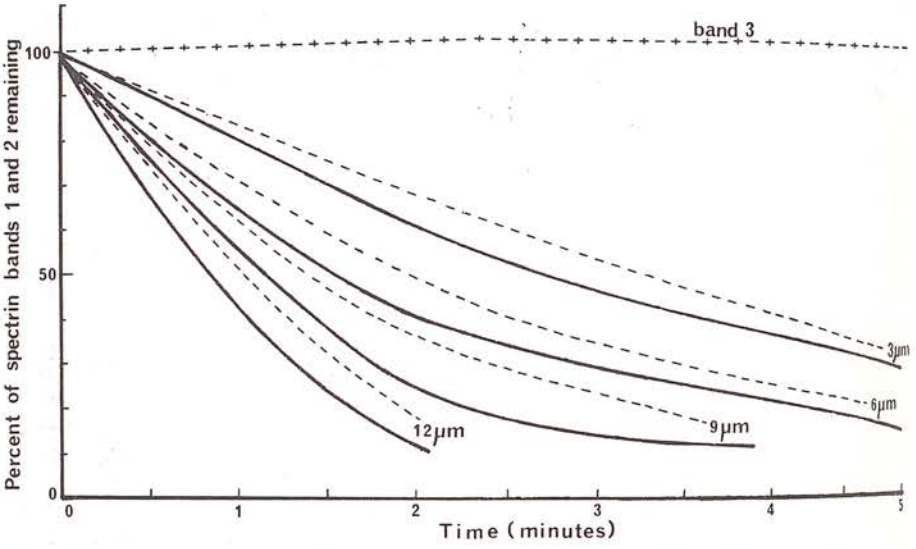

Fig. 3. Curves showing the breakdown of spectrin bands 1 and 2 of erythrocyte ghosts as a function of time and intensity of ultrasonication, in comparison to band 3. Solid line, band 1; broken line, band 2.

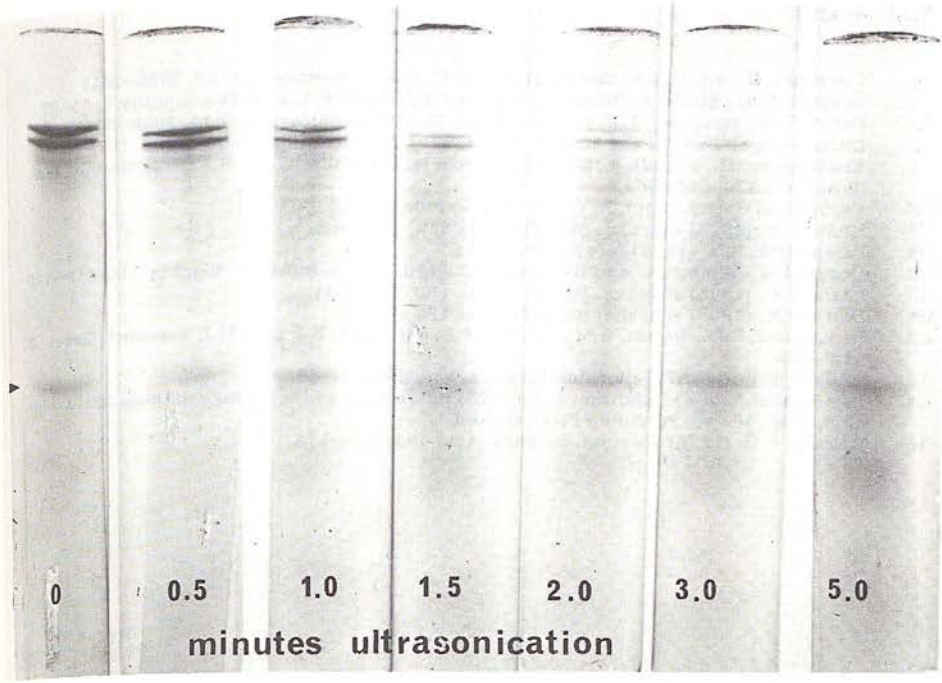

Fig. 4.SDS polyacrylamide gel electrophoresis patterns of purified spectrin obtained by sucrose density gradient centrifugation, subjected to ultrasonication at 3 μm.

The breakdown of the spectrin polypeptides that occurs when suspensions of intact haemoglobin-free biconcave erythrocyte ghosts or isolated spectrin are subjected to carefully controlled ultrasonication has been shown to be directly related to the intensity of the ultrasonication and to the length of time during which the ultrasonication was applied. Only when relatively pure samples of spectrin are available is it possible to see clearly the initial breakdown products of the spectrin dimer, which are ultimately broken down into small molecular weight polypeptides (see Fig. 4). Proteolytic digestion of erythrocyte membranes [13] is known to give rise initially to high molecular weight breakdown products from spectrin, which gradually decrease in size. The conclusion that spectrin contains intramolecular bonds that are liable to ultrasonication might draw support from the apparent N-terminal [3–5] and immunological heterogeneity [14] of spectrin, although it has been suggested that both these observations could be due to spectrin cleavage by endogenous protease activity. It has been proposed by Ralston [15] that spectrin may be in an expanded state when in low ionic strength solutions, which could account for its susceptibility to ultrasonication. Experiments performed using ghosts and isolated spectrin in the presence of phosphate buffered physiological saline did not alter the stability of spectrin during ultrasonication. The complete resistance of the high molecular weight multisubunit protein apoferritin to ultrasonication at an intensity of 12 μm, indicates that at least some non-membrane proteins are not dissociated or cleaved by ultrasonication.

of discretely spaced molecules to regions containing single

References

1 Fairbanks, G., Steck, T.L. and Wallach, D.F.H. (1971) Biochemistry 10, 2606—2617
2 Marchesi, S.L., Steers, E., Marchesi, V.T. and Tillack, T.W. (1970) Biochemistry 9, 50—57
3 Fuller, G.M., Boughter, J.M. and Morazzani, M. (1974) Biochemistry 13, 3036—3041
4 Dunn, M.J., McBay, W. and Maddy, A.H. (1975) Biochim. Biophys. Acta 368, 107—119
5 Knufermann, H., Bhakdi, S., Schmidt-Ullrich, R. and Wallach, D.F.H. (1973) Biochim. Biophys. Acta 330, 356—361
6 Furthmeyr, H. and Timpl, R. (1970) Eur. J. Biochem. 15, 301
7 Hulla, F.W. (1974) Biochim. Biophys. Acta 345, 430—438
8 Kirkpatrick, F.H. (1976) Life Sci. 19, 1—18
9 Dodge, J.H., Mitchell, C. and Hanahan, D.J. (1963) Arch. Biochem. Biophys. 100, 119—130
10 Harris, J.R. (1968) Biochim. Biophys. Acta 150, 534—537
11 Harris, J.R. (1969) Biochim. Biophys. Acta 188, 31—42
12 Kirkpatrick, F.H., Woods, G.M., LaCelle, P.L. and Weed, R.I. (1975) J. Supramol. Struct. 3, 415—425
13 Wallach, D.F.H. (1972) Biochim. Biophys. Acta 265, 61—83
14 Bog-Hansen, T.C. and Bjerrum, O.J. (1973) in: Protides of the Biological Fluids, 21st Colloquium, pp. 39—43, Pergamon Press, Oxford
15 Ralston, G.B. (1976) Biochim. Biophys. Acta 455, 163—172

Biochimica et Biophysica Acta, 537 (1978) 495—500

BBA Report

BBA 31264

THE SUBUNIT COMPOSITION OF TWO HIGH MOLECULAR WEIGHT EXTRINSIC PROTEINS FROM HUMAN ERYTHROCYTE MEMBRANES

J.R. HARRIS and I. NAEEM

Biomembrane Unit, Division of Biochemistry, Faculty of Science, North East London Polytechnic, Romford Road, London E15 4LZ (U.K.)

(Received April 24th, 1978)

Summary

Purified hollow cylinder (22.5 S) and torus protein (9.0 S) from human erythrocyte membranes, together with the intact membranes, have been dissociated using 2% sodium dodecyl sulphate and electrophoresed in the presence of 0.1% sodium dodecyl sulphate. The torus protein gives rise to a single subunit migrating slightly ahead of band 8 of the polypeptide profile of the intact membranes ($M_r \approx 20\,000$) and the hollow cylinder gives rise to two main subunits, which migrate slightly behind that of the torus protein. It is clearly shown that neither protein is related to erythrocyte membrane spectrin (bands 1 + 2) or actin (band 5).

The hollow cylinder (22.5 S) and torus protein (9.0 S) complexes from human erythrocyte membranes (ghosts) were discovered using electron microscopy by Harris [1] and most of the subsequent investigations have been of an ultrastructural nature [2—6]. A thorough biochemical characterization of the purified proteins has not been possible to date owing to difficulties in obtaining adequate quantities of the two proteins in a suitable state for such studies. This paper presents electrophoretic data on the purified hollow cylinder and torus proteins, in the native state and following dissociation with sodium dodecyl sulphate (SDS). The subunit molecular weights obtained after dissociation are correlated with the total polypeptide molecular weight profile of human erythrocyte membranes, similarly treated.

The electrophoretic distribution of the polypeptides of SDS solubilized human erythrocyte membranes was initially defined by Fairbanks et al. [7] and has subsequently been shown to be highly reproducible by many groups

Abbreviations: SDS, sodium dodecyl sulphate; EDTA, ethylenediamine tetraacetic acid.

of workers. Although there has been some criticism of the allocation of precise molecular weights to the polypeptide bands on the electrophoretograms, it is widely accepted that, with the exception of glycopeptides, these figures are reasonably accurate. Owing to some confusion in the literature over the apparent similarity of the hollow cylinder and torus proteins and their relationship to erythrocyte membrane spectrin (bands 1 + 2) [8] and actin (band 5) [9], it is considered important that these issues be clarified.

Haemoglobin-free erythrocyte membranes were prepared by the procedure of Dodge et al. [10], as modified by Harris [3]. The hollow cylinder and torus proteins were extracted by a slight modification of the distilled water

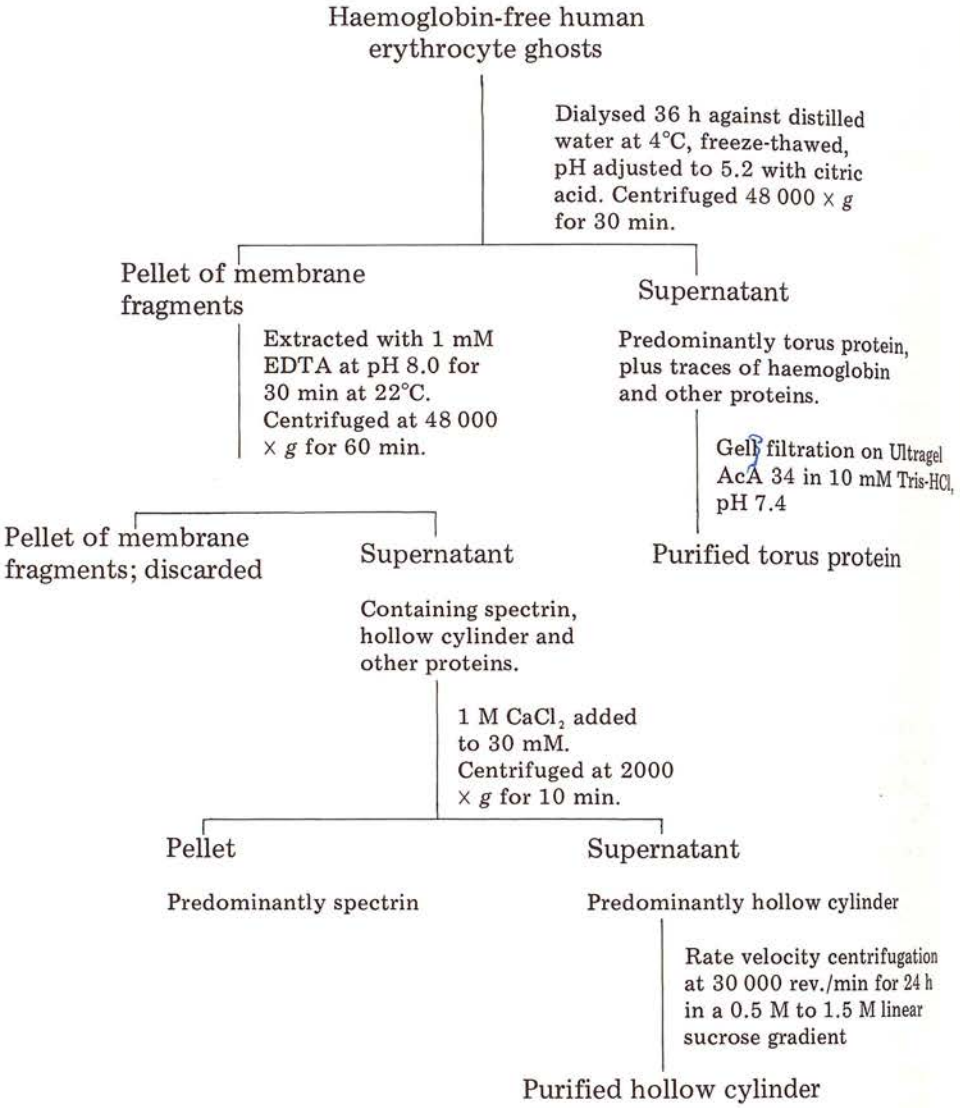

Chart 1. Purification of human erythrocyte ghost hollow cylinder (22.5 S) and torus (9.0 S) proteins.

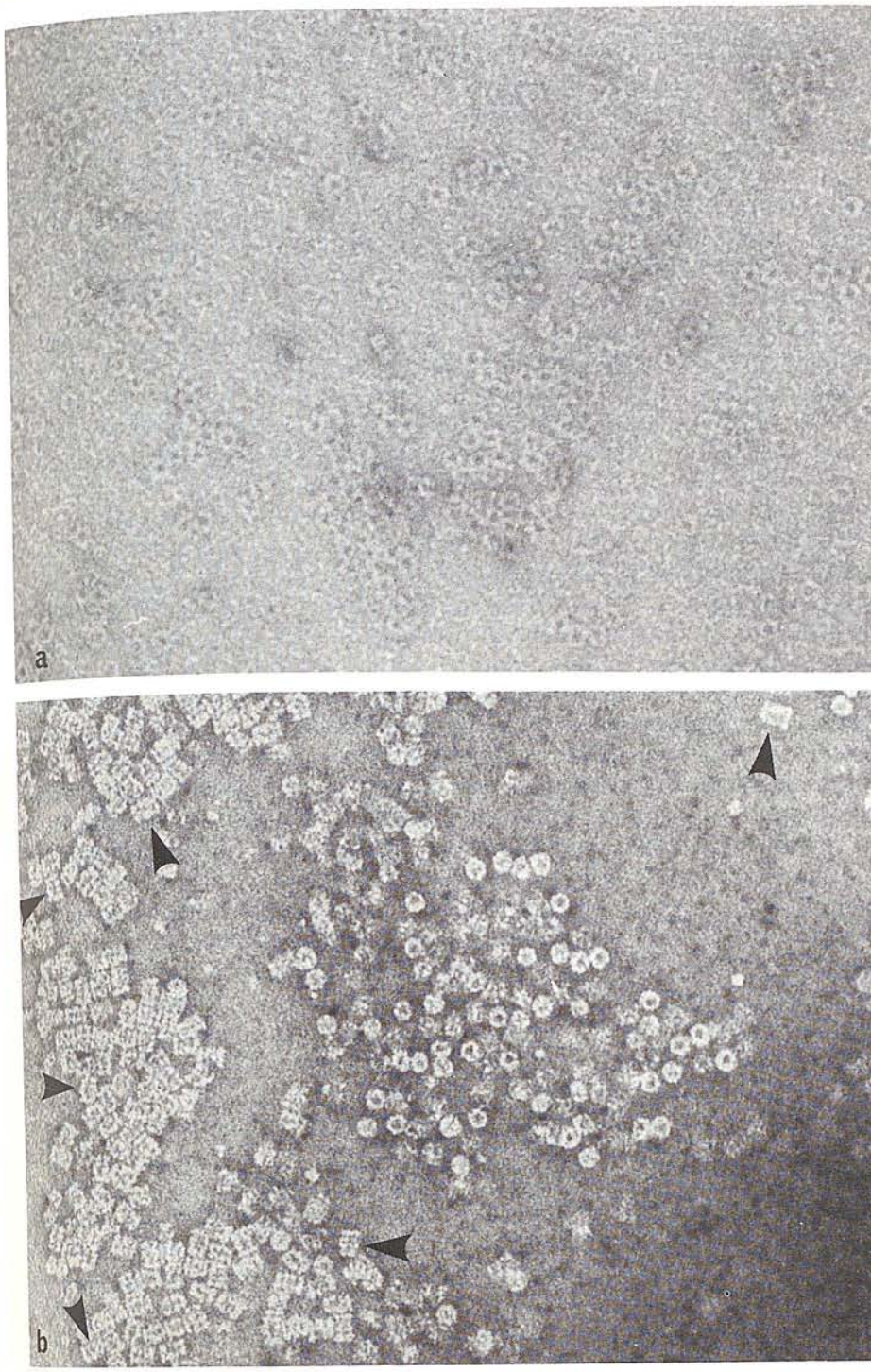

Fig. 1. Purified torus protein (a) and hollow cylinder protein (b) negatively stained with 1% uranyl acetate using the mica-carbon film technique. × 200 000.

dialysis and freeze-thaw treatment previously described (Chart 1). After dialysis against distilled water for 36 h at 4°C the membrane suspension was rapidly frozen using liquid nitrogen and after 30 min thawed in a 37°C water bath. The pH of the suspension was then adjusted to 5.2 with 1 M citric acid prior to centrifugation at 48 000 × *g* for 30 min, to remove the membrane fragments. The supernatant contained the torus protein, together with traces of haemoglobin and other proteins which can be separated from the torus by gel filtration chromatography on either Biogel P300 or Ultragel AcA 34. The membrane fragments were then extracted for 30 min at 22°C with 1 mM sodium ethylenediamine tetraacetic acid (EDTA) at pH 8.0, and centrifuged for a further 60 min at 48 000 × *g*. The supernatant from this centrifugation contains predominantly spectrin plus the hollow cylinder. The spectrin was precipitated selectively by the addition of 1 M calcium chloride to give a concentration of 30 mM, leaving the hollow cylinder in solution. Final purification of the hollow cylinder was achieved by rate velocity centrifugation on a 0.5 M to 1.5 M linear sucrose density gradient [4].

Fig. 1 shows negatively stained electron micrographs of the purified torus and hollow cylinder proteins, and Fig. 2 shows 7% polyacrylamide gel electrophoretograms of these proteins in their native state. Following dissociation by heating at 100°C for 1 min in the presence of 2% SDS, 1% 2-mercaptoethanol, and electrophoresis in the presence of 0.1% SDS, erythrocyte membranes, the torus and hollow cylinder proteins reproducibly exhibit the polypeptide distributions shown in Fig. 3. The gels (a) and (e) in Fig. 3 are of erythrocyte membranes, with the polypeptide bands numbered 1 to 8, and their approximate molecular weights are indicated. The position of the subunit of haemoglobin is indicated by Hb. Gel (b) is of purified torus protein and (c) is of torus protein plus haemoglobin. It can be concluded that the torus protein has a single subunit of molecular weight approximately 20 000

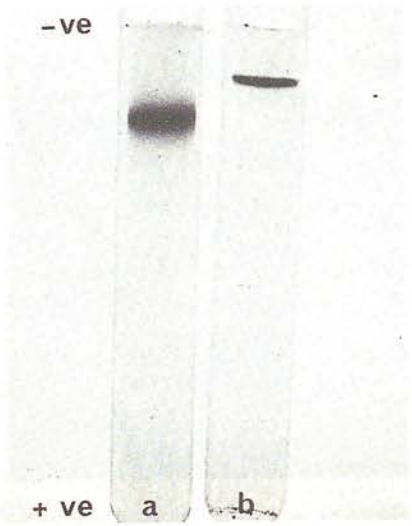

Fig. 2. 7% polyacrylamide gel electrophoretograms in a 50 mM Tris-HCl (pH 8.0) continuous buffer system; gel (a) torus protein, gel (b) hollow cylinder protein.

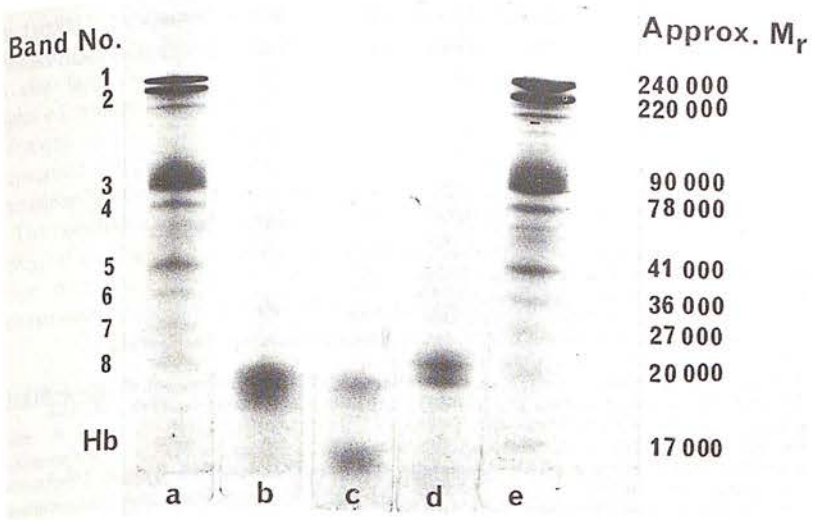

Fig. 3. 7% polyacrylamide gel electrophoretograms in a 0.1% SDS, 50 mM Tris-HCl (pH 8.0) continuous buffer system; gels (a and e) 2% SDS dissociated erythrocyte membranes, (b) purified torus protein SDS dissociated, (c) torus protein plus haemoglobin SDS dissociated, and (d) purified hollow cylinder protein SDS dissociated.

which migrates slightly ahead of polypeptide band 8 of erythrocyte membranes. The purified hollow cylinder, on the other hand, gives rise to two polypeptides (gel d), which migrate slightly behind that of the torus protein; a minor polypeptide band is also present between bands 4 and 5 of the total. It is likely that on the SDS electrophoretograms of the intact erythrocyte membranes the subunits of the torus and hollow cylinder proteins would not be present in sufficient quantities to be resolved as separate bands: the two proteins may therefore, due to band spreading during electrophoresis, be jointly approximated by band 8. The presence of more than one main subunit in the hollow cylinder protein supports the interpretations placed on the electron microscopic images of this protein, which show the central region of the side-on image to be clearly distinct from the end regions [6,11] (arrowed in Fig. 1b). It is apparent from the electrophoretic data that the torus and cylinder proteins are not composed of identical subunits, as was implied in previous publications [1—3,12], yet queried in others [11]. This conclusion is supported by the Ouchterlony double diffusion analysis performed on the native proteins, in which no antigentic cross-reactivity was detected [13]. The suggestion that the torus and hollow cylinder proteins may be equivalent to either spectrin or actin is clearly shown to be incorrect. This is in agreement with the more recent conclusions of Ralston [14] who calculated approximate sedimentation coefficients for the torus and hollow cylinder proteins and claimed that they were too large for identity with spectrin. Although Kirkpatrick et al. [9] indicated that at pH 5.2 the polypeptide band 5 (actin) was the main protein to remain in the supernatant of the EDTA extract, this is contrary to our results. Nevertheless, on treating the acid precipitated pellet with calcium the hollow cylinder protein has been

shown to remain in solution, in agreement with the later results of Kirkpatrick et al. [15], which do not, however, show clearly which electrophoretic band should be allocated to this protein.

References

1 Harris, J.R. (1968) Biochim. Biophys. Acta 150, 534—537
2 Harris, J.R. (1969) J. Mol. Biol. 46, 329—335
3 Harris, J.R. (1969) Biochim. Biophys. Acta 188, 31—42
4 Harris, J.R. (1971) Biochim. Biophys. Acta 229, 761—770
5 Harris, J.R. (1971) J. Ultrastruct. Res. 36, 587—594
6 Harris, J.R. and Kerr, J. (1976) J. Microscopy 108, 51—59
7 Fairbanks, G., Steck, T.L. and Wallach, D.F.H. (1971) Biochemistry 10, 2606—2612
8 Ralston, G.B. (1975) Aust. J. Biol. Sci. 28, 259—266
9 Kirkpatrick, F.H., Woods, G.M., LaCell, P.L. and Weed, R.I. (1975) J. Supramol. Struct. 3, 415—425
10 Dodge, J.T., Mitchell, C. and Hanahan, D.J. (1963) Arch. Biochem. Biophys. 100, 119—134
11 Harris, J.R. (1971) Biochem. J. 122, 38—40
12 Howe, C. and Bächi, T. (1973) Exptl. Cell Res. 76, 321—332
13 Harris, J.R. (1974), in Methodological Developments in Biochemistry, (Reid, E., ed.), Vol. 4, pp. 393—404, Longmans
14 Ralston, G.B. (1976) Biochim. Biophys. Acta 455, 163—172
15 Kirkpatrick, F.H., Woods, G.M., Weed, R.L. and LaCelle, P.L. (1976) Arch. Biochem. Biophys. 175, 367—372

very highly purified and concentrated liquid suspensions. In addition, rod-like and filamentous viruses can be prepared to give large paracrystalline arrays or two-dimensional sheets of ordered structures. Recent modifications to the technique and a possible interpretation of the specimen preparation mechanism will be discussed together with limitations in resolution imposed by the specimen itself.

The relatively large areas of these highly ordered biological specimens provide ideal electron micrographs for image processing methods. Examples of 'averaged' or reconstructed images from the above arrays will be shown.

REFERENCES

Horne, R. W. and Pasquali-Ronchetti, I. (1974) A negative staining-carbon film technique for studying viruses in the electron microscope. I. Preparative procedures for examining icosahedral and filamentous viruses. *J. Ultrastruct. Res.* 47, 361.

Horne, R. W., Hobart, J. M. and Pasquali-Ronchetti, Ivonne (1975) Application of the negative staining-carbon technique to the study of virus particles and their components by electron microscopy. *Micron* 5, 233.

Horne, R. W., Hobart, J. M. and Markham, R. (1976) Electron microscopy of tobacco mosaic virus prepared with the aid of negative staining-carbon film techniques. *J. gen. Virol.* 31, 265.

Some Problems associated with the Production of Paracrystalline Arrays of Protein Molecules

J. R. Harris
Biomembrane Unit, Division of Biochemistry, North East London Polytechnic, Romford Road, London E15 4LZ

Application of the carbon film-negative staining technique of Horne and his colleagues to purified protein molecules, in an attempt to produce paracrystalline molecular arrays, has revealed certain fundamental technical problems when asymmetrical proteins are processed. The proteins that have been studied in this investigation are apoferritin, the 22.5S hollow cylinder and the 9.0S ring protein extracted from human erythrocyte membranes, the 22S cylindrical complex from *Bordetella pertussis* and human serum α_2-macroglobulin.

Protein solutions at a concentration of 1.0 to 10.0 mg/ml were mixed with the equal volume of 2% ammonium molybdate (pH 7.0), spread as a thin film on freshly cleaved mica, air dried, and coated with a thin layer of carbon. The carbon layer with adhering protein molecules was then picked up on holey carbon support films, after floating off on a solution of 1% uranyl acetate.

Apoferritin was found to give rise to a variety of electron optical images, ranging from a single layer spread of discretely spaced molecules to regions containing single and multiple layers of ordered paracrystalline arrays and randomly packed arrays. The cylindrical protein complexes from *Bordetella pertussis* and human erythrocyte membranes were found to preferentially orientate themselves on their ends and on their sides, and it has not yet proved possible to make the molecules selectively orientate themselves in one or other of these positions. Thus, for these two molecules in the main only randomly packed arrays have been observed. The single ring protein from human erythrocyte membranes presents much the same problem, in that it tends to lie flat when there is a dilute protein concentration, but once the concentration increases molecules are supported on their sides, which destroys the production of regular arrays. The α_2-macroglobulin, which has an extremely complex and as yet not precisely understood quaternary conformation, exhibits a similar randomness of molecular packing.

It can be concluded that proteins with a symmetrical quaternary conformation are more suitable for the production of paracrystalline arrays by the carbon film-negative staining technique. It may, nevertheless, be possible by varying the staining conditions (type of stain, concentration, pH and time of exposure to stain) to selectively orientate asymmetrical molecules in one particular position and thereby produce regular molecular arrays.

Advanced Techniques in Electron Microscopy of Animal Viruses

M. V. Nermut
National Institute for Medical Research, Mill Hill, London NW7 1AA, UK

Because of their size and chemical composition, animal viruses are most sensitive to surface tension forces which during air-drying cause their distortion or even disruption. The following preparation techniques prevent such drying artefacts: freeze-drying, freeze-fracturing and critical-point-drying.

Freeze-drying: Most enveloped viruses display considerable pleomorphism when air-dried on the grid, but are usually spherical when freeze-dried. It has been shown by Williams in 1954 and Nermut and Frank in 1971 that the diameter of influenza virus is 25 to 30% larger after air-dry negative staining than after freeze-drying. The surface knobs of oncogenic RNA-viruses and their icosahedral cores have convincingly been demonstrated only by means of freeze-drying (Nermut, 1977). Recently, we have obtained similar results with Bunyamwera virus.

Icosahedral viruses are less sensitive to air-drying especially in the presence of negative stain. But they are usually disrupted on the grid when previously stored at 4°C for a few days. Freeze-drying and shadowing can reveal fine structural details on the surface of adeno-viruses equivalent to those seen by negative staining (i.e. 2.0-2.5 nm resolution).

The application of *freeze-fracturing* in virus research is hindered by (i) small size of most viruses (problem of resolution), (ii) path of the fracture plane: enveloped viruses fracture 'preferentially' through their lipid membrane so that no internal structure is revealed; naked viruses either do not fracture at all or fracture 'randomly' across, which can lead to incorrect interpretation unless complementary replicas are available.

The 'preferential' fracture path through virus envelopes can be altered by fixation with formaldehyde (not glutaraldehyde) so that the virus interior can occasionally be seen (e.g. in influenza virus or Sendai virus). High resolution shadowing of freeze-fractured envelopes reveals 'intramembranous particles' both in Sendai and in influenza virus, which indicates that the glycoprotein spikes span the virus membrane.

Br. Poult. Sci., 12: 95-99. 1971 *Longman: printed in Great Britain*

THE PREPARATION OF NUCLEATED ERYTHROCYTE GHOSTS FROM AVIAN ERYTHROCYTES

J. R. HARRIS [1]

Department of Zoology, University of Edinburgh

AND

J. N. BROWN

Department of Physiology, University of Edinburgh

Received for publication 2nd July 1970

SYNOPSIS

A method is described for the preparation of erythrocyte ghosts, which are haemoglobin-depleted, from domestic fowl and turkey erythrocytes. These erythrocyte ghosts retain their ellipsoid shape and their nuclei, which are shown to possess the typical double nuclear membrane. In the cytoplasmic compartment of the ghosts, mitochondria have been clearly observed. There is little or no indication of endoplasmic reticulum. Filamentous structures have been seen adhering to the outer nuclear membrane, the mitochondria and the inner surface of the plasma membrane. These filaments may extend between the plasma membrane and the surfaces of the nucleus and mitochondria, thereby providing a form of structural anchorage for these organelles. It is a consistent observation that the nucleus of the intact erythrocyte and its ghost always occupies a central position, so some structure must be holding the nucleus otherwise one would expect to occasionally find it positioned off-centre. Significantly, very few of the filament structures are observed at the extremities of the avian erythrocyte ghost, well away from the nucleus.

INTRODUCTION

This study was undertaken to answer several questions related to the ultrastructure of the avian erythrocyte. It has been known for a considerable time that avian erythrocytes are respiring cells, yet thin sections of these cells have not given a positive conformation of the presence of mitochondria (Harris, unpublished observations). Mitochondria have, however, been observed within amphibian erythrocytes (Davies, 1961). It was thought that the major factor hindering the observation of mitochondria within avian erythrocyte was the presence of copious haemoglobin, and that in the absence of haemoglobin any mitochondria present should be revealed more clearly. No method has yet been published for the preparation of erythrocyte ghosts from avian erythrocytes by

[1] Present address: Department of Cancer Research, University of Nottingham.

osmotic haemolysis, so a scheme was developed for their preparation from fowl and turkey erythrocytes, in the hope of being able to resolve the above problem.

At the same time, very little information has been obtained by thin sectioning of intact erythrocytes on the presence of other cytoplasmic organelles such as endoplasmic reticulum and lysosomes. Also, it has not been explained why the nucleus of the avian erythrocyte invariably occupies a central position within the cell. Information on these problems was also hoped to be gained by an electron microscopic study of the avian erythrocyte ghost.

MATERIALS AND METHODS

The preparation of erythrocyte ghosts. The method is summarised for convenience in Table 1. Firstly heparinised whole blood was centrifuged at 2000 × *g* for 10 min. and the serum and buffy coat removed by aspiration. The packed cells were washed twice in 1·0 per cent saline with centrifugation at 2000 × *g* for 10 min. The cells were haemolysed by the addition of 10 volumes of 10 mM Tris-HCl buffer (pH 7·4) containing 4 mM $MgCl_2$. The ghosts were sedimented at 23,000 × *g*

TABLE 1

The preparation of avian erythrocyte ghosts

Turkey or domestic fowl

Whole blood (heparinised)

Centrifuged 2000 × *g* for 10 min.

Serum and buffy coat removed by aspiration; discarded.

Packed erythrocytes
Washed 2 × in 1·0 per cent NaCl at 4° C with centrifugation at 2000 × *g* for 10 min.

Supernatants; discarded.

Washed packed erythrocytes
Haemolysed by the addition of 10 vol 10 mM Tris-HCl (pH 7·4) containing 4 mM $MgCl_2$, at 4° C centrifuged at 23,000 × *g* for 10 min.

Supernatant decanted; discarded.

Packed erythrocyte ghosts

Fowl erythrocyte ghosts
Washed alternately in 5 vols 10 mM Tris-HCl buffer (pH 7·4) containing 4 mM $MgCl_2$ with and without 0·3 M sucrose, with centrifugation at 23,000 × *g* for 10 min. Finally resuspended in the sucrose buffer

Turkey erythrocyte ghosts
Washed 6 or 7 times in 5 vols 10 mM Tris-HCl buffer (pH 7·4) containing 4 mM $MgCl_2$ and 0·3 M sucrose, with centrifugation at 23,000 × *g* for 10 min.

Haemoglobin-free fowl erythrocyte ghosts (creamy-white in colour).

Haemoglobin-free turkey erythrocyte ghosts (almost pure white).

for 10 min and the supernatant decanted. The ghosts were then resuspended in 10 mM Tris-HCl buffer (pH 7·4) containing 0·3 M sucrose and 4 mM $MgCl_2$. The turkey ghosts were washed repeatedly in this buffer until free of haemoglobin. To obtain haemoglobin-free fowl erythrocyte ghosts it was found to be necessary to wash the ghosts alternately in the Tris-HCl buffer, with and without sucrose.

The presence of magnesium cations was found to be essential to preserve the integrity of the erythrocyte nuclei. During the development of this method the state of integrity of the erythrocyte ghosts and their nuclei was monitored after each wash by phase contrast microscopy (at a magnification of 1000 times). Routinely, approximately 1·5 l of turkey blood were processed, but only 150 ml quantities of fowl blood were used.

Fixation and embedding. Fixation was performed by the addition of 2·0 ml 2 per cent glutaraldehyde in Palade buffer (Palade, 1952), at pH 7·4, to 0·5 ml of erythrocyte ghosts. The ghosts were left at room temperature for 1 h and then pelleted by centrifugation at $1000 \times g$ for 10 min. The ghost pellet was post-osmicated in 1 per cent osmic acid in Palade buffer for 1 h, dehydrated by passing through graded ethanols and finally epoxypropane, before embedding in TAAB epoxy-resin.

Thin sectioning. Thin sections were cut with a Porter-Blum MT-2 ultramicrotome, using glass knives. Sections showing a silver-white interference colour were mounted on L.K.B. type 400 grids without a supporting membrane. Post-staining was performed using uranyl acetate in 50 per cent ethanol, followed by Reynolds' lead citrate (Reynolds, 1963).

Negative staining. Samples of the avian erythrocyte ghost preparations were negatively stained with 2 per cent ammonium molybdate (pH 7·0) without prior fixation.

Electron microscopy. Electron microscopic examination of the ghost preparations was performed with an A.E.I., E.M. 6B. The instrument had an accelerating voltage of 60 kV, a 150 μm condenser aperture and a 50 μm objective aperture. Electron optical magnifications of 7,500, 30,000 and 50,000 diameters were routinely employed. The magnification scale of the electron microscope was found to have an error of less than 2 per cent by calibration with a replica containing 2160 lines/mm. Photographs were taken on Ilford $3\frac{1}{4}$ in $\times$ $3\frac{1}{4}$ in plates, " Special Lantern Contrasty ".

RESULTS

The avian erythrocyte ghosts prepared by the method described above have been studied in the electron microscope by thin sectioning and negative contrast staining. Plate-Figure 1 shows a sample of fowl erythrocyte ghosts negatively stained with ammonium molybdate. The electron opaque nuclei often appear distorted, but nearly always occupy a central position within the ghost. The plasma membrane appears to be relatively smooth, though sharp folds can be observed which are due to the collapse of the ghost on to the carbon backing film. Negative staining does not reveal any cytoplasmic organelles within the avian erythrocyte ghost. Thin sectioning, on the other hand, has clearly revealed the presence of densely stained mitochondria within the cytoplasmic compartment of these ghosts (Plate-Figure 2). Another feature revealed by thin sectioning is the typical double nuclear

membrane. The inner nuclear membrane is almost hidden by the dense chromatin, but the outer nuclear membrane is clearly seen.

Surrounding the outer nuclear membrane and the mitochondria can be seen many tenuous fibrillar structures (Plate-Figures 3 and 4). These fibrils appear to pass from the surfaces of the nucleus and mitochondria to the adjacent plasma membrane. Very few of these fibrils are to be found within the extremities of the avian erythrocyte ghost, well away from the nucleus and mitochondria (Plate-Figure 2).

DISCUSSION

Methods have been known for a considerable time by which haemoglobin-free erythrocyte ghosts can be made from mammalian erythrocytes, but prior to this investigation no published method had appeared for the preparation of ghosts from the nucleated avian erythrocyte. The method outlined in this paper for their preparation is based essentially on the methods employed for the preparation of mammalian erythrocyte ghosts (Dodge, Mitchell and Hanahan, 1963; Marchesi and Palade, 1967; Harris, 1969), with the incorporation of precautions to stabilise the cell nuclei. The most important of these precautions is the presence of magnesium cations in the haemolysing and washing buffers.

It is readily apparent that much more ultrastructural detail can be obtained from the study of the avian erythrocyte ghost than from the intact erythrocyte. It must, however, be stated that the method used for preparing these ghosts may have induced morphological alterations within cellular organelles. Bearing this criticism in mind, it nevertheless appears that the cell nuclei and mitochondria do not appear to suffer any major trauma by the preparative procedure. Some lesions must be produced in the plasma membrane to permit the escape of haemoglobin and other soluble molecules. Possibly even ribosomes escape during the washing procedure, if they are not bound to intracellular membranes. The plasma membrane as a whole does, however, retain its original shape, as is the case with the mammalian erythrocyte ghost. At high magnifications the thin sectioned plasma membrane shows the typical *unit membrane* profile, which is not clearly distinguishable in thin sections of the intact avian erythrocyte. Similarly, the nuclear membranes and mitochondria are found to show up clearly within the erythrocyte ghost, but not within the intact erythrocyte, due again to the presence of the very high concentration of haemoglobin in the cytoplasm which tends to hide these structures.

The fibrillar structures observed to extend from the erythrocyte ghost nuclei and mitochondria to the adjacent plasma membrane may have undergone some disruption during the swelling produced by haemolysis. It is proposed that these fibrils may act as supports for the nucleus and possibly also for the mitochondria. Since the nucleus of the avian erythrocyte ghost remains in its central location, sufficient of these fibrils must remain intact throughout the preparative procedure, to hold the nucleus in this position.

ACKNOWLEDGEMENTS

The authors wish to thank Dr D. J. Bell, Physiology Department, University of Edinburgh, for the encouragement and advice he has given throughout this

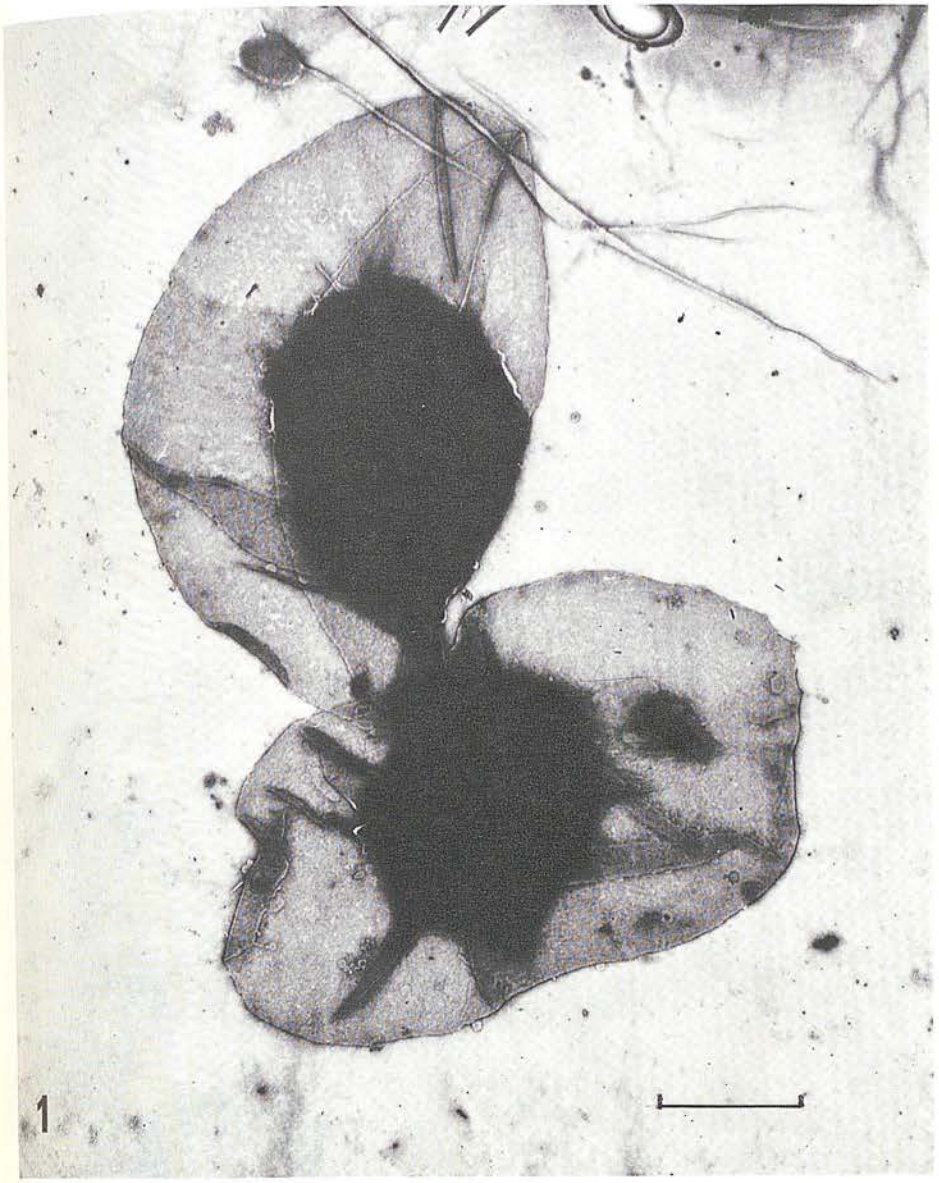

FIG. 1.—Ghosts from domestic fowl erythrocytes negatively stained with 2 per cent ammonium molybdate (pH 7·0). The scale marker indicates 2 μm.

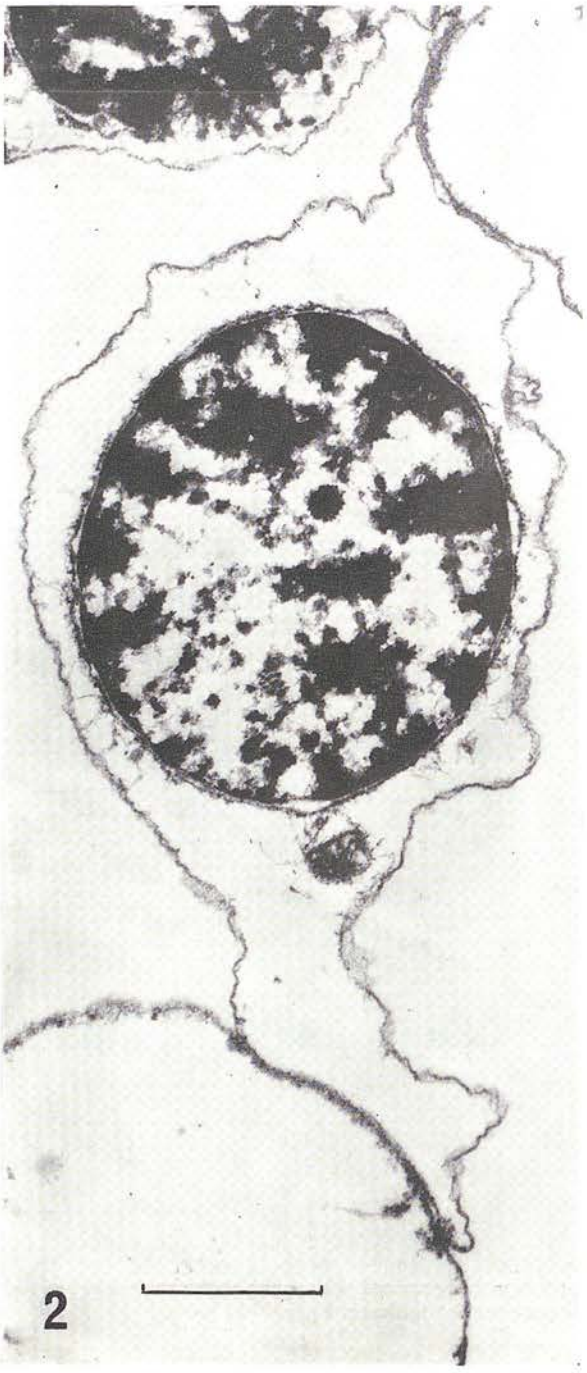

FIG. 2.—A thin-sectioned turkey erythrocyte ghost. The scale marker indicates 1 μm.

FIG. 3.—Part of a thin-sectioned turkey erythrocyte ghost showing mitochondria surrounded by fibrillar structures. The scale marker indicates 200 nm.

FIG. 4.—Part of a thin-sectioned turkey erythrocyte ghost showing fibrillar structures passing from the outer nuclear membrane to the plasma membrane. The scale marker indicates 200 nm.

study and British United Turkeys Ltd and Dr P. E. Lake for supplying turkey and fowl blood.

REFERENCES

DAVIES, H. G. (1966). Structure in nucleated erythrocytes. *J. biophys. biochem. Cytol.*, **9**: 671-687.

DODGE, J. T., MITCHELL, C. D. AND HANAHAN, D. J. (1963). The preparation and chemical characteristics of haemoglobin-free ghosts of human erythrocytes. *Archs Biochem. Biophys.*, **100**: 119-130.

HARRIS, J. R. (1969). The isolation and purification of a macromolecular protein component from the human erythrocyte ghost. *Biochim. biophys. Acta*, **188**: 31-42.

MARCHESI, V. T. AND PALADE, G. E. (1967). The localization of Mg-Na-K-activated adenosine triphosphatase on red cell ghost membranes. *J. Cell Biol.*, **35**: 385-404.

PALADE, G. E. (1952). A study of fixation for electron microscopy. *J. exp. Med.*, **95**: 285-298.

REYNOLDS, E. S. (1963). The use of lead citrate at high pH as an electronopaque stain in electron microscopy. *J. Cell Biol.*, **17**: 208-212.

J. ULTRASTRUCTURE RESEARCH 36, 8–23 (1971)

Fractionation of the Avian Erythrocyte: an Ultrastructural Study

J. R. HARRIS[1] AND J. N. BROWN

Department of Zoology and Department of Physiology, University of Edinburgh, Edinburgh, Scotland

Received July 7, 1970 and in revised form November 3, 1970

A method is described for the preparation of hemoglobin-depleted erythrocyte ghosts from chicken and turkey erythrocytes by osmotic hemolysis followed by repeated washing. These ghosts retain the shape of the intact erythrocyte and also the cell nucleus. Electron microscopy has shown the presence of mitochondria and the outer nuclear membrane, both of which tend to be hidden when the hemoglobin is present. Also, fibrils have been observed surrounding the mitochondria and nuclei. Fibrils appear to pass between the plasma membrane, and these organelles may provide an anchorage mechanism, particularly for the nucleus, which always occupies a central position within the ghost as it does in the intact erythrocyte.

By means of a controlled ultrasonication treatment, it has been possible to disrupt the plasma membrane of the avian erythrocyte ghost while leaving the nucleus intact. A nuclear fraction and a crude membrane fraction which contains mitochondrial and plasma membrane fragments have been otained. Most of the nuclei do not have a continuous outer nuclear membrane, which thus appears to be an extremely frail structure. Some of the plasma membrane and mitochondrial fragments had fibrils still attached.

The results are discussed in relation to the ultrastructure of the avian erythrocyte. In particular, possible functions of the hitherto unknown fibrillar structures are expanded upon in relation to the positioning of the cell nucleus and the cell shape.

Recently, a method has been developed for the preparation of hemoglobin-depleted nucleated erythrocyte ghosts from chicken and turkey erythrocytes (*7*). By means of a controlled ultrasonication treatment, monitored either by phase contrast or dark field microscopy, it has been possible to disrupt selectively the plasma membrane of these ghosts, leaving the nuclei intact. The nuclei were then separated from the membrane fragments by centrifuging at low *g* and purified by repeated resuspension and centrifugation at low *g*, until judged to be free of membranal contamination by phase contrast microscopy.

[1] Present address: Department of Cancer Research, University of Nottingham.

Of the standard cellular disruption techiques that have been applied to avian erythrocytes, ultrasonication has not found general usage. Pestle and blade homogenization were employed by Zentgraph et al. (*17*) and pressure homogenization by Davoren and Sutherland (*3*). It was, however, maintained by Hughes and Cunningham (*8*) that ultrasonication could provide an easily controllable method for producing cell disintegration. In our hands it has been possible to apply ultrasonication successfully to ghosts derived from very large quantities of blood (up to 1.5 liters). With careful light microscopic monitoring the risk of applying too much ultrasonic energy can be avoided. By skimming off the loose pellet of undisrupted ghosts from the firm pellet or crude nuclei obtained after the initial ultrasonication, it is possible to resubject them to ultrasonication without disrupting any of the nuclei that have had sufficient ultrasonication to break their surrounding plasma membrane.

The method to be described gives a high yield of clean nuclei. Purity is assessed at the time of preparation by phase contrast microscopy and subsequently in the electron microscope by the absence of plasma membrane fragments. The membrane fraction obtained after ultrasonication was shown by electron microscopy to contain predominantly plasma membrane fragments, with a few mitochondria. The further purification of this membrane fraction has not been pursued.

MATERIALS AND METHODS

Turkey blood was obtained from British United Turkeys Ltd., Fenton Barns, East Lothian. Approximately 2–liter quantities were collected in to heparinized 1% saline direct from the carotid arteries at the time of slaughtering and were filtered through glass wool before proceeding further. Chicken blood was obtained from the Poultry Research Centre, Edinburgh, by the courtesy of Dr. P. Lake. This blood was collected directly into heparinized 1% saline from the wing veins of male birds. Approximately 20 ml was removed per bird. Usually 100–150 ml of chicken blood was used.

The preparation of avian erythrocyte ghosts. The turkey and chicken blood was initially centrifuged at 2 000 *g* for 10 minutes and the serum and buffy coat were removed by aspiration. The packed erythrocytes were then washed two times in 1% saline with centrifugation at 2 000 *g* for 10 minutes. Hemolysis was then brought about by the addition of 10 volumes of 10 m*M* Tris–HCl buffer (pH 7.4) containing 4 m*M* $MgCl_2$. The ghosts were then sedimented at 23 000 *g* for 10 minutes and the supernatant was decanted. The ghosts were then resuspended in 10 m*M* Tris–HCl buffer (pH 7.4) containing 0.3 *M* sucrose as well as 4 m*M* $MgCl_2$. The turkey ghosts were washed repeatedly in this buffer until hemoglobin-free. To obtain hemoglobin-free chicken erythrocyte ghosts it was found to be necessary to wash the ghosts alternately in the Tris-HCl–$MgCl_2$ buffer, with and without sucrose. Chart 1 outlines the various stages of the treatments given to the blood throughout the preparation of the erythrocyte ghosts.

The presence of 4 m*M* $MgCl_2$ throughout the above procedure is essential for the

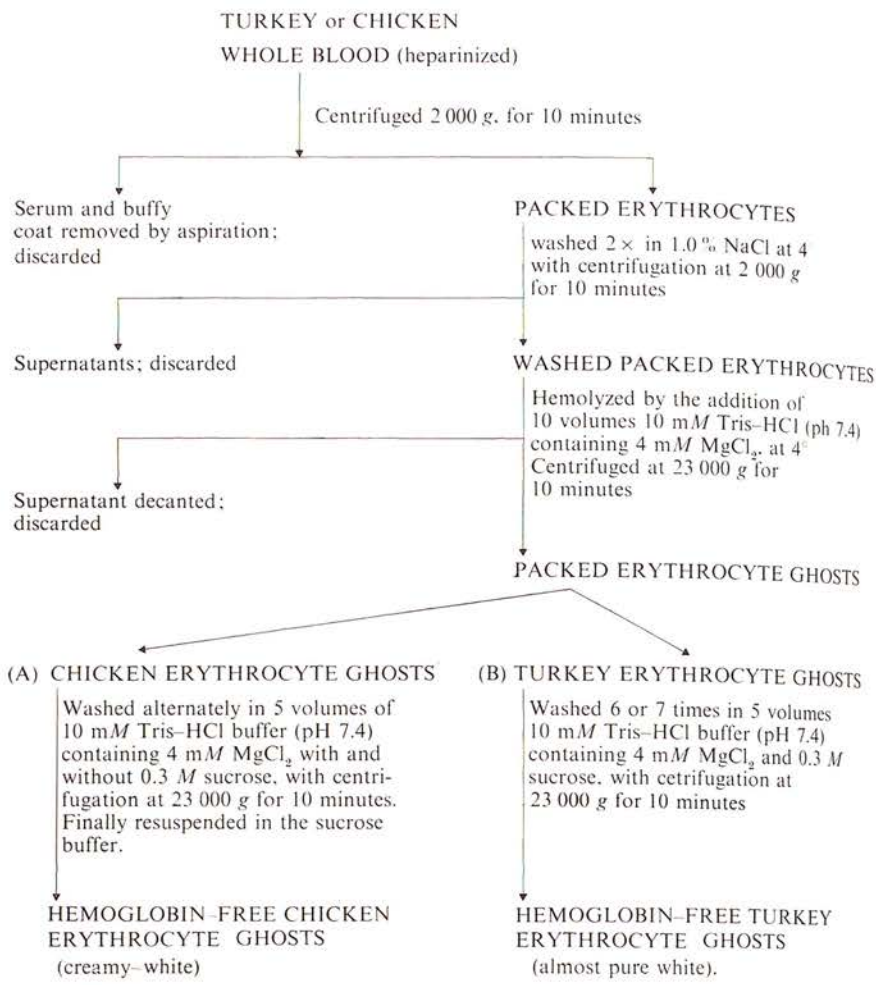

CHART 1. The preparation of avian erythrocyte ghosts.

maintenance of the integrity of the nuclei, which otherwise tend to burst (*6*), the chromatin escaping into the cytoplasmic compartment of the ghosts. The presence of the 0.3 *M* sucrose, although desirable, is not so critical as the 4 m*M* $MgCl_2$.

The disruption of avian erythrocyte ghosts by ultrasonication. The method developed for the disruption of the hemoglobin-depleted chicken and turkey erythrocyte ghosts is summarized in Chart 2. Approximately 100–ml volumes of the erythrocyte ghosts suspended in 10 m*M* Tris–HCl, pH 7.4. containing 4 m*M* $MgCl_2$ and 0.3 *M* sucrose at 4°C, were subjected to 60–second ultrasonication at an amplitude of 4 μ, with the M.S.E. 100-W Ultrasonic Disintegrator. The suspension was then centrifuged at 2 000 *g*, for 10 minutes and the cloudy supernatant was carefully decanted. The upper loose pellet of unbroken

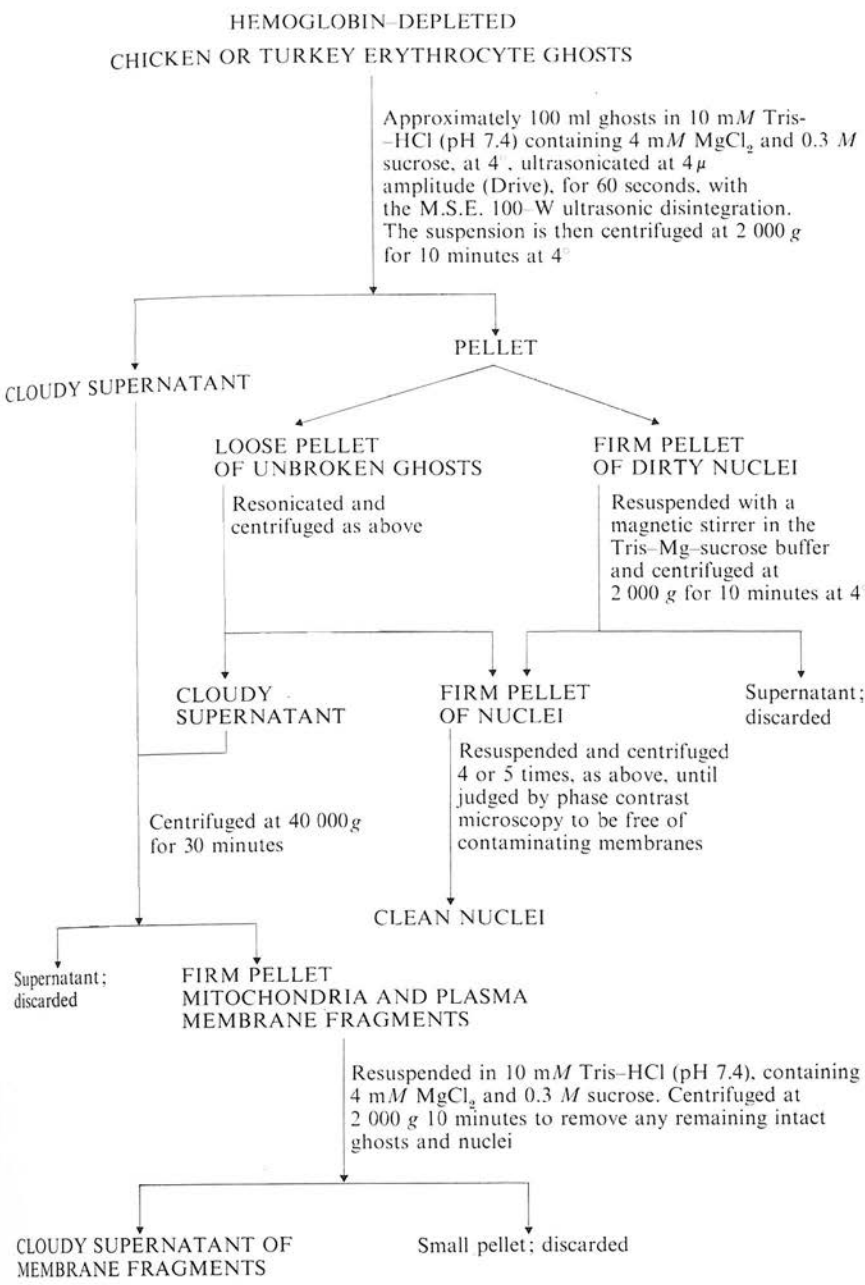

CHART 2. The disruption of the avian erythrocyte ghost by ultrasonication.

erythrocyte ghosts was then separated from the lower firm pellet of nuclei and resubjected to ultrasonication, and centrifugation, as above. The pooled pellets of crude nuclei were then resuspended with a magnetic stirrer in the Tris–HCl–$MgCl_2$–sucrose buffer and recentrifuged at 2 000 *g* for 10 minutes. This resuspension and centrifugation was repeated until observation by phase contrast or dark field microscopy showed the absence of free membrane fragments and membrane pieces attached to the nuclei.

Phase contrast or dark field microscopy provided a reliable method for assessing the disruption produced by a given amount of ultrasonication during the initial development of this technique. The ease with which unbroken ghosts could be separated from the crude nuclei ensured that the amount of ultrasonication could be minimized, and the risk of subjecting nuclei to an excessive amount of ultrasonication thereby avoided.

The cloudy 2 000 *g* supernatants obtained following the ultrasonication treatment were recentrifuged at 40 000 *g* and the clear supernatant was decanted. The pellet of plasma membrane and mitochondrial fragments was resuspended in the Tris–HCl–$MgCl_2$–sucrose buffer and centrifuged at 2 000 *g* for 10 minutes to remove any remaining ghosts and nuclei. The cloudy supernatant from this final centrifugation was decanted, and the small pellet was discarded.

Fixation and embedding. Fixation was performed by the addition of 4 volumes of 2% glutaraldehyde in Palade buffer (*11*) to 1 volume of the avian erythrocyte ghosts, nuclei, or membrane fraction. The material was left at room temperature for 1 hour and then pelleted by centrifugation at 1 000 *g* for 10 minutes. The pellets were postosmicated in 1% osmic acid in Palade buffer for 1 hour, dehydrated by passage through graded ethanols and finally epoxypropane, before embedding in TAAB epoxy resin.

Thin sectioning. Thin sections were cut with a Porter–Blum MT–2 ultramicrotome, using glass knives. Sections showing a silver-white interference color were mounted on LKB type 400 grids without a supporting membrane. Poststaining was performed using uranyl acetate in 50% ethanol, followed by Reynolds' lead citrate (*12*).

Negative staining. Samples of the avian erythrocyte ghost and plasma membrane preparations were negatively stained with 2% ammonium molybdate, pH 7.0, without prior fixation.

Electron microscopy. Electron microscopic examination of the various erythrocyte ghost, nuclei, and membrane preparations was performed with an A.E.I., E.M. 6B. The instrument had an accelerating voltage of 60 kV, a 250–μ condenser aperture and a 50–μ objective aperture. Electron optical magnifications of 7 500, 30 000, and 50 000 diameters were routinely employed. The magnification scale of the electron microscope was found to have an error of less than 2% by calibration with a replica containing 2160 lines/mm. Photographs were taken on Ilford 3¼–inch plates, "Special Lantern Contrasty."

FIG. 1. A phase contrast micrograph of a hemoglobin-free turkey erythrocyte ghost preparation. × 2 000.

FIG. 2. A thin-sectioned turkey erythrocyte ghost. × 21 000.

FIG. 3. Fibrillar structures surrounding a mitochondrion inside a turkey erythrocyte ghost. × 105 000.

FIG. 4. Fibrillar structures extending from the outer nuclear membrane to the plasma membrane of a turkey erythrocyte ghost. × 105 000.

FIG. 5. Part of a chicken erythrocyte ghost. Negatively stained with 2% ammonium molybdate (pH 7.0). × 30 000.

FIG. 6. Part of the nuclear membrane from a turkey erythrocyte ghost nucleus that had undergone disruption. The nuclear pore complexes are visible as are fibrillar structures (arrowed). Negatively stained with 2% ammonium molybdate (pH 7.0). × 30 000.

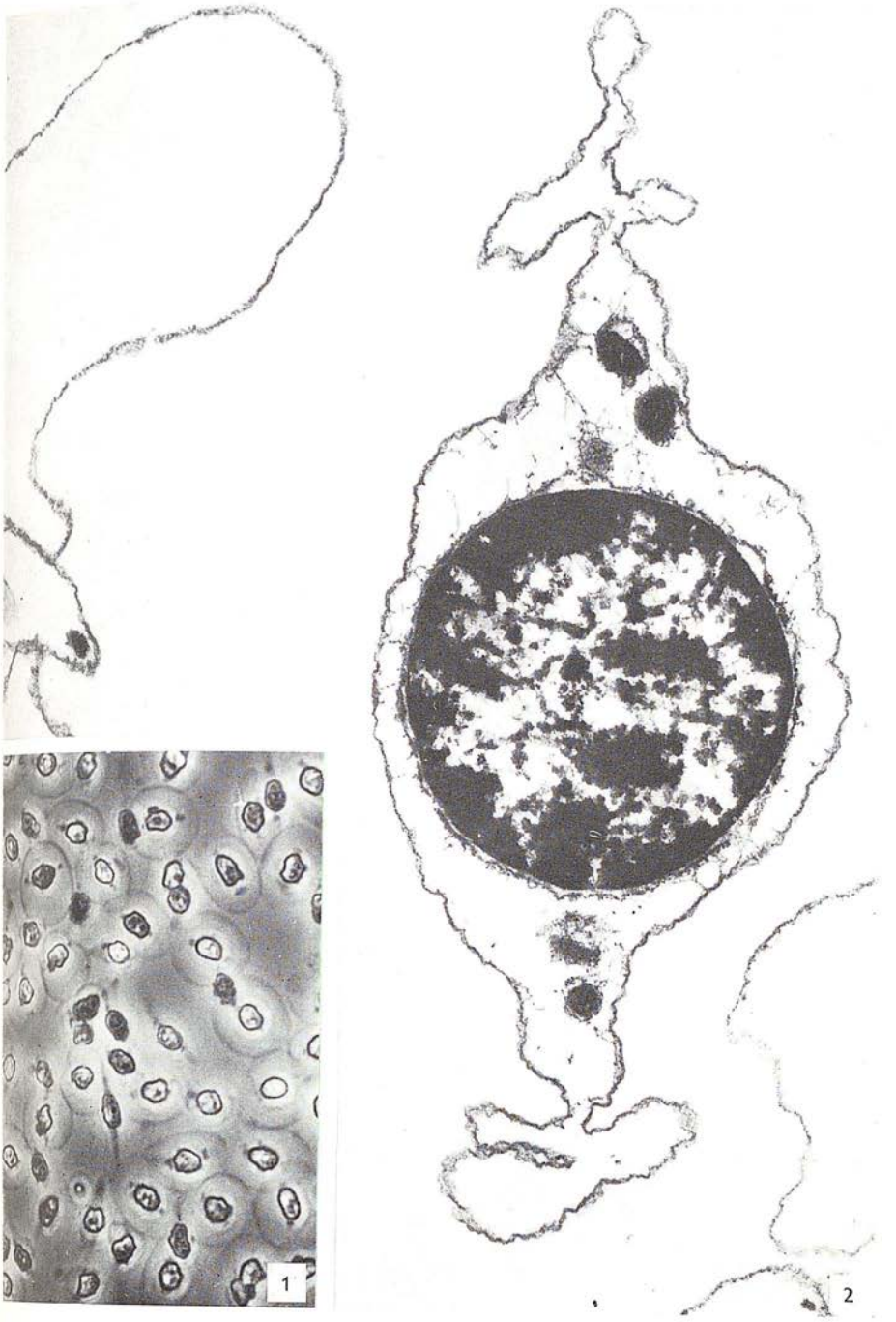
1
2

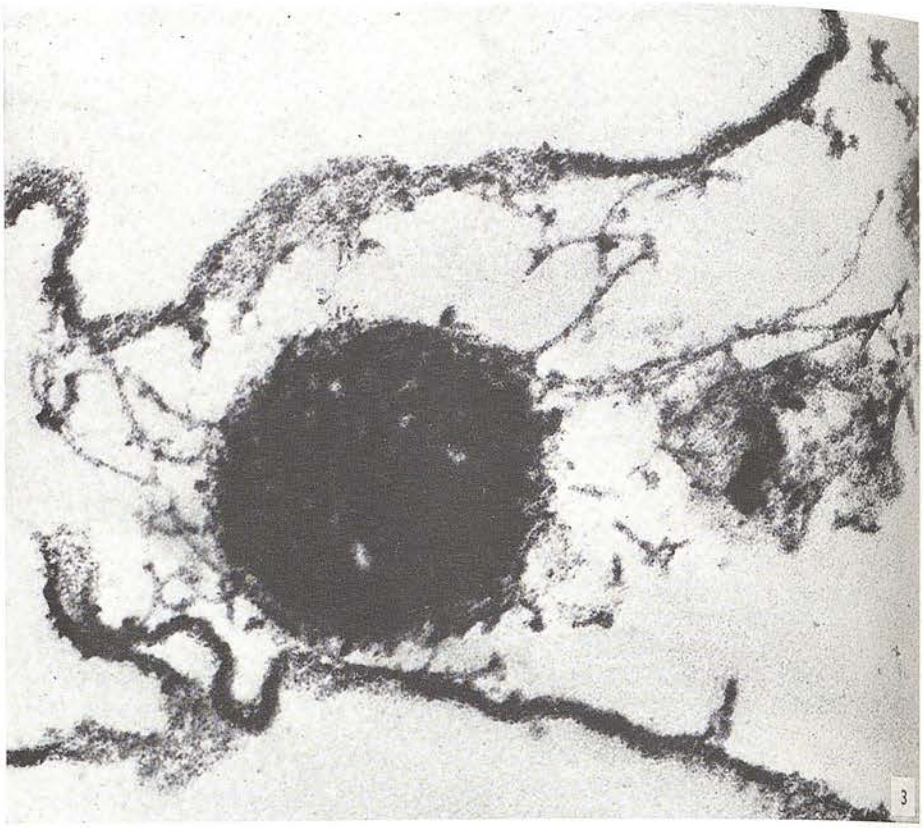
3

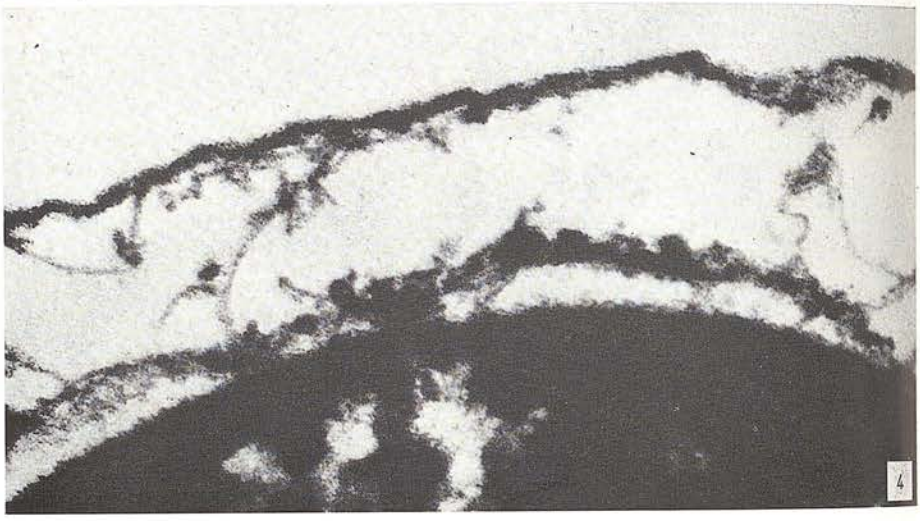
4

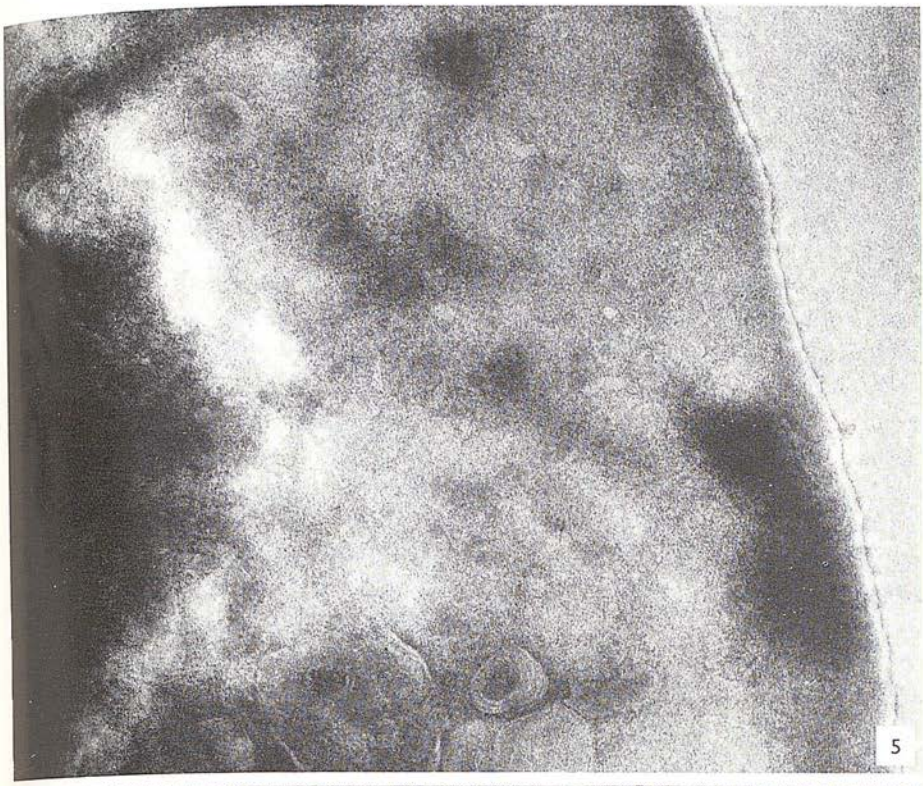

5

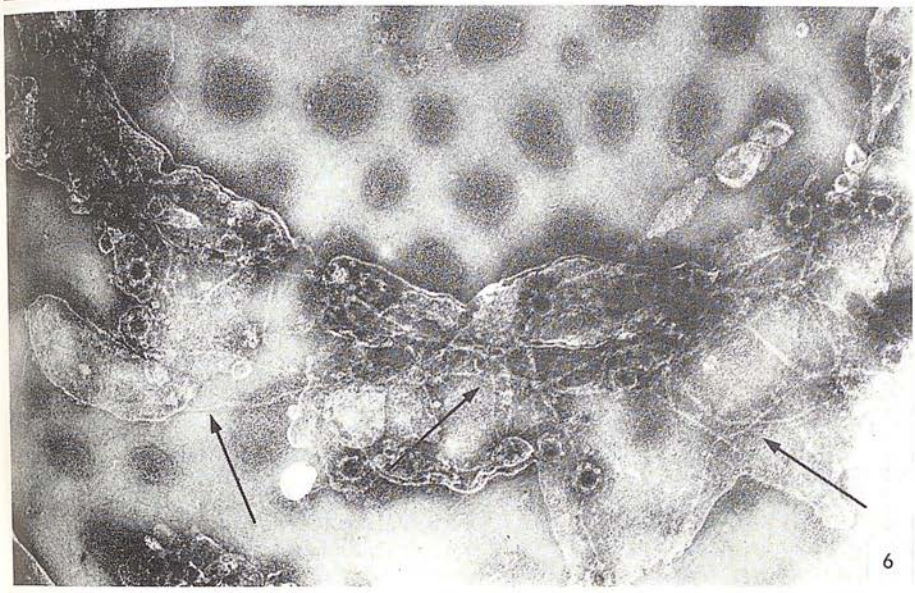

6

RESULTS

The avian erythrocyte ghost

The product obtained from the avian erythrocyte after hemolysis and subsequent washing until hemoglobin-free, is termed an erythrocyte ghost preparation, following the terminology currently employed when a similar procedure is applied to the mammalian erythrocyte. These avian erythrocyte ghosts retain the centrally positioned nucleus and the elongate ellipsoid shape of the intact erythrocyte, see Fig. 1, which is a phase contrast micrograph of a turkey erythrocyte ghost preparation. Electron microscopy has confirmed this light microscopic image and has considerably extended ultrastructural knowledge of the avian erythrocyte (*6*, *7*).

The thin-sectioned avian erythrocyte ghost (Fig. 2) shows many features which are not clearly observable in thin sections of the intact erythrocyte. First, the plasma membrane, which in thin section of the intact erythrocyte is almost completely hidden by the hemoglobin, is readily observed. At high magnifications the plasma membrane shows the typical unit membrane structure. Second, within the cytoplasmic compartment of the erythrocyte ghost occasional mitochondria can be seen. These mitochondria are often extremely electron dense, the cristae being less clearly defined than those in mitochondria of other avian tissues. Third, the tenuous outer nuclear membrane is readily visible, although the inner nuclear membrane remains almost hidden by the adjacent chromatin. There is a notable absence of endoplasmic reticulum and other cytoplasmic membrane systems. However, it is a reproducible observation that many fibrillar structures surround the mitochondria and also appear to extend from the outer nuclear membrane to the adjacent plasma membrane (Figs. 3 and 4).

Negative staining shows the plasma membrane of the avian erythrocyte ghost to be relatively smooth and featureless (Fig. 5). Sharp folds are present due to the ghost collapsing onto the carbon backing film. No detail can be seen within the nuclei, unless they happen to have burst, in which case the nuclear membrane can be recognized owing to the presence of the nuclear pore complexes (Fig. 6). Apart from the nuclear pore complexes, many fibrillar structures (approximately 100 Å in diameter, and up to 1 μ in length) can be seen on the nuclear membrane fragments. These fibrils are thought to be equivalent to those which are observed to extend between the outer nuclear membrane and the plasma membrane of thin-sectioned

---

FIG. 7. A phase contrast micrograph of turkey erythrocyte nuclei obtained by ultrasonication. ×2 000.

FIG. 8. Thin-sectioned turkey erythrocyte nuclei (as in Fig. 7). ×6 000.

FIG. 9. A thin-sectioned turkey erythrocyte nucleus showing clearly the outer nuclear membrane with a few fibrils attached. ×40 000.

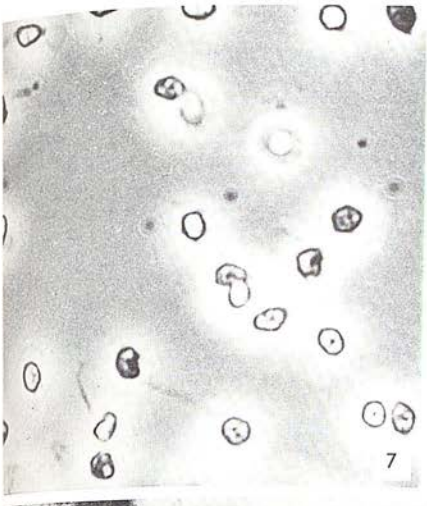
7

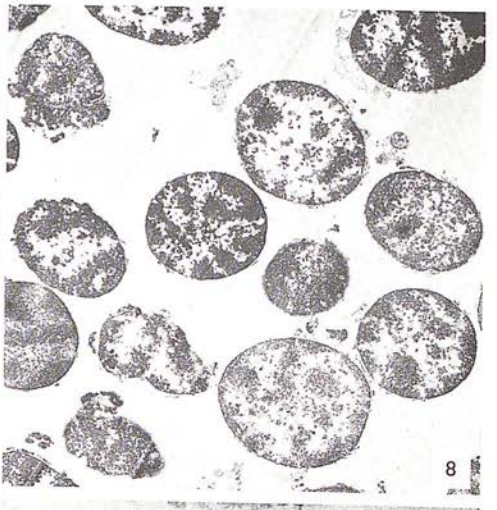
8


9

avian erythrocyte ghosts. It has not been possible to recognize mitochondria within the avian erythrocyte ghost by negative staining. This may be because the mitochondria, which contain tightly packed cristae, are not penetrated or surrounded to any extent by negative stain.

The nuclear fraction

Once the appropriate amount of ultrasonication required to disrupt the plasma membrane of the avian erythrocyte ghosts had been determined by careful phase contrast monitoring, the actual separation and purification of the nuclei by repeated washing and centrifugation at low *g* was a relatively simple procedure (Chart 2). The conventional method for purifying nuclei, i.e., by sedimenting them through dense sucrose, did not appreciably increase the purification obtained, since even the ghosts were found to pellet along with the clean nuclei. Figure 7 is a phase contrast micrograph of a purified preparation of nuclei, and Fig. 8 the corresponding material after embedding and thin sectioning. It is seen that most of the nuclei have lost their outer nuclear membranes, in agreement with the observations of Zentgraf et al. (*17*), who stressed the high fragility of the chicken erythrocyte outer nuclear membrane. By the method described in Chart 2 there were always a few nuclei that possessed an intact outer nuclear membrane (Fig. 9).

Work currently in progress is directed at obtaining a nuclear membrane preparation from these avian erythrocyte nuclei, and the following preliminary results have been obtained. First, by applying further ultrasonication the nuclei can be disrupted resulting in small pieces of nuclear membrane which nevertheless still possess nuclear pore complexes (Fig. 10). Enzyme treatment with DNase at 4° is also under trial. To date it has been possible to obtain morphologically intact nuclear ghosts (Figs. 11 and 12), but they can be seen to be heavily contaminated with chromatin.

The membrane fraction

The hemoglobin-free membrane fraction obtained after the ultrasonication treatment (Chart 2) has been studied by thin sectioning and negative staining. As expected, negative staining reveals membrane vesicles of varying size (Fig. 13). Mitochondrial fragments were recognized by the presence of Fernández-Morán

FIG. 10. Fragments of turkey erythrocyte nuclear membrane obtained by ultrasonication. Negatively stained with 2% ammonium molybdate (pH 7.0). × 40 000.

FIG. 11. A thin-sectioned turkey erythrocyte "nuclear ghost" obtained after DNase treatment of the nuclear preparation. Granules of chromatin line the inner surface of the inner nuclear membrane. The arrow indicates a nuclear pore. × 41 250.

FIG. 12. A thin section tangential to the surface of a "nuclear ghost" obtained after DNase treatment of a preparation of turkey erythrocyte nuclei. The arrows indicate nuclear pores. × 41 250.

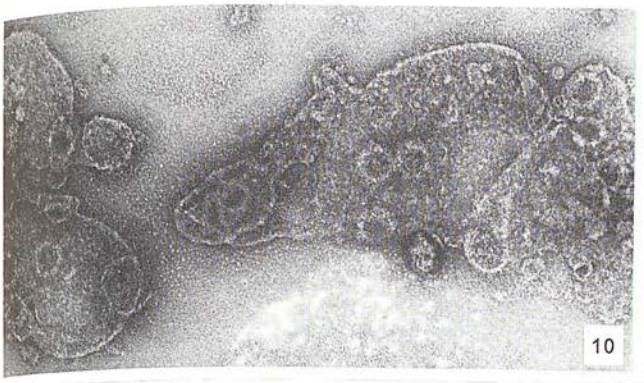
10

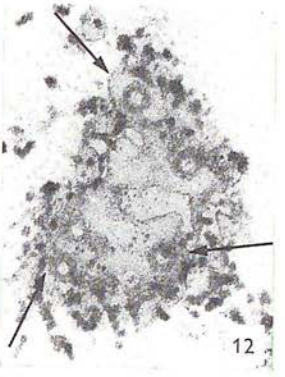
12

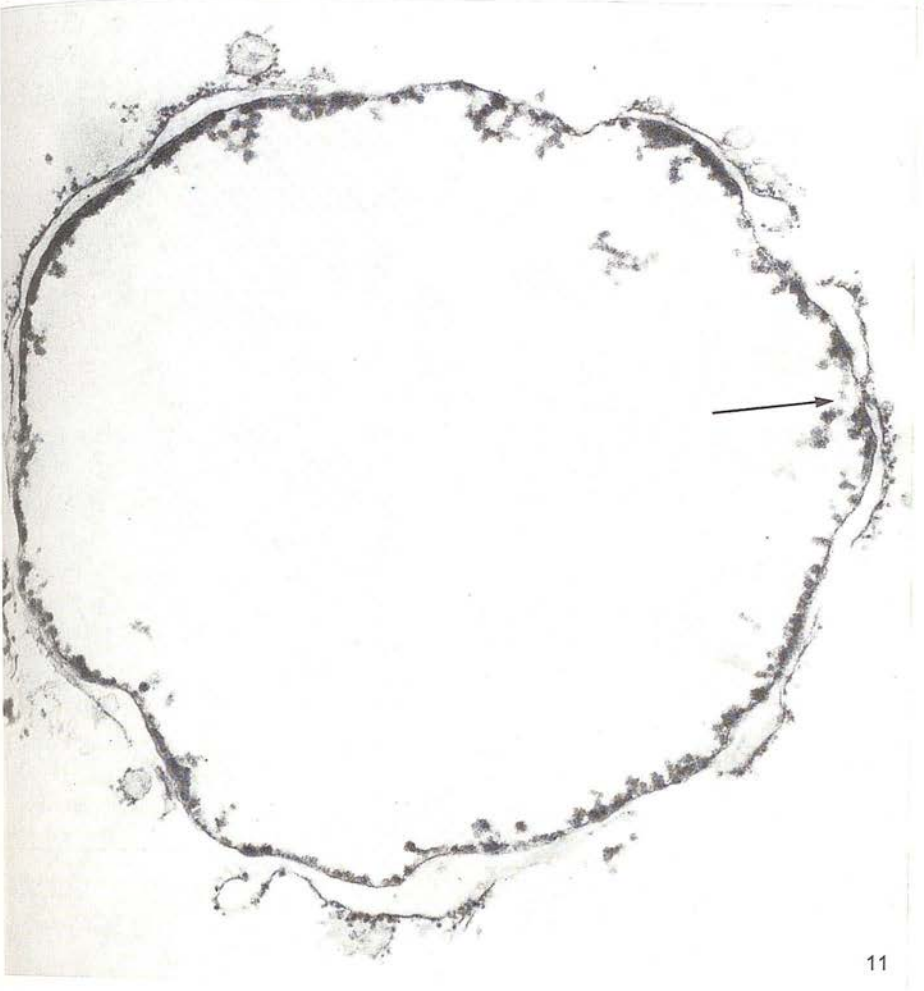
11

particles, and the fibrillar structures were observed occasionally, although they tended to be hidden by the vast excess of plasma membrane fragments. Thin sectioning, on the other hand, revealed more clearly the presence of mitochondria and membrane fragments with fibrils adhering to them (Fig. 14).

DISCUSSION

Electron microscopic study of the hemoglobin-free avian erythrocyte ghost, produced by osmotic hemolysis and repeated washing, reveals ultrastructural features which may tend to be hidden by hemoglobin in the intact erythrocyte. There have nevertheless been several earlier studies made using intact nucleated erythrocytes (*2*, *4*, *5*, *14*), some of which indicate the outer nuclear membrane and the presence of mitochondria. A method for producing chicken erythrocyte ghosts by treating erythrocytes with Sendai virus at 37° was employed by Schneeberger and Harris (*15*), but these workers did not expand greatly on ultrastructural detail, other than by noting that occasional mitochondria were present. The statement by Davoren and Sutherland (*3*), that on exposure to hypotonic conditions, the cell envelope of the avian erythrocyte collapses around the heavy nucleus, is not confirmed by the present study, since the avian ghost has been shown to retain the overall shape of the intact erythrocyte. The hypotonic conditions employed do not appear to cause serious alteration to the cell nuclei and mitochondria. It cannot, however, be ruled out that the initial osmotic shock, which produces one or more lesions in the plasma membrane, may not result in some damage to the nucleus and mitochondria which cannot be detected by electron microscopy. The swelling of the erythrocytes prior to hemolysis would be likely to break some of the fibrillar structures if they do, as suggested, extend between the outer nuclear membrane and the plasma membrane.

From the light and electron microscopic observation that the avian erythrocyte ghost nucleus tends to occupy a central position, it is thought reasonable to propose that some structural anchorage must be present. Since there are no cytoplasmic membrane structures present which could provide positional restriction for the ghost nuclei, it is thought that the fibrillar structures may fulfill this role. Recently Koehler (*9*) has shown by freeze cleaning that membrane associated fibrils (400–500 Å long) are located on the internal surface of the frog erythrocyte plasma membrane, but he was unable to detect any fibrils in chicken erythrocytes.

FIG. 13. The membrane fraction from ultrasonicated chicken erythrocyte ghosts. Negatively stained with 2% ammonium molybdate (pH 7.0). × 40 000.

FIG. 14. Thin-sectioned membrane fraction from turkey erythrocyte ghosts. Mitochondria and fibrils can be seen as well as plasma membrane fragments. × 37 500.

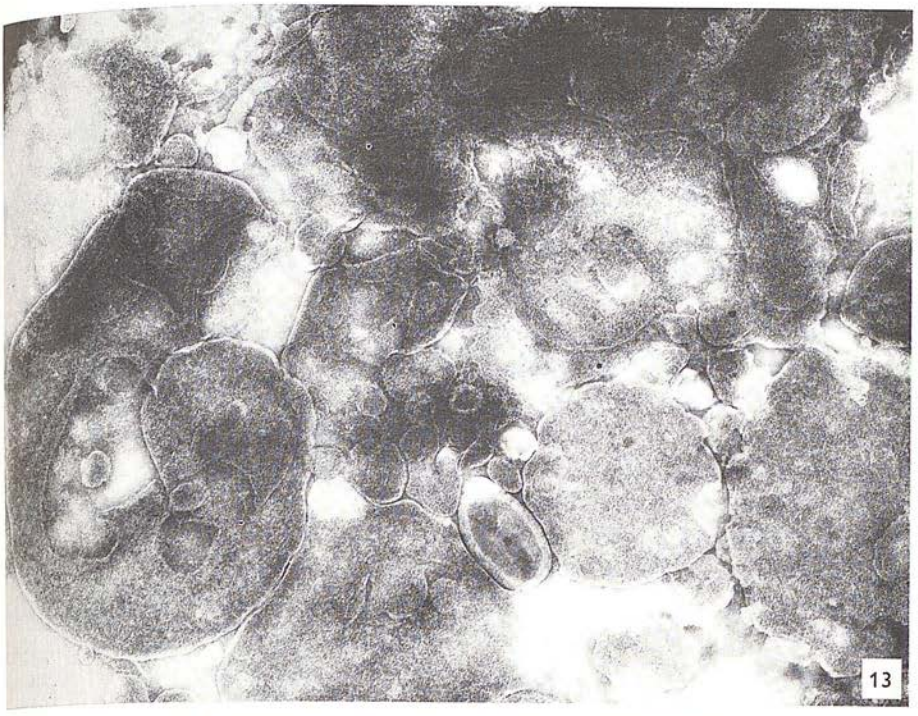

13

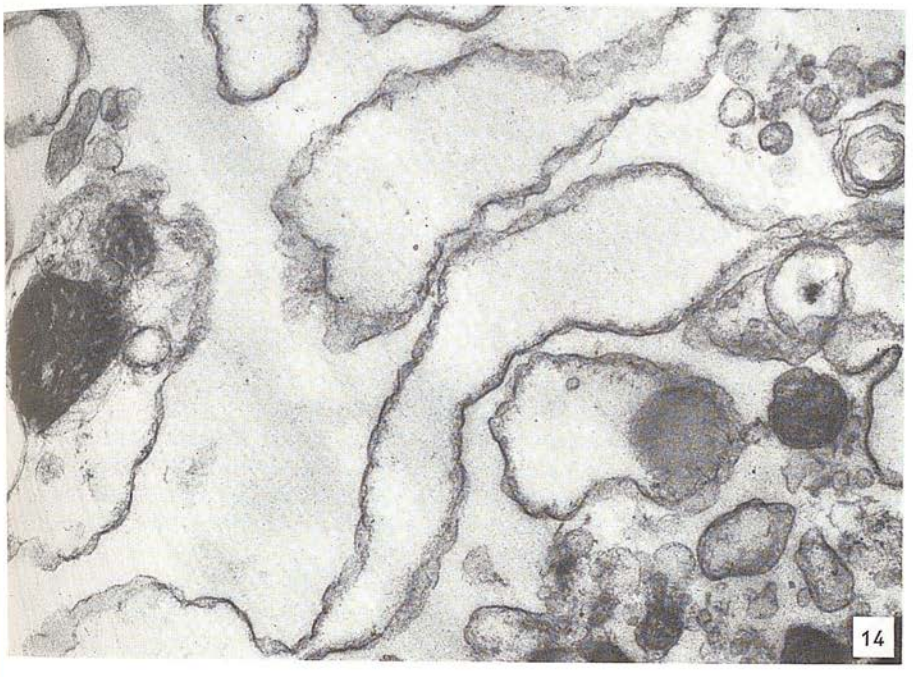

14

The nuclei prepared by the ultrasonication method presented above are generally in a good state of preservation, even though many of them have lost their outer nuclear membrane. Naturally, if too much ultrasonication was applied, a greater proportion of the nuclei appear to be damaged than if the appropriate amount of ultrasonication to only break open the plasma membrane was given. Perhaps the most important aspect of the ultrasonication method is the ease with which it can be controlled, subject to monitoring by light microscopy. Also, the fact that very large quantities of nuclei can be easily obtained may make the technique extremely valuable for providing nuclei for biochemical studies.

The membrane fraction can likewise be obtained in large quantities, and if required could easily be fractioned further to separate mitochondrial fragments from the plasma membrane fragments. Contrary to the pressure homogenization method of Davoren and Sutherland (*3*), which shattered the cell membrane to a "fine debris" (quote), the ultrasonication treatment results in membrane fragments of a wide size range. The presence of fibrils on one side of some of the membrane fragments conforms with the observations made on the avian ghost.

Whether or not these fibrils play a role other than that of supporting the nucleus and possibly the mitochondria, such as maintaining the overall shape of the plasma membrane, cannot yet be proposed with any certainty. There is currently much discussion in relation to the presence of fibrous proteins on the inner surface of the mammalian erythrocyte membrane (*10*, *13*, *16*) which may play a structural role in helping to maintain the biconcave disk shape of the erythrocyte. Behnke (*1*) has suggested that marginal microtubules probably do not play an important role in maintaining the shape of the fowl erythrocyte, although they may do so for some amphibian erythrocytes and blood platelets. It may therefore be reasonable to suggest tentatively that the attachment of the plasma membrane adjacent to the nucleus by fibrillar structures could assist in maintaining the shape of the avian erythrocyte as well as holding the nucleus in position.

REFERENCES

1. BEHNKE, O., *J. Ultrastruct. Res.* **31**, 61 (1970).
2. DAVIES, H. G., *J. Biophys. Biochem. Cytol.* **9**, 671 (1961).
3. DAVOREN, P. R. and SUTHERLAND, W. E., *J. Biol. Chem.* **238**, 3016 (1963).
4. EVERID, A. C., SMALL, J. V. and DAVIES, H. G., *J. Cell Sci.* **7**, 35 (1970).
5. FAWCETT, D. W. and WITEBSKY, F., *Z. Zellforsch. Mikrosk. Anat.* **62**, 785 (1964).
6. HARRIS, J. R., *In* Physiology and Biochemistry of the Domestic Fowl. Academic Press, New York, in preparation.
7. HARRIS, J. R. and BROWN, J. N., *Brit. Poultry Sci.* **12**, 95 (1971).
8. HUGHES, D. E. and CUNNINGHAM, V. R., *Biochem. Soc. Symp.* **23**, 20 (1963).

9. KOEHLER, J. K., *Z. Zellforsch. Mikrosk. Anat.* **85**, 1 (1968).
10. MARCHESI, V. T. and PALADE, G. E., *J. Cell Biol.* **35**, 385 (1967).
11. PALADE, G. E., *J. Exp. Med.* **95**, 285 (1952).
12. REYNOLDS, E. S., *J. Cell Biol.* **17**, 208 (1963).
13. ROSENTHAL, A. S., KREGNOW, F. M. and MOSES, H. C., *Biochim. Biophys. Acta* **196**, 254 (1970).
14. SCHJEIDE, O. A., MCCANDLESS, R. G. and MUNN, R. J., *Growth* **28**, 29 (1964).
15. SCHNEEBERGER, E. E. and HARRIS, H. J., *Cell Sci.* **1**, 401 (1966).
16. ZELANDER, T. and ERICSSON L., *J. Ultrastruct. Res.* **12**, 240 (1965).
17. ZENTGRAF, H., DEUMLING, B. and FRANKE, W. W., *Exp. Cell Res.* **56**, 333 (1969).

34 The Ultrastructure of the Erythrocyte

J. R. HARRIS[1]

Department of Zoology, University of Edinburgh, Edinburgh, Scotland

I. The Intact Avian Erythrocyte

Thin sections of the mature avian erythrocyte tend to show very little ultrastructural detail. The haemoglobin-filled cytoplasm usually draws away from the nucleus, leaving a gap. The typical double nuclear membrane is seldom observed. Some organelles resembling mitochondria are occasionally visible within the cytoplasm, but they are never entirely convincing (Fig. 1). There are rarely indications of endoplasmic reticulum or other intracellular membranes (Fig. 2), and even the plasma membrane is usually hidden by the haemoglobin. A recent study by Behnke (1970) has, however, shown that marginal microtubules can be detected within the fowl erythrocyte (Fig. 3). These avian microtubules are apparently much more labile than those present in amphibian erythrocytes, and may not contribute towards the maintenance of the cell shape, as they undoubtedly do in some amphibian erythrocytes and blood platelets.

II. The Avian Erythrocyte Ghost

In order to investigate more precisely the ultrastructure of the avian erythrocyte, a method for the preparation of haemoglobin-depleted

[1] Present address: Department of Cancer Research, University of Nottingham.

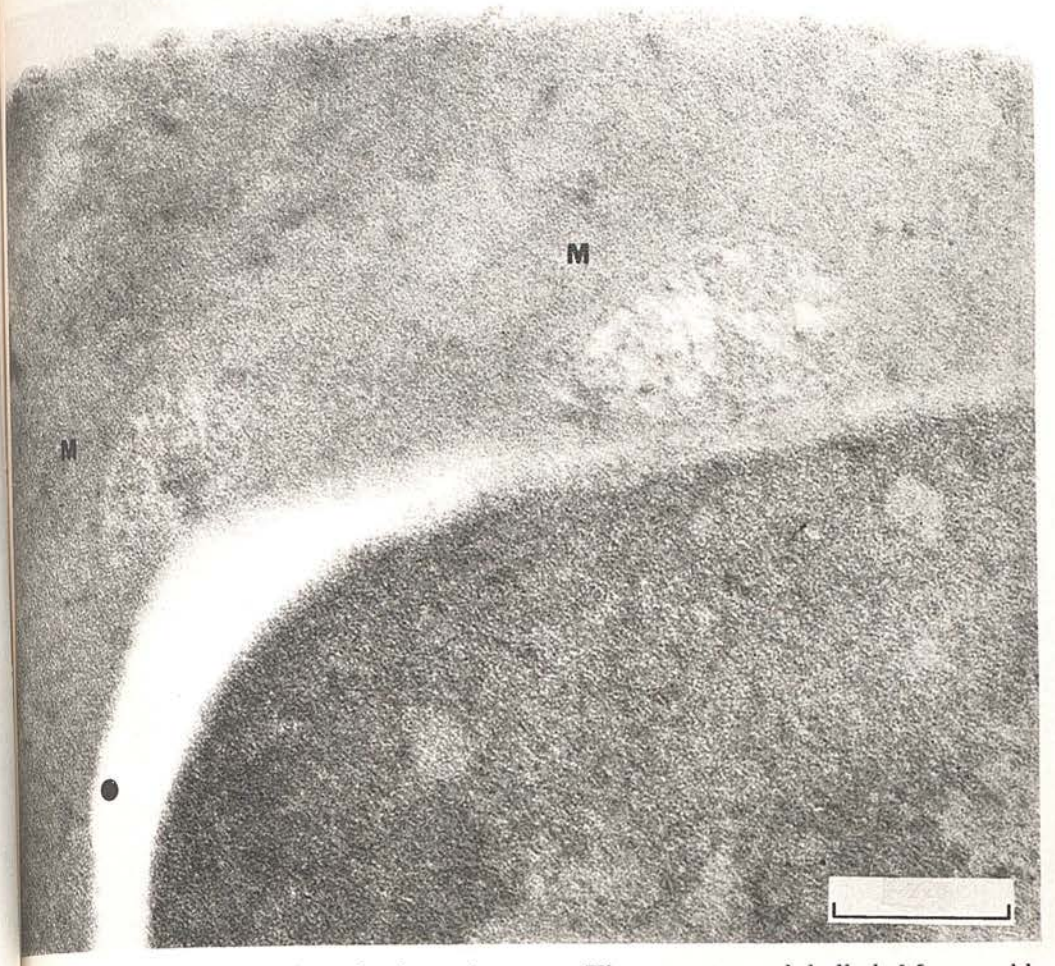

Fig. 1. A thin section through a fowl erythrocyte. The structures labelled M resemble mitochondria. There is a noticeable gap between the nucleus and the haemoglobin-filled cytoplasm. Neither the nuclear membranes nor the plasma membrane are clearly defined. The scale marker indicates 200 nm.

erythrocyte ghosts from fowl and turkey erythrocytes has been developed by Harris and Brown (1971). This method follows the concepts employed in recent years by several groups of workers for the preparation of haemoglobin-free mammalian erythrocyte ghosts (Dodge *et al.*, 1963; Marchesi and Palade, 1967; Harris, 1969). Basically, washed fowl or turkey erythrocytes are haemolysed in a Tris-HCl buffer (pH 7·4) containing 4 mM $MgCl_2$, and are then repeatedly washed in the same buffer containing 0·3 M sucrose as well as 4 mM $MgCl_2$. No aggregation problems are encountered on resuspending the ghosts for each successive wash. The final product can be obtained in a haemoglobin-free condition. Phase-contrast microscopy provides a rapid means of monitoring the integrity of the ghosts throughout the preparation. This technique reveals that the avian erythrocyte ghosts retains the nucleus and also the ellipsoid shape of the intact erythrocyte (see Fig. 3).

Fig. 2. Fowl erythrocyte showing a degenerating mitochondrion (M) and a Golgi apparatus (GA). Fixed by glutaraldehyde/osmium; × 64,000. It is extremely rare to be able to see mitochondria in the erythrocyte when haemoglobin is present. By courtesy of W. G. Siller, Poultry Research Centre, Edinburgh.

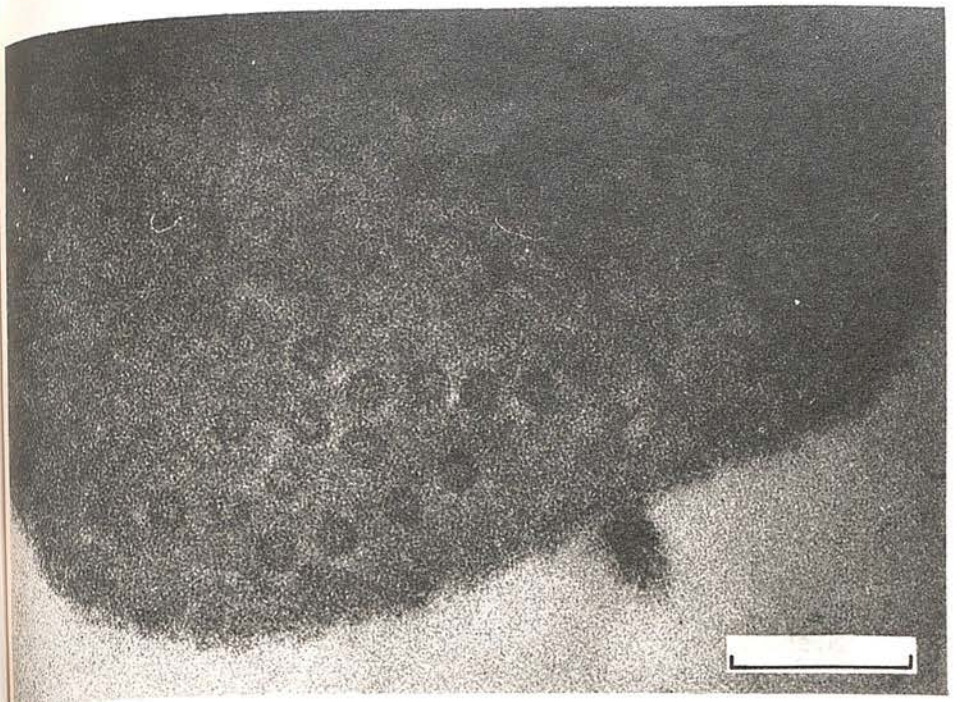

Fig. 3. A thin section of part of a fowl erythrocyte showing the terminal microtubules. The scale marker indicates 100 nm.

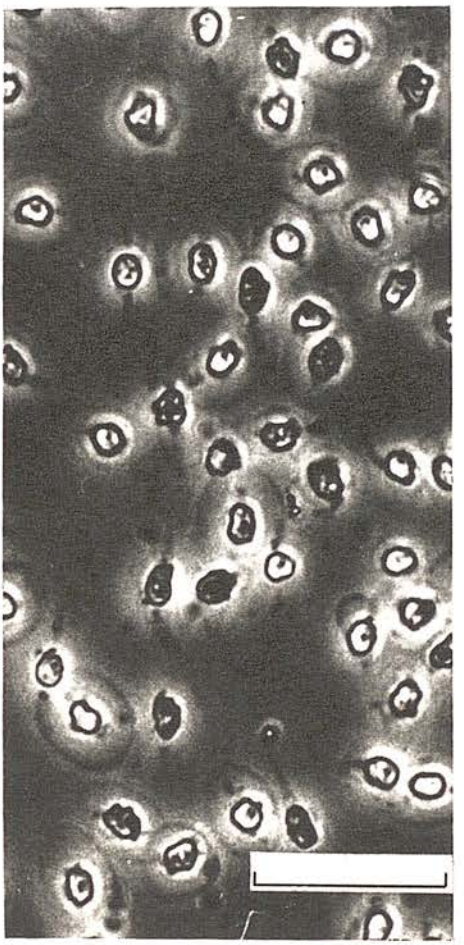

Fig. 4. A phase contrast micrograph of a preparation of haemoglobin-free turkey erythrocyte ghosts. The scale marker indicates 20 μm.

III. Electron Microscopy of the Avian Erythrocyte Ghost

Electron microscopy has confirmed the observations made by light microscopy and has been able to extend considerably ultrastructural knowledge of the avian erythrocyte.

A. THE NUCLEUS

A thin section through a turkey erythrocyte ghost is shown in Fig. 5. The absence of haemoglobin is immediately noticed as is the centrally positioned nucleus, which can be seen clearly to have an outer nuclear membrane. The inner nuclear membrane is almost hidden by the closely adhering chromatin. The state of granularity of the chromatin was found to vary with the concentration of magnesium in the suspending buffer. The preparation from which the ghost in Fig. 5 was taken contained 4 mM $MgCl_2$ and the chromatin is condensed and granular. In the absence of magnesium, the chromatin appears very diffuse and often the nuclei burst allowing the chromatin to enter the cytoplasmic compartment of the ghost (see Fig. 6).

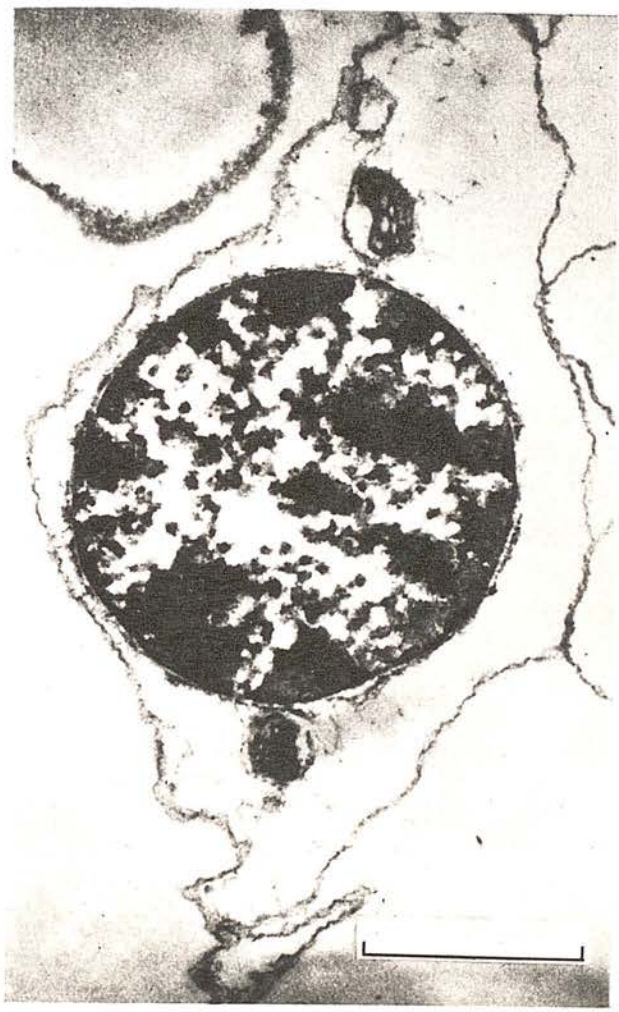

Fig. 5. A thin section through a turkey erythrocyte ghost. The scale marker indicates 1 μm.

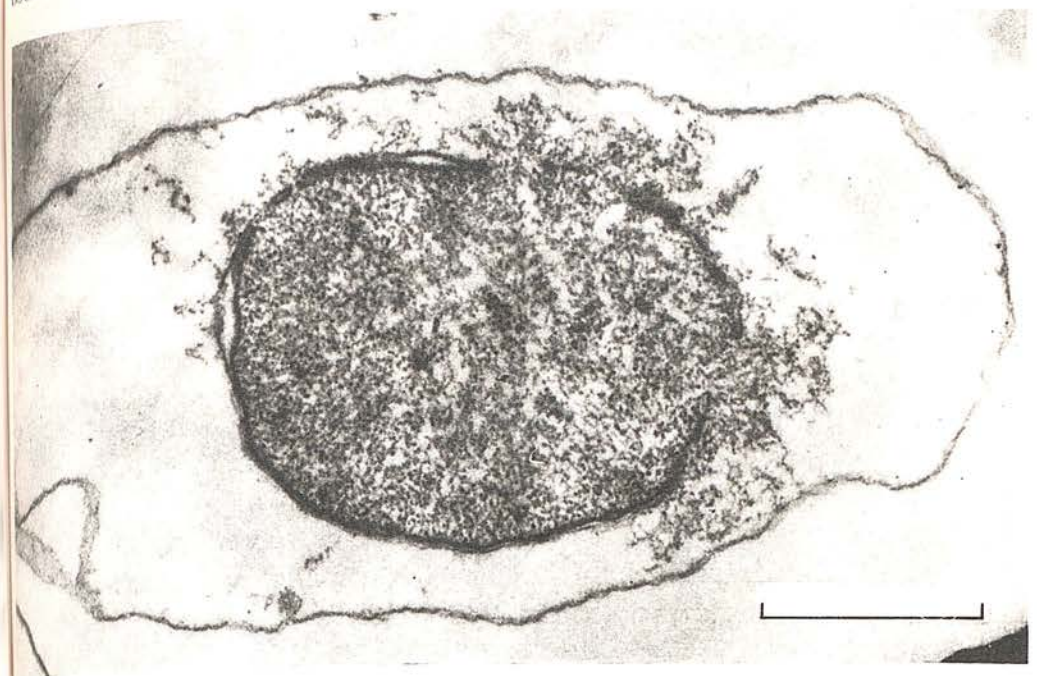

Fig. 6. A thin section through a turkey erythrocyte ghost. This preparation contained no magnesium, and the chromatin is seen to be escaping from the nucleus into the cytoplasmic compartment. The scale marker indicates 1 μm.

B. THE PLASMA MEMBRANE

As mentioned above, the plasma membrane of the intact avian erythrocyte is not easily distinguishable in thin sections. However, once the haemoglobin has been liberated the plasma membrane becomes readily visible as shown in Fig. 5. At higher magnifications the typical "tram-line" profile of the thin-sectioned membrane is visible in regions where the membrane lies parallel to the electron beam (see Fig. 7). The hazy membrane image results from the membrane twisting within the thin section. By negative contrast staining with ammonium molybdate the plasma membrane of the avian erythrocyte ghost can be seen to have a very smooth surface texture (see Fig. 8). The pit-like structures observed by Harris and Agutter (1970), on human erythrocyte ghosts by negative staining, are not present on either fowl or turkey erythrocyte ghosts.

C. THE MITOCHONDRIA

Within the cytoplasmic compartment of the ghost shown in Fig. 4 can be seen densely stained mitochondria. The christae within these mitochondria do not appear as clear as those observed in the mitochondria of other cell types. A possible reason for this is that the erythrocyte mitochondria may store iron which can then be supplied for haemoglobin synthesis. Biochemical evidence has shown that the mature avian erythrocyte is still slowly synthesising haemoglobin. There is, however, a notable absence of endoplasmic

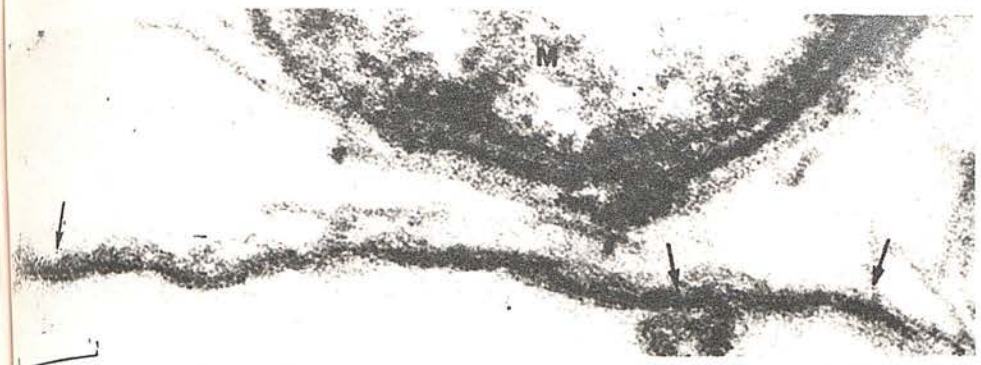

Fig. 7. A region of turkey erythrocyte plasma membrane where the typical "tram-line" membrane profile can be seen (arrowed). The scale marker indicates 100 nm.

Fig. 8. Part of the plasma membrane of a fowl erythrocyte ghost, negatively stained with ammonium molybdate (pH 7·0). The scale marker indicates 1 μm.

g. 3. Part of a thin-sectioned turkey erythrocyte ghost. Fibrillar structures can be seen to
between the outer nuclear membrane and the plasma membrane. The scale marker
icates 200 nm.

reticulum within the avian erythrocyte ghost. Free ribosomes would in all probability escape along with the haemoglobin during the washing procedures applied to the ghosts.

D. THE FIBRILLAR STRUCTURES

Surrounding both the nucleus and the mitochondria within the avian erythrocyte ghost can be seen many fine fibrillar structures, apparently extending between these organelles and the adjacent plasma membrane. Figure 9 shows a high magnification of a region in which there are fibrils passing from the outer nuclear membrane to the plasma membrane. Significantly, there are very few of these fibrils within the extremities of the ghost; that is within the terminal regions, well away from the nucleus. It might thus be reasonable to postulate that these fibrils provide some kind of support or anchorage for the nucleus and possibly also the mitochondria. By both phase-contrast microscopy and electron microscopy the nucleus of the intact avian erythrocyte and its ghost is observed to be centrally located within the cell, so some structural component must hold the nucleus in this position. The swelling to which the cells are subjected during haemolysis might be expected to damage some of the fibrils if they are supports for the nucleus, but apparently sufficient are left intact to hold the nucleus at the centre of the ghost.

IV. General Discussion

From the results briefly presented above, it is readily apparent that the electron microscopic study of the avian erythrocyte ghost reveals much more ultrastructural detail than does the study of the intact erythrocyte. The method used for producing the erythrocyte ghosts is, however, open to several criticisms. Firstly, severe alteration might be produced by the initial haemolysis, within the intracellular organelles as well as to the plasma membrane. Secondly, the removal of the normal internal environment and its replacement by the Tris-HCl-$MgCl_2$-sucrose buffer, may again cause organelle disruption or fail to preserve the organelles in their normal ultrastructural condition. Finally, the haemolysis may permit the escape of small intracellular organelles, such as ribosomes, if they are not membrane bound.

Answers to some fundamental questions regarding the ultrastructure of the avian erythrocyte have nevertheless been suggested. Biochemical evidence has indicated that avian erythrocytes are respiring cells, yet as shown above, electron microscopy of the average intact erythrocyte does not convincingly show the presence of mitochondria. The presence of mitochondria within the avian erythrocyte ghost is, however, clearly shown. Likewise, the typical double nuclear membrane and the plasma membrane which are not

clearly definable in thin sections of avian erythrocytes, are clearly visible in thin sections of the avian erythrocyte ghost. The explanation put forward for the function of the hitherto unknown fibrils surrounding the nucleus and mitochondria within the avian erythrocyte ghost remains tentative. It is difficult to envisage their fulfilling a role other than that of providing a holding or anchorage mechanism for these organelles, though they may concurrently help to maintain the shape of the erythrocyte. The absence of the marginal microtubules within the avian erythrocyte ghost strongly suggests that they have undergone dissociation during the haemolysis and washing procedures. The dissociated form will, in all probability, be lost together with the haemoglobin and other soluble cytoplasmic components.

Acknowledgements

The author wishes to make it known that this study was undertaken at the suggestion of Dr. D. J. Bell, Department of Physiology, University of Edinburgh. The collaboration and technical assistance provided by Mr. J. N. Brown throughout the investigation is gratefully acknowledged. Electron microscope facilities were provided by Professor W. E. Watson, Department of Physiology, University of Edinburgh.

References

Finke, O. (1970). *J. Ultrastruct. Res.* **31**, 61–75.
Fridge, J. T., Mitchell, C. and Hanahan, D. J. (1963). *Archs Biochem. Biophys.* **100**, 119–130.
Harris, J. R. (1969). *Biochim. biophys. Acta* **188**, 31–42.
Harris, J. R. and Agutter, P. (1970). *J. Ultrastruct. Res.* **33**, 219–232.
Harris, J. R. and Brown, N. (1971). *Br. Poult. Sci.* **12**, 95–99.
Marchesi, V. T. and Palade, G. E. (1967). *J. Cell Biol.* **35**, 385–404.

Micron, 1978, Vol.: 9, pp. 117–125.
© Pergamon Press Ltd. Printed in Great Britain

0047–7206/78/0901–0117 $02.00/0

ULTRASTRUCTURAL AND BIOCHEMICAL STUDIES ON AVIAN ERYTHROCYTE PLASMA MEMBRANE AND NUCLEAR ENVELOPE

JAMES R. HARRIS, PAUL S. AGUTTER* and JEREMY F. MILNE

Biomembrane Unit, Division of Biochemistry, North East London Polytechnic, Romford Road, London E15 4LZ, England

(*Received* 19 *January* 1978; *received for publication* 7 *March* 1978)

Abstract—Procedures are described for the isolation and purification of chicken erythrocyte plasma membrane and nuclear envelope. The membranes have been studied by electron microscopy using negative staining with ammonium molybdate and conventional thin sectioning. Polyacrylamide gel electrophoresis of the sodium dodecylsulphate solubilized membranes shows that the nuclear envelope and the plasma membrane are composed of different proteins. Chemical analysis of the membranes shows that there is a low, but constant, amount of nucleic acid present. Enzymic analysis for ATPase shows that both the nuclear envelope and plasma membrane contain the magnesium stimulated ATPase, but only the plasma membrane ATPase shows further stimulation in the presence of sodium and potassium.

INTRODUCTION

The mature avian erythrocyte has a metabolically dormant nucleus with respect to messenger RNA synthesis. It is, therefore, of interest to perform biochemical and ultrastructural studies on avian erythrocyte nuclear envelope and to compare these results with those obtained from the nuclear envelope of more active tissues such as mammalian liver and amphibian oocytes. In addition, the availability of avian erythrocyte plasma membrane for comparison with the nuclear envelope and with the plasma membrane of the erythrocytes of other species, is of considerable importance.

The procedures used for producing haemoglobin-free chicken erythrocyte ghosts by osmotic haemolysis and repeated washing (Harris and Brown, 1971a) and for releasing the nuclei of these erythrocyte ghosts by controlled ultrasonication (Harris and Brown, 1971b) have been further extended as a comparative study of the plasma membrane and nuclear envelope. A new method for the isolation of the nuclear envelope has been developed, which uses as a starting material the purified nuclei produced by the ultrasonication treatment. Plasma membrane fragments are also released by the ultrasonication, along with mitochondria and trace quantities of other organelles. The nuclear envelope, which is obtained following dispersal of the chromatin and digestion with deoxyribonuclease consists of nuclear 'ghosts' and torn membrane sheets on which the nuclear pore complexes are readily detected by negative staining electron microscopy. Both the plasma membranes and nuclear envelopes are finally purified by isopycnic banding on sucrose gradients. This floatation procedure is considered to be the most satisfactory method for removing contaminants of higher or lower density than the membrane species sought, and has been used successfully by the authors for obtaining the nuclear envelope from rat liver and hepatoma (Price *et al.*, 1972; Harris and Milne, 1974).

Several studies have been undertaken on plasma membranes and nuclear envelopes from chicken erythrocytes (Blanchet, 1974; Weise and Ingram, 1973; Zentgraph *et al.*, 1971). The procedures described employ the use of high speed blade homogenization (Zentgraph *et al.*, 1971), the French pressure cell (Blanchet, 1974) and nitrogen cavitation (Weise and Ingram,

*Present address: Department of Biology, Napier College of Commerce and Technology, Colinton Road, Edinburgh EH10 5DT, Scotland.

1973) to produce disruption of intact erythrocytes rather than haemoglobin-free erythrocyte ghosts. One of the major problems that all investigators interested in this system have to face is the presence of contaminating material in their 'purified' membrane samples. This may be in the form of residual haemoglobin or other cytoplasmic proteins, residual chromatin, or cross-contamination because of the incomplete separation of the plasma membrane from the nuclei during the homogenization treatment. The presence of plasma membrane in samples of nuclei purified following pressure homogenization (Blanchet, 1974) is readily detectable in the published thin sections of this material. Only samples of nuclei which show no such contamination have been included in the present investigation. Extensive trial experiments have been performed in an attempt to separate the chromatin from the nuclear envelopes of chicken erythrocyte nuclei. Basically a low ionic strength treatment is given to the nuclei in the absence of divalent cations, which bring about a decondensation of the chromatin (Harris and Milne, 1975). The chromatin is then solubilized by digestion with deoxyribonuclease I, in a manner similar to that employed for the isolation of rat liver nuclear envelope (Harris and Milne, 1974). Incomplete release of chromatin was encountered, which resulted in the nuclear envelope passing completely through a 1.0M to 2.0M sucrose gradient, until heparin was added to the buffer system used for decondensing the chromatin. Heparin was found to assist the dispersal of the chicken erythrocyte chromatin, in agreement with the observations of Bornens (1973), who claimed to be able to solubilize the chromatin of rat liver nuclei with this reagent. It should be noted that the technique of ultrasonication has been used to release the nuclear envelope of mammalian liver (Agutter, 1972; Franke *et al.*, 1970; Kashnig and Kasper, 1969), but in view of the fact that this procedure produces extensively fragmented material it is not considered to be a desirable approach in the present context, as the aim of the studies has been to produce intact nuclear envelope 'ghosts' and large sheets of torn nuclear envelope.

Studies very similar to our own have been performed by Jackson (1975) who dispersed the chromatin of chicken erythrocyte ghosts with sodium tetrathionate and phenylmethane-sulphonyl fluoride prior to digestion with deoxyribonuclease. It is notable, however, that Jackson (1975) did not separate the plasma membrane from the nuclei prior to performing this treatment. He therefore investigated material that must be considered a mixture of plasma and nuclear membranes.

MATERIALS AND METHODS

Preparation of haemoglobin-free erythrocyte ghosts

The procedure developed by Harris and Brown (1971a,b) has been used. Chicken blood was collected directly from the carotid arteries into heparinized phosphate buffered saline (PBS, Oxoid) at the time of sacrifice. The erythrocytes were then washed three times with PBS at 3000 rev/min (1000*g*) at 4°C in the Beckman J-21 centrifuge using the JA-10 rotor. The buffy coat of white cells was removed at each wash. The washed packed cells were then split into 40ml quantities and either used directly or stored at −20°C until required. The erythrocytes were haemolysed by the addition of 400ml 10mM Tris–HCl buffer (pH 7.4) containing 4mM magnesium chloride to stabilize the nuclei. The erythrocyte ghosts were then washed repeatedly in the haemolysis buffer with 250mM sucrose present at alternate washes until free from haemoglobin, with centrifugation at 5000 rev/min (2000*g*) for 10min at 4°C.

Preparation of purified nuclei and a crude plasma membrane fraction from haemoglobin-free erythrocyte ghosts

The nuclei of haemoglobin-free chicken erythrocyte ghosts were released by bringing about disruption of the plasma membrane by ultrasonication. Erythrocyte ghosts (derived from 40ml packed cells) were made to 80ml in 250mM sucrose, 10mM Tris–HCl (pH 7.4), 4mM magnesium chloride and treated for 2min at an amplitude setting of 6μm in the MSE 150watt ultrasonic disintegrator. The material was cooled throughout this procedure by an ice bath. The suspension of disrupted ghosts was then centrifuged at 3000rev/min (1000*g*) in the Beckman JA-20 rotor at 4°C, for 10min. The cloudy supernatant, which contains predominantly plasma membrane fragments and the few mitochondria of the chicken erythrocyte was decanted leaving a firm pellet of nuclei. This pellet was then washed two times at 3000rev/min with the sucrose buffer and the slightly cloudy

supernatants containing plasma membrane were pooled with that from the first centrifugation, leaving a pellet of creamy-white nuclei. When studied by thin sectioning the absence of intact erythrocyte ghosts and plasma membrane fragments is readily apparent. The nuclei show the presence of both the outer and inner nuclear membranes.

Preparation of purified plasma membrane

The pooled 3000rev/min supernatants taken following the ultrasonication treatment were centrifuged for 30min at 20,000rev/min (48,000*g*) in the JA-20 rotor. A firm pellet was obtained which was light brown-yellow in coloration. This material was resuspended in 2ml 10mM Tris–HCl (pH 7.4) and layered over a linear 1.0 to 2.0M sucrose gradient prepared in the same buffer. After centrifugation for 16hr at 25,000rev/min (83,000*g*) the single broad band of membrane positioned approx one-third of the way down the gradient at an isopycnic density of 1.175 ± 0.004 was taken as purified plasma membrane. Traces of dense material at the bottom of the gradient were discarded. The plasma membrane was washed two times with 10mM Tris–HCl (pH 7.4) at 20,000rev/min (48,000*g*) for 30min to remove the sucrose. The material was then used directly for the biochemical and electron microscopic studies or was stored at $-20°C$ as 0.5ml aliquots. The yield of material was approx 0.2mg plasma membrane protein derived from 1.0ml packed erythrocytes.

Preparation of purified nuclear envelope

The nuclei obtained from 40ml of packed erythrocytes were suspended in 800ml of 2mM sodium phosphate buffer (pH 7.4). The suspension immediately became gelatinous because of the dispersal of the chromatin and this was increased further by the addition of heparin to a concentration of 12.5 U/ml. After 5min at room temperature the extremely viscous dispersion was treated with deoxyribonuclease I (Sigma type DN-100) at a concentration of 10μg/ml for 20min at 30°C. After 5min incubation 0.2ml of 1.0M $MgCl_2$ was added, giving a magnesium concentration of 0.25mM, to activate the deoxyribonuclease. By phase contrast micronuclear 'ghosts' can be observed, which are readily distinguished from intact nuclei.

After the incubation period the nuclear envelopes were pelleted by centrifugation at 10,000rev/min (12,000*g*) for 30min and then washed three times in 10mM Tris–HCl buffer (pH 7.4) with centrifugation at 20,000rev/min (48,000*g*) for 5min. Most of the solubilized chromatin is released during these centrifugal washes, and a further purification of the nuclear envelope is achieved by isopycnic banding on a 1.0 to 2.0M linear sucrose gradient prepared in 10mM Tris–HCl buffer (pH 7.4). Centrifugation was performed for 16hr at 25000rev/min (83,000*g*). The nuclear envelope banded approximately one-third of the way down the gradient at a density of 1.165 ± 0.008. Some material always extended further down the gradient, and undoubtedly represented nuclear envelope that contained greater quantities of bound chromatin than the main band of membrane. A small pellet of material was usually present and was discarded. The nuclear envelope band was washed two times with 10mM Tris–HCl (pH 7.4) at 20,000rev/min (48,000*g*) for 10min to remove the sucrose. The material was then used directly or stored at $-20°C$ as 0.1ml quantities. The yield of nuclear envelope was approx 0.1mg envelope protein derived from 1.0ml packed erythrocytes.

Electron microscopy

Negatively stained specimens were prepared on carbon coated grids using the plasma membrane and nuclear envelope material directly after the removal of sucrose by centrifugal washing. The single drop technique (Harris and Agutter, 1970) was used for applying the membrane suspension and negative stain (2% ammonium molybdate, pH 7.0). For thin sectioning the membrane material was fixed overnight at room temperature in Dalton's Chrome-Osmium (Dalton, 1955), dehydrated with graded ethanols and epoxypropane before embedding in TAAB epoxy resin. Thin sections were cut using glass knives with a Reichert OM U2 ultramicrotome and were post stained with uranyl acetate and lead citrate. Specimens were studied in a Philips EM 301S electron microscope at an accelerating voltage of 80kV. Photographs were taken on Ilford 3¼in. × 4in. plates, type EM6.

Polyacrylamide gel electrophoresis

40μl quantities of the membrane samples, at a protein concentration of approx 2.0mg/ml, were

solubilized by the addition of 10μl 10% sodium dodecyl sulphate, 5% 2-mercaptoethanol in 5mM Tris–HCl (pH 8.0) by heating for 1min in a boiling water bath. 10μl and 20μl quantities were then electrophoresed at 3mA per tube on 7% polyacrylamide gels in a 50mM Tris–HCl buffer system at pH 8.0. The buffer in the cathode compartment contained 0.1% sodium dodecyl sulphate and that in the anode compartment contained Tris–HCl alone. After the current had passed for 1hr the gels were removed and fixed for 1hr in 20% trichloracetic acid, washed for 4hr in 10% acetic acid, 20% methanol, 70% water and then stained overnight in the same solvent mixture containing 0.01% Coomassie blue dye. Background stain was then removed by washing in the acetic acid methanol mixture and the pattern of protein bands recorded on 35mm film (Ilford, type FP4).

ATPase assay

Approximately 0.1mg quantities of membrane protein were incubated with 1.0mM tetrasodium ATP, 1.0mM magnesium chloride, 25mM triethanolamine–HCl buffer (pH 7.5) for 30min at 35°C. The reaction was stopped by cooling in an ice bath and the release of inorganic phosphate from ATP determined by the method of Wohler and Wollenberger (1958).

Chemical analysis

Protein was determined by the method of Lowry *et al.* (1951), as modified by Maddy and Spooner (1970). Lipids and nucleic acids were separated by precipitating 0.2ml quantities of the membrane suspension (protein concentration 2.0mg/ml) with 1.0ml of 10% trichloracetic acid. The precipitate was washed once with cold methanol and then three times with a 2:1 chloroform–methanol mixture. The methanol and chloroform–methanol extracts were pooled and mixed with an equal volume of 1.0% sodium chloride, following the method of Folch *et al.* (1956). The mixture was spun in a bench centrifuge to separate the phases and the top aqueous phase, along with the material at the interface, was discarded. The remaining chloroform phase, containing the extracted lipids was evaporated to dryness using a rotary film evaporator. The dried lipids were then hydrolysed by heating with 0.4ml of concentrated (7.2M) perchloric acid. The inorganic phosphate thus released was determined by a modification of the method of Berenblum and Chain (1938). The solution was made up to 2.6ml with distilled water, and 1.5ml of 0.012M ammonium molybdate 2.25M sodium chloride was added. After mixing 4.0ml of ethyl acetate was added, the two phases mixed and allowed to separate. The upper ethyl acetate layer was drawn off and 5.0ml 40% stannous chloride–2.8% sulphuric acid–2.0M sodium chloride was added. The solution was mixed and left to stand for 10min. The upper layer was drawn off and the absorbance at 700nm measured immediately. The phosphate content thus determined was multiplied by 25 to give an estimate of the phospholipid content of the samples (Kopacyzk *et al.*, 1966). The pellet remaining after the final chloroform–methanol wash of the trichloroacetic acid precipitate was resuspended in 1.0ml of 1.0M perchloric acid and incubated at 70°C for 20min. The solution was then made up to 2.0ml with 1.0M perchloric acid and two samples of 1.0ml taken. One sample was analysed for DNA by the method of Giles and Myers (1965) and the other for RNA by the method of Ashwell (1957) using orcinol. The coloration produced by DNA in the orcinol reagent was taken into account.

RESULTS

Electron microscopy

The purified chicken erythrocyte plasma membranes and nuclear envelope have been studied by conventional thin sectioning and by negative staining with ammonium molybdate. Figures 1 and 2 show representative regions of thin sectioned plasma membrane and nuclear envelope, respectively. The plasma membrane is mostly in the form of enclosed vesicles, whereas the nuclear envelope tends to be in the form of torn sheets. This interpretation is supported by negative staining. Figure 3 shows plasma membrane vesicles and Fig. 4 shows torn pieces of nuclear envelope, negatively stained with 2% ammonium molybdate. Nuclear pore complexes are visible in Fig. 4. Some relatively intact nuclear ghosts are present in the nuclear envelope suspension, along with the torn membranes, as shown in Fig. 5. In general, the nuclear pore complexes appear to be partially disrupted, in that some of the annular material as well as the central granule appears to have been lost. It is readily apparent that there is a

Fi

Fi

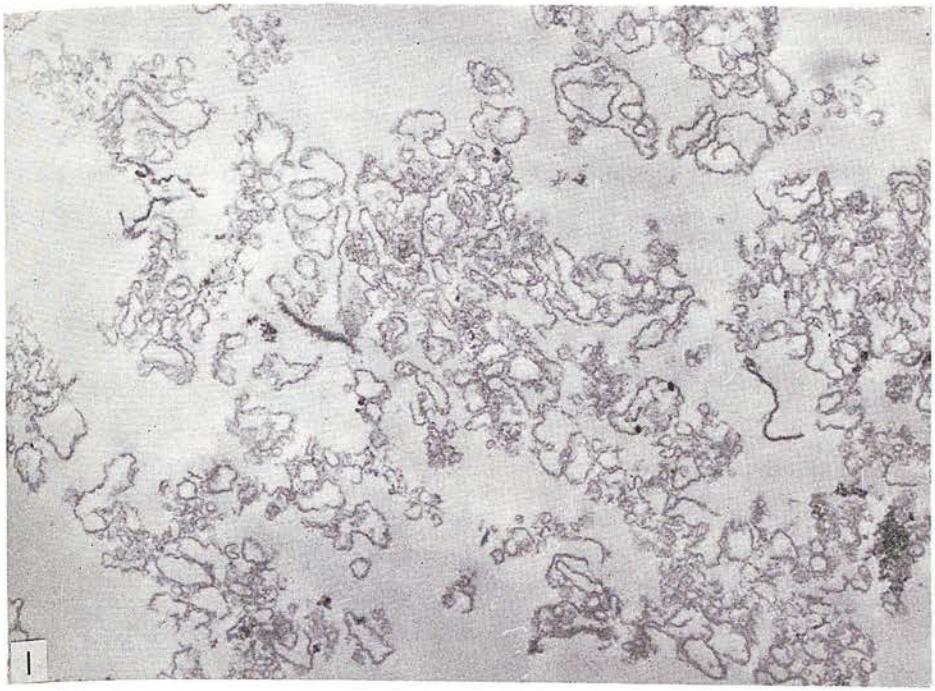

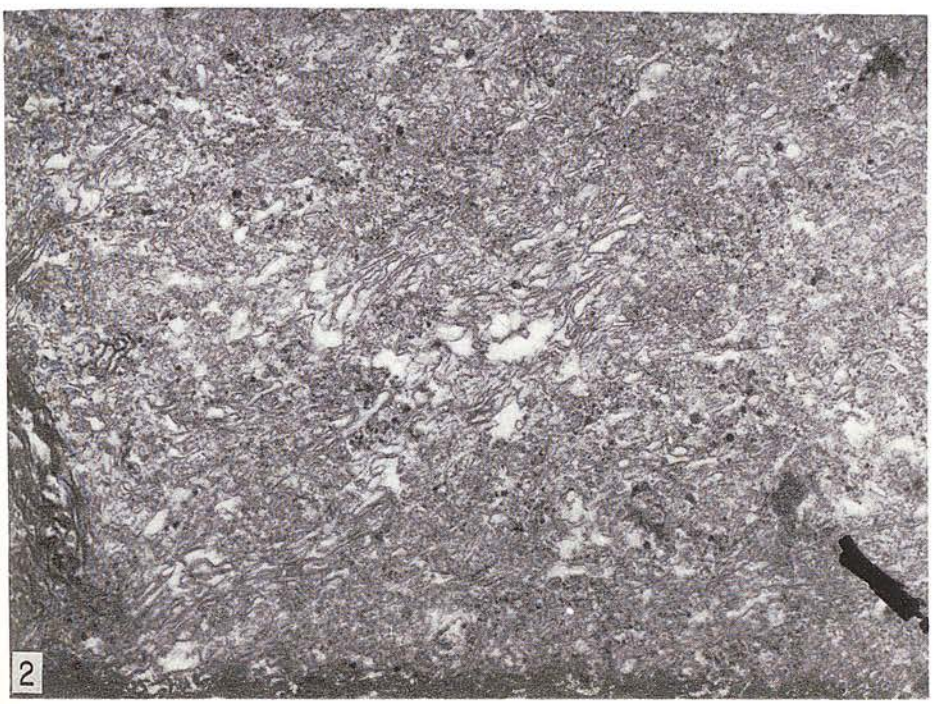

Fig. 1. Thin sectioned chicken erythrocyte plasma membrane after purification by isopycnic banding on a sucrose density gradient. ×18,000.

Fig. 2. Thin sectioned chicken erythrocyte nuclear envelope after purification by isopycnic banding on a sucrose density gradient. ×18,000.

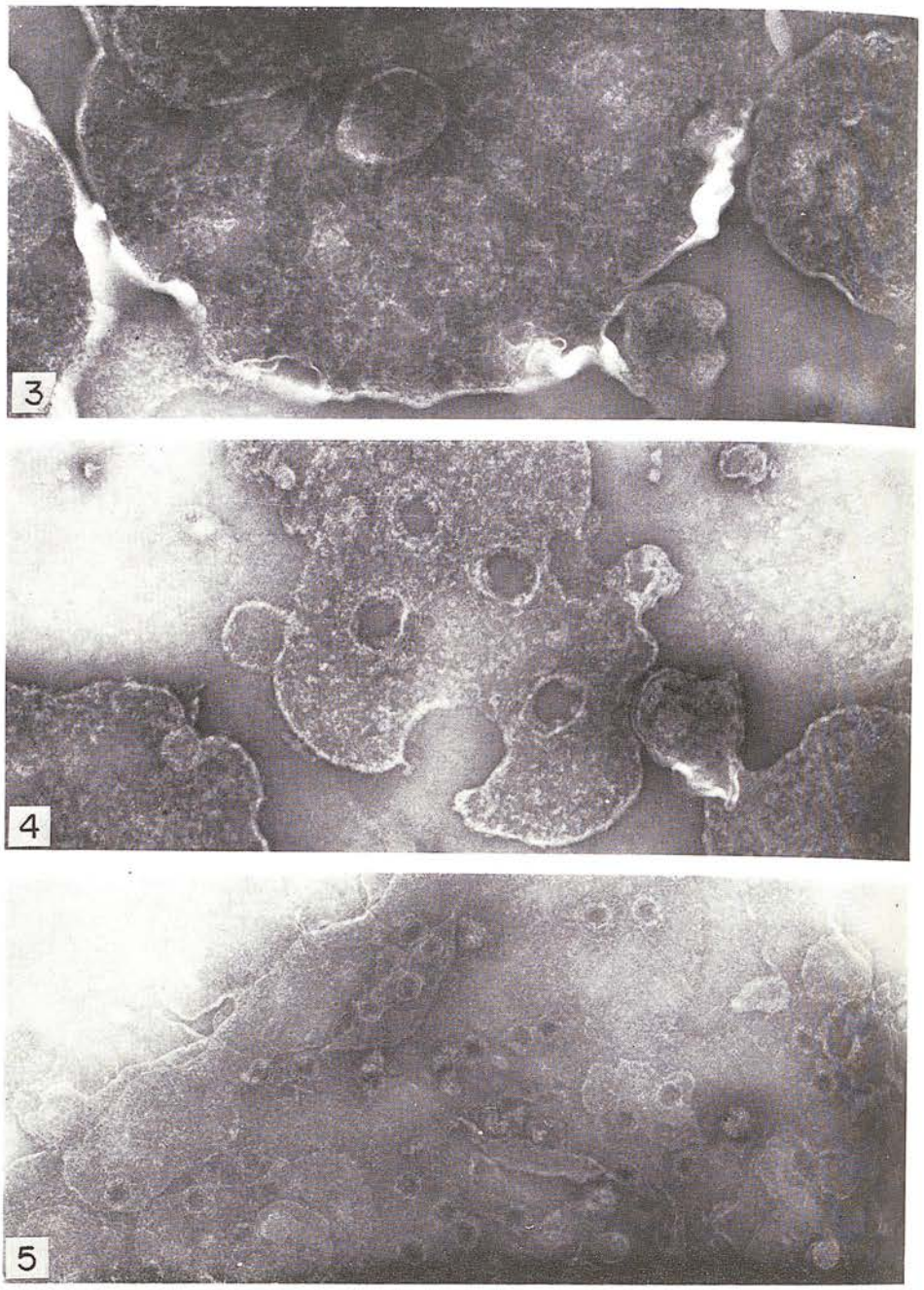

Fig. 3. Purified chicken erythrocyte plasma membrane, negatively stained with ammonium molybdate. ×94,000.

Fig. 4. Purified chicken erythrocyte nuclear envelope, negatively stained with ammonium molybdate. ×94,000.

Fig. 5. Part of a purified chicken erythrocyte nuclear ghost, negatively stained with ammonium molybdate. ×46,000.

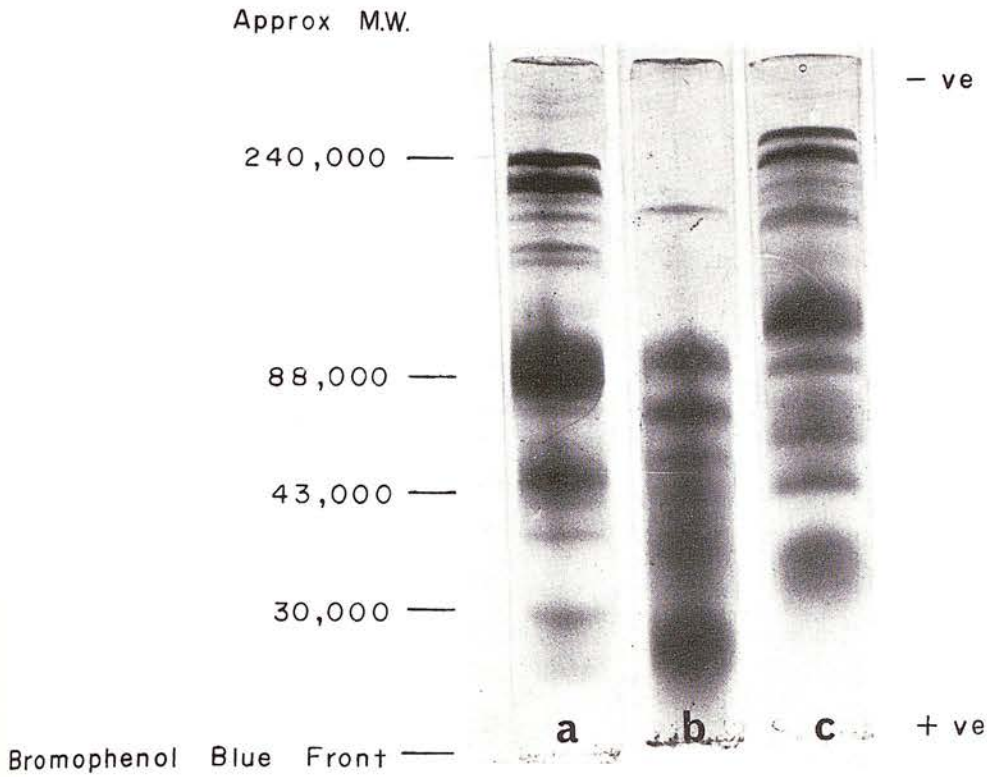

Fig. 6. Sodium dodecyl sulphate polyacrylamide gel electrophoresis of purified chicken erythrocyte plasma membrane (a), nuclear envelope (b), and plasma membrane plus nuclear envelope (c).

relatively small number of nuclear pore complexes per unit area of membrane compared with the nuclear envelope of most other nucleated cells. For this reason the nuclear pore complexes of avian erythrocyte nuclear envelope are not as readily detected by thin sectioning as are those in the nuclear envelope of most other cell types, and their apparent absence in Fig. 2, is therefore, not unreasonable.

Polyacrylamide gel electrophoresis

Polyacrylamide gel electrophoresis in the presence of sodium dodecyl sulphate (SDS) has been performed with the membrane samples. Figure 6 shows representative gels of the purified chicken erythrocyte plasma membrane (a), the nuclear envelope (b), and the mixture of the two (c) in which the nuclear envelope is retained within the plasma membrane ghost. It is clearly seen that the polypeptide composition of the nuclear envelope is very different to that of the plasma membrane.

ATPase activity

Chicken erythrocyte plasma membrane and nuclear envelope samples have been assayed for the presence of magnesium-dependent, calcium-dependent and sodium plus potassium stimulated magnesium-dependent adenosine triphosphatase activities. The results are shown in Table 1. It is seen that both the nuclear envelope and plasma membrane contain a similar amount of magnesium stimulated ATPase activity. Only the plasma membrane shows further stimulation

Table 1. Adenosine triphosphatase activity of chicken erythrocyte plasma membrane and nuclear envelope

	Nuclear envelope	Plasma membrane
Mg-ATPase	11.5 ± 3.1	12.8 ± 4.9
NaKMg-ATPase	11.0 ± 3.4	15.4 ± 3.7
Ca-ATPase	1.9 ± 0.8	3.7 ± 1.6

Activities are expressed as μmoles inorganic phosphate liberated per mg protein per hour, ±1 SEM for 8 determinations.

when sodium and potassium are added. Both membrane types have a low calcium stimulated ATPase activity. The value of $11.5 \pm 3.1\mu$moles Pi/mg protein/hr for the magnesium ATPase of chicken erythrocyte nuclear envelope compares with the values 16.4 ± 4.1 for rat liver and 10.1 ± 3.7 for pig liver nuclear envelope.

Chemical analysis

The composition (protein, phospholipid, DNA and RNA) of the chicken erythrocyte plasma membrane, nuclear envelope and nuclear envelope retained within the plasma membrane ghost is shown in Table 2. The values differ considerably from those of Zentgraf *et al.* (1971), who obtained a lower phospholipid content and higher DNA and RNA content.

Table 2. The phospholipid, DNA and RNA content of chicken erythrocyte plasma membrane and nuclear envelope expressed per mg membrane protein

	Phospholipid	DNA	RNA
Plasma membrane	0.31	0.02	0.02
Nuclear envelope	0.27	0.03	0.03

DISCUSSION

The procedures described in the present publication for the purification of chicken erythrocyte plasma membrane and nuclear envelope succeed in avoiding most of the problems of cross-contamination mentioned in the introduction. Residual haemoglobin is eliminated by initially preparing haemoglobin-free erythrocyte ghosts. The ultrasonication treatment applied to these erythrocyte ghosts produces a very high degree of separation of plasma membrane from nuclei, such that thin sectioned samples of nuclei do not show more than trace quantities of contaminating membrane. The problem of chromatin contamination is more difficult to avoid. Even prolonged incubation with deoxyribonuclease does not lower the DNA content of the nuclear envelope; in fact the material usually becomes very aggregated under these conditions. Both Zentgraf *et al.* (1971) and Blanchet (1974) appear to have faced similar problems in this respect, and produce nuclear envelope with a significantly higher density and nucleic acid content than that produced by our procedure. Our purified plasma membrane of density 1.175, is of cream colouration and the nuclear envelope, of density 1.165 is of pale yellow colouration. The corresponding figures of Blanchet (1974) are 1.16 and 1.21, and both the plasma and nuclear membranes contain significant amounts of haemoglobin.

Our ultrasonication treatment has been found to be easy to control and it reproducibly produces an almost complete separation of plasma membrane from the nuclei (Harris and Brown, 1971b). In our hands, blade homogenization (Zengraf *et al.*, 1969, 1971) did not achieve the same degree of separation. This problem was largely ignored by Jackson (1975), who studied the material obtained following deoxyribonuclease treatment of the nucleated erythrocyte ghosts. Jackson (1975) claimed that the SDS polyacrylamide gel electrophoresis patterns of the nuclear envelope were dominated by the plasma membrane bands. While this is undoubtedly true, as shown by our own gel (Fig. 6c), it is highly desirable to also show the patterns given by purified plasma membrane and nuclear envelope (Fig. 6a and b).

The fragility of the nuclear envelope of the chicken erythrocyte is not unexpected following the observations of Zentgraf *et al.* (1971) on its fragmentation during blade homogenization. The nuclear pore complexes may well act as regions of stabilization for the overall maintenance of nuclear 'ghost' integrity. This may explain why it is easier to obtain intact nuclear 'ghosts' from a tissue such as liver (Harris and Milne, 1974) which has large numbers of nuclear pore complexes per unit of area nuclear surface than from the chicken erythrocyte nucleus. This interpretation is supported by the conditions under which the nuclear envelope remains inside the plasma membrane ghost (Harris, 1978), and is thereby given structural protection by the surrounding plasma membrane. In addition, the nuclear pore complexes remain in a superior state of preservation in these latter conditions indicating that either the ultrasonication treatment or the subsequent separation of the two nuclear membranes during the isolation procedure may destabilize the pore complexes on the purified nuclear envelope. The octagonal symmetry of the nuclear pore complex is readily apparent from the purified nuclear envelope, although there does appear to be a considerable loss of annular material.

When studied in the electron microscope the purified plasma membrane isolated by our procedure does not show the presence of mitochondria, which are released along with the

plasma membrane when the erythrocyte ghosts are subjected to the ultrasonication treatment (Harris and Brown, 1971b). The SDS polyacrylamide gel pattern of the purified nuclear envelope material (Fig. 6a) shows a very different pattern to the plasma membrane, indicating the non-similarity of the polypeptide composition of these two membrane types. This is not unexpected since they are functionally very different and can be readily distinguished from one another in the electron microscope by negative staining, if not by thin sectioning.

In general, our ATPase activity figures for nuclear envelope are in agreement with other workers in that there is no sodium plus potassium stimulation of the magnesium–ATPase. Our figures are considerably higher than those of Zentgraf *et al.* (1971) and slightly higher than those of Blanchet (1974). This may be an indication of the destructive effect of the high ionic strength treatment used by Zentgraf *et al.* (1971) during their isolation procedure for nuclear envelope, although a similar treatment was used by Blanchet (1974). The lower isopycnic density of our nuclear envelope compared with that of Zentgraf *et al.* (1971) and Blanchet (1974) can be accounted for by the presence of a higher proportion of phospholipid and a lower proportion of nucleic acids (Table 2). The electron micrographs of both these groups show the presence of chromatin contamination in their nuclear envelope, which is largely absent from our material.

Technical difficulties at the moment appear to preclude the possibility of obtaining nuclear envelope from the chicken erythrocyte which is totally in the form of nuclear 'ghosts', although this aim has been partially achieved by the method presented in this publication.

Acknowledgements—This work is supported by the Medical Research Council and The Royal Society.

The technical assistance provided by Mr. J. Murdock and Mr. J. Kerr is gratefully acknowledged.

REFERENCES

Agutter, P. S., 1972. *Biochim. biophys. Acta*, **255:** 397–401.

Ashwell, G., 1957. In: *Methods in Enzymology*, Colowick, S. P. and Kaplan, N. O. (eds.), Academic Press, London, Vol. 3, 73–105.

Berenblum, I. and Chain, E., 1938. *Biochem. J.*, **32:** 295–298.

Blanchet, J. P., 1974. *Exptl. Cell Res.*, **84:** 159–166.

Bornens, M., 1973. *Nature*, **244:** 28–30.

Folch, J., Lees, M. and Sloane-Stanley, G. H., 1956. *J. biol. Chem.*, **226:** 497–509.

Franke, W. W., Deumling, B., Ermen, B., Jarasch, E. D. and Kleinig, H., 1970. *J. Cell Biol.*, **46:** 379–395.

Giles, K. W. and Myers, A., 1965. *Nature*, **206:** 93.

Harris, J. R., 1978. *J. Cell Sci.*, (in press).

Harris, J. R. and Agutter, P. S., 1970. *J. Ultrastruct. Res.*, **32:** 219–232.

Harris, J. R. & Brown, J. N., 1971a. *Br. Poult. Sci.*, **12:** 95–99.

Harris, J. R. and Brown, J. N., 1971b. *J. Ultrastruct. Res.*, **36:** 8–23.

Harris, J. R. and Milne, J. F., 1974. *Trans. biochem. Soc.*, **2:** 1251–1953.

Harris, J. R. and Milne, J. F., 1975. *J. Physiol.*, **251:** 25P–26P.

Jackson, R. C., 1975. *J. biol. Chem.*, **250:** 617–622.

Kashnig, D. M. and Kasper, C. B., 1969. *J. Biol. Chem.*, **244:** 3786–3792.

Kopacyzk, K., Purdue, J. and Green, D. E., 1966. *Archs. biochem. Biophys.*, **115:** 215–275.

Lowry, O. H., Rosebrough, N. J., Farr, A. L. and Randall, R. J., 1951. *J. biol. Chem.*, **193:** 265–275.

Maddy, A. H. and Spooner, R. S., 1970. *Vox. Sang.*, **18:** 34–41.

Price, M. R., Harris, J. R. and Baldwin, R. W., 1972. *J. Ultrastruct. Res.*, **40:** 178–196.

Weise, M. J. and Ingram, V. M., 1973. *Fedn. Proc. Fedn Am. Socs. exp. Biol.* **23:** 673 abs.

Wohler, B. E. and Wollenberger, A., 1958. *Biochem. Z.*, **329:** 508–520.

Zentgraf, H., Deumling, B. and Franke, W. W., 1969. *Exptl. Cell Res.*, **56:** 333–337.

Zentgraf, H., Deumling, B., Jarasch, E-D. and Franke, W. W., 1961. *J. biol. Chem.*, **246:** 2986–2995.

J. Cell Sci. **34**, 81–90 (1978)
Printed in Great Britain © *Company of Biologists Limited 1978*

THE PREPARATION AND ULTRASTRUCTURE OF AVIAN ERYTHROCYTE NUCLEAR ENVELOPE ENCLOSED BY THE PLASMA MEMBRANE

JAMES R. HARRIS

Biomembrane Unit, Division of Biochemistry, North East London Polytechnic, Romford Road, London E15 4LZ, England

SUMMARY

A procedure is described for the preparation of avian erythrocyte nuclear envelope ghosts which remain enclosed by the ellipsoid plasma membrane. Haemoglobin-free nucleated chicken erythrocyte ghosts are treated in a low ionic strength buffer plus heparin which brings about decondensation of the chromatin. This is followed by solubilization of the chromatin by digestion with pancreatic deoxyribonuclease-1. When studied by light microscopy using either phase-contrast or Nomarski interference optics, the ellipsoid plasma membrane is clearly seen to remain with the collapsed nuclear envelope trapped inside. This interpretation is supported by negative-staining electron microscopy using ammonium molybdate, which in addition reveals the presence of the nuclear pore complexes. The suggestion is advanced that structural protection is provided for the fragile nuclear envelope system by the surrounding plasma membrane, which might account for the final nuclear envelope being in the form of relatively intact ghosts with well defined nuclear pore complexes. The nuclear envelope is highly fragmented when the plasma membrane is absent, the nuclear pore complexes showing appreciable breakdown. Thin sectioning supports the results of negative staining and in addition shows the nuclear envelope retained within the plasma membrane to be composed of both inner and outer nuclear membranes, but the nuclear pore complexes are not clearly defined.

INTRODUCTION

The procedure previously used for the production of haemoglobin-free avian erythrocyte ghosts (Harris & Brown, 1971*a*, *b*), which retain their nuclei has been further developed in an attempt to release the chromatin from the nuclei retained within the plasma membrane ghosts. It was hoped that the morphological juxtaposition of the 2 nuclear membranes and the integrity of the nuclear pore complexes might be retained under these circumstances. The direct treatment of isolated avian erythrocyte nuclei in an attempt to obtain intact nuclear envelopes (Harris, Agutter & Milne, 1978) has proved to be only partially successful, in that the final product consists primarily of fragmented nuclear envelope containing damaged nuclear pore complexes.

The protective action afforded by the plasma membrane surrounding the fragile nuclear envelope throughout the low ionic strength swelling in the presence of heparin and the deoxyribonuclease digestion used to release the chromatin, is considered to be of prime importance. This is particularly so since the overall treatment is basically the same as that applied to isolated nuclei. It will be shown that the nuclear envelope

enclosed by plasma membrane produced by this treatment is in a superior morphological condition to that isolated directly from nuclei (Harris *et al.* 1978). Despite the fact that the procedure presented below does not produce nuclear envelope as highly purified as that from isolated nuclei, it is clearly shown that it does provide material suitable for detailed electron-microscopic investigations of the extremely fragile nuclear envelope of the avian erythrocyte,which unfortunately cannot be quantitatively obtained in the form of purified intact nuclear envelope ghosts, as is possible from other tissues (Harris, 1978; Harris & Milne, 1974; Kay, Fraser & Johnston, 1972).

Several investigators other than the author and his colleagues have performed biochemical studies on avian erythrocyte plasma membrane and nuclear envelope (Zentgraph, Deumling, Jarasch & Franke, 1971; Shelton, 1973; Blanchet, 1974; Jackson, 1975; Jackson, 1976*a*, *b*; Caldwell, 1976; Weise & Ingram, 1976; Shelton, Cobbs, Povlishock & Burkat, 1976). It is clear that in most cases the plasma membrane is separated from the nucleus by procedures such as homogenization, ultrasonication and nitrogen cavitation. Although Jackson (1975) did perform studies with deoxyribonuclease-treated nucleated chicken erythrocyte ghosts, he did not include any electron micrographs of his material.

The available publications dealing with avian erythrocyte nuclear envelope which do include electron micrographs support the interpretation that this membrane system is very fragile. The inner and outer nuclear membrane and nuclear pore complexes are generally not definable by thin sectioning of isolated nuclear envelope fragments, but Harris *et al.* (1978) clearly show the location of damaged nuclear pore complexes by negative staining.

EXPERIMENTAL METHODS

Preparation of nuclear envelope within plasma membrane

Chicken erythrocyte ghosts were prepared by the method of Harris & Brown (1971*a*, *b*). The treatment of these nucleated haemoglobin-free erythrocyte ghosts with deoxyribonuclease permits the release of solubilized chromatin from the nuclei, which in turn escapes from the cytoplasmic compartment through lesions in the surrounding plasma membrane. Erythrocyte ghosts from 40 ml of packed cells were washed twice at 3000 rev/min (1000 **g**) for 5 min with 10 mM Tris-HCl buffer (pH 7·0). The slightly gelatinous pellets were then pooled and made up to a volume of 400 ml with the Tris-HCl buffer. To disperse the chromatin further, heparin was added to a concentration of 20 U./ml and deoxyribonuclease-1 (Sigma DN-100) was added to give a concentration of 20 μg per ml. The gel dispersed rapidly, and to activate the enzyme 0·04 ml of 1·0 M magnesium chloride was added, giving a final concentration of 0·1 mM. After 10 min incubation at room temperature with gentle stirring, the suspension was centrifugally pelleted and washed with 10 mM Tris-HCl (pH 7·4), twice at 10000 rev/min (12000 **g**) for

Fig. 1. Chicken erythrocyte plasma membrane ghosts containing nuclear envelope ghosts, as observed by light microscopy using, A, Nomarski interference optics, compared with the initial nucleated erythrocyte ghosts, B. × 3000.

Fig. 2. Chicken erythrocyte plasma membrane ghosts containing nuclear envelope ghosts, as observed at low electron-optical magnification. Negatively stained with 2% ammonium molybdate (pH 7·0). Arrowheads indicate the location of the nuclear envelopes. × 8000.


1A


B

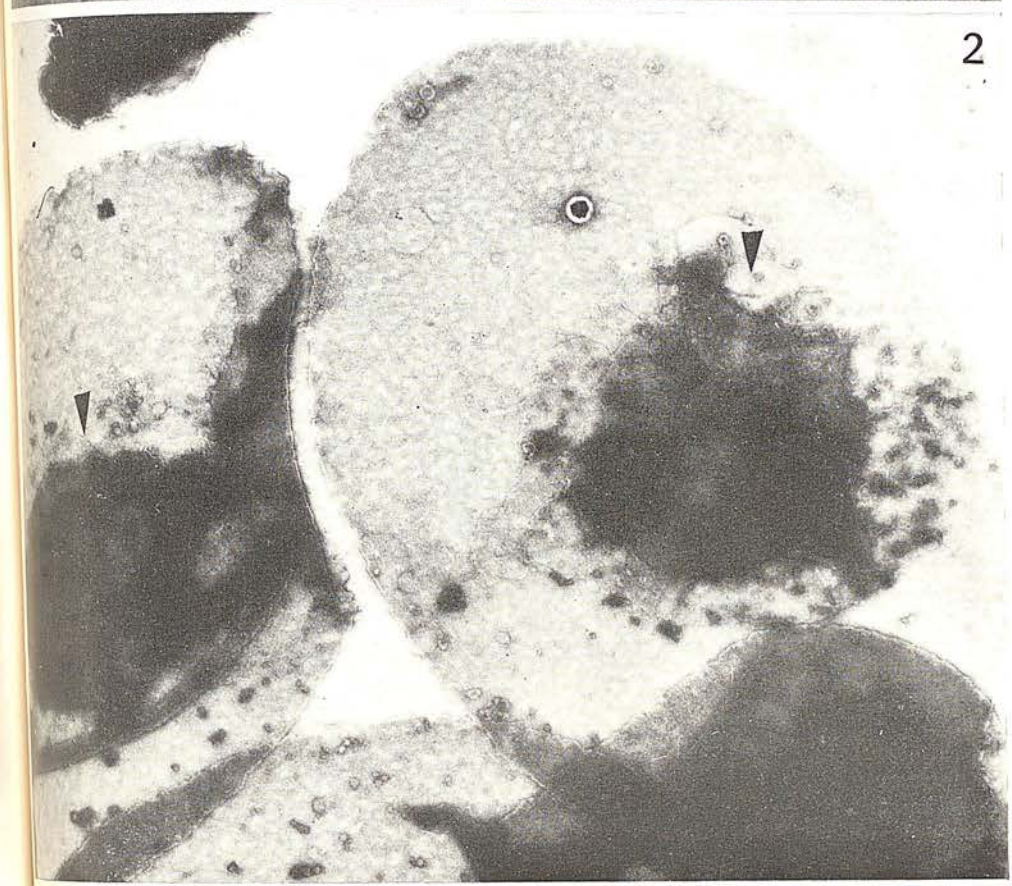
2

10 min and 6 times at 20000 rev/min (48000 g) for 5 min to remove most of the solubilized chromatin. The membrane material was then purified by isopycnic banding on a 1·0 to 2·0 M sucrose gradient prepared in 10 mM Tris-HCl (pH 7·4). Centrifugation was performed for 16 h at 25000 rev/min (83000 g). The erythrocyte plasma membrane ghosts containing nuclear envelope banded at a mean density of 1·18, were removed and washed centrifugally in 10 mM Tris-HCl buffer (pH 7·0) to remove the sucrose prior to performing processing for electron microscopy.

Electron microscopy

Negatively stained specimens were prepared on carbon-coated grids using the nuclear envelope material directly after the removal of sucrose by centrifugal washing. The single-drop technique (Harris & Agutter, 1970) was used for applying the membrane suspension and negative stain (2 % ammonium molybdate, pH 7·0) to the grids. For thin sectioning the membrane material was fixed overnight at room temperature in Dalton's chrome-osmium (Dalton, 1955), dehydrated with graded ethanols and epoxypropane before embedding in TAAB epoxy resin. Thin sections were cut using glass knives with a Reichert OM U2 ultramicrotome and were stained with uranyl acetate and lead citrate. Specimens were studied in a Philips EM 301S electron microscope at an accelerating voltage of 80 kV. Photographs were taken on Ilford $3\frac{1}{4} \times 4$ in. (8·25 × 10·2 cm) plates, type EM 6.

RESULTS AND DISCUSSION

The erythrocyte plasma membrane ghosts containing nuclear envelope ghosts readily seen by light microscopy using phase contrast or Nomarski interference optics, see Fig. 1. Electron microscopy confirms and extends the light-microscopic observations. By negative staining, the ellipsoid outline of the plasma membrane is clearly revealed as is the position of the nuclear envelope trapped inside, see Fig. 2. Small, dense mitochondria can be seen adjacent to the nuclear envelope. If the nuclear envelope is adequately spread rather than folded, it is possible to see the distribution of the nuclear pore complexes over the whole area of the flattened envelope (Fig. 3).

At higher electron-optical magnifications (Fig. 4) it can be seen that the nuclear pore complexes possess pronounced annuli with indication of the 8 annular subunits. It is proposed that the apparent morphological integrity of the overall nuclear envelope and the nuclear pore complexes under these conditions may well be due to the structural protection afforded by the surrounding plasma membrane throughout the isolation procedure. Nevertheless, a few free nuclear envelopes were always detected (Fig. 5), which may be derived from nuclei released during the haemolysis of the erythrocytes. It might be expected that the ultrastructural detail of the free nuclear envelope as revealed by negative staining would be significantly better than that of the nuclear envelope entrapped by the plasma membrane, owing to the absence of the plasma membrane layer above and below the nuclear envelope. On close comparison

Fig. 3. Part of a chicken erythrocyte plasma membrane ghost containing a nuclear envelope ghost which is adequately flattened so that the distribution of the nuclear pore complexes can be clearly seen. Arrowheads indicate densely stained mitochondria. Negatively stained with 2 % ammonium molybdate. × 34000.

Fig. 4. Part of the nuclear envelope ghost shown in Fig. 3, revealing detail of the nuclear pore complexes. Negatively stained with 2 % ammonium molybdate. × 94000.

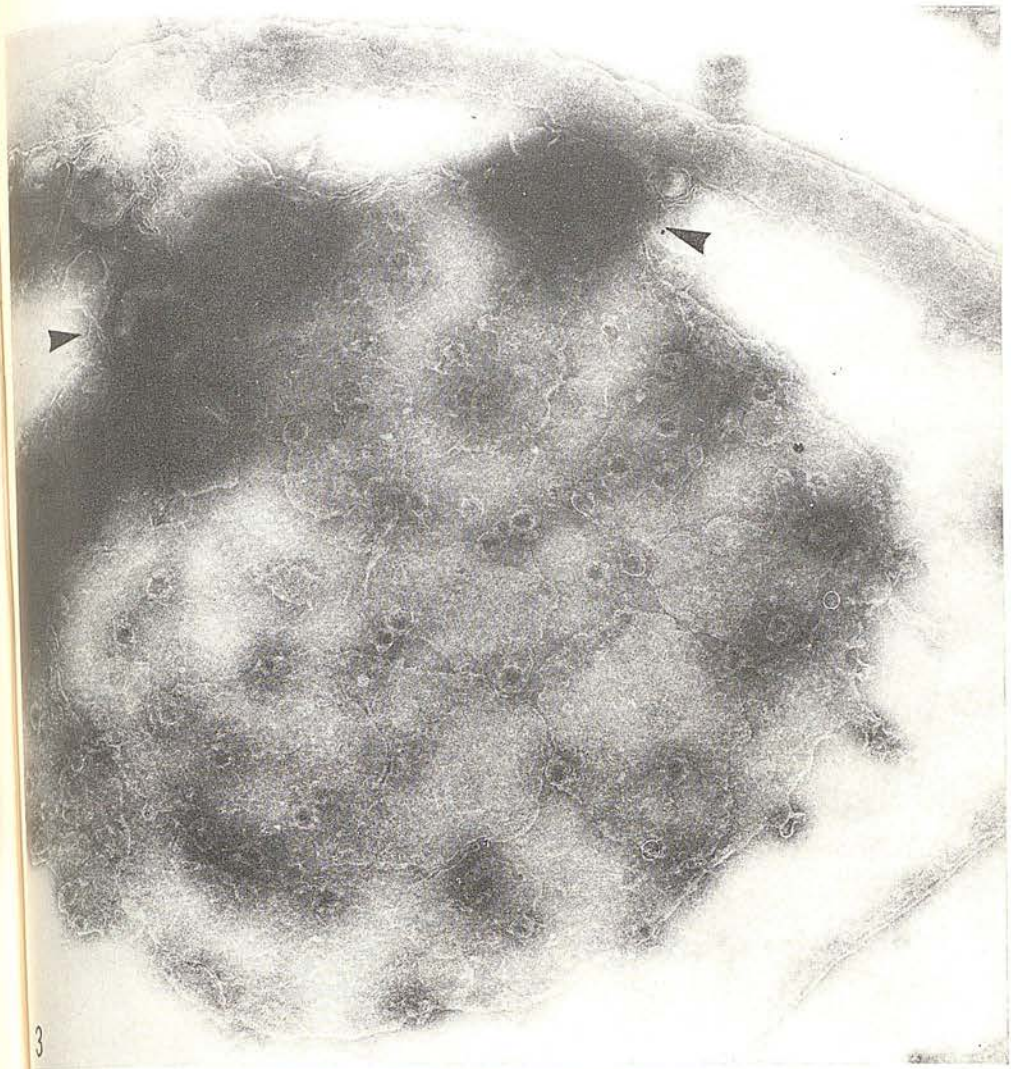

3

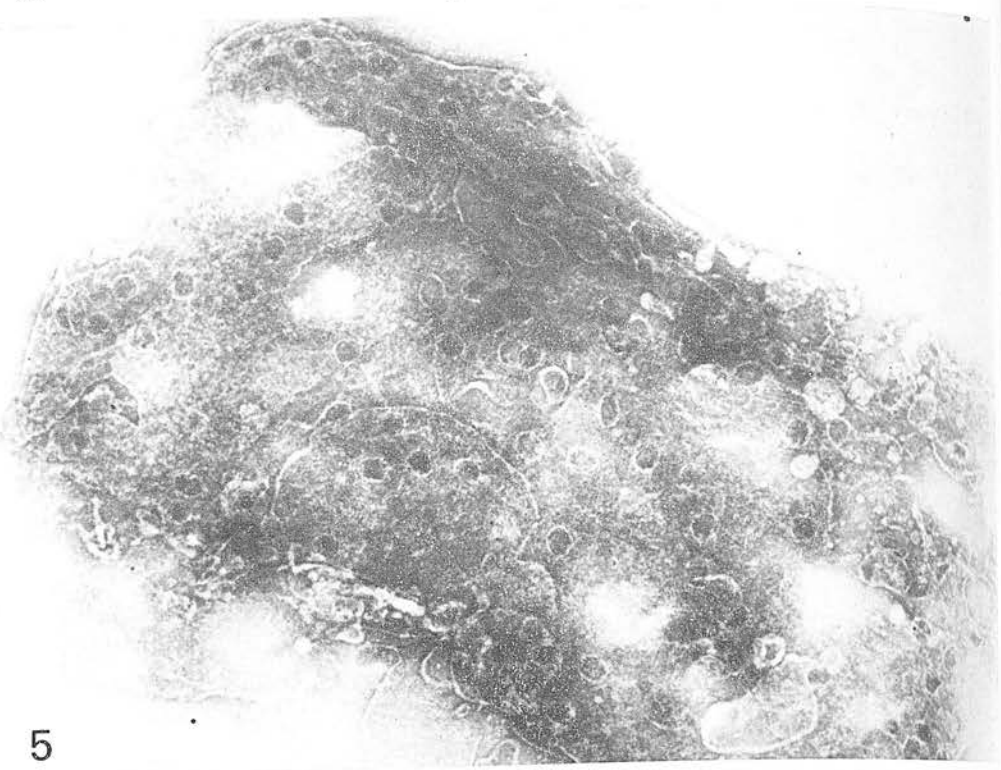

5

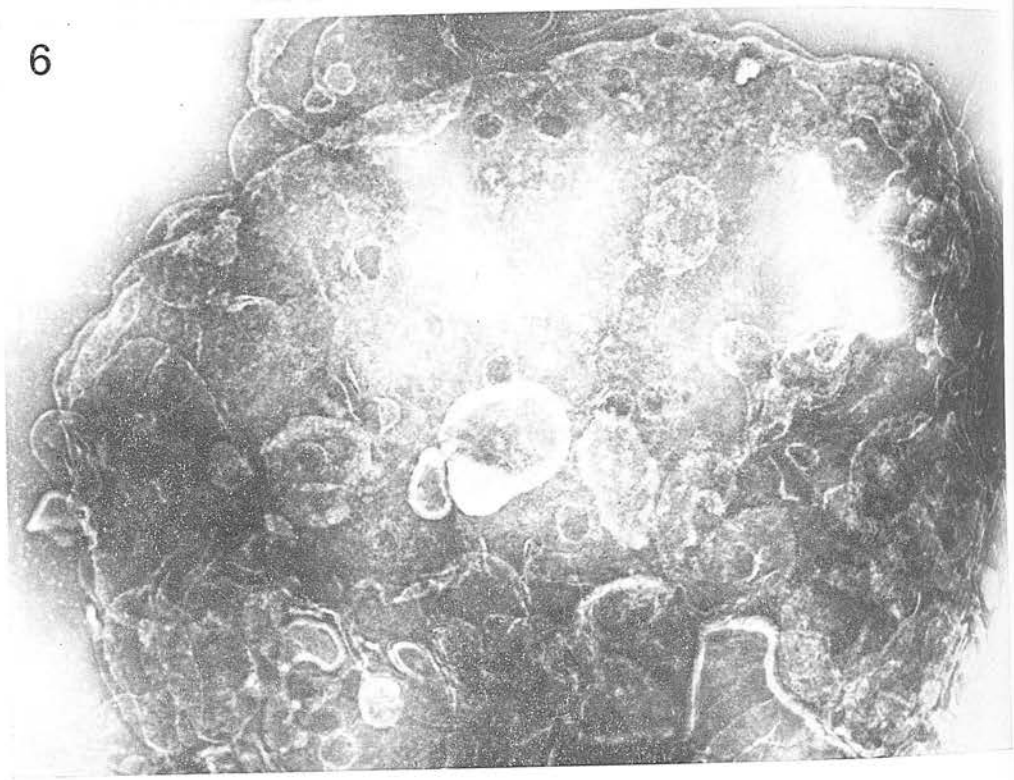

6

of the images of the entrapped nuclear envelope (Figs. 3, 4) with that of the free nuclear envelope (Fig. 5), and with the nuclear envelope obtained directly from purified nuclei by the swelling treatment in the presence of heparin followed by deoxyribonuclease digestion (Harris *et al.* 1978) as shown in Fig. 6, it is apparent that the nuclear envelope in Figs. 5 and 6 is considerably more damaged than that in Figs. 3 and 4, but that the nuclear envelope surface shows only marginally greater detail. What is of greater significance is the distortion of the nuclear pore complexes and the apparent loss of much of the annular material in Figs. 5 and 6. It should be emphasized again that the preparative procedure applied to purified nuclei does produce nuclear envelope in a predominantly fragmented state, rather than as nuclear envelope ghosts.

When thin-sectioned, the nuclear envelope entrapped within the plasma membrane can be seen to retain both the inner and outer nuclear membranes (Figs. 7, 8). The outer nuclear membrane is extremely tenuous and the inner nuclear membrane appears denser due to residual chromatin particles attached to its nucleoplasmic surface. This chromatin could be intimately associated with the inner nuclear membrane, but it is more likely to be a contaminant due to incomplete release during the deoxyribonuclease digestion. The location of the nuclear pore complexes is difficult to define by thin sectioning owing to the low pore density, as shown in Figs. 3–6. This reduces the chance of any one nuclear pore complex being located within the plane of the section under study, while at the same time being oriented appropriately to give the circular image of a tangentially sectioned pore complex or the 'press-stud' image of the perpendicularly sectioned pore complex (Figs. 7, 8).

The use of heparin for the release of chromatin from nuclei was introduced by Bornens (1973) and has recently been extended as a detailed production of nuclear envelope from rat liver nuclei (Bornens & Courvalin, 1978). One point of significance that emerges from this work is that the nuclear pore complex annuli are completely removed, resulting in thin-sectioned rat liver nuclear envelope showing smooth-edged pores with no indication of the annular subunits. Hildebrand & Okinaka (1976), who applied a heparin treatment to cultured cell nuclei, commented that their fragmented nuclear envelope contained few nuclear pore complexes, whereas they were clearly distinct on the intact nuclei, again indicating the disruptive action of heparin. Despite this criticism of the use of heparin it appears from the results presented above, that when the fragile avian erythrocyte nuclear envelope is protected by the surrounding plasma membrane throughout the preparative procedures, the effect of heparin is less marked than is the case when isolated nuclei are treated by the same procedure.

The availability of relatively intact avian erythrocyte nuclear envelope ghosts

---

Fig. 5. An isolated nuclear envelope ghost, free from plasma membrane. The nuclear pore complexes appear to be distorted and have less annular material than those visible in Figs. 3, 4. Negatively stained with 2 % ammonium molybdate. × 46000.

Fig. 6. A nuclear envelope ghost prepared from purified nuclei. Note the similarity to the envelope in Fig. 5, in particular the presence of distorted nuclear pore complexes deficient in annular material. Negatively stained with 2 % ammonium molybdate. × 64000.

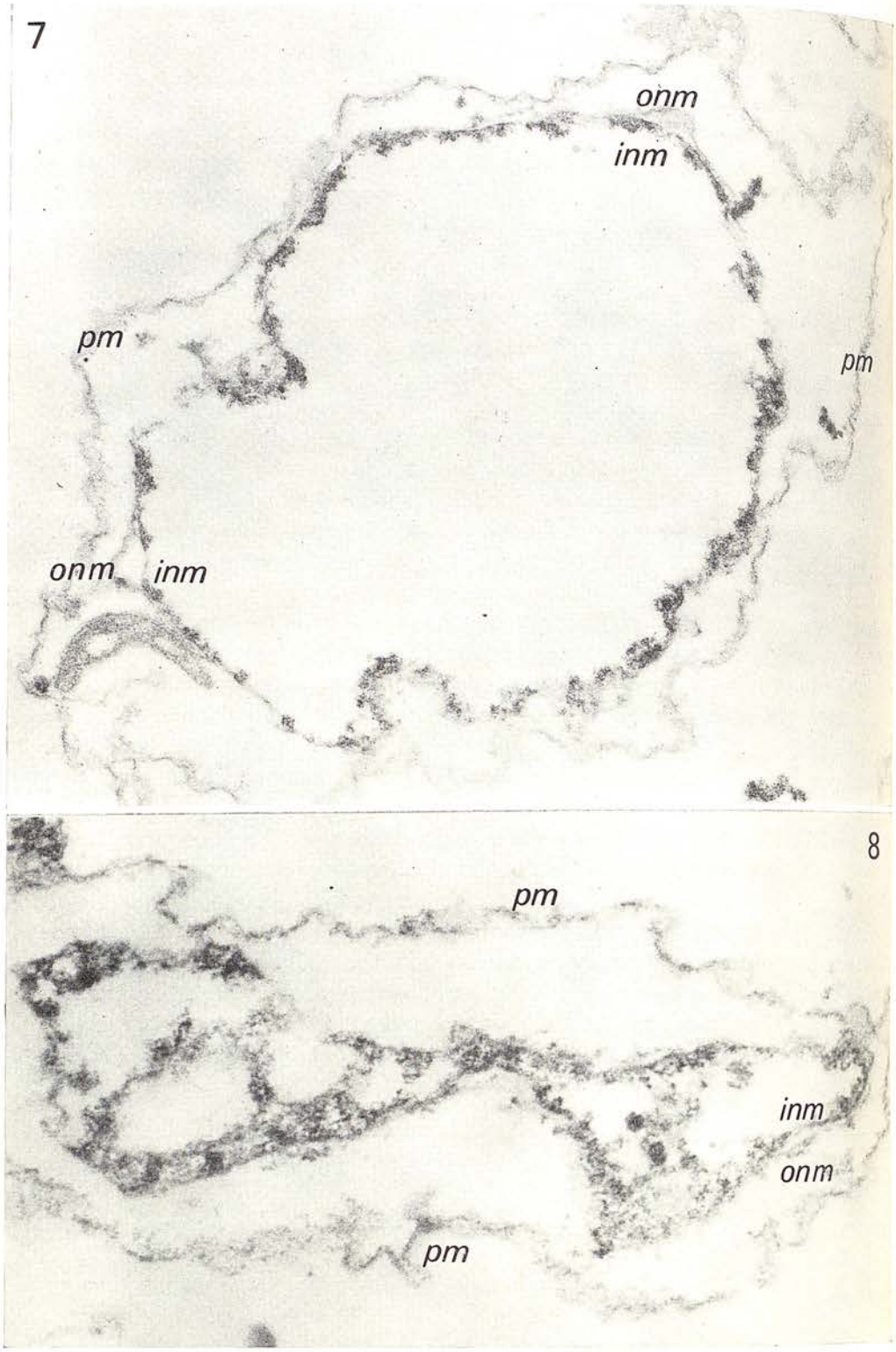

Figs. 7, 8. Thin-sectioned chicken erythrocyte plasma membrane ghosts containing nuclear envelope ghosts. Residual chromatin is seen to be adhering to the nucleoplasmic surface of the inner nuclear membrane (*inm*). The tenuous outer nuclear membrane (*onm*) is visible in places. The plasma membrane is indicated by *pm*. ×34000 and 78000, respectively.

enclosed by plasma membrane ghosts may provide a system for investigating the permeability of the nuclear envelope to macromolecules. The system may similarly be of application to cell fusion studies and nuclear reactivation following fusion, where it is of interest to know whether the nuclear pore complex density increases on reactivation of the avian erythrocyte RNA metabolism. There is also considerable scope for further ultrastructural and biochemical study, particularly in relation to cellular development of the avian erythrocyte, membrane receptors and the nuclear envelope pore complex-lamina which has been shown by Aaronson & Blobel (1975) to remain after the extraction of rat liver nuclear envelope with the non-ionic surfactant Triton X-100 and high salt concentration. This latter aspect has been investigated electrophoretically by Shelton (1976). Although preservation of the morphological integrity of the nuclear envelope and the nuclear pore complexes has been emphasized throughout this publication, it must be stated that there is considerable value in having available highly purified yet fragmented nuclear envelope containing damaged pore complexes, for comparative biochemical studies, particularly if these fragments can be classified as being predominantly inner or outer nuclear membrane.

This work has been supported by grants from the Medical Research Council and The Royal Society. The technical assistance of Mr J. Murdock and Mr J. Kerr is gratefully acknowledged.

REFERENCES

Aaronson, R. P. & Blobel, G. (1975). Isolation of nuclear pore complexes in association with a lamina. *Proc. natn. Acad. Sci. U.S.A.* **72**, 1007–1011.

Blanchet, J. P. (1974). Chicken erythrocyte membranes: comparison of nuclear and plasma membranes from adults and embryos. *Expl Cell Res.* **84**, 159–166.

Bornens, M. (1973). Action of heparin on nuclei: solubilization of chromatin enabling the isolation of nuclear membranes. *Nature, Lond.* **244**, 28–30.

Bornens, M. & Courvalin, J. C. (1978). Isolation of nuclear envelopes with polyanions. *J. Cell Biol.* **76**, 191–206.

Caldwell, A. B. (1976). Proteins of the turkey erythrocyte membrane. *Biochemistry, N.Y.* **15**, 2711–2718.

Dalton, A. J. (1955). A chrome-Osmium fixative for electron microscopy. *Anat. Rec.* **121**, 281 (Abstr.).

Harris, J. R. (1978). The biochemistry and ultrastructure of the nuclear envelope. *Biochim. biophys. Acta* **515**, 55–104.

Harris, J. R. & Agutter, P. S. (1970). A negative staining study of human erythrocyte ghosts and rat liver nuclear membranes. *J. Ultrastruct. Res.* **33**, 219–232.

Harris, J. R., Agutter, P. S. & Milne, J. F. (1978). Ultrastructural and biochemical studies on avian erythrocyte plasma membrane and nuclear envelope. *Micron* (in press).

Harris, J. R. & Brown, J. N. (1971 *a*). The preparation of nucleated erythrocyte ghosts from avian erythrocytes. *Br. Poult. Sci.* **12**, 95–99.

Harris, J. R. & Brown, J. N. (1971 *b*). Fractionation of the avian erythrocyte: an ultrastructural study. *J. Ultrastruct. Res.* **33**, 8–23.

Harris, J. R. & Milne, J. F. (1974). A rapid procedure for the isolation and purification of rat liver nuclear envelope. *Trans. Biochem. Soc.* 1251–1253.

Hildebrand, C. E. & Okinaka, R. T. (1976). A rapid method for preparation of nuclear membranes from mammalian cells. *Analyt. Biochem.* **75**, 290–300.

Jackson, R. C. (1975). The exterior surface of the chicken erythrocyte. *J. biol. Chem.* **250**, 617–622.

JACKSON, R. C. (1976*a*). Polypeptides of the nuclear envelope. *Biochemistry, N.Y.* **15**, 5641–5651.

JACKSON, R. C. (1976*b*). On the identity of nuclear membrane and non-histone nuclear proteins. *Biochemistry, N.Y.* **15**, 5652–5656.

KAY, R. R., FRASER, D. & JOHNSTON, I. R. (1972). A method for the rapid isolation of nuclear membranes from rat liver. *Eur. J. Biochem.* **30**, 145–154.

SHELTON, K. R. (1973). Plasma membrane and nuclear proteins of the goose erythrocyte. *Can. J. Biochem.* **51**, 1442–1447.

SHELTON, K. R. (1976). Selective effects of non-ionic detergent and salt solutions in dissolving nuclear envelope proteins. *Biochim. biophys. Acta* **455**, 973–982.

SHELTON, K. R., COBBS, C. S., POVLISHOCK, J. T. & BURKAT, R. K. (1976). *Archs Biochem. Biophys.* **174**, 177–186.

WEISE, M. J. & INGRAM, V. M. (1976). Proteins and glycoproteins of membranes from developing chick red cells. *J. biol. Chem.* **251**, 6667–6673.

ZENTGRAPH, H., DEUMLING, B., JARASCH, E. D. & FRANKE, W. W. (1971). *J. biol. Chem.* **246**, 2986–2995.

(*Received* 21 *April* 1978)

J. ULTRASTRUCTURE RESEARCH 33, 219–232 (1970)

A Negative Staining Study of Human Erythrocyte Ghosts and Rat Liver Nuclear Membranes

J. R. HARRIS[1] AND P. AGUTTER

Department of Zoology, University of Edinburgh, Scotland

Received November 4, 1969, and in revised form February 2, 1970

An electron microscopic study of membrane features has been performed using negative staining. Hemoglobin-free human erythrocyte ghosts and membranes from rat liver nuclei have been observed in the electron microscope after negative staining with ammonium molybdate and the uranyl acetate–oxalic acid complex, both at pH 7.0.

The surfaces of partially empty nuclear envelopes have been shown to be covered with pores approximately 500 Å in diameter and surrounded by annuli approximately 250 Å wide. Many of the annuli appeared to be composed of eight subunits. Individual annuli have been found to separate themselves from the overall membrane sheet in regions where the membranes have undergone disruption.

Hemoglobin-free human erythrocyte ghosts have been shown to possess membrane holes or pits, approximately 140 Å in diameter. These pits are very similar to those formed by complement hemolysis, but are fewer in number and may be slightly larger. The erythrocyte pit structures have much smoother edges than the nuclear pores and do not appear to be composed of subunits, though this cannot be ruled out.

Apart from the pit structures the surface of the erythrocyte ghost has an overall fine structure. Within this fine structure individual protein molecules have been located, though it has very often been difficult to obtain sufficient contrast around the molecules owing to the double layer of membrane beneath them on the specimen grid. The uranyl complex provided a superior contrast to ammonium molybdate at this order of resolution, though it tended to impart a more granular texture to the electron images than did ammonium molybdate.

The results presented are discussed in relation to the possibilities and limitations of the negative staining method when applied to membrane systems.

In the present investigation, membranes obtained from human erythrocyte ghosts and rat liver nuclei have been studied by negative staining with ammonium molybdate and the uranyl acetate–oxalic acid complex.

It has been proposed independently by Muscatello and Horne (*22*) and Munn (*21*) that ammonium molybdate has desirable negative staining properties for the study

[1] Present Address: Department of Cancer Research, University of Nottingham, England.

of membrane systems. Mitochondrial and microsome preparations were investigated and a good preservation of membrane structure claimed. A negative staining study of low molecular weight proteins has been performed by Mellema *et al.* (*19*) using the uranyl acetate–oxalic acid complex which can be brought to neutral pH with ammonia without precipitation. This stain, which offers excellent electron contrast, has not yet been used to any extent on membrane systems.

In order to reveal detail on or within a membrane surface, a negative stain must be able to surround or penetrate to some degree any fine structure that is present. While penetrating a membrane surface, a negative stain may structurally alter components of the surface and thus create artifacts. A comparative study using different negative stains may show that some stains cause more membrane disruption than others (*12, 21, 22*). At the last resort it may, however, become impossible to rule out the possibility that a negative stain which is considered to have desirable staining properties is not causing changes within a membrane at the molecular level. Such changes could occur either before or during the drying of the stain–membrane mixture on the specimen grid. With these reservations in mind it is nevertheless generally accepted that negative stains have the ability to preserve and reveal structural detail within biological material.

MATERIALS AND METHODS

Preparation of human erythrocyte ghosts. Human erythrocyte ghosts were prepared by modification of previously published methods (*13, 14*). Seven-day-old packed erythrocytes (group O + ve, in acid–citrate–dextrose) were obtained from the Blood Transfusion Unit of the Royal Infirmary, Edinburgh. The erythrocytes were washed three times in isotonic phosphate buffer (pH 7.0) at 4°C, with removal of the supernatant and buffy coat by aspiration. Hemolysis was then brought about by the addition of 5 volumes of 0.01 *M* phosphate buffer (pH 7.4) at 4°C. The ghosts were collected by centrifugation at 12 000 rpm (23 000 *g*) in the M.S.E. 6 × 250 ml angle rotor for 30 minutes. After 6 or 7 washes in the same buffer, ghosts of creamy-white coloration were obtained which appeared intact in the electron microscope by negative staining (*14*).

Preparation of rat liver nuclei. Nuclei were prepared from rat liver by modification of the methods of Sporn *et al.* (*26*), and Widnell and Tata (*28*). The livers of four overnight starved rats were removed as quickly as possible after sacrificing the animals and placed in ice-cold homogenizing medium (0.3 *M* sucrose and 0.003 *M* $MgCl_2$ in 0.03 *M* phosphate buffer at pH 6.1) and were minced for 2–3 minutes, with a scalpel. All subsequent operations were

FIG. 1. A typical nuclear ghost. The large circular structures are flaws in the carbon backing film. Negatively stained with 2 % ammonium molybdate (pH 7.0). × 10,000.

FIG. 2. Part of a "nuclear ghost" that has undergone disruption. Negatively stained with 2 % ammonium molybdate. × 10,000.


1


2

carried out at 0–5°C. The fluid was then decanted and the minced liver resuspended in fresh homogenizing medium (5 ml/g tissue). The suspension was homogenized in a Potter-Elvehjem homogenizer with a loose-fitting pestle rotated at about 1000 rpm. Four up-down movements of about 30 seconds each were used. After filtration through 8 thicknesses of cheese cloth the homogenate was centrifuged at 1600 rpm (approximately 600 *g*) in the 8 × 50 ml swing-out rotor of the M.S.E. Mistral 4L centrifuge for 10 minutes. The pellet was resuspended in 0.03 *M* phosphate buffer (pH 6.1) containing 0.003 *M* $MgCl_2$, and sucrose added to 2.2 *M* concentration in centrifuge tubes. It was then centrifuged for 90 minutes at 25 000 rpm (55 000 *g*) in the Spinco No. 30 rotor, and the pellet of nuclei resuspended in the homogenizing medium after removal of the supernatant. The nuclei were further purified by 4 or 5 washes in the homogenizing medium, with centrifugation at 1600 rpm for 10 minutes each time.

A limited degree of nuclear disruption was brought about by resuspending the nuclei after the final wash in 0.01 *M* phosphate buffer (pH 6.1) which contained 0.002 *M* $BaCl_2$. This salt presumably does not have the same nuclear stabilizing power as $MgCl_2$; it was also found to act successfully as a bacteriostatic. After being stirred magnetically for 16–20 hours at 5°C samples were taken for electron microscopy. Negative staining revealed that approximately 5 % of the nuclei had lost a substantial portion of their contents.

Negative staining solutions. Ammonium molybdate was dissolved in water and the pH adjusted to 7.0 with ammonium hydroxide. The volume was then adjusted to give a 2.0 % (w/v) solution. The uranyl acetate–oxalic acid complex was prepared according to Mellema *et al.* (*19*). The pH was adjusted to 7.0 with ammonium hydroxide and the volume finally adjusted to give a solution 2.0 % (w/v) in uranyl acetate and 0.08 *M* in oxalic acid. Sodium phosphotungstate was prepared by dissolving phosphotungstic acid in distilled water and adjusting the pH to 7.0 with sodium hydroxide. The volume of the solution was then adjusted to give a solution 2.0 % (w/v) in phosphotungstate.

Negative staining technique. Single drops of the membrane suspensions were picked up on carbon-coated specimen grids from a strip of Parafilm. Most of the fluid was then drawn off by touching the side of the grid with a filter paper and a drop of the negative staining solution likewise picked up. The excess stain was then drawn off with a filter paper and the thin film of stain and membrane material allowed to dry. The procedure was carried out at room temperature.

Electron microscopy. Electron micrographs were taken with an AEI EM 6B, operating at 60 kV with a 50-μ objective aperture. The magnification scale of the microscope was calibrated using a carbon grating containing 2160 lines/mm. Ilford 3¼ × 3¼ inch plates, Special Lantern Contrasty, were used in the microscope camera.

FIG. 3. A higher magnification of a disrupted region of "nuclear ghost." Negatively stained with 2 % ammonium molybdate. Arrows indicate the subunits of a pore annulus. Some of the pores have electron transparent material at their centers. × 50,000.

FIG. 4. Part of a "nuclear ghost." Negatively stained with a 2 % solution of the uranyl acetate-oxalic acid complex (pH 7.0). × 30,000.

FIG. 5. Part of a thin-sectioned nuclear ghost. The plane of sectioning is tangential to the membrane surface. Positively stained nuclear pores are visible (arrowed). × 50,000.

FIG. 6. Part of a thin sectioned nuclear ghost showing the double nuclear membrane (*ONM*, outer nuclear membrane; *INM*, inner nuclear membrane). Contamination is present on both membranes. × 50,000.

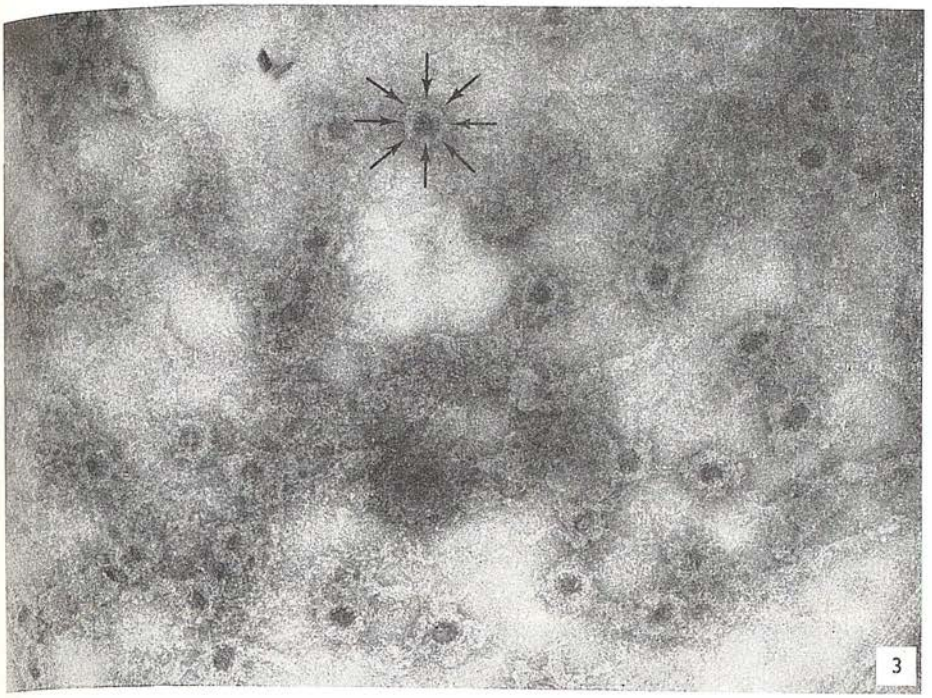
3

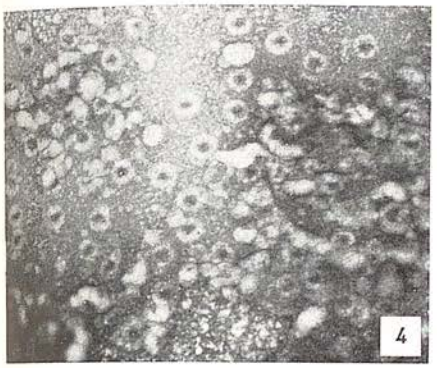
4

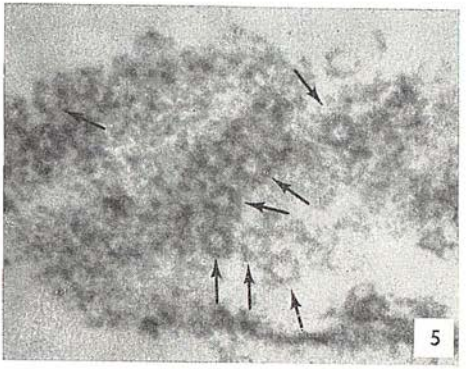
5

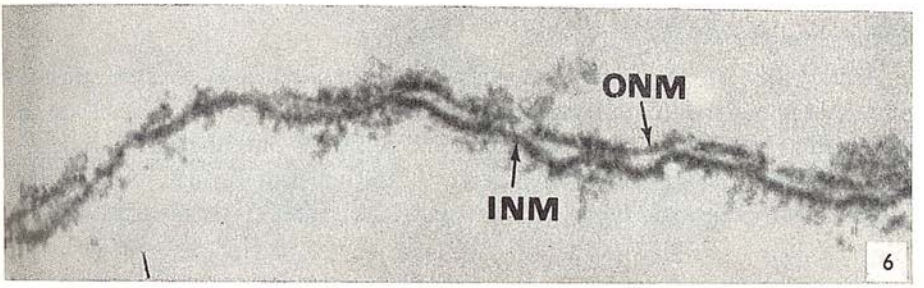
ONM
INM
6

OBSERVATIONS

Nuclear membranes

The small percentage of nuclei which were observed in the electron microscope to have lost a considerable portion of their contents were selected for this study. These "nuclear ghosts" were easily distinguished from intact nuclei, which were electron opaque bodies showing no surface detail by negative staining. The relatively empty "nuclear ghosts" and torn membrane sheets revealed membrane features even at electron optical magnifications as low at 5000 diameters. Figure 1 shows a typical "nuclear ghost" negatively stained with ammonium molybdate. In regions where the electron beam has penetrated the membrane material, the nuclear pores are clearly visible. These pores consist of electron transparent annuli filled with electron opaque stain. A smaller amount of stain surrounds the annuli. The annuli have an inner diameter of approximately 500 Å and an outer diameter of approximately 1000 Å.

In places the nuclear membranes appear to be undergoing fragmentation. This resulted in the isolation of the annuli, which must have a greater structural rigidity than the surrounding membrane (Fig. 2). This disruption was probably caused by the spreading forces applied to the nuclear membrane at the time the excess fluid was drawn off the specimen grid. At higher magnifications the annuli of the nuclear pores often appeared to be composed of 8 or 9 subunits (Fig. 3) in agreement with the observations of Gall (*9*) and Franke (*7*, *8*). The annuli sometimes appeared to be distorted. This again may be due to the spreading or disruption forces applied during the preparation of the negatively stained specimens. Essentially similar results were obtained using the uranyl acetate–oxalic acid complex (Fig. 4), but sodium phosphotungstate revealed the nuclear pores less clearly.

When thin-sectioned, the nuclear membranes were shown to be double and to have many positively stained annuli showing in regions where the plane of sectioning was tangential to the membrane surface (Figs. 5 and 6). These observations supported the negative staining study and indicated that on the negatively stained "nuclear ghosts" there must very often have been at least four layers of membrane, except where the membranes had undergone disruption.

Erythrocyte ghosts

Hemoglobin-free human erythrocyte ghosts were studied by negative staining with ammonium molybdate and the uranyl acetate–oxalic acid complex. These ghosts appeared as intact membrane sacs which had collapsed onto the carbon backing film. They thus presented a double layer of membrane material through which the electron beam had to penetrate. Figure 7 shows part of a typical erythrocyte ghost negatively

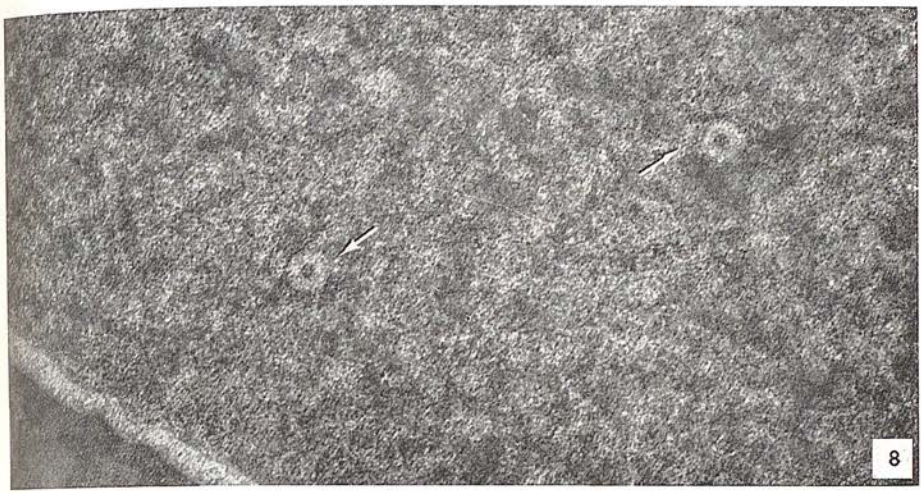

FIG. 7. Part of the surface of a human erythrocyte ghost. Negatively stained with 2 % ammonium molybdate. The arrows indicate pit structures. × 150,000.
FIG. 8. Part of the surface of a human erythrocyte ghost. Negatively stained with a 2 % solution of the uranyl acetate-oxalic acid complex. The arrows indicate pit structures. × 150,000.

stained with ammonium molybdate. The membrane surface contains many electron transparent rings or pitlike infoldings into which the negative stain has penetrated. These pits have an outer diameter of approximately 300 Å and an inner diameter of approximately 140 Å. They are randomly dispersed over the membrane surface and are found in very variable numbers on any one erythrocyte ghost. Sometimes the central hole of the pits appears less distinct. This may be because these pits are very slight infoldings containing little stain.

When negatively stained with the uranyl acetate–oxalic acid complex (Fig. 8), the pitlike structures appear similar to those observed with ammonium molybdate staining. The pitlike structures have also been observed with sodium phosphotungstate staining (*11*), but this stain tends to cause a rapid disruption of the nonfixed erythrocyte membrane, as suggested by Haggis and Harris (*12*).

Detail of the erythrocyte ghost surface

The membrane surface surrounding the pit structures (Figs. 7 and 8) has an unevenness of texture that makes it readily distinguishable from the carbon background. A survey of this surface has been made in an attempt to locate the hollow cylinder protein molecules previously isolated from erythrocyte ghosts (*13–15*). These molecules can be released from intact erythrocyte ghosts when they are made to undergo fragmentation by distilled water dialysis followed by a freeze-thaw treatment. Figure 9 shows a representative negatively stained field containing the isolated and concentrated hollow cylinder protein. Most of the molecules are oriented on their side, giving rectangular profiles (approximately 170 Å by 130 Å) with four cross striations. When oriented on their ends they appear as rings (approximately 130 Å in external diameter).

If located on or in the erythrocyte membrane, it is likely that these molecules will be revealed less clearly in the electron microscope than when they are in the isolated state. The structures indicated by the circles (Figs. 10–12) have rectangular and ring-like profiles and may represent hollow cylinder protein molecules situated on the membrane surface. Some individual molecules have been observed on the background (Figs. 10 and 11, arrowed) so it cannot be stated without reservation that the particles seen on the membrane surface are in their true locations. They may have been released by the negative stain and have settled randomly on the membrane before the stain dried.

DISCUSSION

The nuclear membrane

Negative staining with ammonium molybdate at pH 7.0 has been shown to reveal clearly the pore complexes situated in rat liver nuclear membrane. The uranyl acetate-oxalic acid complex at pH 7.0 was also found to be a successful stain though it pred-

uced a more granular background. The annuli of the nuclear pore complexes tend to be broader and more irregular than those observed by other workers, who used phosphotungstate as the negative stain, usually following osmic acid fixation (*7–9*, *30*, *31*). The octagonal symmetry of the annuli proposed by Gall (*9*) has been supported by the results presented in this study. The "subunits" of the annuli are approximately 250 Å in diameter, and their edges appear to be continuous with the surrounding membrane. The fact that the annuli are able to separate themselves from the surrounding membrane (Figs. 2 and 3) does suggest, however, that they have a greater structural rigidity than the membrane. This apparently mechanical disruption of the nuclear membrane by the negative staining procedure was also observed by Gall (*9*).

The nuclear pores trap a considerable quantity of negative stain which makes them stand out very clearly. Some of the pores have central electron transparent spots (Fig. 3), which is in agreement with thin-sectioning studies (*18*, *25*) that suggested the existence of material within the nuclear pore. The permeability studies of Wiener *et al.* (*29*) strongly suggest that some form of barrier exists within the nuclear pores. Yet on the other hand an accumulating amount of evidence suggests that there may be nuclear-cytoplasmic transport of material via the nuclear pores (*25*). When nuclear membrane preparations containing less nucleoprotein contamination are obtained, the negative staining technique should be able to resolve more detail within the nuclear pore complexes than has been possible in this study. It is probably reasonable to consider that the nuclear pore complexes perform important cellular functions for which they are structurally specialized.

The erythrocyte ghost

Most previous studies on erythrocyte ghosts by negative staining have shown the membrane surface to be relatively smooth and featureless (*12*, *22*). Nevertheless, Haggis (*11*) has shown that erythrocyte ghost fragments negatively stained with sodium phosphotungstate possess pit structures similar to those observed on the surface of intact erythrocyte ghosts in the present study. After treatment with the plant glycoside saponin, erythrocyte ghosts have been shown by negative staining to be covered with an almost hexagonal array of 85 Å holes (*6*). This observation, however, was very rapidly explained by Bangham and Horne (*2*) and Glauert *et al.* (*10*),

FIG. 9. A representative field of the isolated and concentrated hollow cylinder protein from human erythrocyte ghosts. Negatively stained with a 2 % solution of sodium phosphotungstate (pH 7.0). ×150,000.

FIGS. 10 and 11. Parts of the surfaces of a human erythrocyte ghost. Negatively stained with a 2 % solution of the uranyl acetate–oxalic acid complex. The circles indicate structures on the membrane surface closely resembling the hollow cylinder protein molecules. The arrows indicate free hollow cylinder protein molecules on the background. ×150,000.

FIG. 12. Part of the surface of a human erythrocyte ghost. Negatively stained with 2 % ammonium molybdate. The circles indicate structures on the membrane surface closely resembling the hollow cylinder protein molecules. The arrows indicate pit structures. ×150,000.

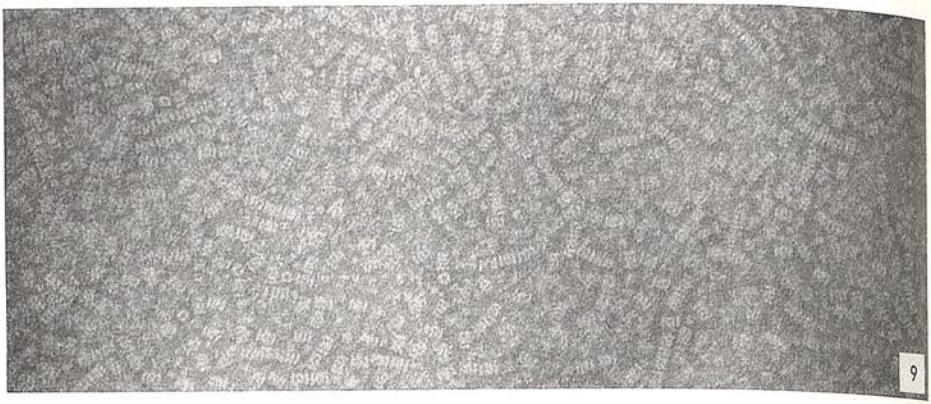
9

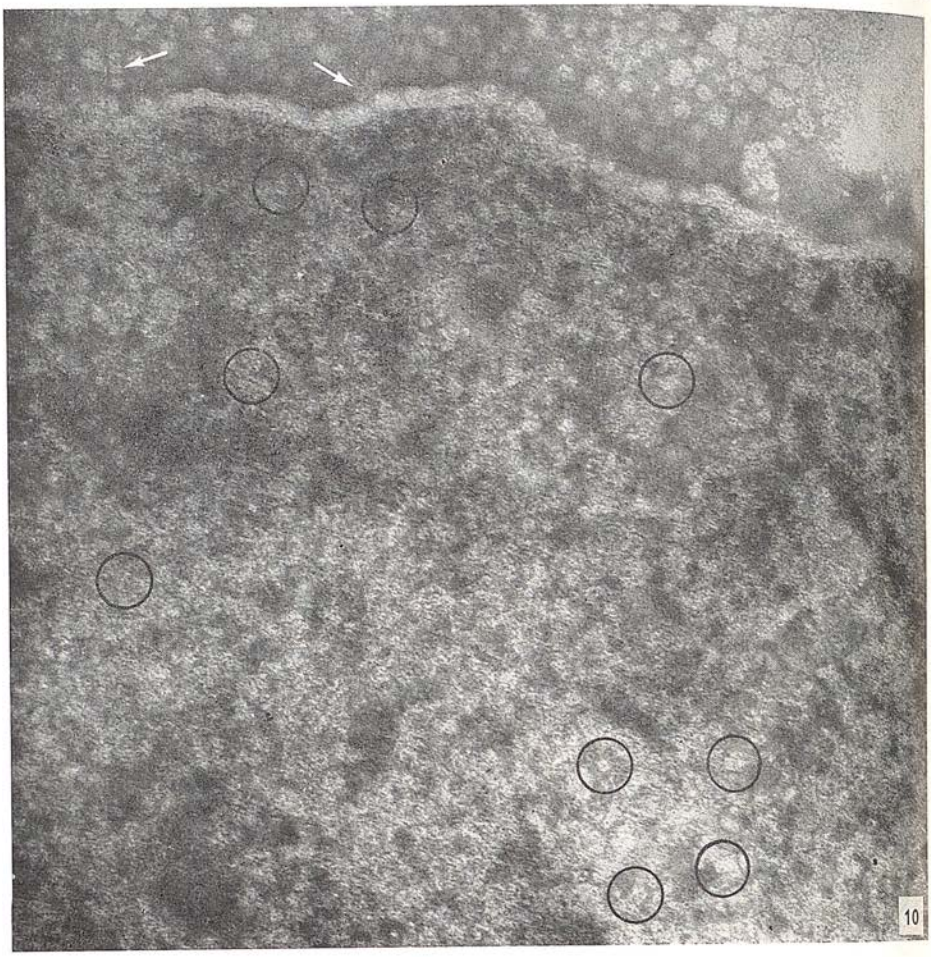
10

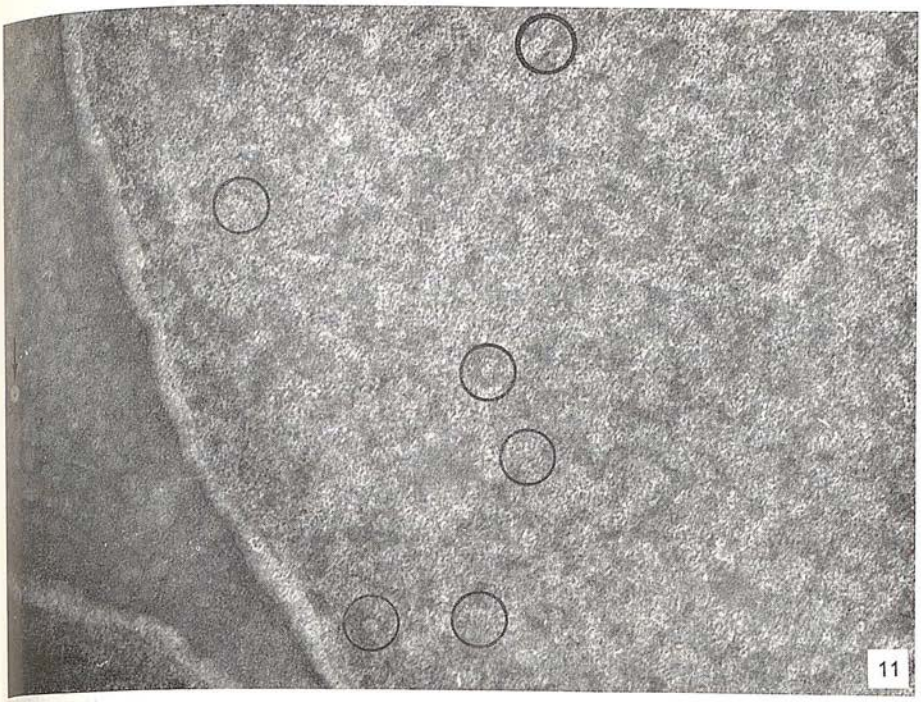

11

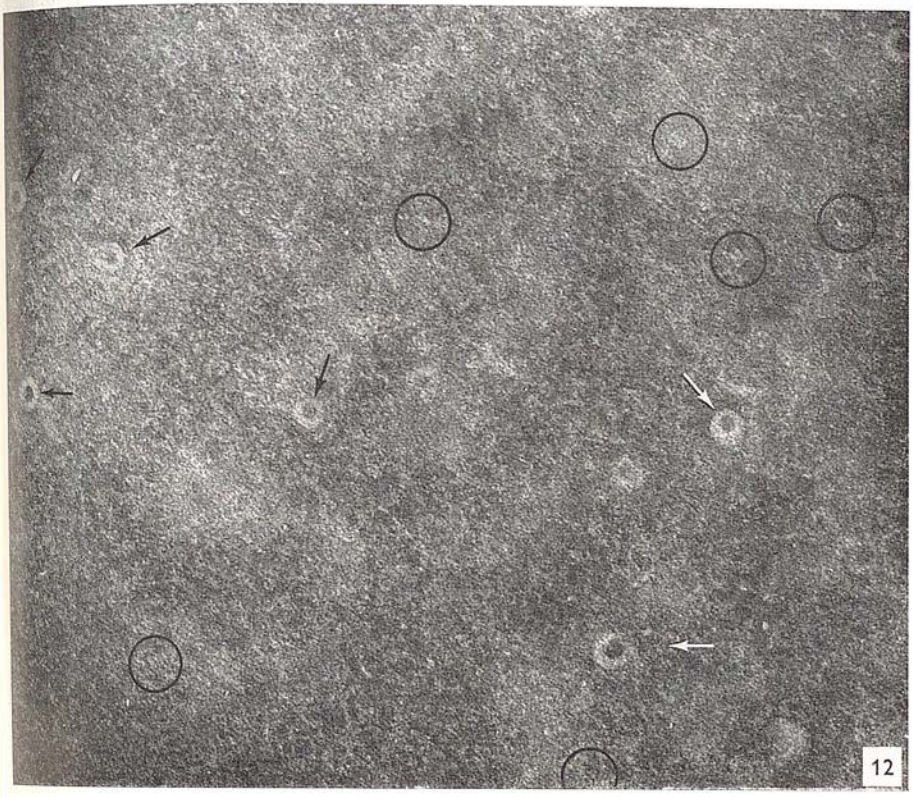

12

who showed the holes to be artifacts produced by the interaction of saponin with the membrane lipids.

Complement hemolysis has also been shown to produce pitlike lesions 80–100 Å in diameter in the erythrocyte membrane (*16*). These pits have also been interpreted as localized changes within the lipid phase of the membrane. The complement-induced membrane pits are very similar to the pits observed on untreated intact human erythrocyte ghosts when negatively stained with ammonium molybdate or the uranyl acetate–oxalic acid complex, but are present in much greater numbers and may be slightly smaller. It is possible that the repeated washings in hypotonic buffer used to obtain hemoglobin-free ghosts may have produced membrane lesions and that the pits on untreated ghosts are membrane artifacts. Because of the close similarity between the two types of membrane pits, it cannot at the moment be claimed that the action of complement is essential for their formation, as claimed by Humphrey and Dourmashkin (*16*) and Coombs and Lackmann (*5*).

The holes or pits observed on the surface of the untreated erythrocyte ghost differ in several respects from the nuclear pore complexes. First, they are considerably smaller, and second, they have very smooth contours. The second difference tends to suggest that the erythrocyte ghost pits are not composed of subunits, though this possibility cannot be ruled out. The variable edge thickness of the erythrocyte ghost pits is also a feature not observed for the nuclear pore annuli. This suggests that the erythrocyte ghost pits may represent localized infoldings of the membrane rather than structures standing up on the membrane surface.

Haggis (*11*) postulated that the pits he observed on ghost fragments might be places where stromalytic outfoldings from the membrane had broken off. The authors consider this to be unlikely since no free stromalytic tubes have been observed on the background adjacent to intact ghosts showing these pits. Also, varying lengths of stromalytic tube have been shown by Baker (*1*) to be left attached to erythrocyte ghosts negatively stained with sodium phosphotungstate.

Fine detail of the erythrocyte ghost surface

Both the negative stains used throughout this study have shown that the surface of the erythrocyte membrane has a detailed fine structure. This fine structure does not appear as an ordered array of subunits, but as an overall random unevenness of texture. It has been possible, however, to locate, with reasonable accuracy, individual particles which closely resemble the hollow cylinder protein molecules previously isolated from erythrocyte ghosts (*13–15*). The clarity of the particles on the membrane surfaces is not as great as when they are in the isolated state. The electron micrographs presented do nevertheless show clearly that the surface of the erythrocyte ghost is not featureless. It is probable that there are a large number of proteins (e.g., blood

group antigens and enzymes) that are located on or within the outer surface of the erythrocyte membrane. These proteins may even be organized in characteristic spatial arrangements, as suggested by Johnson (*17*) for the enzymes located on the surface of hamster intestinal microvilli. Proteins on or in the surface of the erythrocyte ghost have beneath them two layers of membrane which will reduce the ability of a negative stain to contrast the proteins. Thus the difficulty regarding the precise location of the protein under consideration by negative staining can be readily appreciated. The fact that some free molecules can be observed on the carbon background adjacent to the erythrocyte ghosts may be indicative of their having been released from the membranes during the negative staining procedure.

Several groups of workers have been able to show membrane-associated molecules or particles by negative staining (*3*, *4*, *17*, *23*, *24*, *27*). Humphrey and Dourmashkin (*16*) were able to visualize a 19 S hemolytic antibody at the edge of sheep erythrocyte ghost fragments, but they stated that it was invisible on the surface of the membranes. The hollow cylinder protein from erythrocyte ghost (22.5 S) has a very easily recognizable rectangular profile when lying on its side and is thus brought just within the range of visualization by negative staining when situated on the erythrocyte membrane surface. The clarity with which membrane associated molecules can be visualized by negative staining depends primarily on the degree to which the particle stands up from the membrane surface and can accumulate stain around itself, and, second, on thickness of the membrane layer or layers beneath the particle.

The efficiency of the two negative stains employed throughout this study has been investigated at different electron optical magnifications. At lower magnifications both ammonium molybdate and the uranyl complex provide adequate contrast. At higher magnifications the uranyl complex appears to afford a superior contrast to ammonium molybdate, but it does at the same time give a more granular texture to the electron image.

In conclusion it can be said that the results obtained using ammonium molybdate are in general agreement with those of other workers (*21*, *22*). Negative staining has been shown to provide a successful means of studying features of membrane material over the entire range of electron optical magnifications now available. At high magnifications negative staining has the ability to reveal detail on or within cellular membranes at the molecular level.

The authors wish to acknowledge the fact that electron microscopic facilities were made available by Professor W. E. Watson, Department of Physiology, University of Edinburgh. They also wish to thank Mr. J. N. Brown for the skillful technical assistance he provided. The helpful comments made by Dr. A. H. Maddy, Department of Zoology, University of Edinburgh, throughout the preparation of the manuscript are gratefully acknowledged. P.A. is a recipient of an M.R.C. training grant.

REFERENCES

1. BAKER, R. F., *J. Ultrastruct. Res.* **11**, 494 (1964).
2. BANGHAM, A. D. and HORNE, R. W., *Nature* (*London*) **196**, 952 (1962).
3. BENEDETTI, E. L. and EMMELOT, P., *J. Cell Biol.* **26**, 299 (1965).
4. BENEDETTI, E. L., BONTE, W. S. and BLOEMENDAL, H., *Lab. Invest.* **15**, 196 (1966).
5. COOMBS, R. R. A. and LACKMANN, P. J., *Brit. Med. Bull.* **24**, 133 (1968).
6. DOURMASHKIN, R. R., DOUGHERTY, R. M. and HARRIS, R. J. C., *Nature* (*London*) 194, 1116 (1962).
7. FRANKE, W. W., *J. Cell Biol.* **31**, 619 (1966).
8. —— *Z. Zellforsch. Mikrosk. Anat.* **80**, 585 (1967).
9. GALL, J. G., *J. Cell Biol.* **32**, 391 (1967).
10. GLAUERT, A. M., DINGLE, J. T. and LUCY, J. A., *Nature* **196**, 953 (1962).
11. HAGGIS, G. H., *Biochim. Biophys. Acta* **193**, 237 (1969).
12. HAGGIS, G. H. and HARRIS, J. R., *Proc. Eur. Reg. Conf. 4th Electron Microsc.* p. 21 (1968).
13. HARRIS, J. R., *Biochim. Biophys. Acta* **150**, 534 (1968).
14. —— *ibid.* **188**, 31 (1969).
15. —— *J. Mol. Biol.* **46**, 329 (1969).
16. HUMPHERY, J. H. and DOURMASHKIN, R. R., *Complement Ciba Found. Symp.* p. 175 (1965).
17. JOHNSTON, C. F., *Fed. Proc. Fed. Amer. Soc. Exp. Biol.* **28**, 26 (1969).
18. KESSEL, R. G., *J. Ultrastruct. Res.*, Suppl. 10 (1968).
19. MELLEMA, J. E., VAN BRUGGEN, E. F. J. and GRUBER, M., *J. Mol. Biol.* **31**, 75 (1968).
20. MERRIAM, R. W., *J. Biophys. Biochem. Cytol.* **11**, 559 (1961).
21. MUNN, E. A., *J. Ultrastruct. Res.* **25**, 362 (1968).
22. MUSCATELLO, W. and HORNE, R. W., *J. Ultrastruct. Res.* **25**, 73 (1968).
23. NISHI, Y., YOSHIDA, T. O. and TAKESUE, Y., *J. Mol. Biol.* **37**, 441 (1968).
24. SATO, Y. and NAGASE, K., *Biochem. Biophys. Res. Commun.* **27**, 195 (1967).
25. SCHARRER, B. and WURZLMANN, S., *Z. Zellforsch. Mikrosk. Anat.* **96**, 325 (1969).
26. SPORN, M. B., WANKO, T. and DINGMAN, W., *J. Cell Biol.* **15**, 109 (1962).
27. THORNLEY, M. J., HORNE, R. W. and GLAUERT, A. M., *Arch. Mikrobiol.* **51**, 267 (1965).
28. WIDNELL, C. C. and TATA, J. R., *Biochem. J.* **92**, 313 (1964).
29. WEINER, J., SPIRO, D. and LOEWENSTEIN, W. R., *J. Cell Biol.* **27**, 107 (1965).
30. WUNDERLICH, F., *Exp. Cell Res.* **56**, 369 (1969).
31. WUNDERLICH, F. and FRANKE, W. W., *J. Cell Biol.* **38**, 458 (1968).

J. ULTRASTRUCTURE RESEARCH 40, 178–196 (1972)

A Method for the Isolation and Purification of Normal Rat Liver and Hepatoma Nuclear "Ghosts" by Zonal Centrifugation

M. R. PRICE, J. R. HARRIS,[1] and R. W. BALDWIN

Cancer Research Campaign Laboratory, The University of Nottingham, University Park, Nottingham, NG7 2RD England

Received October 27, 1971, and in revised form February 1, 1972

A method is presented for the isolation of nuclear membranes in the form of large fragments and intact nuclear "ghosts" from normal rat liver and an aminoazo dye induced rat hepatoma.

The preparation involves overnight incubation at 4°C of the nuclear pellet suspension from hypotonic homogenates, followed by rate-dependent fractionation on a sucrose gradient in an A-XII Zonal rotor. The fraction sedimenting between mitochondria and nuclei was observed using phase contrast microscopy to be rich in large membrane fragments and nuclear "ghosts". Isopycnic centrifugation of this fraction on sucrose gradients, in conventional swinging-bucket and zonal rotors resulted in a purification of the nuclear membranes. No significant difference in the density of normal rat liver and hepatoma nuclear membranes was detected.

The purity and homogeneity of the nuclear membranes was confirmed by electron microscopy using both thin sectioning and negative contrast staining. Both electron microscopic techniques revealed the presence of pore complexes on the nuclear membranes, there being a marked absence of membranes not displaying these morphological features in the purified preparation. An assessment of the degree of contamination of the membranes with chromatin was obtained by thin sectioning and by measurement of DNA : protein ratios in purified preparations of both nuclear membranes and intact nuclei.

The method developed for the preparation of nuclear membranes is an extension of those devised for the isolation of plasma membranes under hypotonic conditions, and the preparative procedures are discussed in relation to previous studies upon both plasma membranes and nuclear membranes. The method is thought to be significant as an addition to the use of rate and isopycnic zonal centrifugation for the purification of cellular organelles.

The importance of cellular membrane systems in relation to intra- and intercellular control and organization has long been appreciated. The long-term aim of all investigators in this field is to correlate membrane structure and composition with func-

[1] Present address: Department of Physiology, Bute Medical Buildings, St. Andrews, Fife.

tion. Each of these separate approaches has produced rapid advances, but as yet they have not been integrated to any significant extent.

In recent years the plasma membrane has been the focus of much attention, and though most of this has been directed toward the erythrocyte membrane, several standardized preparative procedures have been developed for obtaining this material from other tissues, in particular rat and mouse liver (*7*, *8*, *14*, *18*, *20*). In contrast to the plasma membrane, studies on the nuclear membrane have been less extensive and only very recently have satisfactory methods been devised for the bulk isolation of this membrane (*1*, *10*, *15*, *21*). The nuclear membrane obtained by these groups was nearly always in a state of considerable fragmentation owing to the vigorous treatments applied during its preparation (i.e., sonication, DNase and high salt), though one of the treatments developed by Zbarsky et al. (*21*) only involved osmotic shock followed by gradient centrifugation.

It was initially during a study of the isolation of plasma membrane from rat liver and an aminoazo dye induced hepatoma by rate-dependent zonal centrifugation that the possibility presented itself of applying a similar method for the preparation of almost intact nuclear "ghosts", directly from the crude nuclear pellets. Our criterion for considering the nuclear membranes obtained by this method to be intact was the presence of "ghostlike" bodies in fractions observed by phase contrast microscopy and electron microscopy. The latter technique gave a good, though qualitative, indication of the contamination of the final material by other membrane species and chromatin. The work to be presented must be considered primarily as the development of a new method, supported by an ultrastructural study, in which the maintenance of the morphological integrity of nuclear membrane has been the prime concern, rather than the preparation of nuclear membrane fragments with a very low DNA content.

MATERIALS AND METHODS

Treatment of normal liver prior to homogenization

Adult male and female rats (Wistar strain) were killed by cervical fracture and the livers were perfused via the hepatic vein with cold 0.15 M NaCl until blanched. After removal, the livers (30–80 g) were finely chopped and all subsequent operations were carried out at 0-4°C.

Treatment of hepatoma prior to homogenization

Hepatoma D23, originally induced by 4-dimethylaminoazobenzene in a male rat (Wistar strain), was maintained by serial transplantation into syngeneic hosts and was harvested after 7-9 days of growth in the peritoneal cavity. The tumor at this stage contained little or no necrosis, and approximately 3–6 g of tissue was obtained from each animal. After re-

moval of the capsular connective tissues, the tumors (20–50 g) were finely chopped. All subsequent operations were carried out at 0–4°C.

After the above treatment, the isolation of nuclear "ghosts" from normal liver or hepatoma followed essentially the same procedures unless otherwise stated.

Homogenization

Chopped liver or hepatoma was passed three times through a tissue press using coarse, medium, and 60-mesh stainless steel grids. Much connective tissue was retained on the grids. Approximately 4 volumes of homogenization medium (1 mM $NaHCO_3$ pH 7.6 for normal liver, 1 mM $NaHCO_3$ pH 7.6 or 1 mM $NaHCO_3$–2 mM $CaCl_2$ pH 7.6 for hepatoma D23) were added per gram of minced tissue, which was then mixed with a spatula. Using a Potter-Elvehjem homogenizer, 10 complete passes were made with a loose pestle (0.4 mm clearance) resulting in a homogeneous suspension containing only a few large clumps of cells. These were removed by filtration through a 60-mesh stainless steel screen. After 5–10 passes with a tight pestle (0.2 mm clearance), a suspension was obtained in which there was approximately 80–90% disruption of cells, as judged by phase contrast microscopy. The suspension was passed twice through a 120-mesh stainless steel screen and centrifuged at 1000 *g* for 12 minutes in an M.S.E. Mistral 6L Refrigerated Centrifuge. The supernatants were discarded and the pellets were resuspended in 50–100 ml of homogenization medium with 1–2 passes of the tight pestle on the Potter-Elvehjem homogenizer. This suspension was stored overnight at 4°C prior to its use as sample in an A-XII Zonal rotor.

Sucrose density gradient centrifugation

A-XII zonal centrifugation. The M.S.E. A-XII Zonal rotor was filled at rest with 1 mM $NaHCO_3$ pH 7.6 and then accelerated to a loading speed of 500 rpm in a Mistral 6L centrifuge. The following sucrose solutions in 1 mM $NaHCO_3$ pH 7.6 were introduced into the rotor: 250 ml 6% (w/w), 100 ml 20% (w/w), 200 ml 20–30% (w/w) linear with respect to volume, 450 ml 30–39% (w/w) linear with respect to volume, and 50 ml 50% (w/w); (an M.S.E. fixed profile gradient former was used to generate the linear gradients). 60% (w/w) sucrose (in 1 mM $NaHCO_3$ pH 7.6) was then pumped into the rotor until the light end of the gradient started to emerge from the center feed line. The sample, 50–100 ml of the 1000 *g* nuclear pellet suspension, was introduced to the center of the rotor followed by sufficient 1 mM $NaHCO_3$ to give a sample plus overlay volume of 150 ml. The rotor was accelerated to 3000 rpm for 40 min. After reduction of the rotor speed to 500 rpm, the contents of the rotor were unloaded by pumping 60% (w/w) sucrose (in 1 mM $NaHCO_3$ pH 7.6) to the rotor edge. Fractions were collected in 25-ml aliquots and examined using phase contrast microscopy. Those fractions containing nuclear "ghosts" were pooled.

S.W. 25.1 sucrose density gradient centrifugation. Pooled fractions from the A-XII Zonal rotor were diluted with 1/3 volume of 1 mM $NaHCO_3$, and centrifuged at 30×10^3 rpm (78 000 *g* av) using a Type 30 rotor in a Model L preparative ultracentrifuge (Spinco Division, Beckman Instruments, Inc.). Pellets were washed once with 1 mM $NaHCO_3$, centrifuged at 10×10^3 rpm (9000 *g* av) for 15 minutes (Type 30 rotor) and resuspended in small volumes of 20% (w/w) sucrose (in 1 mM $NaHCO_3$). Aliquots, 2 ml, were layered upon linear sucrose density gradients (30–60%, w/w, sucrose in 1 mM $NaHCO_3$) in SW 25.1 rotor cellulose nitrate centrifuge tubes. Centrifugation was carried out for 16 hours at 25×10^3

rpm (64 000 *g* av) in the Model L centrifuge to obtain isopycnic banding of nuclear membranes. Fractions were collected in approximately 1-ml aliquots using an M.S.E. tube piercer, and each was examined using phase contrast microscopy. Those fractions containing nuclear "ghosts" were pooled, diluted with 1/3 volume of 1 mM $NaHCO_3$ and centrifuged for 30 minutes at 30×10^3 rpm (78 000 *g* av) (Type 30 rotor). The membranes were washed twice by centrifugation at 10×10^3 rpm (9 000 *g* av) (Type 30 rotor) for 15 minutes. The final pellet, resuspended in a small volume of 1 mM $NaHCO_3$ (approximately 5 ml) was taken as the purified nuclear "ghost" preparation.

B-XIV zonal centrifugation. In three experiments, the pooled fractions (approximately 400 ml) from the A-XII Zonal rotor, containing the nuclear "ghosts" were applied directly to an M.S.E. B-XIV Zonal rotor in an M.S.E. Super Speed 65 Preparative Ultracentrifuge. Initially the rotor was filled at rest with 60% (w/w) sucrose in 1 mM $NaHCO_3$ pH 7.6, and precooled to 4°C. At a loading speed of 2000 rpm, 60% (w/w) sucrose was displaced from the rotor edge by pumping the gradient, sample and overlay to the center of the rotor in the following order: 100 ml 44% sucrose (w/w), 50 ml 40% sucrose (w/w), both in 1 mM $NaHCO_3$ pH 7.6, 400 ml pooled nuclear "ghost" fractions from the A-XII Zonal rotor (approximately 30%, w/w, with respect to sucrose concentration) and 25 ml of 1 mM $NaHCO_3$. Since the capacity of the B-XIV Zonal rotor is 650 ml, this procedure leaves a cushion of 75 ml 60% (w/w) sucrose remaining on the periphery of the rotor. Centrifugation was carried out at 30×10^3 rpm for 16 hours to obtain isopycnic banding of the nuclear "ghosts". The contents of the rotor were unloaded at 2000 rpm by pumping 60% (w/w) sucrose to the rotor edge. Fractions were collected in 10 ml aliquots, examined using phase contrast microscopy and those containing nuclear "ghosts" were pooled, diluted with 1/3 volume of 1 mM $NaHCO_3$, and centrifuged at 30×10^3 rpm (78 000 *g* av) for 30 minutes (Type 30 rotor). The membranes were washed twice with 1 mM $NaHCO_3$ at 10×10^3 rpm (9 000 *g* av) for 15 minutes. (Type 30 rotor). The pellet was resuspended in a small volume (approximately 5 ml) of 1 mM $NaHCO_3$ and this was taken as the purified nuclear "ghost" preparation.

All gradients after centrifugation were examined spectrophotometrically using either an ISCO UV Analyser and chart recorder to obtain a continuous plot of OD 280 nm or by using a Unicam SP 500 Spectrophotometer to determine individual optical density measurement at 280 nm upon each fraction. The sucrose concentration of each fraction was obtained by measurement of refractive index using an Abbé refractometer.

Preparation of normal liver and hepatoma D23 nuclei

All sucrose solutions used in the isolation of normal liver and hepatoma D23 nuclei were prepared in a buffer consisting of 1 mM $NaHCO_3$–2 mM $CaCl_2$–2 mM $MgCl_2$, pH 7.6. Minced normal liver or hepatoma, prepared as described above was dispersed in 0.25 M sucrose (approximately 4 volumes of medium added per gram of minced tissue). Disruption of cells was carried out using a Potter-Elvehjem homogenizer. The conditions of homogenization were essentially identical to those described above for the isolation of nuclear "ghosts", with the exception that 3–5 passes with a 0.1 mm clearance pestle had to be included to achieve 80–90% disruption. A nuclear pellet was obtained by centrifugation at 1000 *g* for 10 minutes in a Mistral 6L centrifuge, and this was resuspended in 60% (w/w) sucrose. The actual concentration of this suspension with respect to sucrose was approximately 56% (w/w). Aliquots, 15 ml, were carefully layered upon 5 ml of 60% (w/w) sucrose in SW 25.1

rotor cellulose nitrate centrifuge tubes. An overlay of 0.25 M sucrose (5 ml) was layered upon the sample zone and the tubes were centrifuged at 25×10^3 rpm (64 000 *g* av) for 100 minutes in the Model L centrifuge. The supernatants were discarded and the pellets of nuclei were resuspended in 1 mM $NaHCO_3$–2 mM $CaCl_2$–2 mM $MgCl_2$. The nuclei were washed twice by centrifugation at 600 *g* for 10 minutes and the final pellet of purified nuclei was resuspended in small volumes (approximately 10–20 ml) of the buffer.

DNA and protein estimations

DNA was measured by the method of Dische (*5*) using calf thymus DNA (Sigma Chemical Co.) as standard. Protein was determined by the colorimetric method of Lowry et al. (*16*) with the Folin-Ciocalteu reagent (B.D.H.) and bovine serum albumin (Rosche Products) as standard.

Negative contrast staining

Following the removal of sucrose from isopycnically banded nuclear membranes, by either dialysis or centrifugal washing, negative contrast staining was performed on carbon-coated specimen grids using 2.0% solutions of sodium phosphotungstate or ammonium molybdate pH 7.0 (B.D.H.) as previously described (*11*).

Thin sectioning

Samples of the normal rat liver and hepatoma nuclei and nuclear membranes were fixed overnight in 1.0% glutaraldehyde (TAAB) at 4°C. This was followed by centrifugation at 1000 *g* for 10 minutes. The pellets were postosmicated in 1.0% osmic acid (B.D.H.) in 0.1 M phosphate buffer pH 7.4 for 2 hours at room temperature. Dehydration was performed by passage through graded ethanols and finally epoxypropane with centrifugation at 1000 *g* for 10 minutes at each step. Finally, the material was dispersed in TAAB epoxy resin, which after overnight penetration was polymerized at 60°C.

Thin sections were cut with an LKB Type III ultramicrotome, using glass knives. Sections were mounted on Micron type 400 grids without a supporting membrane. Post staining was performed using uranyl acetate in 50% ethanol.

Electron microscopy

Electron microscopic examination of the thin-sectioned and negatively stained specimens was performed with a Phillips E.M. 300 electron microscope. Photographs were taken on Ilford 3.25 × 4 inch E.M.6 plates.

RESULTS

Production of nuclear "ghosts"

Mild hypotonic homogenization of normal rat liver and hepatoma D23 in 1 mM sodium bicarbonate buffer was used to produce a well dispersed suspension in which there was 80–90 % cellular disruption, as judged directly by phase contrast microscopy. Filtration through fine stainless steel meshes ensured the removal of any large clumps of cells and most of the collagen fibers. The gelatinous nuclear pellet from liver homo-

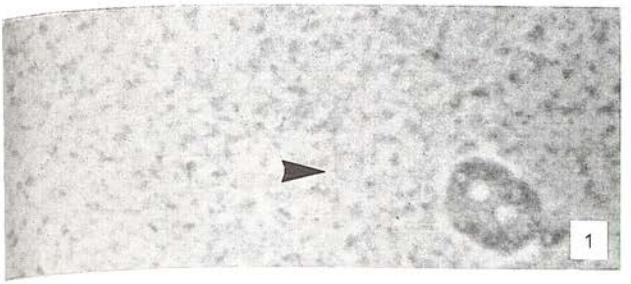

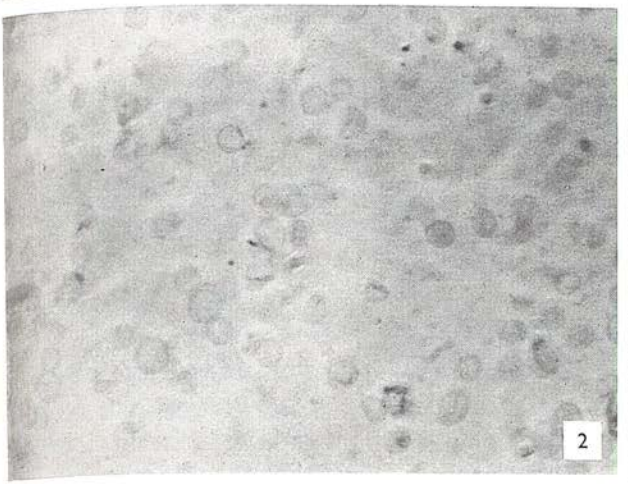

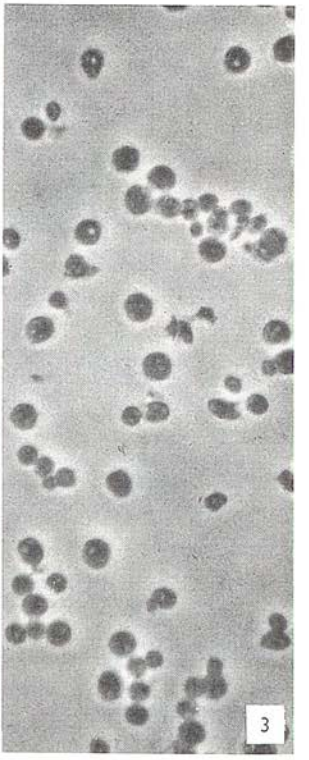

FIG. 1. Normal rat liver 1000 *g* pellet suspension, after incubation overnight at 4°C. One nuclear "ghost" (arrowed), together with an undisrupted cell are clearly visible. Detail is lost, however, owing to Brownian motion of the membranous and mitochondrial background. Phase contrast. ×400.

FIG. 2. Normal rat liver nuclear "ghosts", purified by rate zonal and isopycnic centrifugation. Phase contrast. ×400.

FIG. 3. Normal rat liver nuclei prepared in isotonic sucrose media. Phase contrast. ×400.
Phase contrast. ×400.

genates was easily dispersed in 1 mM bicarbonate buffer using 1 or 2 passes of the tight homogenizer pestle. With hepatoma D23 preparations this procedure resulted in an immediate aggregation of material into a gelatinous mass in which few free nuclei or cells could be seen by phase contrast microscopy. The presence of 2 mM calcium chloride in the 1 mM bicarbonate homogenization and resuspension buffer prevented this aggregation of material, but greatly diminished the yield of purified nuclear "ghosts", which were also found to retain a considerable quantity of chromatin. A well dispersed suspension of the hepatoma D23 nuclear pellet could, however, be obtained simply by incubation of the aggregated gelatinous material overnight at 4°C.

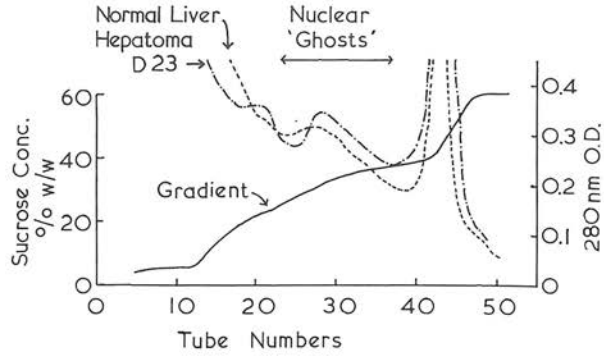

CHART 1. The fractionation of normal rat liver and hepatoma D23 nuclear pellet suspension on the M.S.E. A-XII Zonal rotor, following overnight incubation at 4°C.

Both the liver and hepatoma D23 resuspended nuclear pellets were thus routinely left overnight at 4°C, and after this incubation period observation by phase contrast microscopy revealed the presence of apparently empty or partially empty nuclei, having a circular appearance similar to erythrocyte "ghosts" but showing no biconcave profiles (Fig. 1). The hepatoma D23 nuclear "ghosts" were often ellipsoid or even cigar shaped, in accordance with the known variability of nuclear shape in this tissue.

Gradient centrifugation

Three major zones of material were resolved following rate-dependent centrifugation in the A-XII Zonal rotor at 3 000 rpm for 40 minutes. Representative OD 280 nm

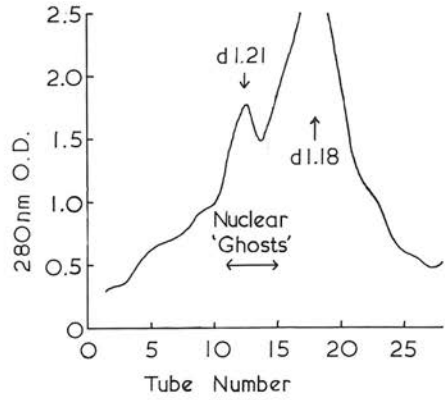

CHART 2. Isopycnic centrifugation in the Spinco SW 25.1 swing-out rotor of pooled A-XII Zonal rotor fractions containing normal rat liver nuclear "ghosts". Purified nuclear "ghosts" were located at density 1.21 ± 0.01. The peak at density 1.18 ± 0.01 consisted predominantly of other subcellular membrane species.

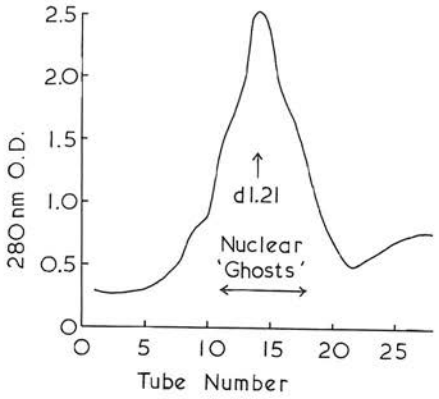

CHART 3. Isopycnic centrifugation in the Spinco SW 25.1 swing-out rotor of pooled A-XII Zonal rotor fractions containing hepatoma D23 nuclear "ghosts". Purified nuclear "ghosts" were located at density 1.21 ± 0.01. No peak at density 1.18 ± 0.01 was resolved in this fractionation. The presence of this latter peak was dependent upon the relative purity of the material taken from the A-XII Zonal rotor with respect to the nuclear "ghosts".

profiles obtained on unloading the A-XII Zonal rotor are shown in Chart 1. Fractionations performed on the normal liver and hepatoma D23 showed a marked similarity, and the procedure was found to be highly reproducible. Within the original sample zone, phase contrast observation revealed material showing a granular appearance typical of mitochondria, together with membrane vesicles. Undisrupted cells and some swollen but intact nuclei banded against the 60% (w/w) sucrose cushion. Between these two regions the gradients contained a broad zone of material that was predominantly membranous consisting of sheets and fragments together with large

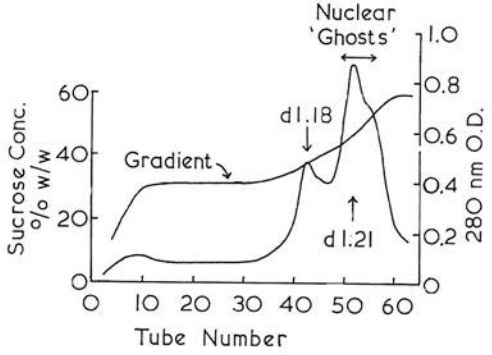

CHART 4. Isopycnic centrifugation in the M.S.E. B-XIV Zonal rotor of pooled A-XII Zonal rotor fractions containing normal rat liver nuclear "ghosts". Purified nuclear "ghosts" were located at density 1.21 ± 0.01. As in Chart 2 a peak at density 1.18 ± 0.01, consisting predominantly of other subcellular membrane species was observed.

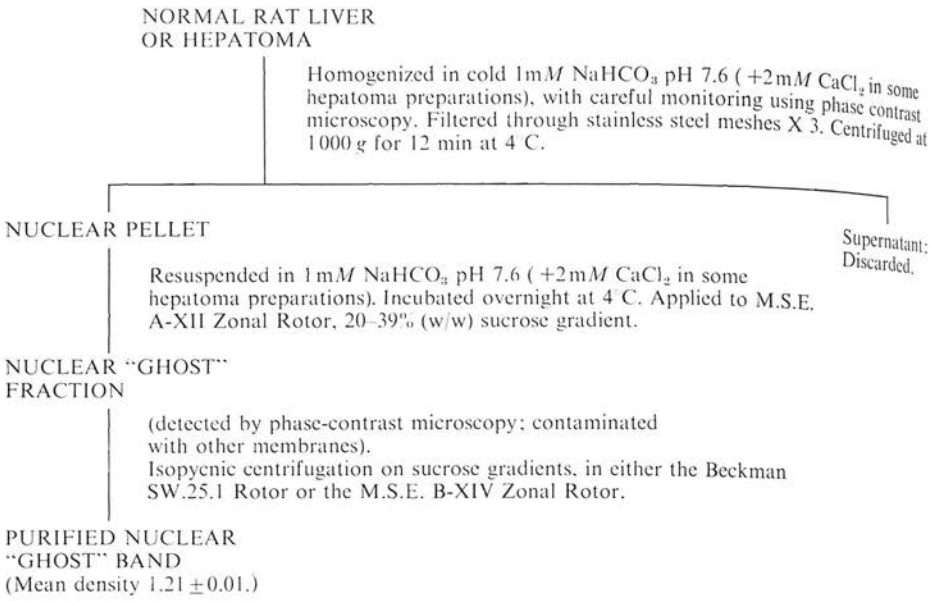

CHART 5. Preparation of nuclear "ghosts" from normal rat liver or hepatoma D23.

numbers of nuclear "ghosts". Hepatoma D23 preparations performed with 1 mM bicarbonate buffer containing 2 mM $CaCl_2$ resulted in the presence of many refractile particles of chromatin along with the membrane material. Low yields of nuclear "ghosts" were obtained under these conditions, and their behavior on isopycnic gradients was found to be highly irregular, indicating a variable residual chromatin content.

Charts 2 and 3 illustrate the results obtained following isopycnic banding of liver and hepatoma D23 nuclear "ghosts", respectively, on sucrose gradients in the Spinco SW 25.1 swing-out rotor. For both liver and hepatoma D23 preparations, a nuclear membrane band was observed midway in the gradient at density 1.21 ± 0.01. A second band of membrane material was detected at density 1.18 ± 0.01 on some isopycnic gradients (Chart 2), and its presence depended upon the relative purity of the material taken from the A-XII Zonal rotor with respect to the nuclear "ghosts".

Phase contrast microscopy of either liver or hepatoma D23 "ghosts" revealed that many of the purified membranes retain a circular profile, while others appear more collapsed and folded (Fig. 2). In comparison with intact nuclei, it is evident that a substantial loss of nucleoplasmic components has been achieved (Fig. 3).

A purification procedure was also developed using the M.S.E. B-XIV Zonal rotor (Chart 4). In this case, a short steep sucrose density gradient was utilized and a large

FIG.
cent
amn

FIG. 4. A normal rat liver nuclear "ghost" obtained by zonal centrifugation followed by isopycnic centrifugation. Two large membrane lesions are present (arrowed). Negatively stained with 2 % ammonium molybdate. pH 7.0. × 22 000.

sample volume was applied (i.e., the pooled nuclear "ghost" fractions from the A-XII Zonal rotor). This eliminated the necessity for sedimenting the pooled membranes prior to the isopycnic banding, and thereby avoided the production of undue mechanical damage to the "ghosts". Here again, a mean peak isopycnic density of 1.21 ± 0.01 was obtained for both the normal liver and hepatoma nuclear "ghosts".

The major features of the preparation are summarized in Chart 5.

DNA:protein ratios

In order to gain an estimation of the loss of chromatin from normal liver and hepatoma nuclear membranes, DNA: Protein ratios were determined and compared with values obtained on purified nuclei. Values of 0.12 and 0.13 for the DNA: Protein ratios of nuclear membranes from liver and hepatoma, respectively, were significantly lower than 0.50 and 0.52 obtained on intact nuclei from liver and hepatoma. These results are indicative of the loss of most of the chromatin from the membranes in agreement with electron microscopic observations (see below).

Electron microscopy

Negative contrast staining

A normal liver or hepatoma nuclear "ghost" was visualized by negative contrast staining as a circular or, more commonly with hepatoma D23, ellipsoid collapsed body, usually with one or more lesions, from which it is presumed that the nucleoplasm had escaped during the preparation (Fig. 4). Even at the low electron optical magnification used in Fig. 4, the nuclear pore complexes are readily visible, as pits containing negative stain, with pronounced annuli around the edge. The presence of these easily recognizable features only on the nuclear membranes enables an assessment of the contamination by other membrane species to be made. Also, the presence of finely dispersed material, probably chromatin, on the carbon background adjacent to the nuclear "ghosts" is readily detected.

At higher electron optical magnifications the nuclear pore complexes can be seen in more detail (Figs. 5 and 6), and a good indication of the overall cleanliness of the membrane surface is obtained. Some of the nuclear pores show the central "spot" (arrowed), and the subunit composition of the annuli is apparent in a few cases. Some loss of image clarity is to be expected since the collapsed nuclear "ghost" presents two layers of double nuclear membrane. An overlapping of some of the nuclear pores on the upper membrane layer with those on the lower membrane can reasonably be expected.

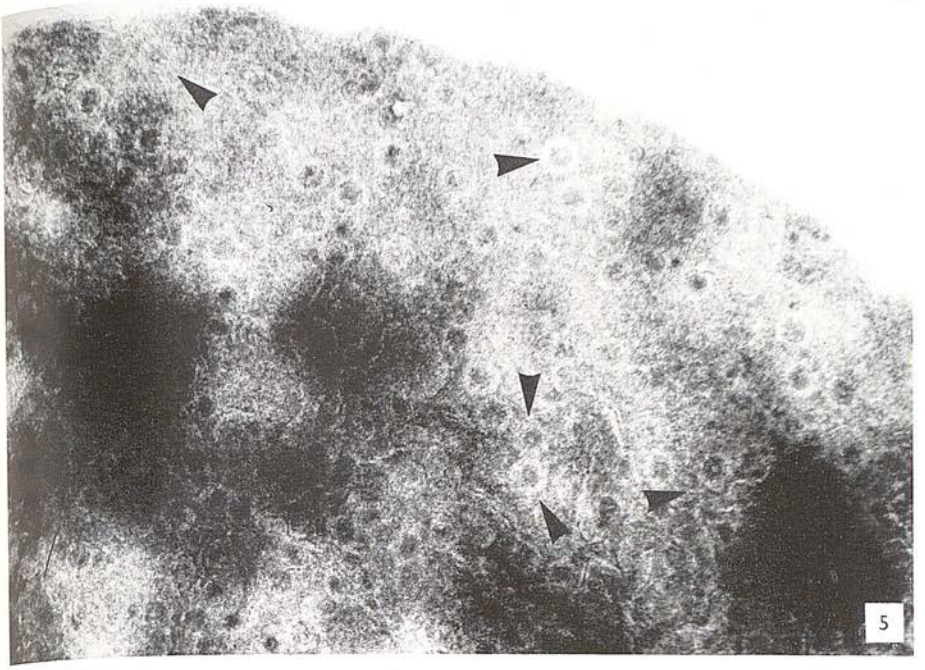

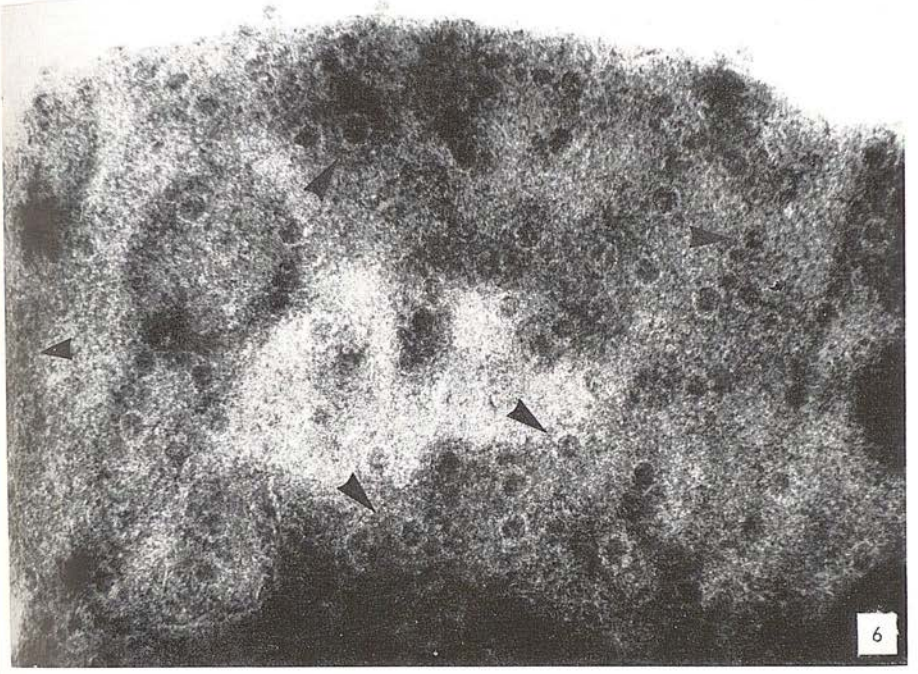

FIGS. 5 and 6. Small regions of purified normal rat liver and hepatoma D23 nuclear "ghosts", respectively. The subunit composition of some of the nuclear pore annuli is apparent, as in the central "spot" of several nuclear pores (arrowed). Negatively stained with 2 % ammonium molybdate, pH 7.0. ×44 000 and ×56 000, respectively.

Thin sectioning

The isopycnically banded nuclear membranes are revealed by thin sectioning as collapsed and folded membranous sheets. Where the membranes are intact and delimiting, without interruption of the more or less circular shape of the nucleus, it is usually possible to distinguish which side of the membranes had previously bordered on the cytoplasm and which on the nucleoplasm. The presence of both inner and outer membranes in hepatoma nuclear "ghost" preparations can be distinguished along segments of the membranes (Fig. 7, arrowed). At this low electron optical magnification, the absence of chromatin and overall homogeneity of the "ghost" preparation is apparent. At higher magnification, the inner and outer nuclear membranes may be more clearly seen in Fig. 8 which shows a rat liver nuclear "ghost". The membranes do, however, tend to have a very irregular beaded electron image (Fig. 8), if compared with the electron images given by most other membrane species. This beaded nature could be due to bound chromatin, to ribosomes, or to true structural features of the membrane. The latter postulation must certainly account for a considerable part of the explanation, since the known presence of nuclear pore complexes will impart to the embedded membrane a greater overall irregularity of the distribution of bound heavy metal atoms, than will occur in most other membranes. Regions of nuclear membrane which are thin-sectioned tangentially to the plane of the membrane surface reveal clearly the presence of positively stained nuclear pore annuli (Figs. 9 and 10, arrowed). In all other regions neither the pores nor their annuli can be located with any degree of certainty, even though from the negative staining results they are known to be present in large numbers.

DISCUSSION

In all previously reported methods describing the isolation of nuclear membranes, the initial step has been to obtain a purified preparation of nuclei. Varied approaches have been devised to produce nuclear disruption and then to isolate a membranous fraction with a low DNA content.

Fairly extensive use has been made of ultrasonication (*10*, *12*, *15*, *17*, *21*), and it appears that in general the membrane obtained is in a state of extensive fragmentation, though the nuclear pore complexes are still present. Enzymatic treatment with DNase, followed by a high salt extraction was employed by Berezney et al. (*1*). This method also produced extremely fragmented membranes, on which the nuclear pore

FIG. 7. Thin-sectioned rat hepatoma D23 nuclear "ghosts" purified by isopycnic centrifugation. Arrows indicate regions where both inner and outer membranes are seen to be present. × 18 000.
FIG. 8. A thin-sectioned normal rat liver nuclear "ghost", purified by isopycnic centrifugation. The inner and outer nuclear membranes (*INM* and *ONM*) are seen to separate from the another in places. × 22 000.

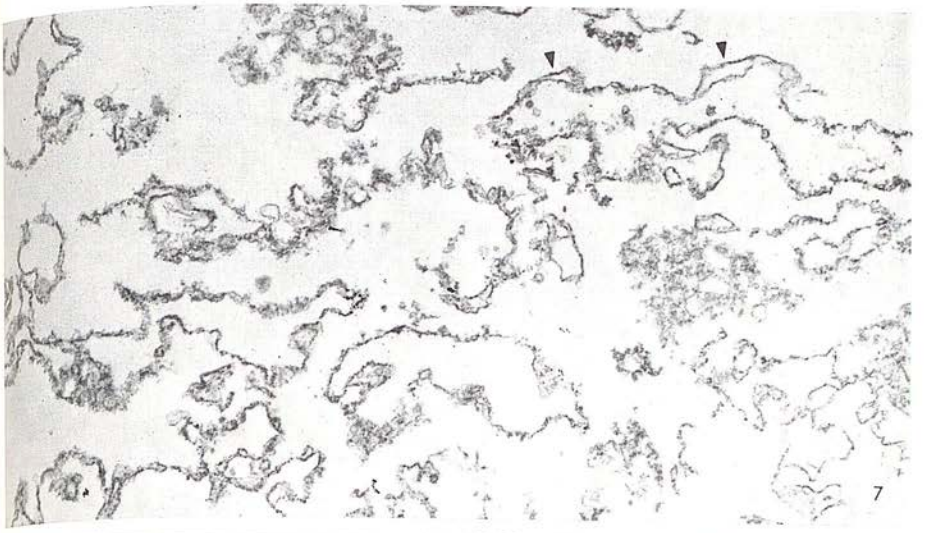

7

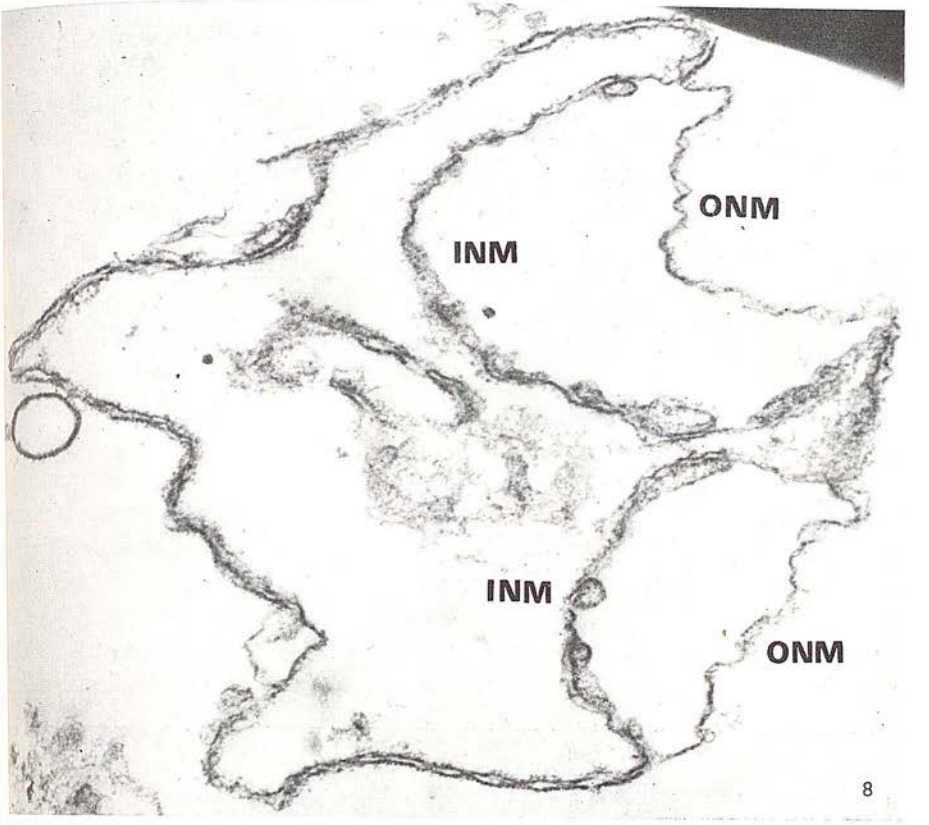

8

complexes appear very distorted. Large quantities of ribosomes, which are known to be associated with the outer nuclear membrane, were also present on their final purified nuclear membrane.

In a paper on the isolation of nuclear membranes from onion root tip nuclei, Franke (*9*) showed that the nuclei would quickly burst if put into a hypotonic medium. The nuclei inside avian erythrocyte "ghosts" have also been observed to burst on omission of divalent cations from the washing buffer (*13*). Similarly, in an investigation of RNA synthesis by purified chick erythrocyte nuclei, Brasch et al. (*2*) have shown that the condensed state of the chromatin is lost under conditions of low ionic strength. Also, the nuclei swell and burst, allowing the "soluble" chromatin to escape. The replacement of the calcium chloride and magnesium chloride in the suspension medium of rat liver nuclei by barium chloride was found by Harris and Agutter (*11*) to produce a low yield of nuclear "ghosts", which were preferentially selected for electron microscopic study by negative staining. (It must be stressed that this barium treatment was not considered to give a membrane preparation.)

The results presented in the current publication indicate that it is possible to prepare nuclear membranes, predominantly in the form of intact "ghosts", directly from the crude nuclear pellets of rat liver and hepatoma homogenates. Briefly, the relatively mild, nondestructive methods of hypotonic homogenization followed by overnight incubation at 4°C and sucrose gradient fractionation were employed to release the bulk of the chromatin from the nuclei. Before expanding the discussion further it is important to critically examine the essential features of this method and to evaluate the experimental conditions which favor the isolation of nuclear membranes. It must immediately be stressed that phase contrast microscopy has provided a very effective tool for monitoring the fate of the nuclei and, together with electron microscopy, has been invaluable in assessing the significance of the various procedures employed.

During initial studies on the large scale preparation of plasma membranes from rat liver and hepatoma, it was found convenient to prepare a nuclear pellet suspension on the day prior to performing an A-XII Zonal fractionation, thus allowing sufficient time to monitor the homogenization procedure with great care. Particular attention was paid to avoid excessive mechanical damage to nuclei, while attempting to prepare a homogenate containing maximum cellular disruption. The use of sodium bicarbonate as a homogenization medium for normal rat liver has been reported in several papers since it was first included in the original procedure of Neville (*18*) for the isolation of plasma membranes from rat liver. It is interesting to note that in this paper Neville makes several pertinent comments on the state of the nuclei, and the

FIGS. 9 and 10. Selected regions of thin sectioned normal rat liver and hepatoma D23 nuclear "ghosts" that reveal the nuclear pore complexes (arrowed). × 28 000 and × 16 500, respectively.

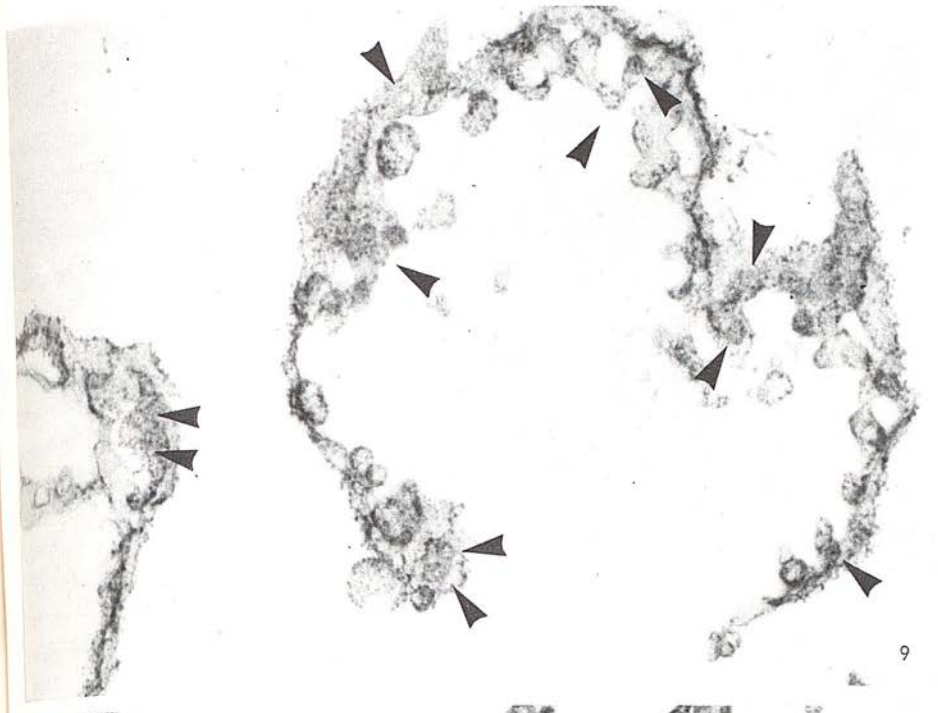

9

10

release of nuclear membranes which he claims undergo fragmentation on repeatedly washing the nuclear pellet with 1 mM bicarbonate buffer. Emmelot and Bos (*7*) state that the addition of 2 mM calcium chloride is desirable when preparing plasma membrane from hepatoma and in some experiments this suggestion was followed. However, owing to the presence of many refractile particles of chromatin in the membrane fractions taken from the A-XII Zonal rotor, this addition is now considered undesirable for the isolation of nuclear membrane.

Perhaps the most critical step in our method is the overnight incubation of the crude nuclear pellets in 1 mM bicarbonate buffer at 4°C. This gives rise to the formation of nuclear "ghosts", which are easily detected by phase contrast microscopy in the suspension to be used as the A-XII Zonal sample. It is probable that other workers using the 1 mM bicarbonate buffer for the isolation of plasma membranes have not observed nuclear "ghosts" in this suspension, since the crude nuclear pellets have not been retained overnight but have been applied to sucrose gradients immediately after resuspension. The hepatoma crude nuclear pellet goes through a gelatinous phase on resuspension in the 1 mM bicarbonate buffer, but this gelatinous state slowly disappears over a period of hours, the material being uniformly dispersed after overnight incubation. This gel-sol phase change was not encountered on resuspension of normal rat liver crude nuclear pellets, though it can be stated that the nuclear pellet does itself appear gelatinous in agreement with the observations of Evans (*8*) and Neville (*18*).

The formation of "ghosts" in the nuclear pellet suspension could be due to a variety of reasons. We consider the nuclei must be losing some mono- and divalent cations which are probably responsible for the initially condensed state of the chromatin. It is reasonable to propose that a loss such as this could take place fairly slowly resulting in a gradual production of nuclear "ghosts" as "soluble" chromatin escapes from lesions in the nuclear surface. There may be a preferential uptake of divalent cations by other membrane components in the suspension, which could aid the dispersal of the chromatin. Wallach (*19*) has stated that homogenization in 1 mM $NaHCO_3$ buffer produces contamination of subcellular membrane components by adsorption of basic nuclear proteins which leads to coaggregation of small and large fragments. The presence of large quantities of other membranes and subcellular debris in the resuspended nuclear pellets may well account for a binding of some "soluble" chromatin as it is being released from the nuclei. Indeed, since the nuclear pellet is such a complex mixture, it is not possible to exclude the involvement of autolytic degradation which may promote the formation of nuclear "ghosts" during the incubation period.

It must be stated that the method for obtaining nuclear membrane developed by Zbarsky et al. (*21*) from purified rat liver nuclei by hypotonic shock does parallel our method to some extent. Work is currently in progress with regard to the application of the principles developed in our method, to the production of nuclear membrane from

purified nuclei. Preliminary results indicate that a long incubation at low ionic strength in the absence of divalent cations is again necessary for the production of nuclear "ghosts".

Although no analytical information has been presented in relation to the percentage of the initial DNA retained in our purified nuclear membranes, the figures for the DNA to protein ratio are significantly lower than those obtained on intact nuclei. The electron micrographs showing the almost complete absence of chromatin inside the nuclear "ghosts" gives support to our claim that the preparation can be considered as reasonably pure. The highly reproducible sucrose banding density of 1.21 ± 0.01 for both normal liver and hepatoma nuclear "ghosts" gives a good indication of the homogeneity of the membrane species and is in close agreement with that obtained by Franke et al. (*10*) for normal rat liver nuclear membrane fragments.

The DNA content of the "ghost" preparation is higher than that obtained by most other workers. In the present state of knowledge we are not in a position to say to what extent DNA is a true component of the nuclear membrane, although there is considerable evidence suggesting that there is a close relationship between chromatin and nuclear membrane pore complexes (*3*, *4*, *6*). Also, it has been claimed that DNA synthesis is associated with the inner nuclear membrane (*17*).

The desirability of using a preparation that consists predominantly of intact nuclear "ghosts" rather than finely fragmented nuclear membranes for the investigation of the ultrastructure, composition, and function of the nuclear membrane is clearly evident. The method presented in this publication is thought to provide membranous material that is not removed as far from the normal physiological condition as that produced by most other methods. This statement is based on the observed overall ultrastructural integrity of the membranes and awaits confirmation at the functional level.

The authors wish to acknowledge the financial assistance of the Medical Research Council and Cancer Research Campaign and also a Government Grant through the Royal Society. Thanks are expressed to Professor H. K. Weinbren, Department of Pathology, for making available the electron microscope facilities, which were provided by the Medical Research Council. Thin sectioning was skillfully performed by Miss B. A. Smith, and help with much animal work was provided by Mrs. M. E. Marshall.

REFERENCES

1. Berezney, R., Funk, L. K. and Crane, F. L., *Biochim. Biophys. Acta* **203**, 531 (1970).
2. Brasch, K., Seligy, V. L. and Setterfield, G., *Exp. Cell Res.* **65**, 61 (1971).
3. Comings, D. E. and Okada, T. A., *Exp. Cell Res.* **62**, 293 (1970).
4. — *ibid.* **63**, 62 (1970).

5. DISCHE, Z., *in* CHARGAFF, E. and DAVIDSON, J. N. (Eds.), The Nucleic Acids, Vol. I, p. 290. Academic Press, New York, 1955.
6. DUPRAW, E. J., *Proc. Nat. Acad. Sci. U.S.A.* **53**, 161 (1965).
7. EMMELOT, P. and BOS, C. J., *Biochim. Biophys. Acta* **121**, 434 (1966).
8. EVANS, W. H., *Biochem. J.* **166**, 833 (1970).
9. FRANKE, W. W., *J. Cell Biol.* **31**, 619 (1966).
10. FRANKE, W. W., DEUMLING, B., ERMEN, B., JARASCH, E. D. and KLEINIG, H., *J. Cell Biol.* **46**, 379 (1970).
11. HARRIS, J. R. and AGUTTER, P., *J. Ultrastruct. Res.* **33**, 219 (1970).
12. HARRIS, J. R. and BROWN, J. N., *J. Ultrastruct. Res.* **36**, 8 (1971).
13. HARRIS, J. R., *in* Physiology and Biochemistry of the Domestic Fowl, Chapter 34, Academic Press, New York 1971, in press.
14. HINTON, R. H., DOBROTA, M., FITZSIMONS, J. T. R. and REID, E., *Eur. J. Biochem.* 12, 349 (1970).
15. KASHNIG, D. M. and KASPER, C. B., *J. Biol. Chem.* **244**, 3786 (1969).
16. LOWRY, O. H., ROSEBROUGH, N. J., FARR, A. L. and RANDALL, R. J., *J. Biol. Chem.* **193**, 265 (1951).
17. MIZUNO, N. S., STOOPS, C. E. and SINHA, A. A., *Nature* (London) **229**, 22 (1971).
18. NEVILLE, D. M., *J. Biophys. Biochem. Cytol.* **8**, 413 (1960).
19. WALLACH, D. F. H., *in* DAVIS, B. D. and WARREN, L. (Eds.), Specificity of Cell Surfaces, p. 129. Prentice-Hall, Englewood Cliffs, New Jersey, 1967.
20. WEAVER, R. A. and BOYLE, W., *Biochem. Biophys. Acta* **173**, 377 (1969).
21. ZBARSKY, J. B., PEROVOSCHIKOVA, K. A., DELEKTORSKAYA, L. N. and DELEKTORSKY, V. V., *Nature* (*London*) **221**, 257 (1969).

J. ULTRASTRUCTURE RESEARCH 48, 17–32 (1974)

A Comparative Study on Rat Liver and Hepatoma Nuclear Membranes

J. R. HARRIS, M. R. PRICE[1] and M. WILLISON[2]

Department of Physiology, Bute Medical Buildings, St. Andrews, Fife, Scotland

Received July 5, 1973, and in revised form February 15, 1974

Using purified nuclear membranes from normal rat liver and hepatoma, a comparative electron microscopic study of the nuclear pore complex has been performed using thin sectioning and negative staining with ammonium molybdate, sodium phosphotungstate, and ammonium uranyl oxalate. In addition, freeze-cleavage studies were performed on whole tissue and on purified rat liver and hepatoma nuclei.

Dimensions of the nuclear pore complexes of rat liver and hepatoma visualised by each technique were compared and no significant difference can be reported. However, the apparent dimensions of the nuclear pore complexes obtained following the different electron microscopic specimen preparation procedures do vary considerably, and suggestions are put forward to account for these differences. It is concluded that no individual electron microscopic specimen preparation method is superior to the others. Each has a contribution to make to the overall understanding of the structure of the nuclear pore complex. Nevertheless, the inherent differences in the preparation methods must continually be borne in mind as must the possibility of artifact production. Of the negative stains used, it is considered that ammonium molybdate revealed the greatest ultrastructural detail.

Following the recently developed method for the purification of nuclear membranes by zonal centrifugation (*18*), an ultrastructural investigation has been performed into the detailed structure of the nuclear pore complexes on rat liver and hepatoma nuclear membranes. The membrane material used throughout this investigation was considered to be of superior purity to that used by Harris and Agutter (*12*) and to be in a better state of morphological integrity than that studied by most other workers.

Along with thin sectioning, three different negative stains have been employed in order to obtain a comparative assessment of their ability to preserve and reveal ultrastructural detail within the nuclear pore complex, at the same time giving a comparison of the dimensions of the nuclear pore complex under different con-

[1] Cancer Research Campaign Laboratory, University Park, Nottingham.
[2] Department of Cell Biology, University of Nottingham, University Park, Nottingham.

ditions. Though many workers have had considerable success using the technique of negative staining with isolated proteins and purified cellular membranes, there is still considerable doubt in the minds of some that the results obtained abound with artifacts. By using different negative stains a more precise interpretation of results can be made by considering the possible interactions of the heavy metal staining anions with membrane components. It might be hoped that information provided by negative staining of purified nuclear membrane will correlate well with that resulting from thin sectioning if the former is to be considered free from artifacts.

There is now an extensive literature relating to thin sectioning studies performed on nuclear membrane pore complexes (*1*, *7*, *8*, *20*). The fine structure thus revealed is usually expressed in terms such as annular subunits, fibrils, tubules, and the central granule of the nuclear pore complex. It is shown in the present study that the results of negative staining largely agree with and supplement those from thin-sectioning studies, although there are slight variations in the interpretations applied to the results following the use of different negative stains.

Freeze-cleavage is currently considered to be the method for preparing electron microscopic specimens which is the least likely to lead to artifact production, as fixation, staining, and dehydration are avoided. The structure and dimensions of the nuclear pore complex as revealed by freeze-cleavage of intact tissue and purified nuclei has been compared with the results following the other specimen preparations in order to assess the amount of detail revealed together with the preservation of pore integrity. Unfortunately, when freeze-cleavage was applied to the purified nuclear membrane, the results obtained were very difficult to interpret since the cleavage planes rarely followed the surfaces of the membranes.

Studying the nuclear pore complex by several electron microscopic specimen preparation methods is likely to provide the best overall interpretation of its detailed structure and should be more accurate and meaningful than the reliance upon any one method alone. Even though the interpretation of negative staining results is difficult, it is nevertheless generally accepted that macromolecules in association with cellular membranes can be revealed by this technique (*10*, *11*).

MATERIALS AND METHODS

The preparation of nuclear membrane. Nuclear membrane from rat liver and hepatoma was prepared by rate zonal centrifugation followed by isopycnic banding, as previously described (*18*).

The preparation of cell nuclei. Nuclei from rat liver and hepatoma homogenates were prepared by conventional centrifugation through 60% w/w sucrose, as previously described (*18*).

Negative contrast staining. Purified nuclear membranes were freed of sucrose by either dialysis or centrifugal washing and were negatively stained with 2% w/v solutions of sodium phosphotungstate and ammonium molybdate (pH 7.0) by the "single drop" method (*12*). Ammonium uranyl oxalate was prepared from uranyl acetate and oxalic acid by the method of Mellema et al. (*17*) and used in the same manner as the other stains.

Thin sectioning. Samples of rat liver and hepatoma nuclear membrane were fixed overnight in 1.0% glutaraldehyde (TAAB) at 4°C and then centrifuged for 10 minutes at 1 000 *g*. The pelleted material was then postosmicated in 1.0% osmic acid in 0.1 M phosphate buffer (pH 7.4) for 2 hours at room temperature. Dehydration was performed by passage of the material through a series of graded ethanol solutions, and finally epoxy propane. The nuclear membrane was then dispersed in TAAB epoxy resin and polymerized at 60°C. Thin sections were cut with glass knives using the LKB Ultrotome 111 and mounted on Micron Type 400 grids. Poststaining was performed using 2% uranyl acetate in 50% ethanol.

Freeze-cleavage. Samples of rat liver and hepatoma tissue, and purified rat liver and hepatoma nuclei were suspended in 10% glycerol and frozen in liquid nitrogen prior to conventional processing in the Balzer apparatus.

Electron microscopy. The material presented was studied in the Philips E.M. 300 electron microscope. Electron micrographs were taken on Ilford 3.25 × 4 inch E.M. 6 plates. The dimensions of nuclear pore complexes were measured by eye to the nearest 0.05 mm using the graticule of a × 5 eye piece micrometer. Mean dimensions and standard deviations were calculated from the measurements of nuclear pore complexes on not less than ten electron micrographs obtained under each of the different electron contrasting conditions presented. The electron microscope magnification was calibrated using a 54,864 line/inch replica grating (E.F. Fullam, Inc., New York).

RESULTS

Freeze-cleavage

The technique of freeze-cleavage reveals the membranes of cell nuclei when applied either to intact tissue or to nuclei that have been obtained by homogenisation of tissue and purified by sedimentation through concentrated sucrose solution. Very often the outer nuclear membrane is torn away in places during the cleavage process, but the nuclear pore complexes remain attached to the underlying inner nuclear membrane. Figs. 1 and 2 show representative electron micrographs of the surfaces of normal rat liver and hepatoma D23 nuclei following freeze-cleavage of intact tissue in both cases. Figs. 3 and 4 show a similar pair of electron micrographs obtained from purified normal rat liver and hepatoma D23 nuclei.

Manual measurement of the diameter of the nuclear pore complexes was made on many freeze-cleaved nuclei and the mean values determined. For normal rat liver the nuclear pore complexes had a diameter of 1 067 ± 36 Å, and those on hepatoma D23 nuclei had a diameter of 1 056 ± 45 Å (see Table I). The apparent difference in the diameters of the nuclear pore complexes on the two types of nuclei are not thought to be significant. The extraction and purification procedures used for

Table I. *The Dimensions (Å) of Normal Rat Liver and Hepatoma D_{23} Nuclear Pore Complexes by Different Specimen Preparation Methods*[a]

Method	NL, OD	NL, ID	D_{23}, OD	D_{23}, ID
Freeze-cleavage	1 067 ± 36	—	1 056 ± 45	—
Thin section	920 ± 34	429 ± 21	959 ± 34	503 ± 33
Negative stain				
Ammonium molybdate	998 ± 25	518 ± 33	926 ± 26	536 ± 34
Uranyl acetate-Oxalic acid	1 135 ± 32	620 ± 14	1 098 ± 25	639 ± 28
Sodium phosphotungstate	944 ± 59	662 ± 65	987 ± 82	586 ± 45

[a] Measurements were made directly on electron micrograph, to the nearest 0.05 mm, using a ×5 graticule micrometer. Standard deviations were calculated from the pooled results of at least ten negatives. In general it must be emphasized that difficulty was encountered owing to the variation in clarity of the nuclear pore complexes on any one electron micrograph, together with the fact that some distortion of the pore complexes was present, in particular when sodium phosphotungstate negative staining had been performed. NL signifies normal rat liver; and D_{23}, hepatoma D_{23}; OD, outer diameter and ID, inner diameter of the nuclear pore complexes.

obtaining the cell nuclei do not appear to cause any alteration to the nuclear pore complexes, though slight overall shrinkage of the nuclei is apparent, in agreement with thin-sectioning studies and phase contrast light microscopy. Freeze-cleavage does not reveal very much in the way of substructure within the nuclear pore complexes. The central granule is occasionally visible as is the annulus, but in general the pore complexes are revealed as circular (octagonal) projections on the surface of the nuclei. The extent of this projection is not readily appreciated from the classical thin section electron microscope image of the nuclear pore complex, although negative staining as well as freeze-cleavage strongly suggests that they are projections. The freeze-cleaved electron image of the nuclear pore complex varies, depending on the angle of curvature of the nuclear surface relative to the angle at which the shadowing metal was evaporated. Thus there will be a varying thickness of shadowing metal on different parts of the nuclear surface which might lead to some error in the measurement of the diameters of the nuclear pore complexes. Nevertheless, the rather large standard deviations quoted are thought to be meaningful, since pore complexes of different diameter are readily detected adjacent to one another by direct observation of electron micrographs.

FIG. 1. The surface of a rat liver nucleus revealed by freeze-cleavage of intact tissue. ×22 000.
FIG. 2. The surface of a rat hepatoma D_{23} nucleus revealed by freeze-cleavage of intact tissue. ×33 000.
FIG. 3. The surface of a purified rat liver nucleus revealed by feeze-cleavage. ×22 000.
FIG. 4. The surface of a purified rat hepatoma D_{23} nuclei revealed by freeze-cleavage. ×28 000.

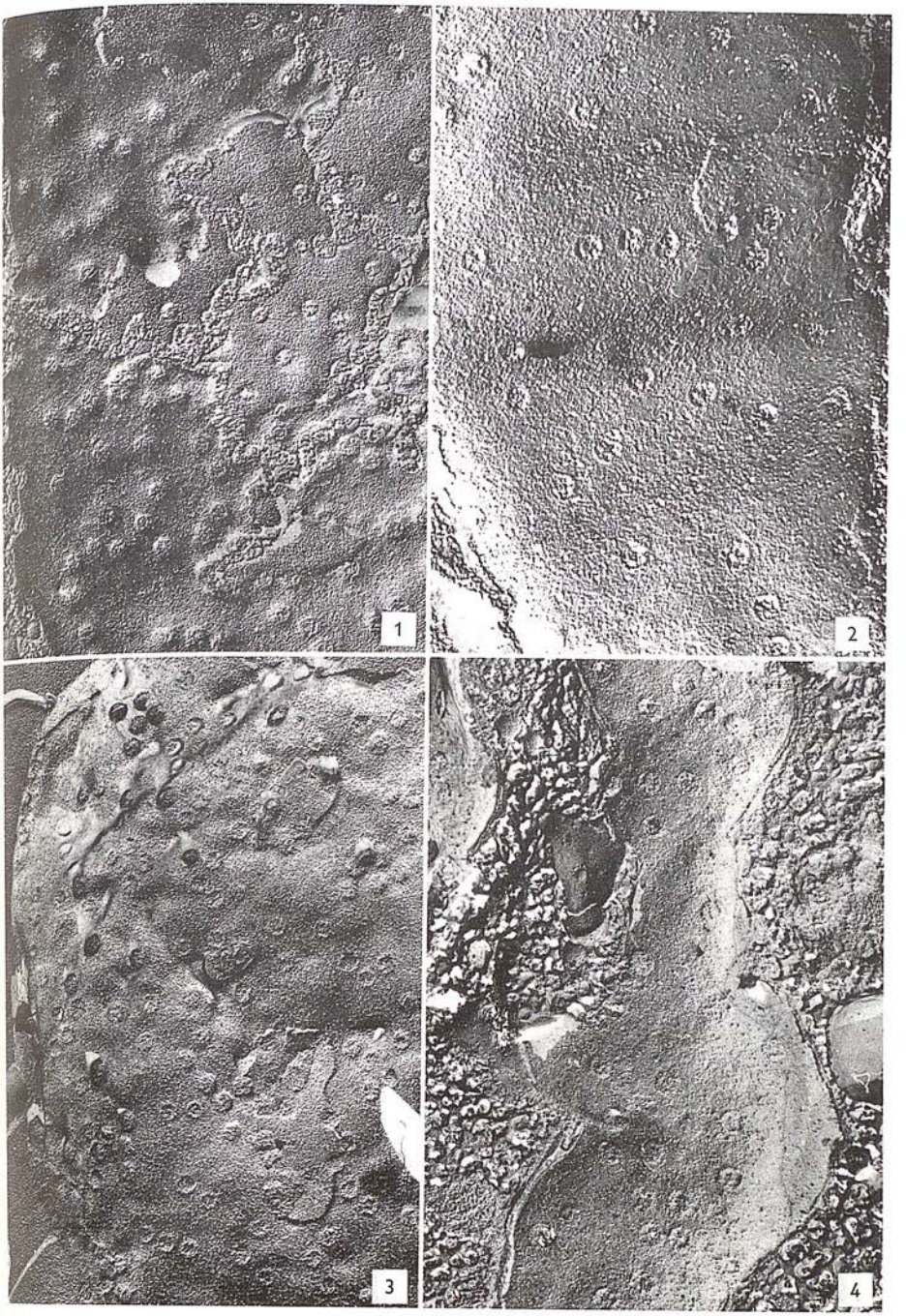
1
2
3
4

Thin sectioning

In thin sections of purified nuclear membrane the nuclear pore complexes are clearly revealed in regions where the plane of sectioning is parallel to the surface of the membrane. Figs. 5–7 show representative areas of thin sectioned rat liver and hepatoma nuclear membrane showing nuclear pore complexes. The central granule of many of the pore complexes is clearly revealed and there is some indication of fibrils and an inner ring of material within the pores. The annuli tend to show the typical octagonal structure originally proposed by Gall (*9*). The dimensions of the thin-sectioned nuclear pore complexes were found to be as follows: (a) normal rat liver: outer diameter 920 ± 34 Å; inner diameter, 429 ± 21 Å; (b) rat hepatoma D23: outer diameter, 959 ± 34Å; inner diameter, 503 ± 33 Å. (see Table I). The apparent difference between the normal rat liver and hepatoma for both the inner and outer diameters of the nuclear pore complexes are not thought to be significant.

Negative staining

Ammonium molybdate. When negatively stained with 2% ammonium molybdate (pH 7.0) purified normal rat liver and hepatoma nuclear membrane is given sufficient contrast for much ultrastructural detail to be revealed. The nuclear pore complexes are penetrated by the molybdate anions and reveal clearly the subunit structured annuli, the central granule, in many cases an inner ring of material and possibly fibres extending from the central granule out to the annulus, see Figs. 8 and 9. Usually the purified nuclear "ghosts" consist of both inner and outer nuclear membranes, so that when the 'ghost' collapses down onto the carbon support film during the negative staining procedure four layers of membrane are likely to be present, through which the electron beam has to pass. Thus it is possible for the nuclear pore complexes in the upper pair of membranes to overlap with those of the lower pair of membranes, resulting in a loss of clarity in the electron image. Occasionally, however, fragments of nuclear "ghost" are to be found on the support films of negatively stained specimens, which will consist either of the intact double nuclear membrane, or possibly the inner or outer nuclear membrane alone. In both cases there is no overlapping of nuclear pore complexes, and thus more detail is likely to be resolved (see Figs. 10 and 11). Under these conditions it must be borne in mind that as the membrane is unstable and breaking up, material might be lost from the nuclear pore complexes, though from an alternative point of view it is also possible that useful information might be obtained on the composition of the nuclear pore complex as it undergoes disruption (*11*).

The dimensions of the nuclear pore complexes when negatively stained with ammonium molybdate were found to be as follows: (a) normal rat liver: outer

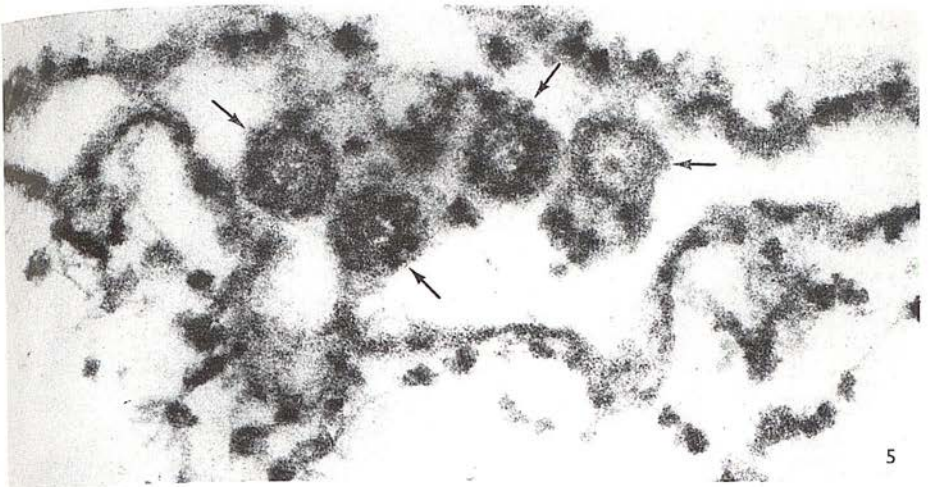

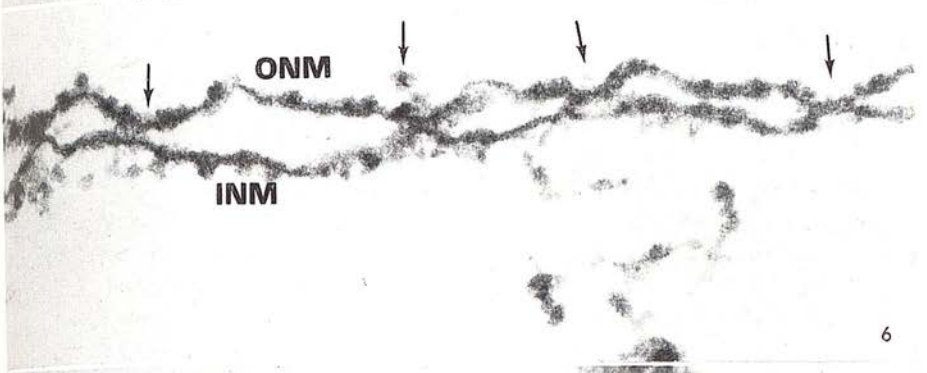

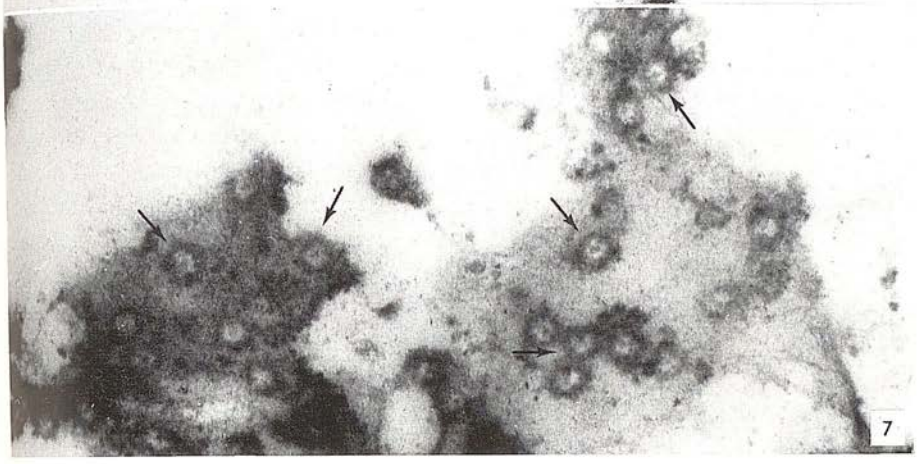

FIGS. 5 and 6. Thin-sectioned rat liver nuclear "ghosts." Arrows indicate the nuclear pore complexes. *INM*, inner nuclear membrane; *ONM*, outer nuclear membrane. × 142 000 and 114 000 respectively.
FIG. 7. Thin-sectioned rat hepatoma D_{23} nuclear membranes showing the nuclear pore complexes (arrowed). × 44 000.

diameter, 998±25 Å; inner diameter, 518±33 Å; (b) rat hepatoma D23: outer diameter, 926±26 Å; inner diameter, 536±34 Å.

The apparent difference in the outer diameter of the nuclear pore complexes may be significant, but it is not supported by the results obtained when sodium phosphotungstate and the ammonium uranyl oxalate were used as the negative stains (see below).

Ammonium uranyl oxalate. When negatively stained with the complex of uranyl acetate and oxalic acid neutralised with ammonium hydroxide, the nuclear pore complexes on purified rat liver and hepatoma nuclear membranes are revealed with excellent electron contrast, see Figs. 12 and 13. The circular annuli have a very pronounced subunit structure, and the central granules are clearly defined. As with ammonium molybdate staining there are indications of an inner ring of material within the nuclear pore annuli, these being more clearly revealed on torn fragments of nuclear "ghost," see Figs 14 and 15. The uranyl oxalate imparts to the surface of the nuclear membrane a more granular texture than either of the other negative stains (this point will be amplified in the discussion).

The dimensions of the nuclear pore complexes when negatively stained with ammonium uranyl oxalate were found to be as follows: (a) normal rat liver: outer diameter, 1 135±32 Å; inner diameter, 620±14 Å; (b) rat hepatoma D23: outer diameter, 1 098±25 Å; inner diameter, 639±28 Å.

Sodium phosphotungstate. The electron optical image of the nuclear pore complex as revealed on purified rat liver and hepatoma nuclear "ghosts" and torn membranes by sodium phosphotungstate negative staining differs significantly from the images given by both ammonium molybdate, and ammonium uranyl oxalate, see Figs. 16–19. First, the pore complexes usually appear to be distorted. They have angular edges and only a minority exhibit the typical circular or regular octagonal profile that is generally proposed as the true structure. Secondly, the edges of the angular nuclear pore complexes appear very narrow and smooth, with no indication of the annular subunits revealed by the other two negative stains. However, within this outer angular profile there is a rim of material which is not so clearly defined as the pore edge and may very well be equivalent to the subunited annuli revealed by ammonium molybdate and ammonium uranyl oxalate. The smooth angular edge to the sodium phosphotungstate-stained nuclear pore complex is likely to be the electron

---

FIG. 8. Part of a rat liver nuclear "ghost" negatively stained with ammonium molybdate. ×171 000.
FIG. 9. Part of a rat hepatoma D_{23} nuclear "ghost" negatively stained with ammonium molybdate. ×56 000.
FIG. 10. Part of a torn rat liver nuclear membrane, negatively stained with ammonium molybdate. ×180 000.
FIG. 11. Part of a torn rat hepatoma D_{23} nuclear membrane, negatively stained with ammonium molybdate. ×80 000.

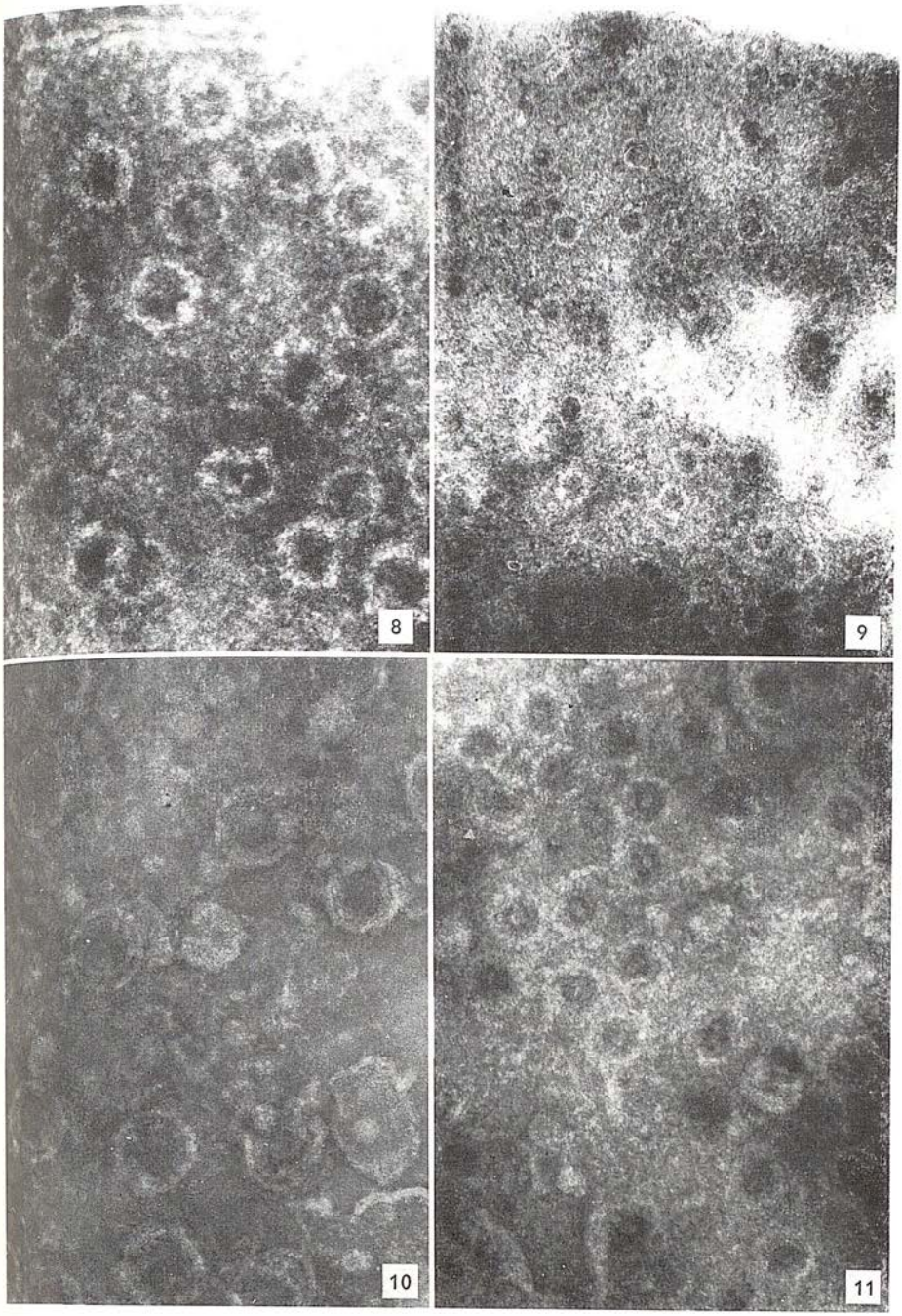
8
9
10
11

image of the region of down folding of the nuclear membrane around the edge of the true annulus (see Discussion for further comment). Thirdly, the region within the nuclear pore complexes tends to show very little detail, the central granules only rarely being visible. The dimensions of the nuclear pore complexes when negatively stained with sodium phosphotungstate were found to be as follows: (a) normal rat liver: outer diameter, 944 ± 59 Å; Inner diameter, 662 ± 65 Å; (b) rat hepatoma D23; outer diameter, 987 ± 82 Å; inner diameter, 586 ± 45 Å.

The large standard deviations are an expression of the distorted shapes of the nuclear pore complexes in this instance. Again there is thought to be no significant difference in the dimensions of the normal rat liver and the hepatoma nuclear pore complexes.

DISCUSSION

The field of nuclear membranes has recently been reviewed by several authors (*5*, *14*, *22*), thus, no attempt will be made to deal with all aspects of this subject. The results presented above will be discussed and compared directly with the publications of other workers that have been concerned with the dimensions of the nuclear pore complex.

Depending on the orientation of a cell nucleus relative to the plane of freeze-cleavage, several different interpretations of the electron microscope image can be made. First, the cleavage plane might pass along the outer nuclear membrane revealing the cytoplasmic surface; if the outer nuclear membrane is split away during freeze-cleavage then the intracisternal surface of the inner nuclear membrane will be revealed. Secondly, if the plane of freeze-cleavage passes along the inside of the inner nuclear membrane then the nucleoplasmic surface will be revealed, and if the inner nuclear membrane is split away then the intracisternal surface of the outer nuclear membrane should be seen. The above argument is based on the proposal that the various planes of cleavage are long the true surfaces of the inner and outer nuclear membrane. This point is disputed by some workers, who claim that cleavage occurs within the membrane and that the true surfaces are revealed only by freeze-etching following the initial cleavage. The problem remains undecided (*13*), but in either case the dimensions of the nuclear pore complexes might be

---

FIG. 12. Part of a rat liver nuclear "ghost" negatively stained with ammonium uranyl-oxalate. × 16 000.

FIG. 13. Part of a hepatoma D_{23} nuclear "ghost" negatively stained with ammonium uranyl-oxalate. × 18 000.

FIG. 14. A torn fragment of rat liver nuclear membrane negatively stained with ammonium uranyl-oxalate. × 24 000.

FIG. 15. A torn fragment of rat hepatoma D_{23} nuclear membrane negatively stained with ammonium uranyl-oxalate. × 44 000.

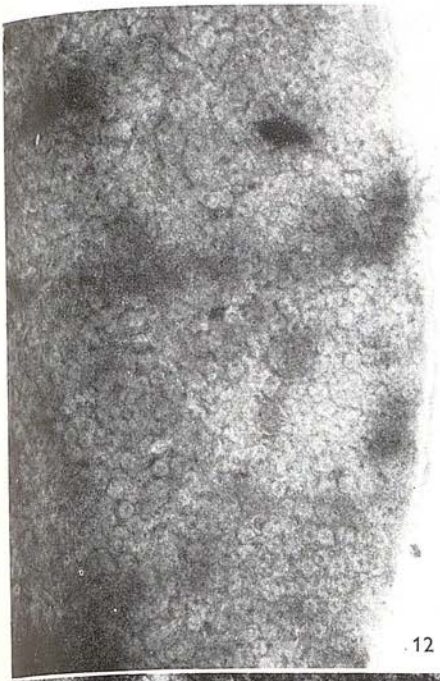
12

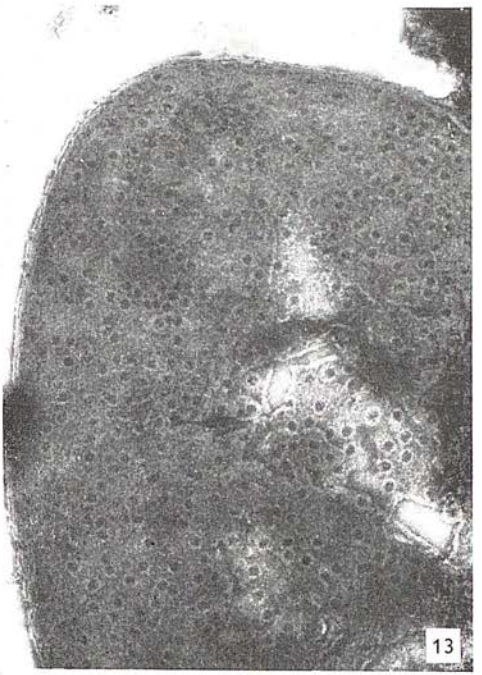
13


14

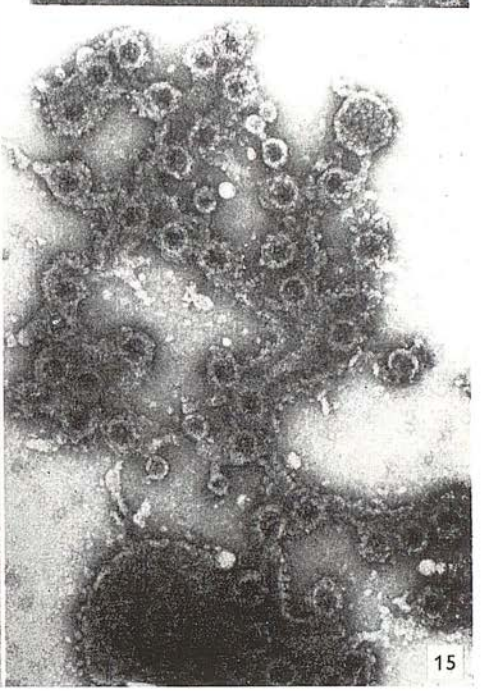
15

expected to be similar, and the theoretical aspects will not be dealt with any further.

The outer nuclear membrane generally appears to be partially torn away by the freeze-cleavage process but the nuclear pore complexes remain attached to the underlying inner nuclear membrane. On the other hand, the inner nuclear membrane when seen from the nucleoplasmic side is usually intact. Perhaps the most important point to be emphasised from the freeze-cleavage results is that the nuclear pore complexes project significantly from the surface of the surrounding membrane. This fact is not so readily appreciated from thin-sectioning and negative-staining results.

The shadowing metal deposited on the freeze-cleaved surface contributes to the apparent diameters of the nuclear pore complexes. From the figures in Table I it is seen that in general the apparent diameters of the nuclear pore complexes following freeze-cleavage are greater than those following thin sectioning and negative staining. These figures are very much in line with those of Maul et al. (*15*), who were studying human melanoma cell nuclei. It must be accepted that freeze-cleavage does not tell us a great deal about the molecular details of the nuclear pore complex. It is, nevertheless, an excellent method for studying the distribution of nuclear pore complexes in different cells and under varying metabolic conditions (*13*, *15*).

The fixation, staining, and dehydration procedures employed prior to thin sectioning may produce overall shrinkage of the nuclear pore complexes. This could explain the fact that the dimensions of thin sectioned nuclear pores obtained in this study are less than those obtained by negative staining and freeze-cleavage. Thin sectioning has revealed several important facts about the nuclear pore complex (*1*) and has confirmed and supported the interpretations put to the results obtained by the other electron microscopic specimen preparation methods. First, that the pore complexes are of octagonal nature with a pronounced annulus. Secondly, that enclosed by the annulus there are other structures which are variously termed diaphragm material, transverse fibres or tubules, cross struts and the central granule or tubule (*1*, *4*, *15*, *16*, *19*). These structures are not fully understood at the present moment, but their presence stresses the multi component nature of the nuclear pore complex.

FIG. 16. Part of a rat liver nuclear "ghost" negatively stained with sodium phosphotungstate. × 28 000.

FIG. 17. Part of a rat hepatoma D_{23} nuclear "ghost" negatively stained with sodium phosphotungstate. × 35 000.

FIG. 18. A torn fragment of rat liver nuclear membrane negatively stained with sodium phosphotungstate. × 22 000.

FIG. 19. A torn fragment of rat hepatoma D_{23} nuclear membrane negatively stained with sodum phosphotungstate. × 53 000.

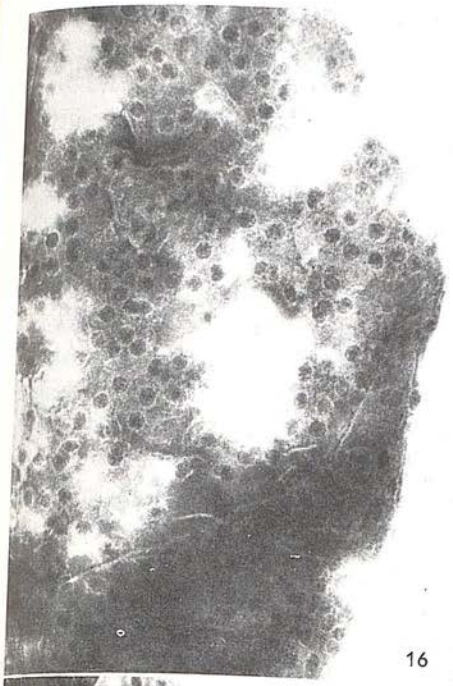

16

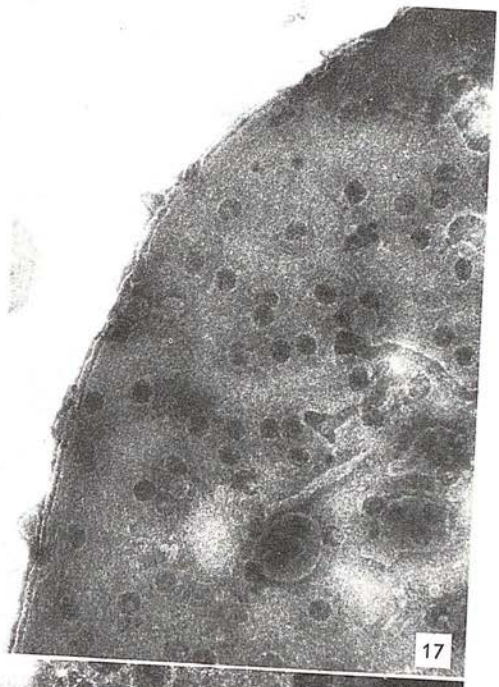

17

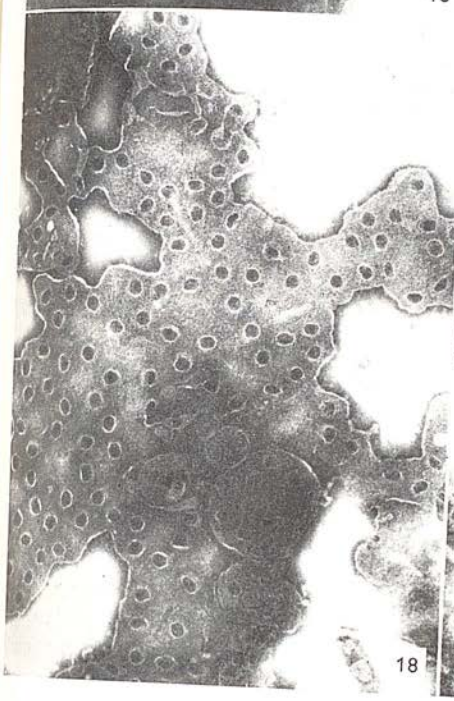

18

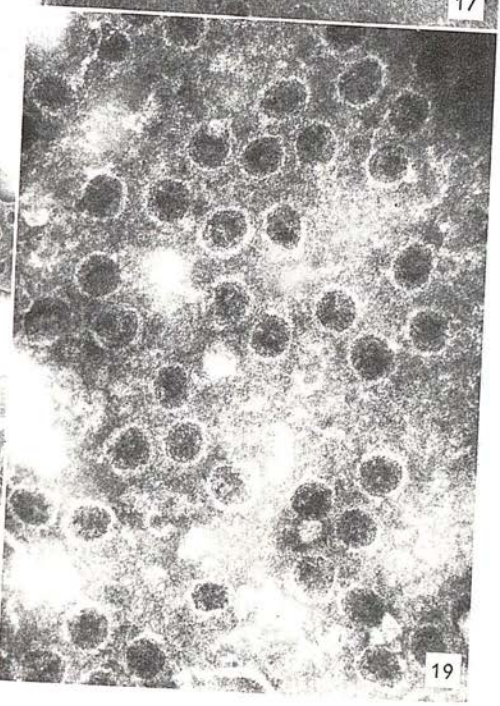

19

The diameter of the thin sectioned nuclear pore complexes given in Table I are very much in line with those given by Abelson and Smith (*1*), though they do vary slightly from the figures of Kartenbeck et al. (*13*). Abelson and Smith (*1*) atttempted to subdivide the pore complex by considering the variation of the electron image of the nuclear pore complex in serial sections. These workers claimed that the central portion of the nuclear pore has a narrower diameter than the cytoplasmic or nucleoplasmic regions on either side. The present thin-sectioning investigation has not been pursued to the same level of interpretation as that by Abelson and Smith (*1*), Englehardt and Pusa (*4*), and Roberts and Northcote (*19*), but support is given to the general conclusion of these workers regarding the ability of thin sectioning to reveal ultrastructural fine detail within the nuclear pore complex. It is though that the results obtained by thin sectioning must be interpreted with extreme caution when one is attempting to derive the molecular detail present within the nuclear pore complex, as emphasised by Wischnitzer (*22*). Most of the models for the nuclear pore complex have, nevertheless, been derived from the thin-sectioned electron image of the nuclear pore complex (*1*, *4*, *7*, *19*, *21*).

The electron optical image of the negatively stained nuclear pore complex will, to some extent, be dependent on the properties of the particular stain employed. Thus, it can reasonably be stated that the penetration of the substructure of the nuclear pore complex by the various negative stains is likely to be different and will depend on the interaction of the complex heavy metal anions with the lipid, protein, nucleic acid, and carbohydrate components of the nuclear membrane. If complete penetration of the nuclear membrane and pore complexes by the negative stains was to occur, then according to the theory behind negative staining no detail would be visible in the electron microscope. As it is, none of the negative stains investigated produces complete penetration, but in practice is thas been found that sodium phosphotungstate, ammonium molybdate and ammonium uranyl oxalate penetrate the nuclear pore complex in a decreasing order. Thus, electron images of the nuclear pore given by sodium phosphotungstate usually have smooth "membranelike" edges with very little detail of the annulus or the structures within the pore visible, due to the extensive penetration of this negative stain within the material of the pore complex (*9*, *22*). Ammonium molybdate appears to penetrate the nuclear pore complex material to a lesser extent and in this instance more detail is revealed. This takes the form of pronounced annular subunits together with an inner ring, fibrils and a central granule. Kartenbeck et al. (*13*) claimed that these structural details could likewise be revealed by phosphotungstate staining, but with this stain detail has been found to be less clearly defined in the hands of the present authors.

With the uranyl-oxalate anion there appears to be even less penetration of the substructure of the nuclear pore complexes than with either of the other

negative stains. This may account for the apparently larger dimensions of the nuclear pore complexes obtained following ammonium uranyl oxalate staining. As with ammonium molybdate, the inner ring of material and the central granule of the nuclear pore are clearly revealed by ammonium uranyl oxalate, which also tends to impart a higher contrast but slightly more granular nature to the electron image than the other two negative stains.

Several previous investigators have used sodium phosphotungstate as the negative staining salt for contrasting nuclear membranes (7–9), it being generally thought that under these conditions the membranous periphery of the nuclear pore complex is revealed rather than the annular material (*9*, *22*), in agreement with the views expressed above. On the other hand, only a few investigators have employed ammonium molybdate to any extent (*11*, *12*, *18*), even though this stain has been used extensively for negatively staining other biological membranes and liposome particles. It is the view of the present authors that ammonium molybdate has the ability to reveal a significant amount of ultrastructural detail within the annulus of the nuclear pore complex (*11*), but also that sodium phosphotungstate and ammonium uranyl oxalate, along with other negative staining salts, are likely to contribute to the overall interpretation of the ultrastructure of the nuclear membrane. In general, the dimensions of the negatively stained nuclear pore complexes given in Table I are in accord with those given by other workers.

Abelson and Smith (*1*) attempted to distinguish between the central membranous region of the nuclear pore and the annular regions on either side which have structural continuity through the octagonal membranous pore. A similar interpretation was advanced by Maul (*15*), who expressed it in terms of an eight-sided symmetry for the membranous pore and an eight-point symmetry for the annulus together with the material within the pore, both of which can be considered as nonmembranous. Franke and Scheer (*7*) also recognised the importance of making a distinction between the nuclear membrane pore, the annular particles and the fibres or minitubule-like structures extending through the pore itself.

The question of the exact biochemical composition of the nuclear membrane remains something of a problem (*2*, *3*, *20*). This is because of the close association of histones, DNA, and RNA with the inner nuclear membrane and of ribosomes with the outer nuclear membrane. Techniques which remove these components from the nuclear membrane generally lead to a breakdown of its morphological integrity as judged by the integrity of the nuclear pore complexes in the electron microscope. It is not unreasonable to consider that the nuclear membrane, as with other membrane species (*5*, *10*), will contain relatively loosely associated components, which may nevertheless be important for its overall structure and function. It is therefore thought desirable at the present state of knowledge to emphasise the

importance of the preservation of the ultrastructural integrity of the nuclear membrane prior to biochemical investigations. The study of the composition and function of this membrane can be considered to have a sound morphological background if applied to purified nuclear membrane which is as close as possible to the normal physiological state in terms of its ultrastructural integrity. An accurate assessment of the effects of any subsequent biochemical treatment can then be made. The techniques of electron microscopy, in particular negative staining which is able to provide detail at the molecular level, will continue to play an important role in the future investigation of the nuclear membrane (*11*). Perhaps the most important gap in our existing knowledge is that of being unable to interpret meaningfully at a functional level the information relating to the fine structure of the nuclear pore complex that the electron microscope has already provided.

REFERENCES

1. ABELSON, H. T. and SMITH, G. H., *J. Ultrastruct. Res.* **30**, 558 (1970).
2. AGUTTER, P. S., *Biochim. Biophys. Acta* **255**, 397 (1972).
3. DEMULING, B. and FRANKE, W. W., *Hoppe-Seyler's Z. Physiol. Chem.* **353**, 287 (1972).
4. ENGLEHARDT, P. and PUSA, K., *Nature* (London) *New Biol.* **240**, 163 (1972).
5. FELDHERR, C. M., *Advan. Cell Mol. Biol.* **2**, 273, (1972).
6. FLEISHER, S. F., ZAHLER, W. L. and OZAWA, H., *in* MANSON, L. A. (Ed.), Biomembranes, Vol. 2, p. 105. Plenum Press, New York, 1971.
7. FRANKE, W. W. and SCHEER, U., *J. Ultrastruct. Res.* **30**, 288 (1970).
8. FRANKE, W. W. and SCHEER, U., *J. Ultrastruct. Res.* **30**, 317 (1970).
9. GALL, J. G., *J. Cell Biol.* **32**, 391 (1967).
10. HARRIS, J. R., *J. Ultrastruct. Res.* **36**, 587 (1971).
11. HARRIS, J. R., *Phil. Trans. Roy. Soc. London* (B) in press.
12. HARRIS, J. R. and AGUTTER, P. S., *J. Ultrastruct. Res.* **33**, 219 (1970).
13. KARTENBECK, J., ZENTGRAF, H., SCHEER, U. and FRANKE, W. W., *Advan. Anat. Embryol. Cell Biol.* **45**, 1 (1971).
14. KESSEL, R. G., *Progr. Surface Membrane Sci.* **6**, 243 (1973).
15. MAUL, G. G., *J. Cell Biol.* **51**, 558 (1971).
16. MAUL, G. G., PRICE, J. W. and LIEBERMAN, M. W., *J. Cell Biol.* **51**, 405 (1971).
17. MELLEMA, J. E., VAN BRUGGEN, E. F. J. and GRUBER, M., *J. Mol. Biol.* **31**, 75 (1968).
18. PRICE, M. R., HARRIS, J. R. and BALDWIN, R. W., *J. Ultrastruct. Res.* **40**, 178 (1972).
19. ROBERTS, K. and NORTHCOTE, D. H., *Microsc. Acta* **71**, 102 (1971).
20. SCHEER, U., *Z. Zellforsch. Mikrosk. Anat.* **127**, 127 (1972).
21. VIVIER, E., *J. Microsc.* (*Paris*) **6**, 371 (1967).
22. WISCHNITZER, S., *Int. Rev. Cytol.* **34**, 1 (1973).

Phil. Trans. R. Soc. Lond. B. **268**, 109–117 (1974) [109]
Printed in Great Britain

Some electron microscopic studies on intact nuclear 'ghosts' and nuclear membrane fragments

By J. R. Harris
Department of Physiology, Bute Medical Buildings, St Andrews, Fife, Scotland

[Plates 38–41]

The electron optical images of negatively stained intact nuclear 'ghosts' are readily identified as flattened and sometimes folded bodies, not unlike those given by mammalian erythrocyte 'ghosts'. Even at low magnifications (× 5000) the nuclear pore complexes are clearly revealed and can therefore be used as morphological markers for nuclear membrane. At higher magnifications the nuclear pore complexes are seen to be composed of an eight-sided annulus surrounding a central granule, an inner ring of material, and possibly radial fibrils.

Very often fine detail appears to be obscured owing to the fact that there are two layers of double nuclear membrane lying flat on the carbon support film. Occasionally the nuclear 'ghosts' appear to be torn apart, in all probability because of the spreading and surface-tension forces applied during the preparation of the negatively stained specimens. In this instance the nuclear pore complexes usually remain intact and the surrounding membrane is disrupted. The nuclear pore complexes are spread as a single layer and greater detail is revealed within the annuli. This is particularly so when partially disrupted nuclear pore complexes are studied.

The octagonal annulus appears to be composed of circular macromolecules approximately 20 nm in external diameter with a 5 nm diameter central hole. These macromolecules are linked together and partly masked by other diffuse material. It is proposed that one or more of these macromolecules underlies each of the eight annular subunits. A model for the nuclear pore complex is presented and compared with those proposed by other authors.

Introduction

A high-resolution electron-microscopic study of the nuclear membrane has been undertaken using the technique of negative staining. Ammonium molybdate has been the main stain employed, although the ammonium uranyl-oxalate complex and sodium phosphotungstate have also been used.

Negative staining has been employed for several years to study the molecular details of virus particles, isolated macromolecules and a wide variety of cellular membranes and membrane-bound organelles. In the hands of the present author it has been successfully applied to the *intact* mammalian erythrocyte 'ghost' and to membrane-associated proteins released from this membrane species (Harris 1969, 1971). It might therefore be reasonably hoped that negative staining would reveal molecular detail within the nuclear membrane, if it is applied to sufficiently purified material. Some progress along these lines has already been achieved, in particular by Franke & Scheer (1970*a*), using phosphotungstate, and Harris & Agutter (1970), using ammonium molybdate. Components of the nuclear pore complex, such as the octagonally subunited annulus, the central granule, inner ring and fibrillar material have been defined, but the actual molecular conformation within these various structures have not yet been precisely described.

The aim of the present investigation has been to obtain a superior degree of molecular interpretation from the electron optical image of the negatively stained nuclear pore complex. From an extensive comparative study of three negative stains – ammonium molybdate, ammonium uranyl-oxalate and sodium phosphotungstate – it was decided that ammonium molybdate revealed the greatest detail within the nuclear pore complex (Harris, Price & Willison, *J. ultrastruct. Res.*, in press), although the uranyl-oxalate complex was found to be almost as good

in that it imparted a superior contrast to the specimen material, but also produced a more granular electron optical image.

It was stated by Haggis (1969) that any disruption of membrane material produced during the preparation of negatively stained specimens for electron microscopy might be advantageous to the study of the component parts of the membrane. Naturally, one has at the same time to be aware of the fact that apart from revealing detail, a process such as this might also destroy molecular organizations and create artefacts. Nevertheless, with these reservations in mind, it will be shown that by carefully studying negatively stained specimens, detail is revealed at the macromolecular level within the nuclear pore complex. The spontaneous disruption of the nuclear membrane and the nuclear pore complex during the negative staining procedure has helped with the interpretation of the electron optical image of the intact nuclear pore complex.

Methods

The preparation of nuclear membranes

Two methods have been employed for the preparation of nuclear membranes. First, the zonal centrifugation method of Price, Harris & Baldwin (1972), which does not require an initial purification of the nuclei. Rat liver and hepatoma tissue was homogenized in 1 mM sodium bicarbonate buffer (pH 7.2), from which the 600*g* nuclear pellet was prepared. Following overnight incubation at 4 °C the nuclear pellet suspension was applied as the sample for low-speed-rate zonal centrifugation. From the zonal rotor the region containing nuclear 'ghosts' and large sheets of membrane was defined by phase-contrast microscopy. Pooled fractions containing nuclear 'ghosts' were then subjected to isopycnic zonal centrifugation, from which purified nuclear ghosts of density 1.21 ± 0.01 were obtained.

The second method, which has been developed more recently owing to the lack of zonal centrifugation facilities, requires initially that the cell nuclei are purified. Rat and rabbit liver were homogenized in 250 mM sucrose–10 mM tris-HCl (pH 7.3)–2mM $MgCl_2$. From the 600*g* nuclear pellet, nuclei were purified by the conventional procedure of sedimentation through concentrated sucrose (58% by mass). The pellet of nuclei was then suspended in the homogenization buffer and centrifuged at 600*g* for 10 min, the pellet then being resuspended in phosphate buffered normal saline containing 2 mM $MgCl_2$ and left overnight at 4 °C. The nuclei were then pelleted at 600*g* for 10 min and resuspended in approximately 50 vol of 2 mM sodium bicarbonate buffer (pH 7.3). The nuclei immediately became swollen and could be observed directly to be bursting by phase-contrast microscopy. The initially dark granular nucleoplasm with its pronounced nucleoli became progressively lighter and the smooth edges of the nuclei became wrinkled and flexible, indicating that lesions must have appeared in the nuclear membrane allowing the nucleoplasm to escape. Nuclei in the actual process of bursting, similar to those from onion root tip observed by Franke (1966), can in fact be seen. Following this lysis treatment the nuclear membrane was pelleted at 48000*g* for 10 min and the chromatin rich supernatant discarded. The pellet was then washed four times in 5 mM tris-HCl (pH 7.3) with centrifugation at 48000*g* for 10 min, and the final pellet resuspended in a small volume (2 ml) of the tris-HCl buffer and centrifuged at 600*g* for 5 min to remove aggregates, the supernatant being taken as partially purified nuclear membrane for electron microscopic study. Further purification was obtained by isopycnic banding on a discontinuous sucrose gradient at density 1.22.

The preparation of negatively stained specimens

The carbon support films were prepared on type 400-mesh copper grids. The method employing single drops of membrane suspension and negative stain, which was originally shown to the author by Dr E. L. Benedetti, was used to prepare the negatively stained membrane material, employing 2.0% solutions of ammonium molybdate, ammonium uranyl-oxalate and sodium phosphotungstate (pH 7.0), as previously described by Harris & Agutter (1970).

Electron microscopy

Specimens were studied in the Philips EM 300 and the A.E.I. EM 6B electron microscope. Electron optical magnifications of 50000 and 60000 diameters were routinely used for studying the detail within the nuclear pore complexes. Photographs were taken on Ilford plates, types EM-5 and EM-6.

The photographic rotation technique for contrast enhancement of Markham, Frey & Hills (1963) was performed using a 360° Perspex protractor mounted on a central pin; structures to be rotated were carefully centred on this pin prior to the rotation and partial exposure procedure.

Results

Nuclear 'ghosts'

At low magnifications the electron optical images of negatively stained nuclear 'ghosts' that have been purified by isopycnic banding on sucrose gradients or by the alternative differential centrifugation method are readily interpreted. Flattened or collapsed bodies not unlike mammalian erythrocyte 'ghosts' are detected on the carbon support film of the viewing grid, which were therefore termed nuclear 'ghosts' by Price *et al.* (1972). These nuclear 'ghosts' are surrounded by and partially coated with the amorphous heavy-metal negative staining salt. This interpretation is based on the extensive knowledge now available on the behaviour of mammalian erythrocyte 'ghosts' under negative staining conditions, and additional support was in fact obtained by the routine monitoring of the material throughout the membrane preparation by light microscopy using phase-contrast and Nomarski interference optics.

Figures 1 and 2 (plate 38) are low electron optical magnifications of single nuclear 'ghosts' from normal rat liver and hepatoma, respectively. The normal rat liver nuclear 'ghost' is seen to have an electron-opaque central region where the membrane is folded over on itself in an intricate manner. The surrounding area in which there is less electron scattering reveals clearly the randomly spread nuclear pore complexes, which can quite reasonably be used as morphological markers for nuclear membranes. The rat hepatoma nuclear 'ghost' in figure 2 is an elongate collapsed body. Most nuclei in hepatoma tissue have extremely distorted shapes. This fact also reveals itself when isolated nuclei and nuclear 'ghosts' are studied by light microscopy or electron microscopy, in that sausage-shaped organelles are found rather than the typically spherical ones obtained from normal liver. In figure 2 fewer membrane folds have been produced during the staining process, and the nuclear pore complexes are visible over almost the whole area of the membrane.

At higher electron optical magnifications more detail can be seen on the surface of the nuclear membrane. First, there is the important fact that the double nuclear membrane is revealed at the edge of the intact 'ghost', where the flattened membranes bend, see figures 3

and 4 (plate 38). The conclusion can thus be drawn that the electron beam does in fact have to penetrate four layers of membrane in order to produce the images shown in figures 3 and 4, and that the central electron-opaque region shown in figure 1 must contain more than four layers of membrane.

Also visible within the nuclear pore complexes is the inner ring of material, just within the annuli and encircling the central granule (figure 5, plate 38). In general, it must be admitted that it is not possible to see very much fine detail within the nuclear pore complexes by increasing the electron optical magnification. A possible reason for this is the presence of the four layers of membrane, together with the probability that there will be overlapping of nuclear pore complexes in the upper pair of nuclear membranes with those of the lower pair, as depicted diagrammatically in figure 6. This will mean that there is an inherent complexity within the system, resulting in a loss of detail in the electron optical image. Nevertheless, as will become apparent from the results presented in the following section, there must be underlying fine structure which is hidden in the areas of overlapping nuclear membrane, from which it cannot be retrieved by the negative staining method.

Nuclear membrane fragments

Along with the relatively intact nuclear 'ghosts' obtained by the purification methods employed for this study, sheet-like fragments of nuclear membrane are also detected on the viewing grids (see figure 7, plate 39). In addition, nuclear ghosts which have apparently undergone disruption during the negative staining procedure are also commonly encountered. Here again, experience stemming from the behaviour of erythrocyte 'ghosts' during the negative staining procedure is paralleled by that of the nuclear 'ghost'. In all probability the nuclear 'ghost', which in aqueous suspension is holding together as a tenuous sack of membrane, is torn apart by the surface of tension and spreading forces applied within the thin layer of fluid on the supporting carbon film at the time of preparing the negatively stained specimens. Figure 8 (plate 39) shows a low magnification field of a nuclear ghost that has undergone disruption. In general, though by no means always, the nuclear pore complexes remain intact within the disrupted region, individual pore complexes and groups being surrounded by a small amount of membrane. At higher electron optical magnifications the detail within the negatively stained nuclear pore complexes becomes more readily apparent than is the case when either intact nuclear 'ghosts' or large torn sheets of membrane are likewise studied, see figure 9

Description of plate 38

Figure 1. A low electron optical magnification of a rat liver nuclear 'ghost' negatively stained with ammonium molybdate.

Figure 2. A low electron optical magnification of a rat hepatoma nuclear 'ghost' negatively stained with ammonium molybdate.

Figure 3. A higher electron optical magnification of part of a rat liver nuclear 'ghost' negatively stained with ammonium molybdate. The double line at the edge of the membrane indicates that both inner and outer nuclear membranes are present.

Figure 4. Part of a rat hepatoma nuclear ghost negatively stained with ammonium uranyl-oxalate. Excellent contrast is produced by this negative stain, which reveals clearly the nuclear pore complexes and the double line at the edge of the membrane, but a greater image granularity is produced than with ammonium molybdate.

Figure 5. Part of a rat liver nuclear 'ghost' negatively stained with ammonium molybdate. Arrows indicate nuclear pore complexes within which the inner ring is visible.

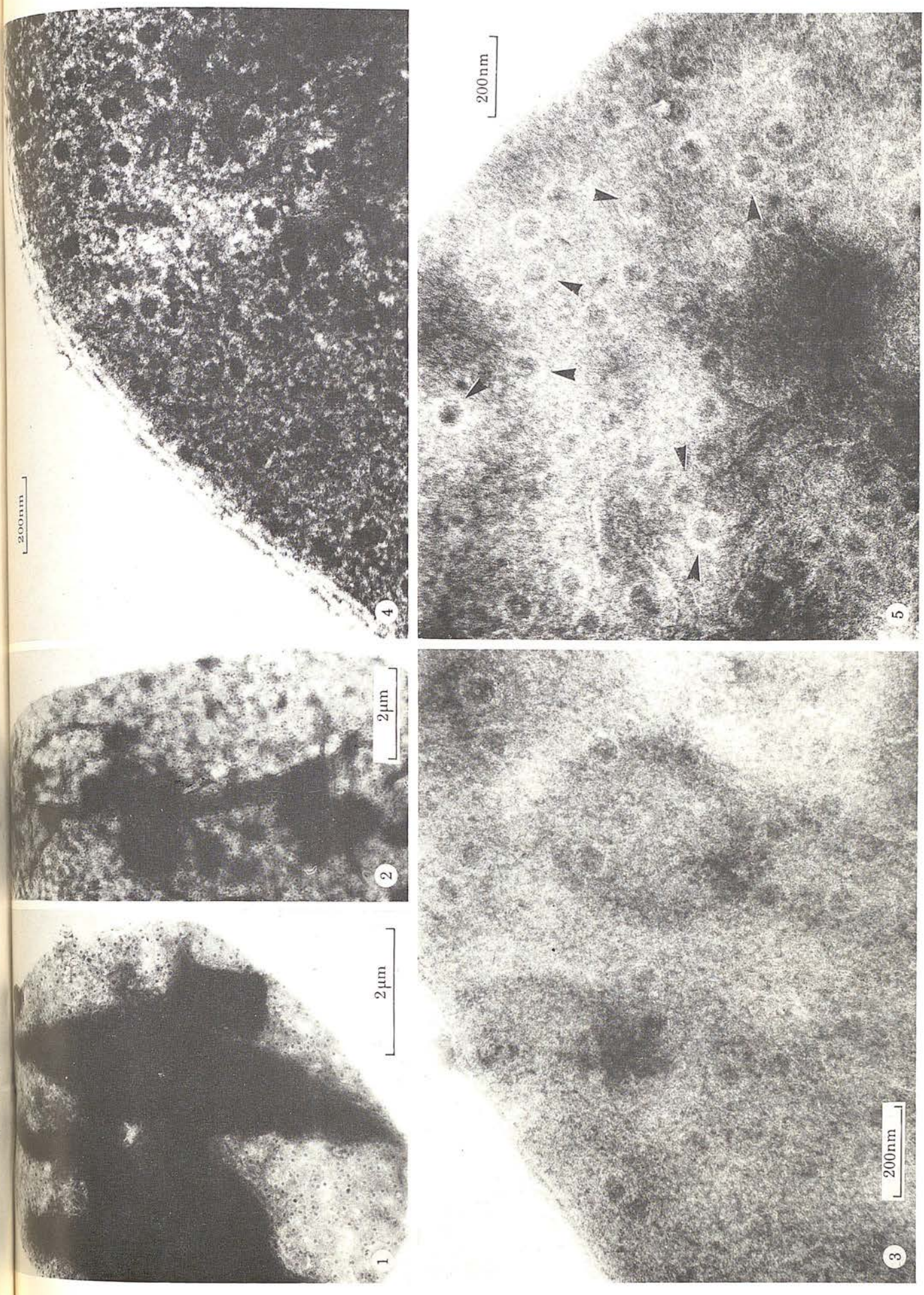

FIGURES 1–5. For description see opposite

(*Facing p.* 112)

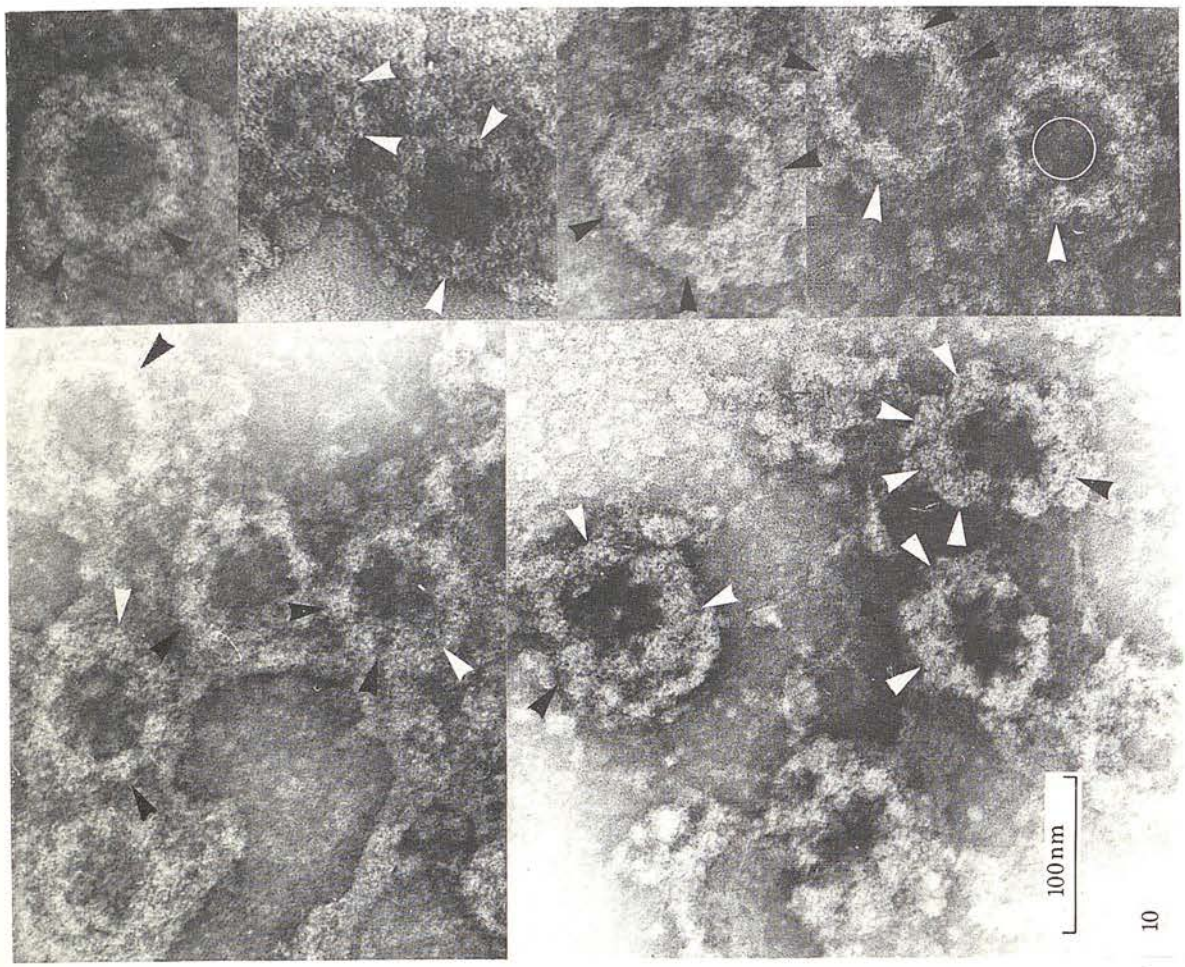

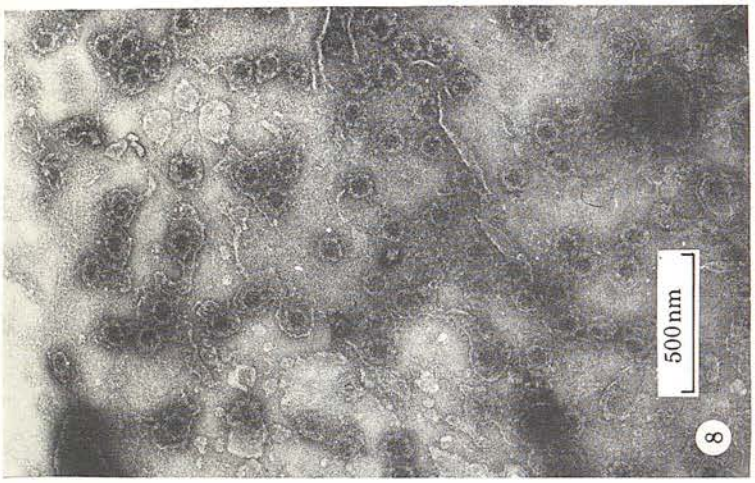

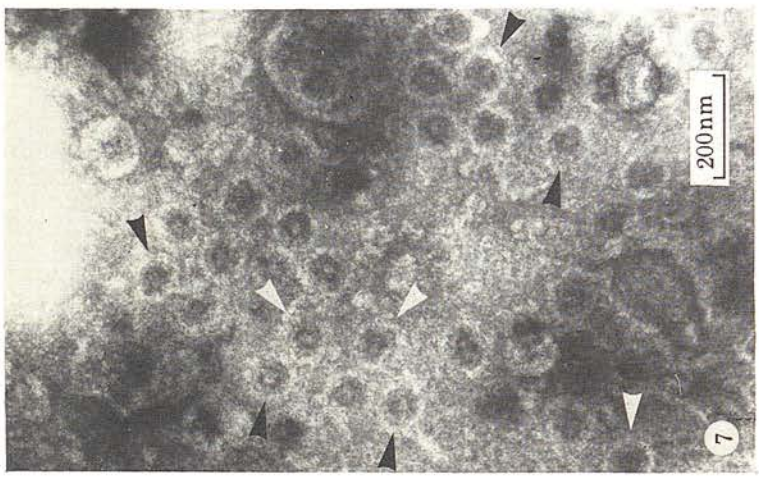

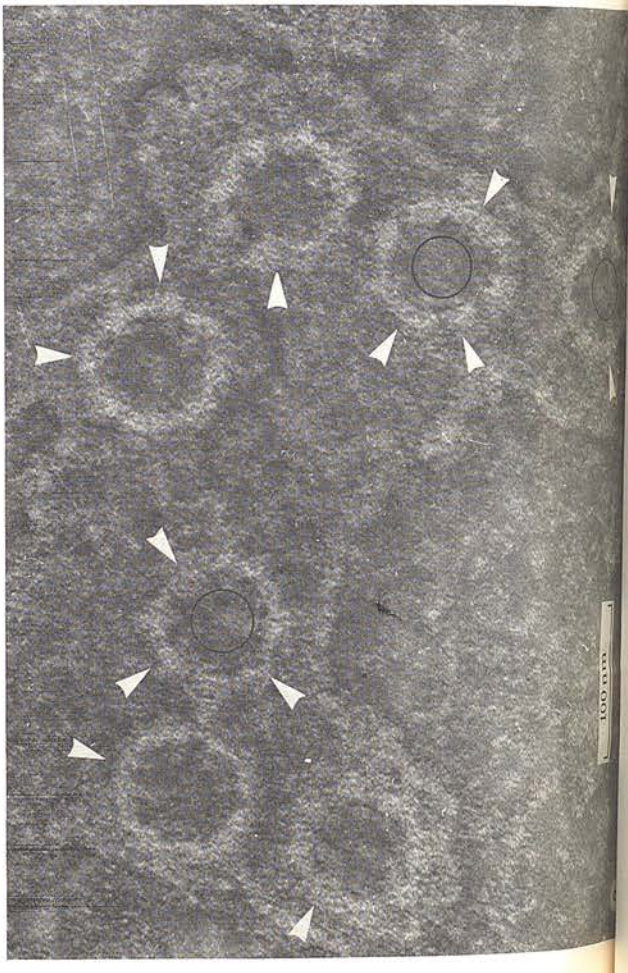

FIGURES 7-10. For description see opposite

(plate 39). Arrows indicate microcylindrical or hollow disk structures with electron-opaque centres which are present within the annular granules of the nuclear pore complexes. These structures appear to underlie each of the eight annular granules. To present these and other features more clearly, composite fields have been prepared by selecting nuclear pore complexes

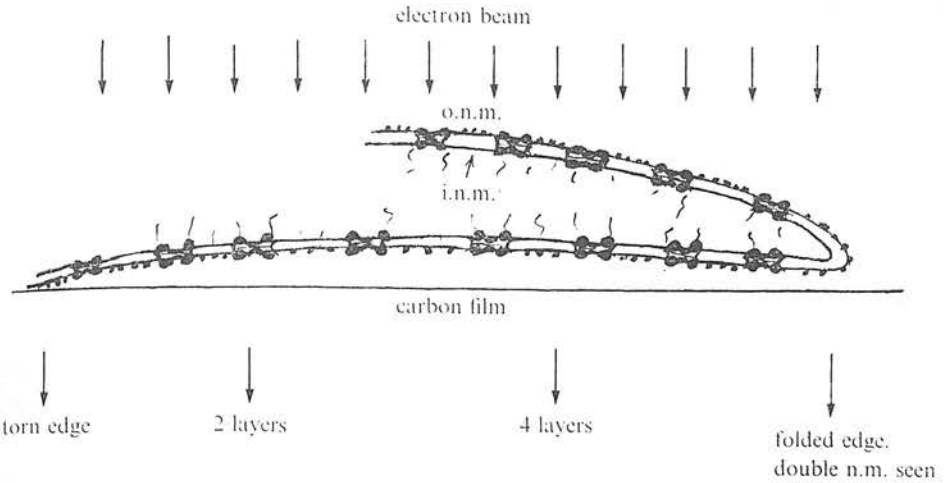

FIGURE 6. A diagrammatic representation of part of a nuclear 'ghost'. The diagram emphasizes the fact that detail in the electron optical image will be lost when pore complexes in the upper layer of double nuclear membrane overlap with those in the lower layer.

from several original electron micrographs, as shown in figures 10 (plate 39), 11 and 12 (plate 40). Arrows indicate the annular granules which reveal the underlying hollow disk or microcylinder-like macromolecule and circles indicate the central granule of the pore complexes, which in many instances also appear as a microcylinder type of structure. This explanation for some of the fine structure within the annulus of the nuclear pore complex is supported by the occasions when partially broken pore complexes have been observed, see figure 13 (plate 40). In these cases some of the diffuse material composing the annuli appears to be splitting away and the hollow disk or microcylinder macromolecules can then be seen more easily.

If the nuclear pore annuli are breaking up, one would expect to fine individual macromolecules actually separated from the pore complexes. This is in fact so, and in figure 14 (plate 41) several of these structures are shown. From isolated macromolecules such as those shown in figure 14 the dimensions of the structure have been determined as follows: external diameter, about 20 nm; internal diameter, about 5 nm. It is suggested that the electron optical

DESCRIPTION OF PLATE 39

FIGURE 7. Part of a torn sheet of rat hepatoma nuclear membrane negatively stained with ammonium molybdate. Arrows indicate nuclear pore complexes showing the inner ring.

FIGURE 8. A low electron optical magnification of part of a rabbit liver nuclear 'ghost' that has split apart at the time of preparing the negatively stained smear of membrane on the carbon support film. Negatively stained with ammonium molybdate.

FIGURE 9. A higher electron optical magnification of part of a rabbit liver nuclear 'ghost' that has split apart, negatively stained with ammonium molybdate. Arrows indicate annular granules of the nuclear pore complex which show an indication of underlying detail and circles indicate the central granule.

FIGURE 10. A compositive field showing nuclear pore complexes which show detail of the annular granules. Arrows indicate granules which show electron-opaque stain filled central regions. Negatively stained with ammonium molybdate.

image just presented is derived from a hollow disk lying on its side with its central hole filled with stain. Alternative electron optical images might be expected if the macromolecule was orientated at different angles relative to the electron beam, but to date the study has not been pursued to this degree of precise interpretation. Thus, no information relative to the height of the hollow disk macromolecule can be presented.

FIGURE 16

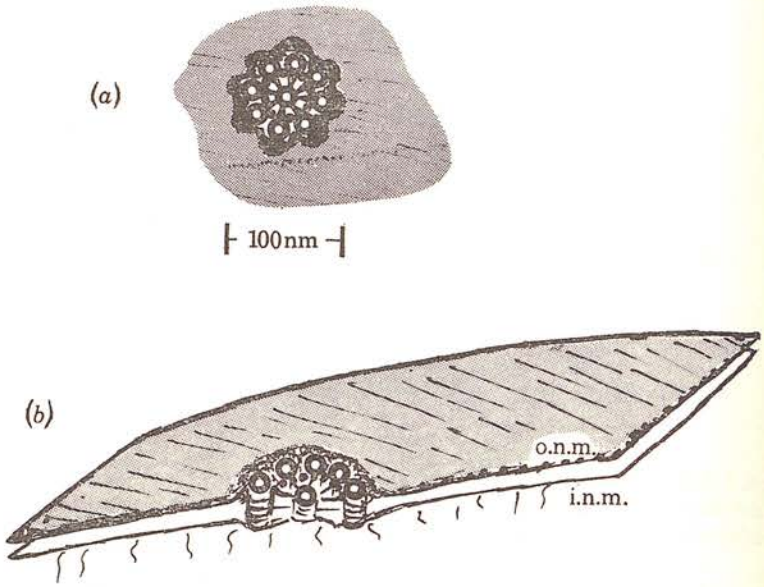

FIGURE 17

FIGURE 16. A model for the hollow disk annular macromolecule derived from the 16-fold rotation symmetry images in figure 15.

FIGURE 17. A schematic model for the nuclear pore complex derived from the results of negative-contrast staining with ammonium molybdate. As the height of the hollow disk annular macromolecules is not known, it cannot be said whether single molecules or stacked molecules are present within the annular granules of the intact nuclear pore complex.

The photographic rotation technique for contrast enhancement has been applied to the annular macromolecule of the nuclear pore complex, for which initial studies immediately suggested the existence of a highly organized subunit structure (see Markham *et al.* 1963) Figure 15, shows the results of this rotation procedure, which strongly suggests that the hollow disk macromolecule has a 16-fold symmetry and that there is in all probability an exceedingly complex organization of subunits within the molecule, as emphasized by the model of the macromolecule derived from the rotational enhancement, shown in figure 16.

From the results presented above, a model for the nuclear pore complex has been drawn. Figure 17*a* shows schematically a face on view of a nuclear pore complex and 17*b* a cut-open

DESCRIPTION OF PLATE 40

FIGURE 11. A composite field of nuclear pore complexes which show the central granule (encircled) to be a hollow cylinder type of structure. Negatively stained with ammonium molybdate.

FIGURE 12. A composite field of nuclear pore complexes selected to show the inner ring and the radial fibrils. Negatively stained with ammonium molybdate.

FIGURE 13. A composite field of nuclear pore complexes which are breaking up. The hollow disk macromolecules can be seen more easily (arrowed). Negatively stained with ammonium molybdate.

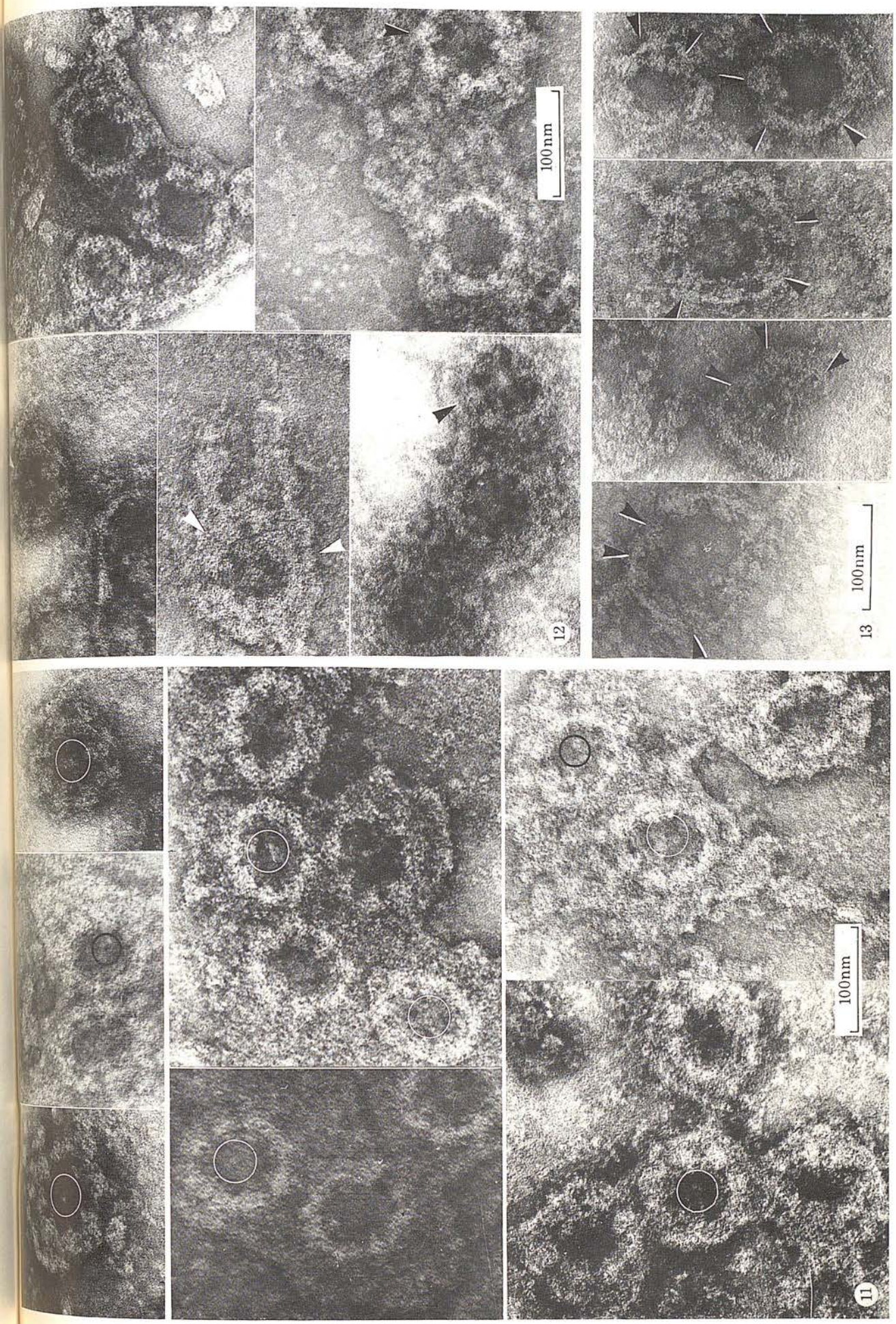

FIGURES 11–13. For description see opposite

(Facing p. 114)

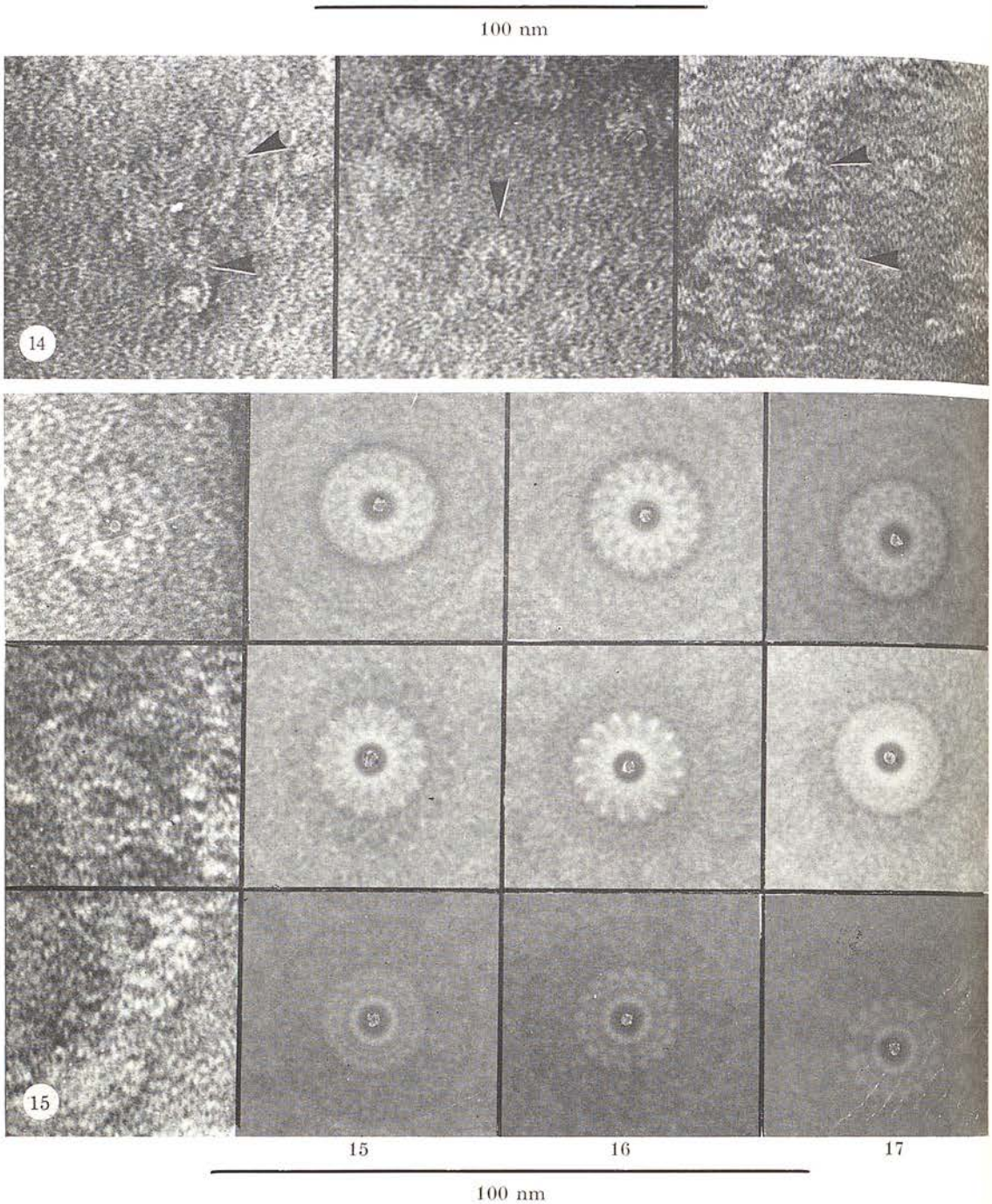

FIGURE 14. Individual hollow disk annular macromolecules which have separated themselves from disrupted nuclear pore complexes. Negatively stained with ammonium molybdate.

FIGURE 15. Application of the photographic rotation technique for contrast enhancement to isolated hollow disk annular macromolecules. The best enhancement is obtained when a rotation of 360°/16° is used, suggesting that there is a 16-fold rotation symmetry within this complex macromolecular structure.

view. The hollow disk macromolecules are positioned within each of the eight annular granules and are shown to have diffuse material surrounding them. Whether or not more than one hollow disk macromolecule is required for the pore complex to extend through both inner and outer nuclear membrane is not yet known. In all probability there will be a stacking of the disks within the annular granules to give the required conformation. The splitting apart of the stacked hollow disks within the nuclear pore annulus during negative staining or the fact that the stack of disks may not be alined parallel to the electron beam could account for some of the difficulty that has been encountered when attempts have been made to try and locate the macromolecules within the intact nuclear pore complex. Additional features included in the model shown in figure 17 are the inner ring of material, the central microcylinder and the radial fibrils, all of which have been detected in the present study, but require further investigation at high electron optical magnification before the validity of their inclusion in the model can be properly assessed.

Discussion

The results presented above are, in the main, preliminary findings. The macromolecular detail revealed within the pore complexes of nuclear membrane when negatively stained with ammonium molybdate has been an extremely reproducible observation. Further high-resolution electron-microscopic and biochemical studies are currently in progress. These studies are directed towards the solubilization of nuclear membrane, followed by the isolation of the macromolecular components of the nuclear pore complex.

From the electron-microscopic point of view it is essential that any biological membrane selected for study should be in a good state of morphological and physiological integrity before any specimen preparative techniques are applied to it. It is considered that the method used for preparing nuclear membrane employed in this study produce a final product which is in a good state of morphological integrity (Price *et al.* 1972), although some residual nucleoprotein remains bound to the membranes. Numerous different approaches have been employed to obtain nuclear membrane by other workers (Agutter 1972; Berezney, Funk & Crane 1970; Franke *et al.* 1970; Kashnig & Kasper 1969; Monneron *et al.* 1972; Zbarsky *et al.* 1969), most of which subject nuclei to a more drastic treatment than does that of the author and his colleagues, and leads to the production of membrane vesicles or tiny fragments rather than nuclear 'ghosts' or large sheets of nuclear membrane. It is impossible at the moment to assess which, if any, of the methods for the isolation of nuclear membrane developed so far really satisfies the criterion of structural and functional integrity which must be strictly adhered to, if possible. This problem is likely to remain a stumbling block in the field of nuclear membranes for some time to come, which will mean that to correlate the results produced by the various groups in the field will continue to be very difficult, until some standard method for the preparation of nuclear membrane becomes widely acceptable.

The results obtained using nuclear 'ghosts' and sheets of nuclear membrane emphasize the possibilities and limitations of the negative staining technique when applied to membranous material. The problem of the overall thickness of the membrane material on the specimen grid is stressed by the multi-layered nuclear 'ghost', within which molecular detail tends to be hidden owing to the overlapping of fine structure in the different layers. It must therefore be concluded that for negative staining to provide the greatest amount of detail it is desirable to have a single layer of membrane material, thereby leading to the production of the simplest electron optical

image. This situation is never realized with the collapsed nuclear 'ghost', with its four layers of membrane or even with the torn sheet where both inner and outer nuclear membranes are present. The detail within the inner or outer nuclear membrane may be masked in the case of the torn sheet, but that within the nuclear pore complex, which extends through both membrane layers as a highly organized structure, should be more easily seen than when they are studied on the nuclear 'ghost'. Despite the arguments expounded above, it has been shown that when nuclear pore complexes within an interfacially disrupted nuclear membrane sheet and also fragmented nuclear pore complexes are studied by negative staining, that a greater amount of information can be gained than can from either the nuclear 'ghost' or the intact sheet of nuclear membrane. Although detail must be present in the latter instances which cannot be retrieved from the electron optical image, the superior methodology of the future with respect to instrumentation and staining may well enable the detail to be seen directly in the intact nuclear membrane. The conclusions relating to the fine structure of the nuclear pore complex are derived in the main from images of partially fragmented complexes. It has been suggested that these images provide an insight into the structure of the intact nuclear pore complex and even though a considerable amount of experimental evidence has been presented to support this derivation, the hypothesis presented is by no means dogmatically stated. Thus, the model for the nuclear pore complex (figure 17) which was drawn to emphasize the electron-microscopic results may have introduced errors or omitted features which may in the future be shown to be important.

The main contribution of the present study has been to show that each of the eight annular granules of the nuclear pore complex does in fact have an underlying hollow disk-like macromolecular configuration which is surrounded by or embedded in other diffuse material. This is a structure not unlike that proposed by Abelson & Smith (1970) from thin sectioning studies. These workers used the term 'subannular minitubules' to describe the detail they claimed to see within the annular subunits of the tissue culture cells they were investigating. In addition, it was claimed by Abelson & Smith (1970) that the central granule of the pore complex was also a tubular structure. This suggestion is supported by the present negative staining study. Thus the model for the nuclear pore complex shown in figure 17 has several features which agree with that proposed by Abelson & Smith. It should perhaps be noted that Wischnitzer (1958) and Vivier (1967) both suggested that the annular granules of the nuclear pore complex were in fact microcylinders.

The models of the nuclear pore complex drawn by Franke & Scheer (1970*a*) and Engelhardt & Pusa (1972) show the annuli to be composed of globular subunits rather than tubule-type structures, as are the central granules. The former authors refer in the text of their paper to the 'inner ring', but do not include it in their model. The results presented in this publication support the existence of the 'inner ring', which has therefore been included in figure 17. One other component of the nuclear pore complex which has received general acceptance are the radial fibrils, which are also included in the model in figure 17. Franke & Scheer (1970) termed these components *internal fibrils*, and Abelson & Smith used the term *struts* and *suspensory apparatus*, the models of both groups including these features.

It should be emphasized that the radial fibrils and central granules have not been detected in all the nuclear pore complexes studied in this investigation. It is likely that in aqueous suspension the nuclear membrane is extremely tenuous and that components are continually being lost from the pore complexes, as we are not yet in a position to define with any degree of

accuracy the optimal ionic composition and pH of the buffer solution required to maintain morphological integrity of nuclear membrane, yet at the same time permit the release of any chromatin associated with the nucleoplasmic surface of the inner nuclear membrane. Several authors have observed differences between nuclear pore complexes (Wunderlich 1969; Speth & Wunderlich 1970; Franke & Scheer 1970*b*; Abelson & Smith 1970), which have usually been accounted for by postulating dynamic metabolic variations.

It is claimed that negative staining has contributed a significant amount to current knowledge relating to the macromolecular organization present within the nuclear pore complex, and that this knowledge could not have been obtained to such a convincing extent by the use of either thin sectioning or freeze-etching. It may be predicted that a superior resolution of detail will be obtained in the future using ammonium molybdate and possibly other negative-contrast stains than has been possible in this publication. Research on nuclear membranes is going through a period that in many ways parallels that on the mammalian erythrocyte membrane during the 1950s when no satisfactory method had been developed for obtaining this membrane species in an intact form yet free from haemoglobin. The methods used by the author and his colleagues (Price *et al.* 1972) to obtain nuclear 'ghosts' by a low ionic strength treatment must be considered as a promising, yet possibly not fully developed system for isolating nuclear membrane which is in a state worthy of further investigation using biochemical techniques and electron microscopy.

References (Harris)

Abelson, H. T. & Smith, G. H. 1970 *J. ultrastruct. Res.* **30**, 558–588.
Agutter, P. S. 1972 *Biochim. biophys. Acta* **255**, 397–401.
Berezney, R., Funk, L. K. & Crane, F. L. 1970 *Biochim. biophys. Acta* **203**, 531–546.
Engelhardt, P. & Pusa, K. 1972 *Nature, New Biol.* **240**, 163.
Franke, W. W. 1966 *J. Cell Biol.* **31**, 619–623.
Franke, W. W., Deumling, B., Ermen, B., Jarasch, E. D. & Kleinig, H. 1970 *J. Cell Biol.* **46**, 379–395.
Franke, W. W. & Scheer, U. 1970*a* *J. ultrastruct. Res.* **30**, 288–316.
Franke, W. W. & Scheer, U. 1970*b* *J. ultrastruct. Res.* **30**, 317–327.
Haggis, G. H. 1969 *Biochim. biophys. Acta* **193**, 237–246.
Harris, J. R. 1969 *J. molec. Biol.* **46**, 329–335.
Harris, J. R. 1971 *J. ultrastruct. Res.* **36**, 587–594.
Harris, J. R. & Agutter, P. S. 1970 *J. ultrastruct. Res.* **33**, 219–232.
Kashnig, D. & Kasper, C. 1969 *J. biol. Chem.* **244**, 3786–3792.
Markham, R., Frey, S. & Hills, G. 1963 *Virology* **20**, 88–102.
Monneron, A., Blobel, G. & Palade, G. E. 1972 *J. Cell Biol.* **55**, 104–125.
Price, M. R., Harris, J. R. & Baldwin, R. W. 1972 *J. ultrastruct. Res.* **40**, 178–196.
Speth, V. & Wunderlich, F. 1970 *J. Cell Biol.* **47**, 772–777.
Vivier, E. 1967 *J. Microsc., Paris* **6**, 371–390.
Wischnitzer, S. 1958 *J. ultrastruct. Res.* **1**, 201–222.
Wunderlich, F. 1969 *Expl Cell Res.* **56**, 369–374.
Zbarsky, J., Perevoschikova, K., Delektorskaya, L. & Delektrosky, V. 1969 *Nature, Lond.* **221**, 257–259.

disulphide bridges in carcinoembryonic antigen (Thomas *et al.*, 1974). When carcinoembryonic antigen modified by treatment with 5.33mM-metaperiodate was hydrolysed in oxygen-free conditions and subjected to acid hydrolysis cystine was detected in a subsequent amino acid analysis, whereas only cysteic acid was obtained from carcinoembryonic antigen treated with 0.533M-metaperiodate.

Oxidative cleavage of the disulphide bonds causes changes in the tertiary structure of the protein core of carcinoembryonic antigen and thereby disorientates determinant groups, whether carbohydrate or protein, and hence decreases the ability of carcinoembryonic antigen to bind to the antiserum.

This investigation was supported by a grant (G793/785/K) to the Chester Beatty Research Institute (Institute of Cancer Research, Royal Cancer Hospital) from the Medical Research Council. The Alexander Keiller Foundation is acknowledged for a fellowship (to P. T.). We would like to thank Miss S. J. Pelly for radioimmunoassays, Mrs. D. Purkiss for amino acid analyses and Dr. M. A. Bukhari for monosaccharide analyses.

Banjo, C., Gold, P., Freedman, S. O. & Krupey, J. (1972) *Nature (London) New Biol.* **238**, 183–185

Gold, J. M., Banjo, C., Freedman, S. O. & Gold, P. (1973) *J. Immunol.* **111**, 1872–1879

Goldstein, I. J., Hay, G. W., Lewis, B. A. & Smith, F. (1965) *Methods Carbohyd. Chem.* **5**, 361–370

Laurence, D. J. R., Stevens, U., Bettelheim, R., Darcy, D. A., Leese, C. L., Turberville, C., Alexander, P., Johns, E. W. & Neville, A. M. (1972) *Brit. Med. J.* **iii**, 605–609

Mach, J. P. & Pusztaszeri, G. (1972) *Immunochemistry* **9**, 1031–1034

Thomas, P., Westwood, J. H. & Foster, A. B. (1974) *Biochem. Soc. Trans.* **2**, 1248–1249

A Rapid Procedure for the Isolation and Purification of Rat Liver Nuclear Envelope

JAMES R. HARRIS and JEREMY F. MILNE

Department of Physiology, University of St. Andrews, Bute Medical Buildings, St. Andrews, Fife KY16 9TS, U.K.

The principles previously developed for the production of nuclear envelopes from rat liver and hepatoma by Price *et al.* (1972) have been modified to enable this membrane material to be obtained rapidly from purified rat liver nuclei by using conventional centrifuge rotors rather than zonal rotors. The underlying factor which has been carried forward in the present method is that rat liver nuclei will swell and release their contents into solutions of low ionic strength in the absence of bivalent cations. A 1mM solution of $NaHCO_3$ (pH7.2) has been used to bring about this release of chromatin (Harris, 1974). In the method of Price *et al.* (1972) nuclear envelopes were isolated by rate zonal centrifugation direct from the 1000*g* nuclear pellet after homogenization in 1mM-$NaHCO_3$ buffer and overnight incubation at 4°C. When applied to purified nuclei, the 1mM-$NaHCO_3$ treatment alone is not satisfactory for producing nuclear envelopes since an unmanageable gel forms as the chromatin is released from the bursting nuclei. This gel can, however, be dissociated by a brief treatment with DNAase (deoxyribonuclease) I. The method given below outlines the details of a procedure which incorporates washing in 1mM-$NaHCO_3$ together with a DNAase I treatment, and leads to the production of intact nuclear 'ghosts' and large torn sheets of envelope from purified rat liver nuclei.

All procedures were carried out at 4°C, unless stated to be otherwise. Purified nuclei were obtained from the livers of six Wistar rats after homogenization in 0.25M-sucrose–1mM-$MgCl_2$–10mM-Tris–HCl (pH7.4) by using an Ultra-turrax type TP 18/2, and sedimentation of the 1000*g* nuclear pellet through 2.2M-sucrose–10mM-Tris–HCl (pH7.4) at 100000*g* for 2h in a Beckman S.W. 27.1 rotor in an L2 65B ultracentrifuge. The

pellets of nuclei were then washed twice at 1000*g* for 5min in the homogenization buffer. The combined pellets of purified nuclei were taken as the starting material for the isolation of nuclear envelope.

The nuclei were resuspended in 40ml of 1mM-$NaCHO_3$ (pH7.2) by shaking, and allowed to equilibrate for 5 min before centrifuging at 31300*g* for 5 min in a Beckman JA-20 fixed-angle rotor in a J-21 centrifuge. The pellet of slightly swollen nuclei was again resuspended in 1mM-$NaHCO_3$ by gentle syringing through a large-diameter needle, and re-centrifuged as above after a further equilibration period of 5min. A very swollen gelatinous pellet was obtained and this was dispersed by the addition of 1mM-$NaHCO_3$ containing DNAase I (Sigma Chemical Co., London S.W.5, U.K., type DN-100) to give 40ml of suspension with an enzyme concentration of 10μg/ml. This suspension was then incubated at room temperature (20°C) for 15–20min. During the incubation period the chromatin excaping from the burst nuclei is degraded by the DNAase, thus allowing the nuclear envelopes to become freely dispersed. The dissolution of the gelatinous state is extremely rapid and nuclear envelopes can be observed by phase-contrast microscopy to become freely suspended. The nuclear envelopes were then repeatedly washed in 40ml of 1mM-$NaHCO_3$ by centrifugation at 31300*g* for 5min. The release of chromatin throughout this sequence is shown in Fig. 1.

The nuclear envelopes from the final centrifugal wash were resuspended in 2ml of 1mM-$NaHCO_3$ and centrifuged at 500*g* for 5min. The small discoloured pellet was discarded and the white supernatant layered over a discontinuous sucrose gradient made up of 10ml of 2.0M-sucrose, 10ml of 1.8M-sucrose, 10ml of 1.5M-sucrose and 6ml of 0.25M-sucrose (all solutions made up in 10mM-Tris–HCl, pH7.4). The gradient was then centrifuged for 90min in a Beckman S.W. 27.1 rotor at 100000*g* (27000rev./min) in an L2 65B ultracentrifuge. A major band of purified nuclear envelope formed at the 1.5M/1.8M-sucrose interface during the centrifugation, as shown in Fig. 2. Prolonged centrifugation did not alter the position of this membrane band and isopycnic centrifugation for 20h at 100000*g* on a continuous sucrose density gradient likewise gave a single membrane band of flotation density 1.21±0.01. Gradient profiles have been recorded as a routine by direct photography and also by passing the contents of the tubes through an LKB Uvicord 11 u.v. absorptiometer coupled to a Bryans model 27000 chart recorder.

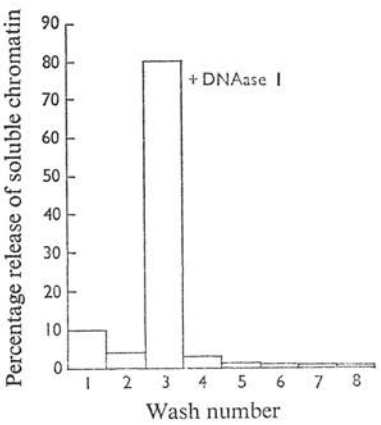

Fig. 1 *Release of chromatin from rat liver nuclei throughout* 1 *m*M-*NaHCO*$_3$ *washes and DNAase treatment*

Results were calculated from the absorbance values at 260nm of the 31300*g* supernatants.

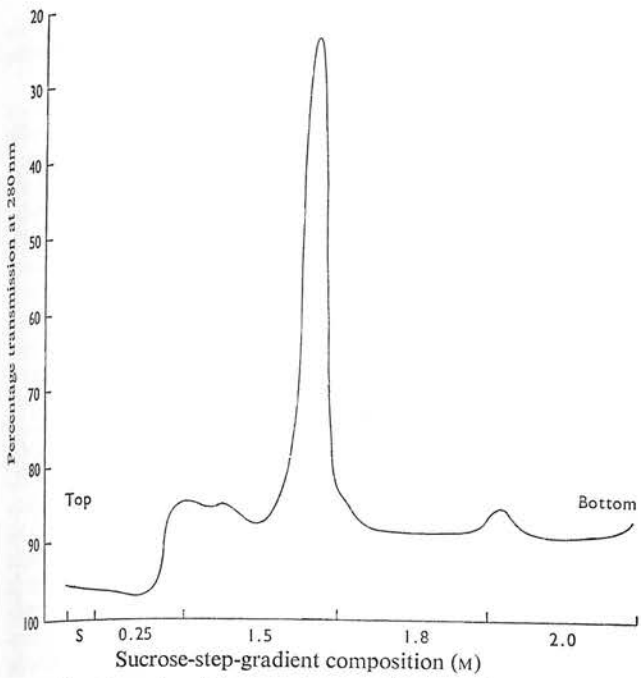

Fig. 2. *Flotation of rat liver nuclear envelope at the* 1.5M-/1.8M-*sucrose interface of a sucrose-step gradient after centrifugation at* 100000*g for* 90*min*

For details see the text. S, Sample.

Nuclear envelope was recovered from the absorptiometer effluent as 40-drop fractions or alternatively the membrane band was removed by hand from the gradients with a Pasteur pipette. Phase-contrast examination of this final membrane material revealed a free suspension of intact nuclear 'ghosts' and large sheets of torn envelope. The assessment was confirmed by electron microscopy by using thin sectioning and negative-staining after the removal of sucrose by washing twice with 1mM-$NaHCO_3$ at 31300*g* for 5min. The absence of mitochondria, rough and smooth membrane vesicles is readily apparent, only sheets of membrane and intact nuclear 'ghosts' showing the characteristic nuclear pore complexes, which can be regarded as morphological markers of nuclear envelope, are present.

Harris, J. R. (1974) *Phil. Trans. Roy. Soc. London Ser. B* **268**, 109–117
Price, M. R., Harris, J. R. & Baldwin, R. W. (1972) *J. Ultrastruct. Res.* **40**, 178–196

Ultrastructural Cytochemical and Metabolic Changes After Nodular Hyperplasia in Experimental Hepatomegaly

NORMAN ROBINSON, JOHN G. NIEVEL and JOHN ANDERSON

Department of Anatomy, The London Hospital Medical School and Department of Medicine, King's College Hospital Medical School, London SE5 8RX, U.K.

Compounds of widely differing chemical structures induce drug-metabolizing enzymes and various morphological and biochemical changes which, after chronic administration, may lead to liver enlargement (Kunz *et al.*, 1966). Phenobarbitone also induces a reversible liver growth and chronic treatment with high dose amounts produces hyperplastic

foci in the enlarged liver. In the present study, we investigated various enzyme activities during hepatomegaly and compared the morphological and biochemical characteristics of the hyperplastic nodules with the normal and enlarged liver.

White female Wistar rats were treated with phenobarbitone (88 mg/kg) in the drinking water for three months. The growth rate, liver size, light and electron-microscopic changes and the activities of succinate dehydrogenase, isocitrate dehydrogenase, lactate dehydrogenase, glucose 6-phosphate dehydrogenase $NADH_2$-diaphorase, acid phosphatase, adenosine triphosphatase, 5′-nucleotidase, α-glycerophosphate dehydrogenase, alkaline phosphatase and monoamine oxidase, were determined histochemically. The animals were starved overnight and killed 18 h after the last dose of phenobarbitone.

Phenobarbitone increases the smooth endoplasmic reticulum in the hepatocyte (Remmer, 1959). Various regions in the phenobarbitone-treated liver contained cells with enlarged cytoplasm and increased number of mitochondria. Infiltration of lymphocytes was widespread and haemorrhages were seen in the sinusoids. The number of mitoses was increased uniformly in the phenobarbitone-treated liver. The RNA and DNA content was higher in the nodules of the enlarged liver. No chromosomal abnormalities were observed. The activities of succinate dehydrogenase, isocitrate dehydrogenase, lactate dehydrogenase, glucose 6-phosphate dehydrogenase and $NADH_2$-diaphorase near the wall of sinusoids was higher in the nodules than in other parts of the enlarged liver. Amongst the oxidative enzymes studied, isocitrate dehydrogenase had the highest activity; α-glycerophosphate dehydrogenase and monoamine oxidase showed no change in the enlarged liver or in the hyperplastic nodules. Parallel with the hypertrophy of smooth endoplasmic reticulum an increase of glucose 6-phosphate dehydrogenase was also detected in the hyperplastic foci. The activity of alkaline phosphatase did not change. However, an increased activity of acid phosphatase, adenosine triphosphatase, and 5′-nucleotidase was observed in the hyperplastic nodules. The marked increase of acid phosphatase in these foci of the enlarged liver was closely related to the perinuclear area. These regions lost the normal hepatic cell morphology.

The observed enzyme changes reflected the increased metabolic activity of the hyperplastic nodules. However, no gross alteration of specific enzyme activities was detected in chronic hepatomegaly.

Kunz, W., Schaude, G., Schimassek, H., Schmid, W. & Siess, M. (1966) *Proc. Eur. Soc. Study of Drug Toxicity* **7**, 138–153

Remmer, H. (1959) *Naunyn-Schmiedeberg's Arch. Exp. Path. Pharmakol.* **235**, 279–290

Plasminogen and Fibrinogen Synthesis in Experimental Hepatomegaly

MICHAEL F. SCULLY, VEEJAY V. KAKKAR snd JOHN G. NIEVEL

Departments of Surgery and Medicine, King's College Hospital Medical School, Denmark Hill, London SE5 8RX, U.K.

Various drugs and lipid-soluble compounds stimulate microsomal protein synthesis in liver, and after chronic administration induce hepatomegaly (Conney, 1967). The toxicological significance of the induced hepatomegaly has not yet been clarified, although differences in the control of macromolecular synthesis during hepatomegaly induced by toxic or non-toxic compounds have been demonstrated (Nievel & Golberg, 1968; Nievel, 1971). Fibrinogen is synthesized by the liver; however, the site of plasminogen synthesis, the other essential component of the fibrinolysis system, is not yet known.

In the present paper we compare the rate of synthesis of fibrinogen, plasminogen and other plasma and liver protein fractions in experimental hepatomegaly.

White female Wistar rats (body weight 100–120 g) were used in these experiments. The animals received a daily intraperitoneal injection of 80 mg of phenobarbitone/kg for 4 days to stimulate ribosomal protein synthesis at a maximum rate and to induce

5 The isolation and characterization of the nuclear envelope

JAMES R. HARRIS and PAUL S. AGUTTER

5.1 Introduction

5.1.1 Terminology

The *nuclear envelope* is morphologically defined as the double membrane which is situated between the nucleoplasm and cytoplasm of eukaryotic cells and which is studded with octagonal structures, known as the nuclear pore complexes. This specialized double membrane system is often simply referred to as the nuclear membrane, both this and the term nuclear envelope being accepted nomenclature. In this review the term *inner nuclear membrane* (INM) which is adjacent to the nucleoplasm, and *outer nuclear membrane* (ONM) which borders onto the cytoplasm (with the perinuclear space between the two membranes) will be used precisely when possible, and the term *nuclear envelope* reserved for the relatively intact isolated double membrane, which is synonymous with the expression nuclear ghost. The term *nuclear envelope* (NE) will also be used to refer to torn sheets of double nuclear membrane (which are thus to be distinguished from sheets of INM or ONM alone). Very often during an isolation procedure the NE undergoes considerable disruption and the INM

and ONM separate from one another. In this instance, the term *nuclear envelope* cannot be applied and the expression '*fragmented nuclear membrane*' or '*inner and outer nuclear membrane fragments*' is more appropriate. The limit of disruption is when membrane vesicularization occurs probably with a concomitant destruction of the nuclear pore complexes.

5.1 2 Some reasons for interest in the nuclear envelope

Interest in the NE as a morphological entity became widespread after the system was identified electron microscopically around 1950 [1–3]. In the last 7 or 8 years biochemical interest in the nuclear envelope has grown rapidly and during this period several widely differing isolation procedures have been published. It should be emphasized at the outset that work in this field is still in its infancy and that it is therefore improbable that any single isolation method can as yet be regarded as wholly satisfactory. Nevertheless, it is accepted that progress towards an understanding of the physiological function of the NE system, together with accurate information on its chemical composition and enzymatic properties is largely contingent on the production of satisfactory isolated preparations.

One major reason for the extensive interest in the NE is its probable involvement in the control of the movement of various metabolites into and out of the nucleus, that is, in nucleo-cytoplasmic interactions [4,5]. Moreover, during cell division, the NE breaks down during late prophase and reforms with a net increase in area and number of nuclear pore complex during late telophase. It is not known for certain whether pieces of NE are attached to the dividing chromosomes or whether the envelope dissociates into 'monomers' which in either case reassociate to give the NE's of the daughter cells.

Available evidence has led some workers to suggest that the ONM may be functionally related to the endoplasmic reticulum [6], as in many cases ribosomes have been detected on its cytoplasmic surface [7] and certain enzyme activites of NE and the endoplasmic reticulum appear very similar. The INM which under physiological conditions is in intimate association with the nucleoplasm, has a layer of heterochromatin along its nucleoplasmic surface termed the internal dense lamina. This layer, which appears to give structural rigidity to the INM, does not cover the inner surfaces of the nuclear pore complexes, which therefore apparently have direct access to the nuclear contents. A possible functional relationship between nucleoplasmic DNA and RNA and the inner nuclear membrane is thus indicated [6]. Much however, remains to be clarified experimentally. One of the main aims of current research on the NE must be to provide some explanation for the existence of the nuclear pore complex in terms of its involvement in the metabolism of the cell.

Permeability studies on intact nuclei [8,9] have shown that most small molecules and many macromolecules can enter and leave the nucleus freely, but such studies have not as yet provided information concerning the movement of RNA and ribosomal ribonuclear proteins from nucleoplasm to cytoplasm, or the

associated feed back of information from the cytoplasm to control gene function. It is probable that knowledge of this and other functions of the NE will be gained from the study of the system in isolation.

5.1.3 Ultrastructural background

The ultrastructure of the NE has recently been reviewed in articles by Feldherr [9], Kessel [10], Wischnitzer [11] and Franke [12]. Some discussion of the ultrastructure of the NE is appropriate at this point since its appearance in the electron microscope at present constitutes the major criterion of acceptability for an isolated preparation. Indeed a large proportion of the information currently available about the system is of an ultrastructural nature.

The term *nuclear envelope* was first used by Anderson in 1953 [3]. Prior to this the existence of the system had been suggested by several light microscopic studies; it was first shown to be a two layered membrane system by the electron microscopic studies of Callan and Tomlin [2]. These workers showed that the NE was associated with, and penetrated by, pore structures currently termed nuclear pore complexes. The discoveries of Callan and Tomlin which were obtained using air dried specimens of isolated oocyte NEs were subsequently confirmed by others using thin sectioning [13–17]. The intimate association of the nuclear pore complex with both INM & ONM has been deduced from many studies on intact tissues [18–22] and isolated NEs [5,23–25]. The double membrane state of the NE seems to be a universal phenomenon, as does the pore complex; but the number of pore complexes per unit area (pore density) varies greatly between species and tissues [14,26–33].

There is evidence that the two membranes of the NE differ considerably in their composition, ultrastructure and stability properties. The ONM is usually studded with ribosomes [7,34] and is removed in nonionic surfactants such as Triton X–100 [35] as well as in low pH media such as 1% citric acid [36], both treatments leaving the INM apparently intact. The closeness of contact between the internal dense lamina, which is also termed the granular perinuclear layer [37] or the peripheral heterochromatin layer [38], and the INM probably confers special properties of organization on the INM and generates a problem of intractable contamination of the NE with chromatin throughout any isolation procedure. The complementary contamination problem regarding the ONM with cytoplasmic material, notably endoplasmic reticulum [34], is also acknowledged. It should, nevertheless, be borne in mind that an apparent ultrastructural continuity between the ONM and the endoplasmic reticulum does not necessarily entail a similarity in composition and enzyme content. The heterogeneity of the latter membrane system within itself is, in any case well established. [39].

Some early accounts of the structure of the nuclear pore complex are remarkably detailed [16,19,40–42]. Recent reports have made use of high electron optical magnifications (derived from thin sectioning, negative staining

and metal shadowing) in attempts to construct models of the nuclear pore complex [20–23,25,43–48]. Briefly, it appears that in all cases the lumen of the pore is surrounded by an annulus which overlaps the membrane margin. This annulus may further be resolved into an octagonal array of annular subunits approximately 25 nm in diameter. The lumen often, though by no means always, contains a central granule which may be attached by fibrils to the annular subunits or to the membrane margin itself. It has been proposed that both the central granule and the annular subunits have a *mini tubule* or hollow cylinder type of structure [20,25,40], and further, that the macromolecular organization underlying the hollow cylinder of the annular subunits may itself have a sixteen fold symmetry [25]. Despite these recent advances the details of the overall structure of the nuclear pore complex are far from clear, particularly when it is desired to express this structure in terms of a macromolecular arrangement. It is perhaps worth re-emphasizing the current view that the nuclear pore complex is likely to constitute more than a mere opening for passive diffusion of protein, RNA or polysomes [48].

The salient features of the NE described above are shown diagrammatically in Fig. 5.1. A selection of electron micrographs of intact nuclei are shown in Fig. 5.2 which illustrates the various aspects discussed.

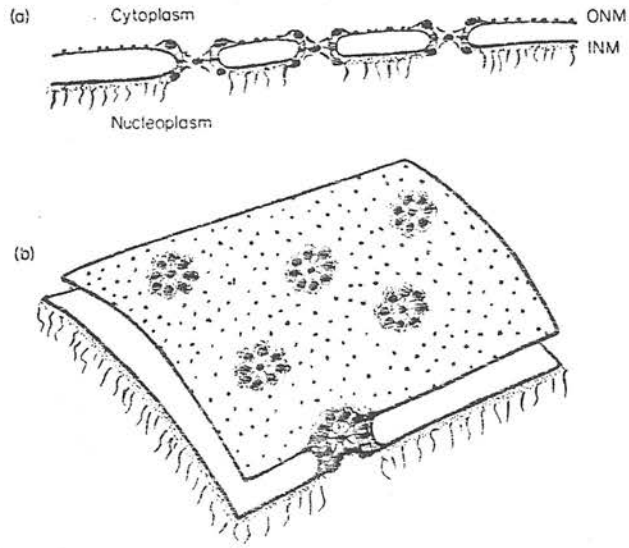

Fig. 5.1 A diagrammatic representation of the nuclear envelope and the nuclear pore complexes. (a) Perpendicular to the two nuclear membranes. (b) Tangential to the two membranes. The cytoplasmic surface of the outer nuclear membrane (ONM) is studded with ribosomes. The annuli of the nuclear pore complexes project from the surface of the ONM and extend through to the inner nuclear membrane (INM). The internal dense lamina and chromatin fibrils are indicated on the nucleoplasmic surface of the INM.

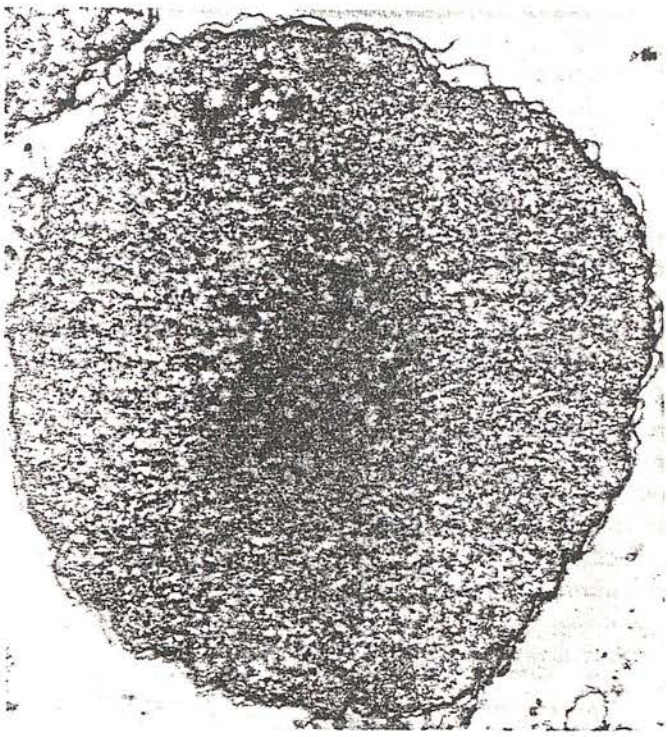

Fig. 5.2a A purified rat liver nucleus revealed by thin sectioning. (x20 000.)

5.1.4 Criteria for evaluating an isolated nuclear envelope preparation

(i) Enzymic markers

To date no acceptable enzymic activity peculiar to the NE has been described; a positive enzymic marker is therefore not at present available. Markers for contamination can, however, usefully be employed. For example, nuclei lack succinate dehydrogenase activity (for assays see [49]), therefore mitochondrial contamination can be estimated. Acid phosphatase can similarly be used as a lysosomal marker [50].

A suitable marker for endoplasmic reticulum has hitherto proved elusive. The NE contains cytochrome b_5 and NADPH oxidase activity [51,52], and glucose-6-phosphatase activity seems to be present [52–54] although it has been reported to be absent in some preparations [55–57]. This absence has been attributed to the inherent instability of glucose 6-phosphatase (R. R. Kay personal communication) and this matter must therefore remain in some doubt. The authors have failed to demonstrate monoamine oxidase activity in their NE preparations, but this is contrary to the claims of Gorkin [58] who showed a

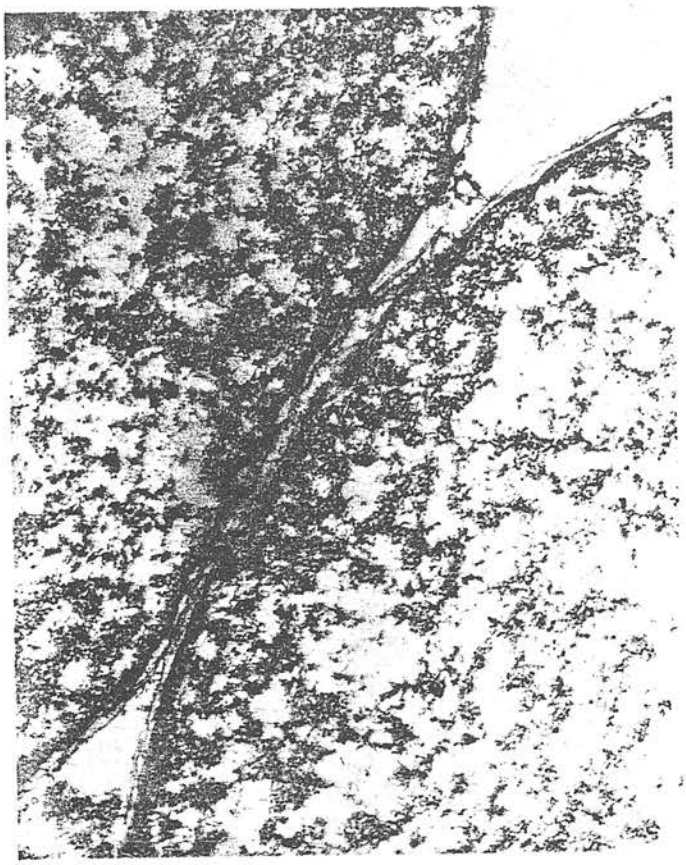

Fig. 5.2b Part of two thin section rat liver nuclei, showing clearly the ONM and the INM with its internal dense lamina of heterochromatin. (x46 000.)

significant increase in the specific activity of monoamine oxidase of rat liver NE over and above that of other cellular fractions. This major difference remains to be settled, but it does perhaps serve to underline the enzymic variability that may follow from the varying membrane isolation procedures. For example, the ultrasonication used by Agutter [57] could well inactivate monoamine oxidase. It must, nevertheless be pointed out that different substrates have been used for monoamine oxidase measurements, and that the enzymes assayed are not necessarily identical. The most comprehensive survey of the enzymes associated with the NE available to date is included in the review by Franke [6].

(ii) Ultrastructural markers

Since the pore complexes are peculiar to NE and the annulate lamellae (which are thought to be derived from the NE's), this morphological feature and the

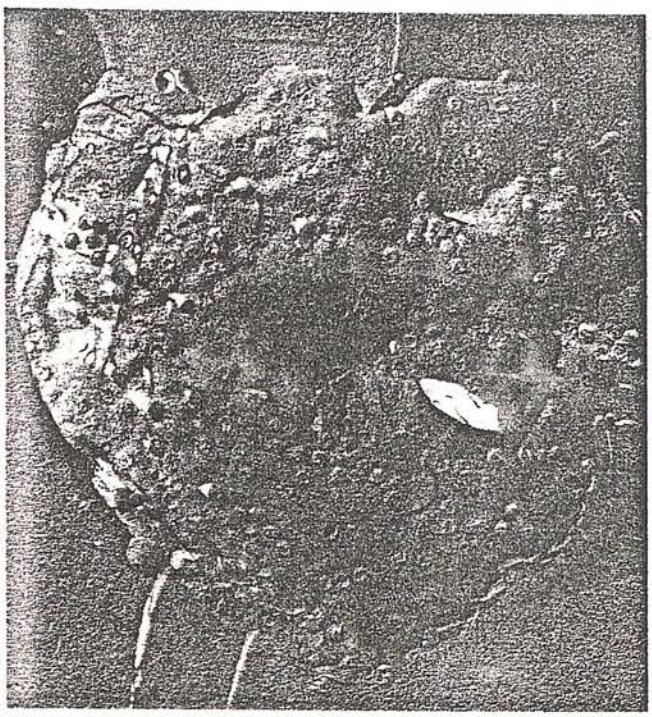

Fig. 5.2c A purified rat liver nucleus revealed by freeze-etching. The nuclear pore complexes are seen to project from the nuclear surface. (x23 000.)

double membrane status of the system have been taken in most laboratories to serve as structural markers for isolated NE in the absence of suitable enzymic markers. Indeed, it must be accepted that both the definition of the isolated NE, and the primary criteria for its evaluation, are based on ultrastructural data. For this reason it is at present essential for those working on the isolation of NE to have a detailed knowledge of those ultrastructural features which are, or should be, visible in the electron microscope under defined conditions of fixation and staining.

Negative staining has been employed with a considerable degree of success to reveal the ultrastructural detail of the NE [5,23–25,45,59]. It is claimed that this technique is able to reveal the macromolecular substructure of the nuclear pore complex [25], although the thickness of these structures presents a considerable obstacle and the results obtained are not as easily interpreted as those obtained with isolated macromolecules [60]. Of the negative stains commonly employed ammonium molybdate appears to provide the greatest detail within the nuclear pore complex [24]. Apart from the integrity of the nuclear pore complex, negative staining readily provides an assessment of the

state of fragmentation of the isolated NE. Thus at low electron optical magnifications the technique can be used as an extension of light microscopy (phase contrast) when preparations of intact nuclear ghosts are obtained and it will also provide a qualitative assessment of the relative proportion of intact nuclear ghosts to torn sheets of NE. Of prime importance is knowledge of whether or not the INM and ONM are both present. This information is obtained from the negatively stained electron optical image of the folded edges of nuclear ghosts or torn sheets, two electron transparent lines being revealed [24,25]. Further to this, a classification can be assigned to a given membrane preparation as to whether it consists of intact nuclear ghosts, large torn sheets of double nuclear membrane (NE), or small fragments or vesicles of nuclear membrane (probably a mixture of both INM and ONM.)

Thin sectioning has been employed for the study of NE for a longer period than negative staining. The conventional fixation and staining methods reveal the double membrane nature of nuclear ghost preparations and the presence of nuclear pore complexes [24,52]. The pore complexes result in two electron optical images, one which shows a coming together of the two nuclear membranes is produced by transverse sections through the membrane, and the other which shows the octagonal densely staining annulus and central granule is obtained by sections parallel to the membranes. Small membrane fragments and vesicle preparations can likewise be appraised by thin sectioning [51,53,56,62–66] but in these cases it is more difficult to assess the state of integrity of the nuclear pore complexes and the presence of both nuclear membranes. Some qualitative indication of the presence of chromatin on the inner surface of the INM is obtained by thin sectioning [24,54,67].

Freeze cleavage and etching have been applied extensively for the study of nuclei within cells [27–33,68–74] and for isolated nuclei [24]. The technique has not yet been widely applied to isolated NE preparations [29,62]. It is doubtful whether, to date, freeze-cleavage has revealed as much structural detail of the NE as thin sectioning and negative staining. It most certainly is of value for the study of the nuclear pore density in different tissues at different stages of the cell cycle and growth, and following the application of stimulatory or inhibitory reagents to cells [28,69].

In general, NE preparations to be acceptable must consist of the two nuclear membranes linked by pore complexes, the annular subunits and central granules of the latter being visible under appropriate conditions of negative or positive staining in the electron microscope. The degree of morphological integrity required as the criterion of a satisfactory envelope preparation remains a matter for the individual worker to decide.

A strong case can be made for demanding that nuclear ghosts or *intact envelopes* are the most desirable state in which the isolated material should be obtained. By analogy more has been learnt about the functional properties of the erythrocyte membrane from studies using resealed ghosts than from studies

with membrane fragments. Yet studies directed towards the biochemical composition of the erythrocyte membrane have made use ghosts and membrane fragments, the same situation apparently existing for studies with the NE.

The foregoing discussion has stressed the primacy of membrane integrity over purity. This would seem to be logically necessary in view of our present level of knowledge of the NE and appropriate in view of the comparative ease with which ultrastructural markers may be demonstrated in this system. Some discussion of purity, although an extremely difficult matter, is clearly relevant to the establishment of our criterion of a satisfactory NE preparation. Two possible sources of contamination will therefore be considered, the nucleoplasm and the cytoplasmic membrane systems.

(iii) Nuclear contamination

On the basis of the assumptions that most or all of the lipid of the cell nucleus is in the NE, and that none or only a small fraction of the DNA is so intimately associated with the INM or pore complex as to be regarded as a structural part of the NE, most workers in this field have sought to produce preparations in which density and DNA content are minimized, and lipid content high. Similar considerations do not apply to RNA since ribosomes are known to be associated with the ONM [7,34]. Some evidence has been presented which suggests that the ONM [75] and the nuclear pore complexes [76] may be rich in RNA.

It must be noted in this context that, while available evidence is consistent with the association of most of the nuclear lipid with the NE [36], the extent of intimate DNA association with the system remains in some doubt [57,62]. The report by Kashnig and Kasper [53] has claimed a DNA-free preparation. In our hands, however, this method has yielded material containing 0.5–1.0% by weight of DNA. It should be pointed out in this context that the diphenylamine assay procedure for DNA developed by Burton [77] and used by Kashnig and Kasper is less sensitive than the modification of this procedure by Giles and Myers [78] used by ourselves; the amount of DNA in the preparation of Kashnig and Kasper is certainly below the detection limits of the Burton method. Further discussion of the problem of whether or not DNA is to be considered as a contaminant or a structural component of the system will be given below.

(iv) Cytoplasmic contamination

The apparent continuity between the ONM and endoplasmic reticulum, by its very nature, constitutes an *a priori* problem of cytoplasmic contamination. Scanning electron microscopy (R. R. Kay personal communication) and freeze cleavage readily indicate that some membranous material often adheres to the surface of purified cell nuclei, which is less apparent by thin sectioning. It does not of course follow that any such contamination will remain attached to the NE throughout its subsequent purification. The problem of cytoplasmic

contamination is made more acute by the lack of a suitable microsomal marker enzyme. Until the extent of microsomal contamination can be reliably estimated, detailed studies on NE composition must be regarded as premature. Apparent similarity between NE and microsomal preparations in terms of protein components may indicate no more than heavy endoplasmic reticulum contamination of the preparation [56,62]. In practice, when intact ghosts and large sheets of NE are isolated, the presence of any membrane material which lacks nuclear pore complexes is readily revealed by negative staining. It is perhaps pertinent that small amounts of collagen can also be detected by this method.

5.1 5 General comments

To summarize the foregoing discussion the following steps are considered vital for the development of a satisfactory NE isolation procedure. (a) Cell nuclei should be obtained as free as possible from cytoplasmic contamination. (b) The nuclear contents (nucleoli, chromatin and dense lamina of heterochromatin) should be rendered soluble and thereby liberate the NE. (c) The required ultrastructural characteristics of the NE should be maintained (double membrane, pore complexes with intact annuli and central granules).

A parallel can be drawn between the release of haemoglobin from mammalian and avian erythrocyte ghosts by osmotic haemolysis [79–81] which leads to the production of haemoglobin-free erythrocyte ghosts, and procedures aimed at bringing about the release of chromatin from nuclei. This comparison suffers from the fundamental fallacy that chromatin, unlike haemoglobin, is not readily soluble under physiological or low ionic strength conditions. As will be seen from the experimental section, additional treatments have been devised to bring about the solubilization of chromatin and in doing so the situation with the lysed or disrupted nucleus may be considered at least partially analogous to the haemolysed erythrocyte.

Most studies on NE have been performed with mammalian liver, that of the laboratory rat being most commonly used, although pig, cattle and rabbit liver have been used in some cases. A small amount of work on the avian erythrocyte NE has been published [66,82]. These dormant nuclei have extremely condensed chromatin which in the experience of the authors is even more intractible than that of liver nuclei. For the sake of completeness it should be mentioned that a considerable amount of work has been done using the large amphibian oocyte NE which is isolated by micro-dissection [5,23,76,83].

5.2 A review of methodology

5.2.1 Isolation of nuclei

All procedures described for the isolation of NE have begun with the isolation of purified cell nuclei (with one exception [61], later modified [84] to include

initial purification of nuclei). Of all the methods available in the literature for nuclear isolation, only those which (a), make use of low shearing stresses during homogenization, ensuring a fairly high yield of unbroken nuclei and (b), utilize centrifugation through dense sucrose media (approx. 2.3 M specific gravity = 1.29) to separate nuclei from all other organelles are applicable. Thus a Dounce- or Potter-Elvehjen homogenizer is greatly preferable to a Waring blender for homogenizing tissue. The recently introduced blade homogenizers of the Polytron and Ultra Turrax type, which can be precisely controlled at low speeds have been found to be successful by the authors, and enable very large quantities of tissue to be rapidly processed. Ultrasonication has also been used to release avian erythrocyte nuclei from erythrocyte plasma membranes [81]. Detergent-containing and organic solvent systems which give highly purified nuclei clearly do so at the expense of the integrity of the NE and should therefore be avoided. Moreover, high ionic strength solution should not be used as these may remove the ONM [85] and undoubtedly disorganize and partially solubilize the chromatin [51,53,56,86]. As previously noted, low pH conditions also remove the ONM [36,75].

The pH of the medium used is most commonly in the range 7.0 to 7.5 [51–53,55,56,61,84] although pH values of about 6.0 have been used [54,57,59], since this minimizes the proteolytic activity associated with crude nuclear preparation [87]. It should, however, be noted that proteolytic activity is not detectable at any pH in nuclei once they have been purified by sedimentation through 2.3 M sucrose. To stabilize the chromatin a divalent cation (Mg^{2+} or Ca^{2+}) should be included in the medium at 1 mM to 3 mM concentration. The original dense sucrose method for isolating nuclei [88] did not use buffer or a divalent cation; subsequent modifications in which pH is controlled and magnesium or calcium is added have undoubtedly improved the yield, integrity, and probably purity, of the preparations.

Homogenization of the tissue in 2.3 M sucrose can lead to undesirable local heating effects, as a result of applying shearing stress to a highly viscous medium. Since maintenance of the temperature in the range 0 to 5°C throughout the procedure is essential, it has become customary to homogenize in dilute sucrose solutions (0.25 to 0.44 M), suitably buffered and containing divalent cations and then to prepare a crude 'nuclear pellet' fraction by centrifugation at 600–1000 x *g*. This nuclear pellet may then be purified further by resuspension in a concentrated sucrose solution (approx. 3.0 M) to give finally 2.3 M sucrose (60% w/w). The nuclei are then separated from all other less dense organelles by centrifugation at approximately 60 000 x *g* for 1 h.

A large number of methods for the isolation of nuclei are available in the literature, all essentially fulfilling the requirements discussed above. The reader not familiar with the field who wishes to consider the relative merits of the most widely used isolation procedures may be recommended to study the purity of the preparations obtained by Blobel and Potter [89], Widnell and Tata [90], Sporn *et al.* [91], Harris and Agutter [59] and Harris [25].

5.2.2 Purity of the isolated nuclei

During the course of isolation nuclei can be routinely examined by light microscopy using phase contrast or Nomarski interference optics and less routinely electron microscopy using thin sectioning or freeze cleavage, in order to obtain a qualitative assessment of purity. In general, mitochondria and other membranous contaminants are not found after pelleting through dense sucrose Visible contamination is normally restricted to small collagen fibres and occasional peroxisomes, which will usually be removed at a later stage if the NE is obtained by density gradient floatation. Glycogen granules can equally be eliminated by starvation of the animals for 16–24 h before sacrifice.

The absence of mitochondria can be confirmed by succinate dehydrogenase assay [49]. 5′-Nucleotidase [92] provides a suitable marker for plasma membrane contamination, and acid phosphatase [50] for lysosomes.

5.2.3 The disruption of nuclei

Isolation of the nuclear envelope is necessarily preceded by disruption of the nuclei; the object of this process is to disperse the nucleoplasm while controlling conditions so as to retain the envelope is a state of maximum integrity. The principle methods used for disruption are outlined below.

Perhaps the simplest approach, which unfortunately is not widely applicable is that of manually bursting and washing the ghosts of nuclei following microdissection. This technique has in fact only been successfully applied to the large nuclei of amphibian oocytes [1,2,5,23,76,83]. Extensive ultrastructural studies have been performed with material isolated in this way, together with microanalysis [83]. An alternative approach using mechanical stress is ultrasonication [54–57,93]. Ultrasonication ruptures the envelopes and under controlled conditions of pH, ionic strength and temperature liberates the envelope fragments from appended heterochromatin without destroying the ultrastructural integrity of the pore complexes.

Treatment of nuclei in low ionic strength solutions in the absence of divalent cations brings about a pronounced swelling due to the change in condensation state of the chromatin [94,95]. The importance of calcium and magnesium in maintaining the condensed state of chromatin [96,97] implies that chelating agents may help to disperse chromatin while leaving the NE intact. This effect may in part account for the chromatin dispersal achieved by Kashnig and Kasper [53] using a 10% w/v potassium citrate solution as well as the heparin treatment of Bornens [64]. In the hands of the authors, low ionic strength treatments in the absence of chelating agents generally lead to the production of an extremely gelatinous suspension of nuclei (see Fig. 5.3), from which the chromatin is escaping, and which can nevertheless be seen to resemble nuclear ghosts. In the procedure devised by Price *et al.* [61], in which the nuclei were not purified, the crude 1000 x *g* nuclear pellet in 1 mM $NaHCO_3$ (pH 7.2) being

used as the starting material for the rate zonal separation of nuclear ghosts the gelatinous state dispersed spontaneously during overnight storage at 4°C. This does not occur if purified nuclei that have become gelatinous and burst after washing in 1 mM $NaHCO_3$ are stored overnight. Dissolution of the gelatinous state can, however, be brought about by a brief treatment with DNAase I [84]. Recently, it has also been observed that when purified nuclei from rat liver are

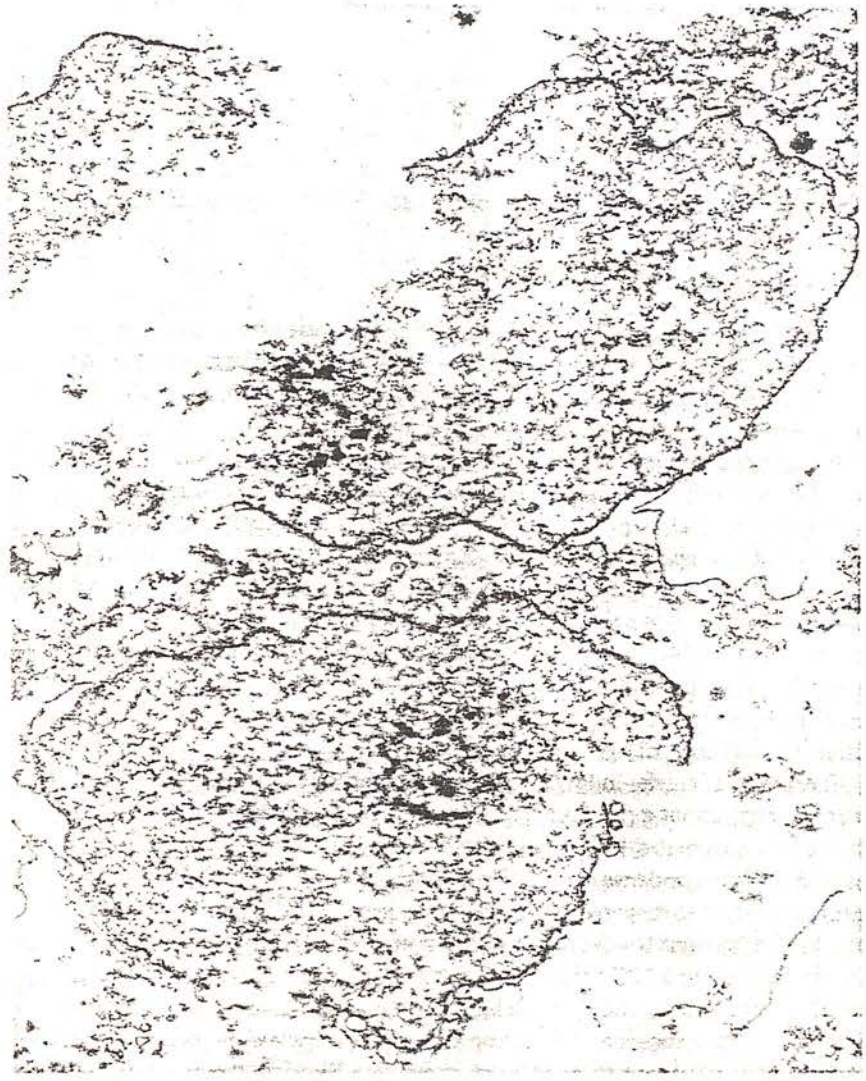

Fig. 5.3 Rat liver nuclei after washing two times in 1 mM sodium bicarbonate (pH 7.2). The nuclei have burst, thus allowing the chromatin and nucleoli to escape. The nuclear envelope does not break up significantly. (x10 000.)

stored overnight at 4°C in 0.25 M sucrose, 2 mM $MgCl_2$, 10 mM Tris HCl (pH 7 4), they will then burst and loose their contents without going through a gelatinous phase when washed in 1 mM $NaHCO_3$ solution (J. R. Harris unpublished observations). Nuclear envelopes (ghosts and large torn sheets) have been isolated by differential centrifugation followed by density gradient floatation of a purified membrane band by both the above procedures (see Section 5.4.3 below). The suggestion may be advanced that in both the method of Price *et al.* [61] and the overnight treatment of purified nuclei in isotonic sucrose containing magnesium chloride, spontaneous breakdown of chromatin occurs due to endogenous DNAase but it is difficult to understand why this should not occur with the purified nuclei after bursting in 1 mM $NaHCO_3$. One possibility is that such endogenous DNAase is Mg-dependent and the sodium bicarbonate treatment has removed much of the chromatin bound magnesium.

An alternative approach stems from the assumption that salt bridges constitute the most significant stabilizing force in chromatin, which suggests that dispersal of the nuclear contents will occur in high ionic strength media Solutions containing 1 mM NaCl [98], 1.5 M KCl [56], 10% tripotassium citrate [53], and 0.5 M magnesium chloride [51] have been employed to disperse nuclei. The nuclear contents are usually made labile either by DNAase treatment or ultrasonication prior to the addition of the high ionic strength medium. Magnesium chloride alone at a concentration of 0.3 M to 0.5 M has been used by Monneron and her co-workers [62] Despite claims that the envelope fragments obtained after such treatments are ultrastructurally acceptable, it is clear the potassium ions in the medium destroy pore complexes [54,57,62] under conditions of neutral pH. Moreover high ionic strength media may remove both lipid and protein components from other membrane systems [99], and possibly also from the NE. After isolation of nuclei in phosphate buffer at pH 6.1 [54,57], high ionic strength treatment was found to destroy the nuclear pore complexes; this apparently is not the case if nuclei are isolated at neutral pH [51,62].

At pH 8.6 nuclei destabilized by mild ultrasonication or DNAase treatment swell irreversibly and the bulk of their contents are solubilized. The explanation for this effect probably lies once again in the disruption of salt bridges stabilizing the chromatin. Kay *et al.* [52] found that after treatment at pH 8.6 almost intact nuclear envelopes could be isolated, which contained ultrastructurally intact pore complexes. Such procedures might, however, be expected to result once again in the loss of membrane components [100], and the departure from physiological pH may produce inactivation of some enzymes, in particular the envelope Mg-ATPase (Agutter, unpublished observations).

Destabilization of chromatin by DNAase, which enters the isolated nucleus readily [101], but which may not have access to the DNA within condensed chromatin or be able to free the envelope of appended heterochromatin, has been employed in combination with the above mentioned approaches. Berezney *et al.* [51] used overnight incubation of nuclei with DNAase at 4°C prior to

final dispersion of the nucleoplasm with 0.5 M magnesium chloride. Kay *et al.* [52] used DNAase at room temperature together with high pH disruption of the chromatin. Comparison of these two publications indicates that the nucleoplasm is very much more DNAase labile at room temperature (20°C) than at 4°C. Differences in enzyme activity alone do not wholly account for this observation; it is probable that the structure of chromatin differs sufficiently at the two temperatures and pH's to retard the digestion of DNA markedly under the conditions used by Berezney *et al.* [57]. The brief DNAase I treatment used by Harris and Milne [84], mentioned above in relation to the low ionic strength and magnesium-depleted conditions, may owe its success to the fact that the chromatin was considerably dispersed prior to the addition of DNAase due to washing in 1mM sodium bicarbonate solution, together with the fact that sufficient magnesium may remain bound to the chromatin to activate the exogenous enzyme.

Despite the success of DNAase treatment for the isolation of nuclear envelope, one report [57] suggests that this enzyme disrupts the nuclear pore complexes and that, concommitant with this disruption, collapse of the double-membrane structure into single-membrane vesicles occurs. Further investigation of this point suggests that the envelopes isolated from nuclei prepared in phosphate buffer at pH 6.0 have DNAase-labile pore complexes, while those from nuclei prepared in Tris buffer at pH 7.4 do not (c.f. ionic strength methods above). Again, alteration of the structure of the nuclear contents seems to be indicated; change of pH effects, presumably an irreversible structural change in the envelope and peripheral heterochromatin which could make the integrity of the nuclear pore complexes dependent on the presence of DNA.

From such observations it may be concluded that the environment of the nuclei during and after isolation has a marked effect on the structure of the nucleoplasm; some changes in this structure are apparently irreversible Such factors are of considerable importance in envelope isolation, since the structure of the nucleoplasm determines the ease with which it can be dispersed under any given conditions. Prior to any procedure for isolation of the nuclear envelope, particular attention must therefore be paid to the conditions under which the nuclei are prepared. Generally, it seems desirable to prepare nuclei in Tris buffer at pH 7.4 in the presence of 2 or 3 mM magnesium chloride, and to pass through the purification procedure as rapidly as possible to minimize degradation due to endogenous proteases in the homogenate and crude 1000 x *g* nuclear pellet

5.2.4 Isolation of the nuclear envelope from disrupted nuclei

Following the disruption of cell nuclei by the above methods, centrifugation procedures are employed to separate the NE from the solubilized chromatin. Differential centrifugation has been employed by several workers [51,52,98], and also used in conjunction with density gradient centrifugation [25,84].

Repeated differential centrifugal washes can be given rapidly, which may be of advantage for enzymological investigations [52]. A major disadvantage is that trace contaminants (e.g. collagen and nucleoli) may be repeatedly packed along with the NE material, which is likely itself to become increasingly fragmented during the successive pelleting and resuspension treatments that are applied to liberate chromatin. Measurements of floatation density naturally require additional gradient centrifugation, usually in sucrose.

It is the opinion of the authors that the use of sucrose density gradient centrifugation following a series of differential centrifugal washes is likely to result in the production of NE of the greatest purity, since contaminants such as other membrane species, collagen and nucleoli as well as residual chromatin are unlikely to band at the same position as the NE on a gradient. This does of course depend on the absence of binding between NE and such contaminants. Nevertheless if one was satisfied that the nuclei used were of maximum possible purity and the disruptive treatment produced complete solubilization of the nucleoplasm, including the heterochromatin of the internal dense lamina then, in theory, repeated differential centrifugation might result in a final membraneous material not markedly more contaminated than that obtained by density gradient centrifugation; unfortunately, in practice these conditions cannot be achieved. In fact Zbarsky *et al.* [55] claimed that repeated isopycnic banding in density gradients was necessary to yield a satisfactory pure NE preparation.

The recent availability of zonal centrifugation rotors has enabled larger quantities of tissue to be processed for the isolation of cellular organelles than is possible with conventional fixed angle and swing out rotors. In addition a superior purification is generally achieved. Low speed rate zonal centrifugation can be considered roughly equivalent to differential centrifugation for purposes of the present discussion. Price *et al.* [61,102] employed this technique using the M.S.E. A–XII Zonal rotor to separate nuclear ghosts from the 1000 x g nuclear pellet of rat liver and hepatoma homogenized in 1 mM sodium bicarbonate (pH 7.2) and kept overnight at 4°C. Contamination of the nuclear ghosts with large sheets of plasma membrane (of equivalent sedimentation coefficient to the nuclear ghosts) necessitated a further isopycnic zonal centrifugation in a high speed B–XIV Zonal rotor, or alternatively in a swing out bucket rotor. In the former instance it was not necessary to pellet the nuclear ghosts taken from the initial rate zonal separation since a large sample volume can be applied on top of a sucrose gradient in the B Zonal rotor. The differing flotation densities of NE and plasma membrane enable a purification of intact nuclear ghosts to be achieved. One major drawback of the use of zonal rotors is the time required in setting up the gradients together with the dismantling and cleaning of the rotors and accessory equipment following each run. Nevertheless, if as suggested above, superior purification and increased quantities if intact nuclear ghosts can be obtained and repeated pelleting avoided, then the use of zonal rotors is amply justified.

5.2.5 Composition of the isolated nuclear envelope

Marked differences in the ultrastructure, chemical composition and enzyme content have been found in the NE material obtained by the various published methods. A comparison of these variables is given in Tables 5.1, 5.2 and 5.3. As indicated previously, most of the procedures described have been established for mammalian liver. Studies have been performed on other tissues, e.g. Ehrlich ascites [55], chicken erythrocyte [67,82,103], calf thymus [66,104] and pea seedlings [54], but in general it is apparent that any one procedure is unlikely to be directly transferable to another tissue without some modification. The results tabulated have been taken only from studies on mammalian liver.

With reference to Table 5.1, protein has been estimated by the method of Lowry *et al.* [105] and DNA by the Burton procedure [77] usually in the modification by Giles and Myers [78]. Using mouse liver, NE prepared by the method of Agutter [57], it has been found that the ratio of satellite DNA to main band DNA in the envelope does not differ significantly from that found in whole nuclei (Agutter, unpublished observations). This suggests that the DNA associated with the NE is a random fraction of total nuclear DNA [57], although the studies of Franke *et al.* [106] have suggested a moderate enrichment of satellite DNA. The RNA present in most NE preparations is possibly, in view of the ribosomes universally found on the ONM, an rRNA fraction. The low RNA content of the NE reported by some authors [55,56,62] may suggest that some or most of these ribosomes have been removed during their isolation procedures.

Detailed studies of the protein [56,62,65] and lipid [107,108] contents of the NE have suggested that it differs from rough endoplasmic reticulum, but that the lipid content correlates well with that of whole nuclei. This latter observation is consistent with the assumption that all the nuclear lipid is associated with the NE, and therefore supports the use of phospholipid recovery from the nuclei as a measure of yield of envelope material.

The flotation densities of the various NE preparations range from 1.16 to 1.21 (Table I). Most values have been obtained in sucrose but determination in sorbitol have produced very much higher figures [54,57]. The range of values undoubtedly emphasizes the varied separation of INM and ONM and integrity of the nuclear pore complexes, together with nucleic acid content. At the moment it must be stated that no absolute figure for the density of NE can be given although the authors have reproducibly obtained the value of 1.21.

All attempts to produce NE have been accompanied by electron microscopic studies, by which means the integrity of the material, as well as the contamination with other organelles, can be qualitatively assessed. In Table 5.2 the ultrastructure of various NE preparations have been categorized in terms of the presence of double or single nuclear membranes, intact ghosts, large and small sheets, and vesicles. Also indicated is the integrity of the nuclear pore complex and the presence or absence of the central granule. Most investigators

TABLE 5.1
Nuclear envelope composition

Tissue used	Percentage by weight: Protein	Lipid: Phospholipid	Lipid: Neutral lipid	DNA	RNA	Density g ml^{-1}	Remarks	References
Bovine liver	75	14	–	0.9	8.9	–	No density gradient used	[51, 102]
Rat liver	62–70	25–33	–	3.5–4.0	3.5–4.0	–	No density gradient used	[52, 113]
Rat liver	59	29	6	0.0	3.1	1.16–1.18	Light band	[53, 65]
Rat liver	62	24	4	0.0	6.1	1.18–1.20	Heavy band	[53, 65]
Rat liver	24–27	21–35	7–15	0.2	2.1	1.16	Light band	[55]
Rat liver	46–48	21–35	7–15	1.3	3.3	1.19	Heavy band	[55]
Pea seedlings	78	4.6	4.0	2.9	7.2	1.24	Gradient in sorbitol	[54]
Pig liver	75	16–18	3	1–2	2.5–3.5	1.21	–	[56, 108]
Rat liver	75	16–18	3	1–2	2.5–3.5	1.21	–	[56, 108]
Rat liver	64	16	7	8	5	1.27	Gradient in sorbitol	[57]
Rat liver	73	23	–	0.6	3	1.17–1.18	–	[62, 104]
Rat liver	75–80	12–19	–	3–4	3–4	1.21	without DNAase*	[25, 61, 84]
Rat liver	75	15	–	3	7	1.21	with DNAase*	[25, 61, 84]

*Figures not previously published.

TABLE 5.2
Yield and ultrastructure of nuclear envelope preparations

Yield (as % of phospholipid	Predominant state of envelope	Recovery of pore complexes		Chromatin contamination	References
		Annulus	Central tubule		
–	Single-membrane vesicles	Trace	None	Very low	[51, 107]
55	Intact double-membrane sheets; nuclear ghosts	Complete	Present	Low	[52, 113]
–	Vesicles; some separation of INM and ONM	Trace	None	Negligible	[53, 65]
13	Envelope fragments	Apparently complete	Present	Extensive	[54]
Very low	Envelope fragments (sheets)	Complete	–	Some	[55]
	Vesicles; separation of INM and ONM	Some	Trace	Low	[56, 108]
50	Envelope fragments (sheets)	Complete	Present	Some	[57]
55–60	Large vesicles; a little separation of INM and ONM	Complete on larger vesicles	Some present	Very low	[62, 104]
12–15	Nuclear ghosts; some envelope fragments	Complete	Present	Low	[25, 61, 84]

have employed both thin sectioning and negative staining to study their NE material [51–57,59–64]. It is considered desirable to detect the presence of both ONM and INM using thin sectioning, although with intact nuclear ghosts negative staining will provide this information [24,25]. Freeze cleavage, which has been applied extensively to intact nuclei has been used by Monneron and her colleagues to assess isolated NE, but it must be admitted that this technique does not provide additional knowledge on either contamination or ultrastructural integrity. It is the opinion of the authors that negative staining with ammonium molybdate reveals the greatest ultrastructural detail within the NE [24,25,59,61].

In Table 5.3, Mg-ATPase, glucose-6-phosphatase, acid and alkaline phosphatase are expressed as μmol Pi released h^{-1} mg^{-1} protein, and NADH, NADPH and glutamate dehydrogenase activities in μmoles of substrate used or product formed h^{-1} mg^{-1} protein. The significance of the presence of most of these enzymes, and many others [6], in the NE is not clear. The basal Mg-ATPase, for example, is not stimulated by the presence of sodium and potassium [55,56,67], and its role in the NE is unknown at this time Discrepancies between certain preparation with regard to Mg-ATPase and glucose-6-phosphatase activity merit further investigation, as does the report by Gorkin [58] that mono-amine oxidase is present in the NE.

5.2.6 Subfractionation of the nuclear envelope

If we accept the evidence that the ONM and INM are dissimilar in composition and possibly function, and that the nuclear pore complex is a distinct and universally found morphological structure which may in fact be considered as a separate organelle [20], there is obvious interest in the possibility of obtaining each of these component parts of the NE as separate entities. This may be achieved either from intact nuclei, or better to avoid nucleoplasmic contamination, from the isolated and purified NE. Zbarsky *et al.* [55] have reported that the ONM and INM can be separated, but details of the method are not yet available. Mizuno *et al.* [63] claimed to be able to isolate the INM, but their criterion of assessment was simply the absence of ribosomes. To the authors' knowledge at the time of writing, there have been no reports of isolation of the pore complex, though the fact that this structure becomes detached from the surrounding NE during certain negative staining procedures [25,109], suggests that isolation is in principle possible.

The major problem to separation of the two membrane leaflets of the NE lies in the difficulty of finding adequate markers (e.g ultrastructural, enzymic and varying flotation density) for these membranes and of assessing cross contamination. This is illustrated in the isolation of an ONM fraction by Busch and his co-workers [75]. The method, based on the finding [36] that citric acid removed the ONM, was applied to whole nuclei obtained by centrifugation of a tissue homogenate through dense sucrose. The objections to such a procedure, if

TABLE 5.3
Enzymes of the nuclear envelope

Fraction	Mg-ATPase[a]	Glucose-6 phospha-tase[a]	Alkaline phospha-tase[a]	Acid phospha-tase[a]	NADH-cyto-chrome *c* reductase[b]	NADPH-cyto-chrome *c* reductase[b]	Glutamate dehydro-genase[b]	Cyto-chrome b_5[c]	Cyto-chrome *P*-450[c]	References
–	6.8	7.0	–	–	49	0.3	–	0.40	0.06	[51, 107]
Heavy	2.3	20.9	–	–	22.3	6.1	–	0.18	0.00	[53]
Light	1.7	15.0	–	–	22.4	6.1	–	0.18	0.22	[53]
–	0.67	0.52	–	–	–	–	–	–	–	[54]
Heavy	13.7	0.16	–	–	5.5	0.6	1.8	–	–	[55]
Light	23.1	0.0	–	–	1.0	0.2	3.0	–	–	[55]
–	5.5–6.8	0.1	1–3	3.1–9.8	5.8	1.2	1.8	0.03	0.03	[56]
–	0.1	–	–	–	10.0	–	–	–	–	[67]
–	–	8.5–11	–	–	12–18	3.0	–	–	–	[52, 113]

[a] μmol phosphate h^{-1} mg^{-1} protein

[b] μmol NAD(P) oxidized or reduced h^{-1} mg^{-1} protein

[c] nmol mg^{-1} protein

the aim is to obtain an acceptable membrane preparation, are several. Firstly, low pH media are known to solubilize several membrane proteins [110,111]. Secondly, contaminants may be removed from the INM and nucleoplasm by the citric acid treatment and readsorbed onto the ONM. Thirdly, since only small membrane vesicles are recovered, it is not certain that the material isolated represent the whole of the ONM or only a specific fraction. Finally, the treatment may well inactivate several enzymes intrinsic to the membrane, for instance glucose-6-phosphatase is known to be inactivated at pH's of less than 5.5 [112].

It is unlikely that any procedure for subfractionation of the NE will meet with widespread acceptance until it uses as starting material an acceptable NE preparation, as previously defined. In addition satisfactory markers for the various fractions must be established and the conditions employed must be mild enough not to inactivate membrane bound enzymes irreversibly or remove components of the individual fractions.

5.3 General discussion

If we accept that the definition of an isolated cell membrane preparation must in some sense be operational, not being guided by such criteria as 'chemical purity', it is very difficult to defend the claim that any membrane isolation procedure is ever wholly satisfactory. Nevertheless, in the case of resealed erythrocyte ghosts and certain mitochondrial preparation, the impressive retention of functional integrity argues for acceptability of the methods involved, even though the detailed composition of the material may not be entirely reproducible. In the case of the isolated NE, claims of functional integrity cannot yet be made and the criterion of ultrastructural acceptability is bound to be subjective and may not satisfy the requirements for all investigations of the system.

The three methods described in detail below were chosen because they appear to be essentially satisfactory within the limitations of current understanding and present day research, and because they entail the use of more or less widely differing ionic conditions. Other methods to which reference has been made in earlier sections, are not necessarily to be dismissed. Nuclear membrane material essentially free from DNA [53], NE fragments still bearing appended DNA [54,57], and the other varieties of preparation which can be obtained from published methods, will certainly find a place in future research on the system. Low-DNA preparations, for example may be useful for studies on the protein components of the NE, since nucleic acids interfere with certain common protein fractionation techniques (e.g exclusion chromatography on Sephadex gel). High-DNA preparations may likewise be useful for investigations on the interrelations between NE and the chromatin.

Some attention must be paid to the difficulties inherent in procedures for isolating the NE. The affinity of DNA for membranes must be accepted as the most difficult problem in the present context. Any membrane that is isolated in

the presence of DNA is liable to be contaminated by this substance, and the problem is particularly severe with the NE since organized heterochromatin is, in the interphase nucleus *in vivo*, contiguous with the INM in the form of the internal dense lamina. It is not clear, however, that the DNA content of isolated NE preparations is necessarily artifactual, or at least wholly artifactual. Dependence of the morphological integrity of the isolated NE on the presence of DNA [57] is found only under specific isolation conditions, but nonetheless DNA may be a genuine component of the NE *in vivo,* and the point remains as yet unsettled. An analogy may be drawn between the involvement of haemoglobin in the structure of the erythrocyte membrane, which likewise remained a matter of controversy for many years [25,116].

The question of the continuity of the ONM with the endoplasmic reticulum also remains as a major stumbling block. It is difficult to claim that any preparation of nuclei, and hence of NE, is wholly free of endoplasmic reticulum Such contamination would be undesirable even if the reticulum and the ONM were of the same composition, a position which is not easy to defend. Perhaps some improved microsomal enzymic marker or an increased use of freeze-cleavage electron microscopy to assess the extent of the endoplasmic reticulum contamination in a nuclear preparation, would assist in overcoming this problem.

The lability of the nuclear pore complex is also a fundamental problem. Excessive mechanical stress as produced by ultrasonication for example, extremes of pH and high ionic strength media, particularly if they contain potassium ions [57], are among the conditions which lead to loss of pore complex. The central granule and the annular subunits tend to disappear and, at best, only the remnant of the pore annulus is retained. Conditions of isolation must, therefore, be carefully defined with respect to pH, ion content and temperature of each medium used, as well as the time of exposure to each medium and the mechanical or other disruption conditions employed, for a completely satisfactory and reproducible NE preparation with stable pore complexes to be obtained. In the three techniques described in detail satisfactory pore complexes have been shown to persist in the final material. Complete loss of pore complexes is usually associated with collapse of the NE into double- or single-membrane vesicles. On the other hand if the pore complexes are present, intact ghosts, large torn sheets and large vesicles may be expected. The undesirable tendency of the membrane system to undergo vesicularization presents the possibility of contamination of the isolated material by foreign soluble proteins and nucleic acids trapped within the vesicles themselves.

In conclusion it must be re-emphasized that studies on the NE are still at an early stage and that considerable methodolgical developments may be expected which should provide a more satisfactory standard isolation and purification procedure. Once this is achieved the results obtained from the various approaches employed for the study of NE (e.g. electron microscopy, chemical

and enzymic analysis, gel electrophoresis) will, hopefully, become more widely uniform and therefore scientifically more acceptable. Extending from the availability of an acceptable NE preparation considerable progress can be expected on the subfractionation of the NE, which in turn should provide some insight into the macromolecular organization of this extremely complex membrane system.

5.4 Experimental procedures for the isolation of the nuclear envelope (NE)

5.4.1 The DNAase/high pH treatment of Kay et al. [52,113]

(i) Procedure

Nuclei are isolated from mouse or rat livers by the method of Widnell and Tata [90]. The nuclei from about 4 g liver are suspended in 1 ml 0.1 mM $MgCl_2$, and freshly dissolved DNAase I (Sigma, electrophoretically pure) is added to give a final concentration of 5 $\mu g\ ml^{-1}$. Four volumes of 10 mM Tris-HCl (pH 8.5), 0.1 mM $MgCl_2$, 5 mM 2-mercaptoethanol, 10% w/v sucrose are added immediately and the suspension mixed and allowed to incubate at room temperature (22°C) for 15 min. This first digestion is terminated by the addition of an equal volume of ice-cold water and a crude nuclear envelope fraction obtained as a pellet by centrifuging at 38 000 x *g* for 15 min. The pellet is resuspended in 5 volumes of the previous digestion buffer, but at pH 7.4, and DNAase added to a concentration of 1 $\mu g\ ml^{-1}$. After incubation at 22°C for 20 min the digestion is terminated as before and purified nuclear envelope pelleted.

(ii) Discussion

The most striking advantages of this procedure are its rapidity (approximately 80 min starting with washed nuclei) and the well preserved ultrastructure of the final NE material which is in the form of ghosts and large sheets (see Figs 5.4 and 5.5). One disadvantage must be the very small yield of material from only 4 g liver. The method may well prove to be very useful for ultrastructural studies and some enzymic investigations. The primary interest of Kay *et al.* was in the DNA polymerase activity associated with the NE, and they claimed that about 1% of the total nuclear DNA polymerase was recovered in the envelope. While so low a yield of the enzyme may not appear significant, it should be noted that an unusually high proportion of the DNA associated with this NE preparation is late replicating. The unusually high glucose-6-phosphatase and NADH oxidase activities (cf. Table 5.3) in the NE may possibly be attributed to the rapidity with which it is obtained and the relative mildness of the procedure, these enzymes being somewhat unstable.

The significance of the inclusion of 2-mercaptoethanol in the digestion

Fig. 5.4 A rat liver nuclear envelope isolated by the method of Kay *et al.* Negatively stained with 2% ammonium molybdate (pH 7.0). (×15 000.)

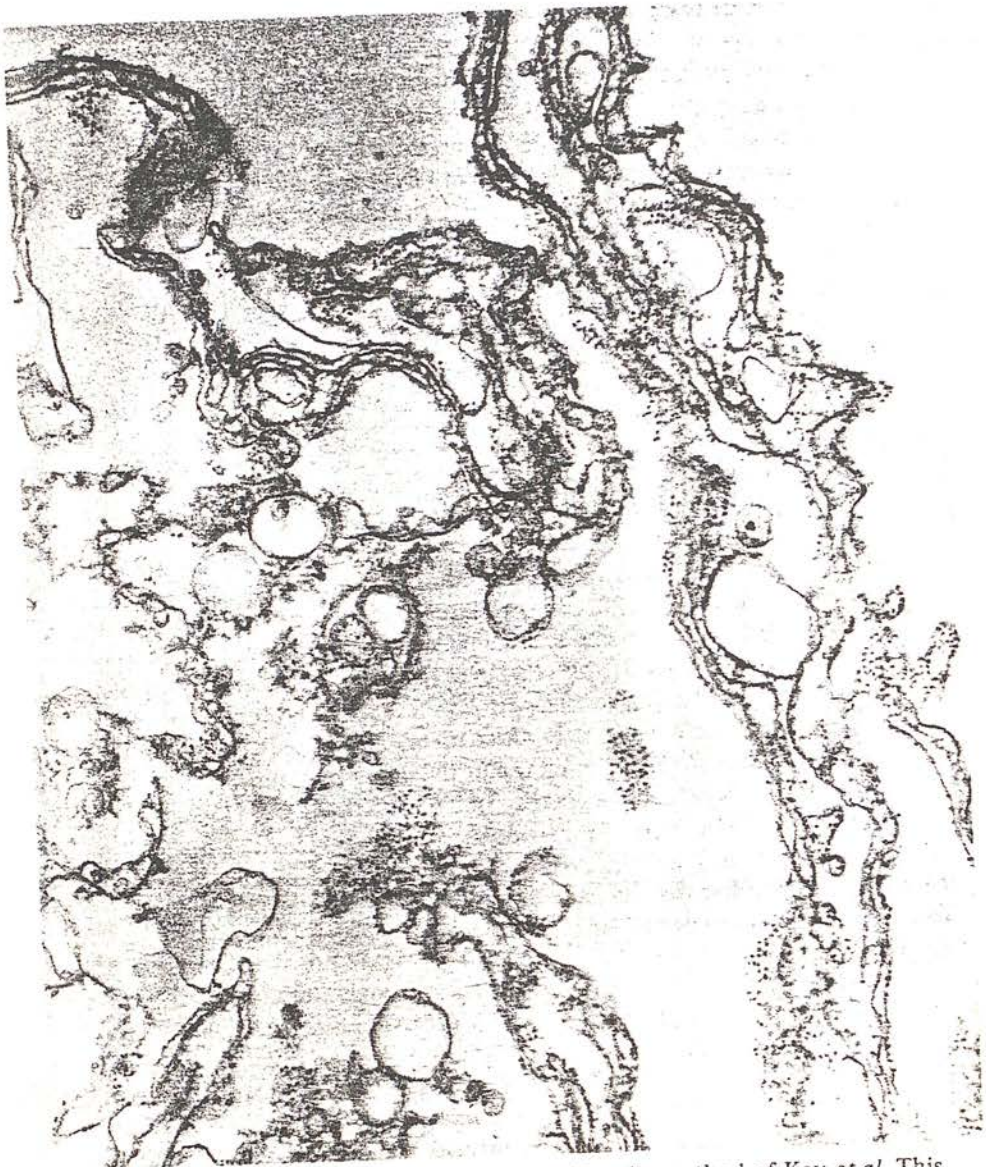

Fig. 5.5 Rat liver nuclear envelope isolated by the method of Kay *et al.* This thin sectional field shows clearly the presence of ribosome particles, but there appears to be considerable separation of the INM and ONM. (x35 000.)

medium is puzzling. The morphology of the isolated nuclear envelope may be improved, but the authors have not found its inclusion to be necessary (see below). 2-mercaptoethanol may interfere with the activity of enzymes which contain disulphide bridges, the presence of which is essential for their activity although it will prevent oxidation of essential sulphydryl groups. Further data on the enzymology in this connection is obviously required. The high pH of the initial DNAase digestion (pH 8.5) could interfere with enzyme activities and, at the molecular level with the structural organisation of the NE. The DNAase treatment renders the quoted DNA content (Table 5.1) somewhat dubious since this value would presumably vary with the length of time of the incubation.

5.4.2 *The high concentration magnesium treatment of Monneron et al.* [62, 104]

(i) Procedure

Nuclei isolated from rat liver homogenates by the method of Blobel and Potter [89] are resuspended to a final concentration of about 30 A_{260} units ml^{-1} in ice-cold 0.05 M Tris-HCl, 0.025 M KCl, 5 mM $MgCl_2$, 0.25 M sucrose (pH 7.5, adjusted at 20°C). 5 ml aliquots of this suspension are centrifuged at 1000 x *g* for 5 min and the pellets resuspended in 1.8 ml ice-cold 0.05 M Tris-HCl, 0.5 M $MgCl_2$, 1.8 M sucrose (pH 7.5). To ensure homogeneous resuspension the pellet is first stirred with 2 or 3 drops of glycerol. The suspension is then mixed 'vigorously' three times, centrifuged at 1000 x *g* for five minutes, and the foamy layer on top of the liquid removed. A linear 20% (w/v) to 55% (w/v) sucrose gradient in 0.05 M Tris-HCl, 0.5 M $MgCl_2$ (pH 7.5) is generated on top of the suspension and the gradient centrifuged at 190 000 x *g* (ave) for 2 h. Nuclear envelope material floats up during this centrifugation and forms a band at a density of approximately 1.179 g ml^{-1}, (see Fig. 5.6). The appearance of the material in the electron microscope is shown in Fig. 5.7.

(ii) Discussion

Monneron and her colleagues indicate that solutions containing high concentrations of mono and divalent metal salts such as KCl, $CaCl_2$, $MgCl_2$ and $MnCl_2$ can be used for the complete dispersal and subfractionation of nuclei. Their NE isolation procedure is best viewed, therefore in the context of total nuclear fractionation The recovery of pore complexes is more convincing than in the closely comparable method of Berezney, Funk and Crane [51], the DNA content is very low (around 0.6%), and the recovery of NE is acceptably high

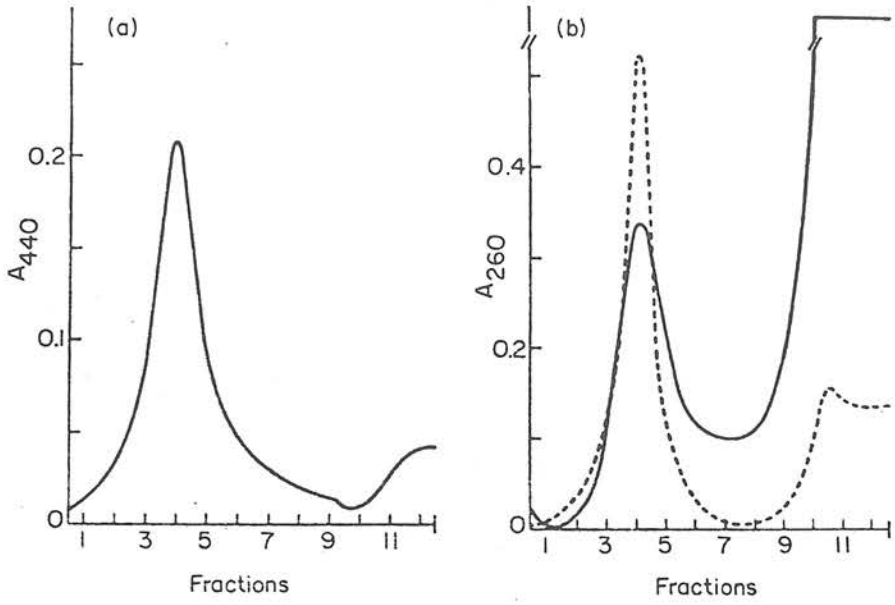

Fig. 5.6 Sucrose gradient analysis of rat liver nuclei treated with 0.5 M $MgCl_2$. Recording was at 440 nm (a) or 260 nm (b). Dotted line represents absorbancy profile at 260 nm of a membrane band collected from gradient, pelleted, and refloated on a sucrose gradient.

(55–60%). As yet, nothing has been reported about the enzyme content of this material, though the preparation time of 3 hours from isolated nuclei and the high ionic strength $MgCl_2$ treatment suggest that any glucose-6-phosphatase and DNA polymerase activities are likely to be lost [52].

Certain features of the procedure indicate that it may be made more generally useful by further modification. Firstly, the NE density varies slightly as the magnesium chloride concentration is varied. (0.3 M $MgCl_2$ gives NE of density 1.169 and 0.7 M gives density 1.184 g ml^{-1}) suggesting that the composition of the envelope material is varying. Secondly, the NE vesicles and sheets produced are of varying size and there appears to be considerable separation of the INM and ONM. In addition, the nuclear pore complexes appear to be at least partially disrupted, as judged by their irregular shapes and lack of central granules in the published electron micrographs.

The destructive effect of high potassium concentration on NE material [54,57,62] is avoided here, and evidence is offered from SDS-polyacrylamide gel electrophoresis that the composition of rough endoplasmic reticulum is very different from that of the NE, in agreement with Bornens and Kasper [65]. Simple treatments such as the one developed by Monneron *et al.* which provide ultrastructurally acceptable envelope fragments with very low DNA content, will probably prove most useful for further

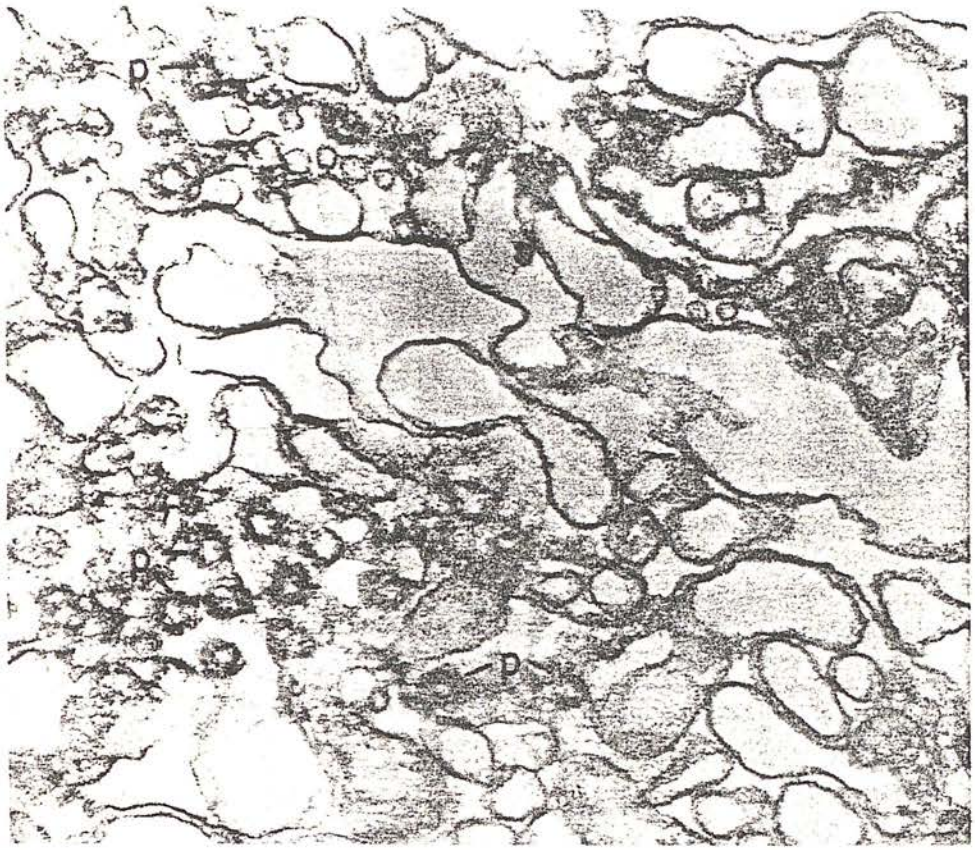

Fig. 5.7 Nuclear envelope material isolated by the method of Monneron *et al.* Recognizable nuclear pore complexes (p) can be seen on many grazing sections of membrane vesicles. There appears to be extensive separation of the two nuclear membranes. (x72 000.)

investigation of the protein components of the NE, since the presence of a significant quantity of DNA renders many techniques of protein fractionation impracticable through its tendency to cause aggregation.

5.4.3 The low ionic strength treatment of Harris et al.[25,61,84)

In its initial form. the low ionic strength treatment developed by Price Harris and Baldwin [61] for the isolation of nuclear ghosts from rat liver and hepatoma is at considerable variance to all other published procedures Firstly, it employs rate zonal centrifugation and isopycnic zonal centrifugation. Secondly, these centrifugation techniques are not applied to purified cell nuclei, but to the

crude 1000 x *g* nuclear pellet obtained following homogenization in 1 mM sodium bicarbonate (pH 7.2) and overnight incubation at 4°C.

Because of the fact that zonal centrifugation facilities are still not widely available, the technique has recently been modified for use with purified rat liver nuclei and conventional centrifuge rotors [84]. It is this latter modification which will be presented below, but discussion will also be made of the original method.

(i) Procedure

The livers from six starved rats are homogenized in cold 0.25 M sucrose, 2 mM $MgCl_2$, 10 mM Tris-HCl (pH 7.4) using an Ultra Turrax type TP18/2 blade homogenizer. The 1000 x *g* nuclear pellet is prepared and resuspended in saturated sucrose to give a concentration of of 2.2 M (59% w/v) with respect to sucrose. The nuclei are then pelleted at 100 000 x *g* for 2 h and then washed two times at 1000 x *g* with the homogenizing buffer.

The purified nuclei are then resuspended in 40 ml 1 mM sodium bicarbonate solution (pH 7.2) by shaking and allowed to equilibrate for 5 min before centrifuging at 31 000 x *g* for 5 min. The pellet of slightly swollen nuclei is again resuspended in 1 mM sodium bicarbonate by gentle syringing through a large diameter needle and after a further period of 5 minutes incubation is recentrifuged as above. A very gelatinous pellet is obtained which cannot be dispersed by further centrifugal washing in 1 mM sodium bicarbonate. Incubation with DNAase 1 (Sigma type DN–100) for 15–20 min at room temperature (22°C) at a concentration of 10 $\mu g\ ml^{-1}$ will however readily disperse the gelatinous suspension of bursting nuclei. Thus during this brief incubation the DNA, which is dispersed and readily available for enzymic degradation, is solubilized, thereby allowing the NE to become freely suspended and therefore separable from the chromatin. It may be noted that the conditions under which the incubation is performed are less than optimal for maximum DNAase activity, which requires the presence of 5 mM $MgCl_2$.

The NE's are then repeatedly washed in 1 mM sodium bicarbonate with centrifugation at 31 000 x *g* for 5 min. The release of chromatin throughout this sequence of washes is shown in Fig. 5.8, which clearly shows the large percentage release of chromatin following the DNAase 1 treatment. The partially purified NE obtained from the final differential centrifugal wash is resuspended in 2 ml 10 mM Tris-HCl (pH 7 4) and is centrifuged for 5 min at 500 x *g* to remove any aggregates. The small discoloured pellet is discarded and the white membrane rich supernatant layered over a discontinuous sucrose gradient made up of 10 ml 2.0 M sucrose, 10 ml 1.8 M sucrose, 10 ml 1.5 M sucrose and 6 ml 0.25 M sucrose (all solutions made up in 10 M Tris-HCl, pH 7.4). The gradient is then centrifuged at 100 000 x *g* for 90 min. A major band of purified NE forms at the 1.5 M/1.8 M interface, as shown in Fig 5.9. Prolonged centrifugation does not alter the position of the membrane band and

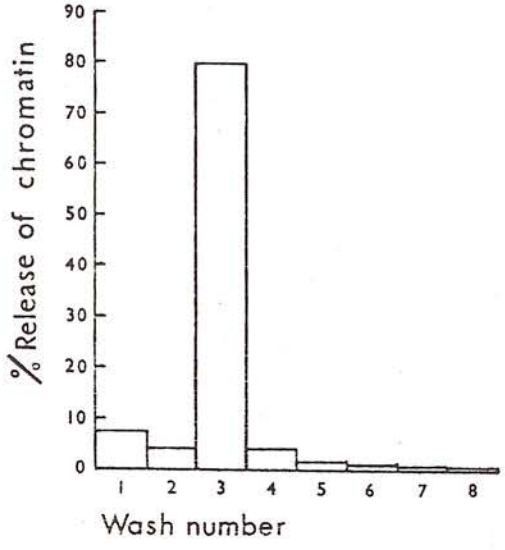

Fig. 5.8 The release of solubilized chromatin (estimated by the absorbance of the 31 000 x g supernatants at 260 nm) throughout the 1 mM sodium bicarbonate (pH 7.2) washing and DNAase I incubation sequence employed for the preliminary separation of rat liver NE from chromatin. The histogram is the mean of three experiments. Note the large percentage release of chromatin following the DNAase I treatment (wash number 3).

isopycnic centrifugation on a continuous sucrose gradient for 20 h at 100 000 x *g* likewise gives a single membrane band of flotation density 1.21 ± 0.01, in agreement with the value obtained by zonal centrifugation method [61]. Fig. 5.10 summarizes the various steps in the above procedure.

Phase contrast examination of the final material reveals a free suspension of nuclear ghosts and large torn sheets of NE, as shown in Fig 5.11. This assessment is supported by electron microscopy using thin sectioning and negative staining after removal of the sucrose by differential centrifugal washing with 10 mM Tris-HCl (pH 7.4) (see Figs. 5.12–5.15).

(ii) Discussion

The underlying premise of the low ionic strength treatment presented above is that in the absence of divalent cations, nuclei will swell and burst thus

Fig. 5.9 The purification of rat liver NE by centrifugation on a discontinuous sucrose gradient. (a) The appearance of a gradient after centrifugation at 100 000 x *g* for 90 min. (b) The absorbance profile of the gradient obtained by passing the tube contents through an LKB UV analyser. The main band of membrane material is located at the 1.5 M/ 1.8 M interface.

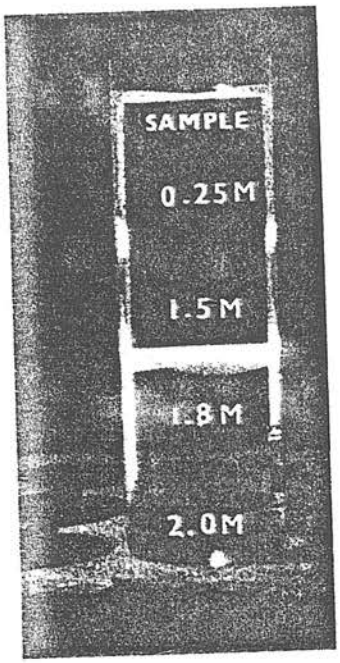
SAMPLE
0.25M
1.5M
1.8M
2.0M

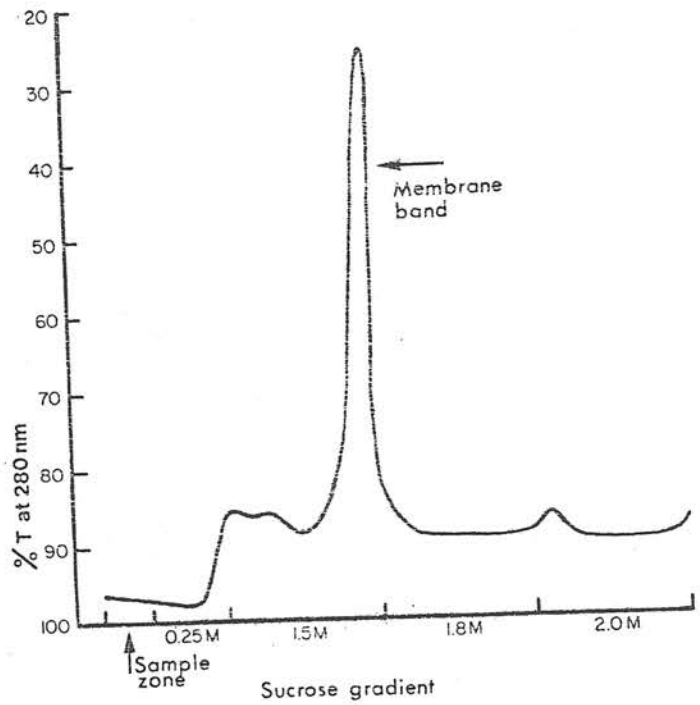
20
30
40
50
60
70
80
90
100
% T at 280 nm
Membrane band
0.25M
1.5M
1.8M
2.0M
Sample zone
Sucrose gradient

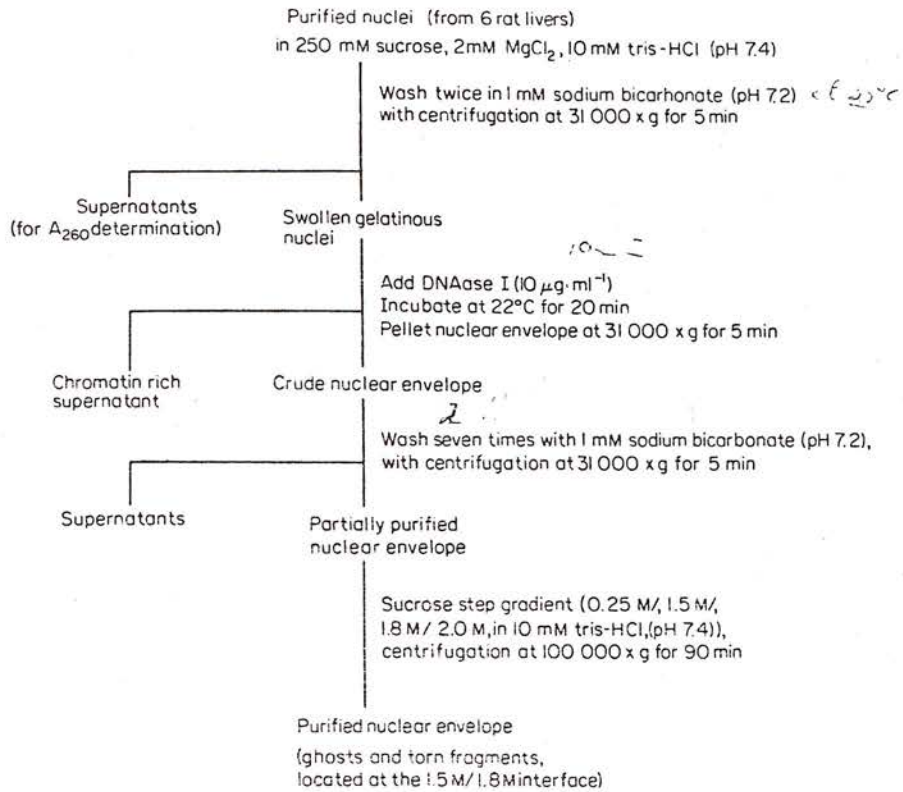

Fig. 5.10 The isolation and purification of rat liver nuclear envelope.

presenting the possibility of isolating relatively intact nuclear ghosts. The studies of Olins and Olins [95] have underlined the changes in the condensation state of the chromatin that can be brought about in rat liver and chicken erythrocyte nuclei by varying the pH, total ionic strength and magnesium concentration and are in general agreement with the concepts presented here. The zonal centrifugation procedure [61], which itself extended from the 1 mM sodium bicarbonate procedure of Neville [114] for the isolation of rat liver plasma membrane, has the considerable advantage that repeated centrifugal packing of the NE material throughout the various steps of the procedure is reduced to a minimum. The disadvantage of the zonal procedure is that it is time-consuming and uses much larger quantities of gradient materials than are required in the variant presented above. Nevertheless, for those with zonal centrifugation facilities available, it is suggested that considerable advantages may possibly be gained as much larger quantities of material can be processed and purified. The authors therefore propose in the future to incorporate the use of zonal centrifugation into the method presented here, in the hope of being able to scale

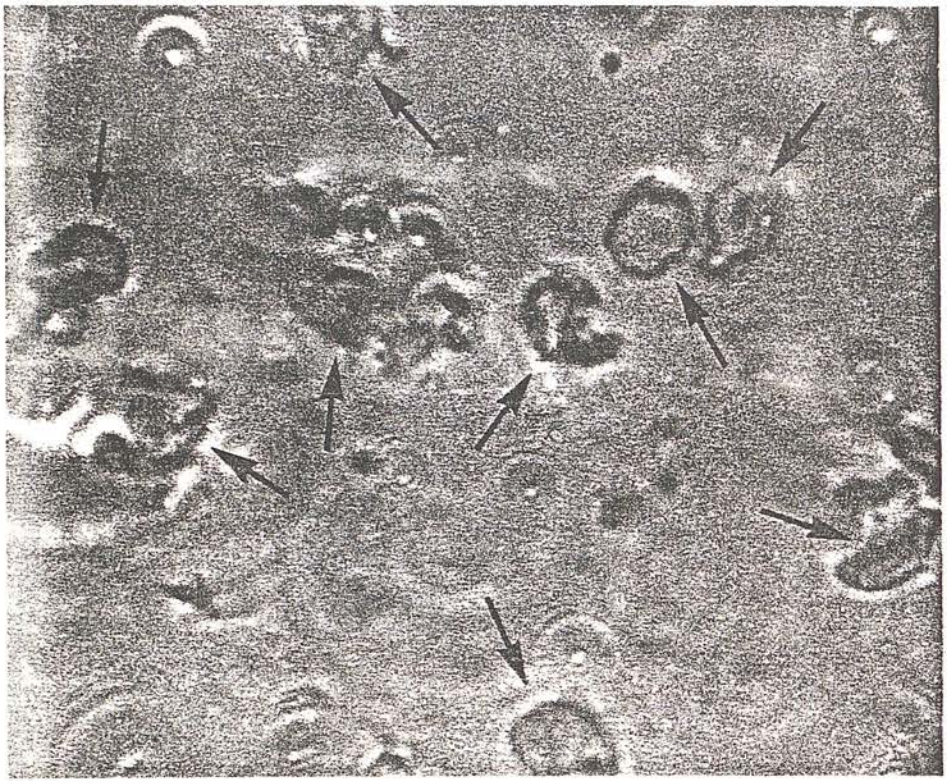

Fig. 5.11 A phase contrast micrograph of purified rat liver nuclear envelope. Arrows indicate intact ghosts.

up the quantity of tissue that can be processed, while retaining satisfactory purification.

Recently, it has been found that the DNAase 1 treatment of the purified nuclei can be omitted if they are stored overnight at 4°C in the homogenization buffer (unpublished observations of the authors). On commencing the sequence of 1 mM sodium bicarbonate washes no gelatinous pellet of nuclei is produced, the material being readily resuspendable at each successive wash. The release of chromatin under these conditions is shown in Fig. 5.16. The behaviour of the material on the sucrose gradient is identical to that obtained following the DNAase I treatment. Further analytical and enzymic studies are in progress to assess whether or not this methodological variant is superior to that requiring the addition of DNAase I, but it may be noted that the overall conditions are brought closer to those employed in the original zonal procedure [61]. It can reasonably be proposed that autolytic digestion of the nuclear DNA will occur during an overnight incubation of 4°C, since it is known that there is an active

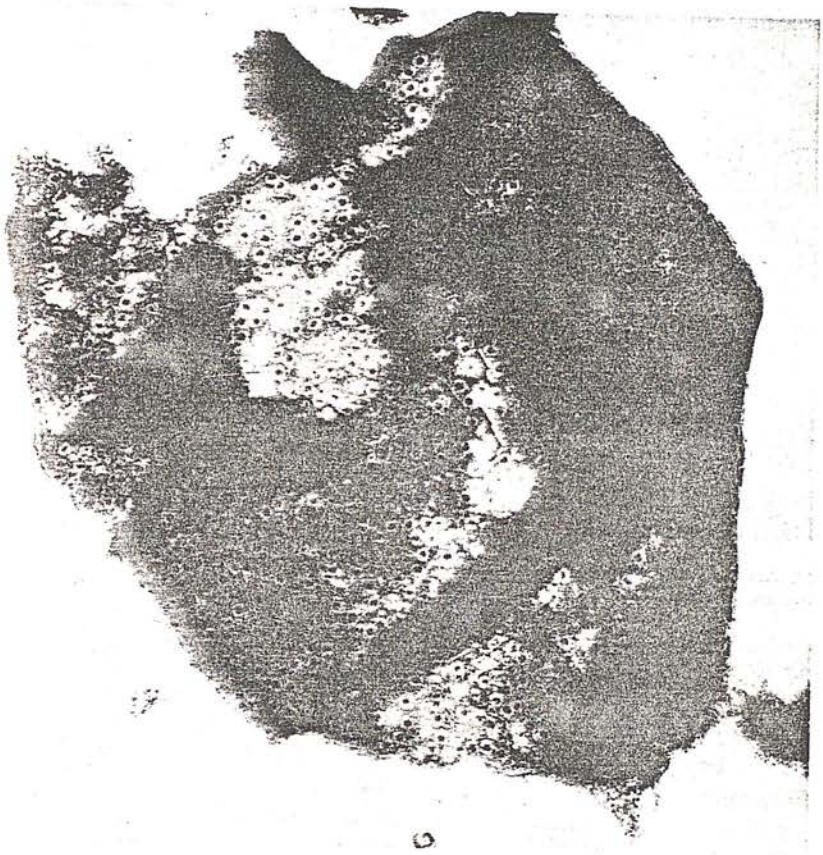

Fig. 5.12 A rat liver nuclear ghost, negatively stained with 2% ammonium molybdate (pH 7.0). ×15 000.

Fig. 5.13 A torn sheet of rat liver nuclear envelope, negatively stained with 2% ammonium molybdate (pH 7.0). ×72 000.

Fig. 5.14 Thin sectioned rat liver nuclear envelope. Regions showing both the INM and ONM are arrowed. x15 000.

Fig. 5.15 A region of tangentially sectioned rat liver nuclear envelope showing the nuclear pore complexes (arrowed). x72 000.

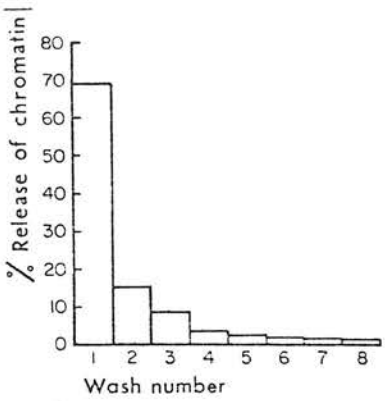

Fig. 5.16 The release of solubilized chromatin from purified rat liver nuclei that had been stored overnight at 4°C in 250 mM sucrose, 2 mM $MgCl_2$, 10 mM Tris-HCl (pH 7.4), when washed with 1 mM sodium bicarbonate (pH 7.2). The washing conditions are the same as those described in the text (cf. Figs. 5.8 and 5.10), but no exogenous DNAase is added. The histogram is the mean of three experiments.

Ca–Mg endonuclease present [115], which will readily attack and digest nuclear DNA *in situ* at 37°C.

The overall aim of the procedure presented is to obtain morphologically intact nuclear ghosts or torn sheets of NE with a low DNA content as rapidly as possible from the time of sacrificing the animals, and this has been achieved. The procedure must be considered to be relatively mild in that it is performed throughout at a pH close to neutrality and that conditions are maintained at 4°C, except for the brief DNAase I treatment. The final NE material is obtained by flotation on a sucrose gradient, which is the most satisfactory procedure for separating NE from trace amounts of contaminants such as collagen, nuclei, peroxisomes as well as solubilized chromatin. One criticism that can be put forward is that the low ionic strength conditions used throughout may release components of the NE. This point can only be answered by extensive comparison of the available methods for the isolation of NE.

References

1. Callan, H. G., Randall, J. T. and Tomlin, S. G. (1949), *Nature*, **163**, 280.
2. Callan, H. G. and Tomlin, S. G. (1950), *Proc. R. Soc. Ser.*, (*B*), **137**, 367.
3. Anderson, N. G. (1953), *Expl. Cell Res.*, **4**, 306.
4. Sharrer, B. and Wurzelmann, S. (1969), *Z. Zellforsch.*, **96**, 325.
5. Franke, W. W. and Scheer, U. (1970), *J. Ultrastruct. Res.*, **30**, 317.
6. Franke, W. W. (1974), *Phil. Trans. R. Soc. Ser. B*, **268**, 67.
7. Wartiovaara, J. (1971), *J. Ultrastruct. Res.*, **36**, 558.
8. Fry, D. J. (1970), *Membranes and Ion Transport*, (Bittar, E. E., ed.), Vol. 2, pp. 259, Wiley Interscience, New York.
9. Feldherr, C. M. (1972), *Adv. Cell and molec. Biol.*, **2**, 273.
10. Kessel, R. G. (1973), *Prog. Surface Memb. Sci.*, **6**, 243.
11. Wischnitzer, S. (1973), *Int. Rev. Cytol.*, **34**, 1.
12. Franke, W. W. and Scheer, W. (1974), *The Cell Nucleus*, (Busch, H., ed.), Vol. 21, Academic Press, New York and London.
13. Hartman, J. F. (1953), *J. comp. Neurol.*, **99**, 201.

14. Palay, S. L. and Palade, G. (1955), *J. biophys. biochem. Cytol.*, 1, 69.
15. Afzelius, B. A. (1955), *Expl. Cell Res.*, 8, 147.
16. Rebhun, L. I. (1956), *J. biophys. biochem. Cytol.*, 2, 93.
17. Watson, M. W. (1959), *J. biophys. biochem. Cytol.*, 6, 432.
18. Wischnitzer, S. (1958), *J. Ultrastruct. Res.*, 1, 201.
19. Vivier, E. (1967), *J. Microscopie*, 6, 371.
20. Abelson, H. T. and Smith, G. H. (1970), *J. Ultrastruct. Res.*, 30, 558.
21. Roberts, K. and Northcote, D. H. (1971), *Microscopica Acta.*, 71, 102.
22. LaCour, L. F. and Wells, B. (1974), *Phil. Trans. R. Soc. Ser. B*, 268, 95.
23. Franke, W. W. and Scheer, U. (1970), *J. Ultrastruct. Res.*, 30, 288.
24. Harris, J. R., Price, M. R. and Willison, M. (1974), *J. Ultrastruct. Res.*, 48, 17.
25. Harris, J. R. (1974), *Phil. Trans. Roy. Soc. Ser. B*, 269, 109.
26. Franke, W. W. (1967), *Z. Zellforsch.*, 80, 585.
27. Branton, D. and Moor, H. (1964), *J. Ultrastruct. Res.*, 11, 401.
28. Maul, G. G., Price, J. W. and Liebermann M. W. (1971), *J. Cell Biol.*, 51, 405.
29. Kartenbeck, J., Zentgraf, H., Scheer, U. and Franke, W. W. (1971), *Adv. Anat. Embryol. Cell Biol.*, 45, 1.
30. Teighler, D. J. and Baerwald, R. J. (1972), *Tiss. Cell*, 4, 447.
31. Lott, J. N. A., Larsen, R. L. and Whittington, C. M. (1972), *Can. J. Bot.*, 50, 1785.
32. La Fountain, J. R. and La Fountain, K. L. (1973), *Expl. Cell Res.*, 78, 472.
33. Markovics, J., Glass, L. and Maul, G. G. (1974), *Expl. Cell Res.*, 85, 443.
34. Parks, H. F. (1962), *J. Cell Biol.*, 14, 221.
35. Sadowski, P. D. and Howden, J. A. (1968), *J. Cell Biol.*, 37, 163.
36. Gurr, M. I., Finean, J. B. and Hawthorne, J. N. (1963), *Biochim. biophys. Acta.*, 70, 406.
37. Bruni, C. and Porter, K. R. (1965), *Am. J. Path.*, 46, 691.
38. Davies, H. G. (1968), *J. Cell Sci.*, 3, 129.
39. Leskes, A., Siekevitz, P. and Palade, G. E. (1971), *J. Cell Biol.*, 49, 264.
40. Wischnitzer, S. (1958), *J. Ultrastruct. Res.*, 1, 201.
41. Gall, J. G. (1956), *J. biophys. biochem. Cytol.*, 2, 393.
42. Gall, J. G. (1967), *J. Cell Biol.*, 32, 391.
43. Roberts, K. and Northcote, D. H. (1970), *Nature*, 228, 385.
44. Hoeijnakers, J. H. H., Schel, J. H. N. and Wanka, F. (1974), *Expl. Cell Res.*, 87, 195.
45. Kessel, R. G. (1969), *Z. Zellforsch.*, 94, 441.
46. La Cour, L. F. and Wells, B. (1971), *Z. Zellforsch.*, 123, 178.
47. Engelhardt, P. and Pusa, K. (1972), *Nature*, 240, 163.
48. Stephens, B. J. and Swift, H. (1966), *J. Cell Biol.*, 31, 55.
49. King, T. E. (1967), *Meth. Enzym.*, 10, 322.
50. Babson, A. L., Read, P. A. and Philips, G. E. (1959), *Am. J. clin. Path.*, 32, 83.
51. Berezney, R., Funk, L. K. and Crane, F. L. (1970), *Biochim. Biophys. Acta*, 203, 53
52. Kay, R. R., Fraser, D. and Johnston, I. R. (1972), *Eur. J. Biochem.*, 30, 145.
53. Kashnig, D. M. and Kasper, C. B. (1969), *J. biol. Chem.*, 244, 3786.
54. Stavy, R., Ben-Shaul, Y. and Galun, E. (1973), *Biochim. biophys. Acta.*, 323, 167.

55. Zbarsky, I. B., Perevoshchikova, K. A., Delektorkaya, L. N. and Delektarsky, V. V. (1969), *Nature*, **221**, 257.
56. Franke, W. W., Deumling, B., Ermen, B., Jarasch, E. D. and Kleinig, H. (1970), *J. Cell Biol.*, **46**, 379.
57. Agutter, P. S. (1972), *Biochim. biophys. Acta.*, **255**, 397.
58. Gorkin, V. Z. (1971), *Experientia*, **27**, 30.
59. Harris, J. R. and Agutter, P. S. (1970), *J. Ultrastruct. Res.*, **33**, 219.
60. Harris, J. R. (1969), *J. Molec. Biol.*, **46**, 329.
61. Price, M. R., Harris, J. R. and Baldwin, R. W. (1972), *J. Ultrastruct. Res.*, **40**, 178.
62. Monneron, A., Blobel, G. and Palade, G. E. (1972), *J. Cell Biol.*, **55**, 104.
63. Mizuno, N. S., Stoops, C. E. and Sinha, A. A. (1971), *Nature*, **229**, 22.
64. Bornens, M. (1973), *Nature*, **244**, 28.
65. Bornens, M. and Kaspar, C. B. (1973), *J. biol. Chem.*, **248**, 571.
66. Jarasch, E. D., Reilly, C. E., Comes, P., Kartenbeck, J. and Franke, W. W. (1973), *Hoppe-Seyler's Z. physiol. Chem.*, **354**, 974.
67. Zentgraf, H., Deumling, B., Jarasch, E. and Franke, W. W. (1971), *J. biol. Chem.*, **246**, 2986.
68. Meyer, H. W., Roth, J. and Block, F. (1972), *Protoplasm*, **75**, 313.
69. Speth, V. and Wunderlich, F. (1970), *J. Cell Biol.*, **47**, 772.
70. Maul, G. G. (1971), *J. Cell Biol.*, **51**, 558.
71. Lui, T. P. (1972), *J. Parasit.*, **58**, 1151.
72. Cole, G. T. and Wynne, M. J. (1973), *Cytobios.*, **8**, 161.
73. Wunderlich, F., Batz, W., Speth, V. and Wallach, D. F. H. (1974), *J. Cell Biol.*, **61**, 633.
74. Moor, H. K., Mühlethaler, H., Waldner, H. and Frey-Wyssling, A. (1961), *Biophys. Biochem. Cytol.*, **10**, 1.
75. Smith, S. J., Adams, H. R., Smetana, K. and Busch, H. (1969), *Expl. Cell Res.*, **55**, 185.
76. Scheer, U. (1973), *Devl. Biol.*, **30**, 13.
77. Burton, K. (1956), *Biochem. J.*, **62**, 315.
78. Giles, K. W. and Myers, A. (1965), *Nature*, **206**, 93.
79. Dodge, J. T., Mitchell, C. D. and Hanahan, D. J. (1963), *Archs. biochem. Biophys.*, **100**, 199.
80. Harris, J. R. (1969), *Biochim. biophys. Acta.*, **188**, 31.
81. Harris, J. R. and Brown, J. N. (1971), *J. Ultrastruct. Res.*, **36**, 8.
82. Blanchet, J. P. (1974), *Expl. Cell Res.*, **84**, 159.
83. Scheer, U. (1972), *Z. Zeliforsch.*, **127**, 127.
84. Harris, J. R. and Milne, J. F. (1974), *Trans. Biochem. Soc.* In press.
85. Callan, H. G. (1952), *Symp. Soc. Expl. Biol.*, **6**, 243.
86. Hunter, A. S. and Hunter, F. R. (1961), *Expl. Cell Res.*, **22**, 609.
87. Dounce, A. L. and Umana, R. (1962), *Biochemistry*, **1**, 811.
88. Chauveau, J., Moulé, Y. and Rouiller, Ch. (1956), *Expl. Cell Res.*, **11**, 312.
89. Blobel, G. and Potter, V. R. (1966), *Science*, **154**, 1662.
90. Widnell, C. C. and Tata, J. R. (1964), *Biochem. J.*, **92**, 313.
91. Sporn, M. B., Wanko, T. and Dingman, W. (1962), *J. Cell Biol.*, **15**, 109.
92. Emmelot, P. and Bos, C. J. (1966), *Biochim. biophys. Acta.*, **120**, 369.
93. Franke, W. W. (1966), *J. Cell Biol.*, **31**, 619.
94. Brasch, K., Seligy, V. L. and Setterfield, G. (1971), *Expl. Cell Res.*, **65**, 61.
95. Olins, D. E. and Olins, A. L. (1972), *J. Cell Biol.*, **53**, 715.
96. Mirsky, A. E. and Osawa, S. (1961), *The Cell*, (Brachet, J. and Mirsky, A. E., eds.), Vol. 2, pp. 677, Academic Press, New York and London.

97. Anderson, N. G. and Wilbur, K. M. (1951), *J. gen. Physiol.*, **34**, 647.
98. Ueda, K., Matsuura, T. and Date, N. (1969), *Biochem. biophys. Res. Commun.* 34, 322.
99. Mitchell, C. D. and Hanahan, D. J. (1966), *Biochemistry*, **5**, 51.
100. Mazia, D. and Ruby, A. (1968), *Proc. natn. Acad. Sci. U.S.A.*, **61**, 1005.
101. Anderson, N. G. (1953), *Expl. Cell Res.*, **5**, 361.
102. Price, M. R', Harris, J. R. and Baldwin, R. W. (1973), *Methodological Developments in Biochemistry*, (Reid, E., ed.), Vol. 3, pp. 159, Longmans, Harlow.
103. Harris, J. R. In preparation.
104. Monneron, A. (1974), *Phil. Trans. R. Soc. Ser. B*, **268**, 101.
105. Lowry, O. H., Rosebrough, N. J., Farr, A. L. and Randall, R. J. (1951), *J. biol. Chem.*, **193**, 265.
106. Franke, W. W., Deumling, B., Falk, H. and Rae, P. M. M. (1973), *Expl. Cell Res.*, **81**, 365.
107. Keenan, T. W., Berezney, R., Funk, L. K. and Crane, F. L. (1970), *Biochim. biophys. Acta.*, **203**, 547.
108. Klenig, H. (1970), *J. Cell Biol.*, **46**, 396.
109. Yoo, B. Y. and Bayley, S. T. (1967), *J. Ultrastruct. Res.*, **18**, 651.
110. Schiechl, H. (1973), *Biochim. biophys. Acta.*, **307**, 65.
111. Maddy, A. H. and Kelly, P. G. (1970), *FEBS Letters*, **8**, 341.
112. Beaufay, H. and De Duve, C. (1954), *Bull. Soc. Chim. biol.*, **36**, 1525.
113. Kay, R. R., Haines, M. E. and Johnston, I. R. (1970), *FEBS Letters*, **10**, 113.
114. Neville, D. M. (1960), *Biochem. Biophys. Cytol.*, **8**, 413.
115. Hewish, D. R. and Burgoyne, L. A. (1973), *Biochem. biophys. Res. Commun.*, **52**, 504.
116. Weed, R. I., Reed, C. Fand Berg, G. (1963), *J. clin. Invest.*, **42**, 581.

Reprinted from (29)
MEMBRANOUS ELEMENTS AND MOVEMENT OF MOLECULES
(Vol. 6 of METHODOLOGICAL SURVEYS IN BIOCHEMISTRY)
edited by E. Reid
Horwood, Chichester, 1977

A Note on

FRACTIONATION OF THE NUCLEAR ENVELOPE

J. R. HARRIS
Division of Biochemistry, Faculty of Science,
North East London Polytechnic, London, U.K.

A simple procedure is now described for the release and separation of the nuclear pore complex from rat-liver nuclear envelope. Already there are several methods for the isolation of the envelope with its firmly associated pore complexes [1-5]. Extensive ultrastructural, chemical and enzymic information is now available on the envelope [6-9], but the function of the pore complex remains unclear. It might be regarded as an independent cellular organelle [9], and is generally held to be a locus for nucleocytoplasmic transport of macromolecules and for the control of this process. Clarification awaits a true isolation procedure, although enrichment has already been achieved [10].

Some early publications on nuclear envelope show that the pore complexes are structurally more stable than the surrounding membrane [11], as confirmed by ourselves [6, 12] and others [3, 13, 14]. The process of ultrasonication can be controlled with respect to intensity, time and temperature, and has been used for the disruption of mitochondria [15] as well as for the production of nuclear-envelope fragments [16-19] and for the separation of chick erythrocyte nuclei [20]. Accordingly, separation of the pore complex from the surrounding nuclear membrane has been attempted by ultrasonicating a suspension of rat-liver nuclear envelope, with careful monitoring by electron microscopy using negative staining in order to assess the degree of separation of the complexes [6]. Ultrasonication might of course disrupt cellular membranes non-selectively and could generate local heat and free radicals [21, 22], but now seems at least partly justifiable because the lipoprotein membrane of the nuclear envelope is disrupted prior to the nuclear pore complex.

PROCEDURES AND RESULTS OBTAINABLE

From a rat-liver nuclear envelope suspension [2] in 10 mM Tris-HCl buffer (pH 7.4), ~1.0 ml portions (protein concentration 5 mg/ml) were treated with the MSE 150 watt Ultrasonic Disintegrator with ice-cooling. The disrupted membrane material was fractionated by centrifugation through linear sucrose gradients prepared from 0.25 M and 1.0 M sucrose in 10 mM Tris-HCl buffer (pH 7.4) with a conventional two-chamber mixing apparatus. Centrifugation was performed in the Beckman SW 27.1 rotor using cellulose nitrate tubes, at 27,000 rev/min (100,000 g_{av}) for 30 min. The contents of the centrifuge tubes were passed

through the LKB Uvicord 11 UV flow analyzer attached to a chart recorder. Fractions of 40 drops were taken by the LKB Ultrorack fraction collector. They were then dialyzed against 5 mM Tris-HCl (pH 7.4) to remove the sucrose prior to preparing negatively stained electron microscope specimens with 2% ammonium molybdate (pH 7.0) using the single droplet procedure [12].

Preliminary experiments using the Sonicor 120 watt ultrasonic cleaning bath containing iced water indicated clearly that the membranous sheets of rat liver nuclear envelope could be made to undergo a gradual fragmentation with release of the nuclear pore complexes. However, subjection to this treatment for up to 2 h did not completely disrupt the nuclear envelope. Fig. 1 shows the envelope after a 1 h treatment in the Sonicor bath. The free nuclear pore complexes have many membranous attachments, besides groups of unseparated pore complexes.

The separation of the latter achieved using the MSE probe-type ultrasonicator was much more rapid and complete. At an intensity setting of 3 μm peak-to-peak, 1.0 ml volumes of the nuclear envelope suspension were treated for a total of 3 min, applied as 10 sec periods of ultrasonication interspaced by 10 sec periods of cooling by a surrounding ice bath. The appearance of the resulting material is shown in Fig. 2. Free nuclear pore complexes are present *(arrowed)* along with small membrane fragments, but there is a complete absence of intact sheets of nuclear envelope and groups of nuclear pore complexes.

Sampling for electron microscopy over a period of time enables the degree of disruption of the envelope to be readily assessed and an ultrasonication time be selected for maximum release of nuclear pore complexes. In general, very few partially broken pore complexes have been detected after this treatment, perhaps reflecting the stability of the octagonal conformation of the pore complex; but completely disrupted pore complexes might not be detectable. With the above conditions, ultrasonication causes only slight inactivation of the nuclear envelope ATPase.

To separate the nuclear pore complexes from the membrane fragments by rate-zonal centrifugation, the ultrasonicated suspension containing free pore complexes was layered over a linear 0.25 M to 1.0 M sucrose gradient, which was centrifuged at 27,000 rev/min ($100{,}000 \times g_{av}$) for 1 h. Fig. 3 shows the distribution of UV-absorbing material in the gradient. Electron microscopy after removal of the sucrose by dialysis showed nuclear pore complexes (Fig. 4) in the fractions sedimenting ahead of the main peak of UV-absorbing material (fractions 6-9, in Fig. 3). The material present in the main peak (fractions 10-15) consists entirely of small membrane fragments, of gradually diminishing size as the top of the gradient is approached (Fig. 5).

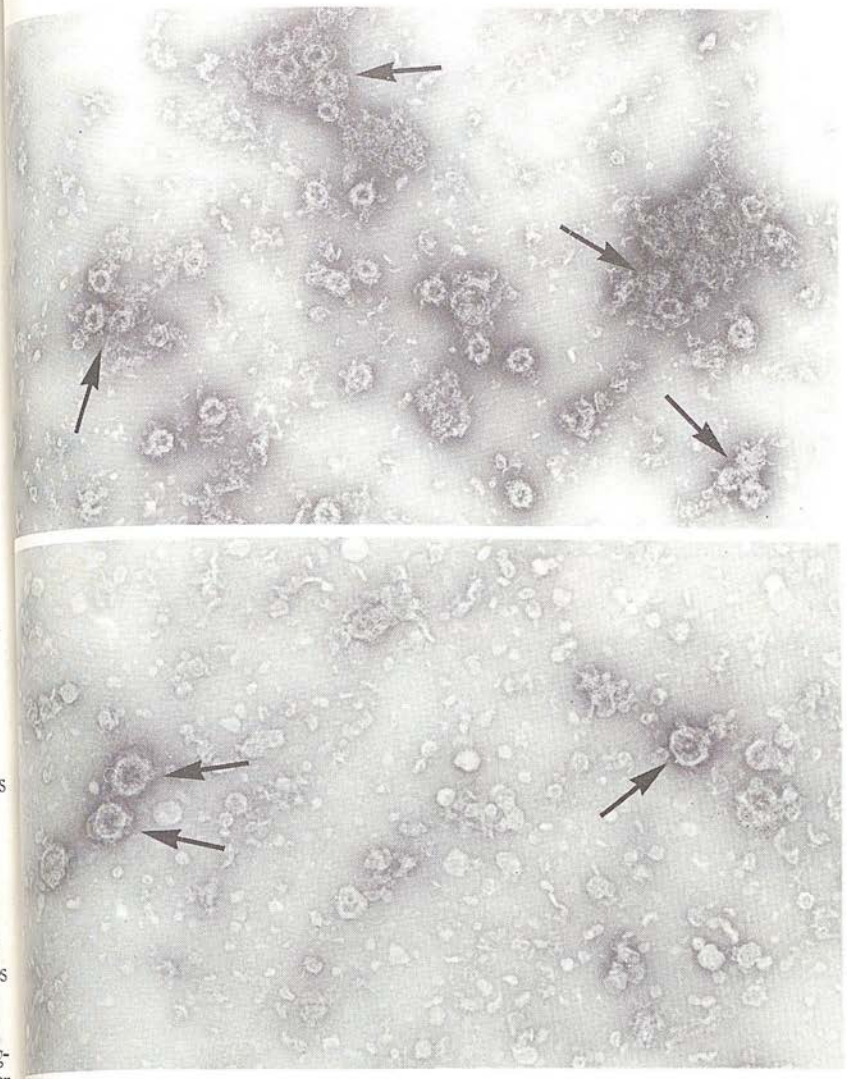

ig. 1 *(upper Plate)*. Nuclear envelope after treatment for 1 h in he Sonicor 120 watt bath-type ultrasonicator. *Arrows* indicate roups of nuclear pore complexes. Negatively stained with 2% mmonium molybdate (pH 7.0). x 39,000.

ig. 2. Nuclear envelope after treatment for 3 min with the MSE robe-type ultrasonicator. *Arrows* indicate free nuclear pore omplexes. Many small membrane fragments are present. Negative- y stained with 2% ammonium molybdate (pH 7.0). x 55,000.

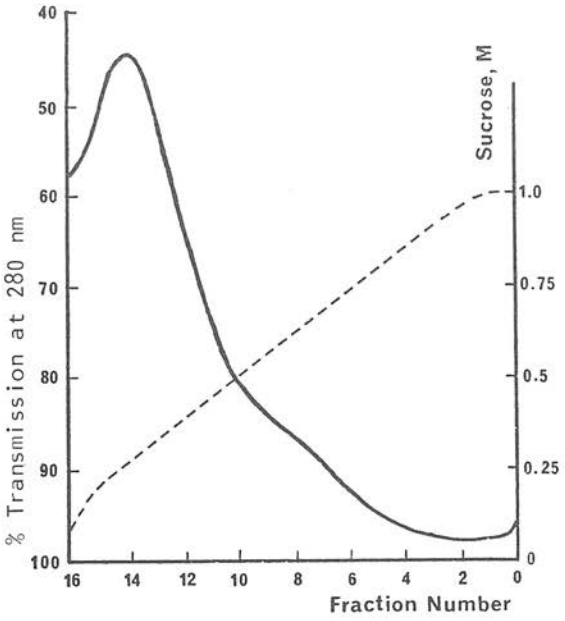

Fig. 3. Distribution of UV-absorbing material after centrifuging the ultrasonicated nuclear envelope suspension through a 0.25-1.0 M sucrose gradient for 1 h at 27,000 rev/min.

CONCLUSION

The sucrose gradient fractions containing nuclear pore complexes cannot be considered to represent a highly purified preparation of these structures, since trace quantities of membrane fragments of similar overall mass are also present. Nevertheless, the procedures described show that ultrasonication will split the nuclear envelope leaving the nuclear pore complexes apparently intact. Also, that simple rate-zonal centrifugation procedures will provide a separation of these pore complexes from most of the nuclear membrane fragments.

Acknowledgements

This work is supported by the Medical Research Council and the Royal Society. The technical assistance of Mrs. I. Stevenson and Mr. J. Kerr is gratefully acknowledged.

1. Price, M.R., Harris, J.R. & Baldwin, R.W. (1972) *J. Ultrastruct. Res. 40,* 178-196.
2. Harris, J.R. & Milne, J.F. (1974) *Trans. Biochem. Soc. 2,* 1251-1253.
3. Kay, R.R., Fraser, D. & Johnson, I.R. (1972) *Eur. J. Biochem. 30,* 145-154.
4. Monneron, A., Blobel, G. & Palade, G.E. (1972) *J. Cell Biol. 55,* 104-125.

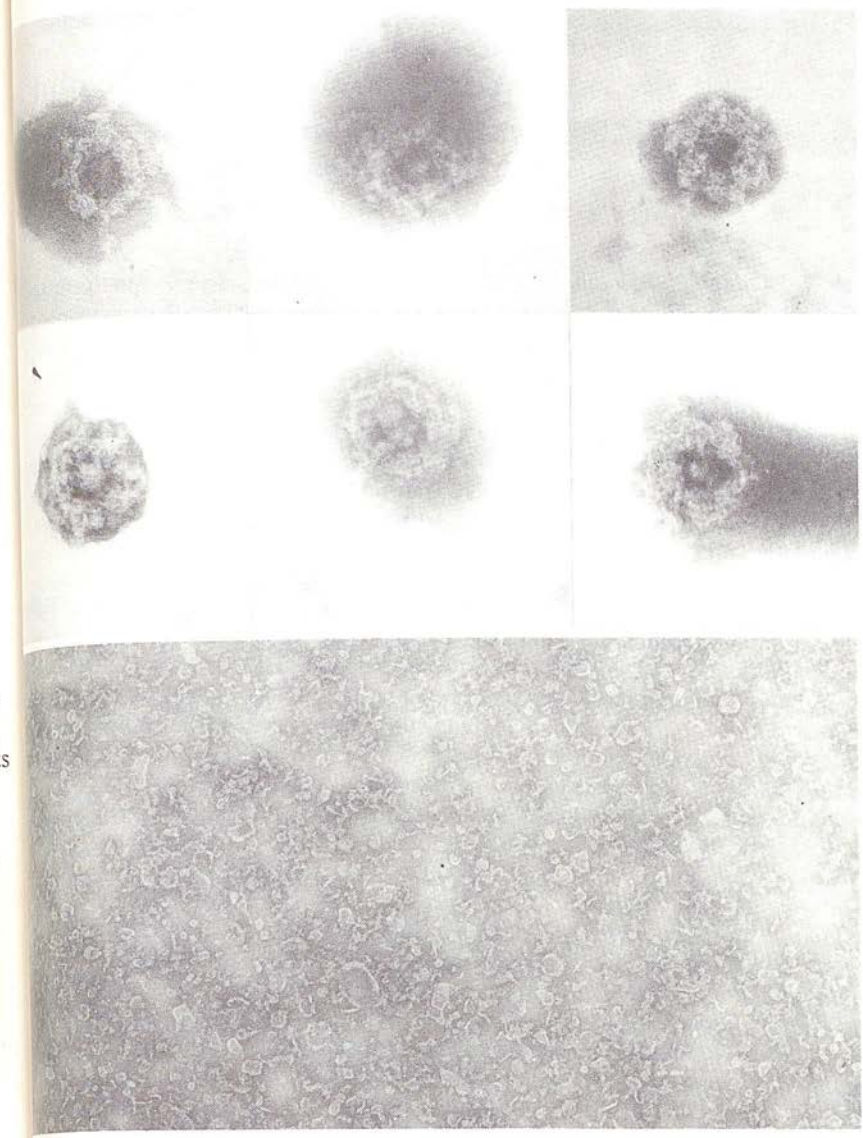

Fig. 4 *(top)*. Representative pore complexes isolated by sucrose density-gradient centrifugation. Negatively stained with 2% ammonium molybdate (pH 7.0). x 136,000.

Fig. 5. The material present in the fractions under the main UV-absorbing peak from centrifugation, in a sucrose gradient, of ultrasonicated nuclear envelope. Small membrane fragments and finely dispersed material are present. Negatively stained with 2% ammonium molybdate (pH 7.0). x 39,000.

5. Franke, W.W., Deumling, B., Ermen, B., Jarasch, E.D. & Klenig, H. (1970) *J. Cell Biol. 46,* 379-395.

6. Harris, J.R. (1974) *Phil. Trans. Roy. Soc. B 268,* 109-117.

7. Franke, W.W. (1974) *Phil. Trans. Roy. Soc. B 268,* 67-93.

8. Wischnitzer, S. (1973) *Internat. Rev. Cytol. 34,* 1-48.

9. Abelson, H.T. & Smith, G.H. (1970) *J. Ultrastruct. Res. 30,* 558-588.

10. Aaronson, R.P. & Blobel, G. (1975) *Proc. Natl. Acad. Sci. U.S.A. 72,* 1007-1011.

11. Gall, J.G. (1967) *J. Cell Biol. 32,* 391-400.

12. Harris, J.R. & Agutter, P.S. (1970) *J. Ultrastruct. Res. 33,* 219-232.

13. Hoeijmakers, J.H.J., Schel, J.H.N. & Wanka, F. (1974) *Exptl. Cell Res. 87,* 195-206.

14. Yoo, B.Y. & Bailey, S.T. (1967) *J. Ultrastruct. Res. 18,* 651-660.

15. Huang, C.H., Keyhani, E. & Lee, C.P. (1973) *Biochim. Biophys. Acta 305,* 455-473.

16. Agutter, P.S. (1972) *Biochim. Biophys. Acta 255,* 397-401.

17. Franke, W.W. (1966) J. Cell Biol. 31, 619-623.

18. Kashnig, D.M. & Kasper, C.B. (1969) *J. Biol. Chem. 244,* 3786-3792.

19. Stavy, R., Ben-Shaul, Y. & Galun, E. (1973) *Biochim. Biophys. Acta 323,* 167-177.

20. Harris, J.R. & Brown, J.N. (1971) *J. Ultrastruct. Res. 36,* 8-23.

21. Wallach, D.F.H. & Lin, P.L. (1973) *Biochim. Biophys. Acta 300,* 211-254.

22. El'piner, I.E. (1964) *Ultrasound Physical, Chemical and Biological Effects,* Consultants Bureau, New York, Chapters 6 and 8.

Comment by G. Siebert.- The use of a protease inhibitor such as phenylmethylsulphonyl chloride – widely applied in chromatin studies – may be helpful for pore-complex isolation, in order to avoid secondary autolytic alteration of the material.

In answer to J.R. Harris, who wondered if nucleoplasmic protein-linked RNA passes to the cytoplasm via the pore complexes (which contain RNA), G.D. Birnie felt this to be plausible, albeit selective, but that direct transfer might also occur across the membranes.

Micron, 1977, Vol. 8: 217–219. Pergamon Press. Printed in Great Britain.

Negative staining of fractionated nuclear envelopes

J. R. HARRIS and P. MARSHALL

Division of Biochemistry, North East London Polytechnic, London, England

Electron microscopic studies on isolated nuclear envelopes (nuclear ghosts) from amphibian oocytes, avian erythrocytes and mammalian liver have been performed for several years, and it is widely accepted that negative staining provides the greatest ultrastructural detail of this two-layered membrane system and its associated press-stud-like nuclear pore complexes. As there is, as yet, no characteristic marker enzyme for nuclear envelopes, the assessment of purity relies heavily on negative staining which readily reveals the presence of any contaminatory membrane fragments which do not carry nuclear pore complexes. Suspensions of our isolated nuclear envelope from rat liver (Harris and Milne, 1974) do not contain any such contaminatory membranes although trace amounts of collagen are detectable.

In line with studies on mitochondria, endoplasmic reticulum and chloroplasts, attempts have been made to sub-fractionate the nuclear envelope of rat liver in order to obtain isolated nuclear pore complexes and fragmented or vesiculated inner and outer nuclear membrane for subsequent biochemical and ultrastructural investigations. Previous negative staining studies using ammonium molybdate (Harris and Agutter, 1970; Harris, 1974) and sodium phosphotungstate (Gall, 1967; Scheer *et al.*, 1976) have indicated that spreading forces applied to the nuclear envelope while preparing the specimen grids, disrupt some of the nuclear membranes such that the membrane sheets become fragmented but the nuclear pore complexes remain relatively intact morphologically. It is likely, therefore, that treatments such as high speed homogenization and ultrasonication may bring about a controllable disruption of the nuclear envelope. In our hands, mild ultrasonication using a bath-type apparatus does not completely disperse the nuclear envelope even over long periods, but a partial release of nuclear pore complexes is obtained. When a probe-type ultrasonicator is used, the nuclear envelope is found to disperse more completely within 3min at the relatively low intensity of 3μm (Fig. 1). For both treatments, the disruption of the nuclear envelope is readily and rapidly monitored by taking consecutive samples throughout the treatment for making negatively stained EM specimens.

Sucrose density gradient centrifugation has been used to separate the nuclear pore complexes, which sediment more rapidly than the small nuclear membrane fragments. Only a partial separation is obtained owing to the fact that a few larger membrane fragments sediment along with the nuclear pore complexes, and some of the pore complexes still have membrane attached. Nevertheless, most of the nuclear pore complexes appear to be in a good state of preservation when studied by negative staining with the central granule and the annular subunits being clearly visible (Harris, 1977). A slightly modified approach currently under investigation employs an initial extraction of the nuclear envelope with a non-ionic surfactant (e.g. Triton X-100 or Nonidet P-40). These surfactants solubilize the outer nuclear membrane and remove the lipids from the inner nuclear membrane but leave behind a 'fibrous' inner nuclear membrane residue with the nuclear pore complexes still attached. Attempts to separate the nuclear pore complexes from this extracted material using ultrasonication followed by gradient centrifugation are in progress and it is hoped that this approach may lead to the isolation of a more highly purified nuclear pore complex fraction than obtained previously by direct ultrasonication of the nuclear envelope.

Perhaps the main area of controversy within the field of nuclear envelope studies is the composition and structure of the nuclear pore complex. Many different diagrammatic models have been produced, none of which can be said to reflect the possible composition of the nuclear complex as a macromolecular organization. It has been proposed by some that the annular material of the nuclear pore complex consists of eight globular particles, whereas others consider it to consist of eight mini-tubule

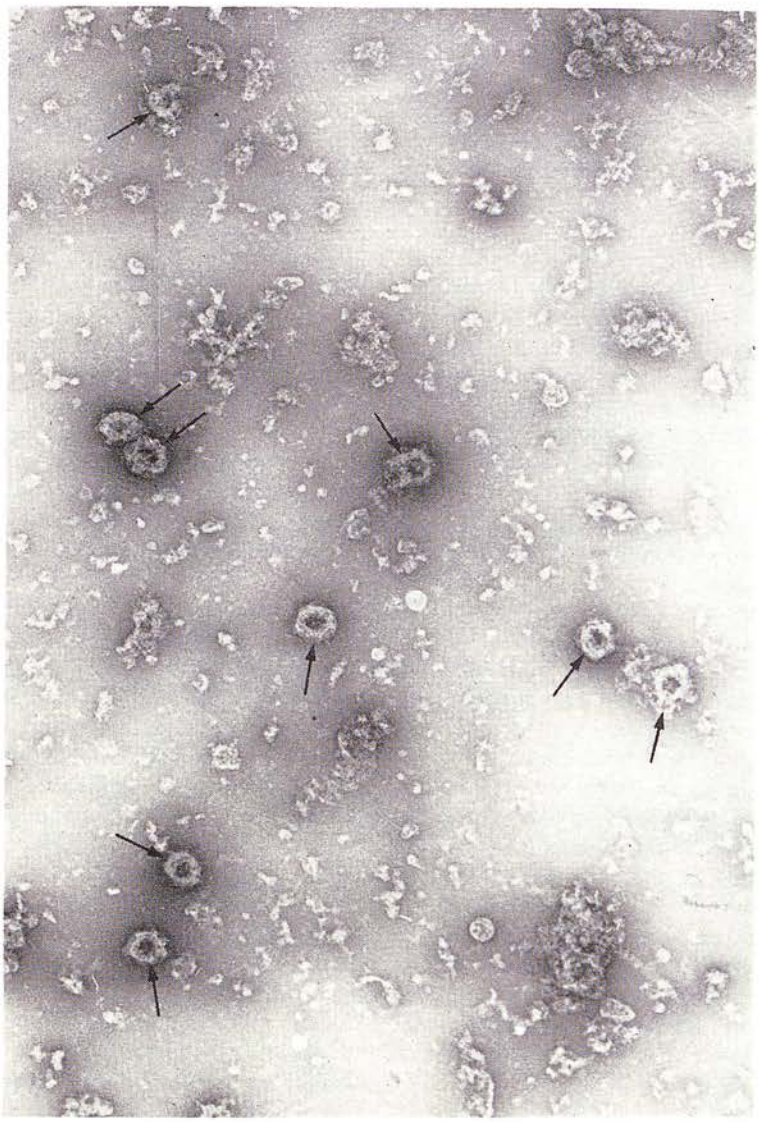

Fig. 1. Rat liver nuclear envelope after ultrasonication using the MSE 150W ultrasonic disintegrator. Negatively stained with 2% ammonium molybdate at pH 7.0. The arrows indicate nuclear pore complexes that have been released. Small fragments of membrane are spread over the background. × 44,500.

or hollow-cylinder components. Evidence from the direct negative staining of nuclear pore complexes separated by spreading and ultrasonication and also from the application of the photographic technique for rotational enhancement of symmetrical structures, indicates that the annular sub-units are hollow rather than globular. Close attention to the published thin-sectioning and negatively stained electron micrographs of others, also provides evidence to support this interpretation. It is hoped that further studies of purified nuclear pore complexes and their controlled dissociation may provide further information of their macromolecular composition.

REFERENCES

Gall, J. G., 1967. *J. Cell Biol.*, **32:** 391.
Harris, J. R. and Agutter, P. S., 1970. *J. Ultrastruct. Res.*, **33:** 219.
Harris, J. R., 1974. *Phil. Trans. R. Soc. B.*, **268:** 109.

Harris, J. R. and Milne, J. F., 1974. *Biochem. Soc. Trans.*, **2**: 1251.

Harris, J. R., 1977. In *Membranous Elements and Movement of Molecules: Techniques*, Reid, E. (ed.), Horwood, Chichester, Vol. 6, pp. 245–250.

Scheer, U., 1976. *J. Cell Biol.*, **69**: 1.

rinted from
hemica et Biophysica Acta, 515 (1978) 55–104
Elsevier/North-Holland Biomedical Press

A 85181

31

E BIOCHEMISTRY AND ULTRASTRUCTURE OF THE NUCLEAR VELOPE

MES R. HARRIS
ion of Biochemistry, North East London Polytechnic, Romford Road, London E15 4LZ (U.K.)
eived May 6th, 1977)

NTENTS

I. INTRODUCTION

Recent interest in the nuclear envelope has culminated in the development of several different procedures for the isolation of this membrane system. The product of these procedures varies from relatively intact nuclear ghosts [1–3] to very small pieces of torn membrane [4–6]. The latter are likely to represent partially degraded nuclear envelope in which there is some separation of the inner and outer nuclear membrane together with some destruction of the nuclear pore complexes, but this may not always be the case [7].

The existence of the nuclear envelope was implied by several early light microscopic studies, but the higher magnifications made available by the electron microscope clearly revealed its presence around cell nuclei. In addition, electron microscopy showed the closely apposed inner nuclear membrane and outer nuclear membrane which are interconnected and penetrated by the nuclear pore complexes. Biochemical progress with the isolated nuclear envelope has relied even more heavily on ultrastructural monitoring than has that with other cellular membrane systems. This is because of the lack of suitable enzymic markers which are characteristic of the nuclear envelope. Enzymology is nevertheless invaluable for the assessment of mitochondrial and lysosomal contamination, whereas electron microscopy is more satisfactory for endoplasmic reticulum contamination, owing to the similarity of enzymes present in the nuclear envelope and endoplasmic reticulum [8]. In intact nuclei the inner nuclear membrane has on its nucleoplasmic surface a layer of heterochromatin and a fibrous layer which varies in thickness in different cells. This fibrous layer which is usually termed the 'internal dense lamina' or 'fibrous lamina', is penetrated by the less dense euchromatin at the locations of the nuclear pore complexes. The outer nuclear membrane is usually coated with ribosome particles on its cytoplasmic surface and the intracisternal space between the two nuclear membranes is in direct continuity with the endoplasmic reticulum cisterna. The nuclear pore complexes are non-membraneous structures that penetrate slightly into the nucleoplasm and cytoplasm as well as passing through the inner nuclear membrane and outer nuclear membrane. It has been proposed that the nuclear pore complexes are composed of eight circularly arranged globular [9–11] or tubular [12–15] subunits along with amorphous and fibrous material. Since the nuclear pore complexes can be considered as subcellular organelles in their own right [1,11,14] and can be isolated from the nuclear envelope as separated entities [16], it is likely that future investigations will provide detailed information on their protein and enzymic composition which may provide some functional explanation for their presence in the nuclear envelopes of almost all cell types. That the nuclear pore complex provides a channel for the passage of material to and from the nucleus is very attractive, but the evidence in support of this hypothesis is not entirely conclusive.

During cell division the nuclear envelope breaks down and re-forms in a controlled manner. This process is not understood, but it is generally thought that the separating chromosomes carry with them fragments of the nuclear envelope which

me together to form the nuclear envelope of the daughter cell nuclei. The precise ge of the cell cycle at which there is a net synthesis of nuclear envelope proteins is t known, but it seems likely to occur during the G_1 phase and the end of S phase, ce there is a two-fold increase in nuclear volume prior to division [17]. In addition, highest rate of nuclear pore complex formation has been shown in synchronised La cells to be within the first hour after division [17], but the mechanism of asiation of the nuclear pore complex components, possibly from a pool of cytosmic macromolecules, is not known.

It has been shown that the distribution and number of nuclear pore complexes unit area of nuclear envelope (the nuclear pore complex frequency) is of considerle significance in relation to the metabolic activity of the nucleus. Cells that are idly synthesising protein such as amphibian oocytes and *Tetrahymena* have a high clear pore complex frequency whereas relatively dormant nuclei such as those of ture avian and amphibian erythrocytes have a very low nuclear pore complex quency. In addition, cells that have been stimulated by metabolic agents such as ncanavalin A and phytohaemagglutinin show an increase in the nuclear pore plex frequency [18,19]. Hormonally and drug-induced changes in the nuclear e complex frequency are likely to be detected, but overall there does not appear to a clear-cut relationship between the nuclear pore complex frequency and the cleocytoplasmic exchange rate or rate of development [20].

Ultrastructural studies have revealed the close similarity of the nuclear enope and the multi-layered membrane system known as the annulate lamella which been detected in many cell types [21]. As there is no available work on isolated purified annulate lamella, biochemical comparisons are not yet possible. The istence of annulate lamella in aggregated HeLa cells [22] may lead to the clarification this interesting area of investigation. The membrane flow hypothesis as put forrd by Morré et al. [23] proposes that the synthesis of cytoplasmic membranes curs in the order nuclear envelope, rough endoplasmic reticulum, smooth endosmic reticulum, Golgi membranes to plasma membrane. In cells that contain nulate lamella it is likely that this cytoplasmic membrane would be positioned tween the nuclear envelope and rough endoplasmic reticulum in the membrane w sequence, but this too remains to be proved experimentally. From ultrastructal and membrane flow considerations a considerable chemical and functional milarity is likely to be present in the nuclear envelope and endoplasmic reticulum. particular it is envisaged that the outer nuclear membrane may have an even closer ntity with the endoplasmic reticulum than the inner nuclear membrane, primarily om ultrastructural evidence. Studies aimed at the sub-fractionation of the nuclear velope into the nuclear pore complex, and inner nuclear membrane and outer clear membrane, followed by ultrastructural and biochemical characterisation, ay well provide further information to support this hypothesis. The relatively gh permeability of the nuclear envelope to all small molecules and macromolecules to an approximate molecular weight of 70 000 has been known for several years 4,25]. It is generally assumed that this low permeability barrier is due to the pas-

sage of molecules through the nuclear pore complex. Although it is clear that the nuclear pore complexes do not have a membraneous diaphragm, they almost certainly do contain fibrous material and in many cases a central granule. Small molecules and macromolecules up to a molecular weight of 70 000 pass across the nuclear envelope by free diffusion, but the involvement of energy dependence mechanisms in nucleocytoplasmic exchanges, particularly for ribonucleoprotein transfers cannot be ruled out at the moment. Such macromolecular transporting systems are unlikely to have similar characteristics to the cation transporting systems of surface membranes apart from the participation of high energy intermediates and complex enzymic sequences.

Electron microscopic histochemistry has suggested that the nuclear envelope ATPase may be located in the nuclear pore complex [26], but this remains to be confirmed by direct enzymic study using isolated and purified nuclear pore complexes. The ATP-dependent release of ribonucleoproteins from cell nuclei [27] could be due to the energy-dependent alteration of the conformation of these nucleic acid-protein complexes or to alteration of the conformation of the nuclear pore complex rather than an energy-dependent transport system. In either case, it is likely that the nuclear pore complexes are involved in the release of ribonucleoproteins from nuclei, and they may therefore represent sites for the control of the synthesis of individual proteins [25].

This brief introduction outlines several important areas of nuclear envelope research, some of which will be dealt with in greater detail below. Almost all aspects of nuclear envelope research have received the attention of other reviewers in recent years [28–35]. It is therefore, the aim of this article to present a slightly more subjective selection of topics and assessment of the field.

II. METHODOLOGICAL CONSIDERATIONS

IIA. Mammalian liver nuclear envelope

Starting with the premise that it is desirable to obtain for most nuclear envelope studies a membraneous material that is in the form of intact nuclear ghosts, we have tried to devise relatively mild procedures by which the nuclear envelope can be released from rat and pig liver nuclei [1,2,15,36,37]. These treatments were derived from the 1 mM sodium bicarbonate homogenization procedure of Neville [38]; rat liver and hepatoma nuclear ghosts were produced along with plasma membrane sheets following low speed rate zonal centrifugation of the crude $1000 \times g$ nuclear pellets, and were subsequently purified by isopycnic centrifugation [36]. This initial procedure has recently been modified to make use of purified nuclei [1,37] by incorporating a short DNAase I (EC 3.1.4.5) digestion along with a series of low ionic strength washes in 1 mM sodium bicarbonate (pH 7.2). The nuclear envelope material obtained by this procedure has been characterised biochemically and ultrastructurally [1,2,37,39]. Although the procedure was developed using rat liver it has

heme 1. The isolation and purification of mammalian liver nuclear envelope.

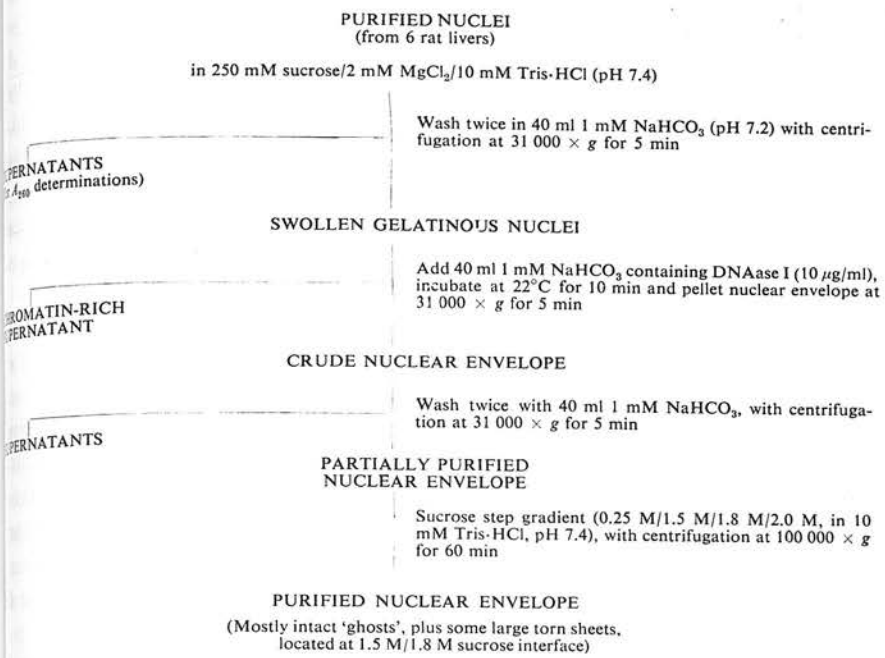

en found to be equally applicable when scaled up to use pig liver [37], the only fference being that the pig liver nuclei were obtained by pelleting through dense crose onto the wall of a zonal rotor, thereby avoiding the use of many individual ntrifuge tubes. An outline of this procedure for isolating and purifying liver nuclear velope is given as a flow diagram in Scheme 1.

The method for isolating nuclear envelope described by Kay et al. [3] bears me similarity to that of the author in that it employs DNAase to disperse the romatin, but differs in that a higher pH is used throughout and the nuclear envelope finally obtained by differential rather than isopycnic centrifugation. This could ve rise to a greater degree of contamination with residual chromatin, nucleoli and llagen. A detailed comparison of the method of Kay et al. [3] and also the high ncentration magnesium treatment of Monneron et al. [4] which produces fragment- nuclear envelope, has been included in the methodological review by Harris and gutter [1]. Despite the fact that low ionic strength conditions have been claimed Scheer et al. [40] to render nuclear envelope unstable, this is not the experience the author and his colleagues who have obtained relatively intact nuclear ghosts hich retain the inner nuclear membrane and outer nuclear membrane with morpho- gically well-preserved nuclear pore complexes (see Section III).

Several other procedures for isolating nuclear envelope have been published, ost of which employ conditions which are considered to be more disruptive than e low ionic strength DNAase treatment of the author and his colleagues [1,2,37]

TABLE I

ULTRASTRUCTURAL FEATURES OF NUCLEAR ENVELOPE ISOLATED BY SEVERAL DIFFERENT PROCEDURES

Tissue	Predominant state of nuclear envelope	Integrity of nuclear pore complexes		Ref.
		Annulus	Central granule	
Rat and pig liver	Intact nuclear ghosts; some large torn double-membrane sheets	Intact	Present	1, 2, 15, 37
Rat liver	Large torn double-membrane sheets and raggy ghosts	Intact	Usually present	3, 133
Bovine liver	Single-membrane sheets and vesicles	Damaged	Not present	6, 48, 121, 122
Rat liver	Small double-membrane sheets and single-membrane vesicles	Apparently intact	Not present	34, 43, 118
Rat liver	Small double-membrane sheets	Intact	Present	7
Rat liver	Single-membrane sheets and vesicles	Intact	Probably present	58
Rat liver	Single-membrane vesicles	Damaged	Not present	4, 93, 94, 99
Rat and pig liver	Highly fragmented single-membrane sheets	Intact	Usually present	5, 103
Calf and rat thymus	Small single-membrane vesicles	Damaged	Not detectable	42
Hen erythrocytes	Small single-membrane sheets	Damaged	Not detectable	55
Pea root tips	Double-membrane sheets	Mostly intact	Not detectable	46

or of Kay et al. [3]. The use of ultrasonication has been favoured by several groups, usually in combination with a high ionic strength extraction [5,41,43] or a low ionic strength extraction [7,44,47]. DNAase digestion has also been used in conjunction with high ionic strength extraction [48–50]. The use of Triton X-100 and other nonionic surfactants cannot be considered as reasonable, as proposed by Wunderlich et al. [28], in view of the fact that the outer nuclear membrane tends to be readily removed by this reagent [51–52] and the inner nuclear membrane is likely to be modified because of the loss of phospholipids [53]. Triton X-100 may, nevertheless, prove to be a useful reagent for subfractionating the nuclear envelope (see Section IVH). Table I indicates the ultrastructural features of the nuclear envelope

lated by several different procedures. Although the ultrasonication and high nic strength treatments do yield nuclear envelope that has a very low DNA con-nt, this material does not generally maintain the overall conformation of nuclear osts, and in some instances there is clear evidence of separation of the inner clear membrane and outer nuclear membrane together with disruption of the clear pore complexes.

Nuclear extractions using salt and Triton X-100 which have been found to ve unsolubilized a residual protein matrix of nuclear acidic proteins [28,52,54] ay indicate a close structural relationship between the inner nuclear membrane d the nuclear pore complexes, which likewise remain unsolubilized, and the nuclear otein matrix. Usually the inner nuclear membrane is seen to have fibres of residual NA attached to it as well as the intranuclear protein matrix. With this fact in nd, it is perhaps reasonable to suggest that it is incorrect to try and obtain nuclear velope with a minimal DNA content, regardless of its morphological integrity. intact nuclei do have DNA closely associated with the inner nuclear membrane, release of this DNA may be partly responsible for the breakdown of the nuclear velope during an isolation procedure.

Although none of the nuclear envelope isolation procedures currently available n be considered to be completely satisfactory, experimental progress does not pear to be unduly limited. The use of nuclear envelope 'material' of slightly fferent ultrastructure and biochemical composition by the various research groups ay even prevent unintentional oversight of further significant features of this mplex membrane system.

B. *Avian erythrocyte nuclear envelope*

Isolation of nuclear envelope from the metabolically dormant nucleus of the ature chicken erythrocyte has been attempted by Zentgraph et al. [55] using a mbination of ultrasonication, high ionic strength and DNAase digestion, and also the author and his colleagues [56] using a low ionic strength treatment to disperse chromatin followed by DNAase digestion. Separation of nuclear envelope from extremely condensed chromatin of avian erythrocyte present greater technical oblems than does the chromatin of liver nuclei. The low ionic strength DNAase atment used by the author has been found to be successful only if the chromatin is oroughly decondensed by the addition of the polyanion heparin [57] prior to the zymic digestion. The final material, which is obtained by isopycnic banding on crose gradients, consists primarily of large sheets of torn nuclear envelope together ith occasional nuclear ghosts (unpublished observations). That this nuclear velope is more fragmented than that from liver nuclei is not unexpected in view of tenuous nature of the outer nuclear membrane [56,58] and the fact that there are ry few nuclear pore complexes per unit area to act as regions of stabilization between two nuclear membranes. The nuclear envelope obtained by Zentgraph et al. [55] ows an even greater degree of fragmentation and contamination with residual romatin than the material obtained by the low ionic strength DNAase procedure,

and the presence of nuclear pore complexes is not shown very convincingly. Jackson [59] has employed a procedure similar to that of Zentgraph et al. [55], but with the omission of ultrasonication. It was maintained by Jackson [59] that the inclusion of protease inhibitors was essential to prevent proteolysis and loss of polypeptide bands on his sodium dodecyl sulphate-polyacrylamide gel electropherograms.

The availability of purified chicken erythrocyte nuclear envelope is extremely useful for comparative studies and will prove to be valuable for the study of nuclear envelope changes that occur following reactivation of chicken erythrocyte nuclei in either heterokaraya [60] or in in vitro nuclear reactivation systems.

IIC. Amphibian oocyte nuclear envelope

The manual microdissection of amphibian oocyte nuclei by the method of Callan and Tomlin [61] has been used by several investigators to obtain nuclear envelope. The isolated nuclei are washed in saline to remove contaminating yolk and are lysed in water to release most of the chromatin. At some stages of oocyte development it is not possible to obtain nuclear envelope free from the nucleoli that adhere to its inner surface. Nearly all of the studies performed on this material have been of an ultrastructural nature, but Scheer [62] attempted to measure the RNA content of single nuclear pore complexes in the nuclear envelopes of *Xenopus* oocytes and obtained the value $0.41 \cdot 10^{-16}$g RNA per nuclear pore complex. Octagonality of the oocyte nuclear pore complex was shown by Gall [63] using negatively stained nuclear envelope. The annuli of the nuclear pore complex did not show up at all clearly in Gall's electron micrographs and he proposed a model for the nuclear pore complex which does not include an annulus. When negatively stained with ammonium molybdate it is found that the nuclear pore complex annuli are much more pronounced (see Section IIIB). Because of the difficulty of obtaining large quantities of oocyte nuclear envelope, it is unlikely that extensive chemical and enzymic analysis will be performed on this material.

III. ULTRASTRUCTURE

IIIA. Thin sectioning

Conventional processing for electron microscopic thin sectioning has provided a wealth of information on the ultrastructure of the nuclear envelope in intact cells and tissues as well as with isolated and purified nuclei and nuclear envelope obtained by the various preparative procedures mentioned above (Section II). Even though negative staining and freeze-cleavage have contributed greatly to the interpretation of the ultrastructural detail of nuclear envelope in recent years, thin sectioning continues to be of importance in almost all investigations on nuclear envelope. The outstanding disadvantage of thin sectioning is that the membrane material has to be chemically fixed and stained, and then dehydrated with organic solvents, any of which are likely to introduce molecular rearrangements as a result of de-

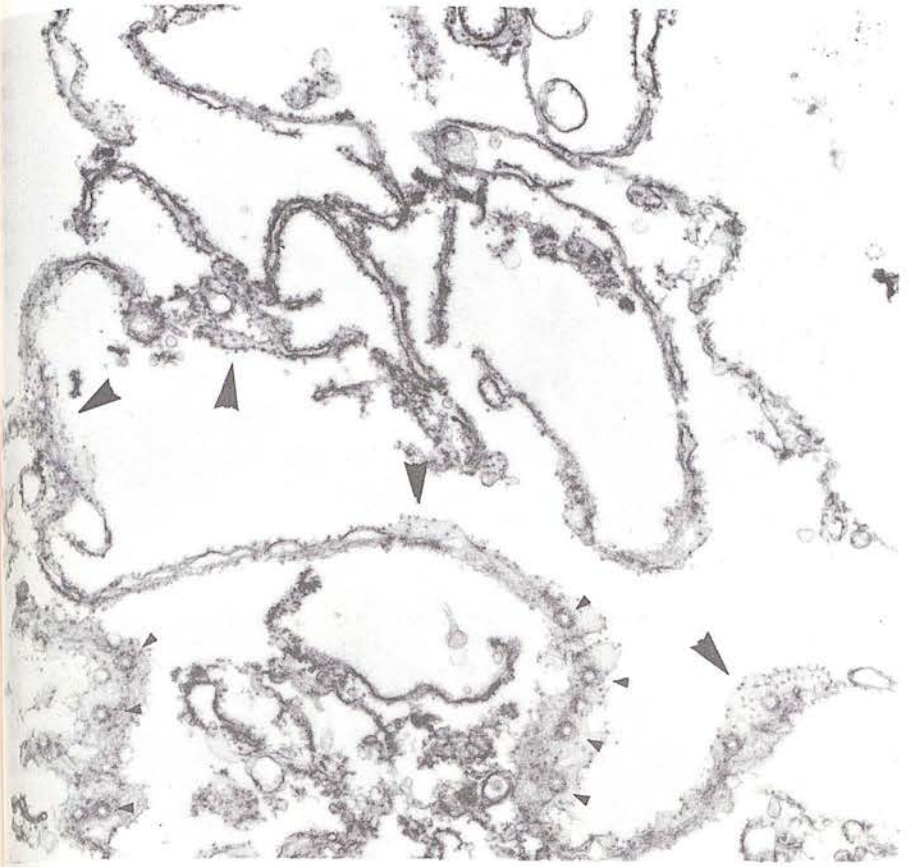

Fig. 1. Thin-sectioned rat liver nuclear envelope. Regions sectioned perpendicular to the plane of the nuclear envelope show the presence of the inner and outer nuclear membrane, and regions sectioned parallel to the nuclear envelope show the nuclear pore complexes (small arrows) and ribosome particles (large arrows). × 30 000.

turation or extraction, whereas negative staining and freeze-cleavage avoid this criticism to some extent. It should, however, be stated immediately that the results obtained by thin sectioning have, in general, been supported rather than opposed by the results of other specimen preparation techniques.

The typical two-layered nuclear membrane system observed around almost all karyotic nuclei is not readily apparent in thin sections of purified nuclear envelope that has undergone a significant degree of fragmentation during the isolation and purification procedure. Likewise, the nuclear pore complexes are less readily detected thin sections of fragmented and vesicularised nuclear envelope. If, however, the clear envelope is in the form of nuclear ghosts and large torn sheets, thin sectioning readily reveals the two nuclear membranes and the nuclear pore complexes. Fig. 1 shows thin-sectioned rat liver nuclear envelope obtained by the low ionic strength DNAase treatment of the author and his colleagues. The regions sectioned per-

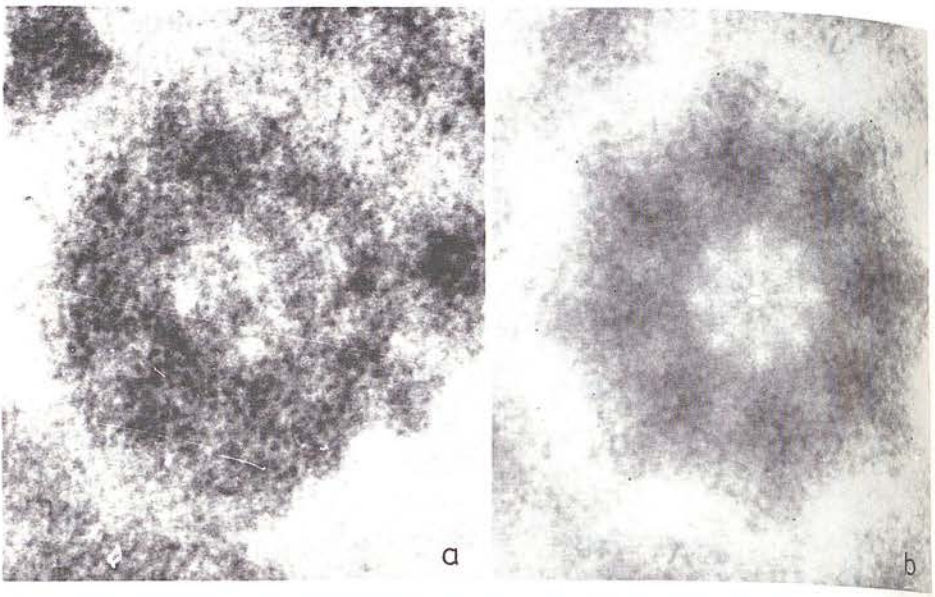

Fig. 2. A thin-sectioned nuclear pore complex subjected to eight-fold rotational image enhancement by the Markham technique 65. The enhanced image (b) shows the presence of eight hollow annular subunits, in agreement with the results of Abelson and Smith [14]. × 550 000.

pendicularly to the plane of the nuclear envelope, which show the inner nuclear membrane and outer nuclear membrane, and the regions sectioned tangentially to the nuclear envelope surface, which show the nuclear pore complex, are clearly defined. The outer nuclear membrane is usually seen to have associated with it discrete ribosome particles and the inner nuclear membrane has traces of residual chromatin. In many instances the nuclear pore complexes show the presence of a densely stained central granule, as shown in Fig. 2a. Image enhancement of the nuclear pore complexes by photographic rotation (Fig. 2b) [14,65] suggests that there are eight subunits present in the annulus in agreement with the interpretations obtained from negatively stained and freeze-cleaved material (see Section IIID).

IIIB. Negative staining

Negative staining has been used for the study of isolated nuclear envelope since the first investigations on this material [45,63,64]. Over the last ten years negative staining has been routinely used by most workers in the field and it has continued to make an important contribution to the understanding of the ultrastructure of the nuclear envelope and the nuclear pore complex in particular [11,15,16]. The author and his colleagues have shown that negative staining with ammonium molybdate reveals greater detail of the nuclear pore complex than does sodium phosphotungstate [15,39,66]. This apparent difference in the electron images may be accounted for by the varying penetration of the heavy metal-containing complex anions into the nucleoprotein annular material of the nuclear pore complexes. It is concluded

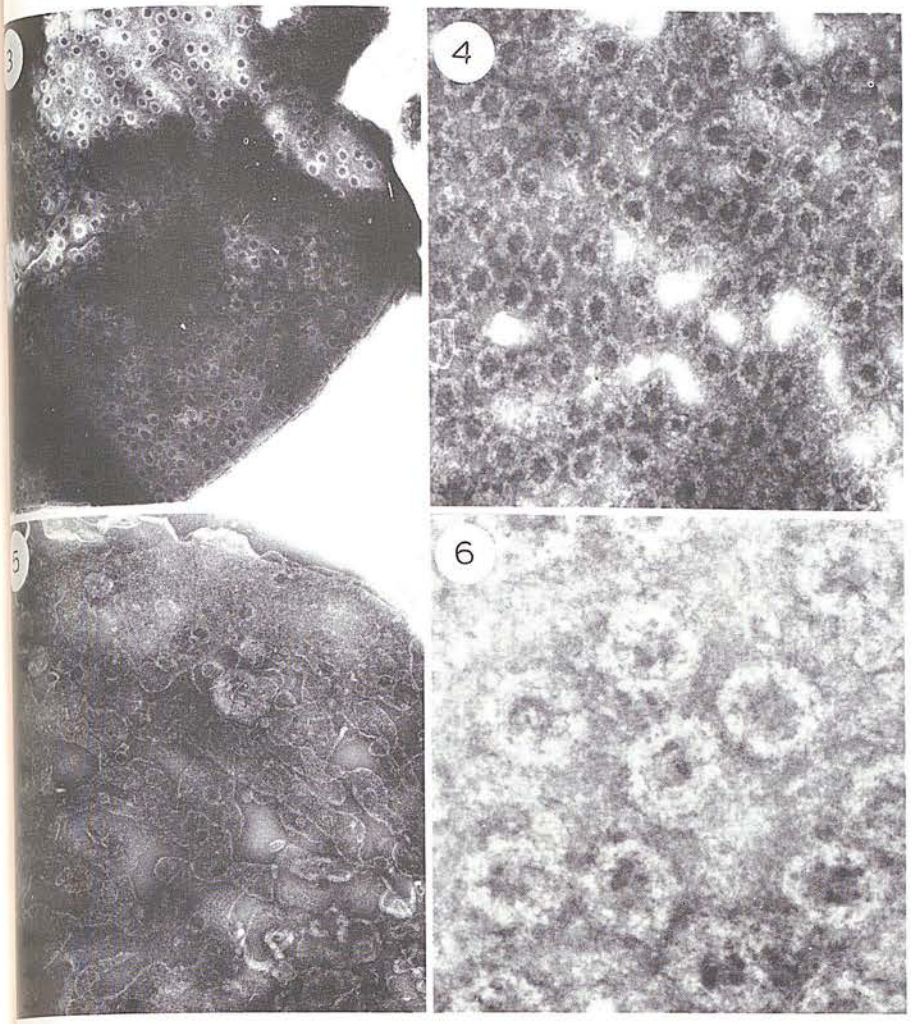

g. 3. A single rat liver nuclear ghost, negatively stained with ammonium molybdate. × 15 000.
g. 4. Part of a *Triturus* oocyte nuclear ghost, negatively stained with ammonium molybdate. 51 000.
g. 5. A single chicken erythrocyte nuclear ghost, negatively stained with ammonium molybdate. 51 000.
g. 6. Rat liver nuclear envelope, negatively stained with ammonium molybdate. × 141 000.

erefore, that the phosphotungstate anion penetrates to a greater extent than the olybdate anion, thereby reducing the detail present in the electron optical image of e nuclear pore complex annulus. Negative staining with phosphotungstate does, wever, clearly reveal the membraneous edge of the nuclear pore complex [5,15,39,]. Despite these observations, Franke and his colleagues have found that phospho- gstate negative staining does reveal considerable detail of the annular material of e nuclear pore complex of amphibian oocyte and *Tetrahymena* nuclear envelope

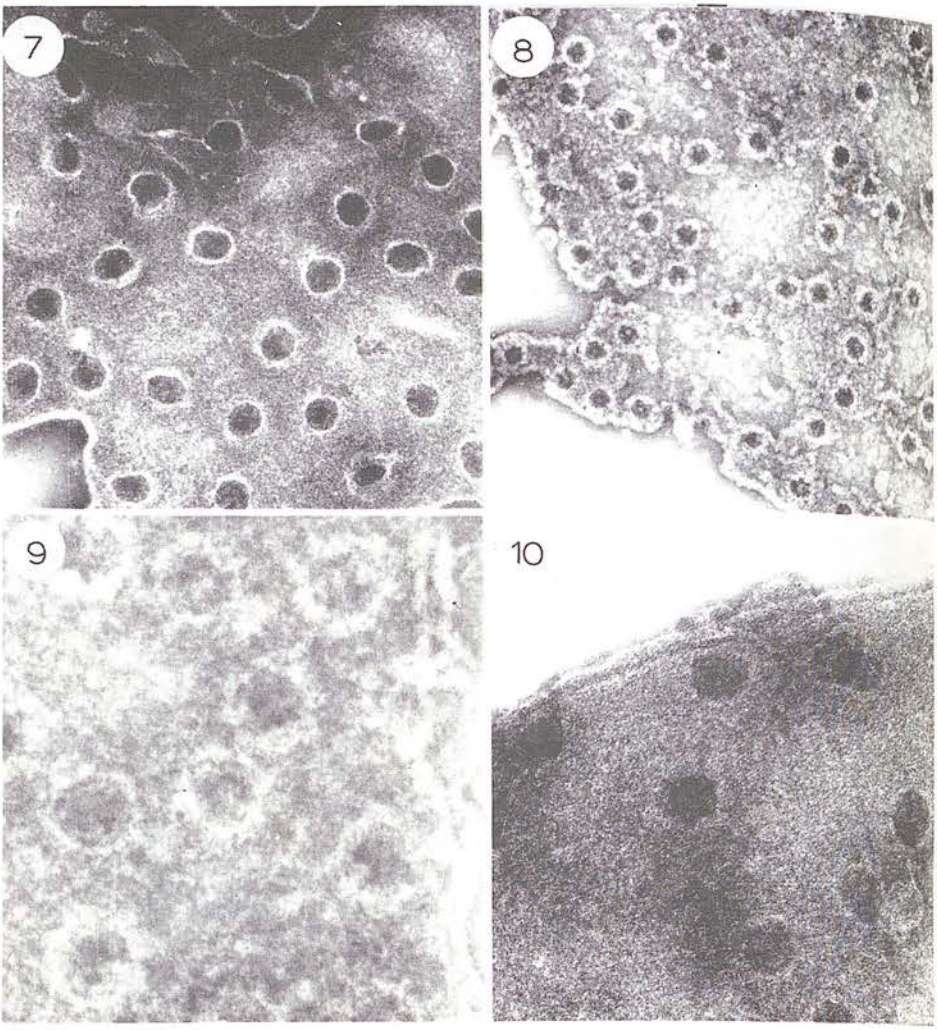

Fig. 7. Rat liver nuclear envelope, negatively stained with sodium phosphotungstate. × 66 000.
Fig. 8. Rat liver nuclear envelope, negatively stained with ammonium uranyl oxalate. × 42 000.
Fig. 9. The edge of a rat liver nuclear ghost, negatively stained with ammonium molybdate. × 141 000.
Fig. 10. The edge of a rat hepatoma nuclear ghost, negatively stained with sodium phosphotungstate. × 105 000.

[9,29,40], but very much less so for that of mammalian liver nuclear pore complexes [5]. In order to assess the integrity of the nuclear pore complex annulus, the author considers that in general it is desirable to perform negative staining with ammonium molybdate, as demonstrated by Figs. 3–5 which show nuclear ghosts of rat liver, *Triturus* oocyte and chicken erythrocyte nuclei.

The complex negative stain ammonium uranyl oxalate, which unlike uranyl acetate, can be adjusted to a neutral pH without precipitation, has been found to

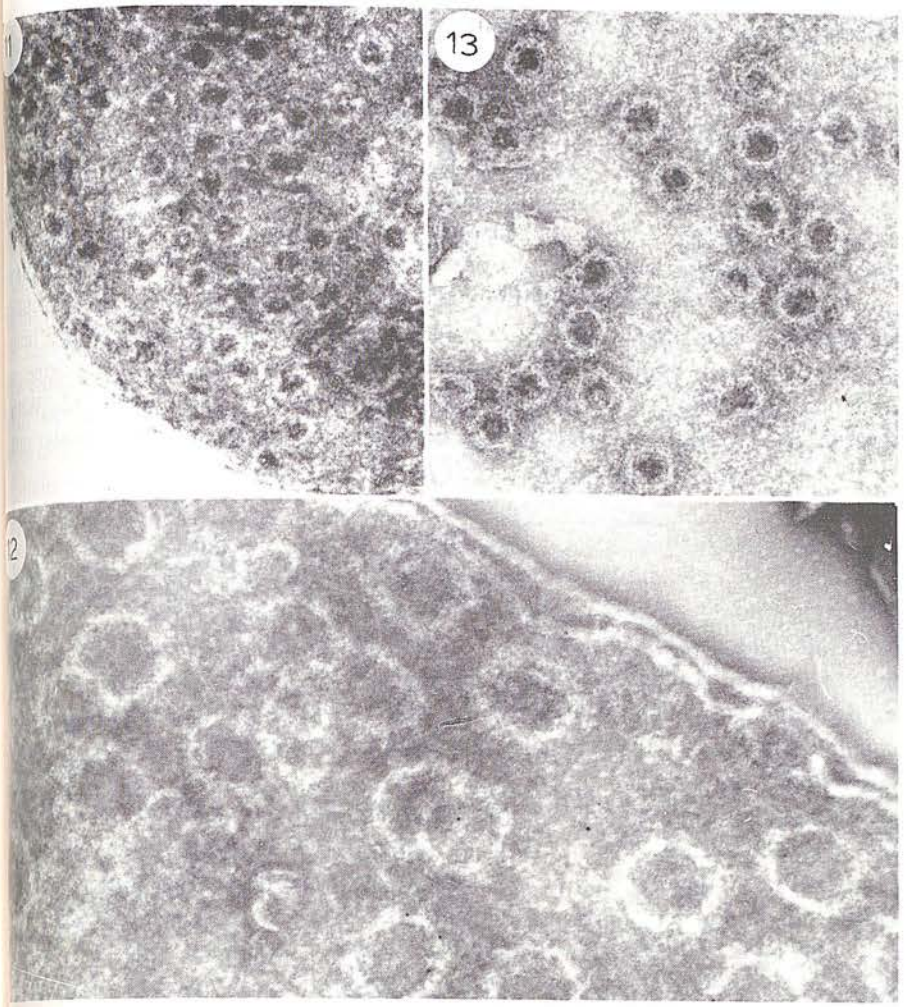

Fig. 11. The edge of a rat hepatoma nuclear ghost, negatively stained with ammonium uranyl oxalate. × 54 000.
Fig. 12. The edge of a rat liver nuclear ghost, showing clearly the overlapping of the nuclear pore complexes in the upper and lower layer of nuclear envelope, negatively stained with ammonium molybdate. × 141 000.
Fig. 13. A single layer of nuclear envelope, negatively stained with ammonium molybdate. × 69 000.

reveal the annulus of the nuclear pore complex with even greater clarity than ammonium molybdate, but the image granularity is also enhanced in an undesirable manner [39,66]. Figs. 6–8 show rat liver nuclear envelope negatively stained with ammonium molybdate, sodium phosphotungstate and ammonium uranyl oxalate, respectively, to emphasise the varying appearance of the nuclear pore complexes described above.

When intact nuclear ghosts or large torn sheets of nuclear envelope are subjected

to negative staining it is always possible to detect a double electron transparent line running along the edge of the nuclear ghost or at a region where a large torn sheet of nuclear envelope folds back on itself to give a double layer. This image, which is given by all the forementioned negative staining salts, is clearly an indication of the presence of both the inner nuclear membrane and outer nuclear membrane. Figs. 9–11 show the edges of nuclear ghosts which demonstrate this negative staining feature. A point to bear in mind in the present context is that with intact nuclear ghosts that have been collapsed onto the carbon support film of an electron microscope grid during the negative staining procedure, there will be two layers of nuclear envelope (i.e. four layers of membrane) contributing to the electron optical image; the nuclear pore complexes in the upper and lower layer of nuclear envelope may therefore overlap resulting in some loss of image clarity, as shown in Fig. 12. With a single layer of nuclear envelope, that has not folded over, a significantly greater image clarity is obtained, as shown in Fig. 13.

IIIC. Freeze cleavage

Owing to technical difficulties freeze cleavage has not been so readily applied to isolated nuclear envelope as to the nuclear envelope of nuclei inside intact cells. When used with isolated fragmented nuclear envelope [4], freeze cleavage does not provide any information that cannot be more readily obtained by either thin sectioning or negative staining. Kartenbeck et al. [67] have recently reviewed the freeze cleavage of nuclear envelope, so the discussion of this approach will be deliberately restricted.

Perhaps the main advantage of freeze cleavage for the study of nuclear envelope is with intact cells, tissues or isolated and purified nuclei. It will provide quantitative information on the nuclear pore complex frequency and distribution, facts which cannot so readily be obtained by thin sectioning or negative staining. Thus the variation of the nuclear pore complex frequency in cells in differing physiological states [68,71], when externally applied cellular stimulation is given using phytohaemagglutinin [18] or by altering the temperature [20,72], as revealed by freeze cleavage, indicates the dynamic nature of the nuclear envelope with respect to the number of nuclear pore complexes per unit area. A comparison of normal and malignant cells has been made using freeze cleavage [39,73], it being claimed that there is a statistically significant increase in the nuclear pore complex frequency in the nuclear envelope of the malignant cells [73]. Although the distribution of the nuclear pore complexes over the nuclear envelope is relatively constant and apparently random, Maul et al. [18] have shown that with rat kidney cells there is a constant inter-pore distance of 130 nm and Roberts and Northcote [74] have shown linear arrays of nuclear pore complexes on freeze-cleaved nuclei of *Equisetum* spores. It has also been reported that the nuclear envelope adjacent to the Golgi apparatus of the algae *Ochromona danicia* has a greater pore density than the rest of the nuclear envelope [75] and in synchronous cultures of *Saccharomyces cervisiae* it has been shown that the nuclear envelope adjacent to the cytoplasmic vacuole is devoid of

clear pore complexes [76]. Other instances of varied pore distribution have also en reported [77,80]. Meyer et al. [81] have claimed to show a network-like distribution of particles on the nucleoplasmic surfaces of the inner nuclear membrane d have suggested that these may be sites where DNA is attached to the membrane. ecause the interpretation of freeze-cleaved images of nuclear envelope is more fficult at this level than for other membranes systems [76,82], considerable care has be taken before making claims such as this, where precise knowledge of the plane cleavage or the amount of etching may not be available. Generally speaking the solution obtained from freeze-cleaved specimens is not quite as good as that from in sectioning and negative staining, but the octagonal symmetry of the nuclear re complex is clearly supported by this technique. [67,73,83]. The ultrastructural tail within the nuclear pore complex and its annulus is usually less evident by eeze cleavage, the nuclear pore complex appearing primarily as stud-like projections shallow depressions which vary with the curvature of the nucleus because of the rying amount of shadowing metal deposited. Occasional observations do show e nuclear pore complex to have pronounced annuli [84]. On avian erythrocyte uclei the nuclear pore complexes do not appear as clearly as they do on other tissues 7]. This may be a reflection of the dormant metabolic state of these cells which has oduced an alteration of the nuclear pore complex or to their stability during eezing. It is, however, clear, that in these cells there is a very low pore frequency, d a similar situation exists on the amphibian erythrocyte nuclear envelope [85].

Apart from the frequency and distribution of nuclear pore complexes, freeze eavage also provides information about the frequency and distribution of intramembrane particles (proteins) revealed on cleavage [72] and membrane surface rticles revealed by subsequent etching. Thus, the future use of freeze cleavage for uclear envelope studies may be predicted to provide information at the molecular vel which will be additional to that obtained by negative staining and by other iophysical and biochemical techniques.

Figs. 14 and 15 show representative areas of freeze cleaved rat liver nuclei. n Fig. 14 the plane of cleavage passes through a nucleus rather than along the nuclear velope and the two nuclear membranes, with the intra-cisternal space between them, re clearly revealed. When the cleavage plane passes along the nuclear envelope a rge area showing the distribution and frequency of the nuclear pore complex is ften obtained (Fig. 15). With isolated and purified nuclei similar results can be btained [39] and a qualitative assessment of the amount of contaminatory material dhering to the nuclei can be made which is complementary to that obtained from hin sectioning.

III. The nuclear pore complex

The nuclear pore complex is widely accepted as a structure of considerable portance, even though this is not at the moment precisely defined. It has even een suggested that the nuclear pore complex might be considered as a subcellular rganelle [1,11,14].

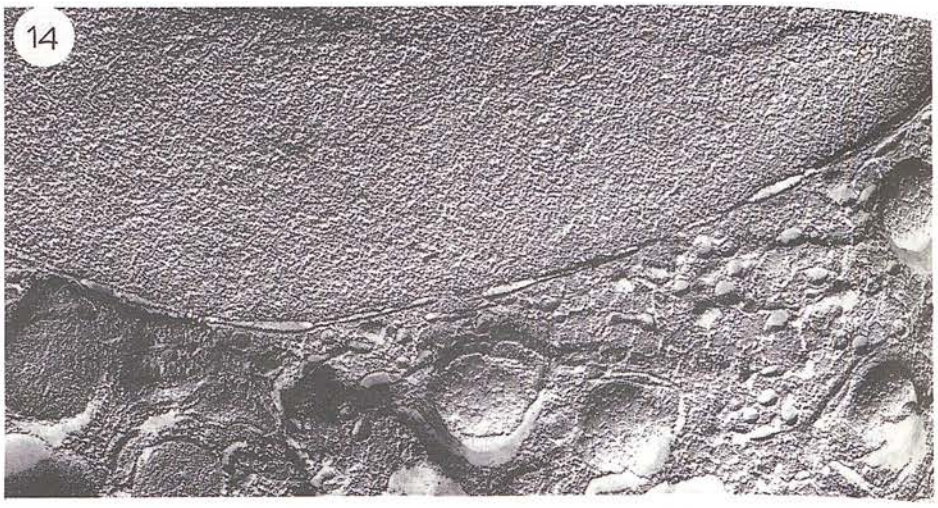

Fig. 14. Freeze-fractured rat liver, showing a region where the fracture plane passes through a cell nucleus. The inner nuclear membrane and outer nuclear membrane are clearly defined. × 33 000.
Fig. 15. Freeze-fractured rat liver, showing a region where the fracture plane passes along the nuclear envelope. × 27 000.

TABLE II

DIMENSIONS OF THE NUCLEAR PORE COMPLEX

Tissue	Inner diam. (nm)	Outer diam. (nm)	Ref.
Thin sectioning			
Acer pseudoplatanus	53	104	11
Triturus oocyte	–	80–100	12
Mouse fibroblast 3T3	–	68–72	14
African green monkey kidney	–	75–80	14
Rat liver	43	92	39
Rat hepatoma D_{23}	50	96	39
Tetrahymena	35	67	69
Echinus oocyte	74	97	88
Freeze-fracture			
Bovine liver[a]	65	100–120	10
Rat liver	–	107	39
Rat hepatoma D_{23}	–	106	39
Tetrahymena	51	78	69
Human melanoblastoma			
Log phase	–	86	73
Stationary phase	–	93	73
Artichoke	68	99	82
Negative staining			
Several amphibian oocytes (PTA)	–	71–75	9
Rat liver (AM)	52	100	39
Rat liver (PTA)	66	94	39
Rat liver (Uox)	62	114	39
Rat hepatoma D_{23} (AM)	52	93	39
Rat hepatoma D_{23} (PTA)	64	110	39
Rat hepatoma D_{23} (Uox)	59	99	39
Mouse liver (PTA)	65	–	45
Triturus oocyte (PTA)	66	–	63
Tetrahymena (PTA)	34	66	69

[a] Air-dried platinum-carbon replica.

AM, ammonium molybdate; PTA, sodium/potassium phosphotungstate; Uox, ammonium uranyl oxalate.

Early thin sectioning [12,86,88] and negative staining studies [45,63,64] indicated that nuclear pore complexes were octagonal structures penetrating through the two nuclear membranes, with annular material projecting into both the nucleoplasm and cytoplasm. This interpretation has been supported by more recent studies, using freeze cleavage [83] as well as other specimen preparation techniques [5,9,11,13–15, 39,74,89]. The dimensions of nuclear pore complexes given in the literature vary considerably with the tissue studied and the electron microscopic specimen technique employed. Table II compares the dimensions of the nuclear pore complex obtained by several authors, using the different specimen preparation techniques.

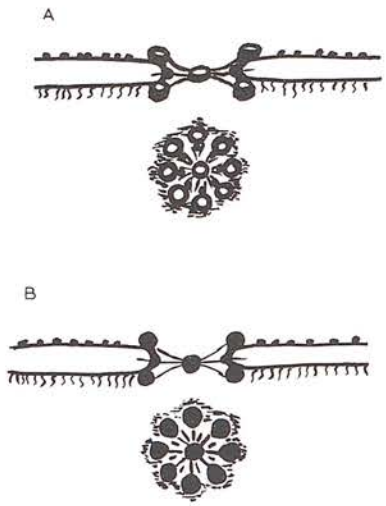

Fig. 16. Diagrammatic models of the nuclear pore complex. Model A approximates to the mini-tubule or hollow annular subunit interpretations, and model B approximates to the compact globular annular subunit interpretation.

Numerous attempts have been made to present diagrammatic representations of the nuclear pore complex that comply with the interpretations the particular investigator derived from his electron micrographs [1,5,8,10,15,29,64,67,74,86–89]. Unfortunately no universally accepted model of the nuclear pore complex has yet been produced, although most of the models have several features in common, such as the octagonal symmetry and the presence of non-membraneous material that passes through the pore with a protruding annulus on either side of the nuclear envelope. A central granule is usually included, which is connected possibly by fibrils to the annular material or the portion of the pore complex that penetrates between the two nuclear membranes. The inner nuclear membrane and outer nuclear membrane appear to fuse with the non-membranous component of the nuclear pore complex, but it is not absolutely clear whether there is a direct continuity between the two nuclear membranes around the edge of the non-membranous material. Thin sections do not show a clear 'unit membrane' in this region, but negative staining with phosphotungstate does reveal a pronounced electron transparent membranous rim at the edge of the nuclear pore complex (see Section IIIB above, and Fig. 7). Perhaps the main area of disagreement centres around the problem of whether or not the annular material of the nuclear pore complex consists of eight globular or hollow, tube-like subunits or 'sub-annuli'. The aim of any nuclear pore complex model must be to represent the structure in terms of a macromolecular organisation, but unfortunately this level of interpretation has not yet been achieved. [11,75].

Fig. 16 shows two models of the nuclear pore complex: Model A approximates to the models of Abelson and Smith [14], Vivier [13], Harris [15], Afzelius [88] and

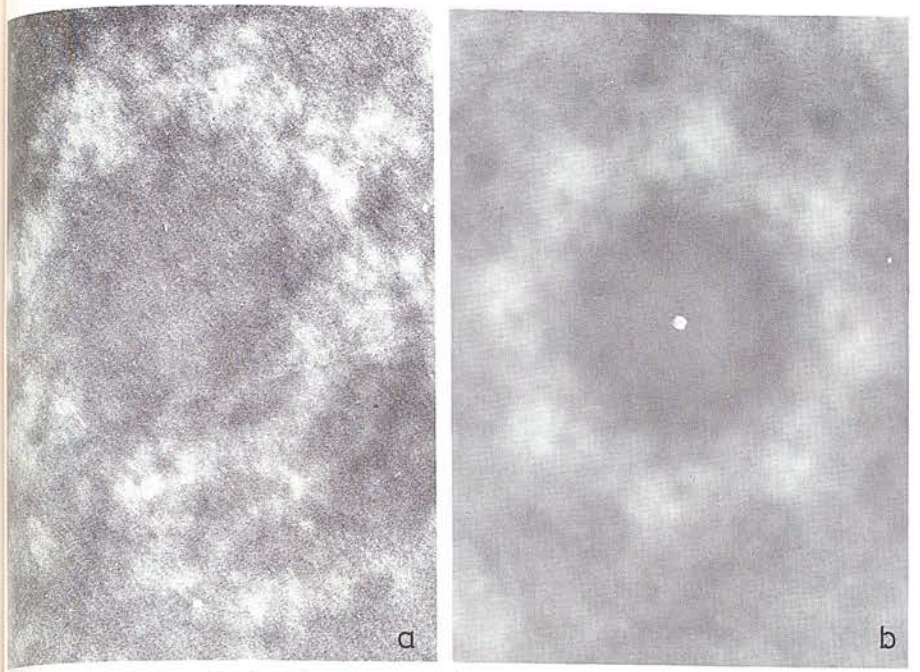

Fig. 17. A negatively stained nuclear pore complex subjected to eight-fold rotational image enhancement by the Markham technique [65]. The enhanced image (b) shows the presence of eight hollow annular subunits, each with an electron-dense centre due to the penetration of negative stain (cf. Fig. 2). × 480 000.

Wischnitzer [12]. Model B approximates to the models of Gall [63], Franke and Scheer [9], Hoeijmakers et al. [10], Wunderlich et al. [28], Roberts and Northcote [74], Stevens and André [86] and La Cour and Wells [89]. As it is impossible from the available evidence to decide which, if any, of the various nuclear pore complex models is likely to be more correct, it is desirable to simply present the various alternatives, in the hope that future investigations will clarify the issue.

From his own experimental work the author favours the interpretation of the nuclear pore complex which proposes hollow annular subunits. Negative staining studies in which samples of nuclear envelope and nuclear pore complexes have undergone partial fragmentation, due to the shearing forces applied to the nuclear envelope at the time of spreading the material on the carbon film of the EM specimen grid, indicate that the nuclear pore complex may well be composed of eight hollow macromolecular annular components [15]. In the intact nuclear pore complex these hollow components are thought to be bound together by the more amorphous outer material of the annulus. Image enhancement by photographic rotation [65] supports this interpretation for both negatively stained and thin-sectioned nuclear pore complexes. With negative staining (Fig. 17) the proposed hollow annular subunits are seen to have electron dense centres, as a result of the negative stain penetrating into the hollow core of the subunit. With thin sectioning the hollow core is revealed

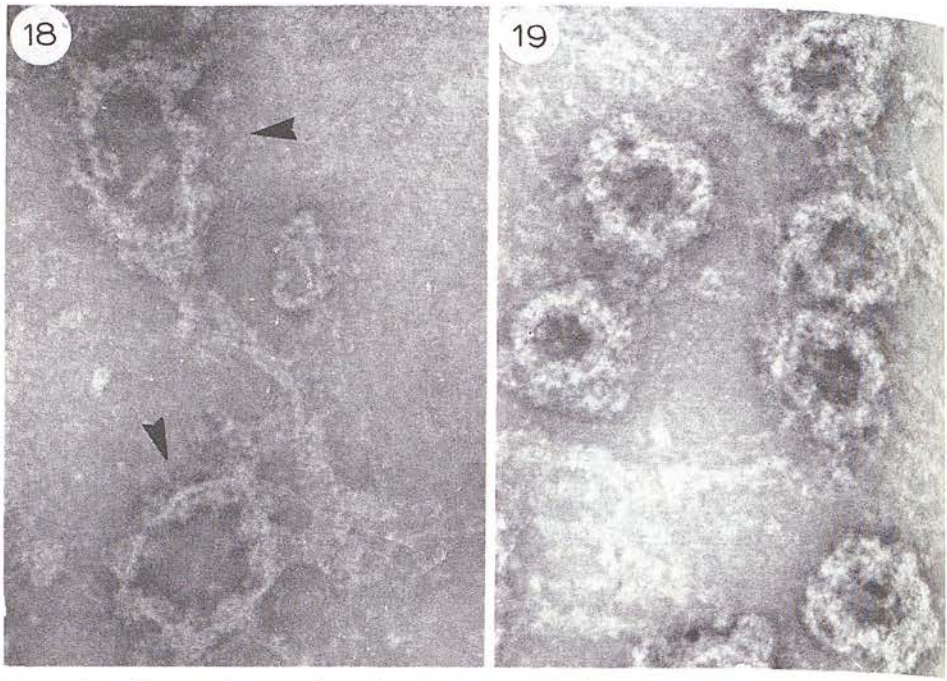

Fig. 18. Rat liver nuclear envelope that has undergone disruption during the negative staining spreading procedure. Two diffuse, possibly fragmenting, nuclear pore complexes are present (arrowed). Negatively stained with ammonium molybdate. × 183 000.
Fig. 19. Rat liver nuclear envelope that has undergone disruption during the negative staining spreading procedure. Several compact nuclear pore complexes are present. Negatively stained with ammonium molybdate. × 183 000.

as an electron-transparent circle surrounded by the electron-opaque positively stained material of the nuclear pore complex annulus as shown in Fig. 2. The published thin-sectioning results of Abelson and Smith [14] using photographic enhancement show the nuclear pore complexes of cultured African green monkey kidney cells to be revealed as eight electrontransparent regions set in an electron-opaque background, and the negative-staining results of Gall using *Triturus* oocyte nuclear envelope [68] show a circle of eight electron-opaque regions set in an electron-transparent background. Even the negative-staining results of Franke [45,64] show an indication of the presence of hollow annular subunits.

In the recent metal shadowing study of Hoeijmakers et al. [10] who spread nuclei from cultured bovine liver cells following isolation in a Triton X-100, Tris · HCl buffer, it was found that there were octagonal annuli and slightly smaller compact circular structures lying adjacent to the nuclei. These two structures were interpreted as being the outer cytoplasmic annulus and the central or inner component of the nuclear pore complex that passes between the two nuclear membranes. In addition, Hoeijmakers et al. [10] claimed to obtain the release of almost intact nuclear pore complex following brief trypsinisation of nuclei. From negative staining studies

sing spread and disrupted nuclear envelope the author has obtained similar results. Fig. 18 shows what might be the outer cytoplasmic annulus of the nuclear pore complex and Fig. 19 shows what might be the central more compact component of slightly smaller diameter. Great care has, nevertheless, to be taken in this context since the larger nuclear pore complex annulus (Fig. 18) could possibly be produced, as a spreading artifact, from the intact nuclear pore complexes.

IIE. Assessment of nuclear purity

Despite the fact that many enzymes have shown to be present in the nuclear envelope by cytochemical techniques and by standard assay procedures, to date no significant increase in the specific activity of any enzyme over and above that of its specific activity in endoplasmic reticulum has been reported in widely reproducible manner. Because of this situation, it is considered that the role of the electron microscope in assessing the purity of nuclear envelope by the detection of membranes containing nuclear pore complex, together with the absence of smooth membranes such as endoplasmic reticulum, Golgi and plasma membrane, which do not show nuclear pore complex, is paramount. Ideally, all that should be detected, by either thin sectioning or negative staining, are intact nuclear ghosts together with large torn sheets, both of which are studded with numerous nuclear pore complexes with the two nuclear membranes morphologically opposed, as they are in the intact cell. The occasional small strand of collagen, which apparently adheres to the nuclear envelope throughout the purification scheme, is the only contaminant that has been found to be present in the material produced by the procedure of Harris and Milne [2]. Mitochondria and lysosomes, which are readily detected by electron microscopy are not present; enzymic assay for succinate dehydrogenase confirms the absence of mitochondria, but there does appear to be a residual non-lysosomal acid phosphatase associated with the nuclear envelope.

If during the isolation and purification procedure the nuclear envelope undergoes a considerable degree of fragmentation it might well be difficult, if not impossible, to adhere the rigorous ultrastructural criteria for nuclear envelope purity presented above owing to the overall similarity of small fragments or vesicles of nuclear envelope that lack nuclear pore complex with other vesicularised cytomembranes. This further emphasises the desirability of obtaining nuclear envelope in the form of intact nuclear ghosts.

IIIF. Cytochemistry of the nuclear envelope

The use of electron microscopic cytochemical techniques has been of considerable value for the study of the endoplasmic reticulum, Golgi, lysosomes, mitochondria and plasma membrane and over recent years cytochemical data has accumulated on the nuclear envelope of intact nuclei. To date very little work has been published on the application of electron microscopic cytochemistry to isolated nuclear envelope. In his review of nuclear enzymes, Verbrodt [90] discusses several enzymes that have been located in the nuclear envelope, and makes the point that almost all the enzymes

TABLE III

ENZYMES DETECTED IN NUCLEAR ENVELOPE BY CYTOCHEMICAL TECHNIQUES

NADP-linked glucose-6-phosphate dehydrogenase
Oxidase (BED* oxidase, in plants)
Endogenous peroxidase
Acetylcholine esterase (in neurones)
Acid phosphatase
Glucose-6-phosphatase
Aryl sulphatase
Nucleoside diphosphatase
Nucleoside triphosphatase (not Na^+/K^+-stimulated)
Cyclic 3′,5′-adenosine monophosphate phosphodiesterase
Cytochrome oxidase (not present in endoplasmic reticulum)
Adenyl cyclase
Thiamine pyrophosphatase
Acetyl-CoA carboxylase
5′-Nucleotidase.

are also present in the endoplasmic reticulum. Of the nuclear envelope enzymes listed in Table III, cytochrome oxidase is the only one that is not detectable in the endoplasmic reticulum.

The location of the nuclear envelope ATPase has interested workers for several years. Yasazumi and Tsubo [91] claimed that the lead phosphate reaction product of the nuclear envelope ATPase was situated beside the nuclear pore complexes. While other workers have clearly shown the presence of the ATPase in the nuclear envelope [92–95], the claim that it is located in the nuclear pore complex is not generally thought to be correct. It is widely accepted that ATPase is a very difficult enzyme to assess cytochemically, in view of its sensitivity to fixatives. The same comment applies to cytochrome oxidase, which has been detected primarily in association with the inner nuclear membrane [96–98]. The plasma membrane marker 5′-nucleotidase has been detected cytochemically in rat liver nuclear envelope [94] and adenylate cyclase has been shown in thymocyte nuclear envelope [99]. It is interesting therefore, that an earlier study on lymphocytes [100] indicated the presence of a cyclic 3′5′-adenosine monophosphatase in the nuclear envelope. A recent report by Yoo and Oreland [101] shows clearly that monoamine oxidase is not present in the nuclear envelope. This observation is contrary to the results of Gorkin [102] using a conventional enzyme assay system, but with *p*-nitrophenylethylamine as a rather unconventional substrate. Using kynuramine as substrate, the author and his colleagues have been unable to detect monoamine oxidase activity in rat liver nuclear envelope (see also Section IVE).

* BED, *N,N′*-bis-(4-aminophenyl)-*N,N′*-dimethylethylene–diamine.

TABLE IV

THE GROSS COMPOSITION OF NUCLEAR ENVELOPE

The results are expressed as percentage of weight.

Reference	Tissue	Protein	Phospholipid	DNA	RNA
Agutter [7]	Rat liver	64.0	23.0	8.0	5.0
Berezney et al. [48]	Bovine liver	70.4	22.7	1.1	5.8
Franke et al. [5]	Rat liver	77.7	16.6	2.0	3.7
Kay et al. [3]	Rat liver	65.7	26.7	3.9	3.6
Kashnig and Kasper [42]	Rat liver	67.4	26.1	0.0	6.6
Milne et al. [37]	Rat liver	75.0	15.0	3.0	7.0
Monneron et al. [4]	Rat liver	73.0	23.0	0.6	3.0
Philipp et al. [104][a]	Onion root tip	67.7	14.9	1.7	5.5
Zentgraf et al. [55][b]	Hen erythrocyte	75.4	13.0	3.8	4.0

[a] Nonpolar lipids account for 10% of weight.
[b] Cholesterol and nonpolar lipids account for 3.7% of weight.

IV. BIOCHEMISTRY OF THE NUCLEAR ENVELOPE

IVA. Chemical composition of the nuclear envelope

The protein, lipid, DNA, RNA and sugar content of isolated nuclear envelope has been determined by several groups of workers [3,7,37,41,46,55,103,104]. Table IV summarises the analytical data of some of these groups. It is significant that the isolation procedures employing high salt and ultrasonication treatments produce nuclear envelope material that has a very low DNA content and often cause fragmentation of the overall nuclear envelope and separation of the inner nuclear membrane and outer nuclear membrane. On the other hand, the low ionic strength isolation procedures [1–3,36,37,56] have a significantly higher DNA content, but at the same time maintain a superior morphological integrity, assessed by the preservation of relatively intact nuclear ghosts possessing both inner and outer nuclear membranes and nuclear pore complexes with clearly defined annuli. In view of the apparent similarity of the nuclear protein matrix [52] and the proteins of the nuclear envelope, procedures such as those using low ionic strength treatments which leave a small amount of residual chromatin attached to the inner nuclear membrane are probably preferable. The microdissection and hypotonic lysis procedure used for obtaining amphibian oocyte nuclear envelope [62] likewise leaves some residual chromatin attached to the inner nuclear membrane. It has recently been shown by Scheer et al. [40] that extraction of *Xenopus* and *Triturus* nuclear envelope with Triton X-100 leaves an inner nuclear membrane residue together with a granulo-fibrilar chromatin residue that is shown to interconnect the nuclear pore complex; the fibrilar nature of the chromatin residue/inner nuclear membrane after extraction of rat liver nuclear envelope with Triton X-100 is, however, less convincing.

Most investigators have detected a significant, yet low, quantity of RNA

TABLE V

PHOSPHOLIPID COMPOSITION OF NUCLEAR ENVELOPE FROM DIFFERENT CELL TYPES

The results are expressed as percentage of total phospholipid.

Phospholipid	Reference: Jarasch et al. [41]	Franke et al. [103]	Kleinig [105]	Kleinig [105]	Kleinig et al. [106]	Khan-dwala and Kasper [108]	Philipp et al. [104]
	Tissue: Calf thymus	Rat liver	Pig liver	Rat liver	Hen erythro-cyte	Rat liver	Onion root tip
SPH	1.7	5.8	2.4	3.2	13.0	2.7	–
PC	68.0	57.7	58.2	61.4	53.0	59.7	25.2
PE	15.0	24.2	25.9	22.7	26.0	18.8	17.1
PS	6.1	1.8	4.4	3.6	–	14.6	2.0
PI		6.4	8.9	8.6	7.1		7.4
PA	1.7	–	<1.0	<1.0	–	–	34.3
LPC	1.7	2.6	<1.0	1.5	–	2.4	3.2
LPE	4.8	2.0	–	–	–	–	3.5
CL	–	–	–	–	–	–	2.1

Abbreviations: SPH, sphingomyelin; PC, phosphatidylcholine; PE, phosphatidylethanolamine; PS, phosphatidylserine; PI, phosphatidylinositol; PA, phosphatidic acid; LPC, lysophosphatidylcholine; LPE, lysophosphatidylethanolimine; CL, cardiolipin.

attached to the nuclear envelope (see Table IV) and Scheer [62] has claimed that most of the RNA of amphibian oocyte nuclear envelope is associated with the nuclear pore complex. While this may well be correct, confirmatory evidence is required from the direct analysis of fractionated nuclear envelope (i.e. nuclear pore complex, inner nuclear membrane and outer nuclear membrane; see Section IVH) as it is likely that at least part of the nuclear envelope RNA can be accounted for by the ribosomes attached to the outer nuclear membrane.

IVB. Lipids of the nuclear envelope

It is widely accepted that most, if not all, of the nuclear lipids are located in the nuclear envelope. Considerable support is given to this premise by the direct comparison of the lipids extracted from intact nuclei with those from isolated nuclear envelope. The various classes of lipid, particularly those in rat liver nuclear envelope, have been studied by several groups [4,103–108]. It is immediately apparent from the data of these workers that the lipid content of the nuclear envelope is very similar to that of the endoplasmic reticulum, in particular that both nuclear envelope and endoplasmic reticulum have a low content of cholesterol and sphingomyelin compared to the plasma membrane and Golgi membranes. Table V summarises the nuclear envelope phospholipid composition obtained by several groups using different tissues.

Information on the major fatty acid composition of the nuclear envelope phospholipids is also available in the literature [104,106].

An interesting finding has been the increased amount of cholesterol ester relative to phospholipids in the nuclear envelope compared to the endoplasmic reticulum [105], but the ratio of unesterified cholesterol remains the same. The very high sphingomyelin and cholesterol content of hen erythrocyte nuclear envelope [106] may indicate that contamination with plasma membrane is present, since residual chromatin may have caused binding of the plasma membrane, as seems likely from the published electron micrographs [55]. This interpretation is further supported by the similarity of the phospholipid fatty acids from the isolated plasma membrane and nuclear envelope of hen erythrocytes [106]. The high amount of phosphatidic acid found in onion root tip nuclear envelope [104] is likely to be suspect, due to the autolytic breakdown of phospholipids by phospholipase D during the isolation procedure. The presence of cardiolipin in onion root tip [104] and bovine liver nuclear envelope [107] may well indicate the presence of mitochondrial contamination.

IVC. Carbohydrate content of the nuclear envelope

Only recently have investigators performed analysis for the sugar content of either isolated and purified nuclei or nuclear envelope. The available information suggests that most of the carbohydrate is associated with the nuclear envelope proteins rather than the lipids [107]. Further support for this is given by the presence of bands stained for glycoproteins on sodium dodecyl sulphate (SDS)-polyacrylamide electrophoresis gels of nuclear envelope [34,109]; the main glycoprotein band is of M_r approx. 160 000, and several minor bands are present in the M_r range 50 000–74 000. Kawasaki and Yamashina [110] have performed carbohydrate analysis with rat liver nuclear envelope which has revealed the presence of mannose, glucose and glucosamine, with smaller amounts of galactose, galactosamine and sialic acid. Removal of the outer nuclear membrane by extraction with Triton X-100 indicates that most of the mannose and glucosamine is located in the outer nuclear membrane, whereas the glucose is present in both inner nuclear membrane and outer nuclear membrane. Recently Franke et al. [103] have analysed their rat liver nuclear envelope for carbohydrates and have obtained a similar pattern to that of Kawasaki and Yamashina [110] although their glucose content is very much lower.

The glycopeptides obtained by pronase digestion of the nuclear envelope have been fractionated [110] to produce a major neutral and a minor acidic fraction. The neutral glycopeptide contains 74% of the total glucosamine and has a molar ratio of 1:3 for glucosamine and mannose, which is similar to that obtained for the neutral glycopeptide fraction from endoplasmic reticulum. Supporting evidence that little sialic acid is present in the nuclear envelope has been provided by the studies of other groups [43,103,107]. Incorporation studies using [^{14}C]glucosamine [110] indicate that the carbohydrate of nuclear envelope is synthesised in situ, in a similar manner to endoplasmic reticulum, but unlike the plasma membrane which receives carbohydrate via the endoplasmic and other cytomembranes. Significantly, Mancini et al.

[111] and Berezney and Coffey [52] have reported that [^{3}H] glucosamine and also sialic acid are incorporated into the nuclear protein matrix, which may further emphasize the similarity between the matrix and the nuclear envelope with respect to its glycoprotein content.

That the carbohydrate residues present in the nuclear envelope are exposed on the surfaces of the membranes is firmly indicated by the binding of plant lectins to purified nuclei [112–114]. Concanavalin A has been shown to bind both the inner nuclear membrane and outer nuclear membrane [114] but it is not entirely clear whether both the intracisternal and cytoplasmic surfaces of the outer nuclear membrane bind Concanavalin A. It does appear that only the intracisternal surface of the inner nuclear membrane binds Concanavalin A, but this could be due to the inaccessibility of the nucleoplasmic surface of the inner nuclear membrane to Concanavalin A. Stoddart and Price [115] using nuclei from rat liver, hepatoma and sarcoma show a reduced quantity of sialic acid and galactosamine residues in the tumour nuclear envelope, by agglutination studies using the carbohydrate-binding protein approtinin and the *Ricinis commuis* lectin.

IVD. Proteins of the nuclear envelope

Studies performed with the aim of obtaining information on the protein or polypeptide content of the nuclear envelope have been, to a large extent, dependent on the application of solubilization procedures with the subsequent separation of the solubilised material by electrophoresis systems. Polyacrylamide gel electrophoresis in the presence of SDS using nuclear envelope solubilised in 2% SDS/1% 2-mercaptoethanol has been the most useful electrophoretic system to date, even though this system does produce complete dissociation of protein and nucleoprotein complexes into unfolded polypeptide chains with release of the nucleic acids [4,37,56, 109,116]. Little success has been obtained using simpler electrophoresis systems that avoid the use of surfactants. Figs. 20a–d show representative samples of rat liver nuclear envelope (a) and endoplasmic reticulum (b), and chicken erythrocyte nuclear envelope (c) and plasma membrane (d) electrophoresed on 7% polyacrylamide gels in the presence of 0.1% SDS. Although there is some similarity between the rat liver nuclear envelope and endoplasmic reticulum, most of the polypeptide bands are clearly different; the chicken erythrocyte nuclear envelope and plasma membrane, on the other hand, show very little similarity. The gel of rat liver nuclear envelope (Fig. 20a) shows a considerable similarity with the one produced by Bornens and Kasper [109], particularly with respect to the sparsity of high molecular weight polypeptides and the preponderance of polypeptides of M_r 50 000–80 000. The presence of two distinct polypeptide bands in the region of M_r 53 000 (arrowed in Fig. 21a) is also shown by Bornens and Kasper [109]. The presence of slightly greater amounts of the low nuclear weight histone bands on the gel of our material compared to that of Bornens and Kasper [109] is reasonable in the light of the fact that the latter was isolated by a procedure involving citrate washing, ultrasonication and high salt extraction.

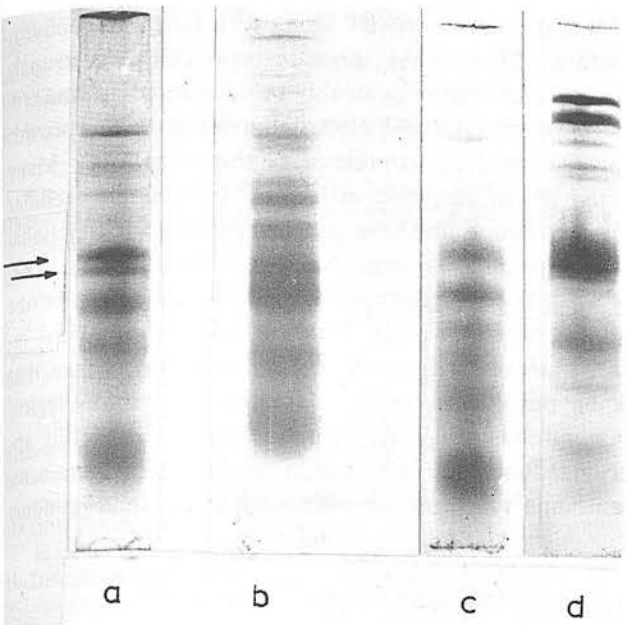

Fig. 20. Electrophoresis on 7% polyacrylamide gel in the presence of 0.1% SDS. a, Rat liver nuclear envelope; b, rat liver endoplasmic reticulum; c, chicken erythrocyte nuclear envelope; d, chicken erythrocyte plasma membrane.

Separation of the nuclear envelope polypeptides has been obtained by column chromatography of SDS-solubilised nuclear envelope on Sephadex G-150 in the presence of SDS [109] and amino acid analysis was performed on the isolated polypeptides. In addition, the suggestion emerged from this study that the RNA component of the nuclear envelope might be associated with the nuclear pore complex, since ribosomes had previously been removed by the citrate washing and the residual DNA and chromatin content was very low because of the high salt extraction.

Not unexpectedly, the nuclear envelope polypeptide bands shown on the polyacrylamide gradient (10–15%) gels of Aarsonson and Blobel [116] reveal a significantly different distribution from those on the single concentration gels. Following Triton X-100 extraction of the nuclear envelope, isolated by the method of Kay et al. [3], it was found [116] that a polypeptide of M_r approx. 50 000 was removed, presumably from the outer nuclear membrane; further extraction with 0.3 M $MgCl_2$ removed a large number of polypeptides, leaving a residue containing four predominant polypeptides. Although many other minor polypeptide bands are still present, it is probably reasonable to conclude that the major polypeptides present in this residue are associated with the nuclear pore complex, since electron microscopy shows the residue to be a single fibrillar lamina with the nuclear pore complex still attached [116]. This treatment is discussed further in Section VIH.

The complete dissociation and denaturation of macromolecular protein complexes into their unfolded polypeptide chains implies that all protein-protein, protein-

lipid and protein-nucleic acid linkages are destroyed, along with functional activity, quaternary and tertiary structure. Thus, while ultrastructural evidence strongly suggests that the nuclear pore complex might reasonably be considered as a macromolecular organisation, SDS-polyacrylamide gel electrophoresis does not provide information on the native proteins and nucleoproteins of this 'organelle'. Many investigators have employed the use of nonionic surfactants to solubilize cellular membranes other than the nuclear envelope, and have obtained isolated and functional enzymes and receptors. These compounds, of which Nonidet P40 and Triton X-100 are perhaps the most widely used, do not produce complete solubilization of the nuclear envelope [40,116] and are, therefore, only likely to be of value for the investigation of the portion of the nuclear envelope, the outer nuclear membrane, that is solubilized. Thus it may be possible to perform comparative enzymological studies on the outer nuclear membrane and endoplasmic reticulum using this approach, but it is unlikely to provide functional information on the nuclear pore complex and the inner nuclear membrane which remain essentially insoluble in nonionic surfactants.

IVE. Enzymes of the nuclear envelope

The enzymology of the nuclear envelope has been dealt with in considerable depth in several recent reviews [8,28,29,34]; to avoid undue repetition of this aspect this section will be restricted to a brief assessment of the overall area with discussion of some of the more recent papers. Franke [29] has listed a large number of enzymes that have been detected in the nuclear envelope. Table VI lists some of the more widely assayed nuclear envelope enzymes, compiled from our own data [37] and the published results of several other groups.

Almost all workers have shown the presence of a Mg^{2+}-stimulated ATPase in the nuclear envelope, which shows no further activation on the addition of Na^+ and K^+. Very variable activity figures have been obtained for glucose-6-phosphatase, but it is generally accepted that this enzyme is present in the nuclear envelope. Figures for the mitochondrial enzymes, succinate dehydrogenase and monoamine oxidase are very low, although Gorkin [102] has claimed to detect an enrichment of *p*-nitrophenylethylamine oxidase in rat liver nuclear envelope, compared to that detectable in the endoplasmic reticulum. This was not found to be the case when kyneuramine was used as the monoamine oxidase substrate, although a significant activity was detected in pig liver nuclear envelope [37]. One area of nuclear envelope enzymology that has received a great deal of attention, particularly from Berezney and his co-workers [6,48,121,122] is the presence of cytochrome oxidase. By carefully monitoring for other mitochondrial markers, such as coenzyme Q, succinate dehydrogenase-associated flavin, rotenone-sensitive NADH-cytochrome *c* reductase and cytochrome *b*, it was concluded that almost 90% of the nuclear envelope cytochrome *c* oxidase could be accounted for by non-mitochondrial activity. Contrary to this observation, Jarasch and Franke [117] claimed to detect much higher quantities of mitochondrial marker enzymes and that the non-mitochondrial component of

TABLE VI

SOME ENZYME ACTIVITIES AND CYTOCHROMES OF MAMMALIAN LIVER NUCLEAR ENVELOPE

Enzymes are expressed as μmol/h per mg protein and cytochromes as nmol/min per mg protein.

ATPase	16.4(R), 10.1(P)[a]; 5.6(R), 6.9(P)[d]; 1.4(R)[e]; 2.4(R)[f]; 6.8(B)[g]; 5.2(R)[j]; 3.2(R)[m]
Glucose-6-phosphatase	15.3(R), 13.9(P)[a]; 9.6(R)[b]; 0.1(R), 0.1(P)[d]; 0.2(R)[e]; 15.2(R)[f]; 7.2(B)[g]; 5.4(R)[j]; 23.4(R)[l]; 51.0(R)[m]
Glucose-1-phosphatase	0.12(R), 0.65(P)[a]
5'-Nucleotidase	1.3(R), 0.4(P)[a]; 3.0(R)[l]; 11.7(R)[m]
Alkaline phosphatase	1.3(R), 1.3(P)[a]; 1.7(R), 2.1(P)[d]
Acid phosphatase	8.5(R), 8.1(P)[a]; 3.2(R), 10.0(P)[d]
Succinate dehydrogenase	0.5(R), 0.9(P)[a]; 0.24(B)[g]; 0.96(R)[h]
Monoamine oxidase	0.0(R), 1.6(P)[a]; 1.0(R)[e]; 0.04(R)[h]
NADH-ferricyanide reductase	15.1(R), 8.1(P)[a]; 155.4(B)[g]; 38.5(R)[k]
NADPH-ferricyanide reductase	6.1(R), 3.9(P)[a]
NADH-cytochrome *c* reductase	16.0(R)[b]; 6.0(R), 2.7(P)[d]; 3.6(R)[e]; 33.1(R)[f]; 50.4(B)[g]; 29.4(R)[m]
NADPH-cytochrome *c* reductase	3.0(R)[b]; 1.1(R), 1.3(P)[d]; 0.4(R)[e]; 6.2(R)[f]; 0.3(B)[g]; 2.8(R)[m]
Cytochrome *c* oxidase	0.6(R)[e]; 0.195(B)[g]; 7.9(R)[h]; 16.0(R)[k]; 1.6(R)[m]
Cytochrome b_5	0.034(R), 0.026(P)[d]; 0.18(R)[i]; 0.33(B)[g]; 0.06(R)[k]; 0.28(R)[m]
Cytochrome a,a_3	0.045(B)[g]; 0.034(R)[h]
Cytochrome *P*-450	0.025(R), 0.026(P)[d]; 0.055(B)[g]; 0-0.22(R)[i]; 0.099(R)[m]

Abbreviations: R, rat liver; P, pig liver; B, bovine liver.

References: [a] Milne et al. [37]; [b] Kay et al. [3]; [c] Gorkin [102]; [d] Franke et al. [5]; [e] Zbarsky et al. [47]; [f] Kashnig and Kasper [43]; [g] Berezney et al. [48, 122]; [h] Jarasch and Franke [117]; [i] Kasper [118]; [j] Kartenbeck et al. [53]; [k] Jarasch [119]; [l] Wilson and Chytil [120]; [m] Sikstrom et al. [93].

nuclear envelope cytochrome *c* oxidase amounted to between 40 and 76% of the total activity. In addition it was shown that 37% of the NADH-cytochrome *c* reductase activity was sensitive to inhibition by rotenone, i.e. that this portion is mitochondrial. Kasper [34] and Berezney and Crane [48] both showed the rotenone-sensitive portion of their nuclear envelope NADH-cytochrome *c* reductase to be much lower. While careful monitoring for the presence of mitochondrial contamination of nuclear envelope using electron microscopy and marker enzymes must continue to be of prime importance, it seems fair to conclude that most of the nuclear envelope cytochrome *c* oxidase is truly endogenous to the nuclear envelope; this statement is given considerable support by the cytochemical studies of Bukhalov et al. [98] which show cytochrome *c* oxidase activity, using the Seligman diaminobenzidine reagent, to be associated primarily with the inner nuclear membrane, and to a lesser extent with the outer nuclear membrane and chromatin of isolated nuclei.

Related studies on the electron transport system of isolated nuclear envelopes

have been performed by Zbarsky et al. [47] and Berezney et al. [122], and are reviewed in detail by Wunderlich et al. [28]. The question as to whether the nuclear envelope provides the mechanism whereby the nucleus can generate its own energy via a respiratory chain is not finally decided. although it is proposed that the presence of cytochrome *c* oxidase [28] may indicate a site of oxidative phosphorylation. The recent claims of Zbarsky et al. [123,124] that 'elementary mushroom-like particles' similar to those seen on mitochondrial christae, can be seen on isolated nuclear membranes of rat liver and spleen cells and that these particles show ATPase activity and are attached to the inner nuclear membrane, must be seen as supportive evidence for an electron transport system. Nevertheless, no published negatively stained electron micrographs of nuclear envelope produced by other groups, including that of the author, show any indication of this feature.

Another area of current controversy has followed from the claim by some investigators [125–131] that the initiation of DNA synthesis and replication occurs adjacent to, or at, the nuclear envelope. The main approaches used in these studies have been autoradiography and the isolation of DNA-membrane complexes from nuclei using the detergent sodium *N*-lauryl sarcosinate. Direct attempts to detect DNA polymerase activity in nuclear envelope have, in general, proved negative [132–135] with the proviso that some late replication of DNA may be associated with the nuclear envelope [132]. Several other papers refuting that DNA replication occurs in the nuclear envelope have also appeared [136–138]. Thus, while Wunderlich et al. [28] come to the conclusion that the bulk of the DNA is not initiated or replicated in association with the nuclear envelope, they do qualify the statement by saying that the available data does not rule out the involvement of the nuclear envelope in replication. More recently the whole issue appears to have reopened with the appearance of several papers claiming that DNA is clearly replicated in or near to the nuclear envelope [139–146]. Perhaps the most significant feature of these papers is that they directly contradict the enzymic data on DNA synthesis in the nuclear envelope [136–138], but it must be borne in mind that the absence of any enzymic activity in an isolated nuclear envelope preparation does not preclude the presence of the enzyme in vivo. The nuclear envelope isolation and purification procedures could remove or inactivate enzymes, due to the high or low ionic strength treatments, ultrasonication or deoxyribonuclease digestion.

At the moment the physiological function of the Mg^{2+}-ATPase of nuclear envelope cannot be fully explained. It is widely accepted that this enzyme is not involved in monovalent or divalent cation transport, but it may be involved in the nucleocytoplasmic transfer of ribonucleoproteins. It has been shown by Agutter et al. [147] that the addition of yeast RNA, polyadenylic or polyguanylic acids stimulates rat and pig liver nuclear envelope nucleoside triphosphatases. Pig liver nuclear envelope adenine, guanine and uridine triphosphatases were stimulated 25, 20 and 31 % by the addition of yeast RNA at a concentration of 50 μg/ml. If the nuclear envelope had been previously incubated with ribonuclease, which produces a significant depletion of the nuclear envelope RNA content, the RNA stimulation of the three

nucleoside triphosphatases became 63, 78 and 60 %, respectively. The suggestion was put forward that the apparent stimulation of nucleoside triphosphatase can be regarded as a protection of the enzyme by RNA. This occurs normally due to the endogenous RNA, and can be enhanced by the addition of exogenous RNA. As this stimulation of nuclear envelope nucleoside triphosphatase by RNA is not paralleled by a stimulation of the endoplasmic reticulum nucleoside triphosphatase by RNA, a tentative proposal was advanced that the RNA or polyguanylic acid-stimulated Mg^{2+}-ATPase activity might be used as a marker enzyme for nuclear envelope [147]. If a significant portion of the nuclear envelope RNA is located in the nuclear pore complex, by implication, it is suggested that the nuclear envelope Mg^{2+}-ATPase might also be located in the nuclear pore complex if there is a functional requirement for RNA. This proposal requires confirmation from Mg^{2+}-ATPase assays performed on isolated and purified nuclear pore complexes and nuclear membrane vesicles depleted in nuclear pore complex (see Section IV) before any conclusive statement can be made as to its validity. The cytochemical results on the location of the nuclear envelope Mg^{2+}-ATPase reaction product are very inconclusive [91–95]; the recent study of Chardonet and Dales [148] on HeLa cells tends to show the localisation of lead phosphate in the vicinity of the nuclear pore complex, whereas the work of Sikstrom et al. [93] shows the lead phosphate to be more evenly spread along the outer nuclear membrane.

IVF. Nucleocytoplasmic transfer of molecules

IVF-1. Ions and small molecules. Most ions and small molecules and many macromolecules rapidly enter and leave the nucleus by diffusion processes not requiring energy. Although it is likely that most of these exchanges occur through the nuclear pore complexes, some might also occur across the inner nuclear membrane, via the intracisternal space to the endoplasmic reticulum cisternae and across the endoplasmic reticulum membrane. Exchanges from the nuclear envelope intracisternal space might also take place directly across the outer nuclear membrane or by blebbing of the outer nuclear membrane [30].

The exchange of water and ions across the nuclear envelope has recently been reviewed by Feldherr [24] and by Fry [149]. It appears that the nuclear concentration of potassium is considerably greater than the cytoplasmic potassium concentration, and that the nuclear sodium concentration is less than that in the cytoplasm [150,151]. Although there is no energy-dependent transport system for sodium and potassium, ultra-low temperature atuoradiographic results [152] indicate that there is a pool of sodium (15 %) in the nucleus which exchanges more rapidly than the remaining 'slow' sodium fraction. There are indications, therefore, that some binding of sodium and potassium by the chromatin may occur, which, together with magnesium and calcium binding is probably important for the maintenance of the normal state of chromatin condensation. This autoradiographic technique has also shown the distribution of sucrose and inulin across the oocyte nuclear envelope, which indicates that the nuclear envelope is of comparable permeability to cytoplasm [28,153]. Using a

microfluorimetric technique Kohen et al. [154] were able to show that iontophoretically injected glycolytic intermediates entered the nucleus in as short a time as 35 ms, thus indicating that for many small molecules the nuclear envelope probably does not constitute a permeability barrier.

IVF-2. Macromolecules. It was shown several years ago by Feldherr [155] that colloidal gold particles of diameter up to approximately 13.5 nm will enter the interphase nucleus of *Amoeba proteus* whereas with *Chaos chaos* the particle diameter for entry is up to approximately 16 nm [156]. Some restriction on the influx, i.e., molecular sieving, probably due to passage through the nuclear pore complexes, starts to occur at particle diameters of around 6 nm in *Periplaneta* oocytes [157]; proteins with diameters less than 4.5 nm penetrated the nuclear envelope freely, whereas those with diameters between 6 nm and 9.5 nm entered at rates varying inversely with the increase in diameter. Thus, the observation that haemoglobin (diameter approximately 7 nm) passes from the cytoplasm to the nucleus of the chicken erythrocyte in less than 1 min is compatible with the diameters for molecular sieving, and this occurs despite the fact that the chicken erythrocyte nuclear envelope has a very low nuclear pore complex frequency. In addition, the autoradiographic approach of Gurdon [158] using ^{125}I-labelled proteins clearly indicates that histones and serum albumin enter *Xenopus* oocyte nuclei, but that ferritin (diameter 12 nm) is excluded. Despite the considerable amout of evidence on the free permeability of proteins up to a molecular weight of approx. 70 000, it has also been shown that histones only enter the nucleus during the S phase of the cell cycle [159], whereas most other proteins enter preferentially during the G_1 phase. Recently, Paine et al. [25], using amphibian oocytes, have shown by ultra-low temperature autoradiography with tritiated dextrans of known diameter that the nuclear envelope has patent pore radii of approx. 4.5 nm and that proteins with radii less than this can move through the nuclear envelope at rates determined by their size. The figure of 4.5 nm for the pore radius is compatible with the central granule or tubule of the nuclear pore complex [14,25] yet there is no evidence to suggest that permeation cannot occur through the region of the nuclear pore complex between the central granule and the annular material, which is generally considered to contain fibril-like structures; permeation might also occur through the annular material, particularly if the tubule hypothesis for the annular structure is correct [12–15,31,32]. It might be reasonable to propose that the channels for the passive size-dependent influx and efflux of molecules to and from the nucleus might not be the same as those used for the energy-dependent translocation of ribonucleoproteins [160]. In the present state of knowledge it is not unreasonable to propose that the overall complexity of the nuclear pore complex might adequately provide independent passive and active transporting systems. Several investigators have shown that the nuclear pore complexes carry a net positive charge, from the binding of negatively charged particles of colloidal gold [161,162]. Thus, the positive charge on the nuclear pore complex would be likely to influence the passive permeability to the larger proteins (6 nm), most of which carry a net negative charge at physiological pH.

Electron microscopic evidence on the transport of nucleolar ribonucleoprotein through the central element of the nuclear pore complex has been presented by Scharrer and Wurzelman [163]. These authors also showed indications of blebbing of the nuclear envelope, and in a following paper [165] that microtubules are associated with the intracisternal space, the perinuclear cytoplasm and the nucleoplasm of African lung-fish oocytes. Sharrer and Wurzelman proposed that these microtubules could serve as a pathway for the transport of nucleolar components, for the direct nucleocytoplasmic passage of materials or represent the localised breakdown of the nuclear envelope at the particular stage of oogenesis at which these microtubules were reproducibly detected. Several other reports of nuclear envelope-associated microtubules have appeared in the literature, some of which dealt with the binding of colchicine, which is, apparently, not as specific a binding as occurs with tubulin (see reviews by Wunderlich et al. [28] and Franke [9,29] for further details).

In view of the probable importance of the nuclear envelope, and the nuclear pore complex in particular, in controlling the active nucleocytoplasmic transfer of ribonucleoproteins, to the extent that it has even been proposed that high molecular weight precursor ribosomal ribonucleoproteins might themselves be considered part of the nuclear pore complex under conditions of low or zero nuclear pore-RNA flow rate [166], interest has recently centred around the presence of an energy-utilising ribonucleoprotein translocation system within the nuclear pore complex. The temperature dependence of nucleocytoplasmic RNA transport [71,160,167] may indicate that ATP is required for this translocation, although Wunderlich et al. [72] do show that morphologically detectable transitions of nuclear envelope structure over the temperature range 20°–16°C, which could represent a 'closing' of the nuclear pore complex 'pores', thus preventing RNA transport, rather than a deficiency of ATP for the transport system.

A recent study of nuclear envelope nucleoside triphosphatases in the presence of several different inhibitors [168] indicates that the Mg^{2+}-ATPase has characteristics unlike the mitotic spindle ATPase or the mitochondrial F-ATPase. Although it is not clear how similar the nuclear envelope Mg^{2+}-ATPase is to that present in the endoplasmic reticulum, the tentative conclusion was drawn that the enzyme might be located in the nuclear pore complex [168]. Even though the cytochemical evidence on this point is inconclusive, the suggestion is given support by experiments performed on the ribonucleoprotein release from isolated rat liver nuclei, which is completely inhibited by the drug quercetin [169], a potent inhibitor of the nuclear envelope Mg^{2+}-ATPase [168]. Several other groups have also performed studies on the nucleocytoplasmic transport of messenger and ribosomal ribonucleoproteins [27,167,171] and it is emphasised that both ATP and cytosol factors (proteins) must be present for there to be a controlled release of ribonucleoproteins from isolated nuclei. It may be significant that cytosol was omitted from the nuclear incubation mixture of Agutter et al. [169] and since no electron microscopic evidence as to nuclear integrity was presented it is not possible to tell whether nonspecific nuclear lysis might have occurred during the incubation. Nevertheless, the interpretation of the kinetics

of the RNA release from nuclei and the Mg^{2+}-ATPase of the nuclear envelope was claimed to provide evidence for their close association. It is disturbing that Goidl et al. [172] have found that RNA, polyuridine and other polyanions induce the release of polyribosome from isolated HeLa cell nuclei in the absence of ATP, apparently by a nonspecific action.

A fundamental statement made by Yannarell et al. [171] is that RNA is always transported from the nucleus as a ribonucleoprotein complex, and that this indicates that nuclear protein synthesis is a prerequisite for messenger and ribosomal RNA transport. The autoradiographic studies of Eckert et al. [173] in which they investigate the inhibition of RNA transport by actinomycin D and cycloheximide support this statement. It was shown that pre-existing nuclear RNA release was prevented by both of these antibiotics at concentration sufficient to inhibit RNA synthesis. An interesting observation made by Hazan and McCouley [174] has been the phenobarbitones stimulated increase in vivo of the energy dependent transport of RNA from the nucleus; the presence of cytoplasmic macromolecules in the nuclear incubation medium was again found to be essential.

This important and rapidly expanding area of nuclear envelope research has recently been reviewed by Franke and Scheer [175] and Franke [176] from whose papers further details may be obtained.

IVG. Comparison of nuclear envelope, annulate lamellae and reticulum

Ultrastructural observations have shown the close morphological similarity of the nuclear envelope and annulate lamella, which is detectable in small quantities in most nucleated cells, but has been studied most thoroughly in the amphibian oocyte and tissue culture cells [21,22,95,177]. The annulate lamella generally consists of several parallel paired membranes, positioned adjacent to the nucleus and which are penetrated by 'pore structures' similar in dimensions and appearance to those found in the nuclear envelope. As mentioned above (Section I), it has not been possible to isolate and purify the annulate lamella in reasonable quantities, and as a consequence no biochemical data is yet available on the annulate lamella for direct comparison with that from nuclear envelope. Scheer and Franke [95] using small quantities of annulate lamella obtained from *Triturus* oocytes claimed to be able to detect Na^+, K^+-stimulated Mg^{2+}-ATPase activity by electron microscopic cytochemistry. Although these workers did not obtain any inhibition of this enzyme on addition of ouabain, they did not perform the incubation in the absence of Na^+ and K^+, so their claim that the annulate lamella ATPase is stimulated by these monovalent cations must be in doubt. It is to be hoped that the future availability of annulate lamella in significant quantities in an isolated and purified state, from tissues such as HeLa cells [22] may make possible the direct comparison of nuclear envelope and annulate lamella at an ultrastructural, chemical and enzymic level.

The situation is very different when comparing the nuclear envelope with the endoplasmic reticulum, on which there is an extensive literature. Several previous reviewers of nuclear envelope [8,29,34] have tabulated the enzymic activities detected

in the nuclear envelope and endoplasmic reticulum. It is apparent that in nearly all cases the nuclear envelope has lower specific activities than the endoplasmic reticulum. Significant deviations from this generalisation are the NADP:4,3-keto-steroid-5-reductase of rat ventral prostrate [43], rat liver aryl sulphatase and glutamate dehydrogenase [47], bovine and rat liver cytochrome *c* oxidase [121,147].

Electron microscopic observation showing the presence of ribosomes on the cytoplasmic surface of the outer nuclear membrane tends to indicate that it is the outer nuclear membrane rather than the inner nuclear membrane which bears the closer resemblance to the endoplasmic reticulum. Thus, if the enzymic activities mentioned above, which differ from those in the endoplasmic reticulum, can be positively shown to be present in the inner nuclear membrane or nuclear pore complex, as in the case for cytochrome *c* oxidase in the inner nuclear membrane [96–98], support will be given to the view that the nuclear envelope should be considered structurally and functionally as three components, i.e. the inner nuclear membrane, outer nuclear membrane and nuclear pore complex.

Sodium dodecyl sulphate-polyacrylamide gel electrophoresis indicates that nuclear envelope and endoplasmic reticulum possess some common polypeptides, but the overall polypeptide composition differs considerably [4,109,120] (see Fig. 20). The immunological investigations of Wilson and Chytil [120] have, likewise, shown that rat liver nuclear envelope and endoplasmic reticulum contain several common antigenic specificities, and also that if rabbit anti-rat nuclear envelope anti-serum was absorbed completely with rat liver mitochondria or endoplasmic reticulum, the remaining antibodies were specific to nuclear envelope. Thus, these remaining nuclear envelope specific antibodies could be used as markers for nuclear envelope, using the complement fixation assay or immunoelectrophoresis, but it is not clear whether the antibodies would be directed primarily against the inner nuclear membrane and nuclear pore complex rather than the outer nuclear membrane. In addition, rabbit anti-serum against rat liver rough endoplasmic reticulum was not absorbed with rat liver nuclear envelope to see if any additional antigens were present in the rough endoplasmic reticulum. Nevertheless, this immunological approach is likely to prove to be very useful for the comparative analysis of nuclear envelope, endoplasmic reticulum and annulate lamella using the immunoferritin labelling technique as well as immunodiffusion and immunoelectrophoresis [178]. As a result of the claim that the nuclear envelope may even carry antigenic components that are present in the plasma membranes, such as the H-2 antigens [179] this approach is likely to supplement conventional enzymic analysis as a means for characterising cellular membranes, and may provide further support for the membrane flow hypothesis [23].

IVH. Subfraction of the nuclear envelope

Stemming from the concept that the intact nuclear envelope be considered as three interconnected components, the inner nuclear membrane, outer nuclear membrane and nuclear pore complex, it is understandable that attempts should be made to obtain each of these components as separate entities for high resolution electron

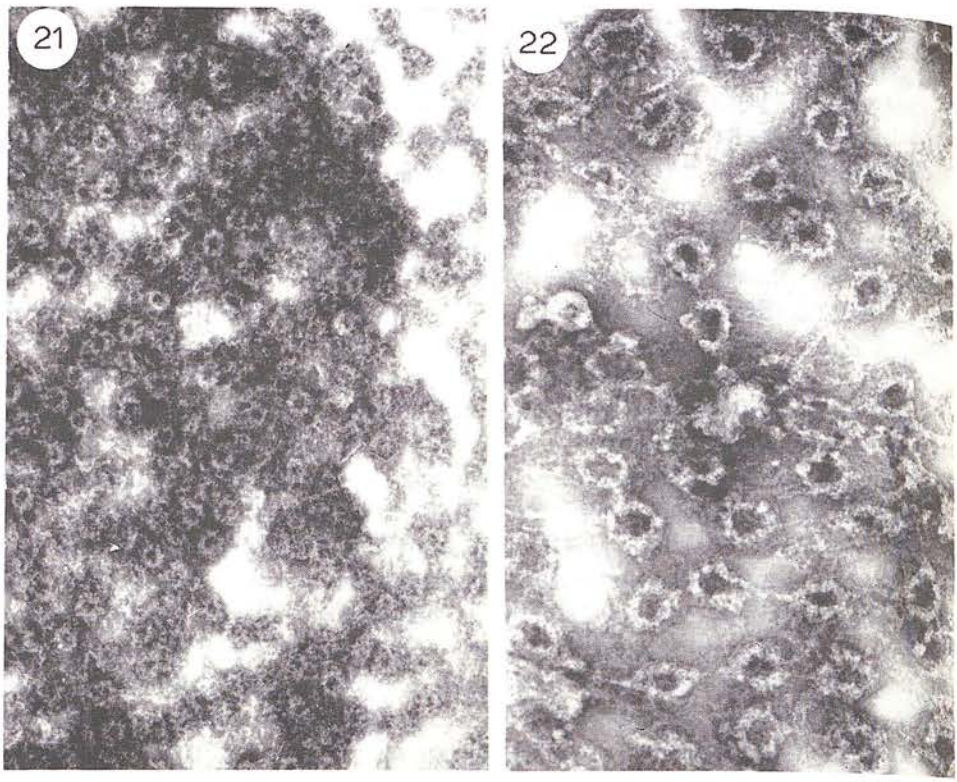

Fig. 21. Part of a rat liver nuclear ghost, after extraction with 1.0% Nonidet P-40. Negatively stained with ammonium molybdate. The double electron-transparent line at the edge of the ghost is absent, but the nuclear pore complexes remain, attached to a diffuse residue of the inner nuclear membrane. × 39 000.

Fig. 22. Part of a *Triturus* oocyte nuclear ghost that has undergone disruption during the spreading procedure used for preparing negatively stained specimens. Many individual nuclear pore complexes can be seen, with a fine network passing between them (cf. Fig. 19). Negatively stained with ammonium molybdate. × 69 000.

microscopic study, chemical, enzymic and immunological analysis. As this type of approach has been used with considerable success for the subfractionation of the mitochondrion, it is likely that the appropriate treatments might be developed for the disruption and fractionation of the nuclear envelope.

The nonionic surfactant extraction procedure applied to nuclear envelope by Aaronson and Blobel [116], Scheer et al. [40] and Harris and Marshall (unpublished observations) and which is thought to remove the outer nuclear membrane along with the lipids of the inner nuclear membrane, leaves an inner nuclear membrane residue that still carries the nuclear pore complexes. Fig. 21 shows a collapsed rat liver nuclear ghost that has been extracted with 1.0% Nonidet P 40. Removal of traces of residual chromatin from rat liver nuclear envelope by 0.3 M $MgCl_2$ treatment, following extraction with Triton X-100, Aaronson and Blobel [116] found that a lamina remained which still carried the stud-like nuclear pore complexes. Although this final material

does show a considerable enrichment of four of the nuclear envelope polypeptides, others being detectable in reduced quantities, the combined Triton X-100 and $MgCl_2$ treatment can only be considered to go part way towards the fractionation of the nuclear envelope since it does not release the nuclear pore complex as isolated entities. The implication was made from the SDS-polyacrylamide gels of Aaronson and Blobel [116] that only one predominant polypeptide was released from the nuclear envelope by Triton X-100 extraction. This result is difficult to accept if the outer nuclear membrane is of similar polypeptide complexity to the endoplasmic reticulum.

An alternative interpretation put forward by Scheer et al. [40] proposes that the nonionic surfactant residue of nuclear envelope consists of thread-like inner nuclear membrane components that interconnect the nuclear pore complex, and that the residue may be of similar composition to the acidic protein matrix of the nucleus [52]. While this proposition seems reasonable and may further emphasise the distinction to be made between the inner nuclear membrane and outer nuclear membrane, it is not yet certain that the nuclear pore complexes bear any compositional relationship to the nuclear protein matrix.

The main approach to the problem of nuclear envelope subfraction employed by the author and his co-workers has been derived from the firm knowledge that the nuclear pore complex possesses a greater structural rigidity than does the surrounding inner nuclear membrane and outer nuclear membrane. This information was obtained from the spreading of nuclear envelope suspensions when preparing negatively stained electron microscope specimens, on which completely shattered nuclear ghosts are frequently detected alongside relatively undamaged ghosts [15,63,66]. This disruption can be readily accounted for by the surface tension forces applied to the nuclear envelopes in the thin layer of aqueous stain that covers the carbon support film of the electron microscope grid at the time of spreading [66]. In the hands of the author the same type of disruption has been found to occur with dilute suspensions of mammalian erythrocyte ghosts, but less so with more concentrated suspensions. The point of significance is that under these spreading conditions the nuclear pore complexes of rat liver nuclear envelope appear to remain essentially intact, although some slight disruption of the nuclear pore complex may also occur (see Figs. 18 and 19). The same situation has been found with *Triturus* oocyte nuclear envelope, as shown in Fig. 22. Essentially the same kind of disruption of oocyte nuclear envelope was obtained by Scheer et al. [40] employing a slightly different spreading procedure on a droplet of water at the relatively high pH of 9.0.

Because of this background knowledge on the relative stability of the nuclear pore complex compared to the inner nuclear membrane and outer nuclear membrane it was considered that either carefully applied highspeed blending using the Ultra turrax homogenizer with a 0.9 cm diameter probe, or ultrasonication using a water bath or probe-type apparatus, might provide the means by which rat liver nuclear envelope could be disrupted in a controlled manner, yielding free nuclear pore complexes and small fragments or vesicles of inner nuclear membrane and outer nuclear membrane. To date, ultrasonication using the M.S.E. 150 W ultrasonic disintegrator

Fig. 23. A sample of rat liver nuclear envelope after ultrasonication for 3 min at an amplitude of 3 μm in the MSE ultrasonic disintegrator. Negatively stained with ammonium molybdate. The arrows indicate free nuclear pore complexes. × 65 000.

has been found to go a considerable way towards achieving these aims [16]. It was previously mentioned that ultrasonication has been used by several workers as part of their procedure for the isolation of nuclear envelope [5,7,34,42,43,103,104] and it is therefore clear that carefully applied ultrasonication does not cause significant damage to the nuclear pore complexes, even though considerable fragmentation of the nuclear envelope sheets occurs and some loss of small fragments and vesicles is likely in these preparations. The published electron micrographs of Franke and his colleagues [5,29,103] show that nuclear envelope fragments obtained by ultrasonication carry only a small number of nuclear pore complexes, and what is perhaps even more significant, a considerable number of fragments carry only one or two nuclear pore complexes.

Although the potential hazards of applying ultrasonication to biological membranes, even under carefully cooled conditions with a low intensity of ultrasonication, are not fully understood, the technique has found widespread usage in recent years for the disruption and subfractionation of mitochondria, chloroplasts, endoplasmic reticulum, mammalian and avian erythrocytes, as well as for the production of liposomes and the solubilization of enzymes [57,180–185]. Experiments performed in the author's laboratory in conjunction with Mr. P. Marshall indicate that the disruption of the rat and pig liver nuclear envelope by ultrasonication can be readily monitored by negative staining electron microscopy. Thus, at an early stage of the ultrasonication treatment a mixture of free nuclear pore complex, small membrane fragments carrying nuclear pore complex and fragments and vesicles that do not carry nuclear pore complex is obtained, which is very similar to the 'intact nuclear envelope' of those groups using ultrasonication as part of their isolation procedure. Gradually a stage is reached where almost complete disruption of the nuclear envelope is obtained, with the release of a high proportion of the nuclear pore complexes. Fig. 23 shows a sample of rat liver nuclear envelope following ultrasonication of 1.5 ml of nuclear

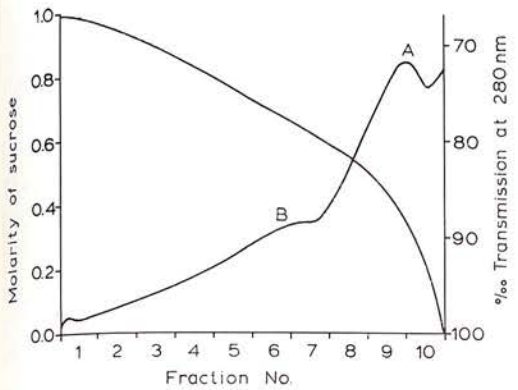

Fig. 24. The distribution of ultrasonicated rat liver nuclear envelope on a 0.25–1.0 M linear sucrose gradient, after centrifugation at 30 000 rev/min (100 000 × g_{av}) for 1 h.

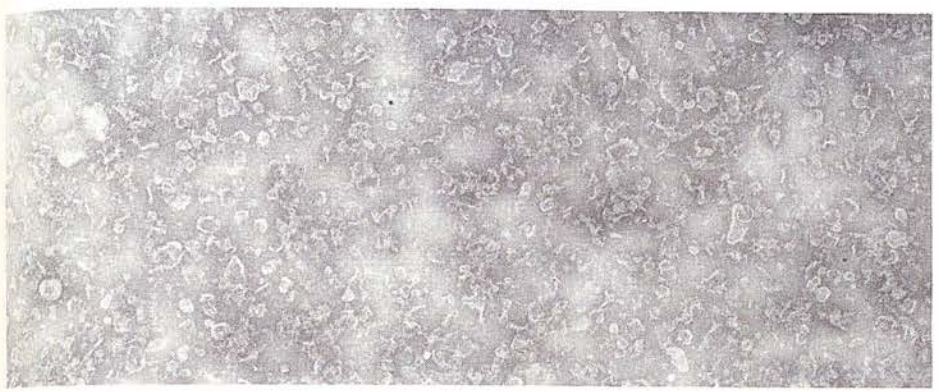

Fig. 25. The material in the fractions under the main peak (A) of the sucrose gradient rate zonal separation of the ultrasonicated rat liver nuclear envelope shown in Fig. 24. Small membrane fragments are visible, which decrease in size towards the top of the gradient. Negatively stained with ammonium molybdate. × 46 000.

envelope suspension in 10 mM Tris · HCl buffer (pH 7.4) for 3 min at an amplitude of 3 μm under ice-cooled conditions using the M.S.E. 150 W ultrasonic disintegrator with the 9.5 mm titanium probe. The probe was cooled in advance, and the ultrasonication applied as 10 s bursts, each followed by a 10 s cooling period. Rate sedimentation on linear 0.25 M–1.0 M sucrose density gradients has made possible the separation of a partially purified nuclear pore complex fraction from the bulk of the small fragments and vesicles of nuclear envelope which do not sediment as rapidly as the nuclear pore complexes. Fig. 24 shows the distribution of material on a sucrose gradient after centrifugation for 1 h at 30 000 rev/min (100 000 × g_{av}) using the M.S.E. 3 × 25 ml swing out rotor. The material under the main peak (A) has been shown in the electron microscope to be small nuclear envelope fragments of increasing size with increasing amount of sedimentation (Fig. 25); that under the

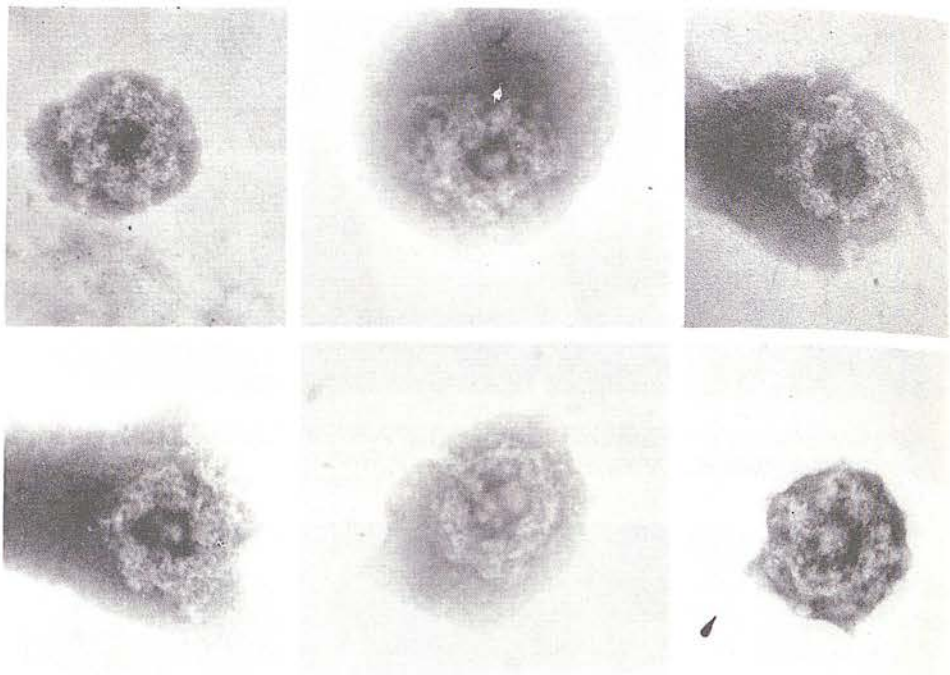

Fig. 26. The material in the fractions under the shoulder (B) of the sucrose gradient rate zonal separation of the ultrasonicated rat liver nuclear envelope shown in Fig. 24. Many individual nuclear pore complexes are present, together with a few larger membrane fragments. Negatively stained with ammonium molybdate. × 160 000.

shoulder (B) has been shown to be rich in nuclear pore complexes (Fig. 26) together with a few larger membrane fragments. Some material pellets through the sucrose gradient and is thought to represent undisrupted nuclear envelope and possibly the denser inner nuclear membrane fragments. In agreement with the electrophoresis results of Aaronson and Blobel [116] we have found that the nuclear pore complexes contain fewer polypeptides than does the intact nuclear envelope, but it must be admitted that the material from our sucrose gradient fractionation does not represent highly purified nuclear pore complexes that are completely freed from attached lipoproteins and larger membrane fragments. It is hoped that by applying ultrasonication to nuclear envelope that has previously been extracted with a nonionic surfactant (Triton X-100 or Nonidet P40) to remove the outer nuclear membrane, a more highly purified nuclear pore complex region will be obtained from the subsequent fractionation by sucrose density gradient centrifugation.

Thus, the possibility of preparing purified inner nuclear membrane, outer nuclear membrane and nuclear pore complexes and their consequent availability for chemical, enzymic and electron microscopic analysis will provide future insight into several of the current problems and controversies over enzyme location and function of the nuclear envelope.

V. FUTURE PROSPECTS AND GENERAL DISCUSSION

VA. The localization of nuclear envelope proteins

Several radioactive labelling procedures for proteins have been successfully applied to erythrocyte ghosts and the plasma membranes of nucleated cells [186]. The introduction of lactoperoxidase mediated iodination by Philips and Morrison [187] has made available a relatively mild enzymic procedure for incorporating ^{125}I or ^{131}I into the tyrosine residues of proteins. Lactoperoxidase has a molecular weight of 78 000 and, therefore, does not penetrate the plasma membrane of intact cells or across the outer membrane of mitochondria or chloroplasts, but it is likely to enter cell nuclei freely (see Section IVF). For this reason, comparative studies using immobilized and free lactoperoxidase are likely to provide useful information, since it can be safely assumed that with immobilized lactoperoxidase only the proteins on the cytoplasmic surface of the nuclear envelope will be labelled. With free lactoperoxidase it is likely that more extensive labelling will be obtained owing to the penetration of the enzyme into the nuclear pore complexes and possibly the nucleoplasm. One complication that has emerged from preliminary studies (Stubbs and Harris, unpublished observations) is that rat liver nuclear envelope contains an endogenous peroxidase which produces a relatively large incorporation of ^{125}I in the control samples. The addition of 5 mM dithiothreitol or 2-mercaptoethanol inhibits the endogenous enzyme and reduces the background incorporation, thus ruling out non-enzymic iodination. Attempts to inactivate irreversibly the nuclear envelope peroxidase using 3-amino-1,2,4-triazole prior to ^{125}I-labelling with exogenous free or immobilized lactoperoxidase are likely, therefore, to assist the interpretation of the SDS-polyacrylamide gel electrophoresis of the iodinated polypeptides. Another approach that has been employed, for comparison purposes, is to iodinate the nuclear envelope proteins using the permeant reagent chloramine T. Advantages derived from the use of this reagent are the speed of the reaction (20 s has been found to be adequate at 4°C) and the tenfold increase of ^{125}I incorporation compared to that obtained by a 30 min incubation with lactoperoxidase. Although there is considerable evidence to suggest that chloramine-T does not alter protein conformation, antigenic and antibody specificity [188–199] there is little literature available on its use for iodinating membrane-bound proteins. As chloramine-T is generally considered to be a very powerful oxidising reagent, it must be used with caution.

By using a combination of different iodination procedures, i.e. chloramine-T, endogenous peroxidase, exogenous free and immobilized lactoperoxidase on intact nuclei, nuclear ghosts and torn sheets of nuclear envelope, it is hoped that it will be possible to interpret the stained and radioactive labelling patterns of the nuclear envelope polypeptides with some degree of precision. Possible complication may well arise from the leakiness of damaged nuclei and nuclear ghosts. The resealing of purified and nuclear ghosts is, therefore, currently under investigation, in conjunction with electron microscopic autoradiography of the ^{125}I-labelled nuclei and nuclear ghosts. The iodination of subfractionated nuclear envelope (Section IVH) will also provide

additional information which should simplify the understanding of the ^{125}I-labelling pattern of the intact nuclei, nuclear ghosts and torn sheets of nuclear envelope, which must present the most complex and highly permeable membranes systems to which these iodination techniques have been applied to date.

VB. The permeability properties of isolated nuclei and nuclear ghosts

A considerable amount of in vivo work has already been performed on the passive permeability properties of amphibian oocyte nuclei [24,25,162] but little or no work has been published on the permeability of isolated and purified nuclei. The recent studies of the RNA release from nuclei [169–171,174] indicate that in vitro experiments can be readily performed using isolated nuclei. It is, therefore, probable that the influx and efflux of macromolecules can be studied using similar in vitro systems. Electron microscopic tracers such as ferritin, peroxidase, haemoglobin and myoglobin, and covalently linked aggregates of these molecules [192,193], should provide useful preliminary information on the permeability of isolated nuclei and nuclear ghosts (cf. ref. 194) prior to more quantitative spectroscopic or radioisotope studies. It is immediately apparent that the difficulties likely to be encountered when attempting to work with resealed nuclear ghosts will be considerably greater than with nuclei. Nevertheless, the likely benefits to be obtained from working with nuclear ghosts rather than intact nuclei, which stem from the avoidance of chromatin-macromolecule interactions that might seriously complicate the interpretation of influx or efflux studies, may make this approach very useful. It may even be possible, for instance, to reseal nuclear ghosts after entrapping radioactively labelled macromolecules such as ribonucleoprotein complexes, in order to investigate their energy dependent translocation across the nuclear envelope. Similarly, the entry of labelled hormone receptor complexes, cytoplasmic macromolecules and growth factors, which may be important components of gene activation and control systems, could be investigated.

VC. The action of drugs on the structure and function of the nuclear envelope

It is likely that the administration of certain drugs to animals, plants and cultured cells will produce structural and functional alterations of the nuclear envelope, as has been extensively documented for the endoplasmic reticulum, the nucleolus and chromatin [195–200]. Thus, carcinogens, pesticides, herbicides and environmental pollutants, together with alteration of the normal hormone and vitamin levels and other dietary constituents may produce detectable ultrastructural changes in the nuclear envelope, such as the loss of ribosomes from the outer nuclear membrane, increased blebbing of the outer nuclear membrane, breakdown of the nuclear pore complexes, loss of heterochromatin from the inner nuclear membrane, as well as subtle changes in the overall stability of the nuclear envelope. Enzymic activities in the nuclear envelope may be lowered or raised and individual intrinsic proteins reduced or increased, in a manner similar to the induction of the endoplasmic reticulum cytochrome *P*-450 drug metabolizing system.

Kasper [34] has found that both phenobarbital and 3-methyl-cholanthrene induce the enzyme aryl hydrolase in endoplasmic reticulum 3.3 and 9.2 times, respectively, whereas with the nuclear envelope, the values are 0.8 and 16.3 times. This indicates that enzyme induction in the nuclear envelope and endoplasmic reticulum does show significant differences, which is emphasised by the results of Alexandrov and Frayssinet [201] using pregnenolone 16α-carbonitrile as well as phenobarbital and methylcholanthrene. Nevertheless, overall similarity of the two membrane types is proposed by Fry and Wishart [202] who showed a comparable phenobarbital induction of UDP-glucuronyl transerase activity in embryonic chicken liver endoplasmic reticulum and nuclear envelope. The cannabinoid alkaloids have been found to alter the binding of ribosomes to the nuclear envelope of infant rat brain [203]. This effect was detectable within 1 h, it was maximal after 3 h and had almost completely diminished after 6 h. Steroid hormones have been found to influence the interaction of ribosomes with rat liver endoplasmic reticulum [204] but it is not known if they likewise release ribosomes from the nuclear envelope. The steroid oestradiol-17β has been found to bind to the nuclear envelope of the bovine endometrium [205] but it is not clear whether such binding sites can be considered as 'receptors'. Reports have appeared indicating that bleomycin [206] and other antibiotics [207] alter the linkages between the DNA and the nuclear envelope. These compounds may therefore be useful for the study of the DNA content of inner nuclear membrane. Regulation of nuclear envelope reformation after mitosis appears to be influenced by chelating agents and the drug chloramphenicol [208]. The effects of low and high protein diets on the induction of endoplasmic reticulum drug metabolizing enzymes in rat liver has been studied by Sachan [209], and here again it will be of interest to see if similar dietary alteration produce detectable changes in the nuclear envelope.

The compound ethionine interferes competitively with all metabolic reactions requiring methionine; in particular, it rapidly produces a reduction of cellular ATP levels due to the formation of the anti-metabolite *S*-adenosylethionine [210,211] and it inhibits RNA and protein synthesis. If administered over long periods ethionine can be classed as a carcinogen, hepatoma developing as a consequence of fatty liver [212]. The shorter term effect of ethionine can be readily reversed by the administration of ATP, adenine or adenine nucleotide precursors which will increase the pool of cellular adenine available for ATP production, thus providing the normal metabolite *S*-adenosylmethionine for methylation reactions. There are strong indications that ethionine causes the release of ribosomes from endoplasmic reticulum [213,214] and it has been found by Milne and Harris [215] that release of ribosomes from the outer nuclear membrane of rat liver also occurs after the administration of ethionine. It has also been found that single injections of ethionine (70 mg/kg) followed by a period of two days prior to sacrificing the rats, results in the production of slightly fragmented nuclear envelope, which is depleted in ribosomes. Negative-stained specimens of this nuclear envelope appear in the electron microscope to be very smooth, the nuclear pore complexes showing with greater clarity than on control

nuclear envelope. When the rats are sacrificed closer to the time of ethionine injections, the isolated nuclear envelope is found to be progressively more fragmented, possibly due to an increased overall fragility of the nuclear envelope such that it is unable to remain as nuclear ghosts throughout the isolation and purification procedure. The nuclear pore complexes, on the other hand, appear to remain morphologically unaltered. This increased fragmentation of the nuclear envelope is prevented if adenine (120 mg/kg) is injected after the ethionine, the nuclear envelope obtained under these conditions being almost completely in the form of nuclear ghosts. An increase of nuclear envelope fragility has also been found under conditions of protein deprivation (rats were kept for 10 days on a protein depleted diet). SDS-polyacrylamide gel electrophoresis of this nuclear envelope and that from ethionine treated rats (rats killed 1–3 h after injection) indicates that there is an increase in the number of high molecular weight polypeptides compared to control nuclear envelope [216], otherwise the overall pattern of polypeptides is not greatly altered.

It is also likely that the investigation of drug action in relation to nuclear envelope structure and function will be successfully performed using established suspension culture cell lines and short-term cultures of hepatocytes. Some of the hazards encountered with in vivo experiments, such as the alteration of hormone levels, may well be avoided but cells in culture are always maintained in a considerably different physiological environment from that present in vivo. Although many drugs may well mediate their effects on cellular membranes by altering metabolic reactions within the living cell, it will be interesting as a further extension of this area of subcellular pathology to see if direct application of certain drugs to isolated nuclear envelope produced alterations such as increased fragmentation and release of bound ribosomes and chromatin in a manner similar to that occurring when drugs are applied to living cells or animals.

VD. Concluding comments

The acquisition of the double-layered nuclear membrane system by eukaryotic cells has undoubtedly conferred decisive evolutionary advantages. Unfortunately, we must admit that in the present state of knowledge many questions relating to the precise functional role of the nuclear envelope in the living cell remain to be answered. For instance, is it correct to propose that the inner nuclear membrane is structurally and functionally distinct from the outer nuclear membrane and do the nuclear pore complexes contain specific enzymes that are important for their role in nucleocytoplasmic exchange processes, or do they function primarily as passive permeability channels? What is the significance of the apparent similarity of protein composition of the nuclear protein matrix and the inner nuclear membrane and is DNA replication associated with both these nuclear components? Can the nuclear pore complex be validly considered as a subcellular organelle in its own right? What, if any, changes occur to the composition and function of the nuclear envelope throughout the cell cycle? This aspect could possibly be investigated if large-scale synchronous cell cultures can be obtained, from which the nuclei and nuclear en-

velope could be isolated at precise stages throughout the cell cycle. The exact relationship of the nuclear envelope and the annulate lamella remains open for further investigations, which should be productive if isolated annulate lamella can be prepared in sufficient quantities for comparative biochemical analysis.

Various immunological approaches have proved to be successful for the study of cell surface and cytoplasmic membranes, and it is likely that this type of approach will likewise prove to be very useful for comparative investigations of the nuclear envelope, endoplasmic reticulum, annulate lamella and all other cytoplasmic membranes. Recent evidence indicates that anti-nuclear envelope antisera from humans with pathological conditions, not as yet clearly defined, and also from some normal humans, cross reacts with the nuclear envelope of mouse and rat cells as demonstrated by immunofluorescence (J. Campbell, personal communication). This result may indicate the presence of common nuclear envelope-specific antigens on different species. If even more specific antisera can be produced against the inner nuclear membrane, outer nuclear membrane, nuclear pore complexes and nuclear protein matrix, the immunofluorescence and immunoferritin labelling techniques, together with immunodiffusion and immunoelectrophoretic analysis, may provide very strong approaches for the further understanding of the molecular composition and function of the nuclear envelope. While there is a large and growing literature on the existence and properties of drug and hormone receptors on cell surface membranes, there is very little information on the presence of such receptors on the nuclear envelope; this is an area of investigation that is likely to be subject to significant expansion in the future.

NOTE ADDED IN PROOF *(Received January 30th, 1978)*

Since completion of the manuscript several relevant articles on nuclear envelope have come to hand. A variant on the heparin treatment for the isolation of nuclear envelope [57] has been presented by Hildebrand and Okinaka [217]. Ultrastructural studies on nuclear envelope have continued to indicate the strength of freeze-cleavage [218–220] as a preparative procedure, as well as thin-sectioning [221–223] and high resolution scanning electron microscopy [224]. The association of DNA synthesis with the nuclear envelope continues to gain support [225–230], as does the location of cytochrome oxidase in the nuclear envelope [231]. The study of RNA transport from nuclei [232–233] likewise continues to be an important area of nuclear envelope research.

ACKNOWLEDGEMENTS

The author has received support for his research on nuclear envelope from The Royal Society and the Medical Research Council. Grateful acknowledgement is made for the helpful criticism made by Dr. D. J. Barber, Mr. P. Marshall, Mr. I. F. Milne and Mr. G. Stubbs throughout the preparation of the manuscript.

REFERENCES

1 Harris, J. R. and Agutter, P. S. (1976) in Biochemical Analysis of Membranes (Maddy, A. H., ed), pp. 132–173, Chapman and Hall, London
2 Harris, J. R. and Milne, J. F. (1974) Biochem. Soc. Trans. 2, 1251–1253
3 Kay, R. R., Fraser, D. and Johnston, I. R. (1972) Eur. J. Biochem. 30, 145–154
4 Monneron, A. Blobel, G. and Palade, G. E. (1972). J. Cell Biol. 55, 104–125
5 Franke, W. W., Deumling, B., Ermen, B., Jarasch, E. D. and Kleinig, H. (1970) J. Cell Biol. 46, 377–395
6 Berezney, R., Funk, L. K. and Crane, F. L. (1970) Biochim. Biophys. Acta 203, 531–546
7 Agutter, P. S. (1972) Biochim. Biophys. Acta 255, 379–401
8 Franke, W. W. (1974) Int. Rev. Cytol. Suppl. 4, 71–236
9 Franke, W. W. and Scheer, U. (1970). J. Ultrastruct. Res. 30, 288–316
10 Hoijmakers, J. H. J., Schel, J. H. N. and Wanka, F. (1974). Exp. Cell. Res. 87, 195–206
11 Fabergé, A. C. (1974) Cell. Tiss. Res. 151, 403-415
12 Wischnitzer, S. (1958) J. Ultrastruct. Res. 1, 201-222
13 Vivier, E. (1967) J. Microsc. 6, 371–390
14 Abelson, P. H. and Smith, G. H. (1970) J. Ultrastruct. Res. 30, 558–588
15 Harris, J. R. (1974) Phil. Trans. Roy. Soc. Lond. B 268, 109–117
16 Harris, J.R. (1977) in Membranous Elements and Movements of Molecules: Techniques (Reid, E., ed), Vol. 6, pp. 245–250, Horwood, Chichester
17 Maul, G. G., Maul, H. M., Scogna, J. E., Lieberman, M. W., Slein, G. S., Hsu, B. Y. I. and Bruon, T. W. (1972) J. Cell Biol. 55, 433–447
18 Maul, G. G., Price, J. W. and Leiberman, M. W. (1971) J. Cell Biol. 51, 405–418
19 Wunderlich, F., Wallach, D. F. H., Speth, V. and Fischer, H. (1974) Biochim. Biophys. Acta, 373, 34–43
20 Lott, J. N. A. and Vollmer, C. M. (1975) J. Ultrastruct. Res. 52, 156–166
21 Kessel, R. G. (1968) J. Ultrastruct. Res. 24, Suppl. 10, 1–82
22 Liebrich, W. and Powetz, N. (1970) Cytobiologie 12, 473–475
23 Morré, D. J. Franke, W. W., Deumling, B., Nyquist, S. E. and Ovtrackt, L. (1971) in Biomembranes (Manson, L. H., ed.), Vol. 2, pp. 95–104, Plenum Press, London
24 Feldherr, C. M. (1972) in Advances in Cell and Molecular Biology, Vol. 2, pp. 273–307, Academic Press, New York
25 Paine, P. L., Moore, L. C. and Horowitz, S. B. (1975) Nature 254, 109–114
26 Yasasumi, G. and Tsubo, I. (1966) Exp. Cell Res. 43, 281–292
27 Raskas, H. J. (1971) Nature 233, 134–136
28 Wunderlich, F., Berezney, R. and Kleinig, H. (1976) in Biological Membranes (Chapman, D. and Wallach, D. F. H., eds), Vol. 3, pp. 241–333, Academic Press, New York
29 Franke, W. W. (1974) Phil. Trans. Roy. Soc. Lond. B 268, 67–93
30 Kessel, R. G. (1973) in Progress in Surface and Membrane Science, Vol. 6, pp. 243–329, Academic Press, New York
31 Wischnitzer, S. (1973) Int. Rev. Cytol. 34, 1–48
32 Wischnitzer, S. (1974) Endeavour 33, 137–142
33 Franke, W. W. and Scheer, U. (1974) in The Cell Nucleus (Busch, H., ed.), Vol. 1, pp. 220–347, Academic Press, New York
34 Kasper, C. B. (1974) in the Cell Nucleus (Busch, H., ed.), Vol. 1, pp. 349–384, Academic Press, New York
35 Fry, D. J. (1975) in Subnuclear Components: Preparation and Fractionation (Bernie, G. D., ed.), pp. 59–105, Butterworths, London
36 Price, M. R., Harris, J. R. and Balduin, R. W. (1972) J. Ultrastruct. Res. 40, 178–196
37 Milne, J. E., Agutter, P. S., Harris, J. R. and Stubbs, G. (1978) Biochem. Soc. Trans., in the press
38 Neville, D. M. (1960) J. Biophys. Biochem. Cytol. 8, 413–422
39 Harris, J. R., Price, M. R. and Willison, M. (1974). J. Ultrastruct. Res. 48, 17–32
40 Scheer, U., Kartenbeck, J., Trendelenburg, M. F., Stadler, J. and Franke, W. W. (1976) J. Cell Biol. 69, 1–18
41 Jarasch, E. D., Reilly, E. D., Comes, P., Kartenbeck, J. and Franke, W. W. (1973) Hoppe-Seyler's Z. Physiol. Chem. 354, 974–986

42 Kashnig, D. M. and Kasper, C. B. (1969) J. Biol. Chem. 244, 3786–3792
43 Moore, R. J. and Wilson, J. D. (1972) J. Biol. Chem. 247, 958–967
44 Yoo, B. Y. and Bayley, S. T. (1967) J. Ultrastruct. Res. 18, 651–660
45 Franke, W. W. (1967) Z. Zellforsch, 80, 585–593
46 Stavy, R., Ben-Shaul, Y. and Galun, E. (1973) Biochim. Biophys. Acta 323, 167–177
47 Zbarsky, J. B., Perevoshchikova, K. A., Delektorskaya, L. N. and Delektorsky, V. V. (1969) Nature 221, 257–259
48 Berezney, R. and Crane, F. L. (1972) J. Biol. Chem. 247, 5562–5568
49 Matsura, T. and Ueda, K. (1972) Arch. Biochem. Biophys. 150, 440–450
50 Ueda, K., Matsura, T. and Date, N. (1969) Biochem. Biophys. Res. Commun. 34, 322–327
51 Tata, J. R., Hamilton, M. J. and Cole, D. R. (1972) J. Mol. Biol. 67, 231–246
52 Berezney, R. and Coffey, D. S. (1976) in Advances in Enzyme Regulation, Vol. 14, pp. 63–100, Pergamon Press, Oxford
53 Kartenbeck, J., Jarasch, E. D. and Franke, W. W. (1973) Exptl. Cell Res. 81, 175–194
54 Berezney, R. and Coffey, D.S. (1974) Biochem. Biophys. Res. Commun. 60, 1410–1417
55 Zentgraph, H., Deumling, B., Jarasch, E. D. and Franke, W. W. (1971) J. Biol. Chem. 246, 2986–2995
56 Harris, J. R. and Brown, J. N. (1971) J. Ultrastruct. Res. 36, 8–23
57 Bornens, M. (1973) Nature 244, 28–30
58 Harris, J. R. (1971) in Physiology and Biochemistry of the Domestic Fowl (Bell, D. J. and Freeman, B. M., eds), Vol. 2, pp. 853–862, Academic Press, London
59 Jackson, R. C. (1976) Biochemistry 15, 5641–5651
60 Appels, R. and Ringertz, N.R. (1975) in Current Topics in Developmental Biology (Moscona, A. A. and Monroy, A., eds), Vol. 9, pp. 137–166, Academic Press, New York
61 Callan, H. G. and Tomlin, S. G. (1950) Proc. Roy. Soc. Lond. B 137, 367–378
62 Scheer, U. (1972) Z. Zellforsch, 127, 127–148
63 Gall, J. G. (1967) J. Cell Biol. 32, 391–399
64 Franke, W. W. (1966) J. Cell Biol. 31, 619–623
65 Markham, R., Frey, S. and Hills, G. J. (1963) Virology 20, 88–102
66 Harris, J. R. and Agutter, P. S. (1970) J. Ultrastruct. Res. 33, 219–232
67 Kartenbeck, J., Zentgraph, H., Scheer, U. and Franke, W. W. (1971) Advanc. Anat. Embryol. 45, 1–55
68 La Fountain, J. R. and La Fountain, R. L. (1973) Exp. Cell Res. 78, 472–476
69 Speth, V. and Wunderlich, F. (1970) J. Cell Biol. 47, 772–777
70 Coleman, S. E., Duggen, J. and Hackett, R. L. (1974) Tiss. Cell 6, 521–534
71 Zerban, H. and Werz, G. (1975) Exp. Cell Res. 93, 472–477
72 Wunderlich, F., Batz, W., Speth, V. and Wallach, D. F. H. (1974) J. Cell Biol. 61, 633–640
73 Svejda, J., Vrba, M. and Blumajer, J. (1975) Neoplasma 22, 385–390
74 Roberts, K. and Northcote, D. H. (1971) Microsc. Acta 71, 102–120
75 Cole, G. T. and Wynne, M. J. (1973) Cytobios 8, 161–173
76 Severs, N. J., Jordan, E. G. and Williamson, D. H. (1976), J. Ultrastruct. Res. 54, 374–387
77 Liu, J. (1972) Parasitol. 58, 1151–1161
78 Hackett, R. L., Coleman, S. E. and Duggan, J. (1975) Am. J. Pathol. 75, 52A
79 Lott, J. N. A., Larsen, P. L. and Whittington, C. M. (1972) Can. J. Bot. 50, 1785–1787
80 Teigler, D. J. and Baerwald, R. J. (1972) Tiss. Cell 4, 447–456
81 Meyer, H. W., Roth, J. and Block, F. (1972) Protoplasma 75, 313–321
82 Servers, N. J. and Jordan, E. G. (1975) J. Ultrastruct. Res. 52, 85–99
83 Maul, G. G. (1971) J. Cell Biol. 51, 558–563
84 Martinez-Palomo, A. Pinto da Silva, P. and Chavez, B. (1976) J. Ultrastruct. Res. 54, 148–158
85 Koehler, J. K. (1972) in Principles and Techniques of Electron Microscopy (Hayat, M. A., ed.), Vol. 2, pp. 53–98, Van Nostrand-Reinhold, New York
86 Stevens, B. J. and André, J. (1969) in Handbook of Molecular Cytology (Lima de Faria, A., ed.), pp. 837–871, North-Holland, Publ. Co., Amsterdam
87 Watson, M. L. (1959) J. Biophys. Biochem. Cytol. 6, 147–155
88 Afzelius, B. A. (1955) Exp. Cell Res. 8, 147–158
89 La Cour, F. L. and Wells, B. (1972) Z. Zellforsch. 123, 178–194
90 Verbrodt, A. (1974) in The Cell Nucleus (Busch, H., ed.), Vol. 3, pp. 309–344, Academic Press, New York

91 Yasuzumi, G., Nakai, Y., Tsubo, I., Yasuda, M. and Sugioka, T. (1967). Exp. Cell Res. 45, 261–276
92 Raikhlin, N. T. and Shubin, A. S. (1970) Folia Histochem. Cytochem. 8, 121–128
93 Sikstrom, R. N., Lamoix, J. and Bergon, J. J. M. (1976) Biochim. Biophys. Acta 448, 88–102
94 Monneron, A. (1074) Phil. Trans. Roy. Soc. Lond. B. 286, 101–108
95 Scheer, U. and Franke, W. W. (1969) J. Cell Biol. 42, 519–533
96 Rupec, M., Bruhl, R. and Sekeris, C. E. (1971) Exp. Cell Res. 66, 157–163
97 Sekeris, C. E., Bruhl, R. and Rupec, M. (1971) Cytobiologie 4, 155–156
98 Bukhalov, I. B., Dmitrjev, H. A., Troitzkaya, L. P., Zbarsky, I. B., Perevoshchikova, K. A., Raikhlin, N. T. and Filippova, N. A. (1973) Cytologia 15, 823–827
99 Monneron, A. (1975) J. Cell Biol. 67, 291A
100 Coulson, A. S. and Kennedy, L. A. (1971) Blood 38, 485–490
101 Yoo, Y. and Oreland, L. (1976) Histochemistry 46, 131–137
102 Gorkin, W. Z. (1970) Experientia 27, 30
103 Franke, W. W., Keenan, T. W., Stadler, J., Genz, R., Jarasch, E. D. and Kartenbeck, J. (1976) Cytobiologie 13, 28–56
104 Philipp, E. I., Franke, W. W., Keenan, T. W., Stadler, J., and Jarasch, E. D. (1976) J. Cell Biol. 68, 11–29
105 Kleinig, H. (1970) J. Cell Biol. 46, 396–402
106 Kleinig, H., Zentgraf, H., Comes, P. and Stadler, J. (1971) J. Biol. Chem. 246, 2996–3000
107 Keenan, T. W., Berezney, R. and Crane, F. L. (1972) Lipids 7, 212–215
108 Khandwala, A. S. and Kasper, C. B. (1971) J. Biol. Chem. 246, 6242–6246
109 Bornens, M. and Kasper, C. B. (1973) J. Biol. Chem. 248, 571–579
110 Kawasaki, T. and Yamashina, I. (1972) J. Biochem. 92, 1517–1525
111 Mancini, P., Heywood, P. and Hodge, L. D. (1973). J. Cell Biol. 59, 214A
112 Kaneko, I., Satoh, H. and Ukita, T. (1972) Biochem. Biophys. Res. Commun. 48, 1504–1510
113 Nicolson, G., LaCorbiere, M. and Delmonte, P. (1972) Exp. Cell Res. 71, 468–473
114 Monneron, A. and Segretain, D. (1974) FEBS Lett. 42, 209–213
115 Stoddert, R. W. and Price, M. R. (1977) Biochem. Soc. Trans. 5, 121–122
116 Aaronson, R. P. and Blobel, G. (1975) Proc. Natl. Acad. Sci. U.S. 72, 1007–1011
117 Jarasch, E. D. and Franke, W. W. (1974) J. Biol. Chem. 249, 7245–7254
118 Kasper, C. B. (1971) J. Biol. Chem. 246, 577–581
119 Jarasch, E. D. (1973) PhD. Thesis, University of Freiburg
120 Wilson, E. M. and Chytil, F. (1976) Biochem. Biophys. Acta 426, 88–100
121 Berezney, R. and Crane, F. L. (1971) Biochem. Biophys. Res. Commun. 43, 1017–1023
122 Berezney, R., Macauley, L. K. and Crane, F. L. (1972), J. Biol. Chem. 247, 5549–5561
123 Zbarsky, I. B., Delektorsky, V. V., Troitskaya, L. P. and Perevoshchikova, K. A. (1973) Cytologia 15, 1453–1457
124 Zbarsky, I. B., Delektorsky, V. V., Troitskaya, L. P. Kuzmina, S. and Perevoshchikova, K. A. (1975) Folia. Biol. 21, 250–255
125 Mizuno, N. S., Stoops, C. E. and Sinha, A. A. (1971) Nature 229, 22–24
126 Mizuno, N. S., Stoops, C. E. and Peiffer, R. L. (1971) J. Mol. Biol. 59, 517–525
127 Hanaoka, F. and Yamada, M. A. (1971) Biochem. Biophys. Res. Commun. 42, 647–653
128 Yoshia, S., Modak, M. J. and Yagi, K. (1971) Biochem. Biophys. Res. Commun. 1408–1414
129 Yoshikawa-Fukada, M. and Ebert, J. D. (1971) Biochem. Biophys. Res. Commun. 43, 133–141
130 O'Brien, R. L., Sanyal, A. B. and Santon, R. H. (1972) Exp. Cell Res. 106–112
131 Jerzamonowski, A. and Toczko, K. (1973) Bull. Acad. Pol. Sci. Ser. Sci. Biol. 21, 404–408
132 Kay, R. R., Haines, M. E. and Johnston, I. R. (1971) FEBS Lett. 16, 233–236
133 Kay, R. R. and Johnston, I. R. (1973) Sub-Cell. Biochem. 2, 127–166
134 Deumling, B. and Franke, W. W. (1972) Hoppe-Seyler's Z. Physiol. Chem. 353, 287–297
135 Franke, W. W., Deumling, B., Zentgraf, H., Falk, H. and Rae, P. M. M. (1973) Exp. Cell Res. 81, 365–392
136 Comings, D. E. and Okada, T. A. (1973) J. Mol. Biol. 75, 609–618
137 O'Brien, R. L., Sanyal, A. B. and Santon, R. H. (1973) Exp. Cell Res. 80, 340–344
138 Wise, G. E. and Prescot, D. M. (1973) Proc. Natl. Acad. Sci. U.S. 70, 714–717
139 Hanania, N. and Harel, J. (1973) Biochimie, 55, 357–359
140 Barrieux, A., Long, G. L. and Garren, L. D. (1973) Biochim. Biophys. Acta 312, 228–242

141 LeBlanc, D. J. and Singer, M. F. (1974) Proc. Natl. Acad. Sci. U.S. 71, 2236–2240
142 Zebovitz, E. and Leong, J. K. L. (1974) Infect. Immunol. 10, 204–211
143 Vig, B. K. (1975) J. Theor. Biol. 54, 191–199
144 Cavalieri, L. F. and Carroll, E. (1975) Biochem. Biophys. Res. Commun. 67, 1360–1369
145 Dye, D. M. and Toliver, A. P. (1975) Biochim. Biophys. Acta 414, 173–184
146 Sparvoli, E., Galli, M. G., Mosca, A. and Paris, G. (1976) Exp. Cell Res. 97, 74–82
147 Agutter, P. S., Harris, J. R. and Stevenson, I. (1977) Biochem. J. 162, 671–679
148 Chardonnet, Y. and Dales, S. (1972) Virology 48, 342–359
149 Fry, D. J. (1970) in Membranes and Ion Transport (Bittar. E. E., ed.), Vol. 2, pp. 259–275, Wiley Interscience, New York
150 Riemann, W., Muir, C. and MacGregor, H. C. (1969) J. Cell Sci. 4, 299–304
151 Century, T. J., Fenichel, I. R. and Horowitz, S. B. (1970) J. Cell Sci. 7, 5-13
152 Horowitz, S. B. and Fenichel, I. R. (1970) J. Cell Biol. 47, 120–131
153 Horowitz, S. B. and Moore, L. C. (1974) J. Cell Biol. 60, 405–415
154 Kohen, E., Siebert, G. and Kohen, C. (1971) Hoppe-Seyler's Z. Physiol. Chem. 352, 927–937
155 Feldherr, C. M. (1965) J. Cell Biol. 25, 43–53
156 Feldherr, C. M. (1966) J. Cell Biol. 31, 199–203
157 Paine, P. L. and Feldherr, C. M. (1972) Exp. Cell Res. 74, 81–98
158 Gurdon, J. B. (1970) Proc. Roy. Soc. Lond. B 176, 303–311
159 Buttler, W. B. and Muller, G. C. (1973) Biochim. Biophys. Acta 294, 481–496
160 Bier, K. (1965) Chromosoma 16, 58–69
161 Goldstein, L. and Trescott, O. H. (1970) Proc. Natl. Acad. Sci. U.S. 67, 1367–1374
162 Feldherr, C. M. (1974) Exp. Cell Res. 85, 271–277
163 Scharrer, B. and Wurzelmann, S. (1969) Z. Zellforsch. 96, 325–343
164 Franke, W. W. and Scheer, U. (1970) J. Ultrastruct. Res. 30, 317–327
165 Scharrer, B. and Wurzelmann, S. (1969) Z. Zellforsch. 101, 1–12
166 Scheer, U. (1973) Dev. Biol. 30, 13–28
167 Horisberger, M. and Amos, H. (1970) Biochem. J. 117, 347–353
168 Agutter, P. S., Sim, R. B. and Harris, J. R. (1978) Biochim. Biophys. Acta, in the press
169 Agutter, P. S., McArdle, H. J. and McCaldin, B. (1976) Nature 263, 165–167
170 McNamara, D. J., Racevskis, J., Schumm, D. E. and Webb, T. E. (1975) Biochem. J. 147, 193–197
171 Yannarell, A., Schumm, D. E. and Webb, T. E. (1976) Biochem. J. 154, 379–385
172 Goidl, J. A., Canaani, D., Boublick, M., Weissbach, H. and Dickerman, H. (1975) J. Biol. Chem. 250, 9198–9205
173 Eckert, W. A., Franke, W. W. and Scheer, U. (1975) Exp. Cell Res. 94, 31–46
174 Hazan, N. and McCouley, R. (1976) Biochem. J. 156, 665–670
175 Franke, W. W. and Scheer, U. (1974) Symp. Soc. Exp. Biol. 28, 249–282
176 Franke, W. W. (1978) Crit. Rev. Biochem., in the press
177 Maul, G. G. (1970), J. Cell Biol. 46, 604–610
178 Bjerrum, O. J. and Bog-Hansen, T. C. (1976) in Biochemical Analysis of Membranes (Maddy, A. H., ed.), pp. 378–426, Chapman and Hall, London
179 Albert, W. H. W. and Davies, D. A. L. (1973) Immunology 24, 841–850
180 Hughes, D. E. and Cunningham, V. R. (1963) in Biochem. Soc. Symp. No. 23 (Grant, J. K., ed.), pp. 8–19, Cambridge University Press, Cambridge
181 Sottocasa, G. L. (1976) in Biochemical Analysis of Membranes (Maddy, A. H., ed.), pp. 55–78, Chapman and Hall, London
182 Depierre, J. and Dallner, G. (1976) in Biochemical Analysis of Membranes (Maddy, A. H., ed.), pp. 79–131, Chapman and Hall, London
183 Huang, C. H., Keyhani, E. and Lee, C. P. (1973) Biochim. Biophys. Acta 305, 455–473
184 Tosteson, D. C., Cook, P. and Blount, R. (1965) J. Gen. Physiol. 48, 1125–1143
185 Tyrrel, D. A., Heath, T. D., Colley, C. M. and Ryman, B. E. (1976) Biochim. Biophys. Acta 457, 259–302
186 Hubbard, A. L. and Cohn, Z. A. (1976) in Biochemical Analysis of Membranes (Maddy, A. H., ed.), pp. 427–501, Chapman and Hall, London
187 Philips, D. R. and Morrison, M (1971) Biochemistry 10, 1766–1771
188 Hunter, W. M. and Greenwood, F. C. (1962) Nature 194, 495–496

189 Marchalonis, J. and Nossal, G. J. V. (1968) Proc. Natl. Acad. Sci U.S. 61, 860–867
190 Caro, R. A., Ciscato, V. A., DeGiaconimi, S. M. V., Quiroga, S. and Radicella, R. (1975) Int. J. Appl. Rad. Isot. 26, 527–532
191 Hutchinson, M. D. and Zeigler, D. W. (1974) Appl. Microbiol. 28, 935–942
192 Wolf, B., Michelin Lauarot, P., Lesnaw, J. A. and Reichman, M. E. (1970) Biochim. Biophys. Acta 200, 180–183
193 Payne, J. W. (1973) Biochem. J. 135, 867–873
194 Brown, J. N. and Harris, J. R. (1970) J. Ultrastruct. Res. 32, 405–416
195 Farber, E. (1971) Annu. Rev. Pharm. 11, 71–96
196 Mull, R. H., Schgaguler, M. and Flemming, K. (1975) Biochem. Biophys. Res. Commun. 67, 849–856
197 Ernster, L. and Orrenius, S. (1965) Fed. Proc. 24, 1190–1191
198 Jakobsson, S. V. and Dallner, G. (1968) Biochim. Biophys. Acta 165, 380–392
199 Simard, R., Langelier, Y., Mandeville, R., Maestracci, N. and Royal, A. (1974) in The Cell Nucleus (Busch, H., ed.), Vol. 3, pp. 447–487, Academic Press, New York
200 Allison, A. C. (1974) in The Cell in Medical Science (Beck, F. and Lloyd, J. B., eds.), Vol. 1, pp. 315–353, Academic Press, New York
201 Alexandrov, K. and Frayssinet, C. (1975) Experientia 31, 778–779
202 Fry, D. J. and Wishart, G. W. (1976) Biochem. Soc. Trans. 4, 265–266
203 Hattori, T., Jakubovic, A. and McGeer, P. L. (1973) Neuropharmacol. 12, 995–999
204 Shinshine, G. H., Williams, D. J. and Rubin, B. R. (1971) Nature 230, 133–136
205 Jackson, V. and Chalkley, R. (1974) J. Biol. Chem. 249, 1615–1626
206 Miyaki, M., Kitayama, T. and Ono, T. (1974) J. Antibiotics 27, 647–655
207 Kravchenko, L. S., Oksman, A. Y., Glubokovskaya, I. O. and Tereshin, I. M. (1976) Biochemistry (USSR) 41, 111–118
208 Chai, L. S., Sandberg, A. A. and Weinfeld, H. (1976) Fed. Proc. 35, 1406
209 Sachan, D. S. (1975) J. Nutr. 105, 1631–1639
210 Kotite, L. and Tarver, H. (1969) Proc. Soc. Exp. Biol. Med. 131, 403–405
211 Baglio, C. M. and Farber, E. (1965) J. Cell Biol. 27, 591–601
212 Farber, E. (1967) Adv. Lip. Res. 5, 119–183
213 Williams, D. J., Rubin, B. R. and Kisilewsky, R. (1972) FEBS Lett. 26, 245–248
214 Kisilevsky, R. and Weiler, L. (1976) Exp. Mol. Pathol. 24, 193–200
215 Milne, J. F. and Harris, J. R. (1977) Proc. Roy. Microsc. Soc., 12, 56
216 Milne, J. F. and Harris, J. R. (1978) Biochem. Soc. Trans., in the press
217 Hildebrand, C. E. and Okinaka, R. T. (1976) Anal. Biochem. 75, 290–300
218 Willison, J. H. M. and Rajaraman, R. (1977) J. Microsc. 109, 183–193
219 Tan, H. K., Harrison, M. and Gralnick, H. R. (1974) J. Natl. Cancer Inst. 52, 1367–1371
220 Severs, N. J. (1976) Cytobios 16, 125–132
221 Bornens, M. (1977) Nature 270, 80–82
222 Feldherr, C. M., Richmond, P. A. and Noonan, K. D. (1977) Exp. Cell Res. 107, 439–444
223 Zatsepina, O. V., Polyakov, V. Yu. and Chentsov, Yu. S. (1976) Cytologia 18, 1433–1437
224 Kirschner, R. H., Rusli, M. and Martin, T. E. (1977) J. Cell Biol. 72, 118–132
225 Infante, A. A., Firshein, W., Hobert, P. and Murray, L. (1976) Biochemistry 15, 4810–4817
226 Ito, K., Arens, M. and Green, M. (1976) Biochim. Biophys. Acta 447, 340–352
227 Yoshida, S., Ungers, G. and Rosenberg, B. H. (1977) Nucleic Acid Res. 4, 223–228
228 Hobert, P., Duncan, R. and Infante, A. A. (1977) Nature 267, 542–544
229 Sinha, A. A. and Mizuno, N. S. (1977) Cell Tiss. Res. 183, 191–201
230 Szekely, J. G. and Copps, T. P. (1976) J. Cell Biol. 70, 466–470
231 Kuzmina, S. N., Kalandarishvili, F. A. and Buldyaeva, T. V. (1976) Biokhimiya 41, 1371–1381
232 Nägel, W. C. and Wunderlich, F. (1977) J. Memb. Biol. 32, 151–164
233 Amano, M., Akino-Sugiyama, T., Munakata-Yoshida, H., Shindo-Okada, N. and Kawahara, A. (1977) Cell Struct. Funct. 2, 91–100

A range of potential substrates of the types:

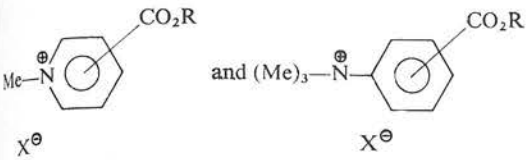

where R is *p*-nitrophenyl or *p*-chlorophenyl, have been synthesized. It is expected that the *p*-isomers will be accommodated in the sites of the co-polymers better than the *m*-isomers. Both the *p*-nitrophenyl and *p*-chlorophenyl series of substrates are subject to nucleophile-catalysed hydrolysis in the presence of mercaptoethanol. Co-poly(acrylic acid–allyl thioacetate) after aminolysis causes a marked enhancement in the rate of hydrolysis of the substrates, but this reaction has not, as yet, been shown to proceed via an intermediate thiol ester.

Kinetic studies need to be performed to examine the reactions of the polymers with the substrates; however, only small enhancements in rate have so far been observed with the *p*-nitrophenyl esters, owing to the high pK_a value of the polymer-bound thiol groups (approx 10.5) and the high rate of aqueous hydrolysis of the *p*-nitrophenyl ester substrates. The use of the less hydrolytically sensitive *p*-chlorophenyl esters may solve this problem.

We thank the Science Research Council for a Postdoctoral Research Fellowship for V. W. P.

Kiefer, H. C., Congdon, W. I., Scarpa, I. S. & Klotz, I. M. (1972) *Proc. Natl. Acad. Sci. U.S.A.* **69**, 2155–2159

Overberger, C. G. & Smith, T. W. (1975) *Macromolecules* **8**, 401–406

Overberger, C. G., Pacansky, T. J., Lee, J., St. Pierre, T. & Yaroslavsky, S. (1974) *J. Polym. Sci.* **46**, 209–225

Van Etten, R. L., Sebastian, J. F., Clowes, G. A. & Bender, M. L. (1967*a*) *J. Am. Chem. Soc.* **89**, 3242–3253

Van Etten, R. L., Clowes, G. A. Sebastian, J. F. & Bender, M. L. (1976*b*) *J. Am. Chem. Soc.* **89**, 3253–3262

Characterization of Mammalian Liver Nuclear Envelope

JEREMY F. MILNE, PAUL S. AGUTTER,* JAMES R. HARRIS and GEOFFREY STUBBS

Division of Biochemistry, North East London Polytechnic, Romford Road, London E15 4LZ, U.K.

We have previously described a rapid procedure for the isolation of rat liver nuclear-envelope 'ghosts' (Harris & Milne, 1974). This method has subsequently been found to be equally applicable to pig liver. Data obtained on the enzymic content of the purified nuclear envelope, the DNA, RNA, protein and phospholipid content and polypeptide composition revealed by sodium dodecyl sulphate/polyacrylamide-gel electrophoresis will be presented below.

The chemical composition of purified rat liver nuclear envelope, expressed as percentage of the dry weight, is as follows: protein, 75%; phospholipid, 15%; DNA, 3%; RNA, 7%. The corresponding values for pig liver nuclear envelope are: protein, 64%; phospholipid, 11%; DNA, 5%; RNA, 4%. These values are in general agreement with those of other workers (Franke *et al.*, 1970; Kay *et al.*, 1972), although there does appear to be a significantly greater amount of DNA retained in the pig liver nuclear envelope.

* Present address: Department of Biology, Napier College of Commerce and Technology, Colinton Road, Edinburgh E10 5DT, Scotland, U.K.

Table 1. *Nuclear-envelope enzymes*

All activities are expressed in μmol/h per mg of protein, and are means $\pm$1 S.E.M. for five determinations.

Enzyme	Specific activity	
	Rat liver	Pig liver
Adenosine triphosphatase (EC 3.6.1.3)	16.4 $\pm$ 3.1	10.1 $\pm$ 2.5
Glucose 6-phosphatase (EC 3.1.3.9)	15.3 $\pm$ 6.3	13.9 $\pm$ 1.7
Glucose 1-phosphatase (EC 3.1.3.10)	0.12 $\pm$ 0.10	0.65 $\pm$ 0.75
5′-Nucleotidase (EC 3.1.3.5)	1.3 $\pm$ 1.1	0.40 $\pm$ 0.25
Alkaline phosphatase (EC 3.1.3.1)	1.3 $\pm$ 0.9	1.3 $\pm$ 1.0
Acid phosphatase (EC 3.1.3.2)	8.5 $\pm$ 2.2	8.1 $\pm$ 1.7
NADH–ferricyanide reductase (EC 1.6.99.3)	15.1 $\pm$ 4.2	8.1 $\pm$ 0.9
NADPH–ferricyanide reductase (EC 1.6.2.4)	6.1 $\pm$ 1.5	3.9 $\pm$ 0.4
Monoamine oxidase (EC 1.4.3.4)	0	1.6 $\pm$ 0.4
Succinate dehydrogenase (EC 1.3.99.1)	0.5 $\pm$ 0.4	0.9 $\pm$ 0.4

Procedures that produce disruption of the nuclear envelope into small sheets and vesicles, in contrast with those that produce nuclear-envelope 'ghosts', tend to give material with a lower DNA content and which at the same time appears to have less-well-preserved nuclear-pore complexes.

Since both morphological and functional integrity of isolated nuclear envelope are of prime importance, it is thought that some residual chromatin contamination can be tolerated. This is particularly so, since attempts to remove residual chromatin by extraction with solutions of high salt concentration (e.g. 2M-NaCl or 2M-KCl) produced fragmentation of the nuclear envelope and the nuclear-pore complexes, with a concomitant decrease in the histone, DNA and RNA content.

Several of the enzymes detectable in rat and pig liver nuclear envelope are listed in Table 1. There is considerable agreement between the two species for the specific activities of the enzymes listed, and in all cases there is no increase in specific activity over that present in the endoplasmic reticulum. We have suggested (Agutter *et al.*, 1977) that an RNA- or poly(G)-stimulated Mg^{2+}-activated nucleoside triphosphatase (e.g. adenosine triphosphatase, EC 3.6.1.3) may possibly be useful as an enzymic marker for nuclear envelope, since this stimulation of nucleoside triphosphatase activity is not detectable in endoplasmic reticulum. We have recently noted, while performing ^{125}I-labelling studies, that both purified rat liver nuclei and nuclear envelope show a significant endogenous peroxidase activity, which produces ^{125}I incorporation into the nuclear-envelope proteins in the absence of exogenous peroxidase (J. R. Harris & G. Stubbs, unpublished work). This endogenous enzyme can be inhibited by the usual reversible inhibitors, such as cyanide, and irreversibly by 3-amino-1,2,4-triazole. Since there have been no reports of peroxidase activity in endoplasmic reticulum that can actively incorporate ^{125}I into protein, the nuclear-envelope peroxidase may prove to be a satisfactory marker enzyme for nuclear envelope.

After solubilization in 2% sodium dodecyl sulphate/1% 2-mercaptoethanol, the dissociated polypeptides of rat and pig liver nuclear envelope gave a very similar and highly reproducible distribution of stainable bands on polyacrylamide-gel electrophoresis in the presence of 0.1% sodium dodecyl sulphate. Fig. 1 shows a densitometric trace from a representative polyacrylamide electrophoresis gel of rat liver nuclear envelope. The leading band of mol.wt. approx. 15000 is co-migratory with chromatin histones, and the double band (arrowed) of mol.wt. approx. 75200 is thought to be the major component of the nuclear-pore complex (P. Marshall & J. R. Harris, unpublished work). The higher-molecular-weight polypeptides are present as a

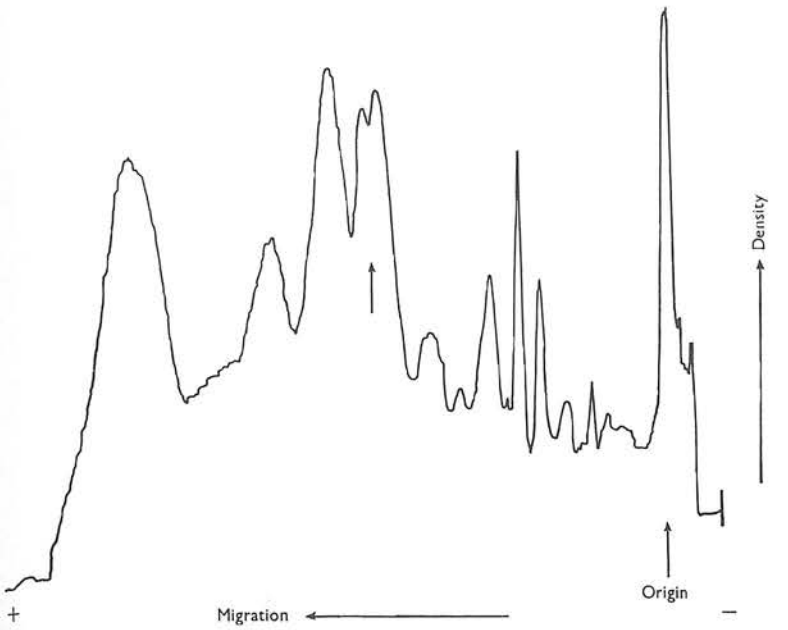

Fig. 1. *Densitometric profile of rat liver nuclear envelope after sodium dodecyl sulphate/polyacrylamide-gel electrophoresis*

relatively small proportion of the total protein and are found to increase in number and proportion when rats are subjected to metabolic inhibitors (Milne & Harris, 1978).

It is hoped that by correlating analytical and enzymic data on the nuclear envelope and endoplasmic reticulum, it may in due course be possible to provide a more clear-cut biochemical distinction between these membrane systems. To date ultrastructural criteria, such as the presence of nuclear-pore complexes, the location of ribosomes on the outer nuclear membrane and the attachment of residual chromatin to the inner nuclear membrane, have been used as the main markers for the assessment of nuclear-envelope purity (Harris & Agutter, 1976). In addition, the suggestion that the nuclear-pore complex may be the location of the nuclear-envelope activated Mg^{2+}-2 activated adenosine triphosphatase (Agutter *et al.*, 1976), and that this enzyme could be involved in the nucleocytoplasmic translocation of ribonucleoproteins, is likely to receive support from subsequent analysis of subfractionated nuclear envelope (Harris, 1977).

This work is supported by grants from the Medical Research Council and The Royal Society.

Agutter, P. S., McArdle, R. J. & McCaldin, B. (1976) *Nature (London)* **326**, 165–167
Agutter, P. S., Harris, J. R. & Stevenson, I. (1977) *Biochem. J.* **162**, 671–679
Franke, W. W., Deumling, D., Ermen, B., Jarasch, E. D. & Kleinig, H. (1970) *J. Cell Biol.* **46**, 379–395
Harris, J. R. (1977) in *Membranous Elements and Movement of Molecules: Techniques* (Reid, E., ed.), vol. 6, pp. 245–250, Horwood, Chichester
Harris, J. R. & Agutter, P. S. (1976) in *Biochemical Analysis of Membranes* (Maddy, A. H., ed), pp. 132–173, Chapman and Hall, London
Harris, J. R. & Milne, J. F. (1974) *Biochem. Soc. Trans.* **2**, 1251–1253
Kay, R. R., Fraser, D. & Johnston, I. R. (1972) *Eur. J. Biochem.* **30**, 145–154
Milne, J. F. & Harris, J. R. (1978) *Biochem. Soc. Trans.* **6**, 308–311

The Relation of Bile Proteins to Serum and Liver Plasma Membrane

BARBARA M. MULLOCK and RICHARD H. HINTON

Wolfson Bioanalytical Centre, University of Surrey, Guildford GU2 5XH, Surrey, U.K.

Although there have been many studies on the low-molecular-weight constituents of mammalian bile, there is no clear agreement on the origin of bile proteins. An obvious source is the outer leaflet of the hepatocyte plasma membrane, and indeed it has been shown that bile is rich in enzymes typical of the plasma membrane (Holdsworth & Coleman, 1975; Evans *et al.*, 1976) and that bile salts are capable of solubilizing membrane proteins (Vyvoda *et al.*, 1977). Moreover, it is clear that the 5′-nucleotidase of bile is immunologically identical with the enzyme present in liver plasma membrane (Evans *et al.*, 1976; Mullock *et al.*, 1977). However, immunological studies have also shown the presence of serum proteins, notably albumin and immunoglobulins, in human bile (Russel & Burnett, 1963). A protein with the immunological properties of serum albumin is also present in rat bile, but its electrophoretic mobility in sodium dodecyl sulphate-containing polyacrylamide gels differs from that of native serum albumin (Evans *et al.*, 1976). Further, the general pattern of rat bile proteins is quite distinct from that of serum proteins (Hinton & Mullock, 1977).

Thus data available at present do not support a single source for bile proteins. It would seem clear that there is some solubilization of proteins, including enzymes such as 5′-nucleotidase, from the bile-canalicular face of hepatocytes, but that such solubilization cannot explain the presence of serum proteins in bile. Two hypotheses that would explain this observation are: (*a*) the 'mistaken' discharge of secretion granules containing serum proteins at the bile-canalicular rather than at the sinusoidal face of hepatocytes; (*b*) the discharge of serum proteins taken up and processed through the lysosomal system, for it has been suggested by de Duve & Wattiaux (1966) that lysosomes discharge their contents into the bile canaliculi. We have now attempted a systematic study of the immunological and electrophoretic properties of the proteins of rat bile with a view to improving our understanding of their origin.

Hooded rats of the University of Surrey strain were used in all experiments. Blood and bile were collected as described earlier (Mullock *et al.*, 1977). Crossed immunoelectrophoresis using single or split antibody-containing gels was carried out as described by Axelsen *et al.* (1973). Anti-(rat serum) was from Mercia (Watford, Herts., U.K.). Anti-(cholestatic rat serum) and anti-(liver plasma membrane) antisera were prepared by using the dosage schedule given by Mullock *et al.* (1977). Two dimensional electrophoresis with the first dimension run in agarose gel and the second dimension in a gradient polyacrylamide gel, was performed as described by Hinton & Mullock (1977).

Crossed immunoelectrophoresis of rat bile proteins against anti-(rat serum) and anti-(liver plasma membrane) revealed the presence of at least 14 proteins (Table 1). No difference was found between the reactions of bile with anti-(rat serum) and anti-(cholestatic rat serum). Of the 14 proteins only one, a relatively minor component, reacted with anti-(liver plasma membrane) and not with anti-(rat serum). Three proteins reacted with anti-(rat serum) and with all preparations of anti-(liver plasma membrane); another protein reacted with anti-(rat serum) and with some anti-(liver plasma membrane) preparations. The relative strength of the reaction of all four proteins with the different antisera suggested that all were, in fact, serum proteins [our anti-(liver plasma membrane) antisera contain antibodies to a number of serum proteins (Issa *et al.*, 1977)]. The remaining nine bile proteins reacted with anti-(rat serum), but not with anti-(liver plasma membrane). Bile lipoprotein (Manzato *et al.*, 1976) did not appear to react with anti-(rat serum) or with anti-(liver plasma membrane), for none of the peaks obtained by crossed immunoelectrophoresis stained with Sudan Black B.

Only nine proteins could be distinguished after two-dimensional electrophoresis of rat bile proteins. By measurement of the electrophoretic mobility in the first (agarose) dimension and by absorption of the bile with immobilized anti-(rat serum) it was possible to correlate most components identified on two-dimensional electrophoresis